Conf.-820827

fe 2.3.1

Proceedings of the DOE Physical and Chemical Energy Storage Annual Contractors' Review Meeting

August 23-26, 1982
Stouffers National Center Hotel
Arlington, Virginia

Published December, 1982

Sponsored by:
U.S. Department of Energy
Office of Energy Systems Research
Division of Energy Storage Technology
Washington, D.C.

DISCLAIMER

This report has been reproduced directly from the best available copy.

Available from the National Technical Information Service, U. S. Department of Commerce, Springfield, Virginia 22161.

Price: Printed Copy A25
Microfiche A01

Codes are used for pricing all publications. The code is determined by the number of pages in the publication. Information pertaining to the pricing codes can be found in the current issues of the following publications, which are generally available in most libraries: *Energy Research Abstracts, (ERA); Government Reports Announcements* and Index (*GRA* and I); *Scientific and Technical Abstract Reports (STAR);* and publication, NTIS-PR-360 available from (NTIS) at the above address.

Conf.-820827

Proceedings of the DOE Physical and Chemical Energy Storage Annual Contractors' Review Meeting

August 23-26, 1982
Stouffers National Center Hotel
Arlington, Virginia

Published December, 1982

Coordinated by:
Courtesy Associates, Inc.
For:
Brookhaven National Laboratory
Upton, New York
Under Contract No. AC02-76CH00016

Sponsored by:
U.S. Department of Energy
Office of Energy Systems Research
Division of Energy Storage Technology
Washington, D.C.

FOREWORD

The Department of Energy (DOE), Office of Energy Systems Research (ESR), conducted an Annual Contractors' Review Meeting during the week of August 23-26, 1982. The meeting was held at the Stouffer's National Center Hotel in Arlington, Virginia, with approximately 200 people in attendance, including contractors, DOE representatives, and interested observers. All of the technology areas within the Physical and Chemical Storage Branch of ESR were reviewed at the single meeting this year. Projects within the following technology areas were presented:

- Chemical/Hydrogen Energy Systems - managed by Brookhaven National Laboratory (BNL)
- Underground Energy Storage - managed by Pacific Northwest Laboratories (PNL)
- Superconducting Magnetic Energy Storage - managed by Los Alamos National Laboratory (LANL)
- Mechanical Energy Storage - managed by Oak Ridge National Laboratory (ORNL)
- Solar Thermal Energy Storage - managed by the Solar Energy Research Institute (SERI) assisted by Sandia Laboratories
- Thermal Energy Storage for Building Heating and Cooling and Industrial Applications - managed by Oak Ridge National Laboratory (ORNL)

The participants in the meeting were welcomed by Dr. James Swisher, DOE Division Director for Energy Storage Technology, and additional comments and guidance were provided by Dr. Rufus Shivers, Physical and Chemical Energy Storage Branch Chief, who served as DOE Chairman for the meeting. Dr. Michael Gurevich, DOE Program Manager, coordinated the technical inputs for the meeting.

Presentations were made by the industrial and university contractors followed by a question and answer period after each presentation. Overview papers by the National Laboratory managers were presented where appropriate. A special Review Committee, invited by DOE, and made up of recognized experts in each of the technology areas, participated in the meeting and evaluated the progress in separate discussion sessions. A separate report of their findings will be provided to DOE for their use.

The proceedings are divided into six sections corresponding to the major technology areas. The papers describe the progress and accomplishments in the projects through mid-calendar year 1982. A project summary sheet is included for each project outlining its goals and tasks as well as providing administrative information. In addition, several papers not formally presented at the meeting have been included.

The 1982 meeting was planned and conducted by Brookhaven National Laboratory program personnel at the request of DOE. We wish to thank the Session

Chairmen from SERI and the National Laboratories for assisting us and coordinating their individual sessions. Special recognition is accorded to Ms. Annmarie Pittman and the staff of Courtesy Associates, Inc. for their support in organizing the meeting as well as the compilation of the proceedings.

We also express our appreciation to the participants in the meeting; contractors, reviewers, and outside guests whose cooperation and interest contributed to a very productive exchange of ideas.

Rufus Shivers, Chief
Physical and Chemical
Storage Branch
Office of Energy Systems
Research
U.S. Department of Energy

Michael F. Bonner
Associate Program Manager
Chemical/Hydrogen Energy
Systems Program
Brookhaven National Laboratory

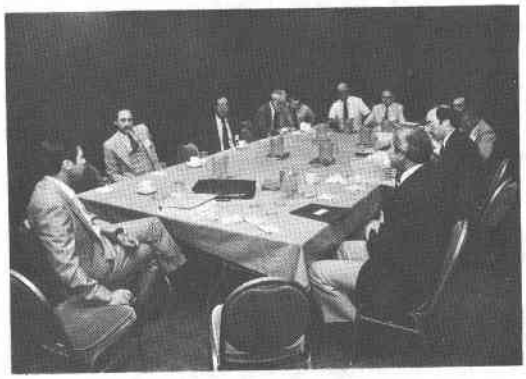


PROJECTION

TABLE OF CONTENTS

TABLE OF CONTENTS

TABLE OF CONTENTS

TABLE OF CONTENTS

TABLE OF CONTENTS

TABLE OF CONTENTS

TABLE OF CONTENTS

TABLE OF CONTENTS

TABLE OF CONTENTS

TABLE OF CONTENTS

TABLE OF CONTENTS

TABLE OF CONTENTS

TABLE OF CONTENTS

TABLE OF CONTENTS

TABLE OF CONTENTS

BROOKHAVEN NATIONAL LABORATORY
CHEMICAL/HYDROGEN ENERGY SYSTEMS
PROGRAM OVERVIEW

Alessio Mezzina
Brookhaven National Laboratory
Upton, NY 11973

1.0 INTRODUCTION

Brookhaven National Laboratory (BNL) provides management, technical oversight, and in-house R&D support to the C/HES Program on behalf of the Division of Energy Storage in the DOE Office of Energy Systems Research. Through FY '82 the program elements have addressed: Hydrogen Production; Storage Systems and Materials; Chemical Heat Pumps and Chemical Energy Systems.

The C/HES Program has undergone changes in direction and emphasis which have reflected the revised federal guidelines. FY 82 has represented the completion of the transition from a near- to mid-term program orientation which had addressed energy conserving commercialization opportunities, to the long-term high-risk/high-payoff criteria currently being applied to program definition.

2.0 PROGRAM DESCRIPTION AND OVERVIEW

2.1 Current Status

- Chemical Heat Pumps/Chemical Energy Storage

This area of investigation is typical of the near- to mid-term thrust of past activities and FY '82 marks the completion of CHP systems development and test efforts.

Rocket Research Corporation is completing the detailed performance mapping of the 150,000 Btu/hr H_2SO_4/H_2O Verification Test Unit by demonstrating temperature amplification over a wide range of thermal inputs and operating conditions. TRW is providing comparative analyses of the H_2SO_4/H_2O CHP and current as well as emerging competitive technology. The project will culminate in a seminar given to industrial users and manufacturers as well as to venture capital interests for the purpose of transferring further pursuits to the private sector.

Southern California Gas Company and Solar Turbine, Inc. are pursuing component development for the metal hydride pair chemical heat pump. These efforts have been redirected in FY 1982 from systems development and testing to fabrication and testing of small metal hydride assemblies to show the effectiveness of heat/mass flow enhancement designs.

Stanford Research Institute has completed preliminary analyses supported by bench-scale testing of a process for recovering hydrogen from H_2S. Technical feasibility has been demonstrted but cost/economic factors associated with the process remain uncertain, to a large extent due to sulfuric acid being identified as a by-product.

o Hydrogen Technology

This area of investigation has been redirected from systems development and testing to long-term base technology development. In FY 82 modest efforts have been applied to characterizing selected components and modules and to set the stage for future exploratory R&D.

Advanced alkaline electrolysis modules are being subjected to endurance tests using advanced electrodes and separator mateials capable of operating at elevated temperatures in order to maximize voltage efficiency at high current densities.

The static feed water electrolysis concept is being developed to show the ability to electrolyze brackish water. Single and multicell module tests are being conducted using electrodes scaled up from 0.1 ft^2 to 1 ft^2.

Several projects are underway in advanced electrolysis research, which represent long-term R&D thrusts. The goal of these investigations is to significantly reduce the voltage requirements for electrolytic hydrogen production. Anode depolarization using low-cost coal derivatives as the oxidizable species and solid oxide electrolyte high temperature (1000°C) electrolysis concepts are being investigated. Investigations into photolytic water decomposition have been limited to development and characterization of heterojunction electrodes. Hole injection has been demonstrated with continued efforts emphasizing increase in efficiency and characterization of stability factors.

A novel hydrogen production concept based upon the catalytic decomposition of water at 500°C using zeolites is being evaluated experimentally to determine prospects for future low-cost hydrogen production when solar, fusion or fission heat sources are made available.

Planning efforts involving the design of facilities and experiments to illustrate photovoltaics/electrolyzer interface have been completed.

Investigation into hydrogen storage and transport have been limited to studies of hydrogen embrittlement and low-cycle fatigue testing of conventional pipeline steels which may be used to transport hydrogen. Experimental testing of laboratory fracture mechanics specimens as well as 4-inch pipe show that cycling over wide pressure swings may result in enhanced propagation of cracks and other defects. These findings are being equated to field experience.

2.2 FY '83 Program Description

The C/HES Program planned for FY '83, consistent with DOE guidelines, will be dedicated to the conduct of R&D in advanced hydrogen production and storage/transport technologies. Efforts will be directed toward selected ongoing projects as well as toward new starts as will have been justified in BNL's technology assessment and planning studies.

2.2.1 Technology Research

Major projects in Technology Research are as follows:

- Catalytic Decomposition of Water Using Zeolites - CCS/TBD
  Efforts will aim toward identification of effective and stable trivalent metal salts as candidate catalysts. Techniques for maximizing thermodynamic efficiencies associated with water management will be developed.

- High Temperature Electrolysis - BNL/TBD
  Investigations will seek to minimize losses at electrode/solid oxide electrolyte interface through use of additives or dopants. Tests will proceed from half-cell through full-cell and multi-cell configurations as modifications are characterized. Materials investigations will include considerations for increasing operating temperature regimes.

- Anode Depolarization - BNL/Texas A&M
  Electrochemical performance improvements attained by introducing oxidizable species at the anode of an electrolyzer are well recognized. Key to development is the identification of an invariant electrolyte. These efforts will be sustained in parallel with work for identifying suitable catalysts and depolarizers.

- Advanced Hydrogen Storage Systems - TBD
  The characterization of metal hydride and microsphere hydrogen storage systems and concepts will be extended to a comprehensive evaluation of novel concepts which will include: cryo-storage in carbon; storage in high-density polymers; storage in liquid organic compounds.

- H_2 Liquefaction Using Magnetic Refrigeration Techniques - LANL
  LANL has conducted preliminary studies over a limited temperature range which show that novel magnetic refrigeration techniques promise a two- or three-fold improvement in efficiency over conventional cryogenic technology. The proposed work will investigate the application of the concept over a wider temperature range (20^{o} to $300^{o}K$) suitable for H_2 liquefaction, and include studies in porous bed heat transfer and materials compatibility.

- Cyclic Reduction/Oxidation of Alkali Metal Compounds - BNL/TBD
  Preliminary systems analyses show favorable thermodynamics at efficiencies approaching 70% if high grade heat is used in highly endothermic reactions where alkali metal compounds are directly reduced to yield energy-intensive and storable products (CO and Na). Sodium can be chemically or electrochemically converted to usable high-grade energy and the oxide can be recycled. Initial efforts will be devoted to experimental verification of the direct reduction process and the development of

Additional work is planned in the areas of:

- Photolytic Decomposition of Water
- Hydrogen Embrittlement
- Conducting Polymers

2.2.2 Exploratory Development

Projects within this category deal with design, fabrication and test of components and subsystems leading to process or systems verification testing, and evaluation.

- Static Feed Water Electrolysis - Life Systems, Inc.
  Single and multicell modules comprised of electrodes scaled up from 0.1 ft^2 to 1 ft^2 will be used to evaluate sea water electrolysis. Pacing problems relate to the presence of organics and their impact on electrochemical performance and stability. Means for maximizing performance efficiency also will be examined by introducing advanced catalyst/electrodes and by operating at elevated temperature.

- Photovoltaics/Electrolyzer Technical Illustration - BNL/TBD
  Designs of the test bed and experiment will be implemented. Initial efforts will be devoted to obtaining key hardware such as the PV array, amplifier/conditioner, electrolyzer and ancillaries and installing the equipment in accordance with the BNL Plan. The test program calls for characterizing the transient performance of the advanced electrolysis system (Advanced Alkaline or SPE) followed by a decision point regarding "stand-alone" testing.

- Advanced Alkaline Water Electrolysis - Teledyne Energy Systems
  Incentives remain to continue testing of advanced components suited to elevated temperature operation of alkaline electrolyzers. IEA participants have emphasized development of advanced separator materials. The TES ARIES test rig can be applied to the conduct of performance verification of such components as a cooperative function within the IEA activity.

3.0 BNL'S MANAGEMENT AND FINANCIAL PERSPECTIVE

3.1 Management Summary

The C/HES Program continues to be organized in three segments:

- Technology Assessment and Planning
- Technology Research
- Exploratory Development

The bulk of the projects are in the research segment as would be expected based on current DOE policy guidance.

3.2 Financial Summary

Figure 1 summarizes the financial aspects of the program showing:

- A modest decrease in overall program spending from $3.2M in FY 1982 to a projected $3.0M in FY 1983.
- The continuing emphasis on H_2 production in terms of number of projects.
- The phase-out of chemical heat pump and large systems development projects.
- Major funding commitments in several new areas, e.g., advanced storage.

The budgets and planning for FY 1983 are preliminary and could change significantly based on actions taken by current administration regarding DOE's status and level of funding.

FIGURE 1

CHEMICAL/HYDROGEN ENERGY SYSTEMS PROGRAM
FINANCIAL SUMMARY
JUNE 1982

Program Activities/Contractor:	Actual FY 1982 Funding ($1000)	Planned FY 1983 Funding ($1000)
1. Technology Assessment & Planning		
• Systems Analysis & Planning (BNL)	110	90
• Support Services (Consultants)	120	100
• Program Admin./Mgmt. (IEA) (BNL)	480	360
• Tech. Assessment (Aerospace)	170	-
• CHP Systems Analysis (TRW)	55	-
Sub Total	935	550
2. Technology Research		
• Cat. Decomp. H_2O-Zeolites (CCS)	44	150
• High Temp. Elect. (BNL/TBD*)	120	200
• Anode Dep. (BNL/Texas A&M)	120	150
• Photolytic H_2 Production (SUNY)	30	100
• Advanced Storage of H_2 (TBD)	-	200
• Magnetic Refrigeration (TBD)	-	250
• H_2 Embrittlement (Battelle)	150	200
• Slurry Hydrides (TBD)	-	50
• Conducting Polymers (TBD)	-	50
• Cyclic Red./Ox. Alkali Comp. (BNL/TBD)	-	150
• H_2 from H_2S (TBD)	-	50
• Advanced Alkaline Mat. (U. Va.)	36	-
• H_2 Recovery from H_2S (SRI)	35	-
• H_2 Production Analysis (LANL)	22	-
• H_2 Purification/Separation (ERG/APCI)	20	-
Sub Total	577	1550
3. Exploratory Development		
• Static Feed Electrolysis (Life Systems)	275	250
• PV Elect. Tech. Illus. (BNL)	190	150
• PV Elect. Hardware (TBD)	-	250
• Adv. Alk. Component Test (Teledyne)	110	100
• Heat/Mass Flow Enhancement (TBD)	234	100
• H_2SO_4/H_2O Chemical Heat Pump (RRC)	477	-
• MH_x Eng. Support (ANL)	44	-
• BHO Contracts/Closeouts	500	50
Sub Total	1830	900
TOTAL	3242	3000

*TBD - To be determined

METAL HYDRIDE/CHEMICAL HEAT PUMP DEVELOPMENT PROGRAM (PART I AND II)

Theresa A. Argabright and David A. Rohy
Solar Turbines Incorporated
P.O. Box 80966
San Diego, CA 92138

Hector A. Madariaga
Southern California Gas Company
Box 3249, Terminal Annex
Los Angeles, CA 90051

INTRODUCTION

Southern California Gas Company and Solar Turbines Incorporated are cooperating in the development and demonstration of a novel metal hydride heat pump (MHHP). The MHHP is a chemical heat pump containing two different metal hydrides. The concept is based on the ability of selected metals to absorb and desorb hydrogen without the consumption of metal or hydrogen. The MHHP can be tailored to provide heating and/or cooling, or temperature upgrading over a wide range of temperatures and, thus, can be used with a variety of heat sources.

In this project, because the MHHP is a cyclical device, heat transfer is considered to be the key technical study area. High heat transfer leads to rapid cycling, high capacity, low hydride inventory per unit output and low system costs. Due to the cyclic nature of this device, the parasitic self-heating and cooling losses of the structure must be reduced. Therefore, the goal of this project is to provide high heat transfer with a low mass unit.

HEAT PUMP CONCEPT

The metal hydride heat pump consists of two different metal alloys that absorb and desorb hydrogen in a controlled sequence. Heat is generated on hydrogen absorption, while desorption is endothermic. The two alloys are maintained separately (Fig. 1) and the hydrogen is thermally driven from hydride A to hydride B and back. The processes are intermittent; continuous output would require dual heat pumps and appropriate controls to establish 180 degrees out-of-phase operation.

There are three heat pump cycles applicable to this study (Fig. 2): refrigeration, heat amplification and temperature upgrade. The MHHP refrigeration cycle uses high temperature heat (T_H) to fire the system, while medium temperature heat (T_M) is rejected to the atmosphere and refrigeration is produced at T_L. For heat amplification, the heat pump operation is identical to the refrigeration cycle, only the temperature use is altered. As in the refrigeration mode, high temperature heat (T_H) is used to fire the system. The low temperature heat (T_L) that was previously used for refrigeration is obtained from a lower temperature, ambient condition source. The medium temperature heat (T_M), which was rejected to the atmosphere in the refrigeration cycle, is used for heating.

In the temperature upgrade cycle, the heat pump operation is reversed compared to the other two modes. Instead of requiring a high temperature heat source to drive the system, this cycle upgrades a medium grade waste heat stream (T_M) to a higher temperature (T_H) without the use of a fossil fuel input. Specifically, this cycle uses an intermediate

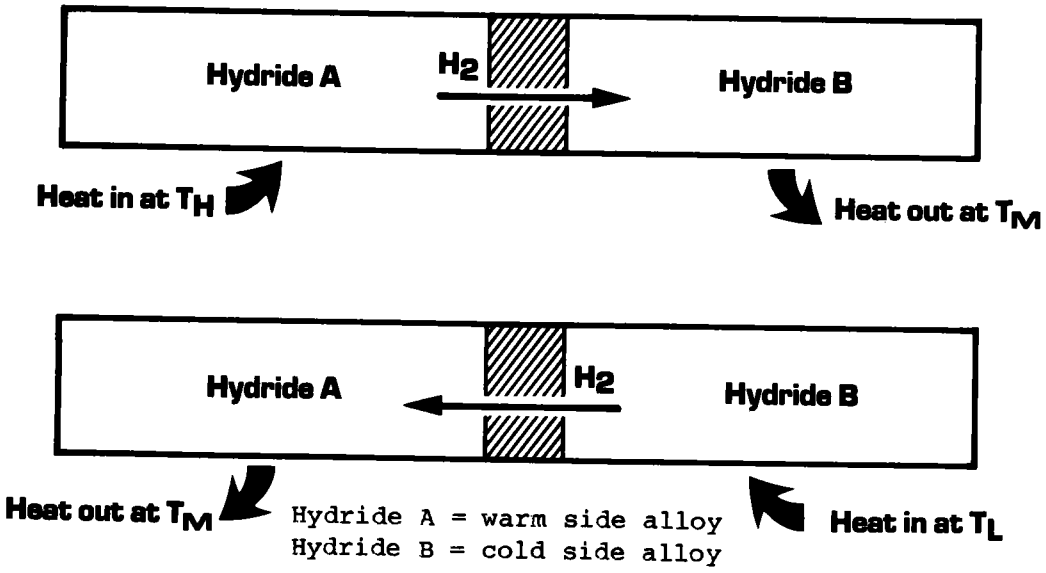

Figure 1. Heat Pump Cycle

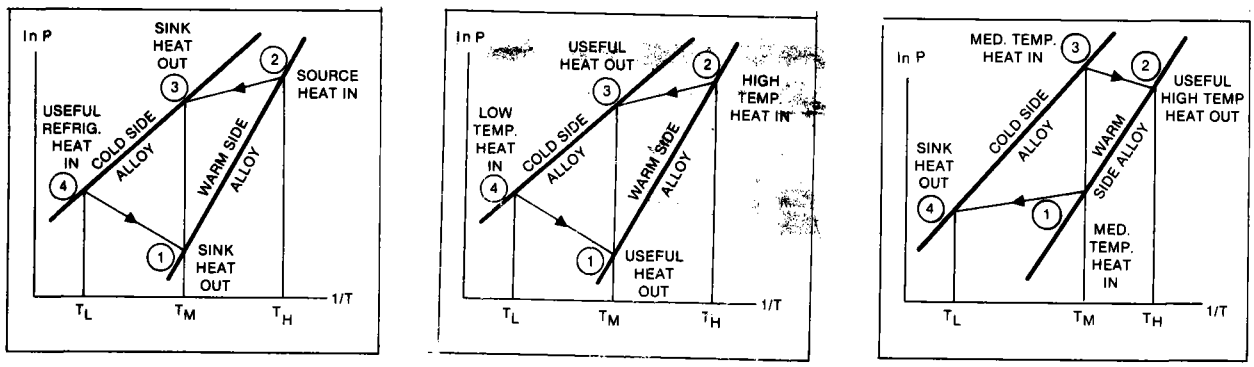

Refrigeration Cycle | Heat Amplification Cycle | Temperature Upgrade Cycle

Figure 2. Heat Pump Cycles: Pressure-Temperature Diagrams

temperature heat source (T_M) and low temperature ambient conditions (T_L) to produce a high temperature process stream (T_H). This cycle was chosen as the focus for the MHHP study.

HYDRIDE MATERIALS

The material requirements for a metal hydride heat pump are specified by the operating temperatures (Table 1). The MHHP requires two different hydrides to work in tandem, one alloy operating on the cold side and the other operating on the warm side. The plateau pressures must be such that the hydrogen will be driven between the two alloys. Hysteresis (difference between the absorption and desorption plateau pressures at a constant temperature) is an important factor, because it tends to lower the maximum ΔT at which the MHHP can operate.

Table 1

Temperature Upgrade Operating Conditions

		Temperature Regime	
Product	T_H	140 - 190°C	(280 - 375°F)
Source	T_M	70 - 110°C	(160 - 230°F)
Sink	T_L	-1 - 40°C	(30 - 110°F)

The alloy pair, $LaNi_5$ (cold side alloy) and $LaNi_{4.5}Al_{0.5}$ (warm side alloy), was selected for use in the MHHP temperature upgrade unit. The selection was based on the several hydride characteristics of the alloys in the intended operating conditions. The alloys will operate in the specified temperature ranges and have low hysteresis losses which allow flexibility in the temperature and pressure operating conditions. The pressure drop between absorption-desorption of the alloys during the heat pump application is in excess of 2 atm. giving enough pressure to move the hydrogen from one alloy to the other. Both $LaNi_5$ and $LaNi_{4.5}Al_{0.5}$ have a relatively high hydride heat of formation allowing for efficient use of the alloy.

HYDRIDE HEAT EXCHANGER

Two parallel design approaches for the hydride heat exchanger were investigated (Fig. 3). Tubular hydride containers were the focus of the first approach. The hydride powder and the heat transfer enhancement

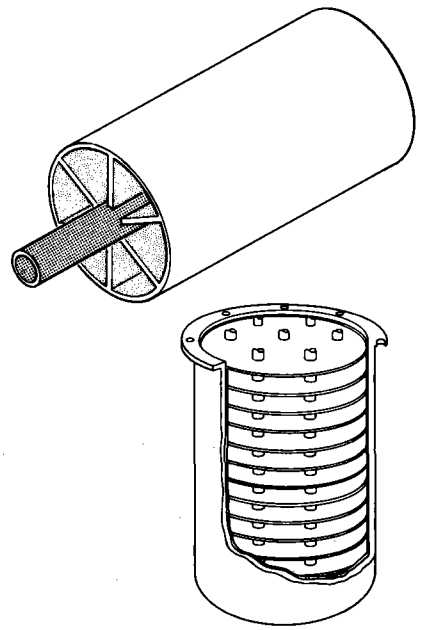

Figure 3. Hydride Heat Exchanger Design - Two Parallel Modeling Paths (not to scale)

device are located inside a tube and the heat transfer media flows externally across the tube. The other approach focused on an externally finned hydride heat exchanger. This model is a tube with external transverse fins in which the working fluid flows through the tube and the hydride powder is packed between the external fins.

A computer model was developed to simulate the thermal processes of the heat exchanger configurations. Many design iterations were executed which incorporated various heat transfer coefficients, tube diameters, temperature differentials and fin geometry. Test rigs were designed and built to verify the computer results.

The results of these studies provided guides for choosing optimum design configurations for each heat exchanger approach. The optimum internal heat transfer device was a nominal one inch OD copper tube with six internal fins. A central cyclindrical filter could be used within the tubular structure as shown in Figure 3. Studies of the external heat transfer device indicated an optimum design geometry of a 0.25 inch copper tube with external copper fins of thickness 0.020 inch, fin spacing of 0.150 inch and a fin height of 0.25 inch.

Table 2 is a comparison of the two optimum designs. The thermal mass ratio is a term which describes the ratio of sensible heat of the hydride powder to the sensible heat of the entire structure including the hydride. The goal is to minimize the sensible heat of the structure and achieve maximum hydride usefulness. The coefficient of performance (COP) is useful in comparing the thermal efficiencies of the two heat transfer configurations. The COP equation for MHHP temperature upgrade cycle is:

$$COP_{\text{temperature upgrade}} = \frac{\text{Net heat output at } T_H}{\text{Net heat input at } T_M} \quad \text{or}$$

$$COP_{upgrade} = \frac{Q_{abs(LaNi_{4.5}Al_{0.5})} + SH_{(LaNi_{4.5}Al_{0.5})}(T_M - T_H)}{Q_{des(LaNi_{4.5}Al_{0.5})} + SH_{(LaNi_{4.5}Al_{0.5})}(T_H - T_M) + Q_{des(LaNi_5)} + SH_{(LaNi_5)}(T_L - T_M)}$$

where Q_{abs} = heat of absorption, Btu

SH = sensible heat, Btu/°F

Q_{des} = heat of desorption, Btu

Based on the more favorable parameters for the externally finned hydride heat exchanger, the decision was made to utilize that design for the MHHP.

FILTER DESIGN STUDIES

It is essential that the fine particles of the two hydrides do not intermix by traveling with the hydrogen gas as it cycles form bed to bed. A particle separator/retainer (or filter) in the hydrogen flow path is

Table 2

Hydride Heat Exchanger Comparisons

Heat Exchanger Configuration	Thermal Mass Ratio	Calculated Cycle Time (minutes)	Specific Heat Rate (Btu/hr-lb Hyd)	Cost ($/Btu/hr)	COP* Temperature Up Grade
Externally Finned Tube	0.75	1.13	2,443	4.25×10^{-3}	0.42
Internally Finned Tube	0.57	1.67	1,554	7.0×10^{-3}	0.38

* maximum possible = 0.55

required to isolate each hydride bed. A critical parameter in the MHHP performance is cycle time and, if the ΔP across the filter is substantial, the result is a long cycle time. Therefore, a filter test rig was fabricated to determine the pressure drop across various hydride powder/filter configurations. Previous filter testing had indicated that the ΔP across a specific filter can vary substantially depending upon the orientation of the filter in relation to the metal hdyride powder.

Previous studies also indicated that one of the most effective filters was a sintered stainless steel filter. Further work in the current program focused on the optimum filtering scheme with regards to orientation and configuration. The goal was to develop a filtering scheme with the following parameters: low pressure drop across the filter, less than 3.45 kPa (5 psi); little restriction of hydrogen gas flow; containment of the hydride powder (no migration of one hydride bed to the other through the filter); long life (clog-free with time); and economical investment.

FINAL DESIGN

The final design of the advanced hydride heat exchanger (Fig. 4) consists of 14 externally finned copper tubes in a staggered tube bundle arrangement. The hydride powder is stored in the annular spacing between the fins, and the heat transfer media, pressurized water, flows through the finned tubes. The 14 finned copper tubes are divided evenly so that 7 tubes function as water inlets and 7 tubes are water outlets. A manifold and flange configuration connect each set of 7 tubes into the appropriate flow path. Solid insulation is placed around the tube bundle. This entire configuration is then loaded into a cylindrical pressure vessel to contain the hydrogen.

The heat exchanger vessel is designed to hold approximately ten pounds of hydride powder. After the pressure vessel is fabricated and pressure checked, the powder is loaded into the vessel through fill ports located on each side of the vessel. The ports are staggered along the vessel wall, three on one side and two on the other. This allows for equal and uniform filling of the hydride powder into the voids between the fins. No welding or processing other than closing the ports with

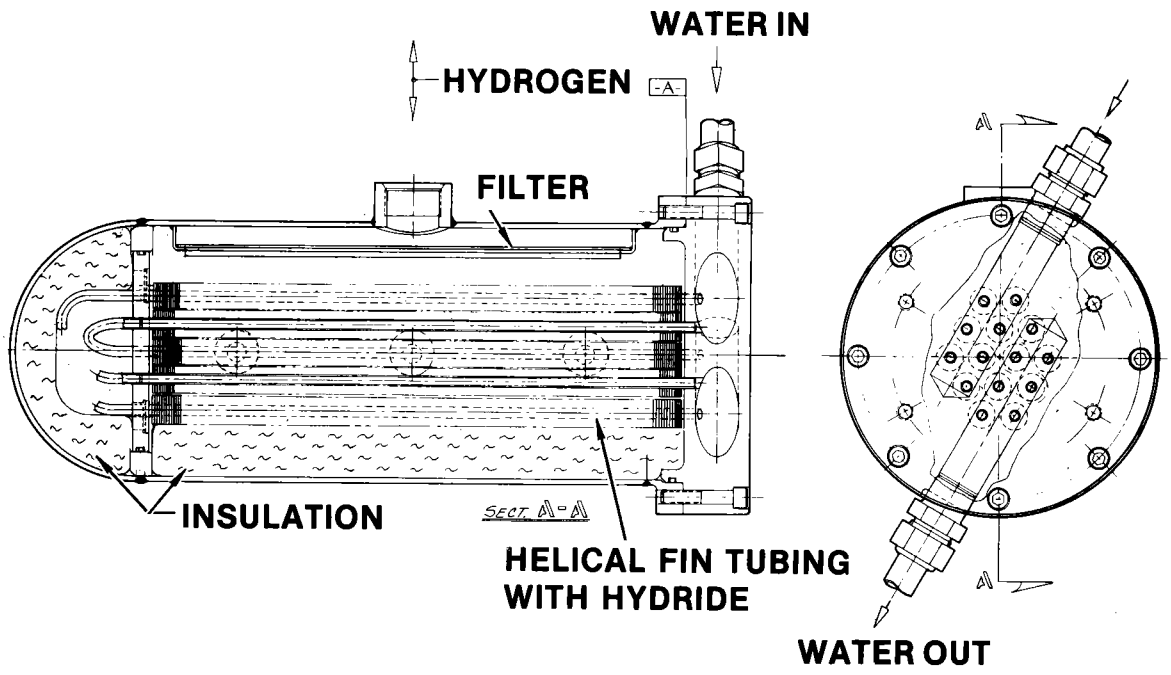

Figure 4. Advanced Hydride Heat Exchanger Schematic

threaded pressure plugs is required. The filter in the hydride heat exchanger module was designed with sufficient area to allow the hydrogen gas to rapidly escape with a low pressure drop. It runs parallel to the tube bundle and is held in place by a stainless steel frame which is welded to the pressure vessel wall.

The MHHP design consists of two pressure vessels connected as a pair. In a temperature upgrade mode, one vessel contains $LaNi_5$ hydride (cold side alloy) packed around the 14 finned copper tubes, while the second vessel contains $LaNi_{4.5}Al_{0.5}$ hydride (warm side alloy) in a similar configuration. The design capacity of this unit is 20,000 Btu/hr of upgraded heat with a calculated cycle time of less than two minutes and a COP of 0.45.

HYDRIDE HEAT EXCHANGER FABRICATION

The construction of the advanced hydride heat exchanger occurred in the Solar Turbines Incorporated Research Laboratories. A search for a vendor to provide 0.25 inch OD copper tubing with 0.25 inch copper fins indicated that this component was commercially unavailable as a standard item. Therefore, Solar fabricated this item in its own lab (Fig. 5). Braze alloys were determined and the entire heat exchanger assembly was brazed together. The external pressure vessel housing was machined, completing the modules.

Due to time restrictions and the need to verify the critical technology of the hydride heat exchangers, the modules are mounted on an existing refrigeration heat pump facility at Solar Turbines Incorporated rather than the temperature upgrade heat pump facility as planned. Testing will be conducted in the refrigeration mode which will verify

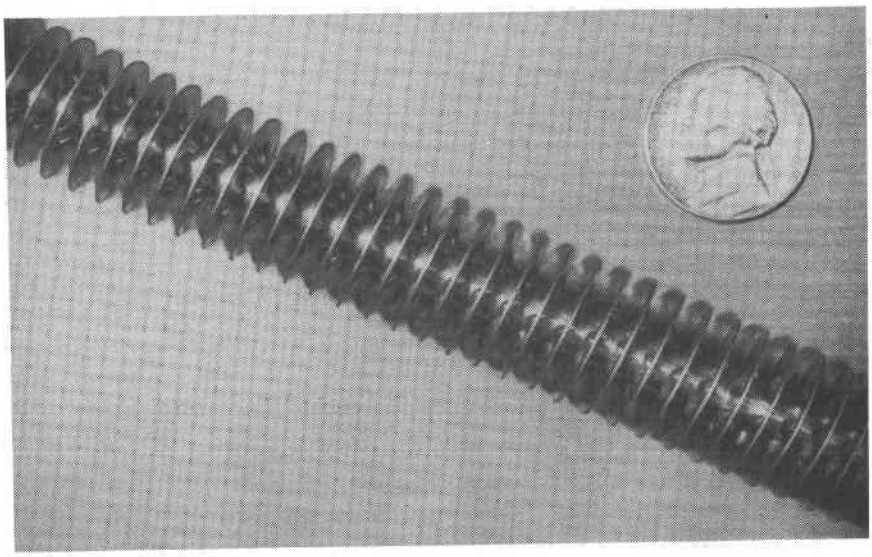

Figure 5. Actual Finned Tube

cycle times and critical heat transfer calculations. Only minor modifications to the advanced hydride heat exchanger are necessary to operate in the refrigeration mode. The heat exchanger pressure vessels remain the same - no design changes are needed. However, the hydride alloys chosen for the temperature upgrade cycle have been replaced with refrigeration alloys. The two alloys well suited for the refrigeration cycle are $LaNi_5$ as the warm side alloy and $MmNi_{4.15}Fe_{0.85}$* as the cold side alloy. The temperature regime is T_H = 200°F as the source heat, T_M = 85°F as the heat sink and T_L = 40°F as the refrigerated product.

Due to the differences in the hydride heat of formation, one vessel will hold 7.3 lbs of $LaNi_5$ and the other will hold 10.3 lbs of $MmNi_{4.15}Fe_{0.85}$. The expected capacity in the refrigeration mode is one ton or 12,000 Btu/hr of refrigeration with anticipated cycle times of less than two minutes. The coefficient of performance (COP) of the MHHP unit for cooling is defined as:

$$COP_{cool} = \frac{\text{Net Heat Input at } T_L}{\text{Net Heat Input at } T_H} \quad ; \text{ or}$$

$$COP_{cool} = \frac{Q_{des(MmNi_{4.15}Fe_{0.85})} + SH_{(MmNi_{4.15}Fe_{0.85})} (T_M - T_L)}{Q_{des(LaNi_5)} + SH_{(LaNi_5)} (T_M - T_H)}$$

The calculated COP for the MHHP refrigeration mode is 0.54. The maximum theoretical COP is 0.74. (This assumes no sensible heat gain or loss.)

---

* Mm = mischmetal

TESTING

Initial tests will be directed toward the verification of performance factors such as heat transfer rates and fluid flow rates. An individual copper finned tube will be encapsulated in a fully insulated stainless steel tube and the voids between the fins will be filled with activated hydride powder. Circulating water will flow through the copper tube and the rate at which heat is transferred from the hydride to the water (due to the absorption and desorption of hydrogen) will be measured.

MHHP module testing will verify over-all cycle perforamnce at the design points. Factors such as heat transfer and fluid flow rates, hydrogen flow rates, pressure, temperature, and cycle times will be monitored and optimized. Phase II testing will be completed by September 1982.

ACKNOWLEDGEMENTS

The authors wish to acknowledge Dr. J. Michael Clinch of Argonne National Laboratory for verification of thermal analysis.

THE SULFURIC ACID/WATER CHEMICAL HEAT PUMP PROGRAM

E. Charles Clark and Thomas R. Duranti
Rocket Research Company
York Center
Redmond, Washington 98052

ABSTRACT

The verification test unit (VTU) designed, built and demonstrated during the previous contract (1) has been tested extensively. System performance measurements using a single simulated waste heat source have been completed and tests using two simulated heat sources of differing temperatures are nearing completion. System thermal COP's ranged from 0.1 to 0.3 during the single source tests. Steady temperature amplification of 60° to 90°F was repeatedly achieved. Preparations are under way to conduct an extended duration test with a total operation time of 100 hours.

INTRODUCTION

The Department of Energy (DOE) has been sponsoring the research and development of chemical heat pumps (CHP) and related energy storage devices for several years.

Chemical heat pumps represent a new technology base with the ability to substantially reduce the consumption of energy in the industrial, commercial and residential sectors. These devices provide an ability to capture low-grade heat rejected from buildings and industrial sources and to reuse the heat at increased temperature levels for confort and water heating or in industrial processing. Chemical heat pumps operate with up to 15 times less electrical power and in higher temperature regimes than conventional heat pumps, thus affording significant performance advantages over the conventional designs. An additional advantage is that energy storage can be incorporated because of the working fluid selection so that intermittent energy source, such as solar energy, can be utilized.

Rocket Research Company has been under contract to explore the design and economics of the sulfuric acid and water CHP since 1976 (1, 2, 3). Nearing completion of this task, under contract to Brookhaven National Laboratory, Rocket Research Company (RRC) has identified the industrial chemical heat pump (ICHP) used to boost the temperature level of industrial reject heat as one of the most promising concepts. While requiring further engineering development for commercialization, the primary proof of concept in terms of materials of construction, system performance and economics has been completed. A verification test unit (VTU) has been constructed with a nominal power rating of 150,000 Btu/hr. Complete performance mapping has been accomplished covering a wide range of system conditions. The current four-task program is organized to conduct performance mapping tests at various source/sink temperature combinations for both single and dual source systems. Additionally, the effects of condenser temperatures have been measured.

SYSTEM DESCRIPTION

The chemical heat pump used for temperature boosting operates essentially as a reverse absorption chiller. Medium temperature reject heat is used to power the system and heat is extracted both at a higher temperature for process use and rejected at near ambient temperature. Figure 1 presents a general schematic and describes the system operation for both the acid and water circuits. For further details on system operation and performance definition, the reader is referred to references 1 and 4.

ACID CIRCUIT

1. **Generator** — Dilute acid is input into the generator where the acid/water separation takes place. Concentrated acid is removed from the bottom and water vapor is removed at the top of the generator. The concentrated acid is cooled by the distillation process.
2. **Acid Heat Exchanger No. 1.** — The concentrated acid from the generator is input into acid heat exchanger No. 1, where it is heated by the waste heat source to regain sensible energy lost in the generator.
3. **Absorber** — Concentrated acid leaving acid heat exchanger No. 1 is input into the absorber along with water vapor transported from the evaporator. The concentrated acid provides a significant chemical attraction for the water vapor, and the water vapor is forced to condense into the acid and dilute it. The resulting dilution process dramatically increases the temperature of the acid solution.
4. **Acid Heat Exchanger No. 2** — Hot dilute acid is routed to acid heat exchanger No. 2 where heat is removed and delivered to a process at a temperature significantly higher than the waste heat source. The dilute acid is then routed to the generator for reconcentration.

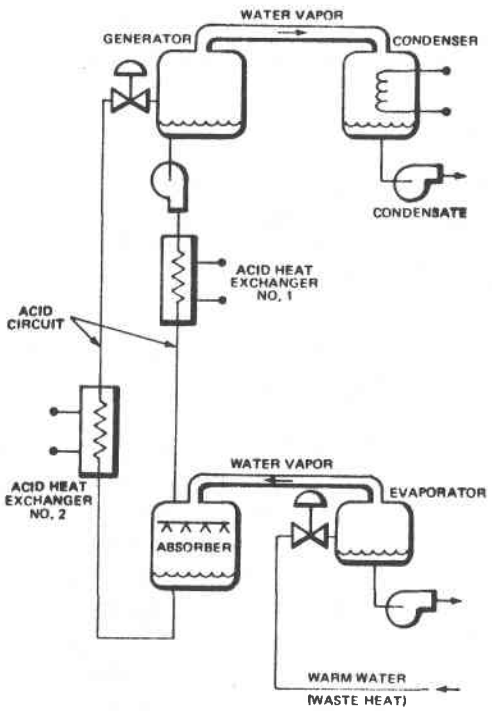

WATER CIRCUIT

1. **Condenser** — Water vapor is removed from the generator by the condensation process. A low-temperature source such as industrial water, groundwater, etc. is used to remove the heat of condensation at ambient temperature. The liquid condensate formed is either routed to the evaporator or discarded, depending on the system design.
2. **Evaporator** — The waste heat source is used to input energy into the evaporator to produce water vapor which is transported to the absorber. If the waste heat source is water (as shown in the schematic), it is input directly into the evaporator where flash evaporation takes place without the necessity for a heat exchanger.

FIGURE 1

INDUSTRIAL CHEMICAL HEAT PUMP OPERATION

VERIFICATION TEST UNIT (VTU)

The VTU designed, built and tested during the previous contract (1) was modified slightly to improve its operational characteristics. The generator, absorber, evaporator and condenser units were left intact. Modifications consisted of improving the acid flow circuit control, acid temperature measurements, and waste heat simulator improvements. Figure 2 presents a picture of the completed system, including the waste heat simulation equipment and plumbing (water heaters shown in right-hand background).

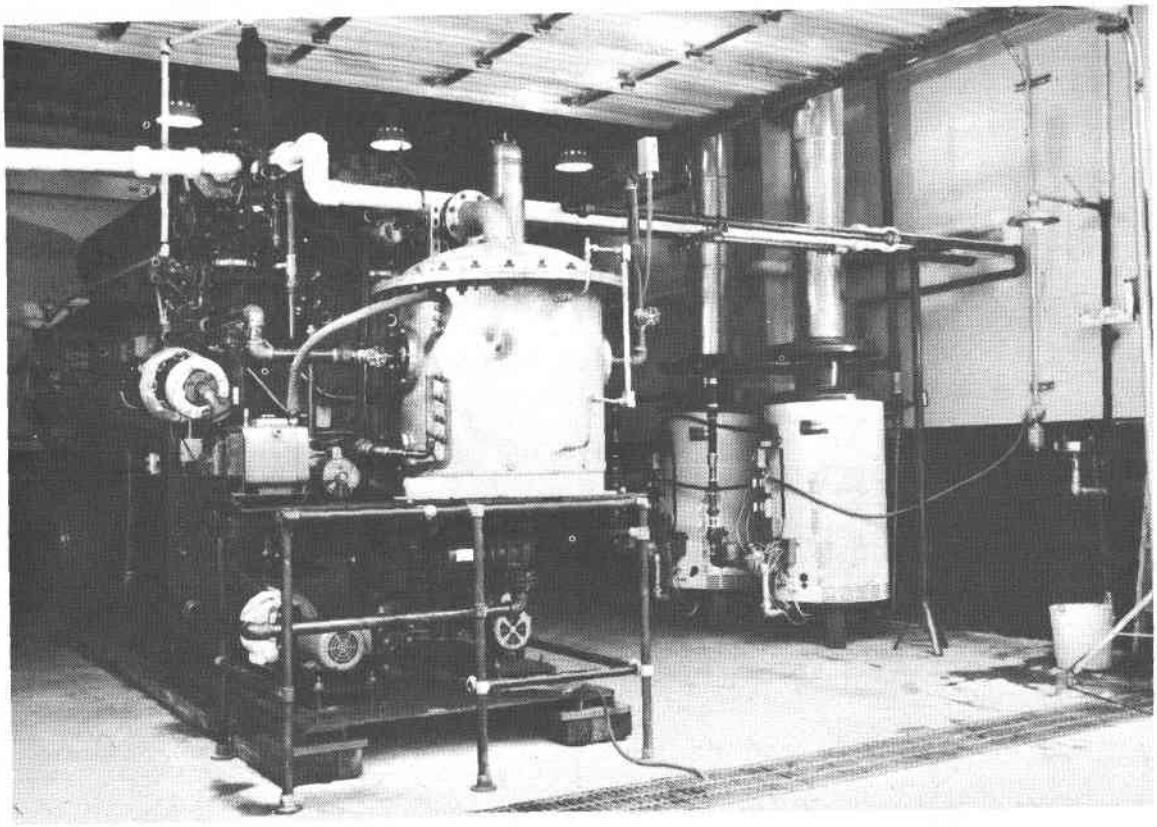

FIGURE 2

VERIFICATION TEST UNIT

Specific modifications to the acid flow loop consisted of adding ullage to the acid flow loops, replacing the control valves, increasing the acid pump rpm for improved flow rates, and replacing the two mechanical vacuum pumps with water aspirators. The additional acid ullage was achieved by replacing the 4-inch-diameter teflon-lined pipe used on the generator and absorber drains with 6-inch-diameter glass pipe. This not only improved the acid flow control between the generator and absorber units, but allowed for visual observation of the acid levels. The acid pump speed was increased by installing a belt-driven linkage which increases the impeller speed from 1,740 rpm to 2,320 rpm, and maintains a 64-foot water head at 15 gpm. To control acid flow rate into the generator and absorber, two manually operated teflon clamp valves were provided upstream of each reactor. These valves were observed to be overly sensitive with a very narrow control band. They were replaced with two Durco teflon-lined plug valves operated with semi-automatic electrical positioners (i.e., the switches are manually operated).

Four thermocouple wells were designed and fabricated from Carpenter 20 to enable direct thermocouple measurement of acid temperatures at each heat exchanger inlet and outlet terminal. The units were designed to ensure that the sensing wells cannot be removed or acid sprayed in the event of a failure.

Additional changes to the waste heat simulation circuits included improving both flow measurement and reliability, as well as the available system NPSH to the waste heat feedwater pump.

A major improvement to the ICHP peripheral equipment has been demonstrated during this study. Formerly, two vacuum pumps in continuous service were needed to scrub inert gases from the generator and absorber. Maintenance of cold traps was particularly time-consuming and expensive. Since a large cooling water flow is required for the condenser (100 gpm) it seemed practical to use a portion of this flow to drive a water aspirator. Two Penberthy-Houdaille 1-1/2-inch inlet water aspirators were installed and have successfully replaced both the generator and absorber mechanical vacuum pumps.

SINGLE-SOURCE TESTING

A total of 11 tests were conducted simulating single-source operation. The first eight tests were conducted with the condenser temperture constant at 62±4°F, while the steam temperature was varied. In the remaining three, performance was mapped at higher condenser temperatures: 81°F $\leq T_c \leq$123°F. Performance parameters such as heat extracted ($\dot{Q}_{HX2}$), COP_t, and temperature amplification (ΔT_A) were measured as functions of source (T_s) and sink (T_c) temperature.

Computer-aided plots of test 82-06, parts 6B and 6C, are given in Figure 3. Temperature responses of several process variables versus elapsed process time (as opposed to real time) illustrate the importance of balancing heat flows in and out of the ICHP. In the first portion of Figure 3, marked 6B, the temperature of the acid decreases continuously at a steam temperature of 176°F. The measured acid concentration diluted from 85 to 63 wt% during this 85-minute period. Although the calculated ΔT_{amp}= 85.7°F, the final equilibrium value was approaching approximately 70°F (see Figure 3). The steam valve was then shut to the absorber and the preheat water temperature in the boiler was increased to ~220°F, allowing acid reconcentration in the generator to 70.5 wt% after 70 minutes. At this higher concentration, an equilibrium ΔT_{amp}= 80°F was attained, given proper $\dot{Q}_{HX1}$ to $\dot{Q}_{HX2}$ balance. Nearly negligible acid dilution reoccurred during portion 6C (68.5 wt% finally).

Figure 4 presents a plot of thermal COP_t as a function of steam temperature supplied to the acid absorber (simulated wate heat). Only data points where thermal equilibrium was closly approached (≥95%) are considered. As shown, two data points exist outside the nominal performance band. This is due exclusively to operating the system in a derated mode (~1/10 of the nominal capacity). During these tests, temperature amplification was being maximized at the expense of output heat flow.

DUAL SOURCE TESTING

Dual source testing began near the end of July of this year. Although data reduction is not complete, quick-look data indicate the system is responding as would be expected. For example, with a 200°F primary source supplied to the evaporator, and a 260°F second simulated

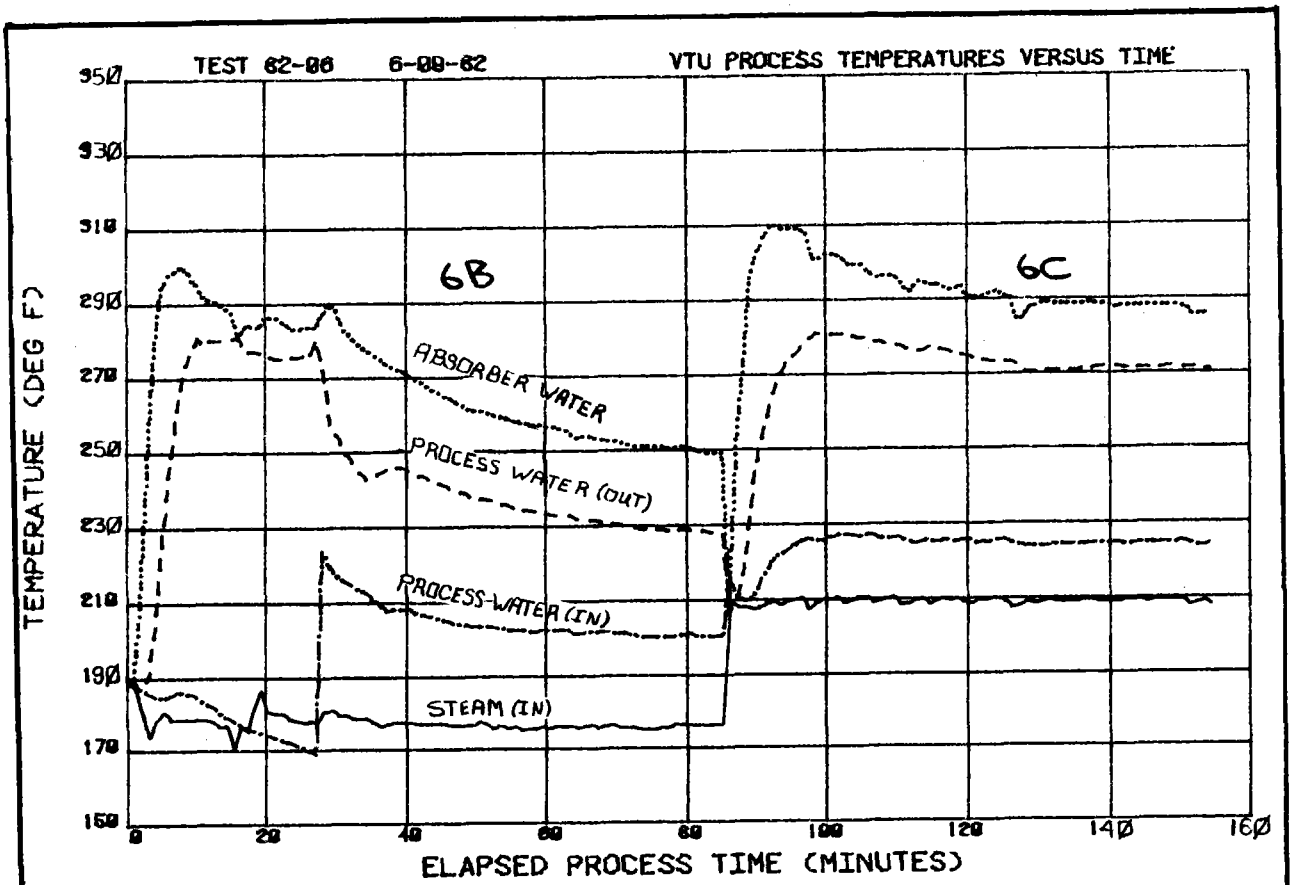

FIGURE 3

INDUSTRIAL CHEMICAL HEAT PUMP

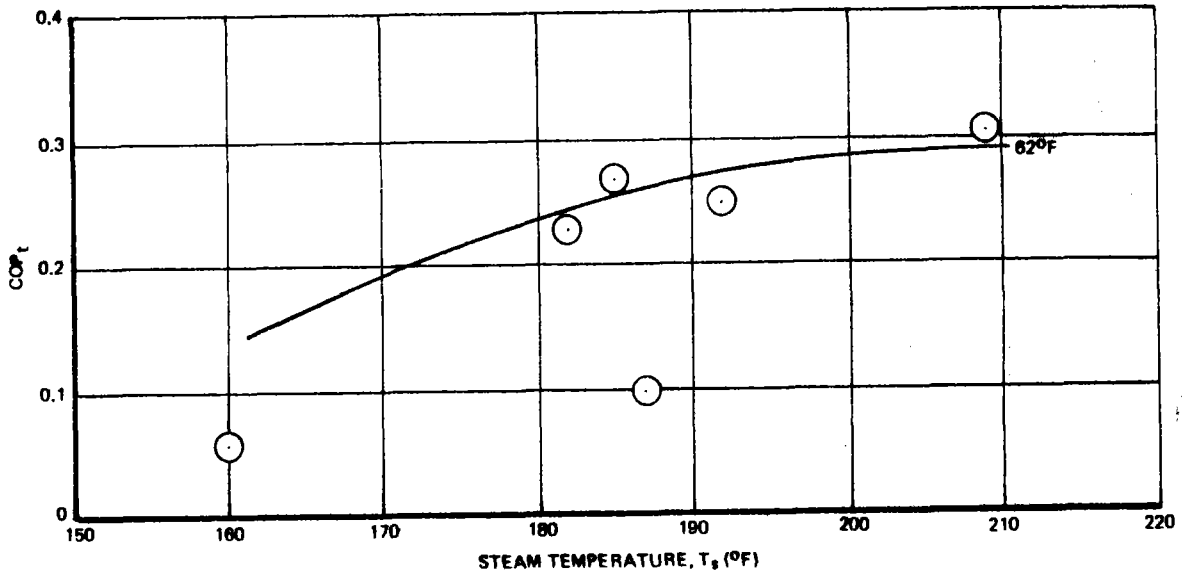

FIGURE 4

THERMAL COEFFICIENT OF PERFORMANCE (COP_t) AS A FUNCTION OF STEAM INLET TEMPERATURE (at CONSTANT T_c)

source supplied to heat exchanger number 1, the absorber temperature output was 290°F at a power level of 150,000 Btu/hr. By reducing the power to 100,000 Btu/hr, a temperature of 305°F was reached.

With no heat removed from the system, an equilibrium acid temperature of 365°F was achieved. A condenser temperature of 80°F was maintained throughout the performance map. Testing is expected to be complete by mid-August after mapping performance at several source temperatures and condenser temperatures of 90°F to 100°F.

EXTENDED DURATION TEST

The final task of the VTU test program is to conduct a 100-hour test with the VTU operating at a fixed set of conditions comprising waste heat source temperatures, condenser temperatures, and heat fluxes. In order to meet or exceed this goal, RRC has designed and fabricated an electronic controller to allow automatic control of the VTU. The test program is scheduled to be completed 30 September 1982.

The VTU controller is a microprocessor system based on the Motorola MC6809. The system operates in either a manual or automatic mode. In the manual mode all system control outputs are based on operator settings entered through a keyboard. In the automatic mode the system calculates the proper acid throttle valve positions required based on measured temperature, flow and pressure conditions within the CHP. This would regulate the system to provide a constant output. Also, an automatic shutdown feature is provided in the event system control cannot be achieved.

CHP conditions are measured via a 12-bit analog to digital converter. Throttle valve position outputs are 4 to 20 mA 8-bit digital to analog converters. Pumps and heaters are controlled via 10A 120 VAC solid state relays. CHP operating conditions and controller status are continuously updated for the operator on a CRT display. Controller internal power is backed up with rechargeable batteries to protect against powerline transients and interruptions.

REFERENCES

1. Rocket Research Company, "Final Report - Volumes I and II - Sulfuric Acid/Water Chemical Heat Pump/Chemical Energy Storage, BNL Contract 494588-S," January 1982.

2. E. C. Clark, "Final Report--Phase II Sulfuric Acid-Water Chemical Heat Pump and Storage System, DOE Contract No. EY-76-C-1185," Rocket Report No. RRC 78-R-595, December 1978.

3. E. C. Clark, "Final Report--Phase II-A, Sulfuric Acid and Water Chemical Heat Pump/Chemical Energy Storage Program, Sandia Contract No. 18-4958," Rocket Report No. RRC 79-R-627, September 1979.

4. E. C. Clark, "The Sulfuric Acid/Water Chemical Heat Pump/Energy Storage Program," Proceedings of the Sixth Annual Thermal Contractors' Review Meeting, September 14-16, 1981.

COST AND ENERGY-EFFECTIVENESS OF CHEMICAL HEAT PUMPS FOR INDUSTRIAL PROCESS HEAT APPLICATIONS

Warren R. Standley
TRW Energy and Environmental Division
McLean, Virginia 22102

ABSTRACT

This paper summarizes the work to date on a study of cost- and energy-effectiveness of the sulfuric acid chemical heat pump (CHP) for recovering industrial waste heat and supplying useful process heat. A previous study of CHPs has indicated that the most effective application for the CHP technologies is very likely in the industrial sector. The current study expands on that conclusion by developing detailed analyses of the sulfuric acid CHP in specific industrial applications. The applications are selected to be recognizable to a broad audience of industrial energy managers and decision-makers, and the analysis is conducted in such a manner as to present that audience with technical and economic parameters with which they are familiar.

INTRODUCTION

A chemical heat pump is a device that extracts thermal energy for a low-temperature source and rejects it to a higher-temperature sink. Unlike vapor-compression heat pumps which use the vapor-liquid phase characteristics of a single working fluid, chemical heat pumps make use of reversible physiochemical reactions between a working fluid (vapor) and one or more stationary phases (solid or liquid). Chemical heat pumps are being developed by DOE because they offer the promise of lower overall cost and greater efficiency for industrial process heat upgrading applications.

Chemical heat pumps must compete with existing industrial process-heat technologies. An applications-specific comparison between the chemical heat pump systems, baseline systems, and emerging technologies will enable the promised benefits of the CHP's to be weighed against the cost of ownership and operation.

In a previous study for BNL, TRW demonstrated that use of the sulfuric acid CHP in a generic application for industrial waste heat recovery to produce process steam could be competitive with both baseline and emerging systems. Compared to a baseline system consisting of steam raised directly in a fuel-fired boiler, the CHP is both cost-effective and conservative of energy resources. The individual CHP was also found to be much more energy conservative than an electrically-driven vapor recompression system. A vapor-driven vapor-recompression system was the most energy-conservative system evaluated, although the practical application of a steam-driven turbine exhausting to very low pressure could reduce the energy efficiency of the system. The concept of vapor recompression is used commercially to conserve energy in evaporation and distillation operations. The concept has been specifically adapted to the industrial waste heat recovery application and, although there is no known commercial system in such an application, the engineering basis is considered valid. The annual consumption of energy resources and levelized annual cost of owning and operating the sulfuric acid CHP and its competitors in the process steam application are illustrated in Figure 1.

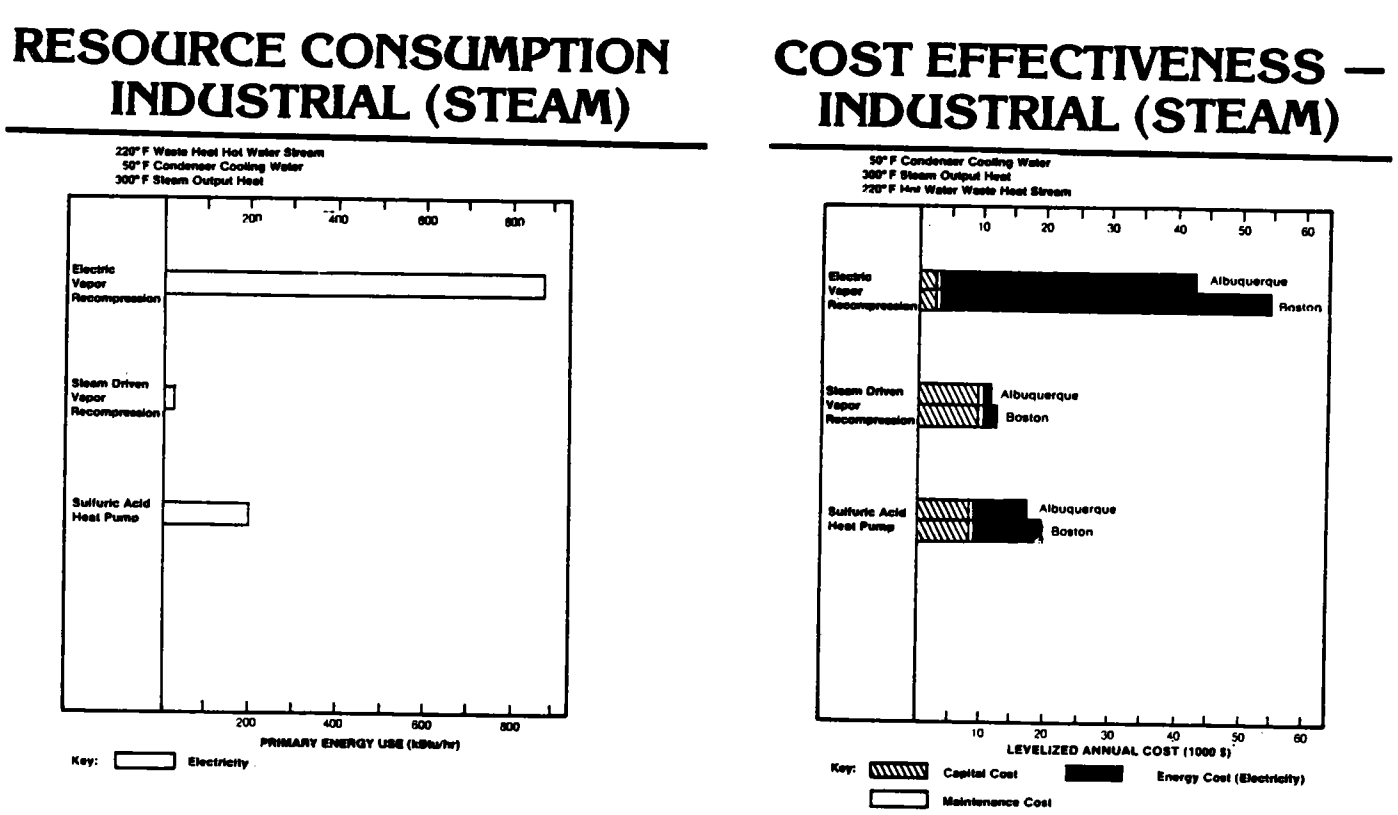

Figure 1. Energy Resource Consumption and Levelized Annual Cost for Several Industrial Heat Pumps Used for Raising 1.0 MBtu/hr of Process Steam

DISCUSSION

The initial study of CHP cost-effectiveness has been expanded to establish a more detailed evaluation of the sulfuric acid CHP in specific, appropriate applications for recovering industrial waste heat and delivering useful process heat. In developing a series of process-specific case studies, the objective was to present a broad audience of industrial energy managers and decision-makers with information regarding the CHP's advantages, presented in a familiar context.

Energy-effectiveness is shown through a comparative analysis of the CHP to both existing and alternative technologies for supplying process energy requirements. The CHP system performance is based on current testing of the verification test unit (VTU) at Rocket Research, with thermal and electrical COP evaluated for each specific application. Performance comparisons are based on direct process energy requirements and auxiliary requirements (electricity, cooling water, ...) for the process operating at constant conditions (e.g., throughput, conversion, or separation) with the baseline technology and with the CHP or alternative energy technology.

Cost-effectiveness is shown through a detailed cash flow analysis of owning and operating the baseline, CHP, or alternative technology. Presenting the results in the form of a return on investment (ROI), payback period, and an equivalent cost of energy saved/displaced is intended to provide a familiar set of parameters to the broadest industrial audience. The analysis includes full use of the current tax advantages provided for energy conservation technologies.

Case studies were defined as the result of a thorough search of the technical literature for "real-world" industrial process which would be recognizable to a broad audience and which would be appropriate applications of the CHP's energy charactersitics. The process-specific aspects that were considered are as follows:

- Reasonable collocation of waste energy source and process energy demand
- Reasonable time synchrony of waste energy source and process energy demand
- Reasonable temperature amplification in the range from $10^{o}F$ to $100^{o}F$
- Impact on auxiliary process requirements such as cooling water
- Impact on process operability or stability
- Nature of the energy saved/displaced.

A representative process application of the CHP is shown in a case study involving distillation of close-boiling materials. This case has broad, direct applications in the refining and petrochemical industries, and the relevance to other industrial operations should be obvious to industrial technical and economic decision-makers.

The specific application is illustrated in Figure 2, and involves a conventional butane splitting operation which is characterized by small differences between top (waste heat) temperature and bottom (process heat) temperature. As practiced, the separation is considered to be difficult, requiring high reflux ratios with associated high waste and process heat duties. A recognized process improvement involving operating at lower pressure to take advantage of improved relative volatility of the components is not usually practiced because it eliminates the ability to use cooling water to condense the overhead product and requires the use of auxiliary refrigeration. The conventional process requires the input of 191 MMBtu of process fuel and the use of nearly one million gallons of cooling water per hour.

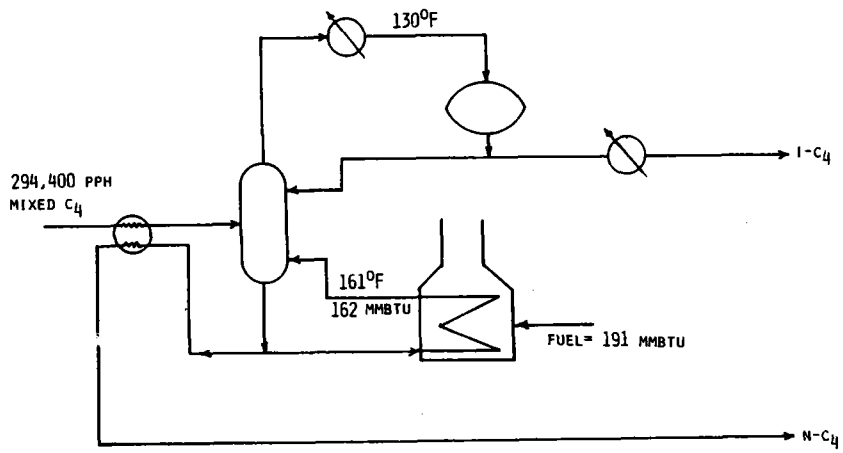

Figure 2. Conventional Distillation Scheme

An alternative energy technology known as a recompression heat pump may be applied to the distillation process, as shown in Figure 3. The overhead vapor product is superheated then compressed using expansion of process steam and a power recovery turbine as the driver. Condensation of the overhead product now takes place at high enough temperature to allow recovery of the heat in the column reboiler. The total steam requirement is only 71.2 MMBtu per hour and the cooling water requirement is reduced by over two-thirds. The approach has the disadvantage of requiring an expensive capital investment, a shift to process steam from on-site fuel gas, and a closing of a process thermal loop which will require closer supervisory control to avoid process instabilities. In spite of the problems introduced, the approach is economically attractive and is frequently cited for this application as well as for similar separations (e.g., butadiene recovery, ethylbenzene-xylene splitting, ethane splitting, and propane splitting).

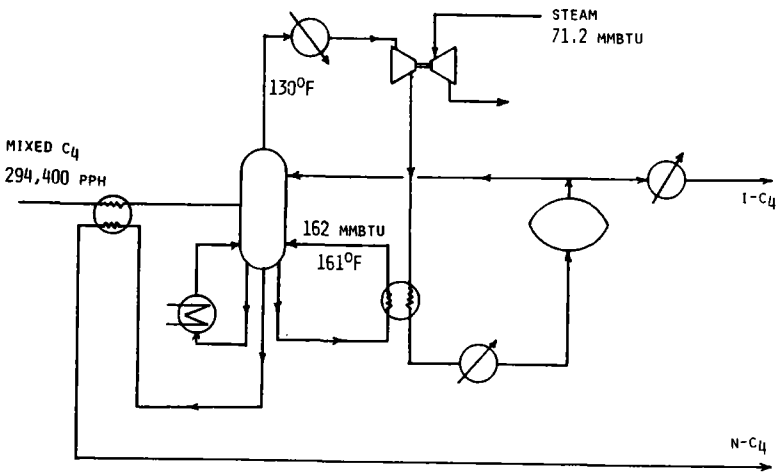

Figure 3. Vapor Recompression Applied to Butane-Splitting

Application of the sulfuric acid CHP to the distillation process is shown in Figure 4. Instead of attempting to replace the existing fired reboiler, the CHP is sized to recover all of the available waste heat from the overhead stream at a thermal COP of about 0.35 to displace fuel at the fired boiler. A closed thermal loop has not been created and process stability is not affected. The process cooling water requirement has been eliminated, and 67 MMBtu of fuel are displaced.

This case study and a similar one based one evaporation as a unit process are being analyzed using the data base developed during the study thus far. Preliminary analysis has shown that the applications have both technical and economic advantages for CHPs, and the study continues to quantify them and present the results in a broadly-understandable form.

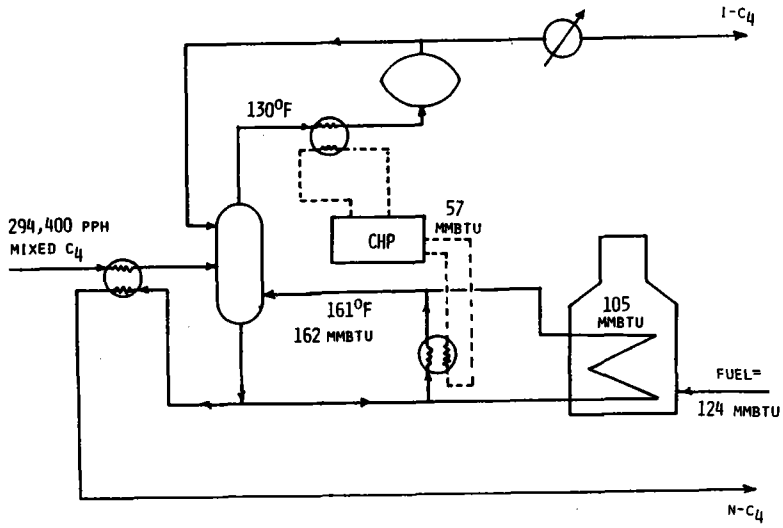

Figure 4. CHP Applied to Butane Splitting

REFERENCES

1. R. Gorman, P. Moritz, and W. Standley, "Chemical Heat Pump Cost-Effectiveness Evaluation: Final Report." TRW Energy Engineering Division for Brookhaven National Laboratory, May 1981.

2. Rocket Research Company, "Final Report - Volumes I and II - Sulfuric Acid/Water Chemical Heat Pump/Chemical Energy Storage, BNL Contract 494588-S," January 1982.

3. E. C. Clark, "The Sulfuric Acid/Water Chemical Heat Pump/Energy Storage Program," Proceedings of the Sixth Annual Thermal Contractors' Review Meeting, September 14-16, 1981.

4. Finelt, S., Hydrocarbon Processing, February 1979, pp 95-98.

5. Galstaun, L. S., et al., Oil & Gas Journal, November 12, 1979, pp 223-226.

6. Barnwell, J., Hydrocarbon Processing, July 1982, pp 117-119.

THE OHZ HYDROGEN PROCESS

C. C. Silverstein
CCS Associates
P.O. Box 563
Bethel Park, Pa. 15102

Introduction

In 1976, Kasai and Bishop patented a process for the catalytic decomposition of water using specially prepared mordenite, one of a large number of natural and synthetic crystalline zeolites known as "molecular sieves" (1). In 1977, they described a representative experiment in which cyclic production of hydrogen and oxygen from the decomposition of water was demonstrated, and presented a theoretical basis for the observed phenomena (2).

The Kasai-Bishop process, which will be referred to hereafter as the OHZ (oxygen-hydrogen-zeolite) process, has the following attractive features:

1. Simplicity - only two basic reactions are involved.
2. No corrosive chemicals - water is the only reactive chemical.
3. Moderate peak temperature.
4. Ease of product separation - water vapor and a carrier gas are the only other substances in the product stream.
5. Environmentally benign - no objectionable substances.

These characteristics strongly suggest that the OHZ process could be simpler, less expensive to develop, and provide hydrogen at a lower cost than alternate hydrogen processes under development. This program was carried out to establish the potential of the OHZ process for further development.

The OHZ Process

The OHZ process consists of two steps, an oxygen production step and a hydrogen production step. Overall, the addition of water and heat yields the hydrogen and oxygen products. The basic reactions are of an oxidation-reduction nature, and occur between adsorbed water molecules and trivalent cations within the pores of a zeolite. The trivalent cations are alternately reduced to the divalent state at elevated temperature, releasing oxygen, and then reoxidized to the trivalent state at a lower temperature, releasing hydrogen.

In their experiments, Kasai and Bishop exchanged several different trivalent trivalent cations into synthetic mordenite. Indium- and chromium-exchanged mordenite were found to participate successfully in the OHZ process, generating hydrogen and oxygen on a cyclic basis.

A schematic of the OHZ process is shown in Figure 1. Hydrated zeolite which has been exchanged with trivalent (M^{+3}) cations is heated to 1000°F-1300°F. The M^{+3} cations are reduced to the +2 valence state, n molecules of water are desorbed, and ½ molecule of oxygen is evolved. The dehydrated zeolite is then cooled to 100°F-300°F, and n+1 molecules of water are added. The M^{+2} cations are reoxidized to the +3 valence state, and one molecule of hydrogen is evolved. Upon heating to the peak temperature, the process is repeated. Overall, the addition of heat and water results in the production of hydrogen and oxygen. The zeolite itself is not involved in the chemical reactions.

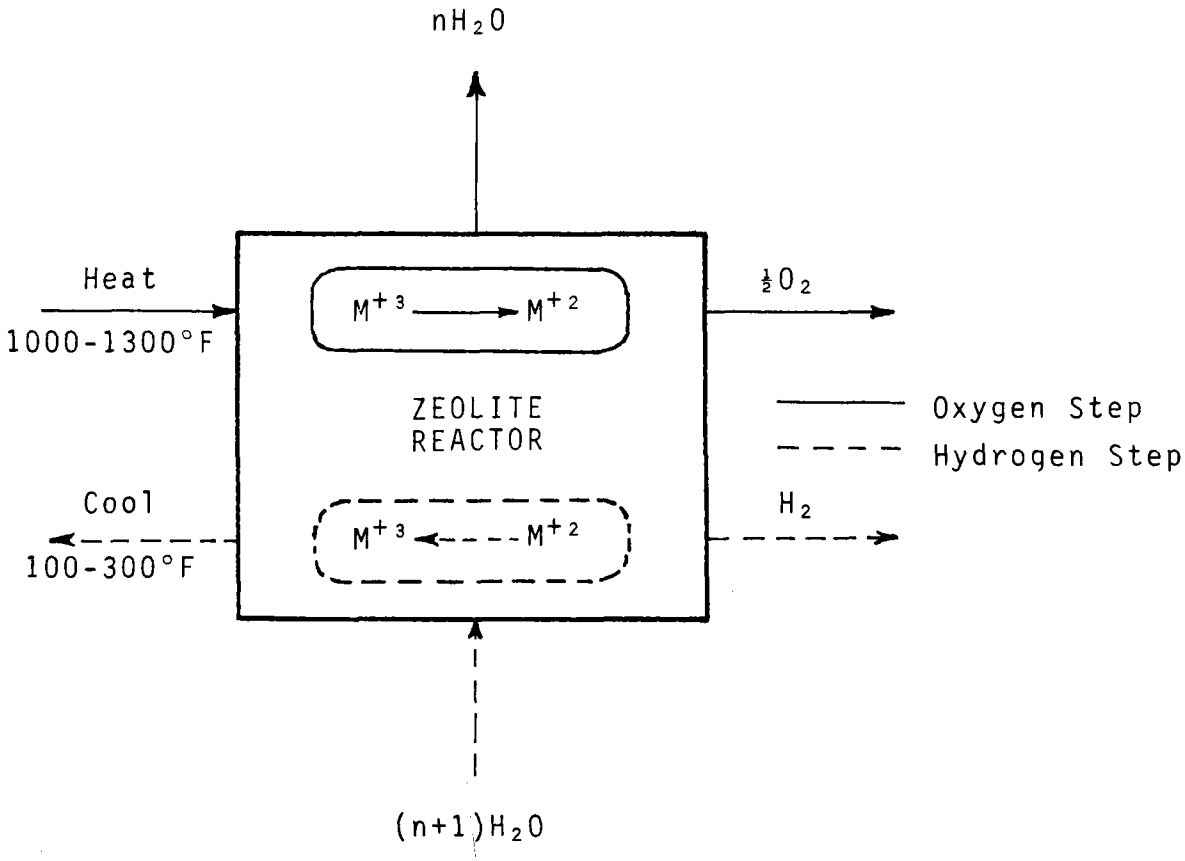

Figure 1. Schematic of OHZ Hydrogen Process

Plant Design Studies

Preliminary systems engineering studies were carried out to obtain design and performance characteristics of a hydrogen plant based on the OHZ process, and to identify process parameter goals necessary for commercial viability. By commercial viability is meant hydrogen production capability on an economically competitive basis.

The studies conducted were of two types. The first type was designed to obtain information on the quantity of materials required for a specified hydrogen production rate, providing a basis for estimates of the contribution of plant capital costs to the cost of the hydrogen product. The second, more extensive, type of study was concerned with determinations of process efficiency, providing a basis for estimates of the contribution of plant operating costs to hydrogen product cost.

A hydrogen production rate of 50 million scfd was selected as the basis of all calculations. This rate is comparable to that required to meet the hydrogen needs of modern refineries (3).

Materials. - The quantity of zeolite and exchanged cation materials required in the OHZ process varies directly as the time needed to complete a single cycle. Therefore, short cycle times are desirable to minimize plant costs. Table 1 gives the zeolite and cation weights for a cycle time of 2 hr. Cation exchange is assumed to be complete, and all of the exchanged cations are assumed to be active.

Table 1. Zeolite and Cation Weights

Material	Weight
Mordenite	6600 ton
Indium	660 ton
Chromium	300 ton

The zeolite (mordenite) weight shown in Table 1 is for the dry, unexchanged form of synthetic mordenite, assuming sodium to be the cation present prior to the exchange with trivalent indium or chromium cations.

Flow Model. - The OHZ process can be broken down into the following steps:

1. Adsorption-hydrogen production
2. Heating-desorption
3. Heating-oxygen production
4. Cooling

Each step takes place sequentially in a bed of trivalent cation exchanged zeolite. The completion of all four steps constitutes a single cycle.

In step 1, a carrier gas containing water vapor enters the bed at the minimum process temperature T_c. The water vapor is adsorbed, hydrogen is emitted, and the heat of adsorption plus the hydrogen heat of reaction is removed by the carrier gas. To avoid condensation of the water vapor, the minimum process temperature T_c is taken to be 10°F higher than the saturation temperature corresponding to the partial pressure of water vapor in the carrier gas. The carrier gas flow rate is adjusted to limit the temperature rise of the gas and bed to 100°F.

In step 2, the bed is heated by hot dry carrier gas to a temperature sufficient to desorb most of the adsorbed water, but not the residual water necessary for oxygen production. In the Kasai-Bishop experiments, oxygen production was noticed at around 600°F. In the model developed here, desorption is assumed to be complete when the bed has been heated to 700°F.

In step 3, the bed is heated further by hot carrier gas to the maximum process temperature, which is taken to be 1300°F, and oxygen is emitted.

In step 4, cold dry carrier gas cools the bed to the minimum process temperature T_c, completing one cycle. The introduction of carrier gas plus water vapor at T_c then initiates the next cycle.

While all the beds in the hydrogen plant could conceivably carry out each process step at the same time, hydrogen and oxygen production would not be continuous and the recovery and reuse of waste heat would be difficult. A more efficient approach is to divide the beds into modules of four beds, each of which is undergoing a different process step at any given time. Then hydrogen and oxygen production from a given module will be continuous, being generated from a different bed of the module during each quarter cycle. In addition, because of the phase difference between the beds, heat recovered from a bed in the cooling phase can be delivered to a bed in a heating phase.

Efficiency. - Plant efficiency is significantly affected by the average content of adsorbed water during step 1. This dependence is shown in Table 2 for a plant with mordenite adsorbing beds and a cycle time of 2 hr. The desirability of operating at a low adsorbed water content is evident.

Cost. - The following assumptions were used to estimate the cost of hydrogen from a 50 million scfd plant using the OHZ process.

1. The only significant operating cost is the fuel cost.
2. The fuel cost is $2/million Btu.
3. The plant operates for 8000 hr/yr.

4. Plant capital costs are amortized at 32%/yr.
5. Zeolite represents 50% to 100% of total plant cost.
6. The zeolite cost is $2-$10/lb.
7. No credit is taken for the value of oxygen produced, or for the waste heat available from the process.

Table 2, Plant Efficiency	
Adsorbed Water	Efficiency
2.5%	55.5%
5.0%	40.9%
10.0%	25.9%

The estimated hydrogen cost was calculated as a function of mordenite cost and the ratio of mordenite cost to plant cost, for 5% water absorption and a cycle time of 2 hr. Results show that OHZ process hydrogen can be produced for less than $10/million Btu, a competitive figure, if the mordenite cost is less than $3.10-$6.60/lb. The present cost of synthetic mordenite is $5-$6/lb, and that of natural mordenite is $0.50-$2/lb.

Concluding Remarks

The OHZ hydrogen process, discovered by Kasai and Bishop, represents a truly unique approach to hydrogen production. The ionizing capability of zeolite cations is utilized to decompose water into hydrogen and oxygen in two thermally distinct steps, which take place in the same bed of zeolite particles.

The evaluation of the OHZ process reported herein has confirmed the attractiveness of the process, and has identified key process goals for commercial viability. It is concluded that further development of the OHZ process is warranted.

References

1. Kasai & Bishop, "Thermolysis of Water in Contact with Zeolite Masses," U.S. Patent 3,963,830, June 15, 1976.
2. Kasai & Bishop, "Thermochemical Decomposition of Water Catalyzed by Zeolites," J.Phys.Chem., Vol. 81, No. 15, 1977, pp. 1527-1529.
3. Heck & Johnson, "Process Improves Large Scale Hydrogen Production," Hydrocarbon Processing, Jan. 1978, pp.175-177.

THE SULFUR-IODINE THERMOCHEMICAL WATER-SPLITTING CYCLE

G. E. Besenbruch, J. H. Norman, L. C. Brown, D. R. O'Keefe,
M. Endo, and C. L. Allen
General Atomic Company
San Diego, CA 92138

ABSTRACT

Experimental work was carried out on process improvement concepts, resulting in an advanced process for treatment of the lower phase (H_2O-HI-I_2) and a liquid HI decomposition process utilizing homogeneous catalysis. Bench-scale testing of Section III improvements was successfully carried out. A flowsheet for a solar thermal powered sulfur-iodine water-splitting process was developed and a cost estimate for hydrogen production completed. The calculated hydrogen costs vary from 18 to 22 $/GJ.

INTRODUCTION

The sulfur-iodine thermochemical water-splitting cycle presents an alternate concept for the production of hydrogen. Its high thermal efficiency (47%) makes it particularly attractive for solar applications, since for a given H_2 production rate the size of the mirror field is directly proportional to the process thermal efficiency. This could result in significantly lower overall plant cost for a process with higher thermal efficiency. General Atomic Company has been working on this cycle since 1974. The main goal for the development effort has been to demonstrate the feasibility of the concept and to improve the system to the state where it can be competitive as an alternate hydrogen production process in the future. The major effort over the last period has been to carry out a flowsheet design and cost estimate for a solar thermal powered water-splitting process. Improvements of the bench-scale system were also investigated, and basic engineering data for the process were gathered.

PROCESS DETAILS

Bench-Scale

The SO_2 removal and I_2 knockout system was placed in a hot box to facilitate operation. The system is shown in Fig. 1. The upper portion of one of the two packed columns in this figure represents a countercurrent inert gas purging system in which the SO_2 is removed from lower phase. This unit, along with the rest of the hot box operation, has been tested with lower phase made in Subunit I. The success of this purge was evidenced by the apparent lack of appearance of sulfur downstream. Analytical results on the iodine for determining its sulfur content have not yet been obtained in this operation, but since moderate quantities of sulfur as well as generated H_2S are easily apparent and neither were detected, it is assumed that the SO_2 removal system was working.

The I_2 knockout columns, redesigned by replacing the three original columns by two longer columns, are also in the hot box. The first column, after gas purging the SO_2, is used to countercurrently contact lower phase with concentrated H_3PO_4 in a Raschig ring packed column. The resulting impure I_2 stream is pumped to the second column where it is washed with water to remove a small amount of dissolved H_3PO_4. This second column is run at 2 atm to keep the water from vaporizing at the operating temperature of 115°C. Pressure is applied to the column with nitrogen gas and is controlled by a pressure regulator valve. The distributions and packing supports in this column were fabricated from Teflon sheets, which also serve as gaskets between column sections. Ball-and-socket ports and thermocouple wells were added to the glass columns that were purchased. Other ports were included for future installation of pressure transmitters, which will ultimately control liquid levels via the pumps.

The hot box, which houses the two columns, was made out of a welded metal framework and insulated. Three glass panels front the box and can be removed easily. Heaters were placed along the walls near the bottom of the box.

The system was run in conjunction with Subunit I and performed as expected, although the test was shortened by an HI_x pump malfunction. The system appeared to operate well with the exception of this pump. It is expected that as soon as adequate pumps are available to move I_2 and HI_x, this system will operate with a minimum of attention. Nevertheless, this unit has not at this point in time fully confirmed the laboratory data concerning these unit operations.

Engineering

The engineering flowsheet for the General Atomic sulfur-iodine thermochemical water-splitting cycle has progressed through several revisions under the dual objectives of maximizing the process efficiency and minimizing the resultant hydrogen cost. While the 1979 flowsheet was designed to match an HTGR heat source, this flowsheet matches the GA process to a solar thermal energy source. A simplified version of this concept is shown in Fig. 2.

The preliminary estimate of the cost of hydrogen from a solar-powered version of the GA sulfur-iodine thermochemical water-splitting cycle is 17.96 to 21.58 $/GJ (constant dollars, July 1980) and is detailed in Table 1. This cost is based on utility financing of a 500 MWT hydrogen plant. It was assumed that solar facilities will be constructed which can deliver thermal energy to the receiver at costs competitive with a nuclear reactor. The plant design was not optimized and this cost estimate is considered to be conservative.

This cost estimate assumes that the plant operates as an independent entity. Solar energy and water are the only inputs to the cycle and hydrogen is assumed to be the only salable product. No credit is assumed for the oxygen product, nor is any value placed upon the waste heat from

the process. It would be improper to call any plant "solar" which receives a significant fraction of its energy input from nonsolar sources, but co-production of hydrogen and either electricity or process heat from an integrated solar plant may be economic. The sulfur energy storage scheme (developed by GA) used to provide both diurnal and seasonal storage of solar energy for this hydrogen plant could produce peaking and evening power from a solar source recycling some of the sulfur dioxide combustion product to the SO_2 disproportionation reactor. Sale of waste heat from the plant may also be possible in special circumstances where a suitable customer is located adjacent to the solar hydrogen plant.

TABLE 1
HYDROGEN PRODUCTION COST

	Yearly Cost (M$ - July 1980)
Capital Charges	30.0 - 43.8
Annual Total Operating Cost Sections I - IV	29.9
Annual Total Operating Cost Sections Va and Vb	6.6 - 13.4
Total	66.5 - 87.1
Yearly Hydrogen Production	5.68×10^6 GJ
Hydrogen Cost Excluding Solar Facilities	11.71 - 15.33 $/GJ
Hydrogen Cost due to Solar Facilities	6.25 $/GJ
Total Cost of Hydrogen	17.96 - 21.58 $/GJ (July 1980)

Process Chemistry

Separation of HI from the H_2O-HI-I_2 phase is the most costly and energy intensive part of the cycle. GA has been working on improvements to the existing process and identified alternatives.

A process has been conceived which combines high-pressure azeotrope shifting, two-phase formation, solvent extraction using a hydrogen halide (HCl or HBr) for HI separation, and some other features to sharply reduce the amount of H_2O distilled in processing HI_x solutions. To establish the feasibility of this process, laboratory experiments were undertaken to study (1) the distribution of HI between a dry hydrogen halide phase and the wet phase, (2) the behavior of I_2 in these phases, (3) the high-pressure distillation to separate H_2O and HBr, (4) the fate of the HBr and the degree of reaction of the reactants in the H_2O-SO_2-I_2 reaction, and (5) the recovery of HBr from these product solutions. Specific experimental work carried out on this process included high pressure distillation of HBr from HBr-H_2O solutions in the apparatus shown in Fig. 3 and phase studies of the HI-H_2O-HBr system and H_2O-SO_2-I_2 eaction studies in the presence of HBr.

Enhanced HI decomposition in the liquid phase has been studied by GA over the last few years. During this period the use of homogeneous catalysis in the decomposition of liquid HI was investigated.

Several dissolved catalysts have been studied in a batch liquid HI decomposition apparatus. In the present case, dry HI liquid was added to various aqueous catalyst solutions, and the decomposition rates were measured on the basis of moles H_2 produced per g active metal. The above rate description would seem to be a much more valid way of presenting the data for homogeneous catalysis than for the heterogeneous cases since supposedly each molecular complex formed is an active center, whereas there is hardly a one-to-one correspondence between active site and metal atom in the heterogeneous case. With water present, a two-liquid system results.

The catalyst solutions employed included:

PdI_2 in hydriodic acid
$PdCl_2$ in hydrochloric acid
$RhCl_3 \cdot 3H_2O$ in hydrochloric acid
PtI_2 in hydriodic acid
$H_2PtCl_6 \cdot 6H_2O$ in water
$Mo(CO)_6$ in hydriodic acid
PbI_2 in hydriodic acid
FeI_2 in hydriodic acid
NiI_2 in hydriodic acid
$MoBr_2$ in hydriodic acid

The iodide and chloride equivalents of the same noble metal were used because initially only the chlorides were readily available from laboratory stock. Later, the iodide equivalents were obtained. There was no discernible difference in the rates at a given temperature between the halide forms. Except for PdI_2 and $PdCl_2$ the compounds are listed in decreasing order of reactivity on a mole H_2 per g metal basis as determined at both 303 and 323 K. Below $Mo(CO)_6$ there was no measurable reactivity. The palladium compounds, although lower in activity than the Rh and Pt compounds, especially at 303 K, do possess a significantly higher activation energy and thus a much higher rate at the projected engineering operation temperatures (up to 424 K). This makes Pd a prime candidate for the process. A higher temperature, higher pressure study of the reactivity of $PdCl_2$ conducted in an all-metal batch system did verify the existence of such a high rate at 348 K.

All of the above compounds except for Pb, Fe, and Ni were studied in both dry (one-phase) and wet (two-phase) environments. In all cases, water was required in order to effect the correct complexing; there was no measurable activity without water present, indicating that the activity surely takes place in the aqueous catalyst carrying phase with HI replenishment taking place from the "dry" HI phase in equilibrium with it. The lower limit of the present measurement capability with the apparatus used is estimated at 1×10^{-6} mole/min·g metal. The reaction was found to be reaction rate limited rather than diffusion rate limited; stirring the mixture did not show a measurable effect, at least for the temperature and pressure conditions of this study.

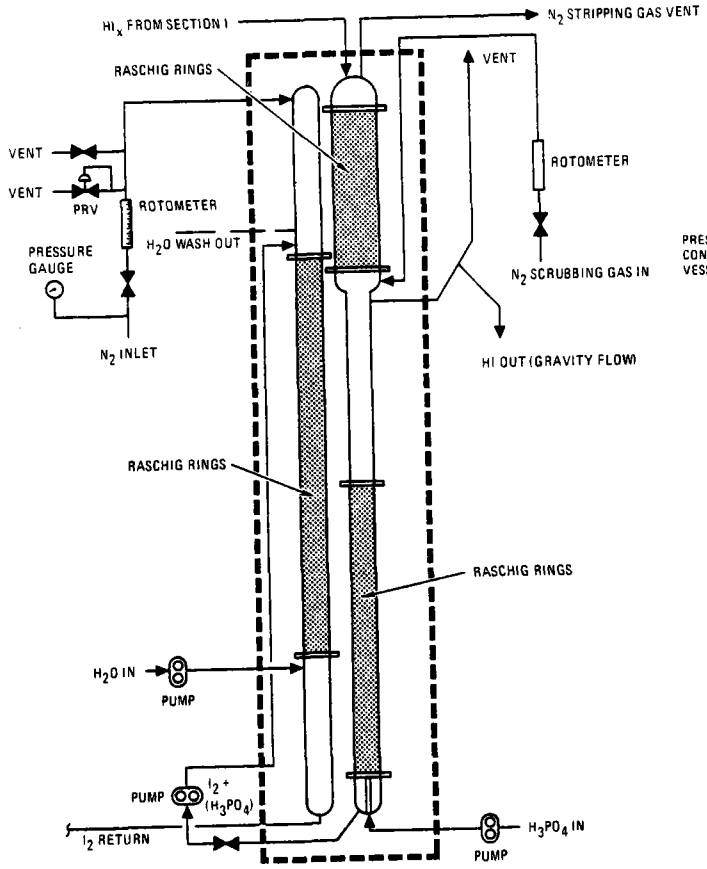

FIGURE 1

BENCH-SCALE DESIGN -- SECTION III DEGASSING AND H_3PO_4 TREATMENT OF HI_x SOLUTIONS

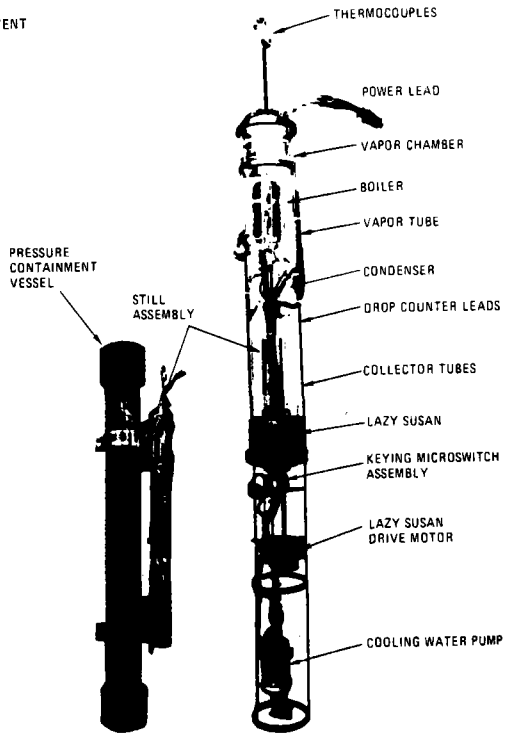

FIGURE 3

HIGH PRESSURE DISTILLATION APPARATUS

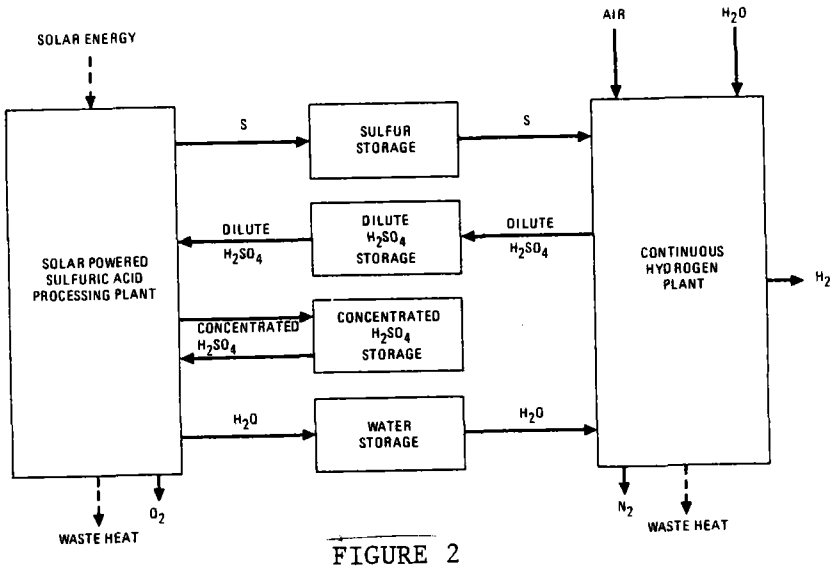

FIGURE 2

SIMPLIFIED DIAGRAM OF SOLAR VERSION OF SULFUR-IODINE CYCLE USING SULFUR STORAGE

RECOVERY OF HYDROGEN FROM HYDROGEN SULFIDE

By
Gopala N. Krishnan and Donald L. Hildenbrand
SRI International
Menlo Park, California

ABSTRACT

A bench scale study was conducted to examine the rate of reaction of hydrogen sulfide with liquid copper for the purpose of recovering hydrogen from hydrogen sulfide. It was found that the reaction rate at 1200°C was rapid and that the conversion of hydrogen sulfide to hydrogen approached the equilibrium level of 99.7%. The rate and the conversion remained constant until nearly all the copper was converted to cuprous sulfide. Using a model based on the Cu-S phase diagram, it was concluded that the gas phase mass transport was the rate-controlling step during most of the reaction period. Preliminary technical and economic assessments were performed for a hydrogen recovery process based on liquid copper and cuprous sulfide intermediates.

INTRODUCTION

A potential source of hydrogen is hydrogen sulfide gas and increasingly large quantities of hydrogen sulfide (10 million tons in 1980) are being generated in the United States and Canada from the processing of sour crude oil and natural gas. Currently, the H_2S is being converted to sulfur by the Claus process during which the hydrogen component is lost as water. It is estimated that potentially 7.7×10^9 cubic meters of hydrogen could have been recovered from H_2S in 1980.[1]

Copper metal can react with H_2S producing hydrogen [$2Cu(\ell) + H_2S(g) \rightleftharpoons Cu_2S(\ell)$]. Because both copper and cuprous sulfide are immiscible liquids above 1130°C, the reactions can be conducted above that temperature as gas-liquid reactions, thereby avoiding diffusion through a solid product. Liquid copper can be recovered from Cu_2S by oxidation with air [$Cu_2S\ (\ell) + O_2(g) \rightleftharpoons 2Cu(\ell) + SO_2(g)$]. The sulfiding and oxidation reactions are thermodynamically favorable. The copper recovery step is identical to the "white metal blowing" step in the commercial production of copper; hence it has been studied in detail. However, the kinetics of reaction of H_2S with liquid copper have not been studied, and a knowledge of the rate of this reaction is essential in assessing the feasibility of a hydrogen recovery process based on liquid copper and cuprous sulfide intermediates. Hence, the major objective of this program is to study on a bench-scale level the kinetics of reaction of H_2S with liquid copper.

BENCH SCALE STUDY

The rate of conversion of H_2S to H_2 were studied in two bench scale reactors having 500 g and 5000 g copper melt capacities, respectively. Technical grade H_2S (99.9% purity) was bubbled through liquid copper at flow rates ranging from 0.025 to 22.5 standard liters per minute (SLM) using lance orifice diameters varying from 0.07 to 0.9 cm. The conversion of H_2S to H_2 was determined by gas chromatographic analysis of the reactor exit gases. Effects of gaseous impurities, diluent inert gases, and cyclic sulfidation-oxidation were also studied.

Results—The rate of reaction of H_2S with liquid copper at 1200°C was found to be rapid. The reaction products were hydrogen and cuprous sulfide. Table 1 summarizes some of the experimental conditions and the observed results. Under most conditions used in this study, the conversion of H_2S to H_2 approached the equilibrium level of 99.7% corresponding to a residual equilibrium concentration of 0.3% H_2S. Lance immersion depths (static) of 0.6 and 4.5 cm were sufficient to obtain near equilibrium conversions at H_2S flow rates of 0.025 and 22.5 SLM, respectively. The conversion of H_2 remained constant until nearly all the copper was converted to cuprous sulfide. The gas orifice diameter did not affect the reaction rate under the bench scale conditions.

Use of low concentrations of H_2S, less than 10% in argon, led to the dissolution of sulfur in liquid copper when the melt was not saturated with sulfur. Under these conditions the observed residual concentration of H_2S varied from < 0.01 to 0.1% depending on the inlet concentration. These residual concentrations were less than that in equilibrium

with cuprous sulfide phase and they appear to represent the equilibrium between the gas phase and the sulfur concentration in the melt in the vicinity of the gas bubble.

The effect of carbonaceous impurities, CH_4 and CO_2 (~ 10 mole %), on the conversion of H_2S was studied. At the reaction temperature of 1200°C, methane dissociated to produce hydrogen and elemental carbon. CO_2 reacted with the H_2 produced from H_2S to form CO and H_2O by reverse water gas shift reaction. These reactions approached equilibrium levels and did not appear to affect the rate of H_2S conversion significantly. Presence of CO_2 along with CH_4 might alleviate the carbon buildup due to carbon oxidation by CO_2 to form CO.

The conversion of O_2 to SO_2 during oxidation of cuprous sulfide was nearly complete and all the cuprous sulfide was converted back to copper. Limited cyclic sulfidation-oxidation experiments indicated no significant effect on H_2S conversion because of cyclic operation.

Analysis—The experimental results were interpreted by a model based on the Cu-S phase diagram. The uptake of sulfur by liquid copper proceeds in three regimes: (1) intially sulfur dissolves in copper up to a saturation limit (~ 1.2 wt%), (2) then an immiscible cuprous sulfide phase is formed, and (3) finally more sulfur is incorporated into the nonstoichiometric cuprous sulfide phase until it reaches a composition of $Cu_2S_{1.09}$. The initial, intermediate, and final regimes account for 5%, 86%, and 9% of the total sulfur uptake, respectively.

It has been generally recognized that, in gas-liquid metal reactions at the high temperatures used in this study, the chemical reaction steps occurring at the interface are rapid and reach equilibrium.[2] The rate is then limited by mass transport either in the gas phase or in the liquid phase.The major portion of the sulfur uptake by the liquid copper melt occurs in a two-liquid phase regime during which sulfur saturated copper is converted to cuprous sulfide. Since the melt is saturated in sulfur, no diffusion is possible in the liquid copper phase; hence, diffusion in the liquid phase must be limited to a very thin layer ($< 10^{-4}$ cm) of cuprous sulfide phase formed at the interface. Because of the small thickness of this sulfide layer, the diffusion rate in the liquid phase is rapid and thus the rate must then be limited by mass transport in the gas phase.

The rate of mass transport in the gas phase (within the bubble) was estimated using a model of unsteady state diffusion within a sphere coupled with a chemical reaction at the interface.[2] From this model it was estimated that the time required for >99% of H_2S to diffuse to the interface varied from about 0.016 s for a 1-cm-diameter bubble to about 0.4 s for a 5-cm-diameter bubble. For large bubbles in which there is substantial internal gas circulation the required residence time for mass transport can be five to ten times less than the above estimated values. The residence times of gas bubbles in the bench scale experiments are sufficiently long (see Table 1) so that under gas phase mass transport limitation equilibrium conversions can be obtained; this agrees with the experimental observation. It should be noted that rate control by liquid phase diffusion can occur in melts not saturated with sulfur (initial regime) and in cuprous sulfide melts (final regime).

The oxidation of cuprous sulfide by air to copper and SO_2 follows a sequence that is the reverse of sulfidation. The conversion of O_2 in air to SO_2 exceeds 90% in many industrial reactors.[3] Under similar fluid dynamic conditions, the gas phase mass transfer coefficient is proportional to the square root of diffusivity. The diffusivity of SO_2 in N_2 at 1200°C (2.0 $cm^2\ s^{-1}$) is about 5 times less than the diffusivity of H_2S in H_2 (10.2 $cm^2\ sec^{-1}$). Thus the gas phase mass transfer rate in bubbles containing H_2S and H_2 must be at least twice as fast as in bubbles containing SO_2 and N_2. The conversion of H_2S to H_2 during reaction with liquid copper should then be equal to or better than the oxygen utilization efficiencies in commercial copper converters. Hence it is possible to obtain a very high conversion (> 90%) of H_2S in a large scale operation.

PROCESS ASSESSMENT

Process Scheme

A simplified flow sheet of the proposed process is shown in Fig. 1. The hydrogen recovery reactors are refractory-lined cyclindrical vessels similar to the "Hoboken type"

copper converters employed in the copper industry. Preheated hydrogen sulfide is blown into molten copper inside the reactors to produce hydrogen and cuprous sulfide. When all the copper is converted into cuprous sulfide the copper is regenerated by blowing air into the sulfide melt. Thus the reactors operate in a cyclic manner producing hydrogen and regenerating the copper. Steam is used to purge the reactor and its lines prior to each changeover from one gas stream to another to avoid formation of any explosive gas mixtures. A 90% oxygen efficiency is assumed, corresponding to the demonstrated attainable performance of commercial copper converters. During hydrogen sulfide blow, where the refractory erosion should be much less severe, thereby permitting use of smaller tuyeres, a hydrogen sulfide conversion efficiency of 98% is assumed.

Impure hydrogen formed in the reactor is partially cooled by preheating the hydrogen sulfide feed and is further cooled in a boiler water preheater. The hydrogen can then be purified of residual hydrogen sulfide in an amine absorption column. The SO_2 produced during the copper regeneration step is cooled in a steam boiler, cleansed of particulates in an electrostatic precipitator, and converted to sulfuric acid in a conventional acid plant.

The flow rates, temperatures, and pressures of various streams in the process are shown in Fig. 1. Using a feed stream containing 90% H_2S, 7% H_2, and 3% hydrocarbons, the process produces 5030 SCFM of 99+% hydrogen, 1200 lbs/min of sulfuric acid and 7940 lb/min of low pressure steam. Table 2 itemizes the capital investment costs for the SRI's hydrogen recovery process. The costs of major equipment items were estimated from published correlations and were adjusted for inflation to a time base of June 1981. A total capital investment of $25.7 million is required for a plant of this size. Table 3 itemizes the production costs. The gross production cost is $7.2 million/year equivalent to $3.04/1000 SCF of hydrogen. Addition of allowance for a 25% rate of return on fixed capital investment brings the hydrogen cost to $5.08/1000 SCF before applying by-product credits. By-Product credits for sulfuric acid (@ $6/ton) and for steam (@ $2/1000 lb) bring the net hydrogen cost to $1.23/1000 SCF.

Assessment

The major technical advantages of this process are rapid reaction rate and very high conversion of H_2S to H_2, so that multiple passes are not necessary. Because the reactions involved are exothermic, no additional heat input is necessary. In fact, a large quantity of excess heat is generated during the process which can be used as process heat or steam or in the generation of electricity.

There are some disadvantages from a technical point of view. The reactions occur at about 1200°C a temperature far higher than normally encountered in petroleum refinery or sour gas processing plants. The residual H_2S (0.3% - 10%) in the impure H_2 stream require further refining to obtain an acceptable hydrogen fuel or feedstock. The cyclic operation requires a complex gas handling systems.

The preliminary estimate shown above indicates that the costs of hydrogen produced by this process can be comparable to the cost of other emerging methods of hydrogen synthesis. The cost of hydrogen was influenced heavily by product credits for steam and sulfuric acid. Hence, a detailed analysis of utilization of steam and marketing of sulfuric acid is necessary for a proper process economic study.

CONCLUSIONS AND RECOMMENDATIONS

The reaction of H_2S with liquid copper at 1200°C was very rapid, and the conversion to H_2 approaches an equilibrium level to 99.7% under bench scale conditions. The reaction rate appears to be limited by the rate of gas phase mass transfer during the major portion of the sulfur uptake.

It is recommended that a detailed study be undertaken to assess the technical and economic aspects of the process. On the favorable outcome of this study, further tests should be conducted with different reactor configurations to determine conversion and reaction rates under large scale operating conditions.

REFERENCES

1. R. W. Bartlett, et al., "Preliminary Evaluation of Processes for Recovering Hydrogen from Hydrogen Sulfide," Final Report to Jet Propulsion Laboratory under Contract No. 955272, SRI International, July 1979.

2. J. Szekely and N. J. Themelis, Rate Phenomena in Process Metallurgy (Wiley Intersicence, New york, 1971).

3. R. E. Johnson, N. J. Themelis, and G. A. Eltringham, "A Survey of Worldwide Copper Converter Practices," in Copper and Nickel Converters, R. E. Johnson, Ed. (The Metallurgical Society of AIME, 1979), pp. 1-32.

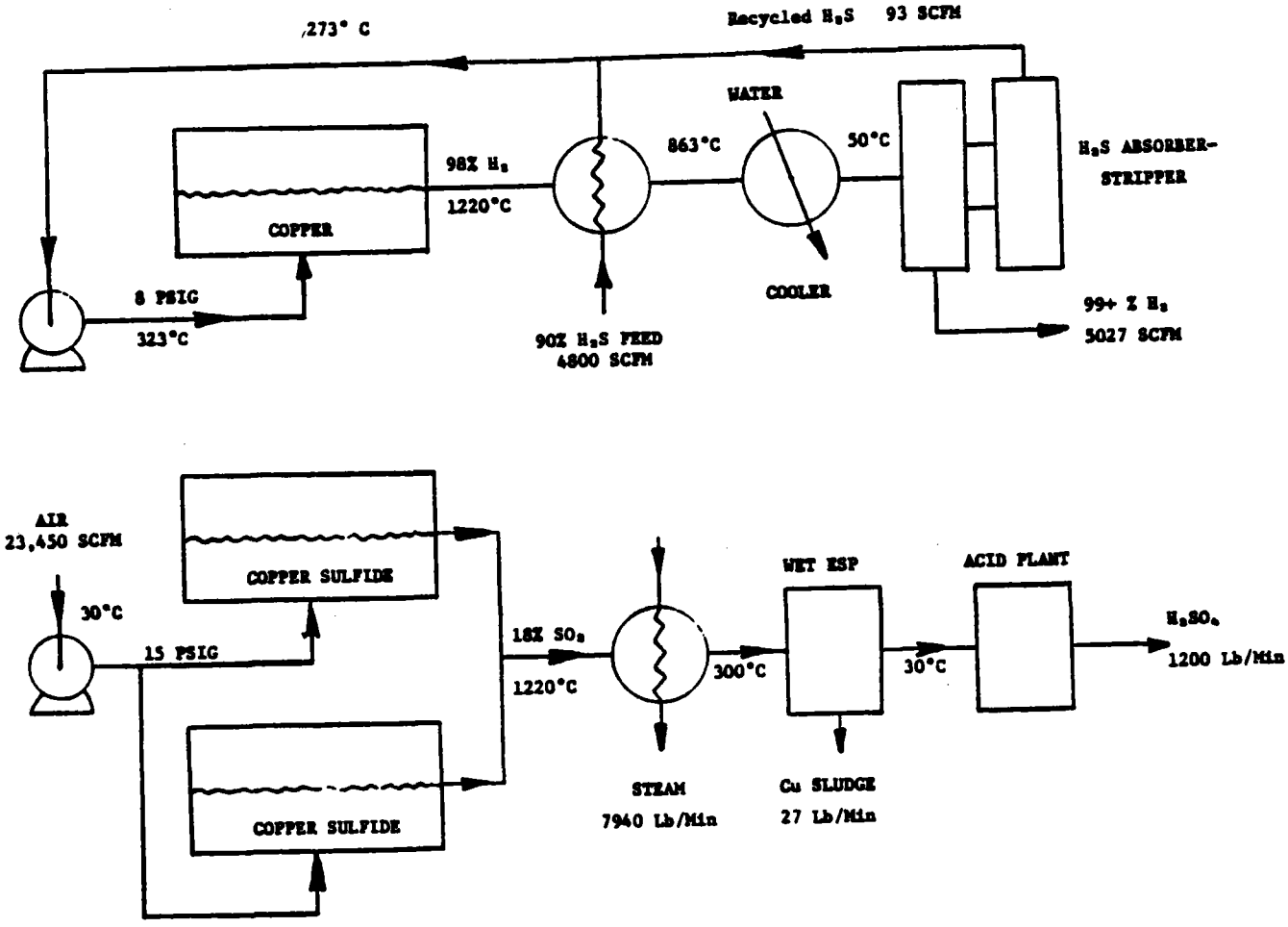

Figure 1. Simplified Flowsheet of Hydrogen Recovery Process

Table 1

Flow Rate (SLM)	Nozzle Diameter ID (cm)	Nozzle Diameter OD (cm)	Conversion of H_2S[a] %	Estimated Bubble Characteristics Diameter (cm)	Velocity ($cm \cdot s^{-1}$)	t_r[b] (s)
0.024	0.9	1.2	99.1	0.9	20	0.033
0.047	0.9	1.2	99.4	0.9	20	0.038
0.14	0.95	1.2	99.85	1.2	22	0.14
0.24	0.95	1.2	99.86	1.3	24	0.13
0.73	0.25	1.0	99.88	1.8	28	0.16
1.03	0.25	1.0	99.88	2.0	30	0.17
0.55	0.07	0.32	99.7	1.4	27	0.15
1.03	0.07	0.32	99.63	1.7	27	0.12
1.97	0.07	0.32	99.7	2.0	30	0.14
6.3[c]	0.7	0.9	99.82	3.3	36	0.15
13.0[c]	0.7	0.9	99.76	4.1	37	0.16
22.5[c]	0.7	0.9	99.5	4.8	39	0.19

[a]Steady state conversion.
[b]Bubble residence time in the melt.
[c]Revise with 12.7 cm diameter reactors; others with 4.4 cm diameter reactor.

Table 2

CAPITAL INVESTMENT

Capacity	250 Tons/day of H_2S
On-stream factor	90%
Time Base	June 1981
C. E. Plant Cost Index	298

Category	Cost (Millions of Dollars)	
Equipment cost FOB		
Reactors (4)	1.5	
Heat exchangers (8)	1.0	
Sulfuric acid plant	2.1	
Others	2.1	
Battery limits investments[a]		16.7
Utilities,[b] facilities[c]	3.5	
Total fixed capital		20.2
Interest,[d] start-up cost,[e] Working capital[f]	5.5	
Total Capital investment		25.7

[a]250% of delivered equipment cost; includes foundation, erection, instrumentation and auxiliary facilities.
[b]5% of battery limits investment.
[c]15% of summ of battery limits investment and utilities.
[d]15%/yr for 1/2 of 18-month construction period.
[e]10% of total fixed capital.
[f]90 day cash expenditure.

Table 3

PRODUCTION COSTS

Category	Cost $Million/yr	Cost $1000 SCF H_2
Labor and maintenance	1.07	0.45
Materials	1.45	0.61
Utilities	0.90	0.39
Overhead,[a] G and A,[b] insurance and taxes,[c] depreciation,[d] and interest[e]	3.8	1.59
Gross Production Cost	7.2	3.04
Return on investment	5.04	2.05
Hydrogen cost	12.24	5.09
By-product credit		
Sulfuric acid, $6/ton	-1.7	-0.72
Steam $2/100 lb	-7.4	-3.13
Net hydrogen cost	3.14	1.23

[a] 80% of labor and maintenance.
[b] 10% of labor, materials and utilities.
[c] 2% of fixed capital per year.
[d] 10% of fixed capital per year.
[e] 12% of working capital per year.
[f] 25% of fixed capital per year.

HYDROGEN EMBRITTLEMENT OF STEEL PIPELINES

J. H. Holbrook, H. J. Cialone, M. E. Mayfield,
and P. M. Scott
Battelle, Columbus Laboratories
Columbus, Ohio 43201

As the world's demand for energy increases and the reserves of non-renewable energy sources are depleted, hydrogen gas could represent an important alternative energy source for the future. In particular, hydrogen gas appears promising as a direct substitute for or supplement to natural gas for both commercial and industrial consumption.

The main advantages of hydrogen are that it is a renewable energy source and also that it is, in principle, transportable by the same methods that natural gas is transported. Another advantage of hydrogen is that, unlike natural gas, it can be stored in large quantities and in small volumes by reaction with certain metals to form hydrides.

The main disadvantages of hydrogen as a viable energy source are that the cost of a unit of energy of hydrogen will be greater than a unit of natural gas, that some design and operating modifications are required of current gas transmission pipelines to optimize them for efficient transport of hydrogen, and that the construction materials used in the natural gas pipeline system are susceptible to degradation by a phenomenon known as hydrogen embrittlement. The issue of optimum pipeline design to maximize efficiency of hydrogen transmission has been treated in detail by other investigators and it is reasonably clear what modifications will be required if hydrogen transport becomes a reality. Also, considerable research activity is currently directed at increasing the efficiency of producing hydrogen to make the cost of hydrogen energy more equitable with natural gas. This paper discusses the work in progress at Battelle's Columbus Laboratories to assess how serious the problem of hydrogen embrittlement will be with transport of hydrogen gas in present and future steel pipelines.

Hydrogen Embrittlement

The ductility and fracture toughness of practically all metals and alloys is reduced by exposure to hydrogen gas. That phenomenon, known as hydrogen-environment embrittlement, has been the subject of hundreds of research papers over the last two decades. Thus, much is known about the phenomenology of hydrogen embrittlement even though the exact mechanisms are still unclear. The severity of hydrogen degradation depends on numerous material and environmental variables. The most important variables are:

Presence of Hydrogen Gas During Plastic Deformation. Degradation is observed only if hydrogen gas is present simultaneously with plastic deformation of a metal (such as at a crack tip). Removal of the hydrogen gas restores normal properties.

Type of Metal. Certain alloys are more susceptible to embrittlement than others, all other conditions equal. Pipeline steels are moderately to strongly degraded.

Yield Strength of Metal. Severity of degradation strongly increases with yield strength of the metal.

Presence of Stress Concentrators. Hydrogen degradation is made more pronounced by the presence of cracks or notches.

Cyclic Loading. The reversed plasticity that occurs with cyclic loading accentuates hydrogen degradation of such properties as low-cycle fatigue and fatigue-crack growth.

Hydrogen Pressure. Severity of degradation increases with hydrogen pressure but not strongly. Usually a square-root-of-pressure dependence or weaker is observed.

Temperature. Hydrogen embrittlement has a non-monotonic temperature dependence. The temperature for maximum embrittlement of almost all metals is in the range -100 C to 100 C.

Rate of Loading. In general, the severity of hydrogen embrittlement increases with decreasing rate of loading (strain rate or frequency). Some exceptions to that behavior have been reported, however, for fatigue-crack growth in hydrogen at very low frequencies.

Hydrogen Purity. Certain impurities in the hydrogen gas inhibit embrittlement. Oxygen strongly inhibits degradation. Carbon monoxide and water vapor also reduce degradation, but not as strongly as oxygen.

Chemical Composition/Microstructure. For a material such as steel, susceptibility to hydrogen embrittlement is only weakly dependent on the specific composition or microstructure, unless variations lead to increases or decreases in the yield strength.

Impact on Pipeline Transmission of Hydrogen

Pipelines are designed to be statically-loaded structures, that operate with pressures that produce no plastic deformation, and that contain no significant stress concentrators. The materials used to construct pipelines are nominally moderate-strength, carbon-manganese steels. Pipes ordinarily have longitudinal seam welds, and girth welds join individual pipe sections. Although the microstructures of the weld metal and heat-affected zones are certainly different than the base metal, the chemical composition and yield strength of the welds are designed to be similar enough to the base metal that differences in degradation by hydrogen of base metal and welds would not normally be expected. Thus, an ideal steel pipeline operated under ideal conditions should not be particularly susceptible to hydrogen embrittlement.

The difficulty with that assumption is, of course, that pipelines and operating conditions are not ideal in practice. In actuality, pipelines experience slow-pressure variations and occasional shutdowns that cause low-frequency cyclic loading; pipelines have stress concentrators, particularly at welds; and pipelines occasionally have hard spots in the pipe wall and hard weld-heat-affected zones, both due to improper heat treatment.

During the period 1974-1981, Sandia Laboratories studied the issues involved with hydrogen compatibility of steel pipelines. Their findings

indicated that the most serious hydrogen-related problems to be overcome were (1) accelerated fatigue-crack growth from internal flaws and (2) the possibility of sustained-load subcritical-crack growth in weld heat-affected zones. Battelle's effort on the current program has been to study further those particular manifestations of hydrogen embrittlement on pipeline steels and welds to provide a more complete picture of the feasibility of transporting hydrogen in present and future pipelines.

Results

Fatigue-Crack Growth

During the program period we have investigated the influence of hydrogen on fatigue-crack growth in pipeline steels using fracture-mechanics specimens and cyclically-pressurized pipe sections with internal starter flaws. An example of the acceleration of fatigue-crack growth by hydrogen is shown in Figure 1. It can be seen in that figure that an environment of 1000 psi hydrogen increases the crack-growth rate in X42 pipeline steel at room temperature by more than an order of magnitude. It should be noted that the data in Figure 1 were obtained from tests with a fixed R-ratio ($R = K_{min}/K_{max}$ where K is the crack-tip stress intensity and is proportional to the load on a cracked specimen). Another important finding from the present work is that the acceleration of crack-growth rate by hydrogen depends strongly on R-ratio at a fixed ΔK (K_{max}-K_{min}) as is shown in Figure 2. The trend shown in Figure 2, where the acceleration of crack growth by hydrogen decreases with increasing R-ratio, is promising for pipeline applications because a crack growing in fatigue due to moderate pressure variations would experience loading at high R-values (P_{min}/P_{max}).

The reduced life of a preflawed A106B steel pipe section cyclically pressurized with hydrogen is shown in Figure 3. The data shown in that figure was taken from tests where the pressure was cycled from 500 to 2000 psi (R = 0.25) with a flaw size that produced an initial ΔK of 12 ksi $\sqrt{in}$ (3-inch flaw, depth 40 percent of wall). It is obvious that the fatigue life is only reduced by about a factor of 3 by hydrogen instead of the 10 or more that would have been expected from the laboratory tests on fracture-mechanics specimens. That observation is also promising for hydrogen pipeline applications because it suggests that low-cycle fatigue life of pipes transporting hydrogen and containing moderate-size internal flaws will not be drastically reduced.

Sustained-Load Subcritical-Crack Growth

In earlier efforts on DOE-sponsored research on pipeline compatibility with hydrogen, Sandia Laboratories had observed indications of time-dependent crack growth in heat-affected zones of fusion welds in X60 pipeline steel. Those heat-affected zones did not have inordinately high hardnesses and were fairly typical of the heat-affected zones of many welds in service. Time-dependent crack growth in hydrogen under sustained loads in typical weldments would cast grave doubts on the possibility of using pipelines to transport hydrogen.

In the past year we have sought to reproduce and quantify the Sandia observations of subcritical-crack growth. We have found that

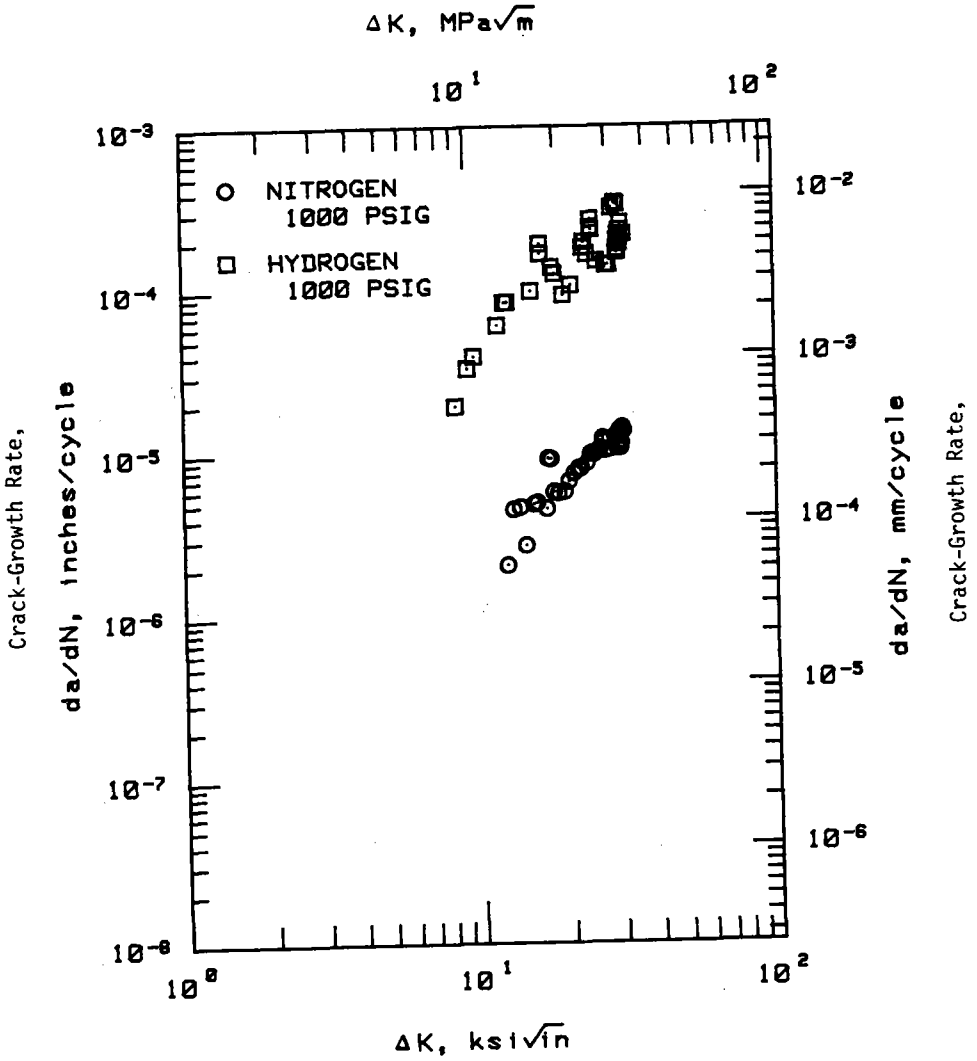

FIGURE 1. FATIGUE-CRACK GROWTH RATE VERSUS CYCLIC STRESS INTENSITY FOR X42 PIPELINE STEEL IN HYDROGEN AND NITROGEN

$R = 0.25$
$\Delta K = K_{max} - K_{min}$
$R = K_{min}/K_{max}$.

sustained-load crack growth does indeed occur in 1000 psi hydrogen in specimens taken from the same weldments that Sandia studied and also from the heat-affected zone of a typical electrical-resistance seam weld from X42 pipe. However, to observe that time-dependent growth in hydrogen, it was necessary to apply loads that resulted in stress intensities that were much greater than would normally be encountered in service. In particular time-dependent growth was not observed in 1000 psi hydrogen until a stress intensity of 70 ksi $\sqrt{in}$ was applied to the specimens which is equivalent to a depth of greater than 50 percent of the wall for a 3-inch long flaw in a typical pipeline operating at 1000 psi. Flaw depths of that magnitude would normally be detected with conventional hydrostatic testing before a pipeline is placed in operation.

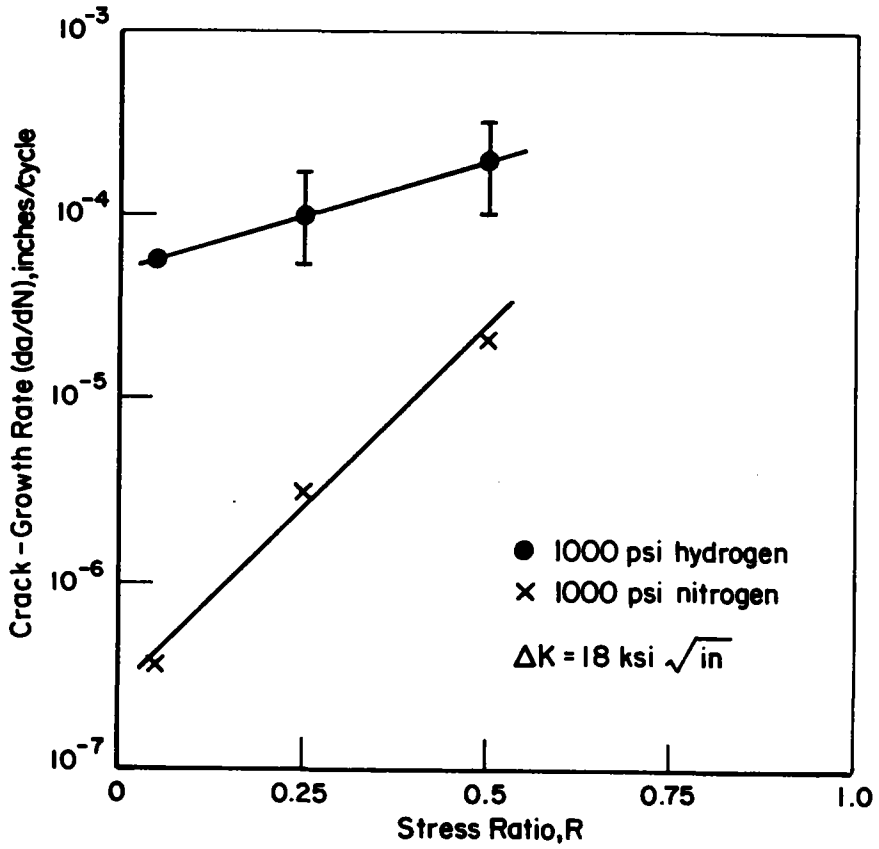

FIGURE 2. FATIGUE-CRACK GROWTH RATE DEPENDENCE FOR X42 PIPELINE STEEL ON STRESS RATIO, R, AT FIXED ΔK

Large values of R-ratio correspond to a large mean stress.

SUMMARY

During the past year we have confirmed that hydrogen gas increases dramatically the fatigue-crack growth in pipeline steels. We have also shown that hydrogen-acceleration of the fatigue-crack-growth rate decreases at large values of R-ratio such as would be produced by moderate variations in operating pressure. We have found that sustained-load subcritical-crack growth does occur in heat-affected zones of typical pipeline welds but only at stress intensities that would not normally be encountered in service.

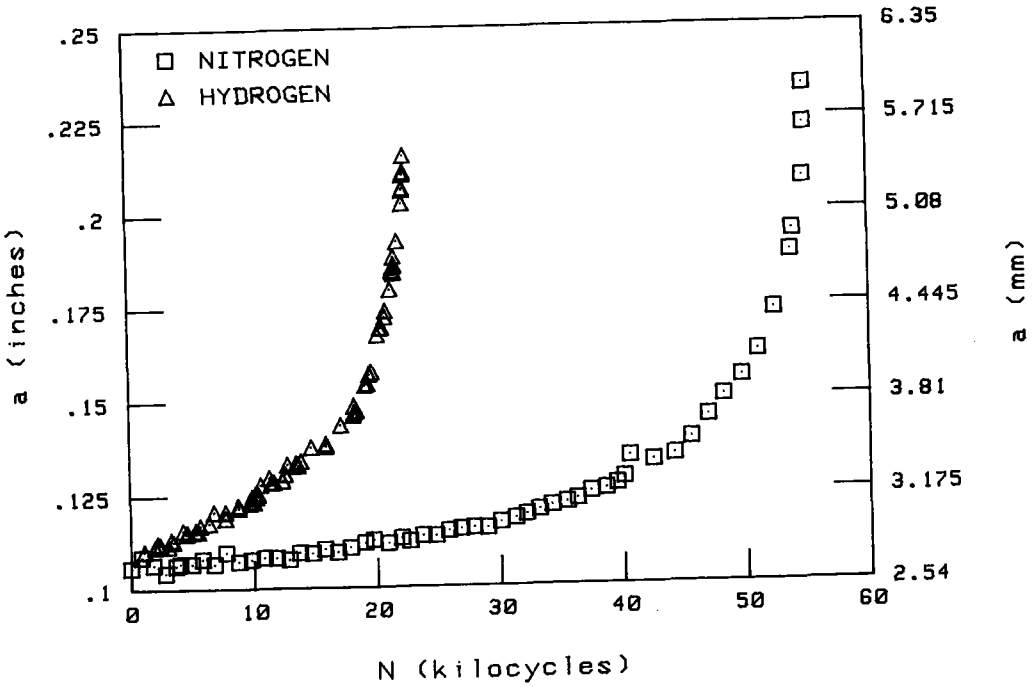

FIGURE 3. CRACK LENGTH VERSUS NUMBER OF PRESSURE CYCLES FOR A106B STEEL PIPE SECTIONS

Maximum pressure was 2000 psi. Minimum pressure was 500 psi.

A TEST BED FOR ADVANCED HYDROGEN TECHNOLOGY: PHOTOVOLTAIC ARRAY/ELECTROLYZER SYSTEM

Gerald Strickland
Brookhaven National Laboratory
Upton, NY 11973

INTRODUCTION

Research on the production of hydrogen from water through the use of renewable-resource energy is one facet of Brookhaven National Laboratory's program dealing with chemical energy storage and subsequent reconversion to a useful form of energy. Solar energy conversion to hydrogen, and its storage, are a logical choice, because hydrogen is a versatile and environmentally desirable energy form. Furthermore, energy reconversion via hydrogen-air fuel cells produces electricity at much higher efficiencies than heat engines, and at greatly reduced emission and noise levels.

The design/planning activity described in this report stems from the United States' participation in the International Energy Agency's (IEA) research and development program on the production of hydrogen from water. The system selected, and defined here for experimental study, consists of a photovoltaic array (PVA) supplying electrical energy to an advanced-technology electrolyzer (ATE) producing hydrogen. The PVA/ATE system is a typical example of solar energy couples which appear to be highly compatible. Solar-cell technology is under development on a number of fronts, the main goal being to lower unit energy costs to acceptable levels. Electrolyzer technology is in a slowly emerging stage of development in the United States. Although the project is a long-term, high-risk venture, it has a very high potential because the technology could represent a valuable export for markets in developing countries.

The primary objective of the project is to establish an integrated test bed that will illustrate advanced technology for the far term. Installation of the test bed would be at the site of the Hydrogen-Technology Advanced-Component Test System (HYTACTS), a service system constructed several years ago and used for testing a hydride-hydrogen storage vessel capable of storing 50 lb of hydrogen as a metal hydride. The HYTACTS provides services essential for hydrogen flow, as well as those for thermal control. Most operations are performed remotely from an indoor control panel outfitted with suitable instrumentation.

The second objective of the project is to test and evaluate the PVA/ATE system under practical conditions. Operation of the ATE in the transient mode, as determined by the local insolation, is the key part of the experimental program. At an appropriate time, IEA participants and interested commercial parties will be invited to operate the system as a tutorial exercise. Subsequently a decision will be made on modifying the system for stand-alone operation. The performance evaluation will aid in guiding system optimization and in planning project activities on renewable-resource energy conversion.

This report presents essential information on the project design/planning activity leading to the installed test bed, and on design of the experimental program leading to system evaluation. The project report (1) contains additional details, specifications for the major components, the construction and experimental schedules, and the manpower and equipment cost estimates.

SYSTEM DESIGN

The functional design is based on coupling the ATE to the PVA via a powe conditioner, with provision for hydrogen storage (existing). A block diagram indicating the relationship of the major components of the PVA/ATE system is shown in Fig. 1. Although the ATE rating is 15-kW (nominal), the PVA rating was limited to 5 kW (peak) in order to restrict the capital investment and physical size of the facility. The power conditioner will provide the necessary additional energy, as rectified alternating current (AC); and it will combine both sources in a manner that will simulate a 100% solar supply. System control and data acquisition are the functions of the microprocessor controller. The hydrogen produced can be stored in hydride form (or vented) until an end-use device, such as a fuel cell, is available for testing. The wind turbine can be evaluated as a supplemental energy source in a follow-on program. An artist's sketch of the installation is shown in Fig. 2.

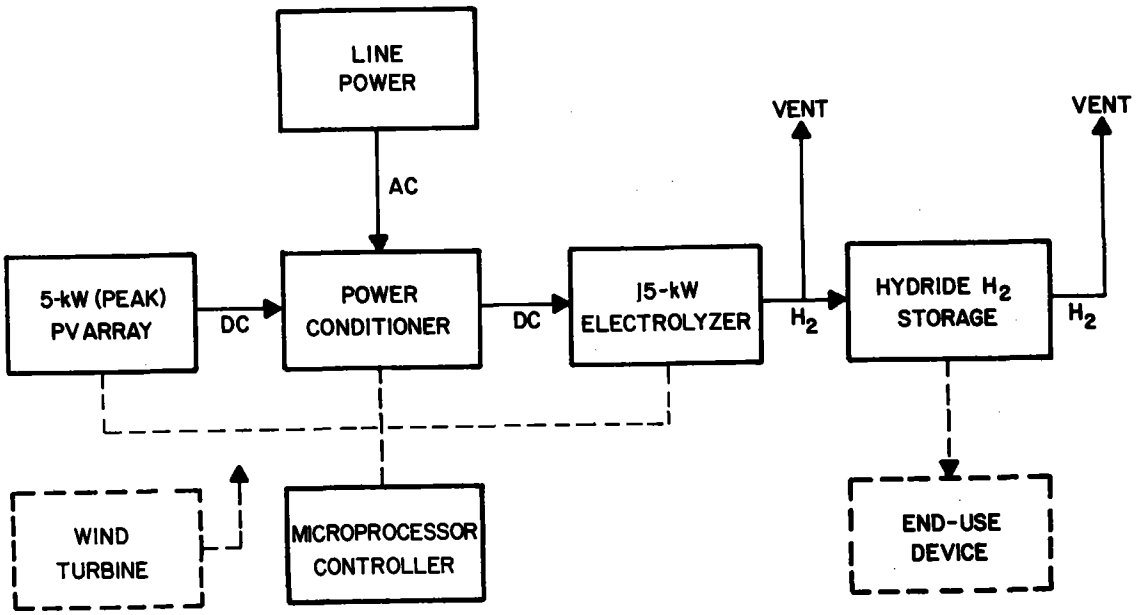

FIGURE 1

DIAGRAM OF PV ARRAY/ELECTROLYZER SYSTEM

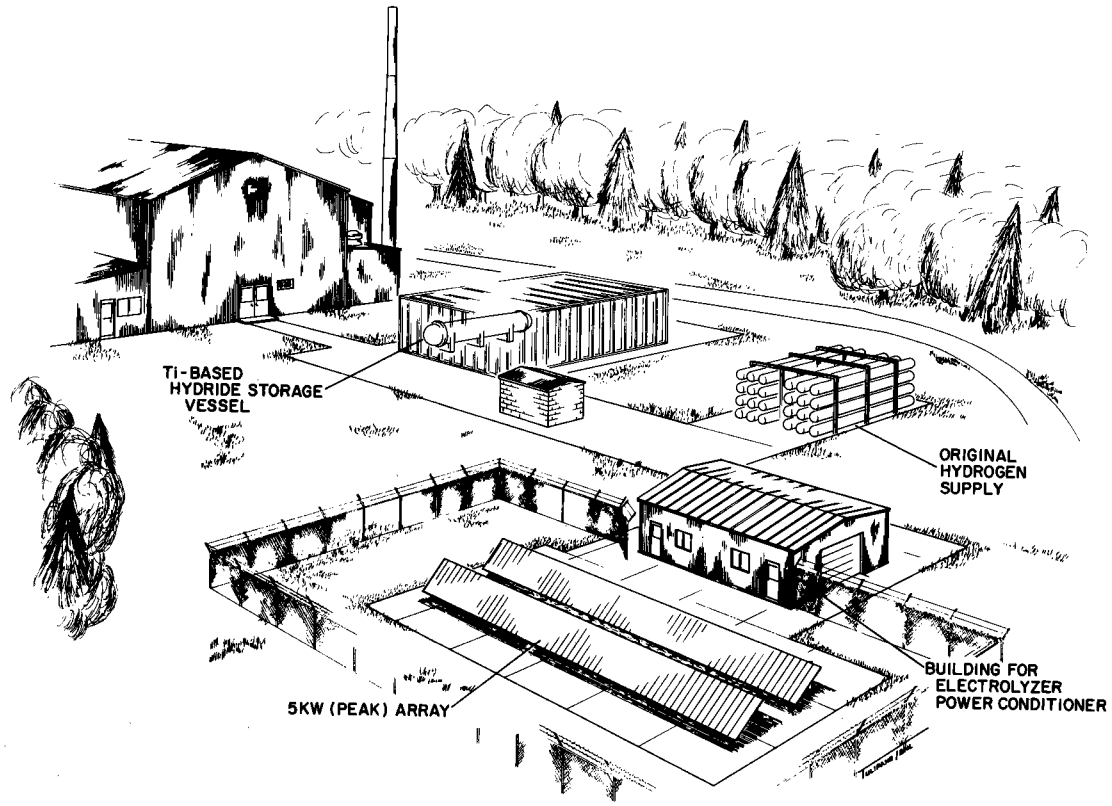

FIGURE 2

ARTIST'S SKETCH OF THE PV ARRAY/ELECTROLYZER SYSTEM

The electrolyzer will be comprised of seven or eight cells in series, each cell having an area in the range of 1 - 1.25 ft^2 so that representative hardware being developed by organizations involved in the DOE/BNL electrolyzer programs can be used. A sample set of electrolyzer performance curves is shown in Fig. 3. These curves have been reoriented to illustrate PVA/ATE interfacing, as explained later. The upper limit presently projected for the cell current is 1000 amperes at about 1.8 volts/cell for an operating temperature of 120°C.

The PVA is comprised of modules which have a DC output which is proportional to the insolation intensity at the solar-cell surface. A choice of flat-panel arrays was made because they are more highly developed and are readily available. Typical 1 x 4 ft. modules have a peak rating of 35-40 watts. That is, when the insolation is 1 kW/m^2, and the module temperature is a nominal 25°C, the peak output is attained. The output is slightly reduced as a function of increasing solar-cell temperature. Modules are arranged on racks, facing south, and are tilted

at a favorable angle to optimize output on a seasonal or annual basis. A set of current/voltage curves for the PVA at various levels of insolation, and two module temperatures, is also shown in Fig. 3. The current provided by the power conditioner is that from the 128 PV modules plus the current derived from the electric-utility source, and it is proportional to the insolation; whereas the voltage is a function of the module temperature. Operation is desired at the knee of the curve where the power output is a maximum. Because a practical upper limit for the local insolation appears to be 0.5 kW/m^2, it was selected as the design point for obtaining an output of 1000 amperes. The peak-power point (14.5 kW) at this level occurs at 14.5 V for a module temperature of

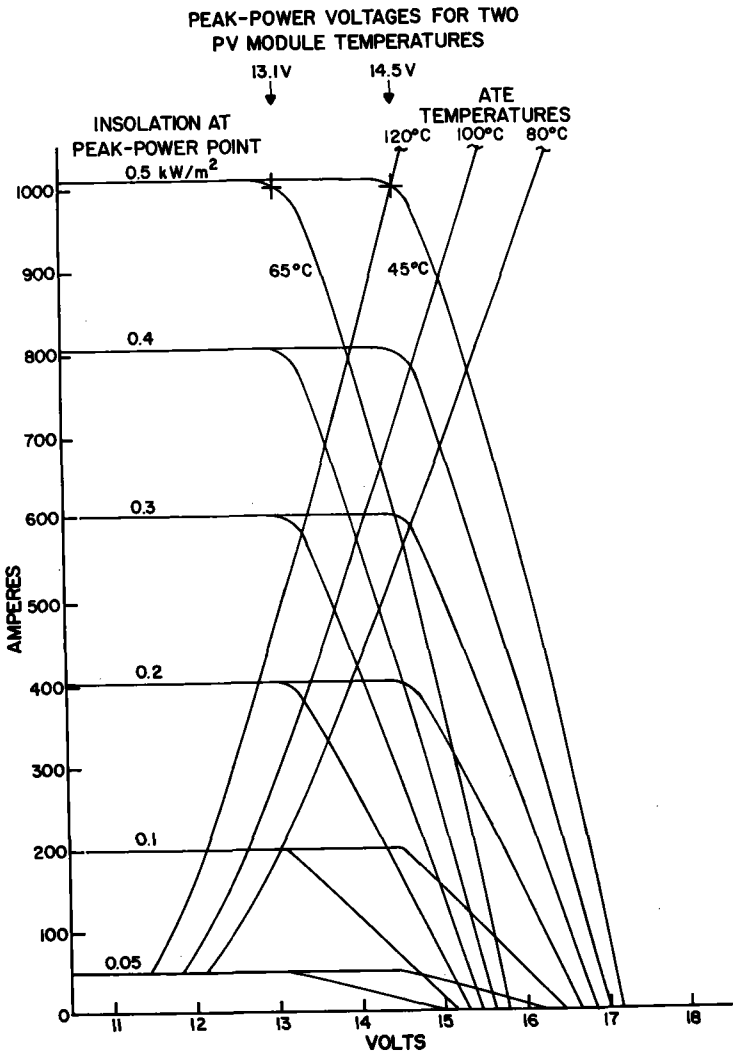

FIGURE 3

TYPICAL CHARACTERISTIC CURRENT/VOLTAGE CURVES FOR THE PVA/ATE SYSTEM ILLUSTRATING POSSIBLE OPERATING POINTS

45°C. This point also lines on the 120°C curve for the ATE; so operation at that point would maximize H_2 output. Other operating points can be determined by examination. Although the voltage match is not optimal improvement will be attainable via power-conditioner control. This current/voltage map is only illustrative, because no provision was made for voltage drops in the busbars and power conditioner. Since the total drop will approach 2 V, it is likely that seven cells will be used in the ATE. The final choice will be made when the characteristics of the procured components are known.

SYSTEM CONSTRUCTION AND OPERATION

The schedule for the three-year program consists of completing all design, construction, and acceptance testing within 12 months after project implementation. Other systems considerations included are participation in a safety review, preparation of operating procedures, and personnel training. The management plan consists of having the fabrication/construction work done via contracts after completion of the design by BNL personnel who would also have an active role in operating the system.

Three ATE operating modes will be used in characterizing system performance. Prior to initiation of the transient-power tests, the ATE will be operated in the "line" (100% AC) mode for the acceptance tests. Baseline testing will immediately follow in order to obtain the initial operating characteristics of the ATE. In the transient mode tests, the PVA output, as determined by the local insolation, will modulate power to the ATE. Subsequently, in the "boost" mode, the PVA output will be supplemented so that the ATE can operate at a preselected power level. A variation of this mode, in which there is a programmed voltage decay will permit simulation of a battery buffer that would function to levelize input to the ATE, if that need becomes essential. The hydrogen storage vessel, of course, functions as the hydrogen supply buffer.

After the formal tests have been completed, the system will be made available to IEA participants and to organizations having a potential interest in hydrogen production. With guidance and support by BNL staff, this opportunity will provide hands-on experience and familiarization, thereby providing technology transfer in a direct and practical fashion. Subsequent activity could involve reducing the number of cells in the ATE in order to illustrate a stand-alone system.

The estimated capital and operating costs, which are about equal, total $700,000 for the first year's effort. Second- and third-year costs involving reduced manpower and nominal maintenance costs are about $200,000.

REFERENCES

1. G. Strickland, "An Integrated Test Bed for Advanced Hydrogen Technology: Photovoltaic Array/Electrolyzer System," - BNL 51577, July 1982.

CHEMICAL/HYDROGEN ENERGY SYSTEMS ANALYSIS

M. Beller
Brookhaven National Laboratory
Upton, New York 11973

Introduction

The major function of this program is to perform systems analyses of selected technologies and programs for which Brookhaven National Laboratory provides management support and technical oversight. The purpose of the analyses is to establish R&D criteria and priorities, and to define the roles of the technologies in terms of their value for long-term payoffs in the energy system.

Four programs have been analyzed in FY 1982. They are:

- Hydrogen recovery from hydrogen sulfide,
- Hydrogen separation using hydride technology,
- Photochemical hydrogen production, and
- Anode depolarization in electrolytic hydrogen production.

Brief descriptions of the analyses and results follow.

Hydrogen Recovery from Hydrogen Sulfide

A process for recovery of hydrogen from hydrogen sulfide uses a molten copper reactor to produce copper sulfide and hydrogen. The copper sulfide is then oxidized by air to produce copper and sulfur dioxide. Since sulfur dioxide is a pollutant, it must be converted to sulfuric acid.

Present technology employs processes which decompose hydrogen sulfide to sulfur and water. Sulfur is a valuable commodity, and water is obviously an innocuous byproduct. The analysis[1] thus focuses on the values of hydrogen and sulfuric acid versus that of sulfur presently derived from hydrogen sulfide.

Sulfuric acid is presently a glut on the market. Twenty percent overcapacity exists in the industry. The acid is highly corrosive, and expensive to transport. It was concluded that the acid is of very low value, and that the potential hydrogen value was equivalent to the value of sulfur from existing processes. On this basis, it was recommended that there was little to be gained by pursuing the process, since disposal of the sulfuric acid presents an added environmental problem. It was suggested that future efforts focus upon a process which produces both sulfur and hydrogen.

Hydrogen Separation Using Hydride Technology

The separation of hydrogen from chemical and refinery process streams is potentially desirable to obtain hydrogen for reuse in plant processes. Although many processes exist for recovering hydrogen from high pressure, high concentration streams economically, there are no successful processes for recovery at low concentrations and partial pressures. Specific metal alloys which form hydrides have been proposed for such use. However, a major problem in this application is poisoning of the alloy by impurities in the waste streams. Overcoming this problem requires the use of a cleanup bed to remove impurities, or the demonstration of economic alloy bed lifetimes.

The analysis[2] analyzed the economics of alloy hydride systems versus the use of steam reformers to reform the entire hydrocarbon stream to hydrogen. Figure 1 summarizes the result of the analysis. The conclusion is that unless a bed life of at least one year can be shown to avoid frequent alloy replacement, the process will not be economic compared to steam reforming of the entire stream.

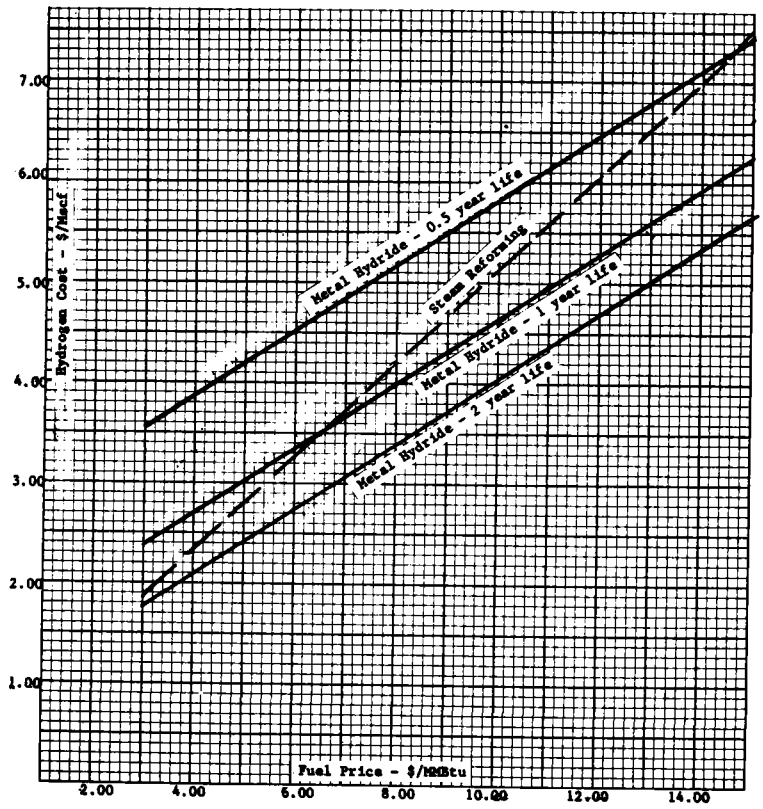

FIGURE 1
ESTIMATED HYDROGEN PRODUCTION COST VS.
COST OF FUEL AND LIFE OF METAL HYDRIDE ALLOY

Photochemical Hydrogen Production

Present work in hydrogen production using photochemical systems was reviewed.[3] Both homogeneous and heterogeneous systems were examined, and their advantages and disadvantages outlined. A breakeven cost analysis was performed to assess the cost requirements for photochemical systems. A list of R&D priorities was formulated, as follows:

1. Efficiencies of 15% or better must be demonstrated for some of these systems, based upon anticipated advances in PV technology with which PC systems may compete.

2. Photochemical agent costs which are lower than DOE PV cost targets are required. An initial goal should be in the order of less than \$500/kW H_2. This again is based on the PV target of \$400/kW, divided by the present electrolytic cell efficiency.

3. If (1) and (2) above can be met, actual solar cell experiments and designs should follow. These experiments are needed to assess whether diffuse radiation is sufficient for significant H_2 production, or if focusing and tracking are required. They also provide information for photochemical cell cost estimates.

4. As advances occur in these systems, more systematic analyses which incorporate better parametric estimates can be done.

Anode Depolarization in Electrolytic Hydrogen Production

A study[4] of the potential for anode depolarizers in reducing the cost of hydrogen production from electrolytic cells was performed. It was concluded that moderate incentives exist to pursue this work, since in the long term, as electricity costs and natural gas prices rise, appreciable decreases in cell voltage requirements can bring electrolytic hydrogen into the cost area of steam-reformed hydrogen (Fig. 2). A set of R&D priorities was also outlined in the study.

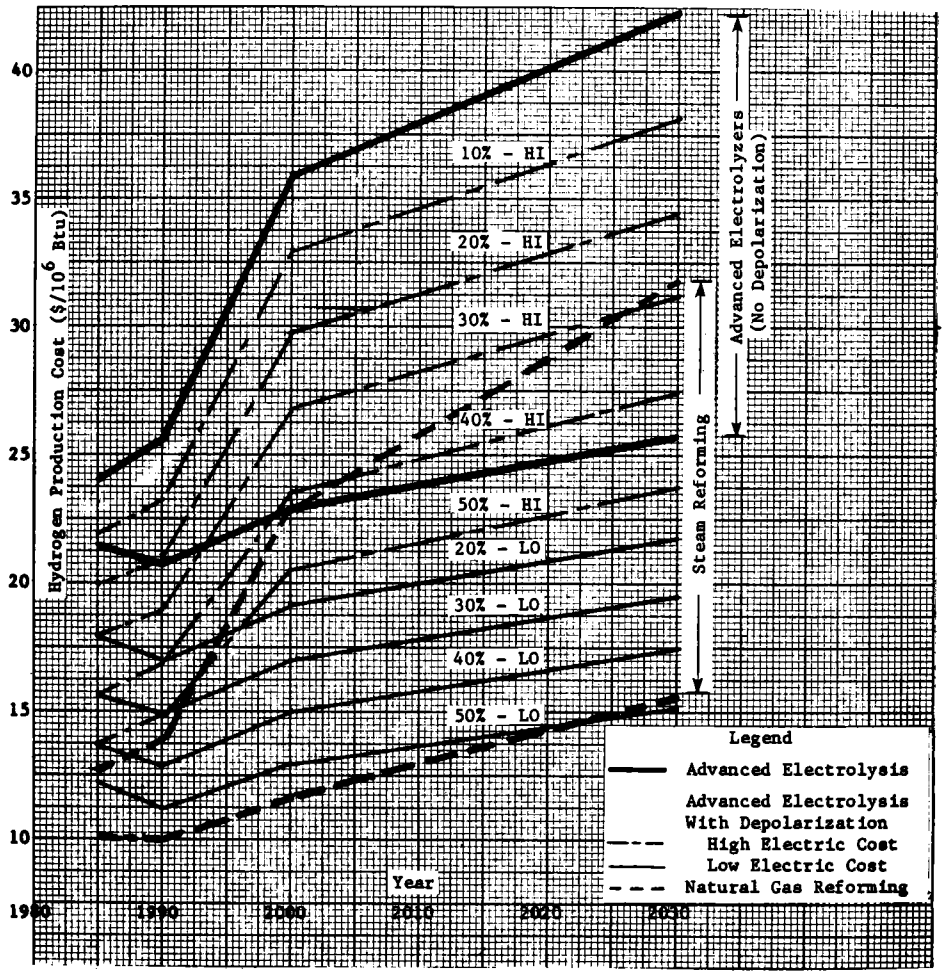

FIGURE 2
HYDROGEN PRODUCTION COSTS OVER TIME

References

1. M. Beller and J. D'Acierno, "Assessment of SRI H_2S Technology," BNL Rept. 30022, Sept. 1981.

2. M. Beller and G. Skaperdas, "Assessment of Metal Hydride Process for Separation of Hydrogen from Waste Streams," BNL Rept. 30678, Dec. 1981.

3. M. Beller, "An Analysis of Photochemical Hydrogen Production," BNL Rept. 31059, March 1982.

4. M. Beller, "Anode Depolarizers in Electrolytic Hydrogen Production," BNL Rept. 51562, June 1982.

ADVANCED CONCEPTS FOR ELECTROLYTIC HYDROGEN PRODUCTION

J. McBreen and C. Y. Yang
Brookhaven National Laboratory
Upton, New York 11973

INTRODUCTION

A major contributor to the cost of conventional aqueous electrolysis is the large decomposition voltage for water. Three methods for reducing these voltages are high temperature steam electrolysis in a solid oxide electrolyte electrolyzer at about 1000°C, electrolysis using anode depolarizers, and photoelectrochemical decomposition of water. This paper discusses research work at Brookhaven National Laboratory (BNL) in the first two areas.

One of the problems in doing electrochemical research on solid oxide electrolyte systems is that unlike aqueous and molten salt systems, the electrochemical techniques do not exist for investigating electrode reactions. To date, much of the work at BNL has been devoted to developing these techniques. This has included the development of a point contact technique for studying the electrode-gas-solid electrolyte interface (1,2). This year this work was extended to include the development of electrochemical techniques for study of the initial stages of oxidation of metals at high temperatures. Techniques were also developed to carry out surface science studies at the solid oxide electrolyte interface under conditions simulating in situ water electrolysis.

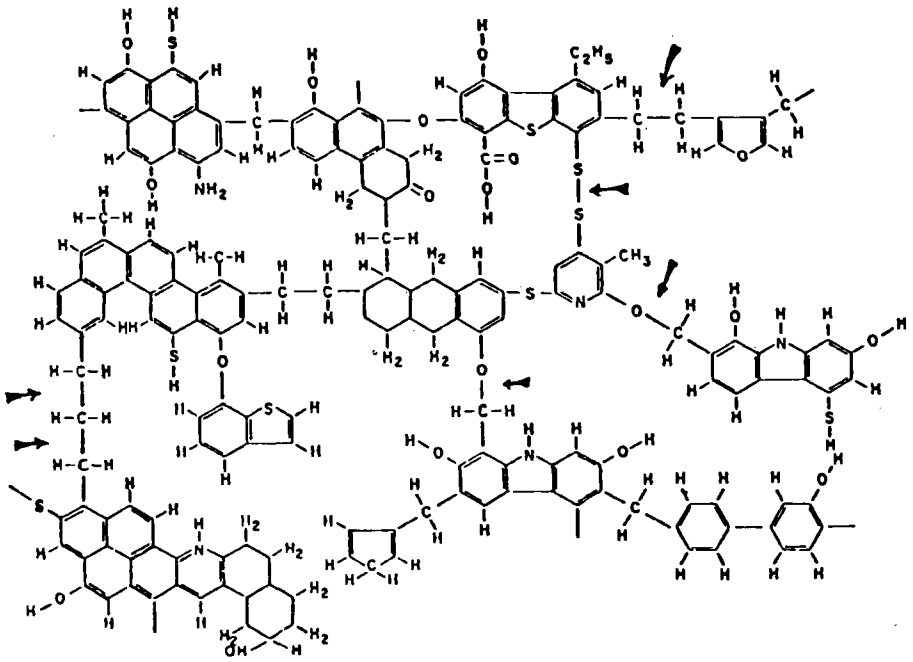

FIGURE 1

A representation of the functional groups in coal (7).

Most prior work on anode depolarizers has been on the use of sulfur dioxide as an anode reactant either in an open or closed cycle (3,4). More recently, coal has been proposed as an anode depolarizer. Results in this area are very contradictory (5,6). Work at BNL, during the year, focused on resolving these discrepancies and on finding simple chemical treatments to enhance the anode depolarization of coal. The ultimate goal of this work is to use a low cost reactant such as coal and produce a useful chemical at the anode while evolving hydrogen at the cathode.

The rationale for the chemical treatment of coal was as follows: Figure 1 is represented by Wiser (7), of the functional groups in coal. The arrows point to a number of weak bonds. These presumably were formed by condensation reactions when coal was formed. Many of these groups are amenable to hydroloysis and sulfur-sulfur bonds can be broken by molten zinc chloride treatments. Accordingly the treatments chosen were hydrolysis by alkali carbonate or treatment with molten zinc chloride. The aim was to liquify a significant portion of the coal. A liquid reactant would be easier to handle because of ease of transport to the electrocatalyst. Solid reactant would require the use of fluidized bed electrodes.

EXPERIMENTAL

1. High Temperature Solid Oxide Electrolyte Studies

1.1 Cyclic Voltammetry on Metal Electrodes at High Temperatures: Experiments on the initial stages of the oxidation of metal were carried out in a simple three electrode cell which can be represented as follows:

$$M\text{-}MO_x \;\Big|\; \frac{Pt}{YSZ} \;\Big|\; M'M'O_y$$

A disc of 8% yttria-stabilized zirconia was used as the electrolyte, and it was sandwitched between two mixed metal-metal oxide electrodes. The test electrode is represented by $M\text{-}MO_x$ where M is Ni, Fe or a Ni-Fe alloy. The counter electrode, which serves as a source or sink for oxygen, is represented by $M'\text{-}M'O_y$ where M' can be Fe or Co. A Pt paste electrode, painted on the side of the electrolyte disc, was the reference electrode. During the cyclic voltammetry measurements purified flowing helium gas was passed through the furnace and the oxygen activity was monitored by oxygen sensors before and after the reaction cell. In a typical experiment, the oxygen partial pressure of the inert gas was 10^{-13} atm at 950°C.

1.2 Surface Science Studies at Elevated Temperatures: The cell used for these studies was a miniturized version of the one described above and is shown in Figure 2. The working electrode in this case was a 1000Å film of either Fe or Ni. The cell could be mounted in a Varian 2001/sec ion pump vacuum system. During electrochemical oxidation, the test electrode was monitored using XPS which was based on a Vacuum Generators Clam electron analyzer and an x-ray source. It was possible to do these measurements at elevated temperatures because the electron analyzer has an electron focusing lens which permitted operation with the lens aperture up to three inches away from the hot electrodes.

2. Anode Depolarizer Studies

Anode depolarizer studies were carried out using formate in alkaline electrolyte, formic acid in acid electrolyte, coal in 5N H_2SO_4, solid residues from hydrolysis or molten $ZnCl_2$ treatments in 5N H_2SO_4, and the liquid extracts from the hydrolysis treatments.

2.1 Formate as an Anode Depolarizer: Experimental work on formate included a brief electrocatalysis study and the construction of a small electrolyzer.

(a) Electrocatalysis Studies: Various Pt, Pd and Pt/Pd alloy catalysts were prepared by a modified version of the method of Grimes and Spengler (8). The catalyst supports were open cell nickel foams. The nickel foam was 2mm thick and had $\sim$40 pores/cm. The nickel was etched in a 1:1 water-concentrated hydrochloric acid mix and then rinsed with cold distilled water. The catalyst plating solutions were prepared from chloroplatinic acid and palladium chloride. The metal content of the solutions was 2mg/ml and the pH was adjusted to one by HCl additions. Plating was carried out by electrochemical displacement. The freshly washed nickel foam was placed in the plating solution and removed when the solution turned to a light yellow-green color. The catalyst loading was 5mg/cm^2. Cyclic voltammetry was carried out on 1cm^2 electrodes in 4MKOH + 4M HCOOK.

(b) Formate Depolarized Electrolyzer: A small formate depolarized electrolyzer was constructed. This is shown schematically in Figure 3. The electrodes consisted of a 7cm diameter nickel foam sandwitched between two nickel screens. These were spot welded to a nickel current collector. The cell body was machined from acrylic plastic, the separator was a 1.3mm asbestos membrane and the electrolyte was 4M KOH + 4M HCOOK. Both electrodes were catalyzed with a 90% Pd-10% Pt alloy catalyst with a loading of 5mg/cm^2. Provisions were made for reference electrode measurements on both electrodes and hydrogen gas collection for current efficiency measurements.

2.2 Coal as an Anode Depolarizer:

(a) Cell for Coal Powders and Solid Residues from Chemical Treatments: The cell for studies of the anode depoalrization activity of coal and solid residues from chemical treatments is shown in Figure 4. The cell was machined from an acrylic block. The coal electrode was prepared by pressing 2g of the powder on to an 80 mesh platinum screen 5cm in diameter. The separator was a Nafion membrane. Provisions were made for a reference electrode capillary behind the coal electrode. All studies were carried out with New Mexico sub-bituminous coal.

(b) Chemical Treatment of Coal: The chemical treatments of coal that were carried out were iron removal, hydrolysis in alkali carbonate and treatment with molten zinc chloride.

Iron was removed from coal by heating it in 50% H_2SO_4 at 120°C for two hours. The coal was filtered and washed through a fiberglass filter in a Buchner funnel. In some cases the coal was washed with oxalic acid.

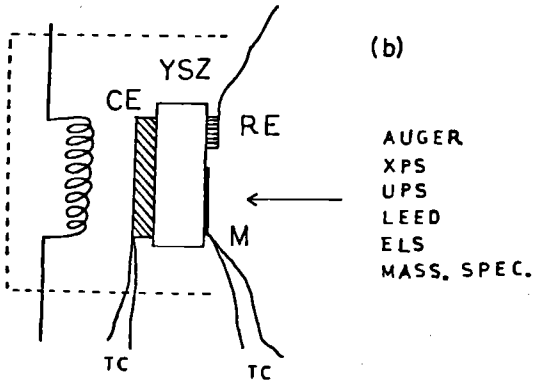

FIGURE 2

CELL FOR SURFACE SCIENCE STUDIES

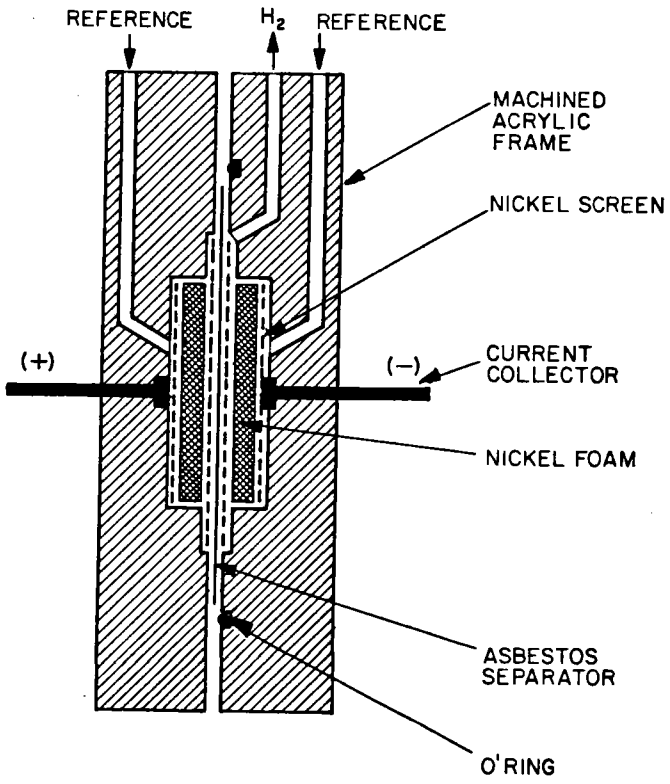

FIGURE 3

FORMATE DEPOLARIZED ELECTROLYZER

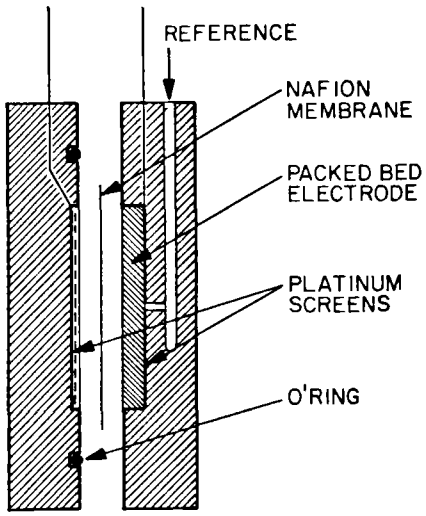

FIGURE 4

SCHEMATIC OF CELL FOR COAL AND SOLID RESIDUE STUDIES

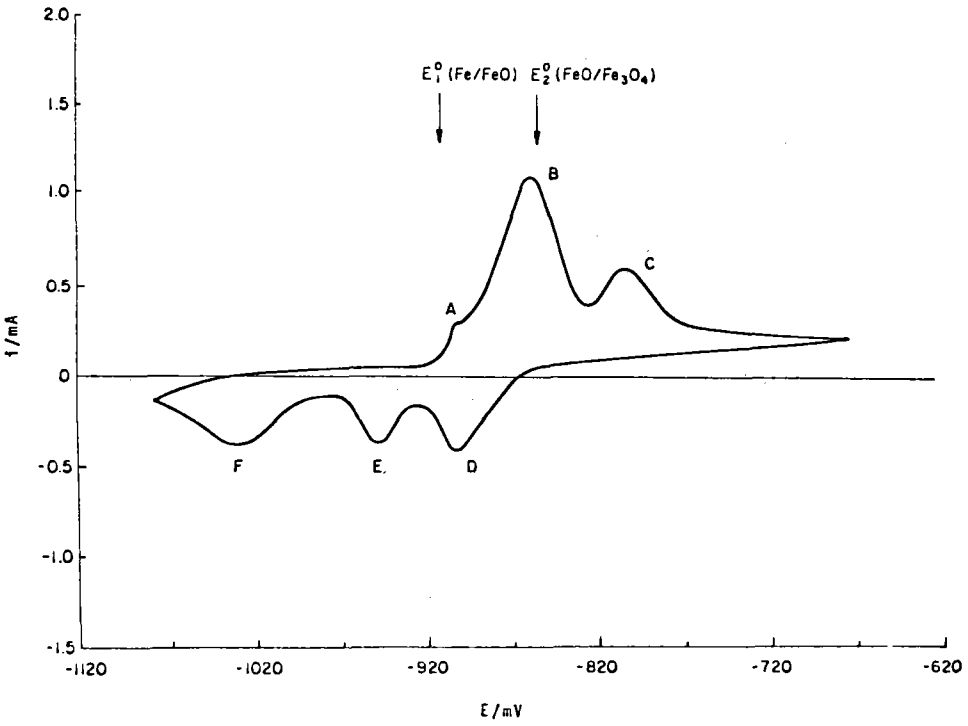

FIGURE 5

CYCLIC VOLTAMMOGRAM ON 0.3cm^2 IRON ELECTRODE AT 740°C; SWEEP RATE = 5mV/sec.

The hydrolysis treatments were carried out in a high pressure vessel for two hours at 300°C. The vessel had a nickel liner. In these treatments 20 ml of a 6.6 molal solution of alkali carbonate was added to 10g of coal that had previously been washed with sulfuric acid.

The molten $ZnCl_2$ treatment was carried out at 300°C for two hours. A PTFE liner was used, and 10g of $ZnCl_2$ was added to 10g of coal.

RESULTS AND DISCUSSION

1. Oxidation of Metals at Elevated Temperatures:

1.1 Cyclic Voltammetry on Iron: Figure 5 is a cyclic voltammogram on an iron electrode at 740°C. Several peaks are present, which indicates a sequence of descrete reaction steps. Peaks B and E are the redox pair for the Fe $\rightleftharpoons$ FeO reaction, and peaks C and D the redox pair for the FeO $\rightleftharpoons$ Fe_3O_4 reaction. The thermodynamic potentials for these reactions are indicated on this figure. Neither the cathodic peak A or the anodic peak F are understood at this time.

1.2 XPS Studies: Figure 6 shows XPS results for an iron film ($\sim$1000Å) at 350°C. Figure 6 (a) is the open circuit data which corresponds to metallic iron. After applying a potential of 200mV anodic to the oxidation potential, for 80 min, the results shown in 6 (b) were obtained. This corresponds to Fe_3O_4. The lower oxide FeO is not stable at 350°C.

With the development of the cyclic voltammetry method for high temperature studies and the cell for surface science studies, it is now possible to carry out in situ surface science studies under conditions simulating water electrolysis at elevated temperatures.

2. Anode Depolarizer Studies:

2.1 Formate Oxidation Electrocatalysis: Figure 7 shows cyclic voltammograms for formate oxidation on uncatalyzed and catalyzed nickel foam electrodes. Uncatalyzed foams have essentially no electrocatalytic activity. The electrocatalytic activity increases in the order Pt < Pd < 90% Pd - 10% Pt alloy. Further increases in the platinum content of the alloy catalyst decreases the activity. Accordingly, the 90% Pd - 10% Pt catalyst was chosen for the small electrolyzer.

2.2 Electrolyzer Performance: Figure 8 shows the performance of the small electrolyzer with a formate depolarizer. The results show that considerable depolarization of the anode was achieved. This was an unoptimized cell and more than half of the cell voltage was due to resistance losses. Gas collection measurements showed that hydrogen was produced at 100% efficiency.

2.3 Anode Depolarization Activity of Coal: Figure 9 shows a cyclic voltammogram for untreated coal. The redox pair of peaks A and B are due to the Fe^{2+}/Fe^{3+} redox couple. Washing of the coal with sulfuric acid eliminates these redox peaks. There is a small oxidation current between 1.2V and 1.4V SCE prior to oxygen evolution. This is due to oxidation of

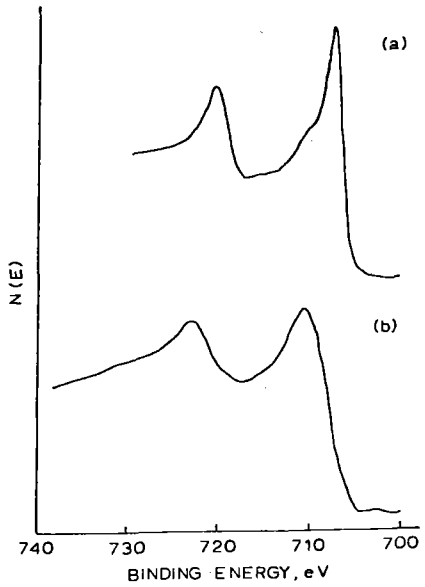

FIGURE 6

XPS SPECTRA OF AN IRON FILM AT 350°C
(a) at open circuit
(b) after 80m at +200mV

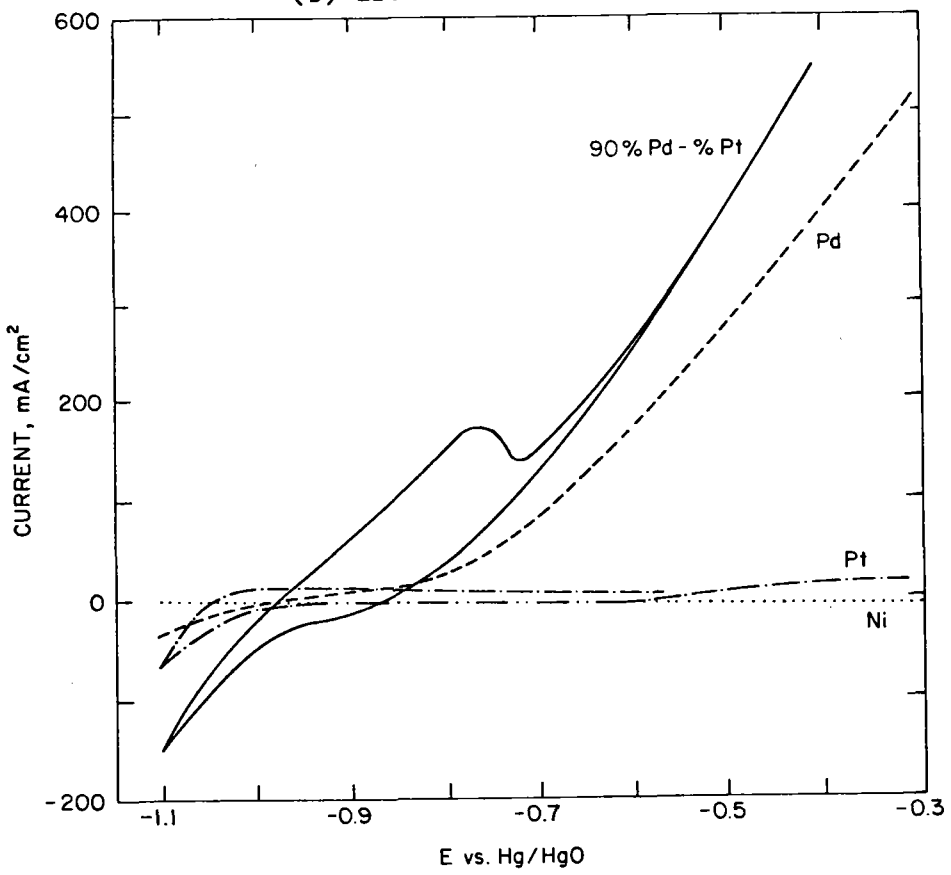

FIGURE 7

CYCLIC VOLTAMMOGRAMS ON 1cm^2 UNCATALYZED AND CATALYZED NICKEL FOAM ELECTRODES IN 4M KOH + 4M HCOOK AT 25°C; SWEEP RATE 10 mV/sec.

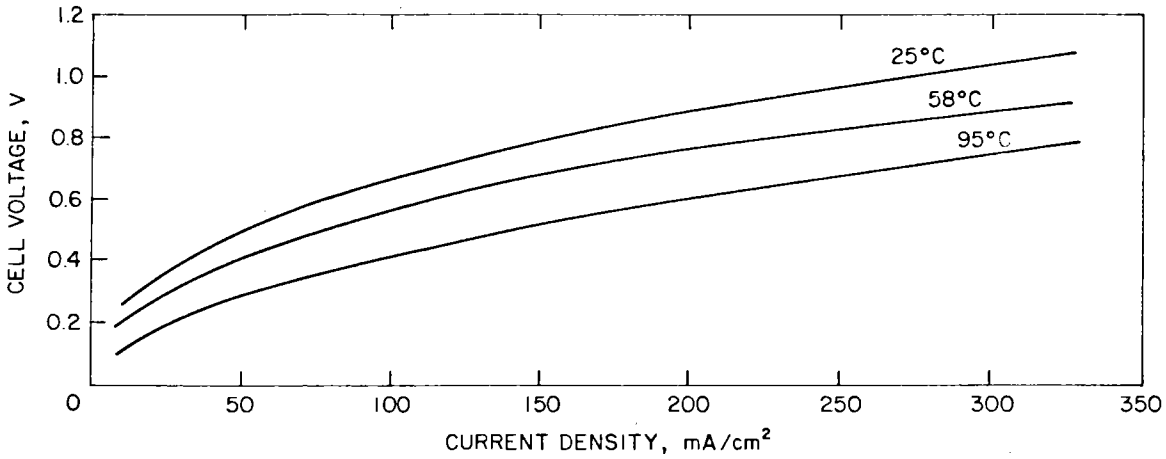

FIGURE 8

PERFORMANCE OF FORMATE DEPOLARIZED ELECTROLYZER

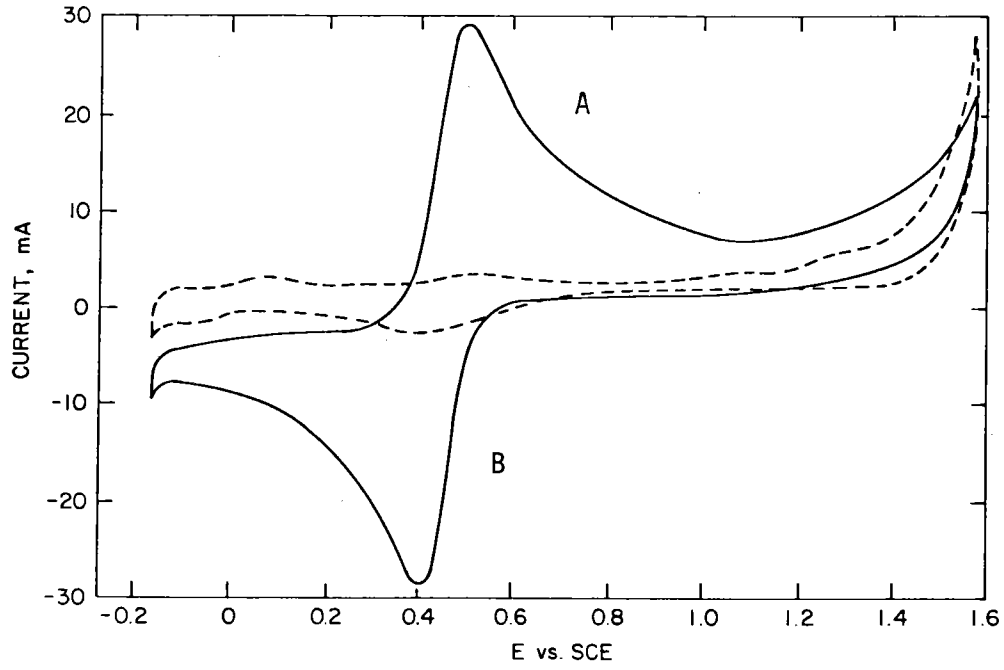

FIGURE 9

CYCLIC VOLTAMMOGRAMS ON COAL ELECTRODES; SOLID LINE UNTREATED COAL, BROKEN LINE COAL WASHED WITH H_2SO_4. ELECTRODE AREA = 20cm^2; TEMPERATURE = 25°C; SWEEP RATE 10 mV/sec.

the coal. The magnitude of this current increases with decreasing particle size of the coal.

Figure 10 shows the effect of K_2CO_3 hydrolysis and Figure 11 the effect of molten $ZnCl_2$ treatment on the oxidation current. These treatments increase the anode depolarization activity of the coal by a factor of twenty to forty.

The alkali carbonate treatments result in liquefaction of some of the coal. The degree of coal breakdown depended on the cation with the degree of liquefaction increasing in the order Na < K < Li < Rb < Cs. In the case of Cs_2CO_3 about 30% of the coal was liquified. This breakdown of the coal resulted in the release of iron that could not be leached out in the first acid treatment. The residual powder, however, did not display very much depolarization activity. Several catalyst materials including Pt, Pd, Pd-Ag alloys and lead ruthrenate were screened as oxidation catalyst for the soluble extracts from the Cs_2CO_3 treatments. Palladium was the only catalyst that displayed any electrocatalytic activity.

The results so far have confirmed that much of the anode depolarization activity of coal is due to iron impurities. However, coal can be oxidized electrochemically at a low rate. This rate can be increased by commination of the coal. Considerable enhancement of the anode depolarization activity can be achieved by simple alkali hydrolysis treatments or treatment with molten zinc chloride.

REFERENCES

1. H.S. Isaacs and L.J. Olmer, J. Electrochem. Soc. 129, 436 (1982).

2. H.S. Isaacs and L.J. Olmer, J. Electroanal. Chem. 132, 59 (1982).

3. W. Juda and D.M. Moulton, Chem. Eng. Progress 63, 59 (1967).

4. P.W.T. Lu, E.R. Garcia and R.L. Ammon, J. Appl. Electrochem. II 347 (1981).

5. R.W. Coughlin and M. Faroogue, Nature 279, 59 (1967).

6. G. Okada, V.Guruswamy and J. O'M. Bockris, J. Electrochem. Soc. 128, 2097 (1981).

7. D.D. Whitehurst, in Organic Chemistry of Coal, J.W. Larsen, Editor, American Chemical Society Washington, DC (1978) pp. 1-35.

8. P.G. Grimes and H.H. Spengler, in Hydrocarbon Fuel Cell Technology, B.S. Baker, Editor, Academic Press New York (1965) pp. 121-130.

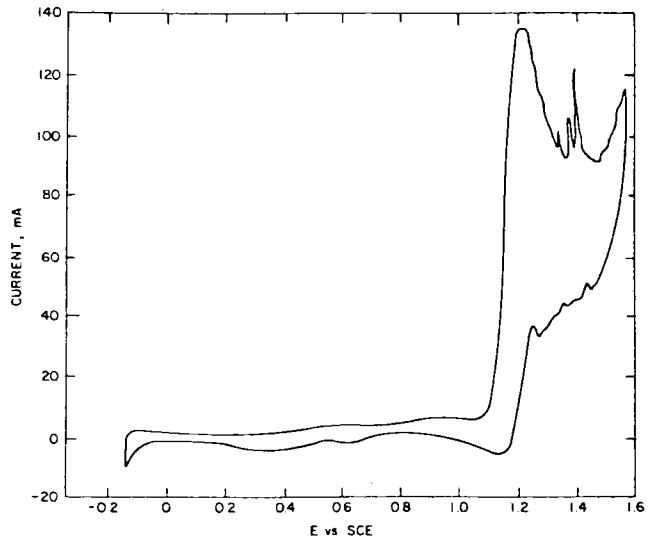

FIGURE 10

CYCLIC VOLTAMMOGRAM ON COAL ELECTRODE TREATED WITH K_2CO_3 AT 300°C FOR 2 HOURS. ELECTRODE AREA = 20 cm^2; TEMPERATURE = 90°C; SWEEP RATE 10mV/SEC.

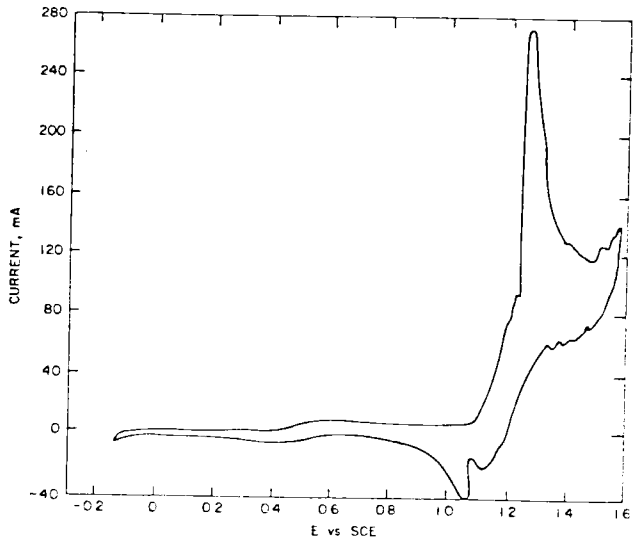

FIGURE 11

CYCLIC VOLTAMMOGRAM ON COAL ELECTRODE TREATED WITH MOLTEN $ZnCl_2$ AT 300°C FOR 2 HOURS. ELECTRODE AREA = 20 cm^2; TEMPERATURE = 90°C, SWEEP RATE 10mV/sec.

STATIC FEED WATER ELECTROLYSIS FOR LARGE SCALE HYRODGEN GENERATION

F. H. Schubert, A. J. Kovach and K. A. Burke
Life Systems, Inc.
24755 Highpoint Road
Cleveland, OH 44122

ABSTRACT

The Static Feed Water Electrolysis concept developed by Life Systems, Inc., over the past 11 years, is being evaluated for application to large-scale hydrogen generation. The inherent potential for low cost and high performance of the alkaline electrolyte-based technique resulted in the continuation of a Department of Energy/Brookhaven National Laboratory-funded program to Life Systems, Inc. The continued efforts addressed four areas: (1) verification of performance of the first 10-to-1 scaled-up cell hardware (0.1_2 ft^2 to 1.0 ft^2), (2) analysis of the data obtained with the 1.0 ft^2 hardware and the development of a Model II 1.0 ft^2 cell capable of high performance, multi-cell stack operation, (3) continuation of the development efforts to operate with impure water feed sources through testing at the 0.1 ft^2 and 1.0 ft^2 level as well as at elevated pressures (up to 200 psia) and (4) initiation of efforts to improve or maintain the present high performance levels, but at potentially reduced capital equipment and operational costs through elevated temperature operation and component/part cost reductions.

This paper presents the results obtained to date in GFY 82.

INTRODUCTION

Life Systems has been working on water electrolysis technology for the past 11 years. During a major portion of this time the electrolysis technology efforts had been focused on generating oxygen to sustain life of spacecraft and aircraft personnel. These applications require high performance water electrolysis systems since power is at a premium. This technology, however, by the nature of its application has been limited to smaller electrode areas (0.1 to 0.3 ft^2) and to stacks of up to 15 cells. Although this technology is extremely attractive, the state of its development requires scale-up at several key areas to realize the performance and cost reduction potentials.

To achieve these goals, Brookhaven National Laboratory (BNL) under sponsorship of the Department of Energy (DOE) had initiated a development program with Life Systems, Inc., in August 1980, to demonstrate the capability of Life Systems' electrolysis concept to satisfy the bulk hydrogen generation requirements of the BNL/DOE chemical/hydrogen energy systems program.

MODEL I 1.0 FT^2 CELL PERFORMANCE CHARACTERIZATION

The larger the electrolyzer cell area the fewer the number of cells that are required to generate a given volumetric rate of hydrogen.

Reduction in the number of cells through increasing the active cell area reduces capital costs and keeps the number of cells within practical limits for large scale gas production.

Sizing calculations for the Life Systems' Static Feed Water Electrolysis (SFWES) style concept were completed during GFY 81 for 1.0, 5.0 and 10.0 ft^2 cells. In parallel, Life Systems designed and fabricated a scaled-up single cell having an active cell area ten times the previous baseline size, or an area of 1.0 ft^2. The major characteristics of this first scaled-up cell hardware are as follows:

• Active Cell Area, ft^2	1.0
• Electrode, Cathode	WCB-2
• Electrode, Anode	WAB-1 (Advanced)
• Nominal Current Density Range, ASF	400 to 800
• Maximum Operating Temperature, F	200
• Maximum Operating Pressure, psig	550

Single cell components along with end plates and end plate support members are shown in Figure 1.

In addition to scaling up the actual cell frame by a factor of 10 (see Figure 2), major efforts were devoted by Life Systems to allow scaling of key cell parts--the asbestos matrix and the electrodes. To fabricate these key parts, required scale-up of existing fabrication hardware. Results of the matrix and electrode scale-up activities are reflected in Figures 3 and 4. With the new hardware up to 1.5 ft^2 active cell areas are possible.

Following successful fabrication of the cell components, (Life Systems-funded) a test program for a 1.0 ft^2 single cell (funded by BNL/DOE) was initiated. The test program consisted of initial checkout testing, 300 hours of parametric testing at 100 to 400 ASF, 100 hours of endurance testing at a constant set of conditions, and 200 hours of exploratory testing from 400 to 1,000 ASF. The cell performance of the 1.0 ft^2 cell using an intermediate performing anode (WAB-1) is shown in Figure 5. Figure 5 shows that the cell scale-up activities were successful in that the performance of the 1.0 ft^2 cells is comparable to the performance range of 0.1 ft^2 cell with similar style electrodes as indicated by the shaded area in Figure 5. The slope of the 1.0 ft^2 cell performance curve is slightly steeper indicating a slightly higher IR voltage loss than encountered at the smaller cell area.

The result of the parametric and exploratory testing, shown in Figure 6, indicate that the overall scale-up of the static feed concept and configuration with this "first generation hardware" (Model I) have demonstrated that the static feed concept is potentially capable of hydrogen production at increased cell sizes and at high current density. No major drawbacks or problems were identified through testing at ambient pressures.

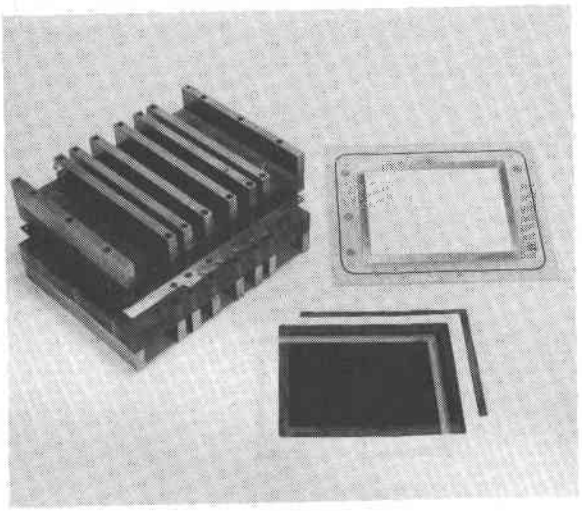

FIGURE 1

SINGLE CELL (1.0 ft^2) CELL COMPONENTS (MODEL 1)

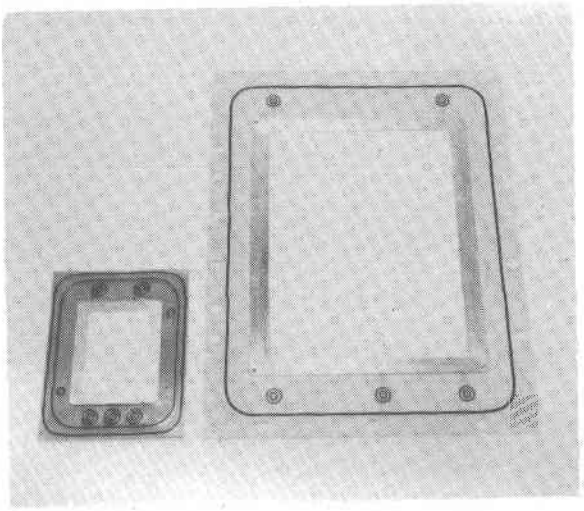

FIGURE 2

COMPARISON OF 0.1 ft^2 AND 1.0 ft^2 POLYSULFONE CELL FRAMES

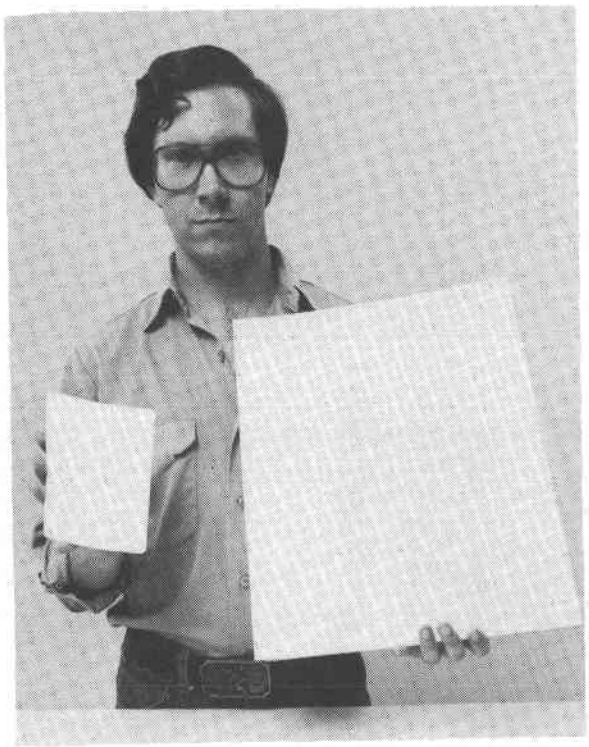

FIGURE 3

ILLUSTRATION OF CELL SEPARATOR SCALE-UP

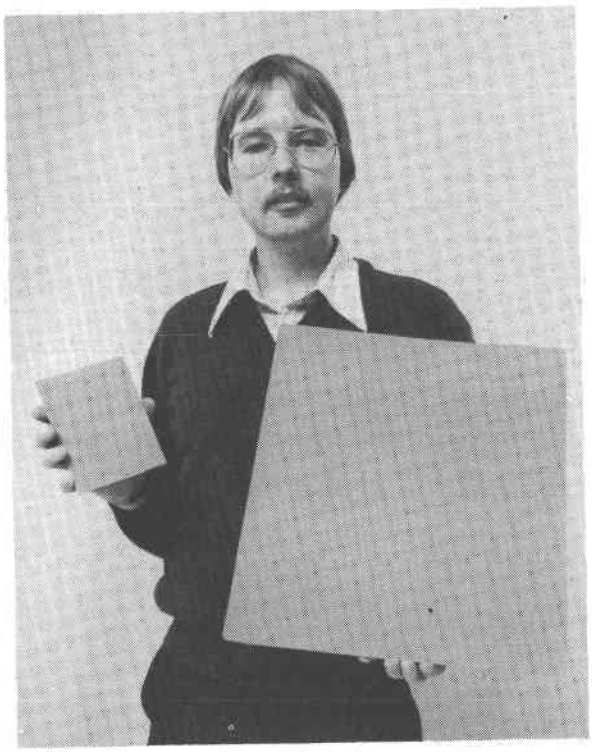

FIGURE 4

DEMONSTRATION OF CELL ELECTRODE SCALE-UP

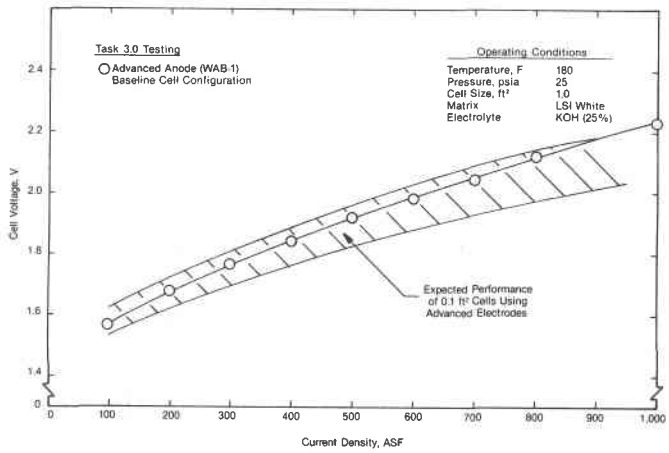

FIGURE 5

CELL VOLTAGE VERSUS CURRENT DENSITY - 1.0 ft^2 CELL (MODEL 1)

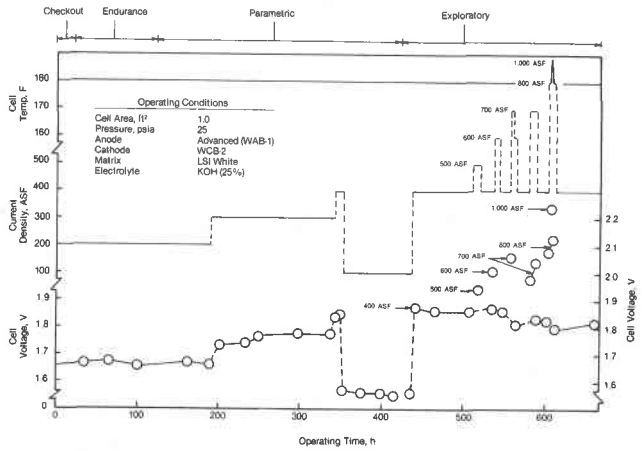

FIGURE 6

CELL PERFORMANCE VERSUS OPERATING TIME - 1.0 ft^2 CELL (MODEL 1)

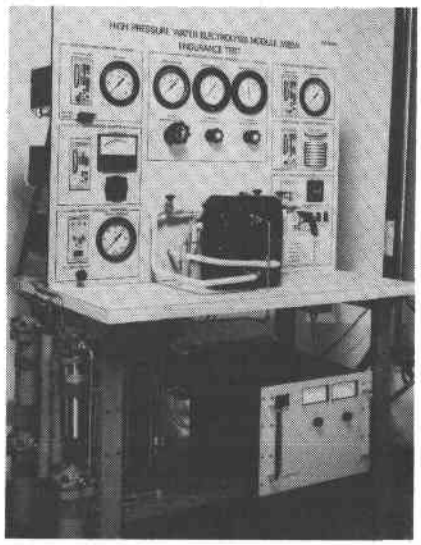

FIGURE 7

HIGH PRESSURE WATER ELECTROLYSIS TEST STAND

The initial test experience with the 1.0 ft^2 single cell did, however, uncover the need for several improvements such as lowering of IR losses, scale-up of the best performing anode (WAB-6), etc., which are scheduled to be incorporated in the second generation (Model II) cell hardware, as described below.

SCALE-UP ANALYSIS/MODEL II HARDWARE DEVELOPMENT

The objectives of this task are to: (1) analyze the test data obtained with the Model I hardware, (2) define and implement modifications and improvements to the Model I hardware to result in the Model II improved 1.0 ft^2 cell design, (3) fabricate and test a multi-cell stack (Model II) and (4) develop the special test equipment to allow the characterization and exploratory testing required with the scaled-up hardware.

To date key improvements needed in the Model I cell hardware have been defined and manufacturing drawings for the Model II have been completed. Modifications and improvements that were addressed are:

- Incorporation of multi-cell current collector design
- Provisions for increased compression and increased thickness in the nickel current collectors to decrease cell IR losses
- Strengthening of anode current collector to allow for the high pressure (550 psig) operation
- Relocation of the static water feed addition point to ensure sufficient lateral diffusion and homogeneity in concentration of the water feed solution
- Incorporation of modifications to the feed membrane to allow operation of the 1.0 ft^2 cell hardware with brackish water sources

Completion of the first multi-cell stack hardware and its subsequent checkout testing is scheduled for late GFY 82.

The multipurpose test stand that provides for characterization and exploratory performance testing of multi-cell 1.0 ft^2 stacks has been designed, fabricated and checked out. The test stand has the capability to test to 200 psig, 200 F and 1,000 ASF for cell stacks consisting of up to six cells. The stand is shown in Figure 7. A 0.1 ft^2 cell stack is shown which was used for test stand checkout purposes.

OPERATION WITH IMPURE WATER SOURCES

A significant part of the present cost of electrolytic hydrogen production is incurred during the purification of the water to contamination of the electrodes and/or cell electrolyte. In the static feed system, however, the liquid water to be electrolyzed is separated from the electrodes and cell electrolyte by a gas compartment containing only water vapor and hydrogen. During the

GFY 81 tasks, Life Systems demonstrated operation with its static feed electrolysis system using unpretreated brackish water prepared from an aquarium sea water mix.

Based on the promising results of the above activities, continuation of exploring the use of impure water feed sources was provided under the current task. Specifically, long-term testing using current baseline 0.1 ft^2 and scaled-up 1.0 ft^2 (Model I) cell hardware is scheduled (greater than 2,500 hours, total). The effects of dissolved organics and inorganics, as contained in actual sea water, will be investigated as well as materials compatibility with the brackish/sea water environments. Testing will be conducted both at ambient and at elevated pressures (up to 200 psig).

Besides the performance test data to be obtained during the testing, other end items of this particular task will consist of definition/chemical makeup of the impure water sources used for testing, definition of allowable ranges of critical system operating parameters, i.e., pressure, temperature, temperature differentials and flow rates, and a list of system hardware modifications required to be compatible with impure water operation.

To date testing is underway using 0.1 ft^2 cell hardware and operating at pressures up to 200 psig. The elevated pressure is not only essential to prevent feed water boiling but is also being explored to determine effects on water feed rate and other cell operating characteristics. Cell performance to date is comparable with other high pressure operational experience. Only several days of testing have been completed at the time of this writing.

PERFORMANCE IMPROVEMENTS/COST REDUCTION INVESTIGATIONS

Electrolytic hydrogen production costs are a strong function of the individual cell voltages and of the parasitic power used by ancillary components. Capital equipment costs, of course, are primarily related to the costs of the electrolyzer stack and the cost of the other system components such as pumps, water purifiers, separators, power conditioning, compressors, etc.

The objective of the efforts to be expended under this task are to maintain or improve the present high performance level of the static feed cells while decreasing projected capital equipment and operational costs. These decreases shall be achieved through actual operation at higher temperatures (>240 F with 300 F as a goal) and projected cost reductions in cell/stack hardware. The simplifications possible with a SFWES at the systems level shall be quantified with respect to ancillary components, parasitic power loads and costs.

The end items of this task shall consist of single cell performance life data using cell separators compatible with projected operation at 240 F (goal of 300 F), a system schematic of a conceptual SFWES using contaminated water sources for feed with heat and mass balances

indicated as well as power requirements defined. A cost analysis of the potential savings for such a simplified SFWES shall also be completed.

To date short-term single cell operation has been achieved at 300 F. Life testing of such a cell is planned to identify long-term effects on the pretreated, reconstituted cell separator used for Life Systems' high temperature cells.

SUMMARY AND CONCLUSIONS

The static feed electrolysis concept using an alkaline electrolyte continues to be a reliable candidate for large-scale, low cost hydrogen production. Its demonstrated performance and inherent system-level simplicity coupled with its use of low cost materials and tolerance to low level purity water, project low capital and operating costs. Activities must be continued in the area of scale-up analyses, performance demonstration and evaluation of operation with impure water sources, as well as quantification of the cost savings to adopt the static feed concept to terrestrial energy applications. The additional activities sponsored by BNL/DOE for GFY 82 are a continuing step in that direction.

REFERENCES

1. Proceedings of the DOE Thermal and Chemical Storage Annual Contractors' Review Meeting, September 14-16, 1981, Washington, DC, December 1981.

2. Burke, K. A. and Schubert, F. H., "Development of Static Feed Water Electrolysis for Large Scale Hydrogen Production," Final Report, Contract BNL-522723-S, TR-470-4, Life Systems, Inc., Cleveland, OH, December 1981.

3. Schubert, F. H. and Burke, K. A., "Static Feed Water Electrolysis for Large-Scale Hydrogen Generation," Proceedings of the Fourth World Hydrogen Energy Conference, pp. 215-224, June 1982.

4. Schubert, F. H., Burke, K. A. and Kovach, A. J., "Static Feed Water Electrolysis Hydrogen Production from Impure Water Sources," Proceedings of Advances in Hydrogen Manufacturers Symposium, March 1982.

ADVANCED ALKALINE WATER ELECTROLYSIS
DEVELOPMENT OF AN ELECTROLYSIS CELL SEPARATOR FOR 125 C OPERATION

John N. Murray
Teledyne Energy Systems
110 West Timonium Road
Timonium, Maryland 21093

ABSTRACT

With the hydrogen technology for 1.7-1.75 volts/cell at 500 ma/cm^2, 100 C demonstrated under previous contracts, the emphasis at Teledyne Energy Systems (TES) during the last year was refocused onto the development of a mechanically stable electrode separator for operation at 125 C. A separator was developed consisting of 20 V/o polybenzimidazole, 80 V/o potassium titanate which appears to satisfy the four separator requirements of low effective resistivity, small pore diameters, a high degree of natural wettability and chemical/mechanical stability in the application environment. Life testing of a two-cell, 300 cm^2 active area module involving the best available technology was initiated in June, 1982 with the plan of operating approximately 2200 hours at 125 C, 500 ma/cm^2 to demonstrate the stability of the technology. Additional investigations into the performance characteristics of the anode have been conducted and have offered new insight into gaining an additional 100 mV per cell.

INTRODUCTION

This report continues from last year's summary report (1) and briefly describes the work at TES during 1981-1982 on the development and testing of an improved electrode separator as part of the contracted effort to the Brookhaven National Laboratory (BNL) as BNL-545767-S. During earlier studies the significance of improving the operating efficiency of hydrogen production via alkaline solution water electrolysis by increasing the operating temperature and by substituting improved electrocatalysts had been demonstrated. A majority of the test data were obtained using the test system dubbed ARIES, constructed as part of an earlier BNL contracted effort. In addition, these data were supplemented with results obtained using 50 cm^2 "minicells" developed under TES funds. Testing to date has shown the use of the C-AN cathode electrocatalyst, a nickel-molybdenum compound coating developed at the British Petroleum Research Centre (2), allowed an improvement from the conventional electrolysis of 64 voltage percent (2.3 volt/cell at 55 C operation) to a voltage efficiency of 82% (1.80 volt/cell) at 100 C as was demonstrated in ARIES test modules No. 13 and 19. A projection of 1.65 volt/cell (90% voltage efficiency) can be made for cell operation at approximately 125 C.

Nearly all conventional alkaline electrolyte electrolysis cells utilize an asbestos electrode separator of one shape or another, the chrysotile asbestos fiber/fibrule having excellent electrical resistance and allowing fabrication of separators with thru-pore sizes sufficiently small to preclude the transmission of the generated gasses. Asbestos separators have reasonable chemical stability in KOH solutions; systems

have been utilized for many years when the operating temperature is maintained below 80 C. Selective dissolution of the SiO_2 component of the magnesium silicate structure has been shown to occur at above 100 C and a reasonably extensive study (3) was conducted relating the corrosion of asbestos as a function of KOH concentration and temperature. The conclusions of that study suggested the asbestos corrosion could be minimized by presaturating the KOH or NaOH electrolyte with silicates. A moderate sized 5 KW system test is underway in France (CGE) (4) to demonstrate these principles at 120 C. Electrode tests with silicate saturated 40 w/o KOH solution at 160 C are also being performed at SODETEG (5). The question of long-term stability will apparently be answered in one or both of these two very interesting experiments.

Of the few inorganic or organic materials which are chemically stable in the 125-150 C region in aqueous KOH solutions, only potassium titanate (K_2TiO_3) polyphenylene sulfide, Teflon (PTFE) and perhaps polybenzimidazole (PBI) are being considered as available today and potentially useful in water electrolysis cells. K_2TiO_3 bonded with PTFE as well as deposited within a porous PTFE matrix had been tested during a previous contracted effort with only limited success because of pore structure problems. Porous PBI separators were found to be somewhat better with a successful test performed at TES using a 75 cm^2 cell at temperatures up to 90 C. However, the subsequent test in the 300 cm^2 ARIES Module No. 12 at 100 C was quite disappointing, the input voltage requirements increasing significantly within 24 hours of operation. The general failure causes were attributed to compressive stress relaxation which perhaps caused two problem--an increase in separator density leading to greater cell ionic resistance and a decrease in compressive loading on the metal-to-metal contacts within the cell leading to increased electronic resistances.

The effort of the last year has consisted in first establishing which of two concepts would resist compressive load relaxation, a higher density, porous, "pure" PBI separator or a PBI separator to which K_2TiO_3 fibers have been added as a spacing agent. With a stable composition then defined, a life test of the advanced electrolysis components at temperatures up to 125 C was then initiated and continues at the time of this paper.

RESULTS AND DISCUSSION

The six-month separator development effort was undertaken in the March to September 1981 time period and the summary report (TES-545767S-7) was prepared and submitted to BNL in December, 1981. Some additional testing regarding the mechanical stability of the porous test pieces was conducted under TES funding and these results are included for appropriate continuity.

Pure PBI separators were prepared for the density range of 30 to 80% and an initial thickness range of 0.05 to 0.3 cm. The thicker pieces were made during the initial fabricating period to verify the fabrication approaches were adequate, a goal of 0.025 cm thickness having been set previously. In general, the pieces were cast from a water slurry, dried, "air roasted" for one hour at 375 C to improve the chemical stability and

finally hot pressed at 150 C for one hour to attain the final required thickness. The electrochemical characteristics of the high density pure PBI separators was found to be significantly poorer than the equivalent 65% dense asbestos separator and the data analysis indicated the higher minicell resistance factor as the primary cause. Gas retention characteristics of the thinner (<0.040 cm) pieces was inadequate and a minimum in-cell thickness of 0.050 cm would appear to be necessary if high (>50 psid) differential pressures must be tolerated. Flat plate compression testing of dry samples at ambient temperature loaded to an approximate 40-50% density showed somewhat high stress relaxation factors which tend to verify the problems noted with the previous test of ARIES Module 12. The more recent testing of separators loaded between screen electrodes indicates the stress relaxation rates to be higher than that of flat plate loading. The air roasting treatment was found to be somewhat beneficial in providing both a greater compressive modulus as well as a piece with half the relaxation rate. The stress relaxation rate was still, however, tenfold higher than the equivalent asbestos separator.

The approach of adding K_2TiO_3 as a spacing agent was reasonably successful. The screening results showing the variation of cell resistance with respect to composition are shown in Figure 1 for four experimental runs. Although there is considerable scatter in the data from cells using the high percentage PBI separators, the favorability of a 10-30 V/o PBI, 70-90 V/o K_2TiO_3 separator was apparent.

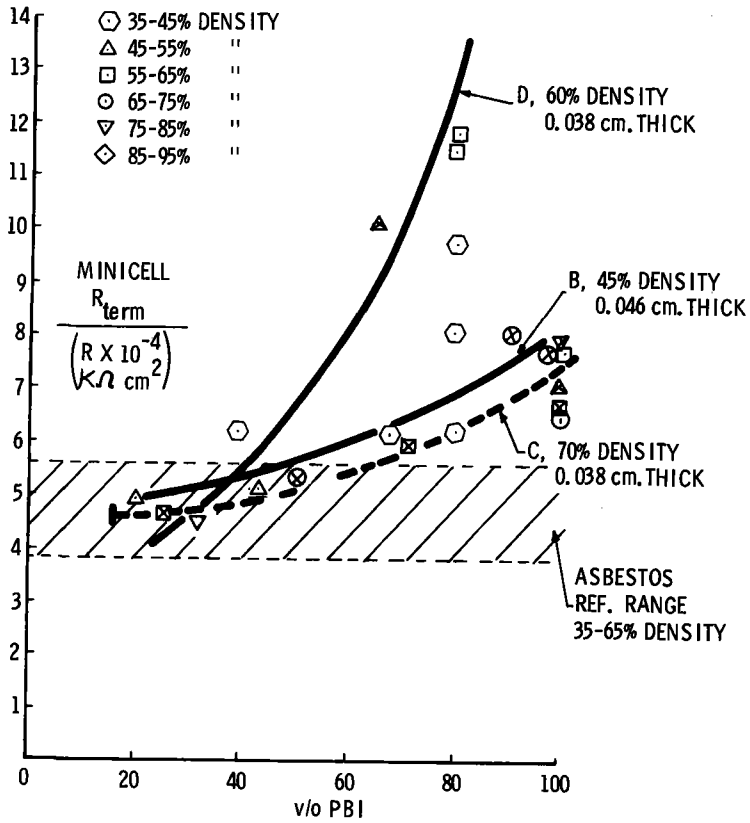

FIGURE 1. SEPARATOR RESISTANCE FACTOR AS A FUNCTION OF PBI-$K_2Ti\ O_3$ COMPOSITION.

Gas retention characteristics were found to be slightly better than for the pure PBI pieces with no particular trend observed as a function of composition. The mechanical strength characteristics were improved by adding the spacing agent as one might expect.

Although the majority of the BNL funded effort has been directed towards an improved separator for 125 C operation, anode development efforts have been continued on a spare time basis. Eight pieces of specially coated 60 x 60 mesh conventional screens were prepared for evaluation by the MPD Technology Corporation (6) and evaluated in the minicell hardware. All the coated test pieces were superior to the uncoated screen, however, the best results were obtained with the lowest catalyzed powder loading, namely 20 mg/cm^2. The 110 mV improvement (373 ma/cm^2, 57 C) decreased in a roughly linear manner to only a 55 mV improvement at 110 mg/cm^2 catalyst loading. The simplified explanation for this behavior would appear to involve an increase in the reactants concentration polarization induced by the decrease in diffusional area as the electrode acquires more catalyst which more than counteracts the decrease in polarization resulting from the increase in electrode surface area. A preliminary evaluation of the polycrystalline nickel whisker deposits prepared at the University of Virginia onto the 60 x 60 mesh at 14 and 30 mg/cm^2 material loadings resulted in no noticeable improvement, possibly caused by the diffusional constraints of the 60 x 60 mesh support. The definition of the appropriate support structure will be completed prior to evaluation of the alternative anode electrocatalysts/surface modification systems.

The current six-month activity is centered on an extended test of the stability of the improved components at temperatures up to 125 C. Two minor modifications had to be made to the ARIES to minimize the shutdown problems encountered in the 1978-1980 test period. Essentially, the small electrolyte pumps associated electrolyte filters and flow switches were removed from the electrolyte loops, circulation of electrolyte being accomplished by the two-phase, gas bubble lift principle. The approach to the water addition sensing was changed to a liquid float, reed switch technique.

The test Module No. 20 consists of two series aligned cells of the same composition and 300 cm^2 active area. The cathodes are the C-AN catalyst coated 60 x 60 mesh screens prepared by BP personnel. The anodes selected for this evaluation are conventional,"uncatalyzed" porous nickel battery plaques. This selection was made for two reasons, the first being a lack of definition of support screen as just discussed, and the second the generally favorable time behavior of the battery plaque anode observed in Module 19 relative to both the conventional screen and an earlier version of the MPD coated anode. Although the 0-4 hour continuous operating data support a superior MPD coated anode, after 100 hours of continuous operation the plaque containing cells were superior by 40 mV (500 ma/cm^3, 100 C). The separators are 20 V/o PBI, 80 V/o K_2TiO_3 pieces, an initial thickness of 0.083 cm with an estimated density of 26.6%. The cell design should result in the separators compressed to 0.038 cm thickness for a density of 55.6%. Three separators, 33 x 33 cm, were prepared at TES with no significant problems noticed excluding a

compositional gradient across the thickness of the piece. The K_2TiO_3 rich phase has been located next to the cathode leaving the PBI rich phase abutting the porous plaque anode.

At the time of writing, Module No. 20 has been on test for 885 hours. The voltage-current density data for the test are presented in Figure 2 for the period after 310 hours of 75 C operation. The data were quite promising and significantly superior to the 1980 experiments with the pure PBI separators. A shift in input voltage requirements occurred during the 660-720 hour period of testing while the module continued to be operated at 100 C, this approximate 100 mV/cell loss not recovered during a 72-hour shutdown or during the subsequent operating temperature increase to 125 C. The voltage has been reasonably stable for 100 hours since the increase to 125 C and the stability of the technology will continue to be evaluated through the end of GFY 1982. Component dimensional and compositional analysis are anticipated to be performed with the results discussed in the technical final report.

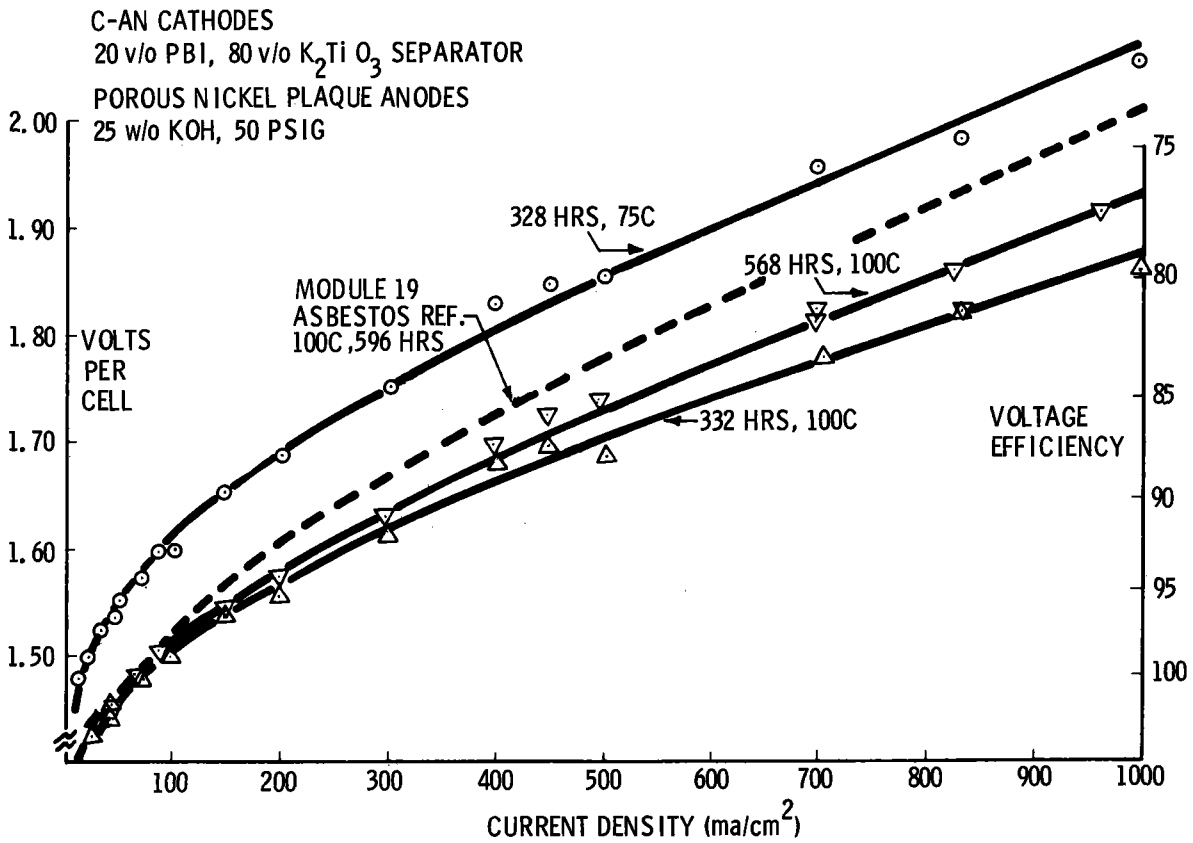

FIGURE 2. VOLT AMP DATA SETS ARIES MODULE 20.

With regard to further work on the cell components, the anode and a more defined specification for the structure as well as analysis of the at least two conflicting parameters of surface area and electrode poros-

ity obviously requires further attention. With proper support specification, the improvements via the new coatings such as the MPD or University of Virginia approaches with pure nickel or the perovskite coating systems as discussed by several authors would perhaps yield benefits commensurate with the additional costs. Testing a thinner (0.025 cm thick) version of the 20 V/o PBI, 80 V/o K_2TiO_3 would also appear warranted when reasonable stability is assured in the Module No. 20 test results and when the fabrication technique has been properly adjusted to result in a separator with better uniformity. Verification of the usefulness of the technology then should probably proceed first within ARIES and then be followed by a larger hardware unit probably involving the 1170 cm^2 cell area hardware.

ACKNOWLEDGMENTS

The experimental work was performed by Mr. C. W. Heusler. As in the past, this manuscript has been improved by the diligence of Ms. M. F. Gembarosky and the artwork is provided by Mr. L. W. Mickle under the supervision of Mr. F. E. Fahdt. The author again appreciates the gratis K_2TiO_3 fibers provided by the Otsuka Chemical Company, Ltd. as well as the cooperation of the several component fabricators and suppliers, including the BP Research Centre, the MPD Technology Corporation, the Celanese Fibers Corporation and the University of Virginia Department of Material Science Applied Electrochemistry Lab. The program is under BNL supervision by Messrs. M. Bonner and A. Mezzina with DOE guidance provided by Drs. M. Gurevich, R. Reeves, and J. Swisher.

REFERENCES

1. CONF 810940, Proceedings of the 6th Annual Thermal and Chemical Storage Contractor's Review Meeting, 14-16 September 1981, Washington, DC.

2. Brown, D. E., et al, "Low Overvoltage Electrocatalysts for Hydrogen Evolving Electrodes," Int. J. Hydrogen Energy, 7, No. 5, pp 405-410, May, 1982.

3. Gras, J. M., and J. J. LeCoz , "Asbestos Corrosion Study in Hot Caustic Potash Solution. Silicate Ions Influence on Electrode Overvoltages," Proceedings of the 2nd World Hydrogen Energy Conference, 21-24 August 1978, pp 255-277, Pergamon Press.

4. Vic, R. L., "Advanced Laboratory Electrolyzer (5kW) Testing," Proceedings of the 4th World Hydrogen Energy Conference, 13-17 June 1982, pp 129-140, Pergamon Press.

5. Prigent, M., and T. Nenner, "Anodic and Cathodic Catalysts for High Temperature High Current Density Alkaline-Water Electrolysis," ibid, pp 299-308.

6. Hall, D. E., "Catalysis of Oxygen Evolution Anodes with $Ni(OH)_2$," Abstract 454, Extended Abstracts, Vol. 82-1, The Electrochemical Society, Inc., Pennington, NJ 08534.

STATUS OF THE DEVELOPMENT OF SOLID POLYMER ELECTROLYTE WATER ELECTROLYSIS FOR LARGE SCALE HYDROGEN GENERATION

J.F. McElroy
General Electric Company
Electrochemical Energy Conversion Programs
Wilmington, Massachusetts 01887

ABSTRACT

During GFY 82, progress continued at General Electric in the development of Solid Polymer Electrolyte Water Electrolysis for Large Scale Hydrogen Generation. The joint Department of Energy, Electric Utility and General Electric Company sponsored program was aimed at performance improvement. A Technoeconomic Study was completed which quantified the cost of hydrogen from SPE water electrolyzers.

In parallel, an Electric Power Research Institute/Public Service Electric and Gas Program concentrated on developing a prototype 500 SCFH system for field evaluation. This system has undergone 2,000 hours of confirmation testing and has been delivered to Public Service Electric and Gas for field evaluation.

INTRODUCTION

The solid polymer electrolyte water electrolysis technology development for large-scale hydrogen generation began in 1975 with a design study for Brookhaven National Laboratory (BNL) and has progressed since then under the sponsorship of the Department of Energy (DOE), the New York State Energy Research and Development Authority (NYSERDA), the Niagara Mohawk Power Corporation (NMPC), the Empire State Electric Energy Research Corporation, the Gas Research Institute (GRI), and the General Electric Company.

The general goals of the program are to develop a water electrolysis technology capable of:

- High overall system efficiency: 85-90%
- Low capital cost: $\leqslant$\$150/kW (1980 dollars)
- Long life: 40,000 operating hours for the cells and 20 years for the system.

This program, encompassing scale-up to cell sizes of 2.5 and 10 ft^2, had progressed through GFY 81 to a point where:

- A 2000 SCFH SPE hydrogen generator system containing a 60-cell module of 2.5 ft^2 cells was successfully operated for greater than 700 hours, and
- 10 ft^2 cell and module design had been completed.

During GFY 1982, effort was continued toward performance improvement, primarily in the areas of improved water distribution and reduced cell impedance. The completed Technoeconomic Study showed that the cost of electric power was the single most important driver in the resultant cost of product hydrogen.

In 1979, a parallel program was started under sponsorship of the Electric Power Research Institute (EPRI) to develop a water electrolysis system for the generation of hydrogen for electric generator cooling. This system utilizes a 1 ft^2 cell appropriate to generation rates in the 100-500 SCFH range.

In 1981, a prototype 500 SCFH system was assembled and a 2,000 hour confirmation test was successfully completed in November, 1981 under the sponsorship of Public Service Electric and Gas. The system is currently being installed into the Sewaren Generating Station in New Jersey.

DISCUSSION OF CURRENT ACTIVITIES

Improved Water Distribution

As previously reported, in the original 2.5 ft^2 cell design, several local areas of membrane attack resulted from non-uniform water distribution. This poor distribution was caused primarily by incomplete forming of the flow field grooves on the oxygen side of the current collectors. In 1981, the 1 ft^2 cell design evolved. In that design preforming of the titanium foil prior to collector molding led to a significant improvement in the uniformity of the flow field. Testing of the 1 ft^2 design in 1981 and 1982 has confirmed the lack of local membrane attack due to flow field malformation caused water starvation.

In 1982 the preforming/molding process developed for the 1 ft^2 cell design was incorporated into the manufacturing process for the 2.5 ft^2 cells. The production run of 2.5 ft^2 current collectors displayed the same fine flow field groove definition that had been achieved in the 1 ft^2 hardware. These 2.5 ft^2 current collectors are currently being assembled into a six-cell module. Confirmation testing of these improved flow field collectors will be accomplished during the last part of 1982.

Reduced Cell Impedance

In 1981, optimized material compounding procedures were introduced into the current collector fabrication of the 1 ft^2 cell design. This resulted in a demonstrated 70 mV/cell improvement at 1000 ASF on a 20-cell module.

In 1982, the optimized material compounding procedures were incorporated into the 2.5 ft^2 collector manufacturing process. The previously mentioned 2.5 ft^2 collector production run incorporating the preformed foils also included the optimized material compounding procedures.

Long Term Life Testing

Endurance testing of 1/20 ft^2 laboratory cells has continued throughout the past year. Highlights of this testing are:

- Over 40,000 hours of operational evaluation has been achieved on a laboratory-size cell configured with porous titanium plate anode support and molded current collectors. (See Figure 1.)

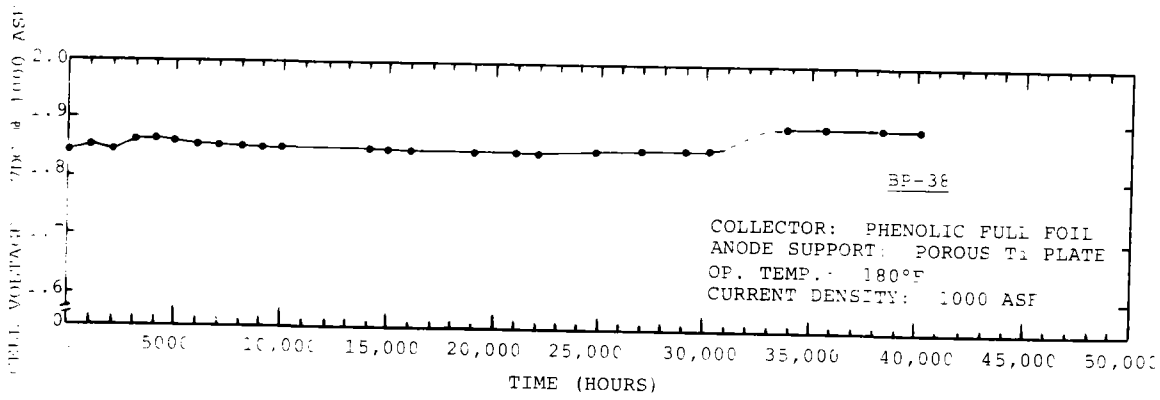

FIGURE 1

CELL PERFORMANCE - CARBON COLLECTOR CELL

- A laboratory-size, four-cell stack has accumulated over 21,000 hours of operational evaluation. The cells are configured with Kynar Fluorocarbon/graphite* current collectors, WE-3 anode catalyst, and porous plate anode supports.

Techno-Economic Study

As part of the 1982/1982 DOE program, a techno-economic study was performed to a) quantify the cost of hydrogen produced by SPE water electrolyzers as a function of design and operational parameters, b) establish the sensitivity of the hydrogen cost to the various parameters, and c) define the operating conditions for the optimum cost of hydrogen. From this study, projected hydrogen gas costs were shown to be relatively insensitive to plant cost. Figure 2 shows that a 3-fold plant cost increase impacts the cost of hydrogen by $< 8\%$. Conversely, variations in the cost of electric power have a very dramatic impact on the cost of hydrogen gas (Figure 3).

SUMMARY

The Technoeconomic Study has revealed that only second order cost of hydrogen improvements are likely through continued research and development. Therefore, the timing seems appropriate for a field demonstration of the large scale (2.5 ft^2 cells) system in an application where the current cost analyses are favorable. Supplementation of natural gas in Up-state New York appears to be one such application.

* Trade Name of Penn-Walt Corporation

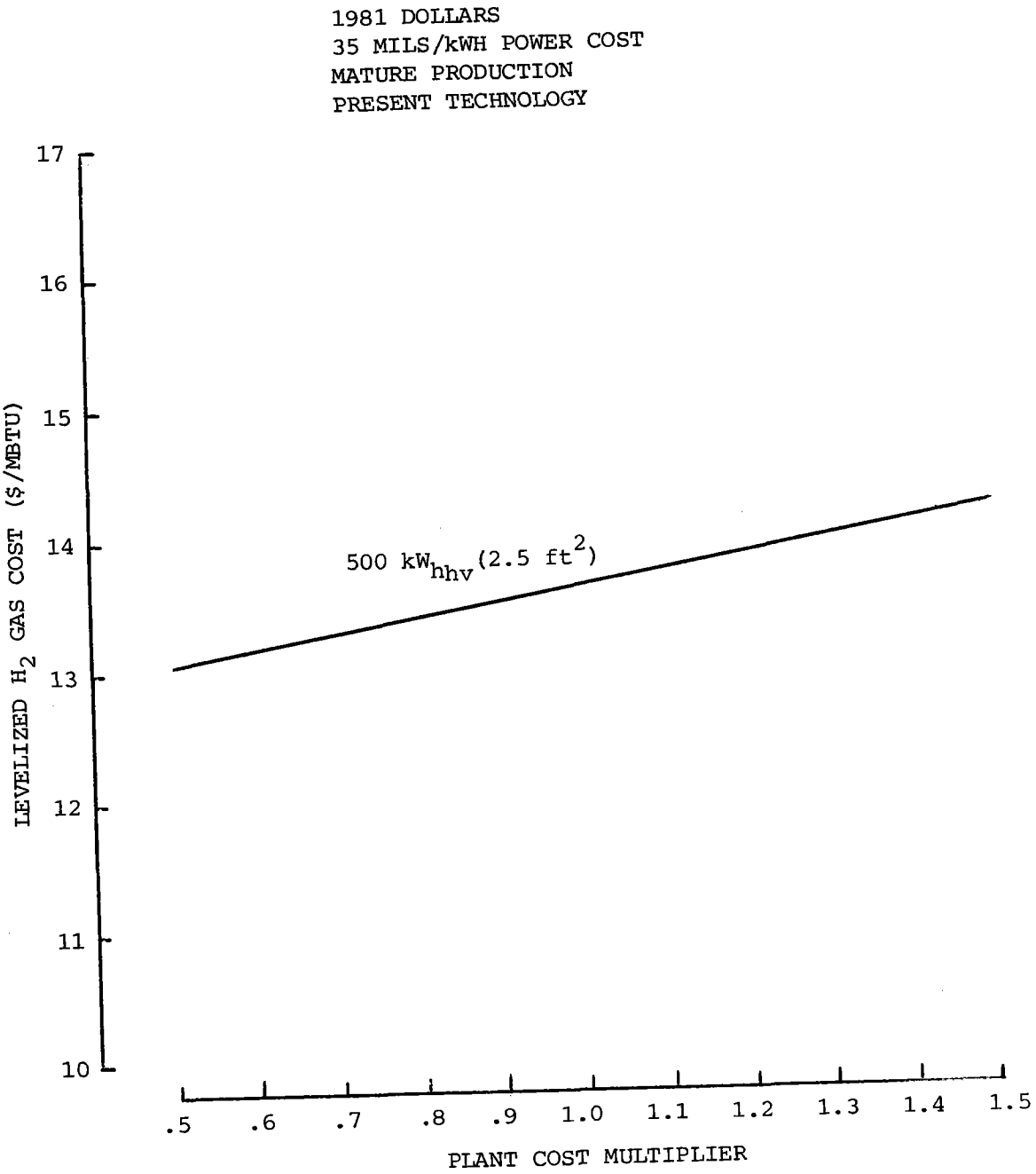

FIGURE 2

GAS COST VERSUS PLANT COST MULTIPLIER

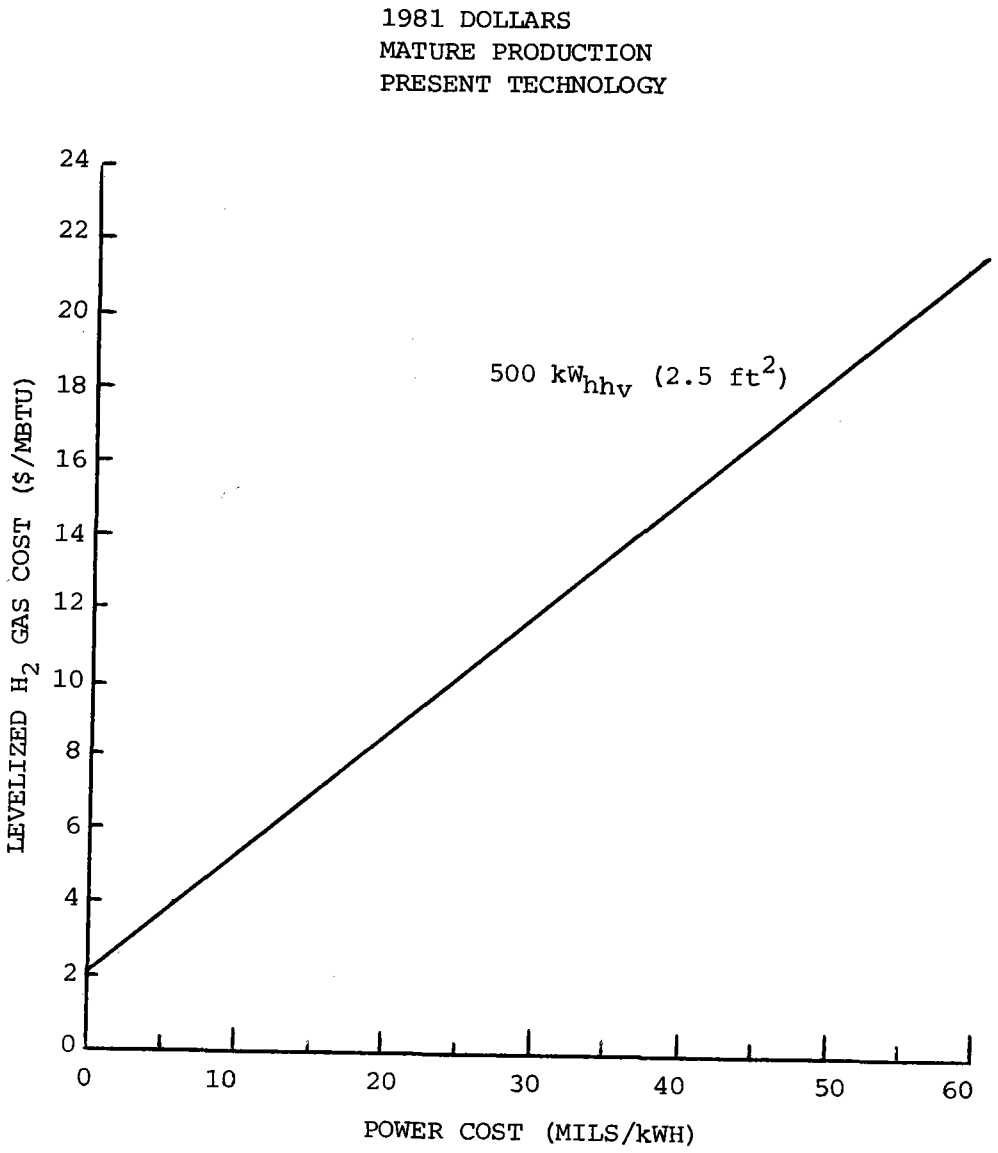

FIGURE 3

GAS COST VERSUS POWER COST

UNDERGROUND ENERGY STORAGE PROGRAM

Landis D. Kannberg
Pacific Northwest Laboratory*
PO Box 999
Richland, Washington 99352

INTRODUCTION

Rising prices and threatened shortages of natural gas and petroleum products are challenging U.S. industry with increasing urgency. Industry, particularly electric utilities, are confronted with the need not only to develop alternative energy sources, but also to find ways of using existing fuel supplies more efficiently.

Studies have shown that two concepts--Seasonal Thermal Energy Storage (STES) and Compressed Air Energy Storage (CAES)--are technically feasible and can offer significant cost savings under certain conditions for utilities, industry, and in some cases commercial building developers and operators. Both of these technologies contribute to the reduction in national consumption of petroleum resources and more efficient utilization of present electric generation capacity. It has been estimated that STES could reduce peak national demand for energy by as much as 7.5% if pursued aggressively. Estimates indicate that CAES could save up to 100 million barrels of oil annually by the year 2000 if vigorously implemented.

Early studies in both STES and CAES by DOE and others identified factors inhibiting entrepreneurial development of these technologies. For STES these factors included technical uncertainties associated with using underground formations, principally aquifers, for cost-effective storage of relatively low-grade thermal energy (both heat and chill). Economic uncertainties were also identified as contributors to hesitant development of STES systems. It was further recognized that currently identified systems would not be feasible in all locations and that new concepts for STES would be explored and developed if promising.

For conventional CAES systems, a key factor is the question of long-term underground reservoir stability. To provide the utilities with a high degree of confidence in the CAES concept, it was necessary to pursue a comprehensive technology research and development program on criteria and guidelines for CAES reservoir design. Another potential deterrent to CAES technology commercialization is the dependence of CAES plants on petroleum fuels. This factor could become a major barrier to large- scale implementation of CAES technology. Thus, it was deemed necessary to identify and examine second-generation CAES concepts, which are less reliant on petroleum fuel.

The Pacific Northwest Laboratory (PNL), operated for DOE by Battelle Memorial Institute, was selected to develop and manage programs in both STES and CAES. The organization of DOE-funded programs is shown in Figure 1.

*Operated for the U.S. Department of Energy by Battelle Memorial Institute under Contract no. DE-AC06-76RLO 1830

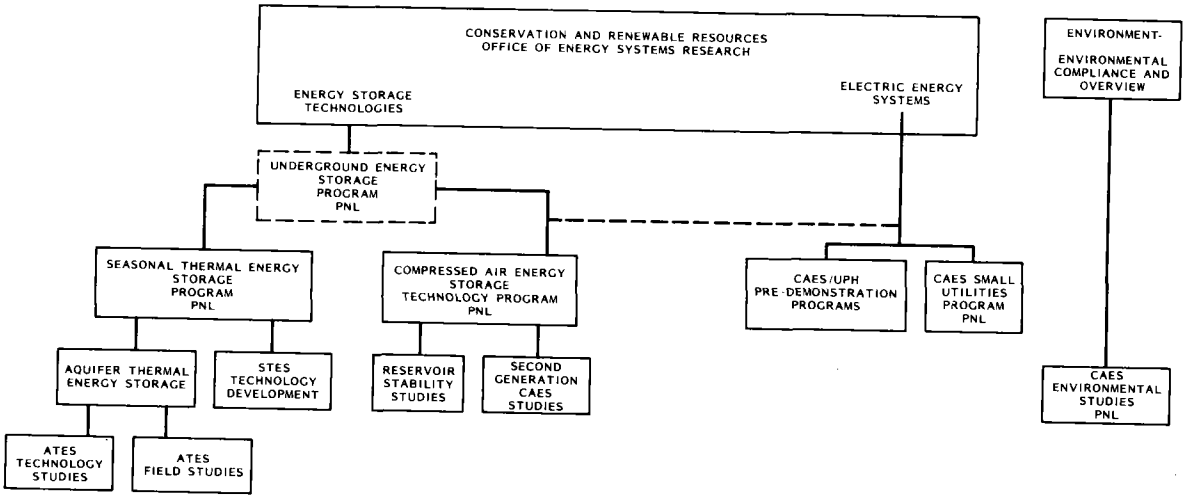

Figure 1. Department of Energy Programs to Pursue Development of Underground Energy Storage

GOAL AND OBJECTIVES

The ultimate goal of the UES Program is to reduce technical and economic uncertainties associated with underground energy storage technologies promising more effective, efficient, and economic utilization of energy resources such that entrepreneurial development is probable.

Pursuant to the principal factors identified as inhibiting entrepreneurial development, separate objectives were established for both STES and CAES. For STES, the objectives are:

- to establish guidelines and methods that improve feasibility and performance and permit the cost-effective appraisal of aquifer thermal energy storage (ATES) for utility, commercial or residential applications

- to screen and, as appropriate, develop promising STES concepts as alternatives to ATES. (This objective includes appraisal of technical, economic, institutional, and environmental issues.)

For CAES, the objectives are:

- to establish stability criteria for large underground air reservoirs in salt domes, hard rock, and porous rock formations that may be used for air storage in utility applications

- to develop advanced CAES technologies that would eliminate the dependence of CAES systems on petroleum fuels.

APPROACH AND STRUCTURE

The STES Program strategy, originally adopted for meeting the objectives identified above, involved development and proof-of-principal testing. Rapid development and implementation of ATES (the most promising STES technology) would be accomplished through small-

scale demonstration projects at sites suitable for eventual commercial development. Technology required to conduct these small-scale demonstration projects would be obtained in a companion effort involving numerical modeling, and laboratory and field testing. A less extensive effort was initiated to identify alternative STES concepts that did not require aquifers. This approach was aggressively pursued at PNL until budget rescissions in April 1981. At that time, FY 1981 funding was reduced; additional funding reductions were projected for FY 1982. In addition, DOE abandoned the approach of using small-scale demonstration type projects. The new favored approach was one in which only high technology, high risk, technical R&D would be performed.

Extensive changes were required in the STES Program as a result of these alterations in budget and direction. Two of the three small-scale ATES demonstration projects (Bethel, Alaska and Stony Brook, New York) were terminated; the third (St. Paul, Minnesota) was redirected toward conducting high-temperature tests. The ATES technology studies were also reduced in scope and funding. More emphasis was to be placed on development of high technology nonaquifer STES systems.

The CAES Program utilized different strategies for reservoir stability studies and second-generation studies. Numerical modeling, laboratory testing, and field testing (if required) would be conducted on an ever-narrowing range of technical issues until reasonable confidence in resulting stability criteria was obtained. Second-generation technologies would be subjected to feasibility analyses, cost analyses, and successive levels of engineering screening and development, as appropriate.

The CAES Program was not as extensively impacted in FY 1981 by budget cuts, or by redirection in FY 1981 and FY 1982, as was the STES Program. Activities in underground pumped hydro (UPH), previously managed by PNL, were terminated as a result of funding reductions in FY 1981 and FY 1982. Continued activities in numerical modeling studies for salt reservoir stability were terminated. Several studies of second-generation technologies were indefinitely postponed as a result of funding reductions.

As a result of these changes in the scope of activities, STES and CAES program efforts were consolidated into the UES Program as depicted in Figure 2. This structure retains STES and CAES Program entities under a single management and administrative center.

PROGRESS IN FY 1982

Significant progress toward program goals was accomplished in both STES and CAES in FY 1982. The major STES accomplishments during FY 1982 were:

- Draft numerical simulation model documentation including sample analyses was completed.
- Reports were issued on state-of-the-art of ATES simulation modeling and heat and mass transfer in unsaturated porous media.

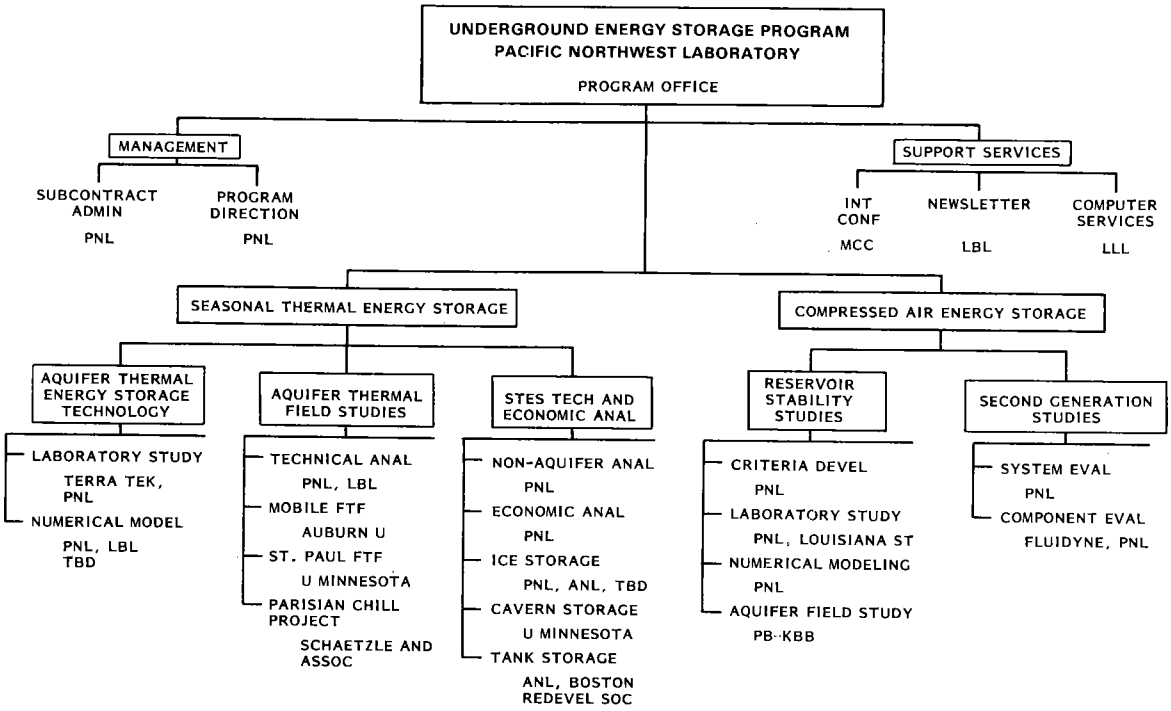

Figure 2. Underground Energy Storage Program Structure After Consolidation

- 82°C true doublet cycle test was completed as well as the injection and storage portions of the 82°C optimized cycle test at the Mobile, Alabama FTF site.
- Numerical model simulation/prediction was completed for both Mobile FTF tests.
- Program plans were completed for converting the St. Paul, Minnesota ATES demonstration project to a high-temperature FTF.
- Construction of all surface and subsurface systems was completed at the St. Paul, Minnesota FTF and initial tests of the system were conducted.
- Although the Stony Brook ATES Demonstration Project was terminated at the end of FY 1981, a reinjection well plugging problem discovered just prior to termination was resolved and corrected in FY 1982.
- The STES Aquifer Properties Test Facility was installed and operated at the St. Paul FTF.
- Development of the AQUASTOR code for simulating ATES cooling/heating systems was completed.
- Technical and economic assessment of six ice storage concepts was completed.

- One season of passive heat pipe ice generation and storage tests was completed at Argonne National Laboratory.

- A contract was awarded to the University of New Mexico to study chill augmentation of stored ice utilizing solar dried molecular sieves.

- The first international conference on underground energy storage, "Managing Energy through Energy Storage, Seasonal Thermal and Compressed Air Energy Storage" was conducted in October in Seattle. A second international conference on a similar theme is being planned for June 1983 in Stockholm, Sweden, by the Swedish Building Research Council.

Significant accomplishments in CAES during FY 1982 include:

- Mine testing of in-situ salt response was completed at the Cote Blanche mine and the CAES salt cavern stability criteria and guidelines were published.

- The CAES hard rock cavern stability criteria and guidelines were published.

- The porous media numerical models were applied to the Pittsfield Aquifer Field Test to assist design and predict performance.

- Combined effects testing of Pittsfield Aquifer Field Test core was conducted in the Porous Media Flow Facility to assess permeability response.

- The injection/withdrawal well and monitoring wells for the aquifer field test were drilled and completed.

- Instrumentation and surface facility design and construction were completed for the Pittsfield Aquifer Field Test.

- Assistance was provided in arranging the transfer of the Pittsfield Aquifer Field Test from DOE sponsorship to Electric Power Research Institute sponsorship.

- Thermomechanical and thermochemical cycling tests were completed on candidate CAES thermal energy storage (TES) materials (jointly supported by DOE and EPRI).

- An engineering assessment of candidate CAES/TES materials was prepared based on testing at PNL and FluiDyne Engineering Corporation.

- Characterization and documentation of the CAES thermodynamic cycle simulation numerical code was completed.

STATUS AND PROGNOSIS

Although there is considerable interest in STES technologies, particularly in Scandinavia, there has been little commercial interest.

Furthermore, technical issues related to geochemistry, long-term well field performance, and accurate predictions of system performance combine with institutional constraints to inhibit the development and implementation of STES technologies by the private sector. Continued research and development by Federal and State governments is essential if the enormous potential of this technology is to be realized. Resolution of the technical issues inhibiting private pursuit of STES technologies has been started and significant progress has been made. Unfortunately, Federal support for this technology is scheduled to end in September of 1983.

Conventional CAES continues to receive strong support by EPRI and at least one utility has awarded contracts for the design and construction of a 220-MW CAES plant in Illinois (Soyland Power Cooperative, Inc.). DOE goals in reservoir stability have been nearly realized with the completion of stability criteria and guidelines for salt and hard rock reservoirs. Efforts leading to the development of stability criteria and guidelines for porous rock reservoirs (notably aquifers) will be continued by EPRI. The development of second-generation CAES systems has moved marginally past the testing of some critical materials for use in CAES/TES components. Extensive long term and combined effects testing is still required before reduced scale, pilot plant design and construction can proceed on adiabatic and hybrid CAES systems. Although EPRI supported earlier studies of second-generation CAES systems including the material testing mentioned above, their current plans do not include near-term work on these systems. All Federal support for CAES research and development will end in September of 1982. It is likely that if current plans are not altered, development of second-generation CAES systems will be delayed at least 5 years.

CONCLUSIONS

Significant changes in the Underground Energy Storage Program were necessitated by budget reductions at DOE. Despite the reduction of major elements of the UES Program, substantial progress was made toward elimination of technical uncertainties inhibiting private sector development of UES technologies.

Significant advances were posted in Aquifer Thermal Energy Storage activities including numerical modeling, laboratory testing, and field testing at modestly elevated temperature water. New concepts were explored for nonaquifer systems including cavern storage and ice storage systems.

CAES reservoir stability studies concluded for salt and hard rock formations with the issuing of stability criteria and guidelines. A facility for testing the injection, storage, and recovery of elevated temperature air in sandstone reservoirs was constructed and plant operation is scheduled for October 1982. Studies of second-generation compressed air energy storage systems were wrapped up with the completion of material screening of thermal energy storage in adiabatic and hybrid plant designs.

Current plans call for the phase out of all Federally supported UES activities in FY 1983.

NUMERICAL MODELING OF AQUIFER THERMAL ENERGY STORAGE

C. F. Tsang and C. Doughty
Lawrence Berkeley Laboratory
University of California
Berkeley, California 94720

C. T. Kincaid
Pacific Northwest Laboratory
Richland, Washington 99352

Introduction

During 1981 and 1982, Auburn University has been performing a three-cycle ATES field experiment in Mobile County, Alabama. Details of the experiment are described elsewhere in this volume. Concurrent with the first two cycles (59°C and 82°C), Lawrence Berkeley Laboratory (LBL) did numerical simulations based on field operating conditions to predict the outcome of each cycle before its conclusion. Prior to the third cycle, a series of numerical simulations were made to aid in the design of an experiment that would yield the highest recovery factor possible.

First-Cycle Prediction

During the first cycle, 25,000 m^3 of water at an average temperature of 59°C was injected over a period of one month into a 21 m-thick aquifer. It was then stored for one month and subsequently produced. The injected water was obtained from a supply well perforated in the same aquifer 240 m away from the injection/production well. LBL was provided with the basic geological, well-test, injection flowrate, and injection temperature data, as well as the planned production flow rate.

The well-test data and geological information were studied and analyzed to obtain reservoir parameters and their range of uncertainty. The parameters used in our numerical simulation are listed in Table 1. Since the supply well is 240 m from the injection/production well and the thermal radius was calculated to extend only about 25 m, it was decided that a radial calculation mesh would be adequate. Based on the flow rates and injection temperature provided, we simulated the experiment using the numerical model PT (formerly called CCC) developed at LBL. The calculated production temperature is presented as curve A in Figure 1, where the experimental result is also plotted. The experimental results were made known to us after we completed and presented our results. The predicted energy recovery factor is 0.620 compared to the experimental value of 0.552. This agreement is satisfactory.

First Cycle: Detailed Comparison Between Theory and Experiment

Next, a series of parameter studies were made comparing the experimental and calculated temperature fields at various times during the first cycle. These studies led us to hypothesize that the aquifer is vertically stratified into three layers, the middle layer (5 m thick) having a permeability 2.5 times that of the upper and lower layers.

Using this model, the first-cycle recovery factor was calculated to be 0.579, calculated production temperature is shown as curve B in Figure 1. Apparently the layered structure of the aquifer noticeably lowers the recovery factor. This is significant because layering is difficult to detect through conventional well-test analysis.

Table 1. Parameters used in the first-cycle prediction numerical simulation.

Thermal conductivity	Aquifer	2.29 J/m.s.°C
	Aquitard	2.56 J/m.s.°C
Heat capacity of rock		1.81×10^6 J/m^3.°C
Aquifer horizontal permeability		63 darcies
Aquifer vertical to horizontal permeability ratio		1:7
Aquitard to aquifer permeability ratio		10^{-5}
Porosity	Aquifer	0.25
	Aquitard	0.35
Storativity	Aquifer	6×10^{-4}
	Aquitard	9×10^{-2}

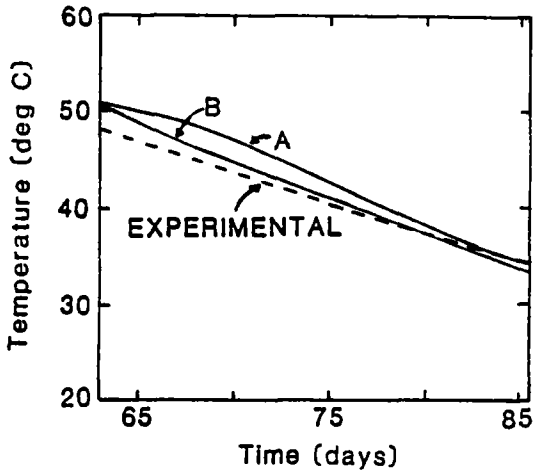

Figure 1. First-cycle Production Temperature.

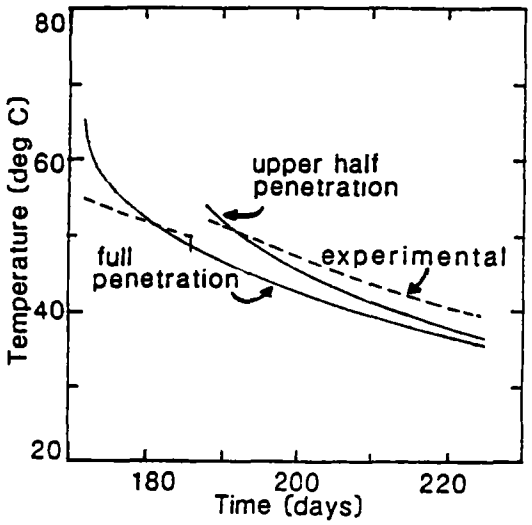

Figure 2. Second-cycle Production Temperature.

Second-Cycle Prediction

The procedure is similar to the first cycle prediction. Only the injection flow rate, temperature history, storage period, and expected average production flow rate were made known to us. The three-layered aquifer model described in the previous section was used for the calculation. Water at an average temperature of 82°C was injected over a period of about 4.5 months. The variable, experimental injection flow rates and temperatures were averaged into five segments for the numerical simulation. The total volume injected, about 58,000 m^3 was considerably larger than the volume injected during the first cycle; hence the thermal

radius extended farther than in the first cycle (to about 38 m). However, this distance is still small enough compared to the distance to the supply well to justify using a radial calculation mesh. After injection, the hot water was stored for 34 days.

The simulation of the original production plan--to produce all the injected water through the fully penetrating well screen that had been used throughout the experiment--was carried out, using a constant fluid flow rate of 200 gpm. The calculated recovery factor is 0.406 and the production temperature is shown in Figure 2.

However, this production plan was changed after two weeks of production. At that time the well was shut down and modified to produce fluid from only the upper half of the aquifer; then production was resumed. This scenario was again simulated using a constant flow rate of 200 gpm. The calculated recovery factor is 0.434; the production temperature is shown in Figure 2. After the second-cycle calculation was completed the experimental results were made known to us: the reovery factor is 0.452, the production temperature is shown in Figure 2. Comparisons between the experimental and calculated temperature fields in the aquifer throughout the second cycle show acceptable agreement.

Second-Cycle Optimization Studies

The recovery factor improvement of about 3% may have been small because the lower part of the modified well screen intersected the high-permeability layer of the aquifer and water may have been selectively produced from this cooler region rather than from the warmer upper region of the aquifer. In order to study the effects of different injection/production schemes, a series of numerical simulations based on the second cycle were run employing different well-screen intervals. Each simulation used a simplified injection history consisting of one constant injection flow rate and temperature. Table 2 summarizes the optimization simulations. Collectively, these results indicate that although buoyancy flow is strong in the aquifer, an improvement of almost 10% can be achieved by selective injection and production schemes.

Table 2. Second-Cycle Summary.

	Well-Screen Interval		
	Injection	Production	ε
Experiment	full	full for 2 weeks upper half thereafter	.452
Prediction	full	full	.406
	full	full for 2 weeks upper half thereafter	.434
Optimizations			
A	full	full	.407
B	full	upper 40%	.466
C	full	upper 20%	.496
D	lower half	upper half	.494
E	upper 20%	upper 20%	.504

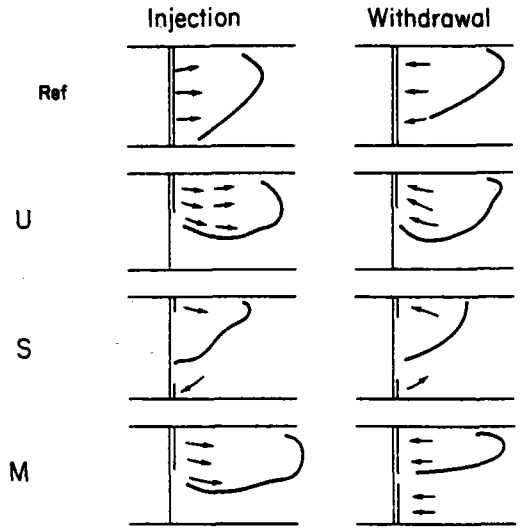

Figure 3. Schematic drawing of the flow fields during injection and withdrawal for the third-cycle design studies.

Third-Cycle Design Studies

Recent work involves assisting Auburn University in its planning for the third-cycle experiment. Alternative injection and production schemes have been studied to maximize the recovery factor for a three-month cycle with constant injection flow rate of 112 gpm and temperature of 82°C. Making use of the knowledge gained from the first- and second-cycle simulations, that buoyancy flow is strong, three approaches have been taken. These are shown schematically in Figure 3, along with a reference case that uses full penetration during injection and production. These three approaches are explained as follows:

1. Simply inject into and produce from the upper portion of the aquifer where most of the hot water would naturally flow because of buoyancy effects (labeled U).

2. Attempt to maintain a compact shape for the injected fluid. Buoyancy flow is counteracted by pumping from the bottom of the aquifer as hot water is injected into the top (labeled S).

3. Inject into the upper portion of the aquifer. Then, while producing from the upper portion, produce (and discard) colder water from the lower portion of the aquifer. Thus the colder water will not be pulled into the upper well where it would lower production temperature (labeled M).

Table 3 summarizes the results of the numerical simulations. For a cycle consisting of one month each of injection, storage, and production, the maximum recovery factor is about 0.52, representing an improvement of about 0.12 over the reference case. However, if the three-month cycle is altered so that two months of injection are followed immediately by one month of production (at twice the injection flow rate) hence doubling the storage volume, a recovery factor of about 0.66 is possible. Hence for this system, the volume of fluid injected is as important as the manner in which it is injected and produced.

Table 3. Third-Cycle Design Studies. T_1 = 82°C, Q = 112 gpm.

I. 1 month each, injection, storage, production V = 18,300 m^3

Case	Well Screen Interval		ε
	Injection	Production	
Ref.	Full	Full	0.404
U1	Upper 40%	Upper 40%	0.448
U2	Upper 40%	Upper 20%	0.501
S1	Upper 20% Lower 20%	Upper 20%	0.516
S2	Upper 20% Lower 20%	Upper 20% Lower 20%	0.487
M1	Upper 40%	Upper 40% Lower 55%	0.500
M2	Upper 40%	Upper 20% Lower 55%	0.521

II. 2 months injection, 1 month production. V = 36,600 m^3, $Q_p = 2Q_i$

U1-2	Upper 40%	Upper 40%	0.609
M1-2	Upper 40%	Upper 40% Lower 55%	0.629
M3-2	Upper 40%	Upper 40% Lower 20%	0.631
M4-2	Upper 40%	Upper 20% Lower 20%	0.661

Conclusion

The successful prediction of the first- and second-cycle energy recovery factors has demonstrated that the main physical processes occurring in the Mobile ATES field are probably well understood and can be properly simulated by the numerical model PT. The third-cycle design studies consider a substantial number of alternative injection/production schemes. Results have been transmitted to Auburn University for consideration in their decisions concerning the third-cycle experiment. This demonstrates the value of numerical modeling. If one were to experimentally carry out all the alternative designs, an order of magnitude increase in budget and time would be required.

Acknowledgements

This work was supported by the Assistant Secretary of Conservation and Solar Energy, Office of Advanced Conservation Technology, Division of Thermal and Mechanical Storage Systems of the U. S. Department of Energy under Contract DE-AC03-76SF00098. This report represents work performed within the Seasonal Thermal Energy Storage Program managed by Pacific Northwest Laboratory.

FIELD AND LABORATORY STUDIES OF SUB-SURFACE WATER INJECTION - SEASONAL THERMAL ENERGY STORAGE PROGRAM (STES)

L. B. Owen[1], S. C. Blair[2] and E. Peterson[1]
[1]Terra Tek Research, Salt Lake City, Utah
[2]Battelle, PNL, Richland, Washington

Introduction

Successful development of the Seasonal Thermal Energy Storage (STES) concept requires a capability to cyclically pump and reinject thermally altered water from subsurface reservoirs. Although subsurface water injection is a common practice, premature failure of injection wells frequently occur. Injection well impairment may result from any one of several mechanism including particulate plugging and scaling of subsurface formations. It is generally recognized that the key to successful injection well performance is careful monitoring of injected water properties and application of water conditioning steps, such as filtration or chemical treatment, when necessary. Quite often, insufficient baseline data on injected water and reservoir properties have been collected to allow an accurate diagnosis of impairment mechanisms after an injection well fails. Application of remedial or workover procedures to restore an impaired injection well is usually expensive with no guarantee of success. In most cases, it is cost effective to evaluate potential water injection problems prior to initiation of large scale injection operations. Pre-injection studies define potential problems and indicate the types of treatment facilities that may be needed to insure adequate performance.

The Seasonal Thermal Energy Storage (STES) project office at the Battelle, Pacific Northwest Laboratory has sponsored development of an Aquifer Properties Test Facility (APTF) to evaluate the effects of thermal cycling on reservoir properties. The APTF laboratory apparatus for testing aquifer materials at elevated temperature and pressure (Figure 1) is now being used to evaluate aquifer material from the University of Minnesota Field Test Facility (FTF).

Injection well impairment has been experienced at STES sites in Mobile, Alabama and Stony Brook, New York. Terra Tek Research, under contract to Battelle, PNL, performed a laboratory evaluation of impairment mechanisms that may have been involved in the failure of the injection well at the Stony Brook site. Terra Tek Research, again under contract to Battelle, PNL, designed, built and installed a portable Field Injectability Test Stand (FITS) at the STES Field Test Facility, University of Minnesota, St. Paul, Minnesota. The injectability apparatus uses membrane filters and core samples as injection formation analogs to evaluate the response of a representative porous matrix to injected water.

Aquifer Properties Test Facility

The APTF is a unique rock mechanics/fluid flow test system that was specifically designed and built by Terra Tek Systems to test rock cores and groundwater solutions under a wide range of conditions including those imposed by a STES facility. This system can monitor fluid flow through core samples under conditions of increased confining pressure,

Figure 1

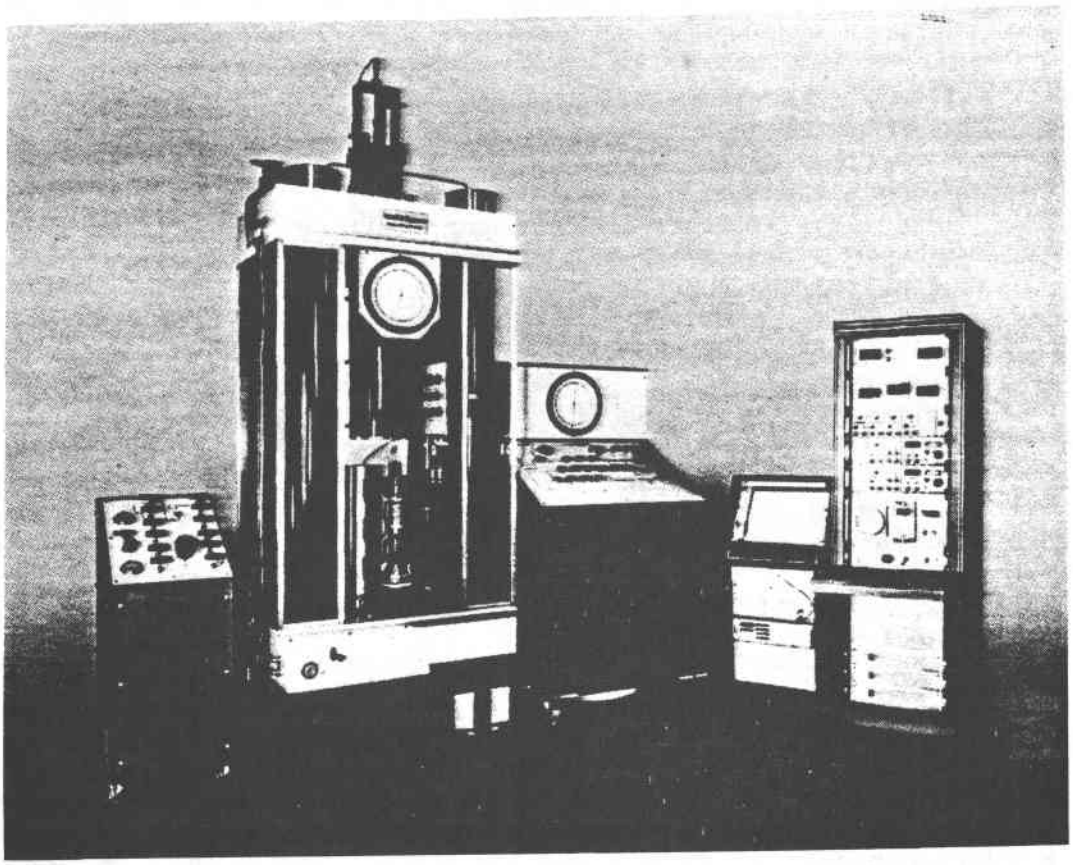

Acquifer Properties Test Facility, for evaluating reservoir properties at elevated temperature and pressure.

temperature, and axial load and is capable of reversed flow through a sample. The APTF has several features which make it a unique system for testing materials for thermal energy storage in aquifers. These include: 1) the ability to provide pressures to 15,000 psi and temperatures to 200°C on core samples as large as 2-1/8 in. diameter by 4 in. long, 2) construction of the permeability fluid loop from chemically unreactive metals in order to accommodate permeability fluids with typical groundwater composition (up to 10% w NaCl), and 3) a high resolution flow meter allowing measurement of flow rates as low as 0.05 ml/sec (±0.0005 gal/min). Fluid sampling ports and micropore filters have also been included in the permeability system so that permeability fluids can be sampled and/or filtered either upstream or downstream of the sample. This system can be used to execute long-term flow experiments (approximately 1 week) as permeability fluid is supplied from a heated 48 gallon tank.

Using the APTF, it is possible to quantify the hydrogeologic properties of aquifer rocks such as permeability and porosity, as well as monitor the geochemistry of pore fluids. In addition, this system can provide a complete suite of physical properties measurements including measurement of Young's modulus, compressibility, mean linear and thermal expansion coefficients, creep, fatigue, thermal spalling and disintegration. The capability for measuring both compressional and shear sonic velocity will be added soon.

The primary thrust of research being conducted on samples from the Minnesota Field Test Facility is to describe the behavior of host aquifer rocks and groundwater solutions under the conditions of increased temperature and pore pressure that will be imposed by the FTF. This research includes studies on each of the following topics: physical properties of the rocks, changes in pore fluid geochemistry after once through flow, particulate carryover, and aquifer characterization. Studies using rock material from the caprock (Franconia formation) and injection/production zones (Ironton formation) at the University of Minnesota STES site are now underway.

Stony Brook Injection Study

A laboratory evaluation of injection well impairment at the Stony Brook STES site was completed by Terra Tek Research. Two injection wells, PI-1 and PI-2, were completed in unconsolidated sands at the Stony Brook site. Well PI-1 was completed with a stainless steel liner, 12 inches in diameter. Well PI-2 was completed with a carbon steel liner, six inches in diameter. The wells were located 280 feet apart. Although well PI-1 performed satisfactorily, well PI-2 rapidly became impaired. Variations in injection reservoir properties were not believed to be a factor. Suggested impairment mechanisms for well PI-2 involved formation fines migration owing to high injection velocities and air entrainment. Corrosion products from the carbon steel liner may also have been a contributing factor. The laboratory study was designed to evaluate the suggested impairment mechanisms and to suggest possible remedial measures that might be employed in the field to improve well performance. Results of the laboratory study are summarized in Figures 2 to 5.

Hydraulic conductivity data for Stony Brook aquifer material and for clean Ottawa silica sand are plotted as a function of pumping flow rate in Figure 2. All conductivity values have been normalized to aid comparison of data and all flow rates are given in PI-2 equivalent values. Initial conductivity of each reservoir material was measured at 10 gpm then simulated pumping flow rates were systematically increased to a maximum value of 200 gpm. Aquifer injection conductivity values were measured at 10 gpm immediately after each increase in pumping rate and these data are shown in Figure 3.

Conductivity of clean Ottawa sand was essentially constant over the range of flow rates investigated while conductivity of the Aquifer sand decreased by 90% at the greatest flow rate. As evidenced by these data, the Ottawa sand matrix is stable at all flow rates but the Aquifer sand matrix changes as flow rates increase. Migration within the Aquifer matrix of flow mobilized particulates is the most likely mechanism for impaired hydraulic properties.

Also presented in Figure 2 are data for an air injection test performed on Aquifer sand. To separate air injection effects from particle migration phenomena, conductivity measurements for this test were performed at 10 gpm. The open and closed triangles seen in Figure 2 show, respectively, conductivity before and after air injection. Injection of air into the Aquifer sand resulted in a 5% loss of conductivity. Additionally, air injection data for clean Ottawa sand showed similar impairment at injection velocities up to 200 gpm.

Injection conductivity data presented in Figure 3 were measured immediately after each pumping increment shown in Figure 2. All injection measurements were performed at 10 gpm and are an indication of backflow recoverability of conductivity in the pumping-damaged Aquifer sand. Each injectivity data point is plotted as a function of the preceding increment of pumping rate.

Injection at 10 gpm results in nearly 100% recovery of conductivity in pumping-damaged Aquifer sand when damage was induced at pumping rates less than 50 gpm. When damage was produced by greater pumping flow rates, only partial recovery of conductivity is achieved with low flow rate backflow. Backflow induced recovery resulted in a final conductivity equal to about 60% of the initial undamaged value.

Figure 4 presents injection conductivity data measured at several systemmatically increasing flow rates. Measurements were performed on an Aquifer sand sample which had been damaged by pumping at 200 gpm. The conductivity value measured at the 200 gpm pumping rate is also shown on the plot of injection conductivity data (solid circle).

Increased injection rates result in significant decreases of conductivity. As injection flow rate approaches the pumping flowrate used to damage the sample, injection conductivity decreases to the original damaged conductivity value. Once particles have been mobilized and have damaged the aquifer matrix, reverse flow through the matrix will not restore original conductivity.

Figure 2

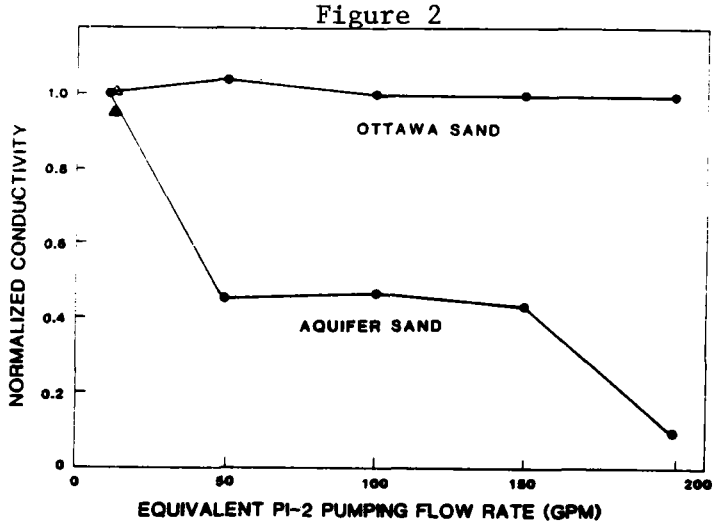

Effect of fluid velocity on the conductivity of clean Ottawa sand and Acquifer Sand. Each conductivity point on the Acquifer Sand curve was immediately followed by a reverse flow of 10 GPM to evaluate recovery - (Figure 3). The triangles indicate the effect of air injection on conductivity; open triangle indicates initial conductivity, solid triangle indicates about 6% decline in conductivity when air was injected with water at a velocity of 10 GPM.

Figure 3

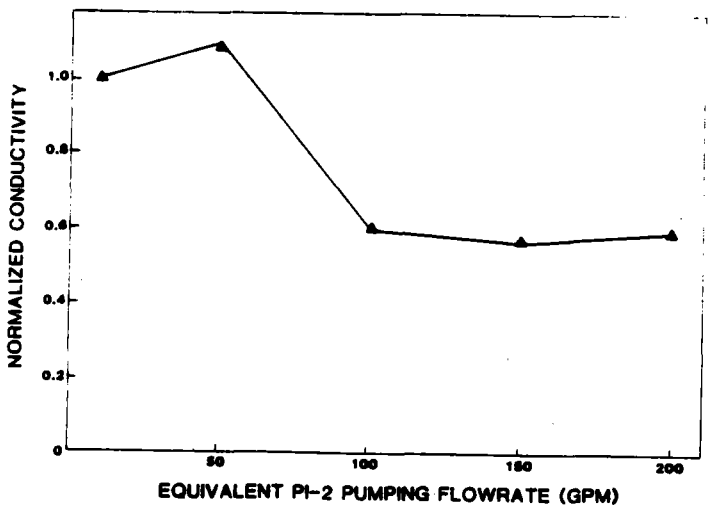

Recovery of conductivity in Acquifer Sand by injection at 10 GPM after pumping impairment at flow rates of 200 GPM. Pumping conductivity data are shown in Figure 2.

Figure 4

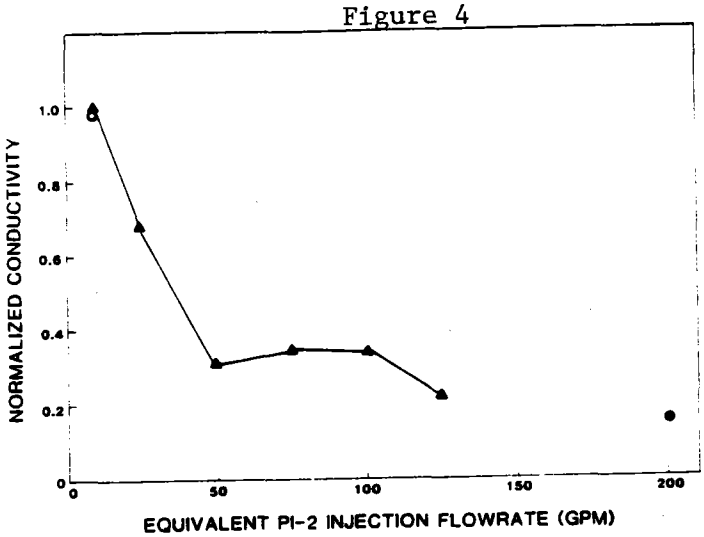

Effect of injection velocities on the conductivity of pre-damaged Acquifer Sand. The acquifer material was damaged by pumping at 200 GPM (solid circle). Recovery of conductivity at a pumping rate of 10 GMP was 60% (open circle). Increasing injection velocities cause rapid conductivity loss.

Figure 5

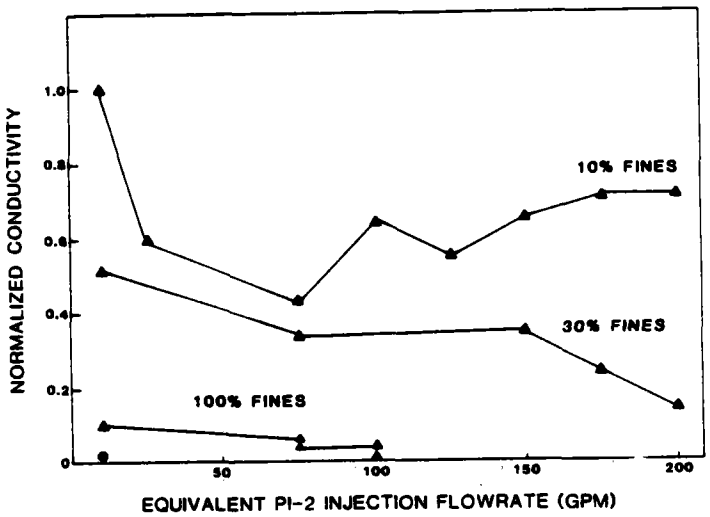

Effect of injection velocity on conductivity of clean acquifer material as a function of the content of dispersible fines in the gravel pack. The significance of the rust injection data point (solid circle) is discussed in the text.

Data presented in Figure 5 show the effects of dispersible Aquifer fines placed in the gravel pack and subsequently mobilized into the Aquifer sand. Aquifer sand used in this test was cleaned of fines by repeated washing in deionized water. Fines placed in the gravel pack were recovered from the decanted water used to wash the Aquifer sand.

Conductivity values measured in this test are flow rate-dependent and are qualitatively similar to those measured in normal Aquifer sand. As the mass of fines in the gravel pack increased, overall conductivity decreased and particle mobilizaton sensitivity to flow continued to persist.

Also included in Figure 5 is the conductivity value measured during the injection of rust. A suspension of rust was injected at 10 gpm into the gravel pack while conductivity was measured. The mass of rust injected was equivalent to approximately 3% of the fines and resulted in conductivity decreasing to 0.016.

The experimental evaluation suggests that impairment of Stony Brook injection well PI-2 was due primarily to mobilization of formation fines. Corrosion products from carbon steel completion liner may also have contributed to the premature failure of the well. Air injection was shown to be a negligible factor in failure of the well.

Field Injectability Test Stand

The injectability test stand is a laboratory or field device that is used to determine the injectability characteristics of fluid streams prior to subsurface disposal (Figure 6). Membrane filters and core samples are used as analogs of subsurface injection formations. Permeability of the analogs can be measured under the conditions of either constant flow or constant differential pressure. Two injection process streams may be monitored simultaneously. Reservoir analogs are maintained at process stream temperature by cylindrical ovens and solid state temperature controllers. Each test channel is equipped with extended range flow metering systems. Both flow channels are also equipped with selectable mini-high pressure, 1 micron pore size cartridge filters which permit evaluation of the effect of pre-filtration on fluid injectability. An on-board vacuum system is available to deaerate the system prior to runs.

The injectability test stand was installed at the University of Minnesota STES test facility in April of 1982. Initial test results indicated that fluid injectability decreased significantly as a function of increasing temperature. Subsequent analysis of filter cakes formed on 0.4 and 10 micron membrane filters indicated that permeability impairment was due primarily to deposition of calcite ($CaCO_3$). Membrane filtration test results are summarized in Figures 7 and 8. These results are consistent with geochemical models which predicted that calcite precipitation would occur when reserovir fluids were heated to temperatures in excess of about 18°C. A water conditioning system is now being installed at the University of Minnesota STES facility to control calcite precipitation. Prevention of calcite formation is essential both in maintaining

Figure 6

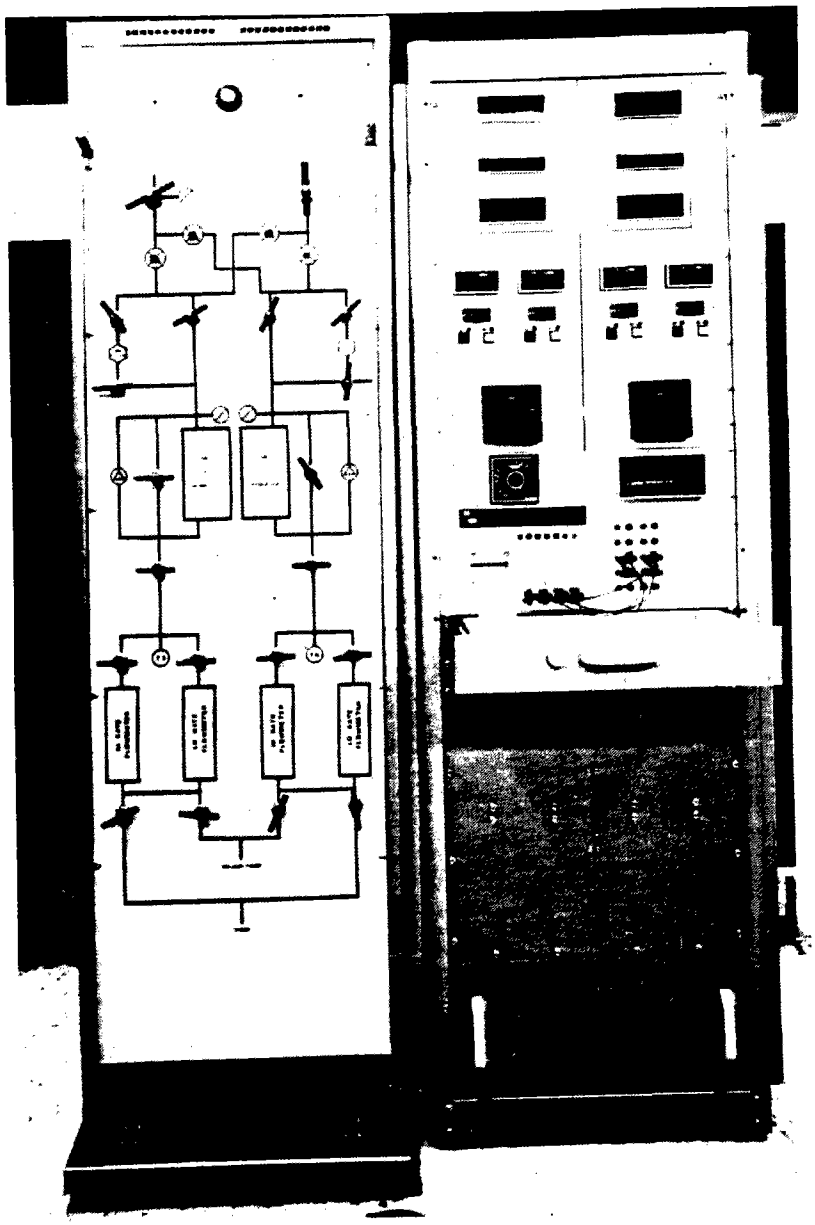

Field Injectability Test Stand

Figure 7

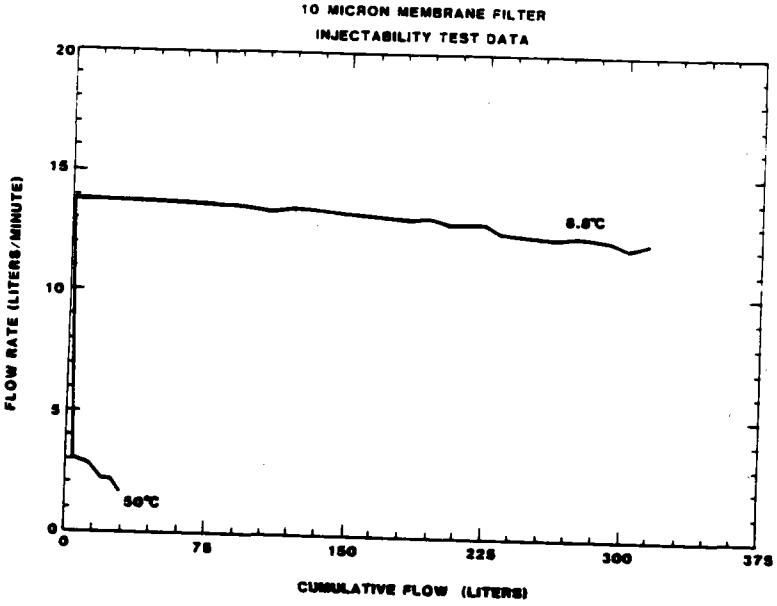

Figure 8

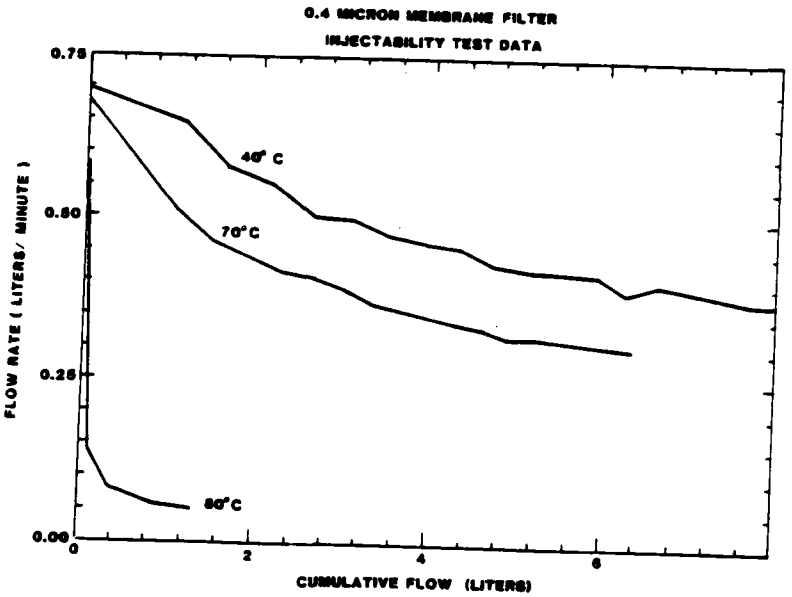

adequate injection well performance, and eliminating scale deposition in surface heat exchangers. Injectability test results also helped prevent premature failure of an injection pump. Several filter residues contained significant amounts of copper shavings. This observation led to the discovery of a defective bearing on one of the site pumps.

Acknowledgements

Dr. M. A. Hoyer of the Minnesota Geological Survey was particularly helpful in assisting with injectability equipment installation and operation at the University of Minnesota STES facility. Mr. T. Holm of the University of Minnesota provided field analytical chemistry support. Mr. W. Deutsch, University of Minnesota, and Mr. T. Holm carried out geochemical and modeling studies of reservoir fluids from the Minnesota STES site. Dr. I. Gyuk, DOE Project Office has been particularly supportive of this work.

MONITORING & ANALYSIS OF A CHILL STORAGE SYSTEM

W. J. Schaetzle* and C. E. Brett**
W. J. Schaetzle & Associates, Inc.
Box 1523
Tuscaloosa, AL 35403

ABSTRACT

Parisian, a major department store in University Mall, Tuscaloosa, Alabama, has a "free cooling" system installed to provide air-conditioning. The system uses a cooling tower during cold weather, below 47°F Wet bulb temperature, to chill water to an average 43°F. The cold water is stored in an unconfined aquifer and recovered as required for air-conditioning on an annual basis. This contract provides monitoring of this system to evaluate system performance.

Instrumentation for monitoring has been selected and is being installed. Water temperatures and integrated flow entering and leaving the air-conditioning cooling coils and the cooling tower are the prime measurements. Power input to all pumps and cooling tower is also measured. In addition, the temperatures leaving and entering the wells and near the bottom of the wells are measured at random intervals. The water levels in the wells are measured at similar times. Store and ambient data are also recorded.

The data is to be analyzed and the cooling performance of the system evaluated. Problems peculiar to this type system will be evaluated.

"FREE COOLING" SYSTEM

The "free cooling" used in this system allows the cold provided by nature in the cold weather period to provide the cooling required on an annual basis. During the cold weather periods, water is withdrawn from an aquifer and chilled in a cooling tower. The cold water is immediately returned to the aquifer, a natural underground porus volume filled with water. The aquifer provides a heat sink in both the water and the rock volume. The cold water is retrieved from the aquifer to meet the demand for air-conditioning. Standard water cooling coils are used to remove the energy from the air. The chiller or refrigeration cycle is completely eliminated. In addition, the normal power input of the chiller no longer needs to be dissipated in the cooling tower.

The operating energy is decreased by the normal power input to the chiller. In addition, the major power reduction occurs during peak hours thereby shaving peak load. Coefficients of performance for air-conditioning (not including the air handler) are expected to be in excess of ten.

*Also Professor of Mechanical Engineering, The University of Alabama, Tuscaloosa, Alabama.
**Also Director of Natural Resources Center, The University of Alabama, Tuscaloosa, Alabama.

DEPARTMENT STORE SUMMARY

Parisian is a major department store specializing in quality clothing and accessories. The management is open to new concepts in all areas. The recently constructed store in Tuscaloosa includes two inches of foam between the inner block wall and the brick outer wall providing a large thermal capacity. An economiser cycle uses cold external air for air-conditioning when outside air temperatures are low enough to permit it. The prime air-conditioning system will be the aquifer system. One hundred percent back-up air-conditioning is available.

The cooling system is designed so that on thermostat demand below 70°F outside ambient a large percentage of outside air is drawn into the building. If the thermostat is not satisfied, the aquifer system is initiated. If the thermostat still cannot be satisfied, the conventional air-conditioning system comes on line.

During winter months, water chilling is initiated at 47°F and below. This is calculated to produce water at an average of 43°F. Approximately 1400 hrs/year are available for chilling. The flow rate set for chilling is 400 gpm or double the normal flow for air-conditioning.

SYSTEM AQUIFER

The aquifer utilized for this project is unconfined and in a unit locally described as terrace deposits of Quaternary age. The terrace deposits lie directly on the Pottsville Formation of Pennsylvanian age. The Pottsville Formation was named for exposures near the town of Pottsville in the anthracite coal fields of eastern Pennsylvania. There are many Pottsville outcrops near the aquifer storage site.

The Pottsville Formation, which underlies the terrace deposits, is relatively impermeable and acts as a barrier to the vertical migration of groundwater in the project area. The aquifer perches on top of the Pottsville Formation and remains relatively stable throughout the year with some seasonal variation in the water table height.

Upper parts of the terrace and alluvial deposits generally consist of clay and silt beds which have weathered to a reddish-brown color in the higher terraces but which are gray in other places. The terrace deposits are commonly less than 50 ft. thick; however, at the storage site the terrace thickness exceeds 80 ft. In samples taken from the wells at the Parisian site there is an abrupt change in lithology at approximately 30 ft. in depth. The upper sediments have high concentrations of clay and are heavily stained with iron; the lower sediments are relatively free from clay and have high concentrations of sand and gravel. The gravel content increases downward until the deposits are nearly pure gravel 10-15 ft. above the Pottsville Formation.

FIGURE 1

GEOLOGICAL LOG
Well Number 4 - Parisian
August 1, 1980

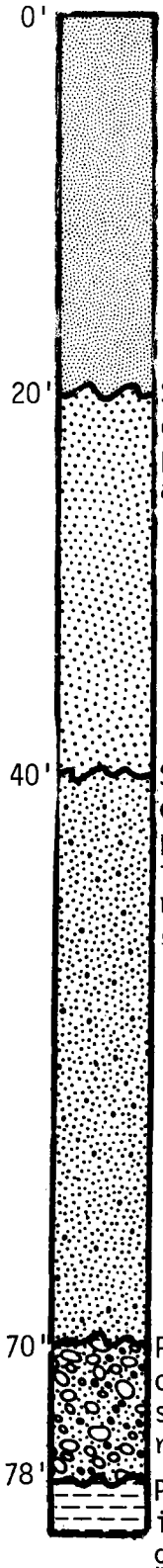

TABLE 1. Driller's Log
Well Number 4 - Parisian
August 1, 1980

0- 1	ft	Black Top Soil
1- 7	ft	Brown Sandy Clay
7- 8	ft	Blue Sandy Clay
8-10	ft	Clay with Pea Gravel
11-13	ft	Tan Clay with Pea Gravel
13-23	ft	Tan Clay with Blue Clay
23-25	ft	Fine Light Tan Sandy Clay
25-30	ft	Light Tan Sand
30-46	ft	Medium to Coarse Sand
46-55	ft	Coarse Tan Sand
55-60	ft	Coarse and Fine Tan Sand
60-62	ft	Fine Tan Sand
62-73	ft	Coarse Tan Sand
73	ft	Rock

A stratigraphic column of the aquifer is shown in Figure 1. A more detailed drillers log is shown in Table 1. A geological survey on the well samples was made to determine primarily sand sizes. This survey result did not note any clay in the samples.

MONITORING INSTRUMENTATION

Figure 2 shows an outline of the store, the aquifer cooling system and monitoring instrumentation. The data is broken into two categories. Some data is monitored every 30 minutes by a Parisian heating and cooling system computer in Birmingham and recorded every two hours. In addition, some data is read manually (normally once a day). Integrated water flow rates are recorded continuously with flow probes and counters.

The resistance thermometers "T_r" for water entering and leaving each side of the building for the air-conditioning water coils, on each side of the cooling tower, and ambient temperature "T_a" are recorded by the computer each half hour. The computer also notes whether the various motors,

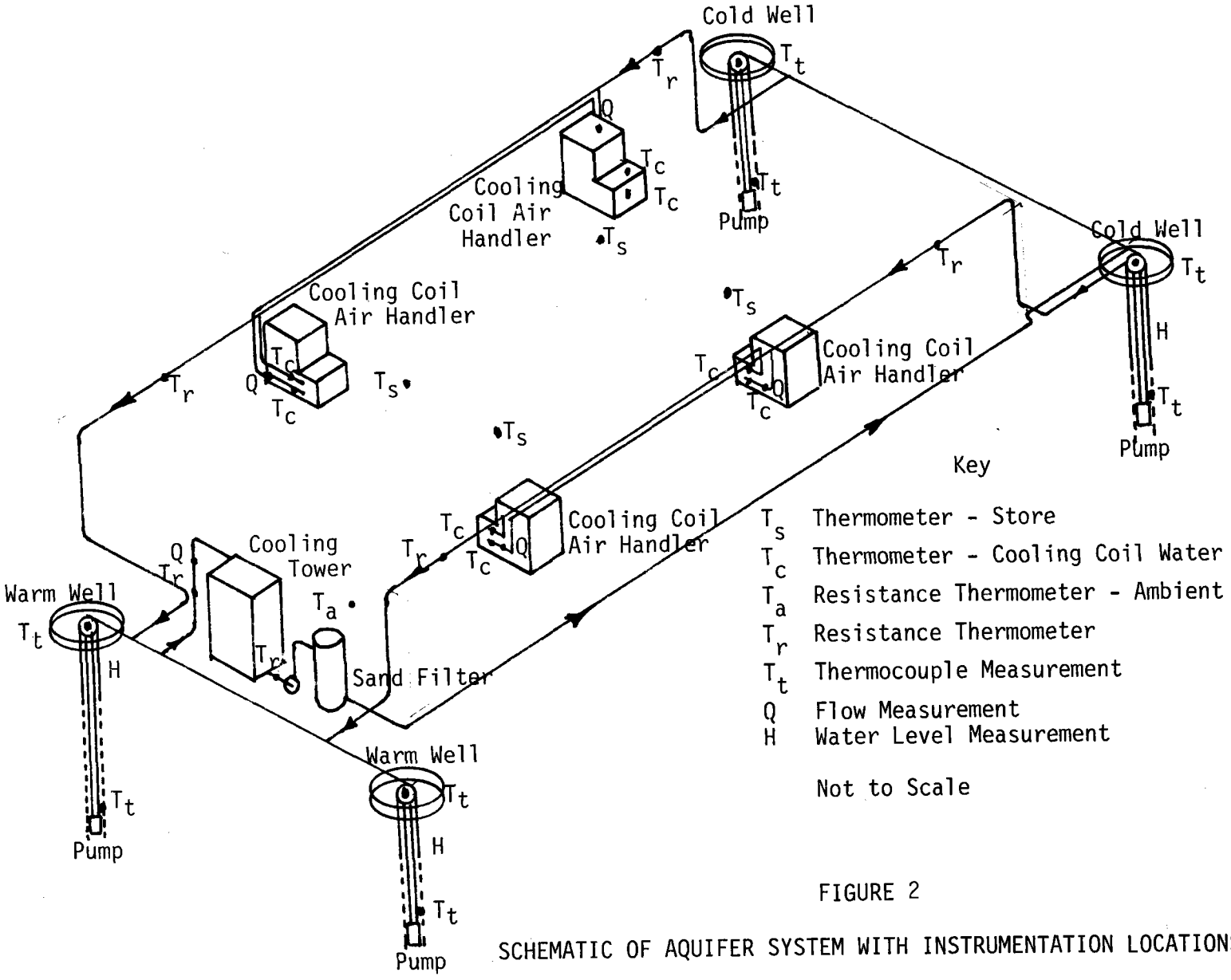

FIGURE 2

SCHEMATIC OF AQUIFER SYSTEM WITH INSTRUMENTATION LOCATIONS

pumps, cooling tower, etc. are on or off each half hour. Water levels are measured by pressure gages.

In addition, thermometers in thermometer wells are installed at the inlet and outlet of each water cooling coil and inlet and outlet of the cooling tower to back up and calibrate the computer read system. Thermometers are also located at four locations in the store. Input energy is determined by multiplying the number of hours of operation of the motor times the power input measured by a watt meter during standard operation.

Each well, Figure 2, has inlet or outlet temperature, temperature at the bottom of the well and water level height manually read (normally once a day). Due to the location of these temperatures, thermocouples are used for the measurement.

PRESENT STATUS

All instrumentation has not been installed at the time this paper is being written but it is expected to be installed by the time of the contractors meeting. Computer output exist back into 1981; however, much of the data is questionable. Present output is being compiled and analyzed. Back data is being organized and studied.

OPERATION OF THE SYSTEM

Water chilling began as the temperature dropped in October 1981 and continued through to Spring 1982 whenever wet bulb temperature was below 47°F. Due to well overflowing on injection and a frozen pipe, part of December 1981 and most of January 1982 were lost. Leaking valves at the cooling coils allowed warm water to pass through the building to the cold wells, bypassing the cooling tower. As a result, the water stored was at a much higher temperature than calculated. Still, over ten million gallons (possibly as much as twenty million gallons) of cold water were stored. It is believed that these problems will be corrected by the coming water chilling period.

For air-conditioning in February, March, and April 1982, the aquifer provided most of the air-conditioning and kept the store below 70°F. Water flow rates and cooling water temperatures were too high and therefore the stored energy was used during this period.

Since then, water temperatures of 64°F to 67°F have been carrying a base load of 40 tons of air-conditioning at a COP of around 10. For the period June 16 to July 15, 1982, the system provided 193×10^6 Btus of cooling for a power input of 23.8×10^6 Btus (6.98×10^3 Kwhr) and a water flow of 4.46×10^6 gallons. Also, maintenance has been much less on the aquifer system than the conventional back-up system.

During the next chilling season, approximately two and one-half to three times as much chilled water will be stored. This should be sufficient for a season's cooling and give an annual COP in excess of fifteen. Nature provides the chilling and the storage.

UNIVERSITY OF MINNESOTA AQUIFER THERMAL ENERGY STORAGE FIELD TEST FACILITY

Matt Walton and Marcus C. Hoyer
Minnesota Geological Survey
University of Minnesota
1633 Eustis Street
St. Paul, Minnesota 55108

ABSTRACT

The University of Minnesota Aquifer Thermal Energy Storage (ATES) Field Test Facility became operational. Experiments demonstrated that the Franconia-Ironton-Galesville aquifer will accept injection of 300 gpm (18.9 l sec^{-1}) at reasonable pressures with a head buildup in the injection well of about 44 psi (31.6 m) over 8 days. Heating of the ground water caused precipitation of carbonate in the piping and injection well, but with proper water conditioning, the system will work satisfactorily at elevated temperatures.

INTRODUCTION

The University of Minnesota Aquifer Thermal Energy Storage (ATES) Field Test Facility is being constructed to gather basic hydrogeological, hydrogeochemical, and hydrogeothermal information to assess the feasibility of using the Franconia-Ironton-Galesville (FIG) aquifer beneath the Twin Cities as a storage medium for heated water. Conceptual design and monitor array were described in detail in the Proceedings of the 1980 and 1981 Contractors' Review volumes.

The facility is a nominal 5-megawatt thermal input/output ATES system using a supply and storage well doublet with a spacing of 255 meters (836 ft). The system is designed for operation at 300 gpm (18.9 l sec^{-1}), a delta T of 66°C, and maximum temperature of 150°C (302°F). It is located near the center of the wide, shallow, multiple-aquifer Twin Cities artesian basin. At the test site the FIG aquifer is about 63 m (207 ft) thick, and lies at depths of 172 to 181 m (564 to 593 ft). Head above the aquifer top is about 125 m (410 ft). Monitor wells are spaced 7 m (23 ft) and 14 m (46 ft) around the heat storage well (well A).

Well A was completed and step-drawdown tests were conducted in October 1981. Construction of the above-ground connections continued and was essentially completed. The Field Injectivity Test Stand, built by TerraTek for Battelle PNL, was delivered, installed, and operated successfully using three sampling points in the system. Testing of the heat exchangers and above-ground monitoring system began in March 1982. Pressure transducers for monitor wells arrived and were tested; the 15 (of 22) which worked were installed. Monitor points without transducers were measured manually.

A 4.5-day pump test on well A (February-March 1982) and a 24-hour pump test on well B (May 1982) were conducted prior to the beginning of water injection. Water samples were taken from the monitor well points and from the pumping wells. Injection tests of ground water at ambient

temperature and the first heated-water injection test were attempted with the available monitor array. Calibration of flow and thermal models, experiments using aquifer water on rock samples, and calculation of chemical equilibria at various temperatures continued through the year.

AQUIFER TEST RESULTS

A 9-day aquifer test was conducted using well A, which was pumped for 4.5 days at an average rate of 340 gpm (21.4 l sec^{-1}).

The FIG aquifer has two hydrologic zones which have been screened in wells A and B. Analysis of the test results indicates that the upper Franconia portion has a transmissivity of 365 ft^2/d (3.9 x 10^{-4} m^2 sec^{-1}) and that the Ironton-Galesville portion has a transmissivity of 690 ft^2/d (7.4 x 10^{-4} m^2 sec^{-1}). Total transmissivity for the layered FIG aquifer yielded 1,055 ft^2/d (1.1 x 10^{-3} m^2 sec^{-1}).

Modeling results show significant, but small, differences from the observed drawdown data. Modifying input parameters continues in order to match the observed results more closely. Anisotropy within the aquifer accounts for some deviations from the modeling result.

INJECTION-CYCLE TEST RESULTS

Two ambient-temperature ground-water injection cycles (hereafter referred to as cold-injection cycles) and one heated ground-water injection cycle were started. Only the second of the cold-injection cycles ran successfully for the planned eight days. Clogging problems curtailed the other test cycles.

The first cold-injection cycle was run using the system as the design engineer had proposed; i.e. the water was introduced to injection well A through the annular space between the column pipe and the outer casing. For the first 24 hours of this test, well B was pumped at 350 gpm (22.1 l sec^{-1}) and water was introduced at well A at a rate of 125 gpm (7.9 l sec^{-1}). Excess flow was discharged to a nearby storm sewer. Flow was then increased into well A over a 30-minute period to 300 gpm (18.9 l sec^{-1}) and the pumping rate of well B was adjusted to an equal rate. This test was terminated after 6.7 hours because of the rate of head buildup in well A (Fig. 1, A-A'), apparently caused by clogging of the aquifer due to air entrainment. Air entrainment occurred because it was impossible to maintain positive pressure on the water entering the annular space of the well. Water supplied for injection had a dissolved oxygen (DO) level of <0.1 ppm and a turbidity value of 0.15 NTU.

Well A was immediately pumped to redevelop it. Pumping at increasing rates continued for 19 hours (Fig. 2). Initial water pumped out was very turbid and frothy. DO levels were >12 ppm and turbidity levels were as much as 163 NTU. DO and turbidity at the cessation of

pumping were <0.5 ppm and 0.29 NTU respectively.

Following an 18.5-hour shutdown and a 30-minute flushing of well A, a second cold-injection cycle began with the water introduced through the column pipe of well A. The column pipe was a completely water-filled system and no air-clogging resulted. This resulted in a completely successful 8-day test (Fig. 1, B-B'). The average injection rate for the 8 days was 295 gpm (18.6 l sec^{-1}). Head build up in well A appeared to approach an equilibrium at about 31.6 meters (44 psi).

According to the plans for the first hot-injection cycle, ambient water was injected for two days to allow comparison with the previously run cold-injection test (Fig. 1, C-C'). At the appointed time, steam was introduced to the heat exchanger heating the aquifer water to 85°C (185°F). Approximately 45 minutes was required to stabilize the steam side of the system. The head dropped immediately by 5 m (7 psi) in the injection well as a result of the decrease in kinematic viscosity of the water from 0.013 to 0.003 stoke as the water was heated by 73°C (Figs. 1 and 3). Approximately 9.3 hours later, a power outage at supply well B required that the steam be shut off and the system be restarted. The spike on Figures 1 and 3 shows clearly the drop in head when injection stopped, and also the resumption of injection about 50 minutes later. From this point on to the conclusion of the test the injection temperature was about 82°C (180°F) and the flow rate approximately 295 gpm (18.6 l sec^{-1}).

Pumping continued until it was clear that clogging was taking place in well A (Figs. 1 and 3). The constant and increasing rate of head buildup in well A, along with the relative head changes in the Ironton-Galesville and the upper Franconia portions of the aquifer suggested that a) the Ironton-Galesville was clogging first, and b) the clogging rate was increasing. Differential pressures across the condenser increased during the heated-water cycle as well, suggesting that precipitation of solids was taking place as the water was heated. Upon shutdown, the injection well recovered rapidly to a head slightly higher than before the test, suggesting that the Ironton-Galesville screen is more clogged than the upper Franconia screen.

Thermocouples at the Ironton-Galesville level of the aquifer in wells nominally 7 meters from the injection well indicated a temperature rise beginning 17 hours after heated-water injection began and climbing to 46°C (115°F) over an 11-hour period at the 744-foot level in well AS1. Only thermocouples in the Ironton-Galesville portion of the aquifer showed a temperature rise during injection.

Attempts to pump well A following shutdown were unsuccessful because bearings on the pump shaft did not work properly when hot. The pump bearings proved to be of the wrong materials and are being replaced. A thermal profile and a television inspection of well A both show that the upper screen in well A is relatively clear, but the lower screen is clogged. The screen in well A will be cleaned before well A is pumped.

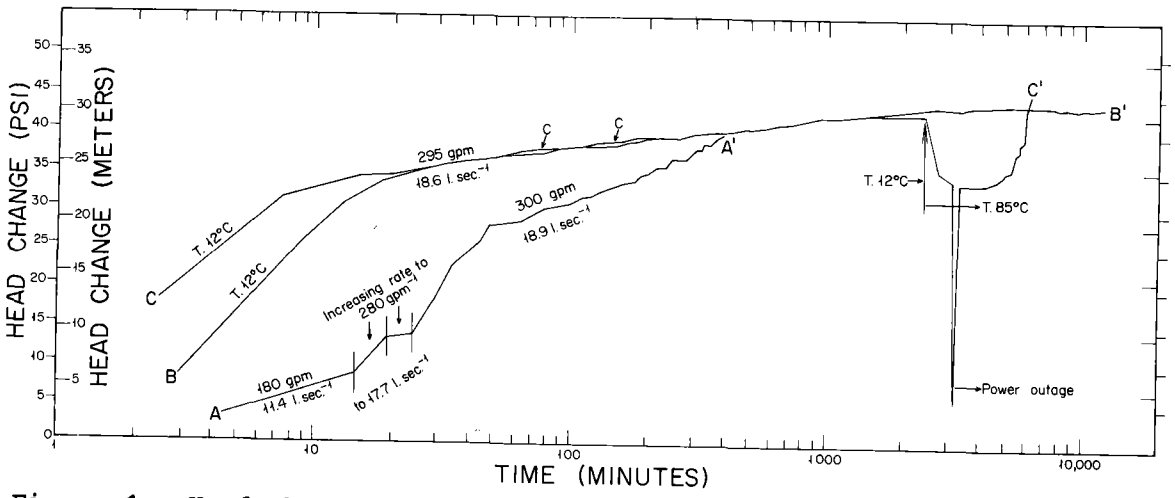

Figure 1. Head changes as a function of time during injection. A-A' -- ambient (12°C) water introduced through annular space (line A-A' begins 24 hours after start of injection.); B-B' -- ambient water introduced through column pipe; C-C' -- ambient water followed by 82-85°C water introduced through column pipe.

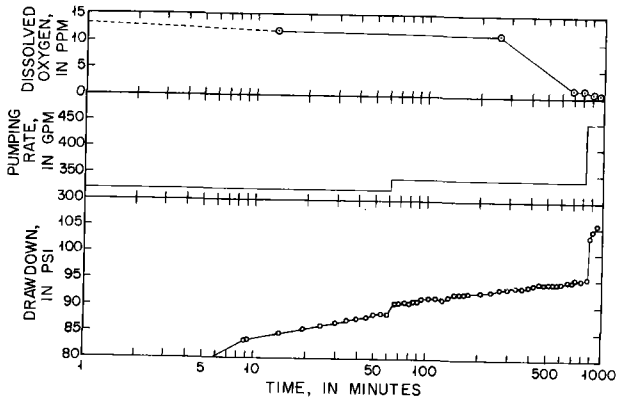

Figure 2. Comparison of drawdown, pumping rate, and dissolved oxygen content during rehabilitation of well A.

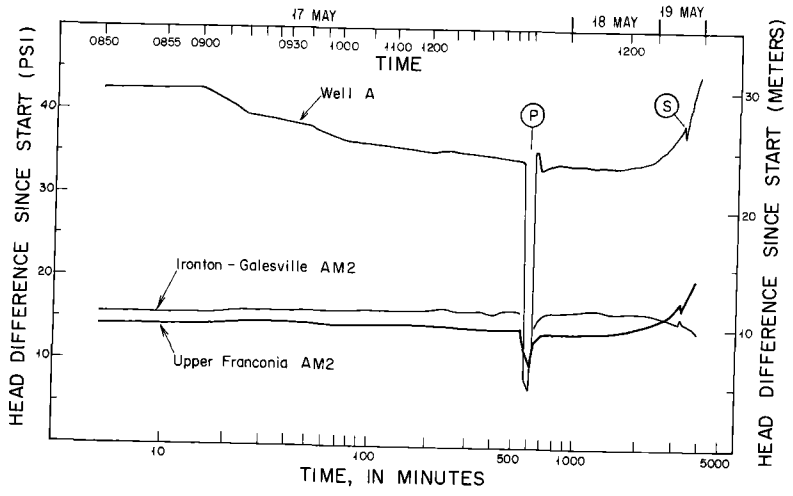

Figure 3. Head changes measured during hot-water injection cycle in well A and well AM2 located 14 meters from well A. P, power outage which interrupted injection; S, steam problem which temporarily lowered temperature of injected water.

WATER ANALYSES AND CHEMICAL MODELING

The ambient ground water is saturated in calcium carbonate; increasing the temperature to 80°C decreases solubility by an order of magnitude. A typical analysis of water from well B was:

pH	7.46	Cl^- (μM)	37.8	Na^+ (mM)	0.21
Eh (mv)	+108	F^- (μM)	11.9	Fe_{tot} (μM)	15.5
SC (mmho cm^{-1})	0.352	NO_3^{-2} (μM)	1.3	Mn_{tot} (μM)	ND
DO (mg l^{-1})	0.6	SiO_2 (μM)	104.3	Hardness (mM)	2.11
NH_3 (mg l^{-1})	ND	Ca^{+2} (mM)	1.37	Oil and Grease (mg l^{-1})	ND
Alkalinity (mM)	4.63	Mg^{+2} (mM)	0.81	TDS (mg l^{-1})	216.2
SO_4^{-2} (μM)	52.8	K^+ (mM)	0.014		

Note: ND not detected

Precipitation of carbonate as $CaCO_3$ and also probably $CaMg(CO_3)_2$ is the principal cause of clogging during heated-water injection. Hot water collected during injection was supersaturated in Ca^{+2} and Mg^{+2}. In experiments using FIG aquifer water and portions of the rock core 75 percent of the Ca^{+2} and Mg^{+2} were removed from solution upon heating. This result agrees with modeling of the rock-water system. Removal of the calcium and magnesium by softening will be necessary for operation at design temperatures. Further testing is planned following installation of the water conditioning system.

Modeling and experiments both suggest that dissolved SiO_2, in whatever form, will not become a problem for a very long time (hundreds of injection/withdrawal cycles).

SUMMARY

Experiments demonstrated that the Franconia-Ironton-Galesville aquifer will accept injection of 300 gpm (18.9 l sec^{-1}) at reasonable pressures with a head buildup in the injection well of about 44 psi (31.6 m). Heating of the ground water caused precipitation of carbonate in the piping and injection well.

Following a long-term pump test of both wells and the testing of the steam side of the system and the Field Injectivity Test Stand on the site, injection tests began. These tests continued until clogging became apparent. Attempts to pump injection well A had to be abandoned because of problems with the pump bearings, which are being replaced.

The extent of aquifer clogging will be assessed when pumping is resumed following cleaning of the well. Carbonate precipitation should be eliminated by treating the water. Resumption of heated-water injection is anticipated in September 1982.

MOBILE FIELD TEST FACILITY

Joel G. Melville, Fred J. Molz and Oktay Güven
Civil Engineering Department
Auburn University
Auburn, Alabama 36849

ABSTRACT

The investigation of potential and application of the seasonal storage of energy as heated water in aquifers has increased in recent years. As energy costs increase aquifer storage can become a more important technique in reducing peak energy demands if aquifer thermal energy systems are clearly understood and utilized at maximum efficiency. Since 1976 Auburn University has conducted field tests in a confined aquifer near Mobile, Alabama. A set of three experimental cycles was begun in 2/17/81. This paper discusses the results of the first and second cycles of experiments. The description of the third, final cycle field procedure and preliminary injection phase data are also presented.

The volume injected in cycle I was 26 x $10^3 m^3$ at an average temperature increment of 58.5°C. The volume injected in cycle II was 58 x $10^3 m^3$ at an average temperature increment of 81.0°C. The recovery efficiencies of cycles I and II were 0.55 and 0.45 respectively.

INTRODUCTION

Theoretical and experimental studies of aquifer thermal energy storage has increased in recent years (refs. 1, 2, 3, 4, 5, 6, 7, 8). In addition there are experiments and prototype applications recently completed, operating, or under construction in Denmark, France, Germany, Switzerland, Sweden, Canada, and the United States. Current information is available in the STES Newsletter.

Beginning in 1976, Auburn University conducted two sets of field experiments reported in the above references and proceedings of the IECEC (refs. 9, 10, 11). A third set of experiments under the current contract, began 3/26/80 to provide extensive field data for storage of heated water in aquifers at elevated temperatures. These data are necessary to improve understanding of the physical phenomena, to calibrate numerical models, and to provide field experience in an experimentally controlled situation. Extensive aquifer testing prior to injection was performed and reported (refs. 12, 13). It has been shown in the first and second cycles that storage of water at increased temperatures results in lower recovery efficiencies due to thermal convection which occurs during the storage phase. In an effort to improve efficiency at the higher temperatures, the third experimental cycle will attempt to selectively recover the warmer water from the upper zone of the aquifer and reject cooler water from near the bottom of the aquifer.

DESCRIPTION OF EXPERIMENTS

In order to test a doublet supply-injection well configuration, a third round of experiments consisting of three injection-storage-recovery cycles was started in early 1981 at the Mobile site. A schematic of the doublet system is shown in Fig. 1. The injection and supply wells fully penetrate the confined aquifer and are separated by 244 m (800 ft).

Fig. 2 shows the location of the supply well, injection well and boiler with respect to the 28 observation wells used to measure temperature, hydraulic head and tracer concentration. The different types of observation wells are indicated on the figure.

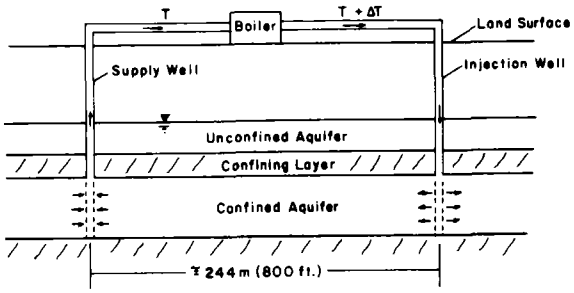

Fig. 1. Diagram of the "doublet" supply-injection well configuration used in the third set of aquifer storage experiments now being performed near Mobile, Alabama.

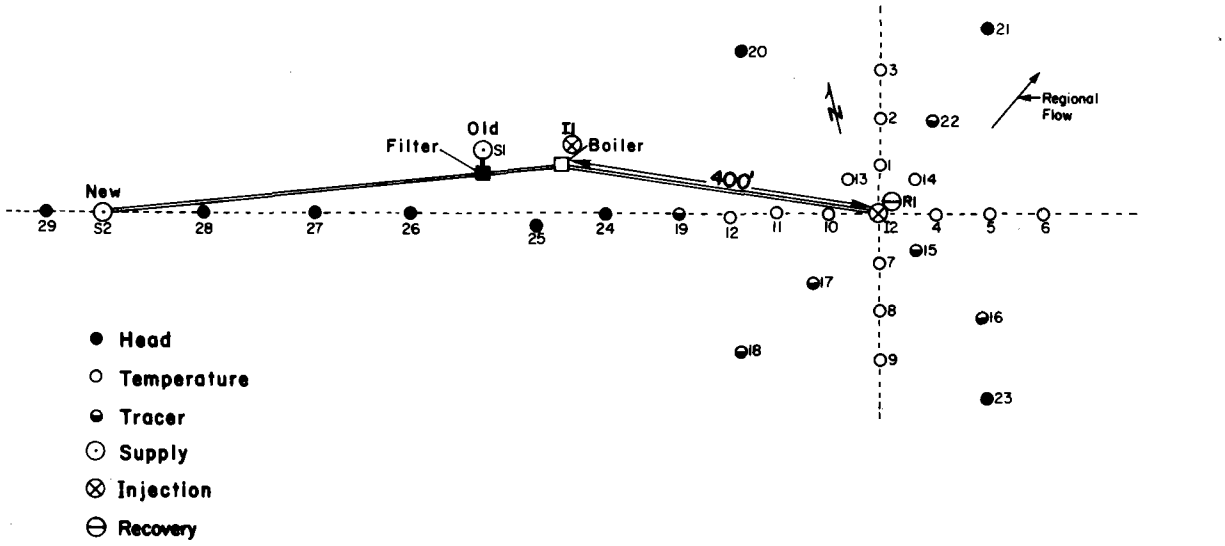

Fig. 2. Top view of the complete well field that has been constructed at the Mobile site. Water is obtained from the new supply well, heated by the boiler and injected into well I2. Water recovered from I2 after storage is injected back into S2 for later use.

Temperature observation wells were constructed (ref. 12) to record temperatures at 6 elevations. A tracer injection experiment was conducted simultaneously with cycles I and II (ref. 12). Extensive pre-injection aquifer testing was also conducted at the Mobile site. Because the data collected in the present experiments are serving as the basis for rather extensive mathematical modeling studies, more than the usual attempt was made to determine accurate hydraulic properties of the storage aquifer and aquitards. These properties included both vertical and horizontal

permeability of the storage aquifer, storativity, and vertical permeability of the upper and lower aquitards. Thermodynamic properties such as thermal conductivity and heat capacity are important also and were measured in previous studies (refs. 3, 13). Results of the aquifer tests are: anistotropy ratio, K_x/K_z = 6.7, horizontal hydraulic conductivity, K_x = 53.6 m/day and a storage coefficient, S = .00049. When laboratory data become available based on samples taken in the field, the aquitard parameters will also be estimated.

RESULTS OF FIRST CYCLE

Shown in Fig. 3 is the cumulative injection volume as a function of time. The horizontal line segments represent shut-down periods due mostly to mechanical problems. During operational periods the average injection rate (slope of line) was very close to 45 m^3/hr. Recovery pumping rates are shown in Fig. 4.

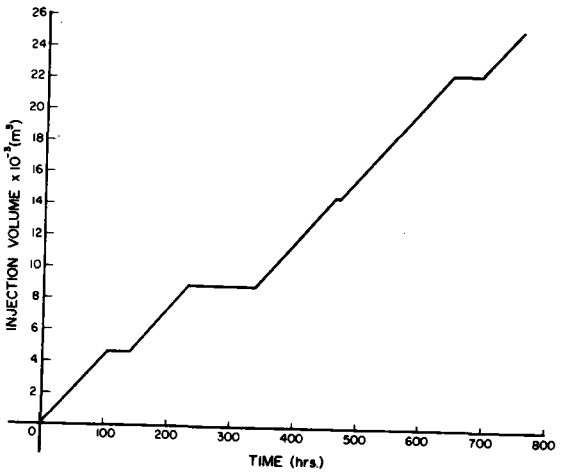

Fig. 3. Plot of cumulative injection volume versus time for the first of three planned injections.

Shown in Fig. 5 is the injection temperature history. This was maintained at a fairly constant value, although there was a drop-off in average temperature of approximately 5°C during the 756 hour injection period due to increasing malfunction of the boiler. Over the entire 756 hour period, the average injection temperature was approximately 58.5°C.

Fig. 6 shows the constant decline of temperature at the recovery well. Some heat loss occurred during the storage phase (755 hours) and constant decline of temperature during recovery indicates that increasing amounts of cool water are pumped from the injection well, probably from near the bottom of the well. Tracer data at the recovery well support the idea that significant convection occurred during the test.

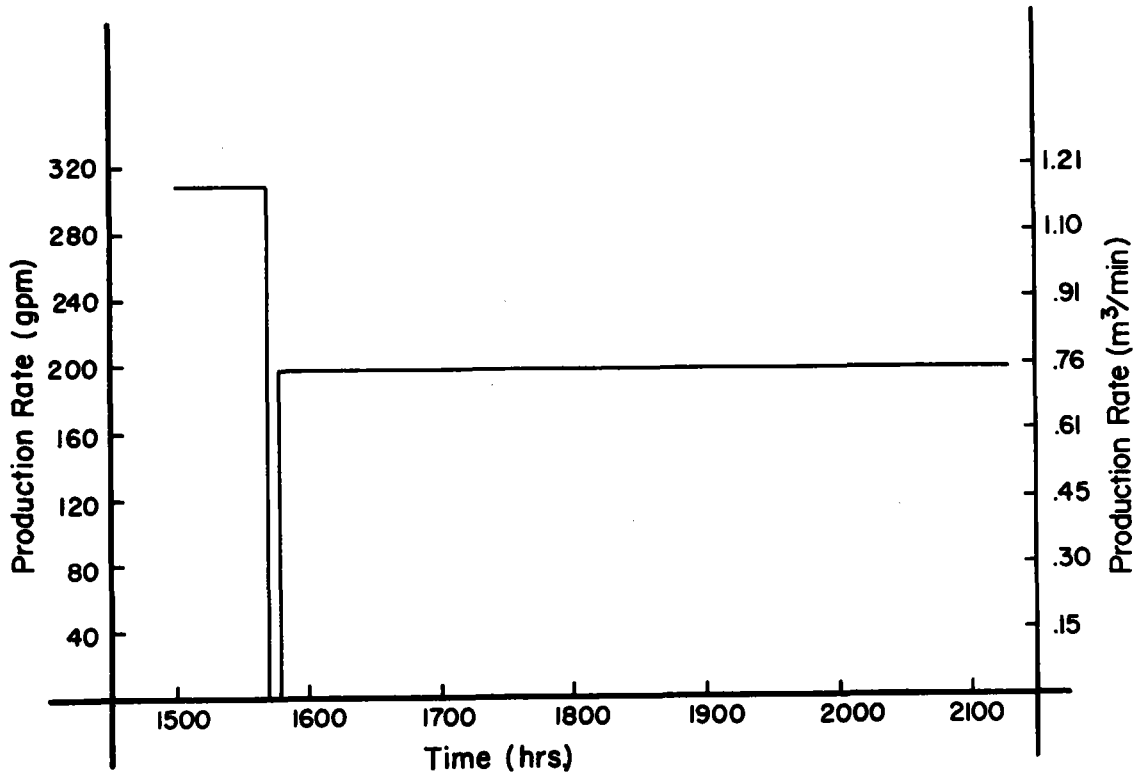

Fig. 4. Recovery well pumping for the first experimental cycle.

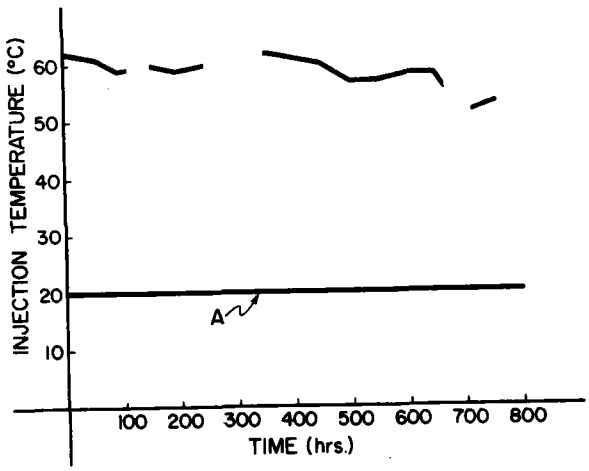

Fig. 5. Plot of injection temperature versus time for the first injection. The horizontal line marked "A" represents the ambient ground water temperature in the storage aquifer.

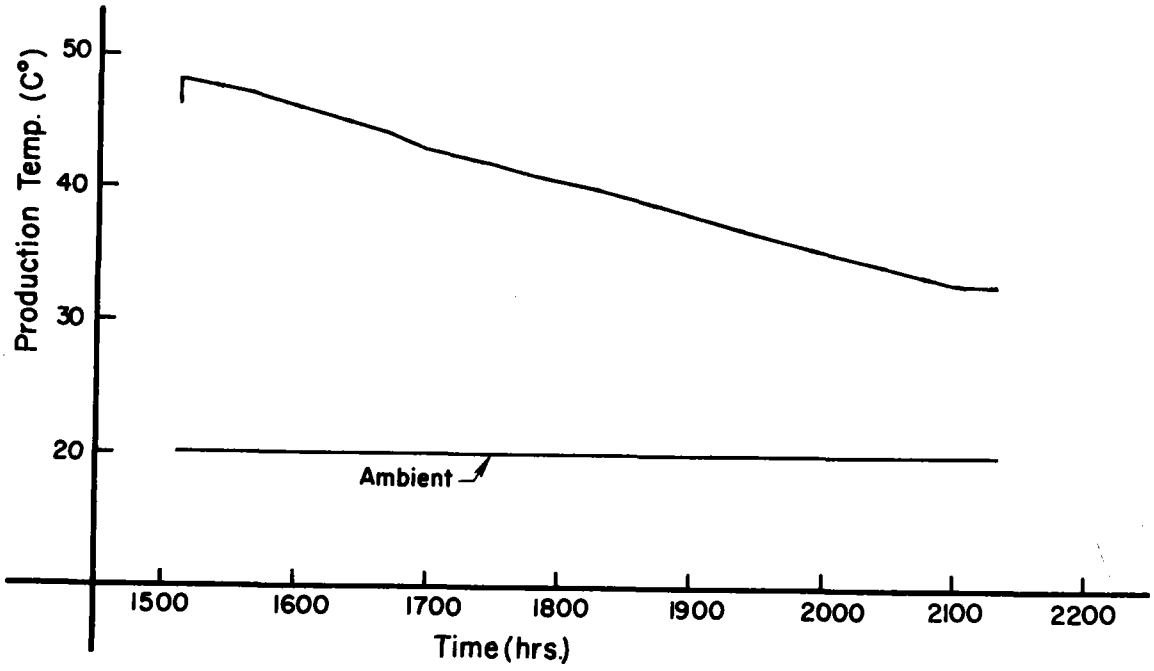

Fig. 6. Recovery well temperature. The horizontal line "A" is the ambient ground water temperature. The energy recovery was 55.3%.

RESULTS OF SECOND CYCLE

Cycle II injection was at an average temperature of 81°C. The purpose of this cycle was to quantify the influence of increased thermal convection caused by higher injection temperature. The injection volume as a function of time is shown in Fig. 7. The total injected volume was 58,063 m^3. The variation of the temperature during injection is shown in Fig. 8. The storage time was 34 days. Variations in the vertical temperature distribution during storage and comparison with tracer concentration measurements clearly indicated significant thermal convection. Production continued over approximately 2 months as shown in Fig. 9.

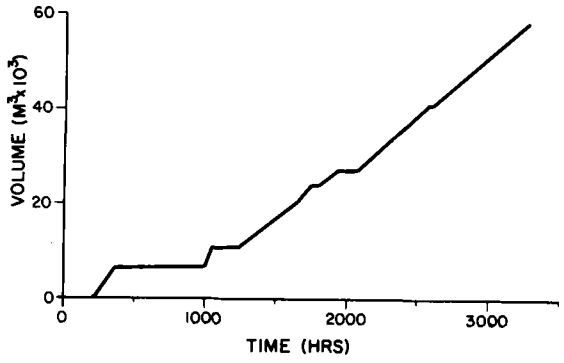

Fig. 7. Cumulative injection volume versus time for cycle II. During the first 1000 hours of the cycle, boiler malfunction continued to be a problem.

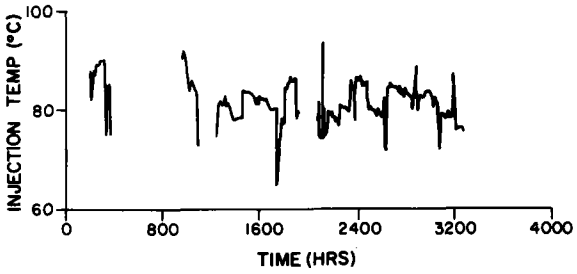

Fig. 8. Cycle II injection temperature as a function of time.

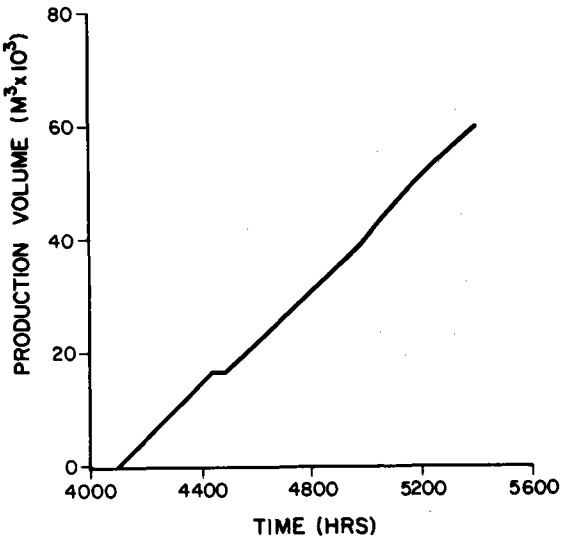

Fig. 9. Cumulative production volume versus time for cycle II.

Production temperature variation is shown in Fig. 10. The peak recovery temperature was 55.1°C. Pumping was continued until a definite recovery trend was established. The temperature distribution in the aquifer indicated that the low recovery temperature was due to the intake of cold native water near the bottom of the aquifer. Projecting a final energy recovery of approximately 40% as compared with 55.3% obtained in cycle I, the detrimental effect of thermal convection was clearly demonstrated. In an effort to improve efficiency, pumping was halted and the well was half filled with sand and a packer was installed above the sand. This modification was intended to withdraw more water from the upper half of the aquifer where the warmer water had migrated. When pumping was restarted, the recovery temperature immediately increased to 52.5°C over the temperature of 49.5°C which existed when initial recovery was halted. Ultimately, the energy recovery was 45.2% based on a recovery volume equal to the injected volume. If modification has been done prior to any recovery pumping, the estimated recovery was 46 to 47%. Based on computer simulations (Lawrence-Berkeley Laboratory, personal communication), the optimum recovery was 51% for practical applications of partially-penetrating recovery wells.

Cycle II was similar to cycle I in that no significant clogging of the injection well occurred. Fig. 11 compares specific capacities for cycles I and II and the specific capacity for an earlier experiment where clogging had to be overcome with frequent backwashing.

Land surface elevations changes induced by the injection have been monitored. For cycles I and II the maximum changes have been 0.43 cm and 1.24 cm respectively. Larger increases are indicated in cycle III. Such changes are significant and potential effect on foundations would have to be considered. Land surface elevation change will be dependent on local stratigraphy. Careful analysis of Mobile data should make it possible to predict potentially large land elevation changes at other sites.

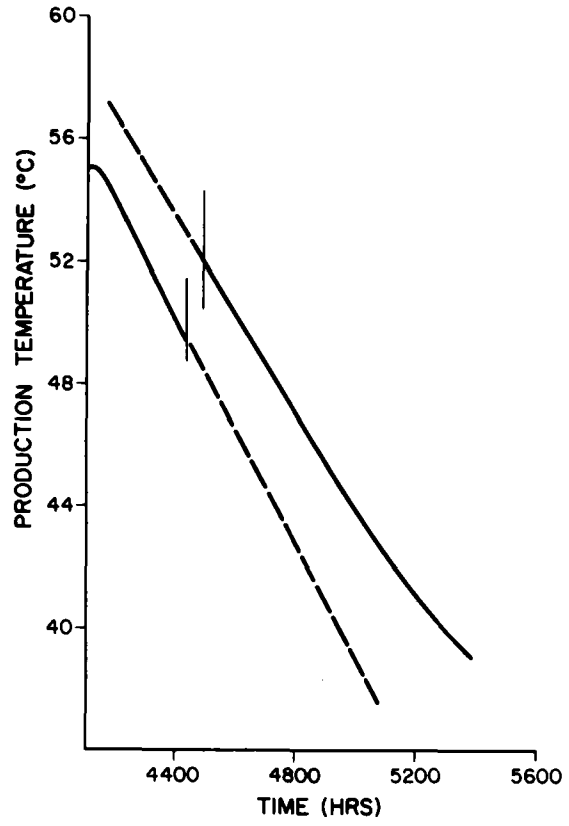

Fig. 10. Production temperature versus time for cycle II. The solid lines represent actual data obtained before and after the recovery well modifications discussed in the text. The broken lines are linear extrapolations of the two segments of data.

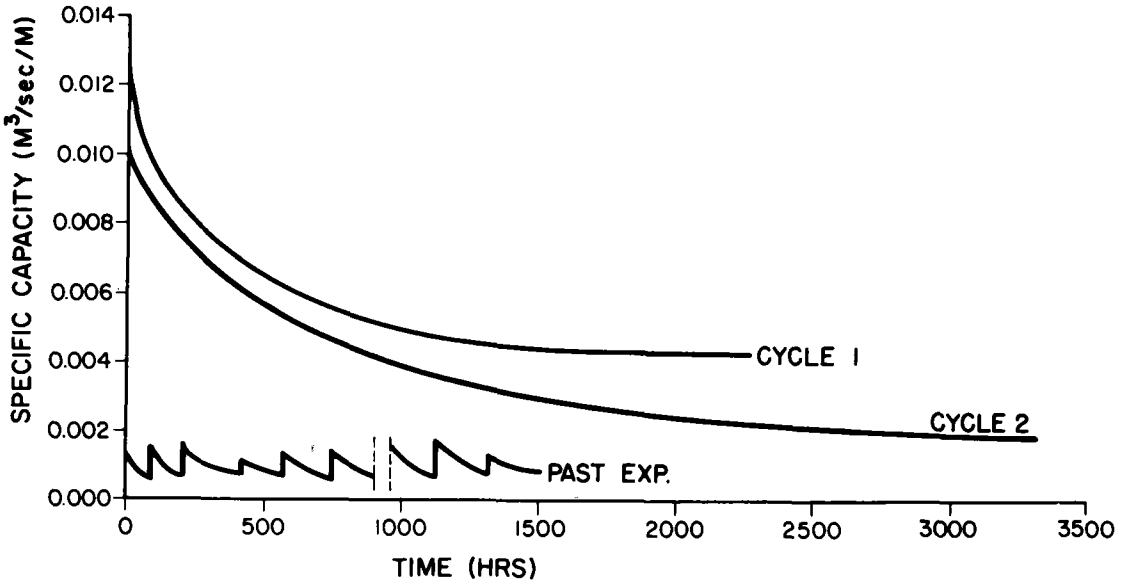

Fig. 11. Specific capacity of the injection-production well during cycle I, cycle II and a previous experiment when clogging occurred due to clay dispersion.

RESULTS OF THIRD CYCLE

It was decided that the third cycle of experiments would be with injection water temperature comparable to the second cycle. Since results of cycle II showed significant thermal convection, the fully-penetrating injection well was modified as described earlier to inject the hot water at the top of the aquifer. Injection of the hot bubble at the top of the aquifer should provide a more stable zone of stored energy. A selective recovery system is being installed. The system consists of the recovery pump in the partially penetrating well which is intended to pump from the upper zone of the aquifer. A second pump, installed in an adjacent well is in a well screened near the bottom of the aquifer. The deeper pump is intended to be pumped at rates to reduce any cold water intake by the recovery pump. The cooler water from the bottom of the aquifer will be rejected.

The third cycle injection was begun 4/7/82 and completed on 7/14/82 with a volume of 56,000 m^3 at an average temperature of 81°C. The injected water is definitely confined to the upper half of the aquifer. The storage period will extend through August and recovery will begin in September, 1982.

CONCLUSIONS

1. Injection temperatures of 58°C and 81°C result in significant thermal convection at the present storage zone location.

2. Because of more thermal convection in cycle II at 81°C, the efficiency dropped to 0.45 as compared to 0.55 obtained in cycle I.

3. No clogging was experienced for any injection under the present contract. This may not hold for long term injection.

4. Tracer studies show significant convection during storage.

5. Dispersion appears to have little effect on efficiency at Mobile.

6. Recovery pumping with fully-penetrating wells results in lower efficiency due to intake of cool ambient water near the bottom of the aquifer.

7. Maximum land surface elevation change was 1.24 cm in cycle II and larger changes are apparent in cycle III.

ACKNOWLEDGEMENTS

This work was supported by the U.S. Department of Energy through a subcontract awarded by the Battelle Pacific Northwest Laboratories (Subcontract B-67770-A-0).

REFERENCES

1. D. Werner and K. Kley. Problems of Heat Storage in Aquifers. Journal of Hydrology, 34, 1977, 35-43.

2. B. Mathey. Development and Resorption of a Thermal Disturbance in a Phreatic Aquifer with Natural Convection. Journal of Hydrology, 34, 1977, 315-333.

3. F. J. Molz, J. C. Warman and T. E. Jones. Aquifer Storage of Heated Water: Part I -- A Field Experiment. Ground Water, 16, 1978, 234-241.

4. F. J. Molz, A. D. Parr, P. F. Andersen, V. D. Lucido and J. C. Warman. Thermal Energy Storage in a Confined Aquifer: Experimental Results. Water Resources Research, 15, 1979, 1509-1514.

5. F. J. Molz, A. D. Parr and P. F. Andersen. Thermal Energy Storage in a Confined Aquifer: Second Cycle. Water Resources Research, 17, 1981, 641-645.

6. S. S. Papadopulos and S. P. Larson. Aquifer Storage of Heated Water: Part II -- Numerical Simulation of Field Results. Ground Water, 16, 1978, 242-248.

7. T. Yokoyama, H. Umemiya, T. Teraoka, H. Watanabe, K. Katsuragi and K. Kasahara. Seasonal Thermal Storage in Aquifer for Utilization. Bulletin, Japanese Society of Mechanical Engineers, 23, 1980, 1646-1654.

8. C. F. Tsang, T. Buscheck and C. Doughty. Aquifer Thermal Energy Storage -- A Numerical Simulation of Auburn University Field Experiments. Water Resources Research, 17, 1981, 647-658.

9. F. J. Molz, A. D. Parr and P. F. Andersen. Thermal Energy Storage in Aquifers: Experimental Study. Proceedings of the 14th Intersociety Energy Conversion Engineering Conference, American Chemical Society, Volume I, 1979, 534-537.

10. C. F. Tsang, F. J. Molz and A. D. Parr. Experimental and Theoretical Studies of Thermal Energy Storage in Aquifers. Proceedings of the 16th Intersociety Energy Conversion Engineering Conference, American Chemical Society, Volume 2, 1980, 1244-1248.

11. F. J. Molz, A. D. Parr, and J. G. Melville. Confined Aquifer Thermal Energy Storage: Mobile Doublet Experiment. Proceedings of the 16th Intersociety Energy Conversion Engineering Conference, ASME, Volume I, 1981, 941-946.

12. F. J. Molz, J. G. Melville, and A. D. Parr. Mobile, Alabama Field Test Facility. Proceedings of the Mechanical, Magnetic and Underground Energy Storage 1981 Annual Contractor's Review, U.S. Dept. of Energy, Washington, DC, August 24-26, 1981.

13. A. D. Parr, F. J. Molz, and J. G. Melville. Field Determination of Aqufier Thermal Energy Storage Parameters. Submitted for publication in Ground Water, July, 1982.

ANALYSIS OF REINJECTION PROBLEMS AT THE STONY BROOK ATES FIELD TEST SITE

Donald J. Supkow, Ph.D. and James A. Shultz
Dames & Moore
6 Commerce Drive
Cranford, New Jersey 07016

Aquifer Thermal Energy Storage (ATES) is one of several energy storage technologies being investigated by the DOE to determine the feasibility of reducing energy consumption by means of energy management systems. The State University of New York, (SUNY) Stony Brook, Long Island, New York site was selected by Battelle PNL for a Phase I investigation to determine the feasibility of an ATES demonstration to seasonally store 17.4×10^4 MBTU (50,000 MWH) of chill energy by injecting chilled water in the winter and recovering it at a maximum rate of 100 MBTU/hr (30 MW) in the summer. The Phase I study was performed during 1981 by Dames & Moore under subcontract to Battelle PLN. The pumping and injection tests were performed using two wells in a doublet configuration (Figure 1). Well PI-1 is a previously existing well and PI-2 was installed specifically for this investigation. Both wells are screened in the Upper Magothy aquifer from approximately 300 to 350 feet below ground surface (Figures 2 and 3). Nine observation wells were also installed as a portion of the investigation to monitor water level and aquifer temperature changes during the test.

The initial portion of the test was performed as anticipated; water was pumped from Well PI-2, chilled to about 41°F and injected into Well PI-1 at a rate of 300 GPM. After a quiescent storage period of 48 days, the chilled water was recovered from Well PI-1 and injected into Well PI-2. However, only a rate of about 100 GPM, could be injected into Well PI-2. Therefore, in order to complete the test in a timely manner, the remaining 200 GPM of recovered water was pumped to waste. Water samples were collected for chemical analysis. The results indicated high qulaity water, however, there were also high concentrations of dissolved oxygen.

Although water had been pumped from PI-2 at a rate of 300 GPM with a specific capacity of about 13.4 GPM per foot of drawdown prior to injection, water could not be injected into PI-2 at the same rate even after some preliminary remedial work. The remedial work consisted of some redevelopment including additional pumping and surging by airlift followed by placement of sodium sulphite, with final jetting and pumping. The particulate material removed was predominantly ferric hydroxide with very little silt or micaceous material. Pumping test data obtained prior to and after redevelopment indicate an increase of 30% in specific capacity to 6.8 GPM per foot of drawdown. However, this is still considerably less than the original specific capacity of 13.4 GPM per foot of drawdown. These data also indicate a well efficiency of greater than 90%. The increase in dissolved oxygen, believed to have occurred during injection of PI-2, may have been responsible for precipitation and accumulation of iron near the interface of the gravel pack and the aquifer. Next a step injection test of PI-2 was performed. The results indicated a drop of injection capacity from about 9 GPM per foot of head to 2.1 GPM per foot of head between Inijection rates of about 100 and 120 GPM. This was considerably less than the pumping capacity. The data suggest that the

injection capacity may be related to the entrance velocity of the water into the well screen and/or aquifer formation.

It should be noted that Well PI-1 did not experience a similar large decrease in injection capacity compared to its pumping capacity. Although direct measurement of the water level in PI-1 was not possible, the water did not rise to the surface in this well during injection. The only known difference between the two wells is the diameter of the screen (12-inch diameter screen in a 30- to 36-inch diameter borehole for PI-1 vs a 6-inch diameter screen in an 11-3/4-inch diameter borehole for PI-2).

The possible causes for decrease in the injection capacity of Well PI-2 which have been considered include air entrainment, degassing of dissolved air, precipitation of iron or other compounds, deposition of sediment pumped along with water from Well PI-1, deposition of sediment derived from the piping system and migration or rearrangement of mineral grains in the filter sand or aquifer formation during injection. Such mineral migration may occur above some critical entrance velocity.

Based upon the results of the preliminary remedial work on Well PI-2, Dames & Moore proposed a more thorough remedial program to Battelle PNL. This work was authorized in June 1982, begun in late July and is ongoing at this time. This work consists of two phases of redevelopment, surging and pumping with a high capacity deep well turbine pump, and if necessary, acid treatment. Each phase will be followed by a step drawdown test to evaluate the specific capacity of PI-2. If after either phase, the specific capacity would be 9 or more GPM per foot for all steps of the drawdown test, a two-day step injection test would be performed at rates up to 300 GPM with water from Well PI-1. If the step injection test is successful, a short non-isothermal doublet test may be performed at the option of Battelle PNL.

During the current program of pumping, development, and testing of these wells, ground water samples will be collected and tested for dissolved oxygen, pH, calcium, magnesium, sodium, potassium, iron, carbonate, bicarbonate, sulfate, chloride, total dissolved solids, and total suspended solids.

The major technical difficulty with ATES systems is predicting and maintaining the specific capacity of injection wells. Hopefully the results of this project will lead to a greater understanding of the mechanics and hydraulics of injection wells, used for ATES projects.

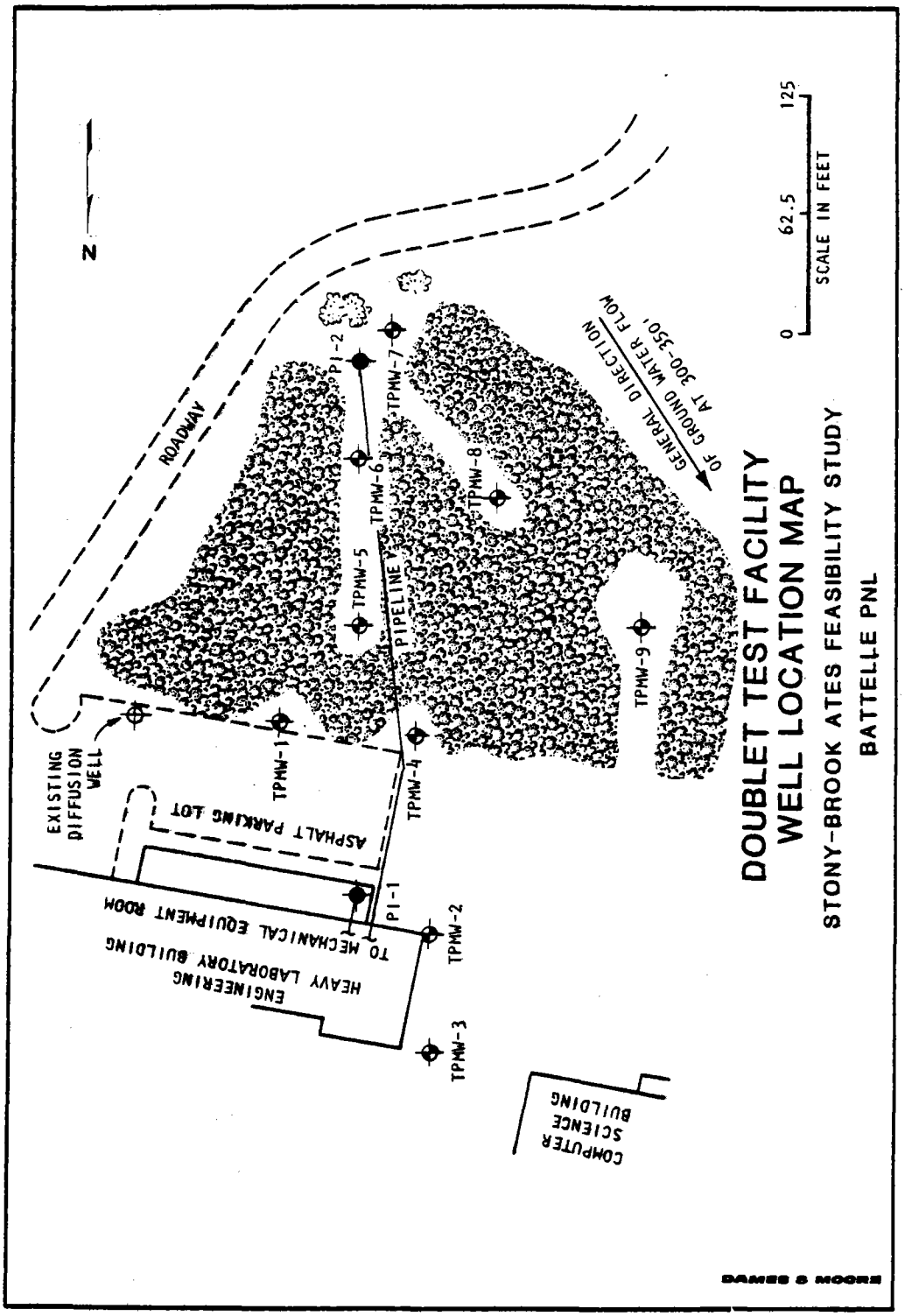
N
ROADWAY
PI-2
TPMW-7
TPMW-6
TPMW-8
TPMW-5
PIPELINE
TPMW-9
TPMW-1
TPMW-4
EXISTING DIFFUSION WELL
ASPHALT PARKING LOT
PI-1
TPMW-2
TPMW-3
TO MECHANICAL EQUIPMENT ROOM
HEAVY LABORATORY BUILDING
ENGINEERING
COMPUTER SCIENCE BUILDING
GENERAL DIRECTION OF GROUND WATER FLOW AT 300-350'
0
62.5
125
SCALE IN FEET
DOUBLET TEST FACILITY
WELL LOCATION MAP
STONY-BROOK ATES FEASIBILITY STUDY
BATTELLE PNL
DAMES & MOORE

FIGURE 1

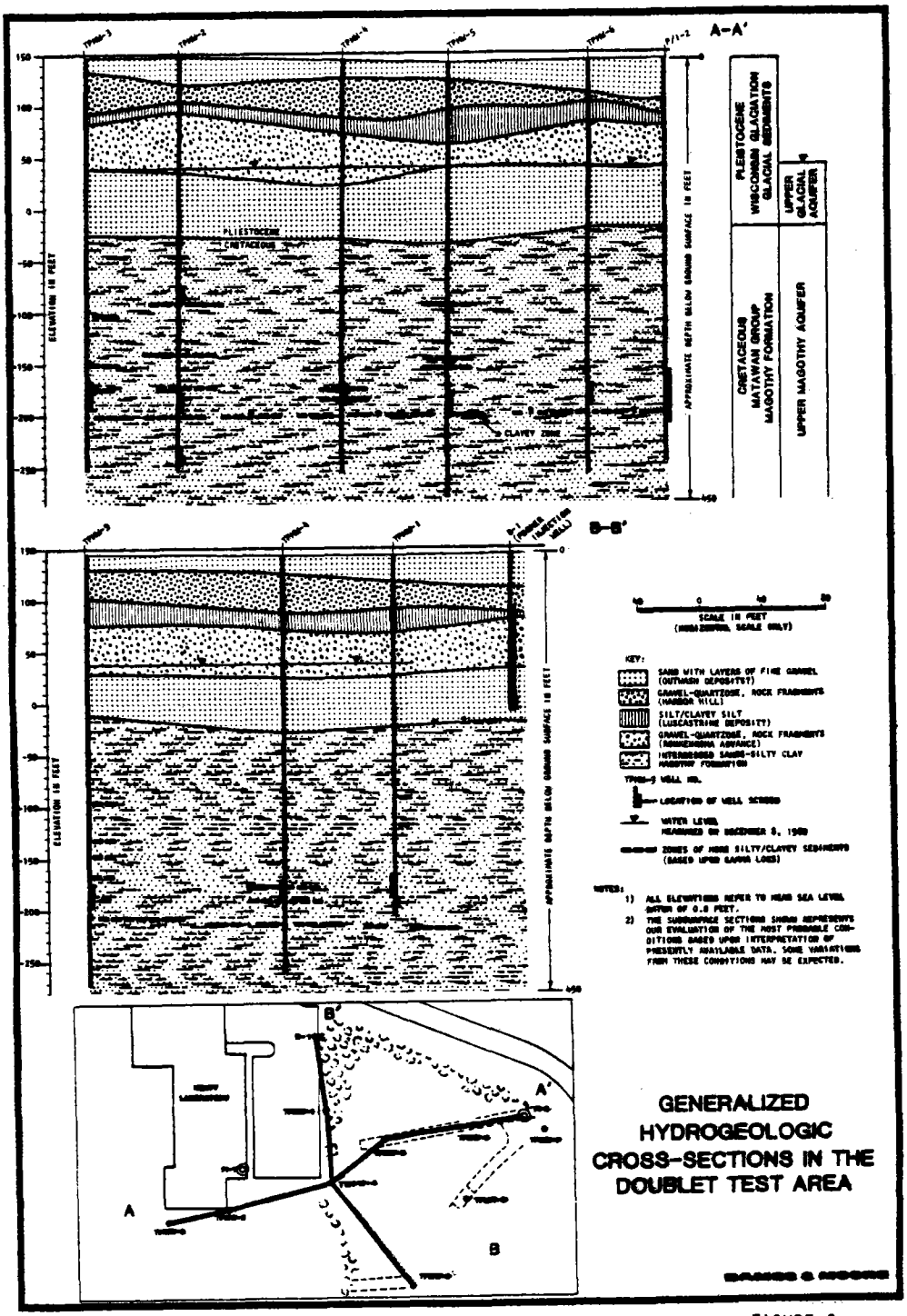
A-A'
B-B'
PLEISTOCENE
WISCONSINAN GLACIATION
GLACIAL SEDIMENTS
UPPER GLACIAL AQUIFER
CRETACEOUS
MATAWAN GROUP
MAGOTHY FORMATION
UPPER MAGOTHY AQUIFER
ELEVATION IN FEET
APPROXIMATE DEPTH BELOW GROUND SURFACE IN FEET
CLAYEY ZONE
SCALE IN FEET
KEY:
SAND WITH LAYERS OF FINE GRAVEL
(OUTWASH DEPOSITS?)
GRAVEL-QUARTZOSE, ROCK FRAGMENTS
(HARBOR HILL)
SILT/CLAYEY SILT
(LUSCASTRINE DEPOSIT)
GRAVEL-QUARTZOSE, ROCK FRAGMENTS
(RONKONKOMA ADVANCE)
INTERBEDDED SAND-SILTY CLAY
MAGOTHY FORMATION
WELL NO.
LOCATION OF WELL SCREEN
WATER LEVEL
MEASURED ON DECEMBER 9, 1980
ZONES OF MORE SILTY/CLAYEY SEDIMENTS
(BASED UPON GAMMA LOGS)
NOTES:
1) ALL ELEVATIONS REFER TO MEAN SEA LEVEL
DATUM OF 0.0 FEET.
2) THE SUBSURFACE SECTIONS SHOWN REPRESENTS
OUR EVALUATION OF THE MOST PROBABLE CON-
DITIONS BASED UPON INTERPRETATION OF
PRESENTLY AVAILABLE DATA. SOME VARIATIONS
FROM THESE CONDITIONS MAY BE EXPECTED.
A
A'
B
B'
GENERALIZED
HYDROGEOLOGIC
CROSS-SECTIONS IN THE
DOUBLET TEST AREA

FIGURE 2

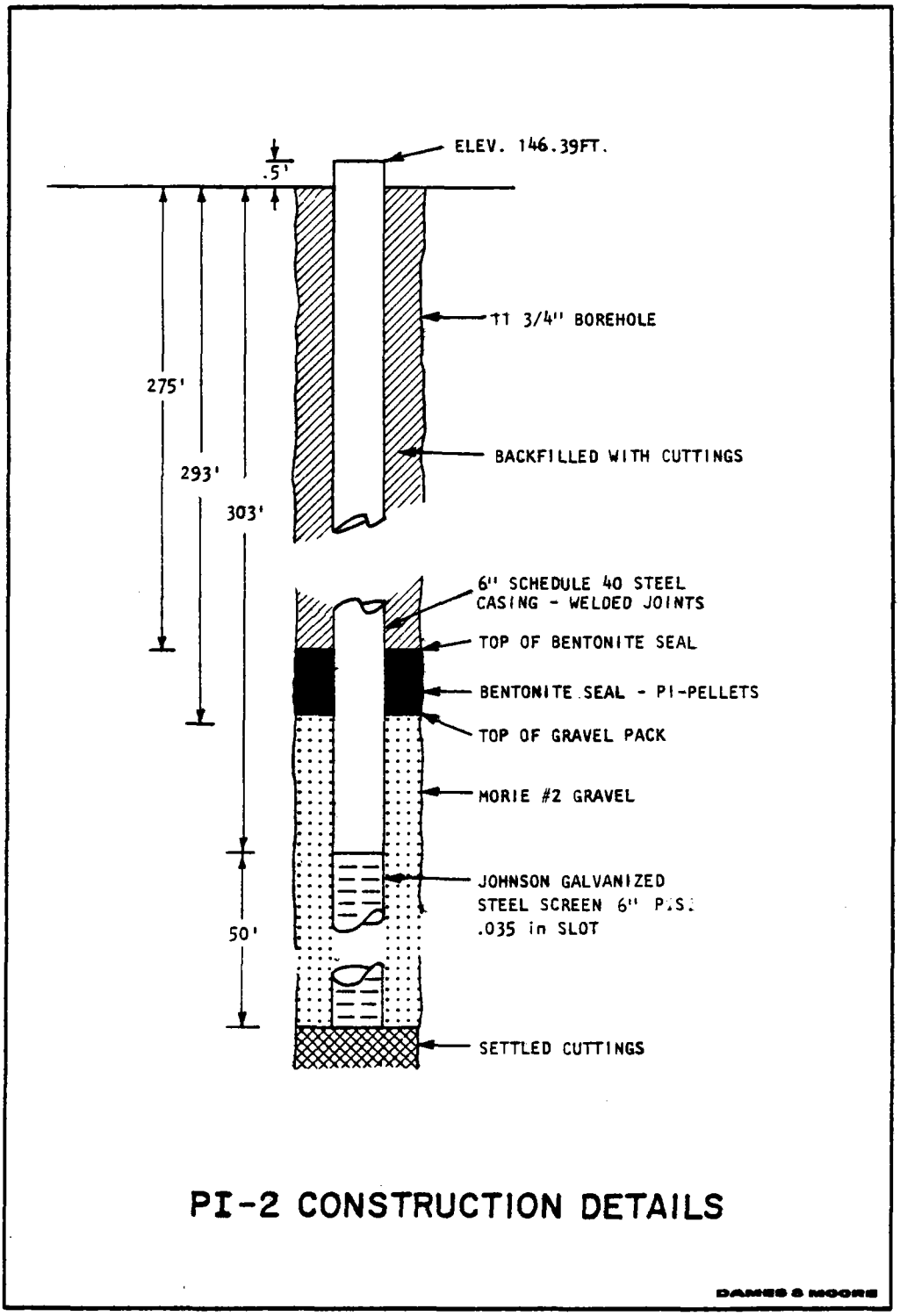
ELEV. 146.39FT.
.5'
11 3/4" BOREHOLE
275'
293'
303'
BACKFILLED WITH CUTTINGS
6" SCHEDULE 40 STEEL
CASING - WELDED JOINTS
TOP OF BENTONITE SEAL
BENTONITE SEAL - PI-PELLETS
TOP OF GRAVEL PACK
MORIE #2 GRAVEL
JOHNSON GALVANIZED
STEEL SCREEN 6" P.S.
.035 in SLOT
50'
SETTLED CUTTINGS
PI-2 CONSTRUCTION DETAILS
DAMES & MOORE

FIGURE 3

HEAT ACCUMULATION AND STORAGE CAPACITY OF THE WATER-FILLED MINES AT ELY, MINNESOTA

Matt Walton and Peter McSwiggen
University of Minnesota
Minnesota Geological Survey
1633 Eustis Street
St. Paul, Minnesota 55108

The iron mines at Ely (Figs. 1 and 2) occupy a doubly plunging isoclinal syncline with a nearly vertical axial plane, forming an irregular, canoe-shaped structure, striking about N.70°E., enclosed within massive Archean greenstone pillow lavas. The ore body was about 10,000 feet (3 km) in length, and was mined to a maximum depth of 1,672 feet (510 m). It was 1,000 to 1,300 feet (300 to 400 m) wide at its widest points. It was thickest in the axial portion or keel of the fold and pinched out on the limbs. Waste rock in the core of the fold subsided as the ore was mined, creating a surface depression that has filled with water since the mines shut down in the 1960's. Figure 2 shows the locations of principal shafts and the outline of the area of subsidence over the underground workings. The Chandler, Pioneer, Zenith, Sibley, and Savoy Mines were connected underground by drifts at various levels for safety and ventilation, but each mine operated from its own shafts and hoists. The water body in the subsidence area is now known as Miners Lake.

A reasonably complete collection of mine maps and sections has been assembled from several sources to provide, at least for the present, an adequate picture of the as-built configuration of the underground workings (Figs. 3, 4, and 5). No topographic data have been found to show the contour of the ground over the mines before subsidence, but it is clear that most of the depression occupied by Miners Lake is due to subsidence, and only a minor amount is due to open-pit mining at the western end of the deposit. Acoustic profiles of the lake, the U.S. Geological Survey 7-1/2-minute topographic map prepared before the water in the mines rose into the subsidence area, and enlarged aerial photographs taken at different dates during the filling of the mines are being studied to evaluate the subsidence of the mine and the filling of the lake since 1965.

Two main shafts are accessible for sounding and water-temperature measurements. Zenith number 3 is a vertical shaft 1,672 feet (510 m) deep in massive greenstone about 1,000 feet south of the subsidence area. It communicates with the ore body and the rest of the mine workings by drifts at approximately 100-foot (30-m) intervals from the 14th level at 1,226 feet (374 m) to the 18th level at the bottom of the shaft. The shaft appears to be free of obstructions, and complete temperature-depth profiles were obtained on July 2 and July 21 (Fig. 6). On July 8 the shaft was inspected to the length of available cable, 1,500 feet (457 m), by a downhole television scanner. The only notable feature was an abrupt improvement in water clarity at a depth of 220 feet (67 m). On August 2 a van Dorn sampler was used to collect two samples from each of the three water masses defined by the inverted thermoclines shown on the temperature-depth profile. Samples are now undergoing detailed analysis.

The Pioneer A shaft is accessible through a 14-inch vent in a 30-foot plug of reinforced concrete and backfill. The shaft is inclined 70° from the horizontal to 703 feet (214 m) and vertical to 1,615 feet (492 m). Temperature-depth profiles (Fig. 6) were measured on July 1 to 1,280 feet (390 m), at which point an obstacle was encountered.

Temperature-depth profiles of Miners Lake were measured on July 2 and again on July 21 at several different stations. A profile at site B-2 (Fig. 2) is shown on Figure 6b. There is a sharp thermocline at a depth of 11 or 12 feet (3.5 m) between water that is 70°F (21°C) or warmer and cold water which decreases to 39°F (3.7°C) at 40 feet (12.2 m), below which the water gradually warms to about 42°F (5.6°C). Comparison with a temperature-depth profile from a large, natural lake near Ely (Fig. 6b) suggests that mixing of surface water is restricted in Miners Lake but that some water from the underground workings mixes with water in the deeper parts of the pond.

A significant contribution of geothermal heat to the water in the underground workings is suggested by the steplike increase in water temperature with depth found in both shafts. However, the reason for the occurrence of sharp inverted thermoclines between nearly isothermal layers of water, rather than a gradual temperature increase with depth, is not understood.

The mine workings and lake appear to be, in effect, an interconnected but isolated water impoundment with no outlet to ground water or surface drainage. When the mines closed and mine drainage by pumping ended during the mid-1960's, the depression now occupied by Miners Lake was dry and overgrown with trees. The watershed draining into it was small, perhaps not more than 25 or 30 percent larger than the actual area of subsidence. Precipitation simply disappeared into the underground workings. In September 1972, the City of Ely completed an addition to its storm sewer system, whereby storm runoff from the western third of Ely discharges directly into the pit. At about this time, standing water began to appear in the deepest part of the pit, about 165 feet (50 m) below the present water level, and the water has continued to rise since then. Records kept since 1980 indicate that the water is rising at the rate of about 7 feet per year and will overflow into Shagawa Lake within the next 2 years. However, the fact that after nearly 20 years the water is still about 3 feet (1 m) below the level of Shagawa Lake strongly suggests that the greenstone formations which surround the ore body are highly impervious, and that the filling of the mine is almost entirely from direct precipitation and local runoff, with little or no contribution from ground water.

Through the initiative of several citizens of Ely and the Reserve Mining Company, a pumping test on the Zenith number 3 shaft is planned for the week of August 16th at no cost to this project. This test should provide information on the degree to which the lake and the Pioneer shaft are hydraulically connected to the Zenith shaft and on the extent to which the Zenith shaft can draw on the warmer stratum of water which appears to exist in the lower part of the mine. Changes in water temperature and composition will be closely monitored during the test.

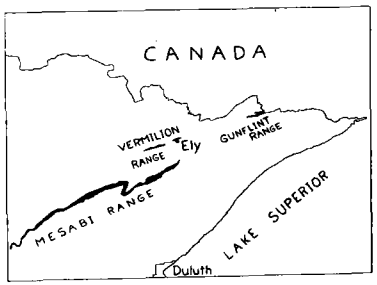

Figure 1. Northeastern Minnesota, showing the location of Ely and the Vermilion iron range.

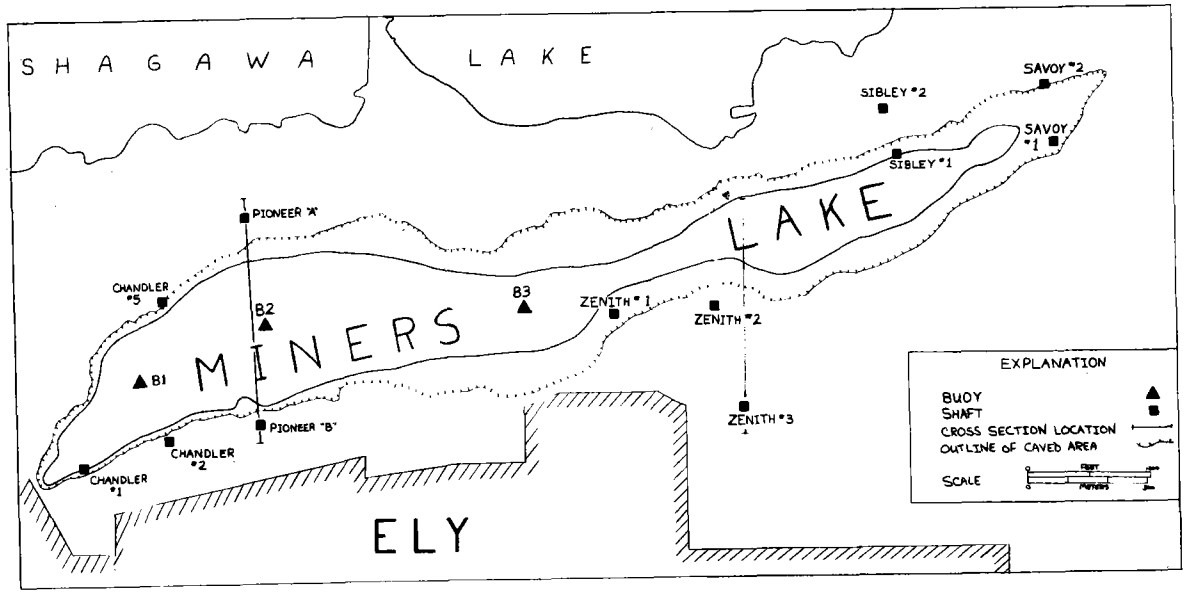

Figure 2. Map of mine sites at Ely, Minnesota.

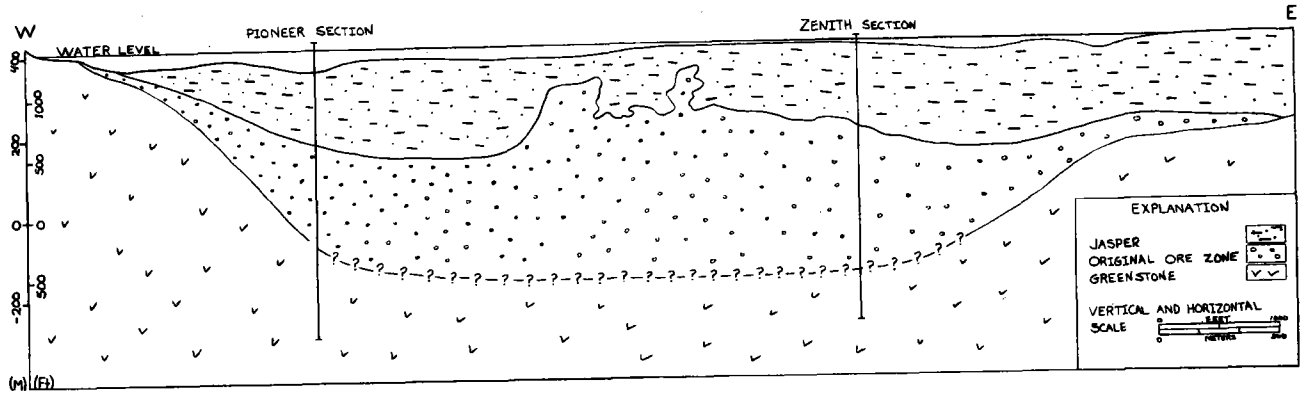

Figure 3. Longitudinal section through the mined area at Ely, Minnesota, from west to east (partly schematic).

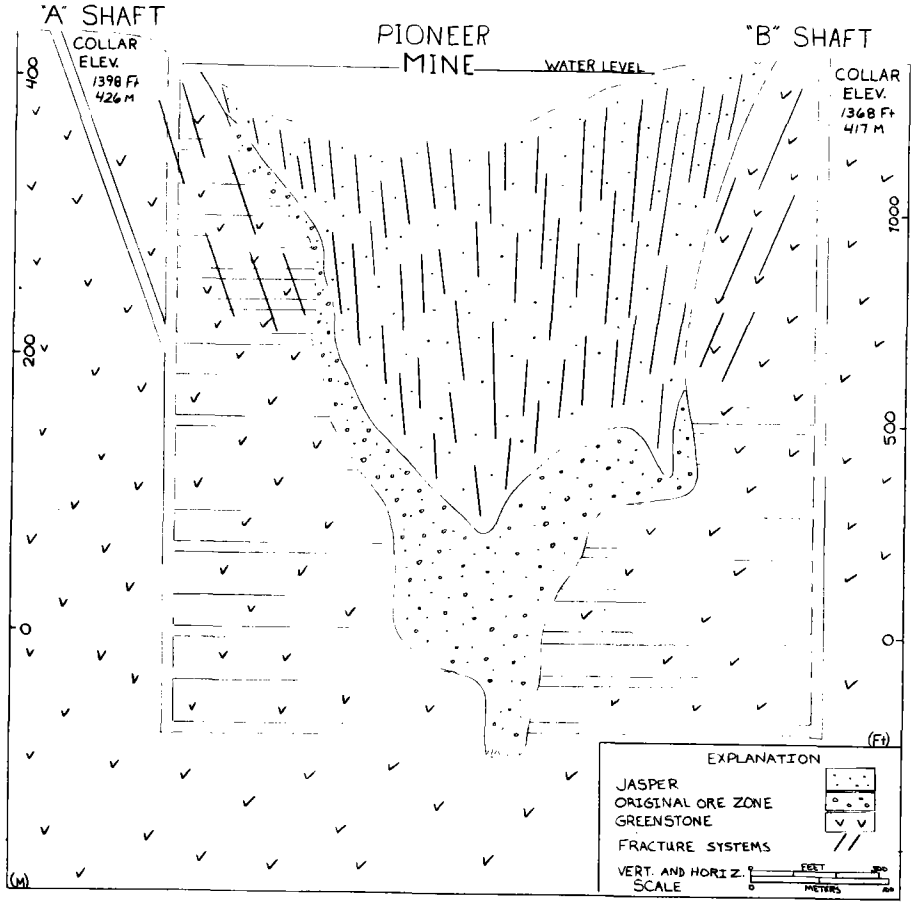

Figure 4. Section through shafts A and B of the Pioneer Mine (facing east).

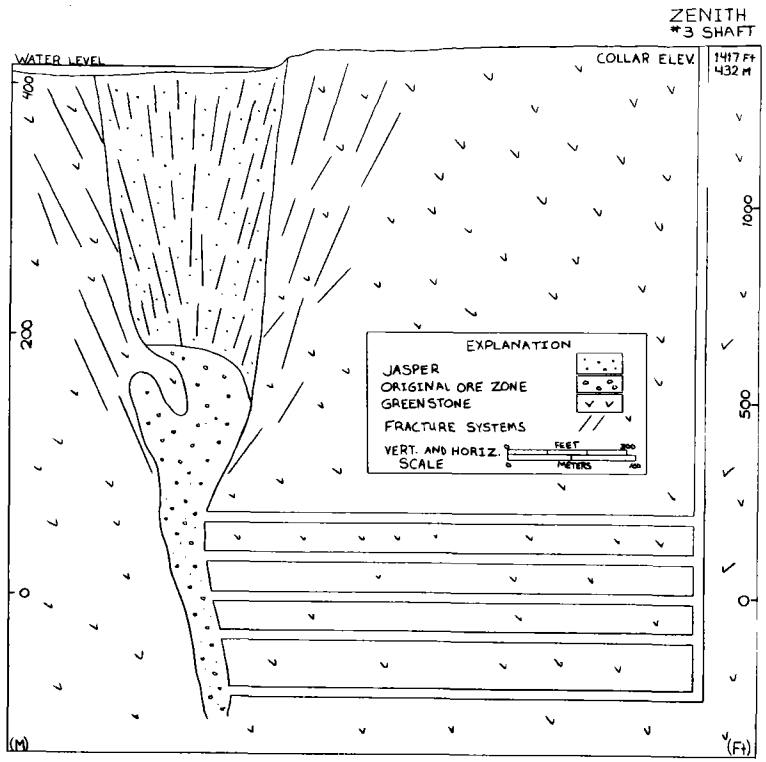

Figure 5. Section through shaft number 3 of the Zenith Mine (facing east).

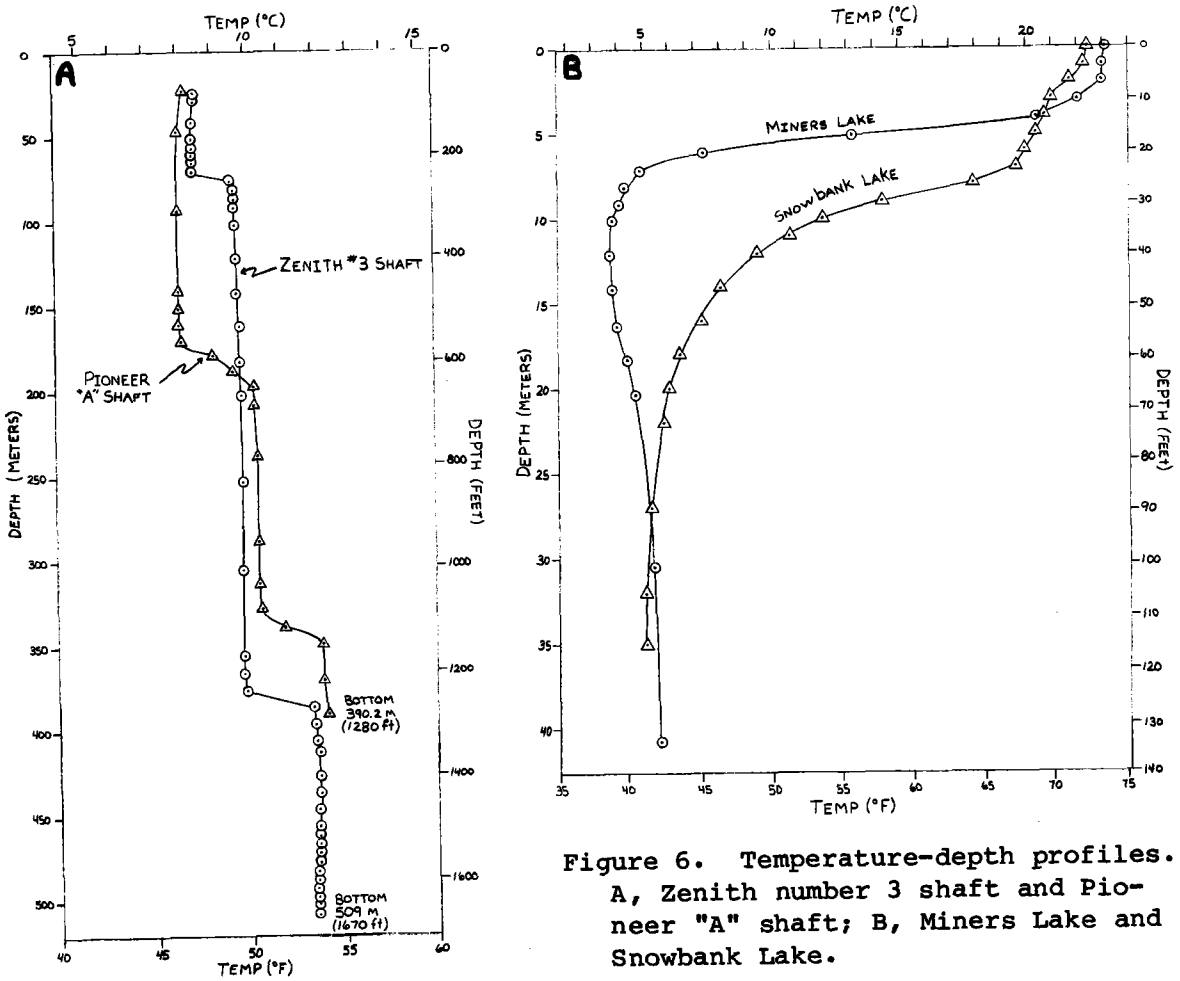

Figure 6. Temperature-depth profiles. A, Zenith number 3 shaft and Pioneer "A" shaft; B, Miners Lake and Snowbank Lake.

Summary and Conclusions

The water-filled iron mines at Ely comprise a large, complex underground system of interconnected shafts and drifts entering at numerous levels into a large, mined-out ore body partly replaced by collapsed rubble. Subsidence has produced a depression occupied by a lake as much as 165 feet (50 m) in depth and 5.3 million ft^2 (493,000 m^2) in surface area. A stepwise increase in water temperatures with depth is found in two main shafts, but the thermoclines occur at significantly different depths in the two shafts. The upper thermocline in the Zenith shaft may be related to the change in water clarity at 220 feet (67 m), and the lower thermocline may be related to the depth of the drifts which communicate with the lower mine workings. The upper thermocline in the Pioneer shaft, which communicates with the underground workings at many levels, is near the point at which the inclined shaft becomes vertical. These results suggest that pumping from the Zenith number 3 shaft could draw on a mass of water in the lower workings at a temperature approaching 54°F (12.2°C). The temperature profiles of Miners Lake indicate that during the summer it could be an efficient solar energy collector, providing sun-warmed surface water to replace chilled water in the underground mines. In short, the results to date imply that the mine can be used to accumulate and store solar and geothermal energy for a heat-pump-based community district heating system.

ICE PRODUCTION AND STORAGE FOR SEASONAL APPLICATIONS, UTILIZING HEAT PIPE TECHNOLOGY

A. J. Gorski, W. W. Schertz
Argonne National Laboratory
Argonne, IL 60439

OBJECTIVE

The objective of this program is to characterize the technical features of formation, collection and storage of ice naturally grown during winter months by means of innovative heat pipe technology.

CONCEPT

The method used freezes ice passively, in the same insulated storage container in which it will be used during the summer cooling season. Unlike methods of old, there are no ice cutting or transportation operations or costs. The essential features of the system follow.

A tank of water is buried underground near or under the building to be cooled. A series of heat pipes extend from the bottom of the tank to above the soil surface. These heat pipes act as very efficient one-way conductors of heat. Along the underwater evaporator section, heat from the water causes thin-film evaporation of the working fluid within the unit. The resulting vapor travels upward and condenses in the above-ground radiator section, releasing the transported heat to the air. During winter months when the ambient temperature is below freezing, the extraction of heat freezes ice along the submerged portion of the heat pipe. When the air is warmer than the water in the tank, the evaporation-condensation cycle stops automatically. The heat pipe thus works as a one-way conductor of heat from the tank to the environment.

As the ice growth increases in thickness, the overall heat transfer coefficient (and system performance) will decrease with time. To avoid this problem, two heat pipe evaporator designs are currently being evaluated. The first design is such that ice would periodically break off and float to the surface of the tank. In this manner, the tank fills with ice from the top down. The advantage would be high system performance; the disadvantage -less than 100% fill factor. To this point in time, only passive release methods have been investigated. Release has been consistent in small-scale experiments but inconsistent in full-scale winter operation. Active release methods will be investigated during the next winter season. The second design uses a large copper coil configuration. Experimental winter results indicate good efficiency and large ice yields. This design will also be evaluated during the next ice growing season. Different coil configurations will be tested for performance and ice yield. Both designs form the ice passively, in the same insulated storage tank, ready for summer cooling applications. Unlike conventional passive cooling techniques developed to date, this system is capable of providing both sensible and latent cooling, i.e., dehumidification can be achieved.

HEAT PIPES

The theory of heat pipe design is well known and will not be considered in detail here. The reader is referred to the book "Heat Pipes," by P. D. Dunn and D. A. Reay (1) or to literature on heat pipes available from the American Society of Mechanical Engineers (2). In addition, a comprehensive heat pipe computer program is available from Los Alamos Scientific Laboratory (3). At the start of this project, the only known example of heat pipe use for freezing was the Trans-Alaska pipeline application. McDonnell-Douglas Corporation supplied nearly 100,000 heat pipes for the pipeline. These heat pipes were used to prevent thawing of the permafrost around the pipe supports for elevated sections of the pipeline. Diameter of the heat pipes ranged from 5 to 7.5 cm and lengths varied from 9 m to 18 m. From this work, we were encouraged that heat pipes similar to what would be required for this program could be built with working lifetimes of the order of 20-30 years.

The ice freezing heat pipe design must satisfy three requirements:

1. The heat pipe must efficiently transfer thermal energy out of the water store and dissipate it to the ambient.

2. The heat pipe must act as a thermal diode and not transfer thermal energy into the storage tank.

3. Since ice growing on the immersed section of the pipe will eventually impede thermal transfer, some method of ice release should be developed, or some economical means of providing large evaporator area provided.

The first requirement is satisfied by the nature of the heat pipe. A simple heat pipe consists of a hollow pipe from which the air has been evacuated, and a small amount of working fluid introduced. The pipe is sealed, and contains no moving mechanical parts. If the lower end of this pipe is heated (or put in a tank of warm water) the liquid vaporizes in the lower (evaporator) section and the vapors rise to the upper end of the pipe. When these vapors contact the top cold end of the pipe, they condense and release the transported thermal energy. The liquid then returns to the lower end by gravity and the process continues. Since the latent heat of evaporation of the working fluid is large, considerable amounts of heat can be transported with a small temperature difference from end to end ($1^{o}C\,\Delta T \sim 5$ psi).

A simple heat pipe as required by this project would use gravity for condensate return to the evaporator section. In this regard, the simple heat pipe as described above could also be denoted as a thermal syphon, or a reflux condensor. We will use the term heat pipe in the course of this report, keeping in mind that this device uses gravity return instead of a wick structure as in a "true" heat pipe. By the use of gravitational condensate return, the device as outlined above will only transfer thermal energy upward and so act as a thermal diode.

The third heat pipe requirement, namely, the periodic ice release from the underwater evaporator section has to our knowledge not been investigated until this program. It is believed that a cost advantage can be achieved if the ice release is successful, however, it may not be required for the success of the concept.

TECHNICAL ACCOMPLISHMENTS

Three full-scale ice releasing and one full-scale coil type heat pipes have been tested during actual winter conditions. Passive ice release was observed during early winter but with a prolonged cold spell, and a uniform 0^{o}_{C} tank temperature, ice lock-on was observed. Comparison studies between the coil configuration unit and the locked-on release unit indicate a performance factor of approximately 4 times for the coil configuration. Using winter experimental data and observations, design decisions have been made for the next system configuration.

The Argonne Ice Storage and Test Facility (AISTF) is now being readied for full-scale system studies during the 1982-83 freezing season. The AISTF has been drained, cleaned, and new system configuration is now being installed.

A computer model has been developed to predict the performance of earth freezing and water freezing by means of pumped heat transfer fluid for five locations in the United States (4). This analysis and assessment is the first step in the development of a more complex computer program modeling heat pipe system for various geographic locations.

Mathematical formalism has been developed for describing heat pipe heat-transfer processes for ice releasing [Roll-Bond™ (5)] and coil type evaporator sections. Four different mathematical analyses have been developed for the two types of evaporator designs.

(1) Ice releasing (Roll-Bond™) evaporator design.
This design consists of a vertical tube with two Roll-Bond™ fins attached vertically, spaced 180° apart. The basic assumption in this case is that the temperature is constant along the vertical length of the tube and equal to the temperature at the mid-point. This is defined as a one dimensional case, solved in rectangular coordinates.

(2) Ice releasing (Roll-Bond™) evaporator design.
This case has the same geometry as above. However, now the temperature is allowed to vary along the vertical length of the tube. This is the two dimensional case, and has been solved also in rectangular coordinates.

(3) Coil evaporator design.
The coil design consists of a series of vertically stacked coil loops. Each loop consists of coil spirals of increasing radius. In this one-dimensional case, cylindrical coordinates, each temperature is allowed to vary radically outward for each given loop. The mathematical formalism for this case has been solved.

(4) Coil evaporator design.
This case has the same geometry as above. However, in addition, the temperature is now allowed to vary in the vertical dimension in addition to the horizontal dimension. The mathematical formalism has been completed, and as far as known, has never been done before.

It is expected that complete computer programs for cases (1) and (3) will be developed by September 30, 1982. Cases (2) and (4) will require additional effort. The mathematical development of the four situations above has been performed by Professor Edgar H. Buyco of Purdue University. The computer analysis is being performed by Professor Arthur E. McGarity of Swarthmore College.

NONTECHNICAL ACCOMPLISHMENTS

The Second Annual Workshop on Ice Storage for Cooling Applications was held at Argonne National Laboratory on May 13-14, 1982 (6). An indication of the growth of this technology is shown by the 100% increase in presentations by active ice researchers from the First Annual Workshop held in 1981 (7).

National and international acceptance of this cooling energy technology is now being expressed by the scientific and industrial sectors. Interactions have started with the American Society of Heating, Refrigerating and Air-Conditioning Engineers, Inc. (ASHRE), on organizing a session on ice storage at one of the upcoming ASHRE national meetings. An ice storage session will also be included at the First U.S.-China Conference on Energy, Resources and Environment, November 7-12, 1982 in Peking, The Peoples Republic of China.

Perhaps the major accomplishment of this program has been the demonstration that -Winter Cold is a Valuable Cooling Energy Resource. With a major commitment to this technology by the northern states, a significant increase in the supply of summer cooling energy can be achieved, as well as the creation of new industry and job opportunities.

REFERENCES

1. P. D. Dunn, D. A. Reay, Heat Pipes, Second Edition, Pergamon Press, 1978.

2. J. Schwartz, "Performance Map of an Ammonia (NH_3) Heat Pipe," The American Society of Mechanical Engineers, Reprint No. 70-HT, September 5, 1970.

3. F. C. Prenger, "Heat Pipe Computer Program (HTPIPE) Users Manual," Los Alamos Scientific Laboratory, LA-8101-M Manual, UC-32 issued November 1979.

4. C. E. Francis, A. E. McGarity, "An Annual Storage Ice System for Cooling Applications," to be presented at the First U.S.-China Conference on Energy, Resources and Environment, November 7-12, 1982 in Peking, The Peoples Republic of China.

5. "Roll-Bond™ Panels," Product of Olin Brass Corporation.

6. A. J. Gorski, "Second Annual Workshop on Ice Storage for Cooling Applications," Argonne National Laboratory, May 13-14, 1982.

7. A. J. Gorski, "First Annual Workshop on Ice Storage for Cooling Applications," Argonne National Laboratory, June 4-5, 1981. ANL-81-45, available from National Technical Information Service, U.S. Department of Commerce.

ADDITIONAL INFORMATION

1. A. J. Gorski, et al., "Long-Term Ice Storage for Cooling Applications Using Passive Freezing Techniques," Proceedings of the Fourth National Passive Solar Conference, October 3-5, 1979, Kansas City, Missouri, p. 462.

2. A. J. Gorski, et al., "Cooling as Means of Passively Grown Ice," AS of ISES Solar Rising Conference, Philadelphia Civic Center, May 26-30, 1981, paper No. 574.

3. C. E. Francis, A. J. Gorski, "Passive and Hybrid Ice Systems for Comfort Conditioning and Chilling Applications," to be presented at the 7th National Passive Solar Conference and Exhibition, August 29-September 1, 1982, University of Tennessee, Knoxville, TN.

ANALYSIS AND ASSESSMENT OF STES TECHNOLOGIES

D. R. Brown, D. E. Blahnik, H. D. Huber
Pacific Northwest Laboratory*
PO Box 999
Richland, Washington 99352

INTRODUCTION

Technical and economic assessments completed in FY 1982 in support of the Seasonal Thermal Energy Storage (STES) segment of the Underground Energy Storage Program included: 1) a detailed economic investigation of the cost of heat storage in aquifers, 2) documentation for AQUASTOR, a computer model for analyzing aquifer thermal energy storage (ATES) coupled with district heating or cooling, and 3) a technical and economic evaluation of several ice storage concepts. This paper summarizes the research efforts and main results of each of these three activities. In addition, a detailed economic investigation of the cost of chill storage in aquifers is currently in progress. The work parallels that done for ATES heat storage with technical and economic assumptions being varied in a parametric analysis of the cost of ATES delivered chill. The computer model AQUASTOR is the principal analytical tool being employed. The results of this analysis were not available at the time this paper was written; however, completion of the draft report is targeted for the end of FY 82.

ECONOMIC EVALUATION OF ATES HEAT STORAGE

Investigation of the cost of heat storage in aquifers began in late FY81. Costs were estimated for point demand, residential development, and multi-district city ATES system using the computer model AQUASTOR. Background information and preliminary findings were reported at the 1981 Annual Contractors' Review; in FY82, the cost effect of varying a wide range of technical and economic parameters was examined. Those parameters found to substantially influence ATES costs were:

- cost of purchased thermal energy
- cost of capital
- source temperature
- system size
- transmission distance
- aquifer efficiency.

The degree to which these parameters affect the costs, individually as well as collectively, is specified in Aquifer Thermal Energy Storage Costs with a Seasonal Heat Source (Reilly, Brown and Huber 1981). Figure 1 compares ATES-delivered energy costs with the costs of hot water generated from more conventional fuel sources. Levelized costs were calculated for electrically-heated water (at $0.05/kWh and 7% annual escalation) and oil-heated water (at $1.00/gal and 8% annual escalation), and an ATES point demand configuration with a 10-MW peak demand and 25% load factor. The figure suggests that an ATES system offers potentially low delivered energy costs, and that system costs are strongly dependent on the cost of purchased thermal energy.

*Operated for the U.S. Department of Energy by Battelle Memorial Institute under Contract no. DE-AC06-76RLO 1830

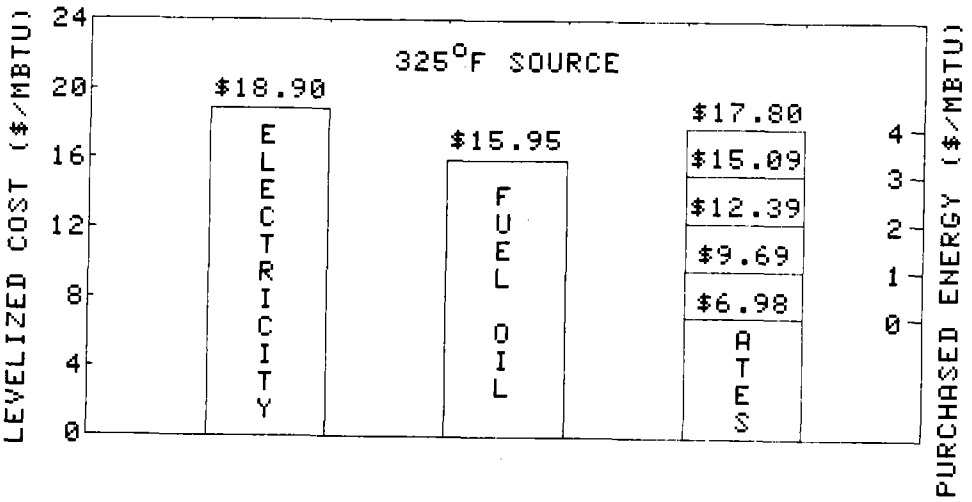

Figure 1. A Comparison of the Cost of ATES Against Conventional Technology

The interplay among cost-influencing parameters is indicated in Figure 2, showing cost components for point demand and multi-district city ATES systems. Capital and thermal energy costs dominate. Capital costs, as a percentage of total costs, increase for the multi-district city due to the addition of a large distribution system. The proportion of total cost attributable to thermal energy would change dramatically if the cost of purchased thermal energy were varied.

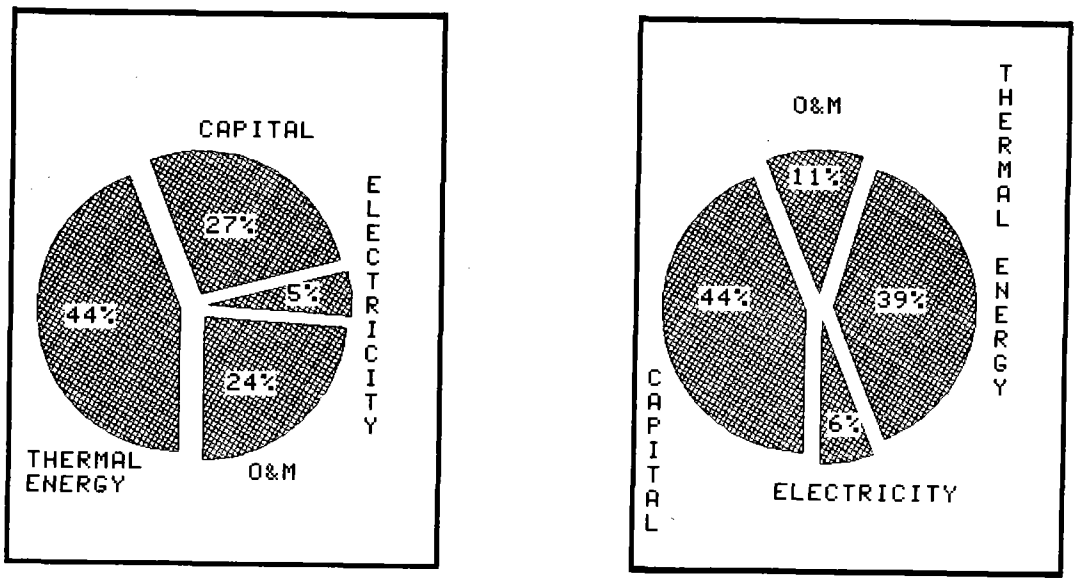

Point Demand

Multi-District City

Figure 2. Aquifer Thermal Energy Storage Component Cost Breakdown

This investigation considered only the storage of energy from a seasonal heat source. Cost estimates were based upon the assumption that all of the energy is stored in the aquifer before delivery to the end user. Systems with near-continuous heat sources would be able to supply some energy directly, and so only a portion of the energy would need to be stored underground. Delivery costs from such systems would be less, because these systems would require less pumping energy, probably a reduction in pipe size and number of wells required, and potentially less heat loss within the aquifer.

DEVELOPMENT OF AQUASTOR

AQUASTOR has been the major tool employed in the investigation of ATES economics at PNL. The model was developed specifically to evaluate the economics of heating or cooling using energy supplied by an ATES system. AQUASTOR optimizes system design and calculates the life-cycle cost of district heating (cooling) using thermal energy supplied by an ATES system coupled to a seasonal energy source. Technical characteristics of supply and distribution systems are combined with financial and tax conditions for the entities operating the two systems into one techno-economic model. This provides the flexibility to individually or collectively evaluate the impact of different economic and technical parameters, assumptions, and uncertainties on the life-cycle cost of providing district heating (cooling) with an ATES system. Development and documentation of the AQUASTOR model was completed in the past year with the publication of User Manual for AQUASTOR: A Computer Model for Cost Analysis of Aquifer Thermal Energy Storage Coupled with District Heating or Cooling Systems (Huber, Brown, and Reilly 1982).

EVALUATION OF ICE STORAGE CONCEPTS

Six seasonal ice generation and storage concepts were technically and economically evaluated at the conceptual design level. The concepts considered represent innovative approaches and techniques of the old idea of gathering and storing winter chill for use during the summer: frozen earth with horizontal tube heat exchanger (HX), ice pond with horizontal tube HX, ice tank with vertical tube HX, ice tank with heat pipe HX, incrementally filled ice pond, and artificial snow pond.

For this evaluation, each concept was designed to deliver an annual load of 10^9 Btu, with a peak load of 1.2×10^6 Btu/h (100 tons). This load size represents a commercial building of median size. The complete cooling system comprises the source (an apparatus using cold winter air to form ice), a seasonal ice storage container, and a supply piping system for transferring the stored chill to a coil in the building HVAC system. System sizing was based on operations in Minneapolis, Minnesota. The Minneapolis climate was chosen for its combination of long, cold winters and a substantial summer cooling load.

Design development for each concept involved calculating the store size, determining the insulation requirements, and sizing the chill transfer equipment. Store size calculations were straightforward, determined primarily by the varying chill capacities (Btu/ft^3) of frozen earth, ice, or snow. Insulation requirements were based on a storage efficiency of 80%, representing a median choice of possible combinations of insulation thickness and store volume.

The method of transferring winter chill from the air to the store is one of the principal distinguishing features of each concept. Three of the concepts use a dual heat exchanger system where heat is removed from the working fluid (50/50 ethylene glycol and water) at an air-cooled coil unit and heat is absorbed by the working fluid through a tubing system within the store. Two of the concepts directly freeze water by either incrementally freezing layers of ice in a pond or creating a mound of ice with a snow-making machine. The other ice storage concept employs a heat pipe to transfer chill from the air to the store. Sizing the dual heat exchanger systems involved an iterative

design process, which considered variable working fluid and ambient air temperatures, tube diameter, spacing, and wall thickness plus thermal transport properties of the working fluid, tubing, and storage medium. Ice/snow formation rates for the other three concepts were based on estimates provided in the literature.

Cost and performance tradeoffs were encountered at almost every decision point in the design development and materials selection process. For example, selection of liner, insulation, and tubing materials has important consequences for ice storage concepts. Liners must isolate the store from its surroundings while withstanding several seasons of freeze-thaw effects. Insulation must maintain its integrity through expansion/contraction cycles and suffer minimal degradation from moisture. Tubing must be selected to meet both structural and heat transfer requirements. Of course, each of the design requirements must be met at a reasonable cost.

Special structural considerations for ice storage concepts involve the expansion/contraction cycle of ice/water mixes and the buoyant loads of submerged icebergs. Allowance for overall expansion was met by including an extra 10% void space in the store containment and tapering the walls outward at slight angles. Major ice loading problems are still possible when the ice logs form on the tubing, especially if differential freezing or thawing occurs. The ice logs create a substantial lifting force on the tubes which must be met by thicker tube walls or a more extensive support system.

In addition to these material and structural problems, several design/cost tradeoffs must be considered in optimizing concept design. Heat exchanger sizes, flow rates, and approach temperatures can be varied for concepts with dual heat exchanger systems. Choosing laminar instead of turbulent flow in the store heat exchanger can result in lower overall piping system cost, even though the store HX itself increases in size and cost. Selection of the appropriate tubing material and configuration must simultaneously consider structural integrity, heat transfer, and cost. Other tradeoffs investigated in this study include liner thickness and material, store geometry, pond cover alternatives, and HX tube orientation.

Both initial capital investment and annual operating and maintenance (O&M) costs were estimated for each concept based on its respective designs. The present worth of each concept was then calculated based on these capital and O&M estimates. The goal of the economic analysis was to provide cost data that are reasonably accurate and allow for equitable comparisons among the concepts.

Capital costs were estimated based on the individual design requirements for each concept. These estimates represent an aggregation of many individual component costs, including charges for contingency, indirects, and land. Land costs were included due to the land-intensive nature of the ice storage systems compared to conventional air conditioning (A/C) systems. Because land costs are extremely site-specific, capital costs and other economic figures of merit are presented both with and without land costs. Table 1 presents capital cost estimates for the six ice storage concepts and a conventional air conditioning system.

TABLE 1. Capital Cost of Ice Storage and Conventional Air Conditioning Systems

Concept	Cost in 1000s of Mid-1981 Dollars	
	With Land	Without Land
Frozen earth	657	595
Ice pond with HX	475	433
Ice tank with HX	584	563
Ice tank with heat pipe	577	554
Incrementally filled ice pond	205	163
Artificial snow pond	219	179
Conventional air conditioning	70	70

Annual O&M costs were disaggregated into operations labor, maintenance supplies and labor, antifreeze (material only; labor for changing antifreeze included in operations), and electricity for pumping. Minimizing annual O&M costs of ice storage systems is essential for them to be competitive with conventional air conditioning (A/C) systems. Ice storage systems are quite capital-intensive compared to conventional A/C systems and must "repay" the incremental investment with annual savings in O&M costs. Annual O&M costs are listed by category in Table 2.

TABLE 2. Annual Operating and Maintenance Costs

Activity	Cost in 1000s of Mid-1981 Dollars						
	A/C	Earth	Ice Pond w/HX	Ice Tank w/HX	Heat Pipe Tank	Inc. Fill Ice Pond	Snow Pond
Operations	0.6	3.3	3.3	3.3	1.9	2.7	4.1
Maintenance	1.1	7.0	5.5	8.0	7.9	2.4	2.7
Antifreeze	0.0	1.2	2.4	1.7	0.0	0.0	0.0
Power	18.0	2.0	2.5	2.5	0.2	0.2	0.6
Total	19.7	13.5	13.7	15.5	10.0	5.3	7.4

Each concept was subjected to a life-cycle (present worth) cost analysis based on the estimates for initial capital investment and annual O&M expenses. Economic assumptions chosen for the analysis are intended to represent the financial situation for a potential ice storage system end user. Values of economic parameters used in the analysis are given in Table 3. Present worth estimates for ice storage and conventional air conditioning systems are presented in Table 4.

TABLE 3. Economic Parameters for Present Worth Analysis

Parameter	Value
Investment tax credit	10%
Debt to equity ratio	50/50
Salvage value	0
Debt rate	10%
Discount rate (before tax)	16%
Effective income tax rate	50%
General inflation rate	6%
Energy escalation rate	8%
O&M escalation rate	6%
System life (years)	20
Price year	1981
Year of operation	1985

TABLE 4. Present Worth of Ice Storage and Conventional A/C Systems

Concept	Present Worth (Cost in 1000s of mid-1981 dollars)	
	With Land	Without Land
Frozen earth	450	394
Ice pond with HX	346	308
Ice tank with HX	421	401
Ice tank with heat pipe	386	364
Artificial snow pond	178	140
Incrementally filled ice pond	159	120
Conventional A/C	155	155

Both the incrementally filled ice pond and the artificial snow pond appear to be strong competitors with conventional air conditioning technology. These two concepts offer comparably low delivered energy costs and a minumum of potential technical difficulties.

The Comparative Analysis of Seasonal Ice Storage Concepts (Blahnik and Brown), documenting this evaluation in detail, will be issued by the end of FY82.

RESERVOIR STABILITY STUDIES: POROUS MEDIA ANALYSIS

T. J. Doherty
Pacific Northwest Laboratory*
Richland, Washington 99352

INTRODUCTION

The Reservoir Stability Studies are within the Compressed Air Energy Storage (CAES) Project of the Underground Energy Storage Program, managed by Pacific Northwest Laboratory (PNL) for the U.S. Department of Energy's Energy Storage Technology Division. A unique aspect of CAES is the use of large geologic containments for air storage. They provide sufficiently economical storage to allow feasibility of CAES for large-scale utility load shifting applications. CAES has significant potential for oil conservation and reduced peaking power rates in this role. Three types of reservoirs are candidates for this use: excavated hard rock caverns, solution-mined salt caverns, and structural traps in aquifers. A wide range of geotechnical information and experience is available to guide the engineering of such storage reservoirs. However, this information does not directly address the technique of air storage, which differs from past experience with such geotechnical structures due to long-term cyclic use for CAES. This use can induce mechanical, thermal, and geochemical responses that must be investigated to ensure the integrity of the storage reservoirs. A comprehensive evaluation using existing information and original research on CAES operational concerns, was required to provide the utility industry with confidence to proceed with CAES. The Department of Energy instituted the Reservoir Stability Studies to meet these needs in 1977. This paper discusses the current status of that work.

PROJECT OBJECTIVES AND STRUCTURE

The Reservoir Stability Studies are based on the premise that long-term reservoir stability is the key technical issue impeding CAES implementation. The objective of the studies is to establish stability criteria and the accompanying technology base for large underground air storage reservoirs used for utility applications. Each of the three reservoir types (hard rock, salt, and aquifer) was the focus of a four-phase effort consisting of 1) a state-of-the-art survey resulting in preliminary criteria, 2) numerical modeling, 3) experimental investigation to address CAES specific concerns, and 4) final field study, if required, to answer remaining technical questions and validate previous work. The preliminary criteria generated early in the project provided both qualitative and quantitative guidelines. These criteria evolved as research and development work was completed. The end product of the research performed on each reservoir type is a document on final stability criteria and guidelines.

PROJECT STATUS

By FY 1982 the Reservoir Stability Studies had completed the generic numerical and experimental work in all three reservoir types. Hard rock caverns studies did not proceed to a field study, but the methodologies developed were applied to existing designs and candidate

*Operated for the U.S. Department of Energy by Battelle Memorial Institute under Contract no. DE-AC06-76RLO 1830

materials to evaluate applicability. This work was completed, and the final version of the stability criteria for hard rock caverns has been published. A summary of this work is provided at this review in the paper by Arlo Fossum of RE/SPEC, Inc.

Early salt research, which concentrated on domal salt structures and materials, was validated by bench-scale testing in the Cote Blanche mine. This work was completed during FY82 and resulted in issuance of a final version of the salt stability criteria. This work is summarized at this review in the paper by R. L. Thoms of Louisiana State University.

Aquifer studies have progressed through preliminary criteria generation, experimental and numerical studies. Effort on aquifer storage is presently in the field study stage. That field study is the only remaining activity in the Reservoir Stability Studies and will, along with its experimental and numerical support functions, draw to a close during the first half of FY83. At that point, continued work will be transferred to EPRI.

The following two sections describe some of the supporting effort in the field study during this period. John Istvan of PB-KBB, Inc. reports on Pittsfield Aquifer Field Test design and construction activities in a paper which is also provided at this review.

EXPERIMENTAL STUDIES

The knowledge of the physical behavior of aquifer sandstone and its potential alteration under CAES conditions is of primary importance in determining long-term reservoir stability. The CAES Porous Media Flow Loop (PMFL), completed in FY81, is being used as a laboratory simulator of anticipated field conditions for the Pittsfield field test. Samples of reservoir material can be tested in the laboratory to provide an understanding of the nature of flow through porous rock, to make lab-field data correlations, and to predict long-term reservoir stability.

PMFL experiments are designed to investigate stress and temperature effects on permeability, fatigue under temperature and stress cycling, and measurement of the rate of desaturation. Work in FY82 has concentrated on the effects of temperature and temperature cycling at in-situ stress conditions on the permeability of Pittsfield-St. Peter sandstone.

Typical Pittsfield samples labeled 655, 657, and 703 from in or near the injection/withdrawal (I/W) borehole were tested. The experimental conditions imposed on the samples (e.g., temperature, pressure) are consistent with expected operating conditions. Each sample was hydrostatically confined to a pressure of 1200 psi and pore gas pressure controlled at 275 psi. Dry air (0 to 1% relative humidity) was injected into the samples and permeabilities were measured at temperatures ranging from 20° to 80°C (70° to 300°F). In steady-state permeability measurements, the reservoir sample was allowed to dwell at each temperature for a period of hours before heating or cooling to the next temperature setpoint. Using the computerized data acquisition

system, instantaneous permeability is also being measured continuously during temperature cycles.

Results of the FY82 experiments are illustrated in Figures 1-3. Figure 1 represents instaneous permeabilities for samples heated at a rate of approximately $1^{o}F$/min. These typical results suggest insignificant changes in permeability on heating from ambient to near $200^{o}F$. In other experiments, samples were cycled between 70^{o} and $350^{o}F$ at a constant confining pressure of 1200 psi. Permeability after a single cycle of the 657 sample (Figure 2) was approximately 15% lower than the initial permeability at ambient conditions. Similar data for three temperature cycles are shown for sample 703 in Figure 3. The greatest permeability reduction occurred during the first heating/cooling cycle. The strain data obtained for these experiments indicate that sample deformation is probably not the cause of the permeability hysteresis. Alternative explanations for this sample behavior are internal rearrangement of sandgrains and migration of fine particules within the rock sample.

NUMERICAL STUDIES

Thermohydraulic, two-phase and phase change models developed at PNL in the past have been used extensively during FY82 to support design and development of the field study and to perform predictions of the tests response. Preliminary analysis has been reported previously. Final predictive analyses are underway. They will be complete prior to the operational phase of the field test. These final analyses are based on the extremely detailed data base ensuing from recent PNL and PB-KBB geologic reservoir characterization. They include refined well completion information, reservoir geometry data and a better characterization of the reservoir vertical stratigraphy in the near-wellbore region. Two fundamental analyses are discussed here: bubble development and isothermal air injection and withdrawal cycling.

Bubble Development

In bubble development, the initial reservoir operation air is injected continuously into the reservoir to develop an adequate storage volume. Initially the reservoir is fully saturated; injected air then displaces a portion of the mobile water. Some water is retained behind the displacement front due to capillary pressure and reduced liquid mobility as the saturation decreases. As a result, the displacement of water by air is represented by a relatively broad front within which the saturation varies from near the irreducible value at the center of the bubble to the fully saturated conditions at the perimeter of the bubble. Bubble development is complete when sufficient air has been injected to preclude large fluctuations in the nominal reservoir pressure during air cycling operations.

The bubble development simulations can be summarized by reviewing results showing the advance of the 50% saturation front with time (Figure 4). The 50% saturation front is shown because there is very little air ahead of the front and liquid mobility is relatively low behind the front. Thus, the 50% saturation front is representative of the true bubble size. The most important result shown here is that a

bubble of adequate size can be obtained with 60 to 75 days of air injection at 1250 SCFM. For the Pittsfield reservoir the volume of the cushion air mass did not determine adequate bubble size. Instead, it was necessary to depress the air-water interface well below the injection/withdrawal zone to minimize the possibility for water coning.

Other important features of the bubble development include the fingering in the high permeability zone below the wellbore. Excessive fingering could result in a loss of closure in the field test. The calculations suggest fingering is not likely to be a problem with careful injection control. If fingering is detected in the field, the model can be used to check injection schedules that may reduce the effect. Note that the final equilibrated bubble is essentially flat and extends to a radius in excess of 400 m.

Isothermal Air Cycling

Following bubble development, cyclic injection and withdrawal of air will be initiated. Several cycles have been evaluated to determine the pressure response and potential for water coning. Water coning in a CAES porous media reservoir can occur due to an imbalance of pressure gradients and water mobility between the injection and withdrawal portions of the daily cycle. The result of this imbalance is a gradual cyclic migration of water toward the wellbore. Operational controls such as periods of reservoir closure and skewed cycles that withdraw air at a slower rate are available to reduce the imbalance causing water coning, but these operational controls must be limited by utility operational needs. Operation without water production depends in practice on low vertical permeability, a feature that is typical in sedimentary strata such as the Pittsfield reservoir.

The air injection/withdrawal cycle that has been decided upon for the field test and analyzed here is 7 hours of injection, 11 hours of withdrawal, and 6 hours of reservoir closure. This cycle will be carried out 5 days per week. On the weekends the reservoir will be closed. This cycle has equal injection and withdrawal mass per day and balanced pressure gradients on alternate sides of the cycle. This result is shown in Figure 5, which indicates pressure gradients during cycling and after 60 days of bubble development. During the injection cycle the pressure difference driving air into the reservoir is approximately the difference between injection pressure and closure pressure. These pressure differences are about equal. The general decay of reservoir pressure is due to continued equilibration of the bubble as it expands against the hydrostatic pressure.

Water saturation profiles below the injection/withdrawal zone are shown in Figure 6 for weeks 1, 5, and 10. There is a large increase in saturation a few meters below the wellbore but this is partially attributable to equilibration of the bubble. The saturation increase in the immediate vicinity of the wellbore is quite small. The low net vertical permeability (135 md) that recent core analysis indicates within the reservoir stratigraphy and the benefit of a skewed cycle apparently may reduce or eliminate water production concerns for the Pittsfield aquifer field test.

CONCLUSION

The Reservoir Stability Studies Project is nearly complete. All hard rock and salt research studies have been completed and stability criteria for these two reservoir types were published in 1982. Generic numerical and experimental work on porous media are complete; these activities now support the field work. The Pittsfield Aquifer Field Test previously completed its exploration, initial permitting and leasing activities. The construction phase of that project including the well field, surface facilities, and instrumentation systems is to be complete at the end of FY82 under the direction of PB-KBB, the operations contractor. This DOE project will be complete in its entirety after a period of field test operations. The aquifer criteria will be published in March 1983.

REFERENCES

Allen, R. D., T. J. Doherty, and R. L. Thoms. 1982. Geotechnical Factors and Guidelines for Storage of Compressed Air in Solution Mined Salt Cavities. PNL-4242, Pacific Northwest Laboratory, Richland, Washington.

Allen, R. D., T. J. Doherty, and A. F. Fossum. 1982. Geotechnical Issues and Guidelines for Storage of Compressed Air in Excavated Hard Rock Caverns. PNL-4180, Pacific Northwest Laboratory, Richland, Washington.

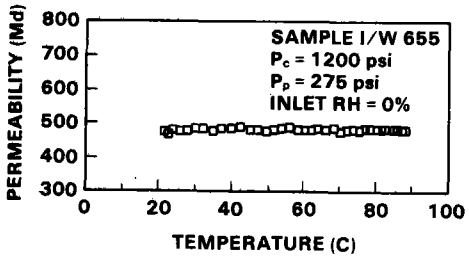

Figure 1. Permeability Versus Temperature

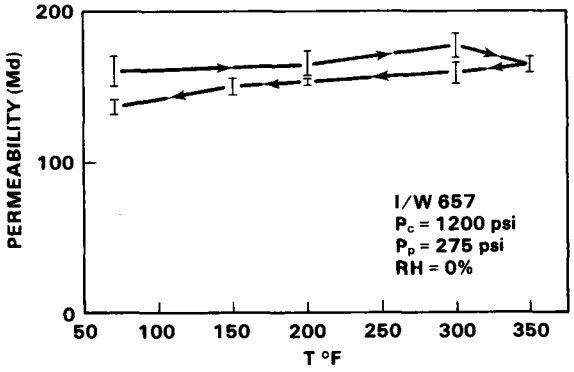

Figure 2. Permeability Versus Temperature, One Cycle

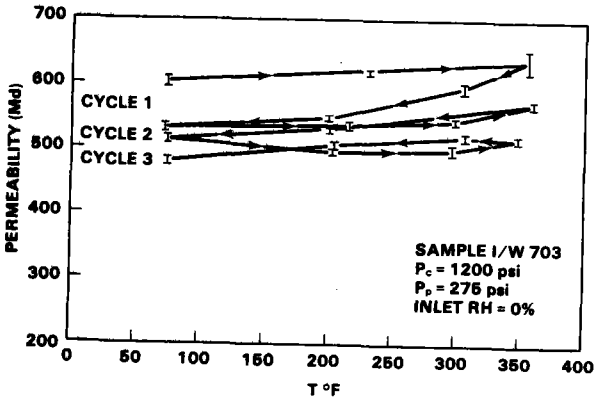

Figure 3. Permeability Versus Temperature, Three Cycles

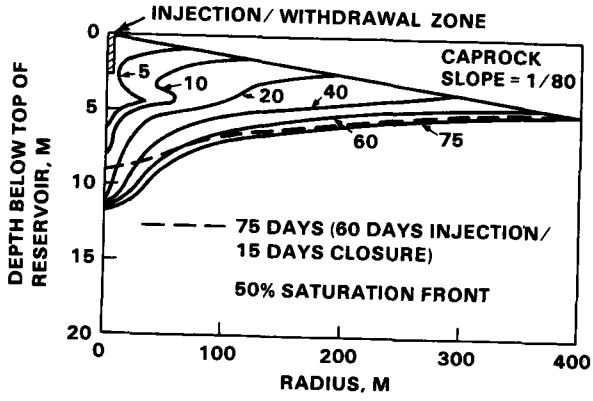

Figure 4. Bubble Development (Stratified Permeability)

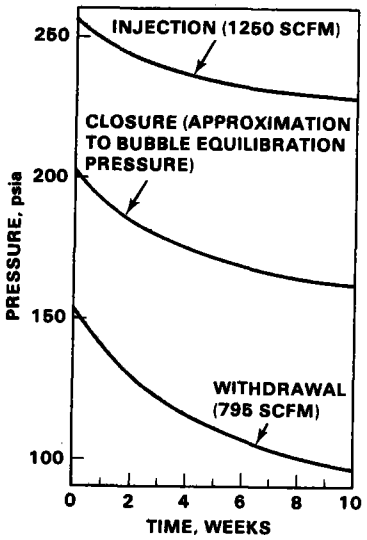

Figure 5. Bottom Hole Pressure During Cycling

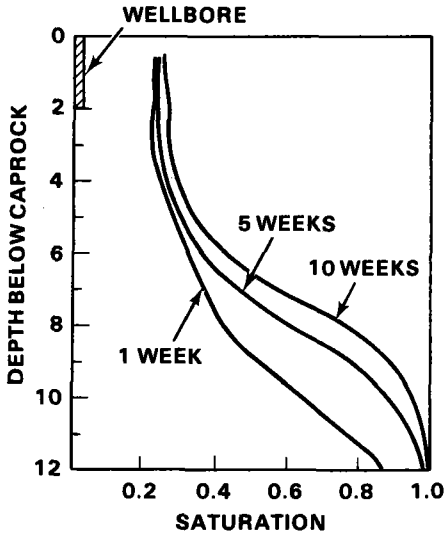

Figure 6. Saturation Below the I/W Well Versus Cycling Time After Bubble Development

SALT STUDIES: CONCLUSIONS

R. L. Thoms and R. M. Gehle
Institute for Environmental Studies
Louisiana State University
Baton Rouge LA 70803

Introduction

This report represents the conclusion of the compressed air energy storage (CAES)program in salt. It includes a brief background of salt cavity studies and utilization for CAES, then focuses on long-term stability criteria for solution mined salt cavities. Summary statements are made on some of the more important criteria and their significance for operational peaking-power plants utilizing salt cavities for CAES reservoirs.

The concluding section of this report incorporates a discussion of the future for CAES in U. S. salt deposits. This discussion is based mainly on technical considerations, since they have been the main consideration in this particular study. Obviously, economic analyses will dominate decisions by utilities on construction schedules for any technically feasible CAES study.

Background of CAES in Salt

The highly successful Huntorf plant in the Federal German Republic (FGR) has demonstrated the advantages of CAES. This plant utilizes two solution mined cavities in the Huntorf salt dome for CAES reservoirs. Herbst and Quast, in separate papers (1, 2) summarized the success of the Huntorf plant during presentations to the 1981 Energy Storage Conference in Seattle.

In the U. S. during the mid-seventies, the Electric Power Research Institute (EPRI) reflected the interest of electrical utilities in CAES by sponsoring work on a conceptual design for a peaking-power plant which utilized solution mined cavities in a Gulf Coast salt dome (3).

As part of the Department of Energy (DOE) sponsored work through Battelle Pacific Northwest Laboratory (PNL), Thoms and Martinez in 1978 published a report on preliminary criteria for stability of CAES cavities in salt (4). Following this preliminary study, a more lengthy and technical test program was undertaken by LSU personnel. About the same time, Serata Geomechanics, Inc. (SGI) personnel dealt mainly with numerical modeling aspects of CAES cavities in salt.

Recently, a report on stability criteria for CAES salt cavities was published by PNL (5). This report summarizes stability criteria from the overview of PNL personnel with input from subcontractors at LSU and SGI in the CAES salt study. The criteria presented in the PNL document are the subject of the next section of this report.

Guidelines for Stability of CAES Salt Cavities

Salt cavities (or caverns) utilized for CAES will undergo daily cycles of air pressure, temperature and humidity. The cyclic, compressible fluid (air) pressurizations of relatively short periods distinguish CAES effects on salt caverns from liquid-filled or seasonally cycled gas storage systems. Cyclic CAES effects on salt caverns potentially could be more damaging than more traditional storage (i.e., hydrocarbons) and thus must be controlled.

The PNL document (5) lists topics evaluated in recent studies that could affect CAES caverns:

- cavern geometry and size
- long-term creep and creep rupture of rock salt
- effects of pressure and temperature loading rates
- low frequency fatigue, coupled with cyclic pressure, temperature, and wetting conditions
- progressive deterioration of salt fabric with possible air penetration
- cavern monitoring methods
- salt properties at nonambient conditions

Several criteria also were identified that could serve as guidelines for long-term stability of salt caverns:

- Cavity floor depths to 1524 m may be acceptable depending on site conditions. For the anticipated maximum operating pressures on 9.0 MPa or less, optimal depth to cavern roof is about 800 m. (Maximum air pressure is to be 1.64 MPa per 100 m of depth.)
- Cavity wall temperatures should not exceed $80^{o}C$.
- Cavity separation (center-to-center) to diameter ratio (SD) should be at least 4. Salt thickness between a cavern wall and the lateral salt dome boundary should be at least 3 times the cavern diameter.
- Minimum thickness of salt above a solution cavity should be 150 m. The ratio of overburden salt thickness to cavity span is to be at least 2.5. Cavern span should not exceed 60 m.
- Cavity height to diameter ratio (H/D) should be in the range of 1 to 5.
- Octahedral shear strength should lie between 3.8 and 5.2 MPa.

- In-situ horizontal stress should not exceed 120% of overburden pressure.
- Depressurization should not exceed 1 MPa/hr.
- Salt cavities must be protected against ground water encroachment.
- Surface subsidence in the region overlying a CAES cavity must not be significant.
- Accessory minerals in salt reduce self-healing of fractures and contribute to irregular cavern shapes. Site selection will take this into consideration.

The listed topics and guidelines (or possible criteria) were intended for cavern designers dealing specifically with CAES applications. Site studies using principles of sound geotechnical engineering, along with some knowledge of CAES technology, would enhance implementation of the guidelines. Some explanatory comments follow on the significance of the guidelines as they relate to implementation of CAES salt caverns.

The cavity (cavern) floor depth of 1524 m reflects a limit on possible pressure difference between the overburden and cavern. The value of 1524 m depends on site conditions (as noted). In some locations a more conservative (smaller) depth may be advisable, particularly if the ratio of lateral/vertical in-situ stress exceeds unity. Maximum pressure difference will be achieved with caverns at atmospheric pressure. This will occur initially following cavity formation and brine emptying by "airlift," and subsequently when the cavern is depressurized for plant maintenance purposes.

The listed maximum cavern air pressure of 1.64 MPa per 100 m of depth is based on guidelines to avoid "fracing" the salt formation. In the geostorage industry working in salt, the value of working cavern pressure per unit of depth is associated with depth to the casing seat. Also, frequently a larger cavern pressure is allowed for dome salt than for bedded salt.

Cavity wall temperatures below 80°C are desirable to control salt creep, which is strongly sensitive to elevated temperatures. Thermal energy storage units between the surface plant and CAES salt caverns would essentially eliminate this consideration.

Cavity separation, minimum salt thickness between caverns ("pillar" or "wall"), and minimum thickness of salt above a cavern ("salt roof") are based upon studies cited in the PNL document (5). In general these guidelines are based mainly on operating experience and analyses for domes. In bedded salt the minimum salt roof thickness may be difficult to achieve because of available bed thickness. Then special consideration must be taken to avoid fracturing the salt formation above and below the caverns. Some states (e.g., Louisiana) have existing regulations for cavern configurations which constrain variance in design.

Ratios of cavern height-to-diameter usually are influenced by amounts of salt available at desirable depths for caverns. Deeper CAES

caverns become expensive because of the large diameter entries that must be drilled. Although an H/D ratio of unity may be most stable (more nearly spherical), many recent controlled storage configurations use H/D values larger than unity, e.g., three to four.

Salt strength and in-situ stress states are site specific characteristics of salt formations. They should be assessed by a coordinated site investigation and complementary rock mechanics study. In particular, near some western U. S. salt deposits, the local geology implies past or ongoing tectonic processes. These sites should be investigated for unusual geostatic stress states that might cause rapid cavern volume loss by creep closure.

Rapid cavern depressurization corresponds to rapid increase in pressure difference, and has caused roof falls in a German test cavern. The depressurization rate of 1 MPa/hr is based on a study cited in the PNL document (5).

Protection of CAES salt caverns from ground water is essential. This is largely a matter of sound drilling and casing programs, and careful maintenance. Control of surface subsidence also is important, although subsidence should be minimal if the previous cavern/salt configurations are observed. However, bedded salt deposits may require violation of the 150 m salt "roof" guideline, as noted previously, and thus might be more susceptible to possible subsidence.

Presence of accessory minerals should be taken into account in cavity formation. Anhydrite and potash are respectively insoluble and more readily soluble minerals frequently found in rock salt formations. Insolubles tend to cause stringers or ledges in cavities that can break off and damage tubing or casing, whereas "washouts" are caused by deposits of more soluble evaporites such as potash.

The PNL document (5) also includes topics other than stability criteria, e.g., a relatively detailed description of cavern formation by soluble mining. Monitoring methods also are noted. These topics will not be covered here because of space limitations.

CAES in Salt: the Future Based on Technical Considerations

From a technical viewpoint, CAES in salt makes a great deal of sense in many parts of the U. S. Conventional pumped-hydro energy storage is not feasible in areas with little topographic relief such as the Gulf Coast and many parts of the Midwest, Southwest, and Western Plains. However, salt deposits with potential for CAES occur in many of these same areas.

The Huntorf plant has demonstrated the advantages of CAES in German salt domes. Tests performed at LSU under the concluding study indicate U. S. Gulf Coast dome salt to be generally equal in performance to the Huntorf salt. Variations exist in U. S. salt formations, especially between bedded and dome salt. Examples can be noted in engineering and geological data available for salt basins through the U. S. National Waste Terminal Storage (NWTS) program for radioactive wastes. In any case, site specific studies must be performed to assess the suitability of a particular location for CAES salt reservoirs.

The U. S. Gulf Coast with its industrial growth and relatively well-known salt domes appears particularly suitable for CAES implementation. Currently this is reflected in advanced activity by electric companies in Alabama (6) and Houston. Other CAES activity has been reported in Mississippi and Louisiana. Planning for CAES also has been reported in the Midwest, and to some extent, in the Southwest.

The authors are of the opinion that satisfactory CAES caverns, based on geotechnical considerations, can be solution mined in many U. S. salt deposits. However, economic considerations obviously will dominate plant construction schedules. When economics indicate a "go-ahead," there exists a positive response on CAES technical feasibility in U. S. salt deposits.

Acknowledgements

This work was supported by the U. S. Department of Energy (DOE) under Subcontract No. B-67966-A-H-0, Laboratory Tests of Rock Salt Subjected to Compressed Air Energy Storage (CAES) Load Environments, through Pacific Northwest Laboratory (PNL), operated for the DOE by Battelle Memorial Institute.

References

1. H. C. Herbst, "The CAES Power Plant - A Tool in the Load Dispacher's Hands in an Electric Utility System", Proc. Inter. Conf. on Seasonal Thermal Energy Storage and Compressed Air Energy Storage, pp. 615-625, CONF-811066, Vol 2, National Technical Information Service, Springfield, VA., 1981.

2. P. Quast, "The Huntorf Plant: Over Three Years Operating Experience with Compressed Air Caverns", Proc. Inter. Conf. on Seasonal Thermal Energy Storage and Compressed Air Energy Storage, pp. 562-573, CONF-811066, National Technical Information Service, Springfield, VA., 1981.

3. G. H. Vosburg, "Conceptual Design for a Pilot/Demonstration Compressed Air Storage Facility Employing a Solution-Mined Salt Cavern", EPRI EM-391, Electric Power Research Institute, 3412 Hillview Ave., Palo Alto, CA. 94304, 1977.

4. R. L. Thoms and J. D. Martinez, "Preliminary Long-Term Stability Criteria for Compressed Air Energy Storage Caverns in Salt Domes", Institute for Environmental Studies, Louisiana State University, 1978.

5. R. D. Allen, T. J. Doherty, and R. L. Thoms, "Geotechnical factors and Guidelines for Storage of Compressed Air in Solution Mined Cavities", PNL 4242 , Pacific Northwest Laboratory, May, 1982.

6. B. Clausen, A. J. Karalis, and E. J. Sosnowicz, "Meeting Low Growth with a Compressed Air Energy System", Proc. Inter. Conf. on Seasonal Thermal Energy Storage and Compressed Air Energy Storage, pp. 626-631, CONF-811066, Vol 2, National Technical Information Service, Springfield, VA., 1981.

HARDROCK STUDIES: CONCLUSIONS

A. F. Fossum
RE/SPEC Inc.
Rapid City, SD 57709

ABSTRACT

The objective of the hard rock reservoir stability studies project was to develop geotechnical criteria for the design and stability of caverns in hard rock formations that would be used to store compressed air for utility load leveling operations. To develop these criteria, a sequence of studies was formulated including state-of-the-art assessment, numerical model development, and an experimental program. This sequence was started in FY 1978 and completed in FY 1981.

During FY 1982, final stability criteria and guidelines were assembled into a report that integrated the geotechnical data base obtained from the sequence of hard rock studies. This document provides a resource that can be used to address concerns regarding long-term cavern stability by those who are responsible for CAES development.

INTRODUCTION

A novel feature of the compressed air energy storage (CAES) concept is that a subsurface cavern is used as a large pressure vessel. Because of its large size, the cavern can be used to store a vast amount of energy in the form of compressed air. Since conventional turbine peaking plants make use of compressed air, it is logical and convenient to store energy in this form. If base load plants not using petroleum fuels are used during off-peak periods to compress the air, then the turbines which use petroleum fuels are not needed to drive air compressors. This concept has the potential for reducing peaking plant consumption of petroleum fuels by more than 60 percent. In addition, this concept offers a number of other advantages over conventional systems used by utilities for meeting peak load requirements (1-2).

Early in the development of the CAES concept, concern was raised regarding the ability of the host rock medium to maintain its structural integrity throughout the operational lifetime of the CAES facility (30 to 50 years). Assurance of adequate reservoir stability was considered crucial to commercialization of CAES systems. Thus, to provide utilities with a high degree of confidence in the concept, a long-term technology research and development program was formulated to develop geotechnical criteria for the design and stability of CAES caverns in hard rock formations. The program included state-of-the-art assessment, numerical model development, and experimental studies. This sequence was started in FY 1978 and completed in FY 1981. In FY 1982 a report (1) was issued providing the final stability criteria and guidelines for use by the engineering community to ensure stable operation of underground CAES reservoirs.

PROJECT DESCRIPTION AND OBJECTIVES

The objectives of this paper are to summarize the results of the overall hard rock studies program and provide an indication of what is happening in the industry for the future.

Work began with the state-of-the-art survey and proceeded to numerical model development and application. While the numerical model development was in progress, generic laboratory evaluations started and led to specific experimental studies. The state-of-the-art survey enabled preliminary stability criteria to be assembled. These criteria were refined in a step-by-step fashion throughout the process and completed at the end of the study sequence. The elements in the study sequence had the following objectives:

- State-of-the-Art Survey: To establish preliminary reservoir stability criteria and identify areas requiring further research and development.

- Numerical Modeling: To develop and use numerical models to evaluate the behavior of CAES caverns in hard rock parametrically under a wide variety of CAES operating and geotechnical conditions; and refine preliminary stability criteria.

- Laboratory Testing: To examine issues not appropriate or amenable to numerical modeling; provide input data for numerical models; and update reservoir stability criteria.

ACCOMPLISHMENTS

At the outset of the project it was concluded that because of the high excavation costs associated with the larger volumes required by other storage schemes, a CAES reservoir in hard rock would probably be a constant pressure, water-compensated cavern. The state-of-the-art survey identified a number of design concerns that follow from the fact that large rock masses have never before been subjected to the daily temperature cycling and wall wetting that would occur during the proposed operating cycle of a CAES facility. These concerns involved the following:

- Cavern geometry and size
- Cavern orientation
- Thermal response
- Low frequency fatigue associated with temperature cycling and wetting
- Air penetration of rock mass
- Hard rock properties at nonambient conditions
- Residual strength of hard rock after failure
- Mineralogical alteration of hard rock under CAES conditions with temperature cycling and wetting
- Air penetration of rock mass
- Hard rock properties at nonambient conditions

- Residual strength of hard rock after failure
- Mineralogical alteration of hard rock under CAES conditions.

To answer many of the questions raised, numerical models were developed with the capability of simulating the excavation processes and cyclic thermoelastic and pressure loading typical of CAES. Parametric analyses of the excavation phase of CAES caverns produced a catalogue of stress concentration factors for single and multiple caverns with different shapes and extraction ratios under a range of initial in situ stress states. This information was related to case history data to determine artificial support requirements for caverns situated at a depth of 750 m in igneous rock. It was found that multiple caverns could be located in competent rock at 750 m without cavern collapse. Substantial strength reductions caused by local rock failure or thermal shock did not alter this conclusion.

Air leakage was found to be affected by stress ratio but was predictable and insignificant for most conditions. A review of European experience supported these conclusions.

Laboratory studies indicated that strength reductions can be expected in the tensile and compressive strengths of rock masses subjected to a CAES cavern environment. The percentage loss of failure strength of the rock decreased with increasing mean stress, and most of the damage caused by thermal shock was caused in the first few cycles, indicating that a rock mass would probably shake down quickly to a stable behavior. It was also shown that foliated and/or jointed rock masses require special attention, and assessment of strength requirements and strength values become quite site specific.

A synthesis of the results that came from each element in the sequence of hard rock reservoir stability studies has been issued in the form of a report (1) entitled, "Geotechnical Issues and Guidelines for Storage of Compressed Air in Excavated Hard Rock Caverns". This report develops and presents geotechnical criteria for the design and stability of CAES caverns in hard rock formations. These criteria involve geologic, hydrological, geochemical, geothermal, and in situ stress state characteristics of generic rock masses. Throughout the text the relevance of each of the criteria to CAES caverns is discussed. The design criteria are established from the viewpoint of 1) the type of CAES system, 2) the desired air volume and pressure, and 3) the thermal/rock mechanics/hydrologic constraints appropriate to the rock mass. These constraints are used in determining optimal cavern shape, cavern orientation, dimensions and spacing, and excavation methods.

The report concludes with a table of guidelines and stability criteria that are currently available to the CAES cavern designer. Categories include general geological environment, hydrology, host rock characteristics, structural characteristics, other geological characteristics, design parameters, and operating parameters.

In summary, the following conclusions regarding air storage in hard rock masses have been identified:

- Rocks must be competent and capable of sustaining openings with minimal support and rock improvement measures. Candidate rock types include granite/granodiorite, quartzite, massive gneiss, dolomite, and limestone.
- Rock masses must be characterized by overall hydraulic conductivities less than 10^{-8} m/sec for water.
- Long-term containment of stored air may not be possible in tightly folded, heavily fractured, jointed, or faulted rocks.
- Cavity geometry and orientation must be selected for minimal support requirements. Important geologic parameters include extent of fracturing, nature of joint surfaces, permeability in zones of weakness, and hydrologic conditions.
- Storage cavern design and construction must minimize slaking, spalling, and loss of ground water above the cavern.
- Cyclic temperature and humidity variations must not significantly decrease rock strength by fatigue.
- Geologic formations with high horizontal in situ stresses are unfavorable. Maximum horiziontal stress should not exceed vertical stress by more than a factor of 1.5.
- The construction cost of CAES caverns can be seriously impacted by conditions such as degree of jointing and faulting and incompetence of the overburden. Access shafts for CAES caverns should not be sunk in areas with more than 50 m of incompetent, water-bearing overburden.

In addition, the following guidelines should be considered when contemplating a CAES reservoir in hard rock:

- Hydrostatic pressure within the host rock should balance the pressure of stored air.
- The "champagne effect", rapid evolution of air in the water column connecting the cavern to the surface lake, must be considered in the design of CAES plants with compensated caverns.
- Unconfined compressive strength should exceed 25 MPa over the cycling life of the caverns.
- The nearest dissimilar geologic formation contact should not be closer than 100 m.
- Areas of active volcanism, faulting, seismic activity, excessive subsurface solution, and subsidence should be avoided.

- Long axes of caverns should be oriented with respect to structural discontinuities and in situ stress fields to maximize stability and minimize construction costs.

- Because of operating requirements, the most likely cavern depths will be 750 to 850 m.

- Air loss should not exceed 1 percent of the storage volume during the storage period.

- Operating pressures, essentially constant, will fluctuate within a very narrow range with differences caused by variations in the effective height of the water-compensating column. The most likely design range for operating pressures is 7.35 to 8.33 MPa. Maximum charging pressure will be 12.0 kPa/m of depth.

- Compensating water temperature may fluctuate between 0 and 30°C, and compressed air will enter the cavern at 30 to 80°C.

- Cavern depressurization should be gradual not exceeding 1 MPa per hour.

The chief geotechnical issues for the development and operation of CAES caverns in hard rock are impermeability for containment, stability for sound openings, and hydrostatic balance.

INDUSTRIAL INTEREST IN CAES

Although several utilities have expressed an interest in CAES development, only one, the Soyland Power Cooperative, Inc., has made plans to construct such a facility. The interested reader is referred to the Technology Assessment Report (2), which describes the design and operational features of the proposed Soyland plant.

ACKNOWLEDGEMENT

This work was supported by the U.S. Department of Energy under Subcontract No. B-B5230-A-0/Prime Contract DE-AC06-76RL0-1830 with Pacific Northwest Laboratory operated by Battelle Memorial Institute.

REFERENCES

1. Allen, R. D., Doherty, T. J., and Fossum, A. F., "Geotechnical Issues and Guidelines for Storage of Compressed Air in Excavated Hard Rock Caverns," - PNL Rept. 4180, Apr 1982.

2. Environmental Science and Engineering, "Technology Assessment Report for the Soyland Power Cooperative, Inc. Compressed Air Energy Storage System (CAES)," - PNL Rept. 4077, Jan 1982.

RSI-PUBL NO. 82-10

CAES IN AN AQUIFER
PITTSFIELD, ILLINOIS

J. A. Istvan
PB-KBB Inc.
P. O. Box 19672
Houston, Texas 77224

A. INTRODUCTION

The purpose of this report is to present and document the operational analysis of the aquifer air storage system under specific site conditions.

Certain assumptions of reservoir properties, such as porosity and permeability were based on laboratory tests performed on core samples recovered during drilling of the wells. The validity of these assumptions can only be verified by actual field testing of the facility.

The program calls for initial development of an air bubble by injection of dried compressed air at a nominal wellhead pressure of 300 psig at about 20°F above ambient. This will have the effect of removing much of the water in the reservoir surrounding the injection well prior to commencement of the injection/ withdrawal cycling at the higher temperatures.

Following development of the bubble and initial cycling, injection will commence with air incrementally heated to 392°F. This heated air will then be cycled as before and vented to the atmosphere during the withdrawal phase.

B. SYSTEM DESCRIPTION

1. Air Injection Cycle (Figure 1)

   During formation of the air bubble, air will be compressed, dried and injected into the reservoir at 300 psig and about 100°F. During the bubble development stage air will not pass through the air heater. Pressure and temperature will be monitored and recorded at the surface, and reservoir data will be measured by the:

   a. sampling logging wells to obtain samples of the formation fluids and measure formation water saturation, and
   b. instrument wells to measure pressure, temperature and water saturation.

2. Heated Air Cycle

   During the periods of hot air injection, air will again be compressed at 300 psig and 100°F. It will then be passed through the air heater for heating to the maximum temperature of 392°F. Air flow out of the heater will be monitored and controlled by a temperature controller to regulate the amount of fuel gas and air fed to the heater. Temperature can be varied by operator with local control up to 392°F and can be maintained at a set point by the temperature controller.

After air exits the heater to the Air Processing and Instrumentation Skid, it passes through an orifice type flow meter for flow measurement. Air pressure, temperature and water content are also measured at this time. Heated air continues to flow through a control valve in the 3-inch injection line to the wellhead and into the reservoir. The Control Valve is a butterfly valve that is normally open during injection and will be closed during the withdrawal cycle to prevent backflow of air to the compressor.

3. Withdrawal Cycle

In the air withdrawal cycle, air flow is reversed, returns from the 3-inch injection tubing to the Return Air Filter and into the Air Return Scrubber. Air is prevented from backflowing through the system by the control valve, actuated by the Injection Status Switch, which routes the air through the filter and scrubber.

After entrained water is separated and drained at the scrubber, return air flow is then measured by a second orifice type flow meter. Air then travels through the Pressure Control Valve and exits through the Air Return Silencer located outside the building.

INSTRUMENTATION AND CONTROLS

A. INTRODUCTION

Task parameters dictate measuring air flow at 1250 scfm at a maximum pressure of 300 psig and at a maximum temperature of 392°F.

B. DEVELOPMENT OF INSTRUMENTS

System requirements included the difficult task of recording relative humidity at the higher temperatures which will be encountered. This required provision for a cooling system to reduce the airstream to less than 140°F prior to air sampling chambers for a relative humidity readout.

C. PROGRAMMABLE CONTROLLER & MICROCOMPUTER

A Kaye Instrument Data Logger has been provided for monitoring and recording the surface instrumentation data. The instrument provides the capability for the operator to select a digital readout of any data on demand by pushbutton selection. The data logger will be programmed to provide a printout, including date, hour and operational modes at periodic intervals.

The subsurface or downhole instrumentation will be recorded in a similar fashion by a microcomputer.

The microcomputer, through proper interface, will serve to provide a permanent repository for the Data Logger outputs by the use of disk drives and 8" disks. The downhole data will similarly be stored by the microcomputer.

D. SURFACE INSTRUMENTATION SYSTEMS

A primary function of the Data Logger is to condition and standardize these signals into acceptable readings. Other functions of the Data Logger are to indicate and print out these readings, to compute corrected values for flow rate and humidity, to alarm whenever a reading exceeds a selected high value and to control sequencing operations such as automatic operation mode switching from injection to withdrawal of air or automatic emergency shutdown.

1. Temperature Measurement System
   a. The temperature of both the injection and withdrawal air is sensed by Transmitter TT-101. The signal is used for recording and in calculating injection and withdrawal air flow rates.

2. Pressure Measurement System
   a. The pressure of the injection air is sensed by Transmitter PT-103. The signal is used for recording and calculating injection air flow rate.
   b. The pressure of the withdrawal air is sensed by Transmitter PT-101. The signal is used for recording and calculating withdrawal flow rate.

3. Flow Rate Measurement System
   a. The flow rate of the injection air is sensed by Transmitter FT-101. Within the data logger, the signal is combined with signals from TT-101 and PT-103 to calculate a corrected flow for material balance.
   b. The flow rate of the withdrawal air is sensed by Transmitter FT-102. This signal is similarly corrected for material balance by inputs from TT-101 and PT-103.

4. Humidity Measurement System
   a. Both injection and withdrawal air streams are sampled through a 3/8" stainless steel tube which passes the air through the coiled section in the Constant Temperature ($100^{o}F$) Conditioning Bath and into the stainless steel sample chamber.
   b. The moisture content of the air in the sample chamber is sensed by Transmitters AT-101 and AT-103, the sample temperature being sensed by Transmitter TT-103.

c. The math package in the Data Logger accepts the signals from the transmitters on the sample chamber and combines these with the output from PT-103 to calculate the relative humidity of the injected air. A separate Data Logger channel will provide a readout of moisture content in PPM.
d. The humidity and PPM readout of the withdrawal air is determined by combining the sample chamber outputs with that of PT-101.

5. Particulate Measurement Systems
   a. Particulates are obtained by opening filters #26-104A or #26-104B. Particle size distribution and bulk loading rate will be determined by standard laboratory procedures.

6. Automatic Operation Mode Switchover System
   Provisions are made to manually set an automatic switchover from injection operation mode to withdrawal mode. The switchover command and time of switchover are entered into the data logger. At the present time, the data logger will align valves and shutdown the compressor and heater to carry out an automatic transfer.

7. Downhole Instrumentation System
   The actual downhole sensors for pressure, temperature, relative humidity and moisture content are shown in Table 1.

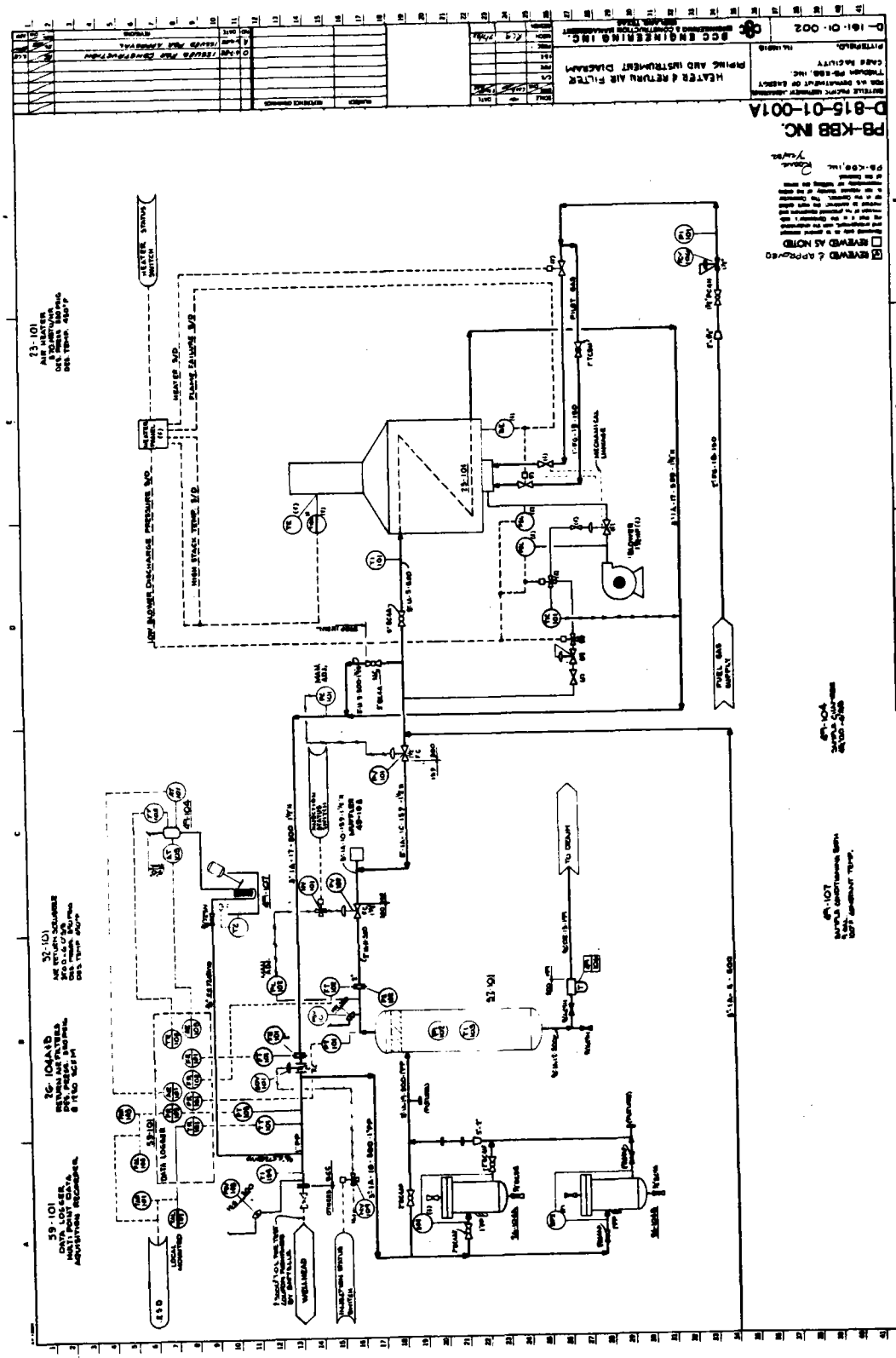

FIGURE 1

Table 1 Sensor characteristics for CAES reservoir monitoring

Sensor Type	Sensor Characteristics under Operational Environment							
	Temperature Range (ambient to)	Pressure Range (ambient to)	Relative Humidity Range	Pore-water Content Range	Accuracy (ambient)	Accuracy (Elevated Temperature/ Pressure)	Exposed Material	Vendor
Temperature								
Platinum resistance element	>200°C	>30 bars	Saturated/ unsaturated vapor conditions	Saturated/ unsaturated liquid conditions	±0.01°C	±0.05°C[a]	Teflon, ceramic, platinum, PVC[b]	Hy-Cal, Engr., Santa Fe Springs, CA
Thermocouple	>200°C	>30 bars	Saturated/ unsaturated vapor conditions	Saturated/ unsaturated liquid conditions	±0.1°C	±0.25°C[a]	Ceramic, Teflon, PVC[b], vinyl[b], chromel, constantan	Wescor, Inc., Logan, UT
Pressure								
Silicon strain gage	200°C	>30 bars	Saturated/ unsaturated vapor conditions	Saturated/ unsaturated liquid conditions	±0.01 bar	±0.05 bar[a]	PVC[b], quartz, titanium, Teflon, stainless steel, epoxy resin	Petur Instrument, Seattle, WA
Relative Humidity								
Thermocouple psychrometer	> 80°C[a]	>20 bars[a]	95%-99.9%[a] (possibly 90%-99.9%[a])	Unsaturated conditions	±0.5%[a]	±1.0%[a]	Ceramic, Teflon, PVC[b], vinyl[b], chromel, constantan	Wescor, Inc., Logan, UT
Cellulose strain gage	>125°C[a]	>30 bars	~0-100%	Unsaturated conditions	±2.0%[a]	±5.0%[a]	Stainless steel, inert cellulose, epoxy resin, Teflon, PVC[b]	Hygrometrix, Inc., Oakland, CA
Pore-water Content								
Thermocouple psychrometer	> 80°C[a]	>20 bars[a]	--	0.8 to >20 bars[a]	±0.2 bar	(a)	Teflon, PVC[b], vinyl[b], chromel, constantan, ceramic	Wescor, Inc., Logan, UT
Resistance block	>200°C	>30 bars	--	0.3 to >15 bars[a]	±0.5 bar[a]	(a)	Fiber glass, PVC[b], Al alloy	Soiltest, Inc., Evanston, Il
Neutron logging device	70°C	>30 bars	Unsaturated/ saturated vapor conditions	Unsaturated/ saturated liquid conditions	±2.0%	not applicable	--	RPR Instruments, Evansville, IN

a. Exact values to be determined during calibration. b. Materials used only where temperatures <100°C.

AN EVALUATION OF THERMAL ENERGY STORAGE MEDIA FOR ADVANCED COMPRESSED AIR ENERGY STORAGE SYSTEMS*

F. R. Zaloudek and K. R. Wheeler
Pacific Northwest Laboratory
Richland, Washington

Lynn Marksberry
Fluidyne Engineering Corporation
Minneapolis, Minnesota

INTRODUCTION

Recent engineering and economic studies (1-4) have examined the feasibility of advanced compressed air energy storage (CAES) system concepts that could improve the fuel and power cost saving potential of conventional CAES systems such as employed at the Huntorf plant in West Germany. These studies identified two advanced system concepts -- the adiabatic and hybrid concepts -- as having sufficient technical and economic benefits to possibly interest U.S. electrical utilities in building such plants in the near future to produce peak and intermediate power (5). However, an important problem is the development of durable and reliable regenerative air heaters. Such air heaters are used in these CAES systems to remove and store the heat of air compression for subsequent use during power generation. Insufficient information is available on the potential long-term (30-year) durability of low cost thermal energy storage (TES) materials under the thermally and chemically aggressive conditions expected in these CAES systems.

This paper describes a study to experimentally evaluate four candidate TES materials identified in early adiabatic and hybrid CAES design studies (3-4):

- sintered iron oxide pellets
- Denstone balls
- cast iron spheres
- crushed rock.

The study sought to identify those materials that could possibly fail quickly or perform poorly under the high temperature, high pressure and thermal cycling conditions expected during CAES plant operation and to recommend TES materials for consideration in planned future pilot plant-scale studies of regenerative air heaters for CAES plants.

THERMAL CYCLE TESTS

Thermal cycle tests were conducted to evaluate the performance and durability of the TES materials under thermal cycling conditions typical of CAES operation.

Thermal Cycle Test Facility Description

The Thermal Cycle Test Facility was designed to simulate the most critical thermomechanical features of a full-scale CAES plant. The test

*Portions of this work were performed for the U.S. Department of Energy under Contract DE-AC06-76RLO-1830 and for the Electric Power Research Institute under Contract RP1699-2.

vessel schematic is shown in Fig. 1. The externally insulated steel vessel was 3 ft in diameter and 20 ft high. An upper and lower stainless steel grate-and-screen assembly enclosed the matrix. A 100,000-lb capacity, hydraulically driven load simulator applied a load to the upper grate by means of push rods to simulate the overburden weight of a typical TES bed. The load applied to a particular TES material was determined through the use of the Janssen equation.

Thermal, hydraulic, and mechanical performance data were obtained from appropriate instrumentation strategically placed on the test vessel. Complete instrumentation details are included in Reference 6. That report also fully describes the exact operational sequence of test vessel components.

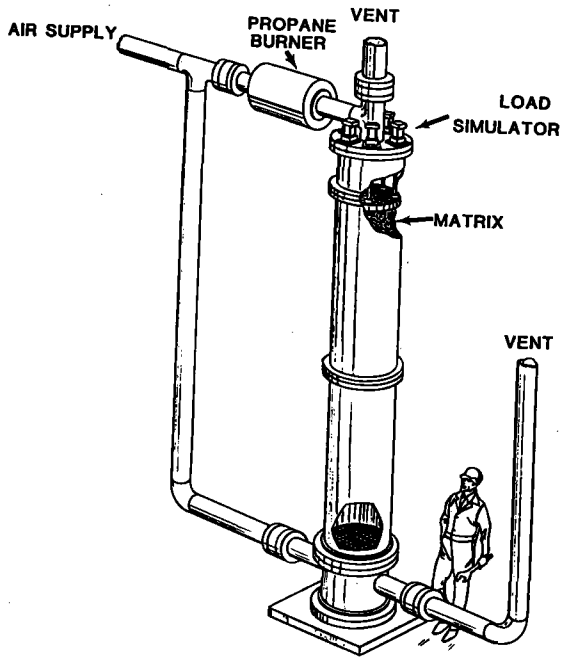

Fig. 1. Thermal Cycle Test Heater

Test Conditions

Typically, a 4- to 5-hour cycle time was required to produce the full range of temperatures in the middle of the test bed at mass velocities typical of projected CAES TES designs. The specific test parameters used for each TES material are noted in Table 1.

Test Parameters	Denstone	Iron Oxide	Dresser Basalt	Cast Iron
Bed height, ft	16.3	15	15.5	10.0
Gas inlet temperature, °F	840	900	900	860
Air inlet temperature, °F	100	105	105	105
Gas flow, lb/h	3300	3800	4000	4300
Air flow, lb/h	3300	3350	3950	4300
Pressure level	Atmos.	Atmos.	Atmos.	Atmos.
Duration, cycles	116	103	104	101
Duration, h	420	480	530	416

Table 1. Test Conditions

Thermal Cycle Test Results

The isothermal pressure loss measurements taken before and after thermal cycling are shown in Fig. 2. Note that the frictional characteristics of the rounded but irregular rock are approximately equal to the spherical Denstone and iron oxide. Although fundamental heat transfer data could not be readily obtained in the high thermal

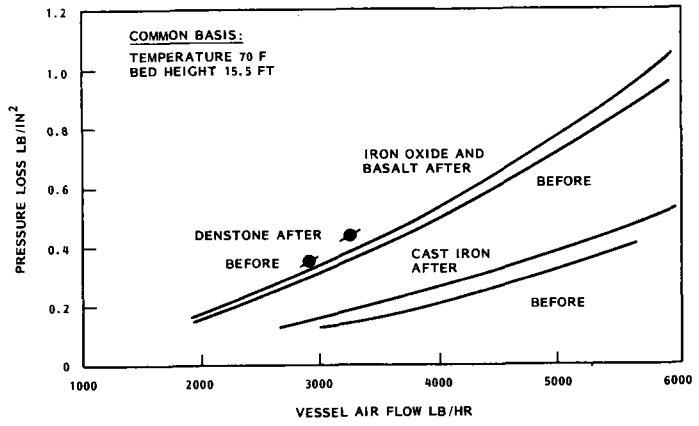

Fig. 2. Isothermal Pressure Loss Comparison

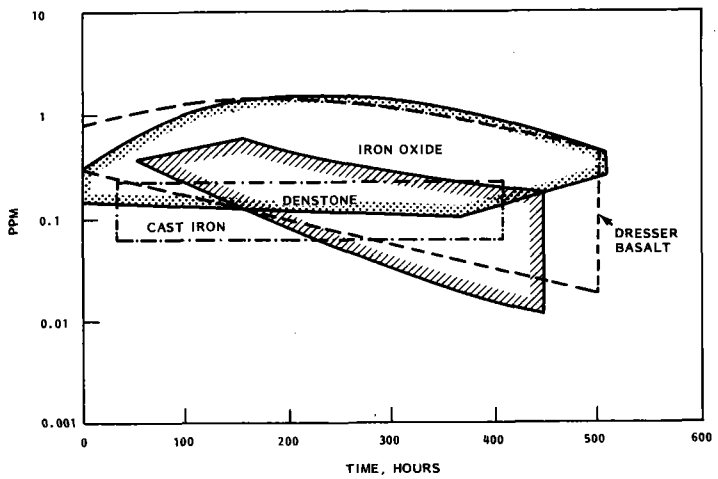

Fig. 3. Elutriated Particle Emission Comparison

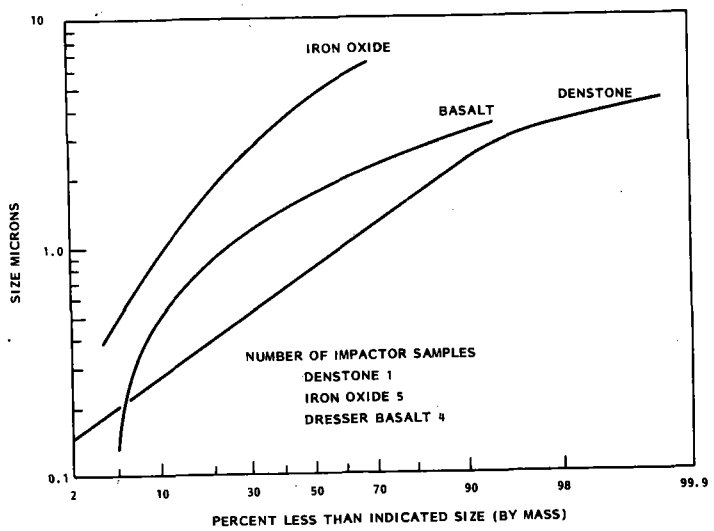

Fig. 4. Approximately Size Distribution Comparison

conductance bed, the implication by analogy is that the thermal performance of rock will also approximate that of 1/2-in. spheres. The iron ball data are lower because of the material's nominal 1-in. diameter. Little difference between pre- and post-test measurements suggests evidence that hydraulic performance did not differ significantly over the test interval.

Particulate elutriation rate measurements taken by the filter samplers are compared in Fig. 3. Multiple filter samples from both the upper and the lower gas discharge lines were combined to give an envelope of data. The rates are apparently not excessive with respect to either turbine wear or bed wastage over a 30-year design life. There are discernable downward trends over time, and a longer test would be required to determine the limiting rates.

The size distribution of the elutriated particles is summarized in Fig. 4. No data are presented for cast iron because the elutriation rates were too small to permit obtaining a significant sample. The particulate sizes for the iron oxide sample are significantly larger than those for the other materials and are in a size range that may cause turbomachinery erosion.

Strain gage data taken throughout the tests revealed no measurable accumulation of vessel strain with the iron oxide, Denstone and crushed rock

samples, although cyclic variations were observed. Therefore, to an accuracy of approximately 50 microstrains, there was no indication of ratcheting for these materials. With the cast iron sample, residual strain gage offsets of 126 to 130 microstrains circumferentially, and 30 microstrains axially were measured suggesting the occurrence of thermal ratcheting.

Following thermal cycling, each test bed was carefully removed and observed for evidence of damage. The only visible damage observed was a few broken pebbles in the Denstone and iron oxide test beds. Free-floating dust was readily observable throughout the bed before and after the thermal cycling test, indicating that even fine particulate may not move freely through the pebble bed matrix.

The principal cast iron alloy utilized in these tests contained 27% chromium for hardness and corrosion resistance. A small quantity of balls made from alloys ranging from 0 to 32% chromium was distributed through the bed near the top. Following testing, severe surface corrosion was observed on all balls containing 21% and less chromium. The corrosion product had the appearance of a red "fuzz" that could be easily rubbed from the surface.

AUTOCLAVE TESTS

The autoclave tests were conducted to evaluate candidate TES materials at two of the more chemically aggressive environmental conditions expected in a CAES TES system. The first was the high temperature and pressure condition experienced in the adiabatic CAES high pressure TES unit. The other was the maximum dewpoint condition experienced in both the adiabatic and hybrid CAES designs. Test conditions chosen to represent these two situations were:

High Temperature	
Pressure	1215 psia
Temperature	896°F
Environment	dry compressed air

Dewpoint Condition	
Pressure	1251 psia
Temperature	280°F
Environment	moist air with simulated SO_2 contamination

The air used in the dewpoint condition tests was intentially contaminated with 0.5 ppm SO_2 to simulate typical industrial pollution. This SO_2 combines with the water present in these tests to form a corrosive acidic environment for the TES materials.

Test Equipment Description

Two autoclaves were used to simulate the high and low temperature conditions. A dry autoclave pressurized to 1215 psia with industrial grade compressed air and heated to 896°F was used to determine the resistance of the TES materials to this accelerated oxidizing condition. Samples of all materials segregated into individual wire

baskets were simultaneously exposed in the unstressed condition in this autoclave. In a second autoclave, 0.1 ft^3 of each material contained in a 3.8-in. OD x 9-in. high column was individually exposed to 280°F moist air at 1215 psia. The sample was axially loaded by a bellows supplied by an external air source to simulate the overburden weight. This autoclave is pictured in Fig. 5.

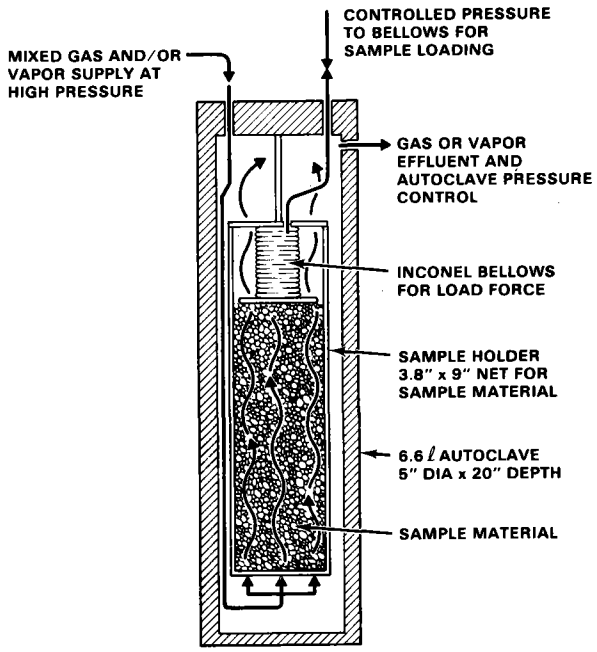

Fig. 5. Simulated TES Material Environment Reaction Column

Material Evaluation

Before testing, all materials were examined to determine internal structures, weight, mechanical resistance to crushing, failure mode under compressive load and chemical composition. The structural examinations showed that the iron oxide pellets had substantial porosity. The Denstone also had large number of voids, but not nearly as many as the iron oxide. All cast iron samples exhibited some shrinkage voids and cracks.

High Temperature Exposure Results

Small samples of all TES materials were exposed 30 days to dry, commercial grade compressed air at 896°F and 1215 psia. After discharge, all materials were evaluated as described above; Table 2 summarizes the results of these examinations.

No significant deterioration of the surface or internal structure of any of the materials was noted. A loosely adherent oxide coating was noted on the cast iron samples having less than 27% chromium content. Microscopic examination of this oxide layer revealed maximum particulate sizes of 1/2 to 1-1/2 microns, which should be small enough to present no serious turbine erosion problems.

The high temperature exposure did produce some statistically significant changes in resistance to crushing loads. The Dresser basalt was observed to increase in strength, while the cast iron samples generally lost strength. The iron oxide sample obtained from Hannah Mining lost strength while the sample obtained from Cleveland Cliffs increased in strength. No change was noted in the strength of Denstone.

Dewpoint Exposure Results

Samples of the TES materials were exposed for 30 days to moist, saturated air at 280°F and 1215 psia. The air was intentionally

Material	Weight Loss (Gain) (%)	Crush Strength (lb) Pre-Test $\bar{x}$	Pre-Test s	Post-Test $\bar{x}$	Post-Test s	Visual Observation	Comments
Iron oxide (Hannah Mining)	0.04-0.27	521	183			No change	
Taconite (Cleveland Cliffs)	0.2	462	150	575	202	No change	Mean crush force significantly increased
Basalt (Dresser)	0.2	1,794	808	2,390	1,194	No change	Mean crush force significantly increased
Denstone	No change	503	117	461	77	No change	Mean crush force not significantly changed
Gray cast iron	(0.8-0.15)	20,880	1,877	-	-	Adherent oxide coating	Oxide particles 3 to 1.5 m (typical)
White cast iron	(0.8-0.15)	28,800	-	-	-	Adherent oxide coating	Same as gray
25% chrome cast iron	No change	52,655	3,366	-	-	Adherent oxide coating	No oxide below iron rich surfaces
27% chrome cast iron	No change	86,360	17,266	62,440	11,903	No change	Mean crush force significantly changed

$\bar{x}$ = mean load
s = standard deviation

Table 3. Changes in Candidate TES Materials after Exposure to Dry, 896°F Air

contaminated with 0.5 to 1 ppm SO_2, which approximated the worst air quality at the Maryland site considered in the PEPCO/EPRI/DOE design study. Water (30 cc) was periodically introduced into the autoclave to moisten the sample and maintain the moist atmosphere.

After exposure, each material was visually examined for evidence of mechanical or chemical change (spallation, surface reaction, etc.). Weight and strength changes were then documented. The results are summarized in Table 3. The observed weight changes of the nonmetals can be explained by the hygroscopic behavior of the particular materials. It should be noted that the iron oxide sample suffered a significant reduction of strength and exhibited spallation and some fracturing of pellets as a result of the exposure.

CONCLUSIONS

The results indicate that iron oxide pellets, the preferred material in the recent design study (3) of adiabatic CAES, may not be the most satisfactory TES material selection. This material produced quantities of large particulates that could threaten CAES turbomachinery. Furthermore, this material lost significant strength in the presence of moisture, which may aggravate the comminution and particulate elutriation process.

Material	Weight Loss (Gain) (%)	Crush Strength (lb) Pre-Test x̄	Pre-Test s	Post-Test x̄	Post-Test s	Visual Observation	Comments
Iron oxide (Hannah Mining)	0.03	521	183	364	139	Fine powder on test vessel surface. Limited fracture in top pebbles.	No evidence of surface reaction. Significant reduction in crush load.
Denstone	0.006	503	117	462	85	No evidence of pebble breakage or spallation.	No significant change in crush crush load. Some brown surface staining.
Dresser basalt	<0.2	1,794	808	1,492	649	No evidence of pebble breakage or surface reaction.	No significant change in crush load.
25% chrome cast iron	No change	52,655	3,366	-	-	Slight brown discoloration on surface.	Very resistant with chrome-rich surface.

$\bar{x}$ = mean load
s = standard deviation

Table 4. Changes in Candidate TES Materials after Exposure to Moist 280°F Contaminated Air

The potential suitability of cast iron balls is also questionable. Evidence of thermal ratcheting was observed in the thermal cycle tests. Both the thermal cycle tests and the autoclave tests showed that this material could oxidize and that relatively small rust particles could elutriate, especially for alloys containing less than 27% chromium. However, these tests were too short to conclusively determine if this behavior eliminates cast iron from the list of acceptable materials.

Both Denstone and Dresser basalt appeared to perform satisfactorily. Both are chemically inert and spallation-resistant. The basalt was observed to increase in strength during high temperature exposure, making it more crush-resistant. Denstone remained relatively unchanged by all conditions imposed on the samples during these tests. Both materials exhibited elutriation rates and particulate sizes within limits of conventional fired turbomachinery. Wastage of the CAES TES system over a 30-year plant lifetime should be no problem.

Because cost is an important factor in TES material selection, Dresser basalt probably has an edge on Denstone. The 1981 prices for Dresser basalt and Denstone were $6.75/ton and $650/ton, respectively, in small quantities. The price of Denstone could probably be reduced significantly in the quantities required for a CAES TES system. However, the Denstone price will never likely become comparable.

Therefore, it must be concluded that Dresser basalt is probably the most attractive of the materials considered for CAES TES systems.

REFERENCES

1. Giramonti, A.J., et al., Technical and Economic Assessment of Fluidized Bed Augmented Compressed Air Energy Storage, Vol. 1-3, United Technologies Research Center, East Hartford, Connecticut, 1980.

2. Giramonti, A.J., and R.L. Sadala, Concept Screening of Coal Gasification Systems, United Technologies Research Center, East Hartford, Connecticut, 1979.

3. Hobson, M.J.. et al., Conceptual Design and Engineering Studies of Adiabatic CAES with Thermal Energy Storage, Acres American, Inc., Columbia, Maryland, 1981.

4. Karalis, A.J., et al., Preliminary Engineering Design and Cost of Advanced Compressed Air Storage (ACAS) A-5 Hybrid, United Engineers & Constructors, Philadelphia, Pennsylvania, 1981.

5. Zaloudek, F.R., and R.W. Reilly, An Assessment of Second-Generation Compressed Air Energy Storage Concepts, PNL-3978, Pacific Northwest Laboratory, Richland, Washington, 1981.

6. Zaloudek, F.R., K.R. Wheeler and L. Marksberry, An Evaluation of Thermal Energy Storage Media for Advanced Compressed Air Energy Storage System, PNL-4390, Pacific Northwest Laboratory, Richland, Washington, 1982.

THERMAL ENERGY STORAGE MEDIA FOR ADVANCED COMPRESSED AIR ENERGY STORAGE SYSTEMS

Lynn Marksberry
FluiDyne Engineering Corporation
Minneapolis, Minnesota

Abstract

Screening tests were performed to compare materials for Thermal Energy Storage (TES) pebble media in advanced Compressed Air Energy Storage (CAES) power plants. Measurements were made of the effects of thermal cycling and bed weight on deterioration of the pebbles. Four materials were tested: Denstone fireclay, iron ore, basalt rock, and cast iron. Each was tested as a pebble bed 0.9m (3 ft) in diameter and 4.6m (15 ft) high. The beds were heated and cooled between 310K (100F) and 750K (900F), at rates that simulated plant conditions, over 100 times at four hours per cycle. The most significant result was the good performance of the basalt rock, which is also the lowest cost material by a large margin.

Introduction

Design studies (1,2) of adiabatic and hybrid CAES systems have indicated that there are technical and economic advantages of storing and reusing the heat of compression developed during the charging phase of the storage cycle. This heat would be stored in large pebble beds and returned to the compressed air during the power generation phase. A typical pebble bed (3) would be 13m (44 ft) in diameter and 20m (65 ft) high. The most severe operating conditions involve daily cycling between 310K (100F) and 750K (900F) at a pressure of about 8.3MPA (1200 psi).

The TES system for an 800 MW plant would require about 100,000T of pebbles, and, in accordance with utility practice, would be designed for a life of 30 years. The large quantity of material and long plant life make the cost of the TES material an important consideration (1,2). Since the combined requirements of size, operating conditions, life, and cost are beyond present day experience with TES systems, the Department of Energy through its Pacific Northwest Laboratory developed a program to screen candidate materials. The objective was to provide a relative ranking of candidate materials. For this purpose tests of limited duration were undertaken. The thermal cycling tests comprised 100 cycles, about one percent of those a full-scale plant would undergo. Longer duration tests would be needed to predict the life of the storage media. For screening purposes the deterioration mechanisms of the pebble bed were divided into those from two sourcess: thermomechanical effects and thermochemical effects.

Thermomechanical effects are caused by the dead weight loads on the pebbles and by the alternate expansion and contraction of the bed during each thermal cycle. Pebbles are especially prone to dusting and breakage under such conditions because of the point-to-point contact. Small dust particles carried out of the bed may cause erosion of the piping, controls, and rotating machinery. Large particles from fracture of pebbles will tend to plug regions of the bed, thereby increasing

pressure drop and reducing its performance as a heat exchanger. The thermomechanical screening tests are reported in this paper.

Thermochemical effects are caused by condensation of water vapor in the bed. The condensate may adversely interact with the pebble material causing a corrosion film and/or a loss of strength. The thermochemical screening tests have been carried out by the Pacific Northwest Laboratory.

Bed Materials

Four materials were selected based upon the results of previous studies (1,2,3); properties are shown in Table 1. These materials range from low cost crushed and tumbled rock to high cost cast iron. They will be discussed in the order in which they were tested.

Denstone (tradename of the Norton Company) is a fireclay pebble used primarily as a catalyst support. The pebbles are manufactured at plants in Ohio and Tennessee. The annual production rate is about equal to that needed for a single 800 MW plant. Thus CAES requirements would probably require additional plant capacity. The current price for 1/2 inch pebbles is about $600 per short ton. Assuming economies of scale for higher production rates, the projected cost for CAES applications is estimated at roughly $500 per ton. The pebbles tested were standard production grade and were tested in the as-received condition.

Iron ore pebbles are prepared from iron ore by crushing, separating out the iron oxides, and sintering into pebble form for handling and shipping. They are made to fairly uniform composition and strength considering the vast quantities involved. A single large plant on the Minnesota iron range will produce over 15 million tons per year. Thus the needs for CAES are, in comparison, insignificant. Further, iron ore pebbles are disbributed throughout the U.S. The current cost is about $50 per short ton and would not be affected by CAES needs. The pebbles tested were produced from magnetite ore in northern Michigan and were donated by the Cleveland Cliffs Iron Company. The pebbles were quite dusty and an attempt was made to reduce the dust by washing with water sprays. There was no apparent improvement.

A study was made to select one or more kinds of natural rocks for which the strength and thermal cycling resistance were judged adequate, and that were available in large quantities at low cost. Information and advice was provided by the Minnesota Geological Survey. An initial conclusion was to avoid rocks containing free quartz. Quartz undergoes a phase transformation, at temperatures just above the range of interest, that is acoompanied by an abrupt expansion. This could cause loss of strength and subsequent deterioration.

The rock tested was Dresser basalt obtained from a quarry in Wisconsin. This quarry ships over one million tons per year, much of it for railroad ballast at $6.75 per ton. The rock has uniform composition and structure and is very strong. The railroad ballast grade was used for the test. This is a crushed rock with sizes from 1.3 to 5cm (1/2 to 2 in) and having sharp edges. The sharp edges were removed by tumbling for one-half hour. The rocks were then

washed with a water spray to remove the dust. Some dust remained which could have been removed with a more thorough washing.

The most expensive material tested was cast iron grinding media manufactured by the American Magotteaux Corp. in Tennessee. Their annual production is about 50,000 tons in the U.S. and Canada and about 200,000 tons throughout the world. The pebbles are spherical in shape and are made in a range of chromium contents. Based upon the recommendation of the manufacturer, a 27% chrome content was selected to minimize corrosion. For grinding media applications the metal is heat treated to increase hardness. This step was eliminated for the present test because some ductility would be beneficial. In addition a few samples of standard grinding pebbles having chrome contents of 8, 12, 21 and 32 per cent were included to determine the level needed to avoid corrosion.

Test Facility and Procedures

The test facility was designed to simulate the most critical thermomechanical features of full-scale operation: the temperature cycling conditions and the dead weight load. Budgetary restrictions imposed three limits: operation at atmospheric pressure, use of dry gases, and reduced bed size. Pressure level does not affect the temperature cycling conditions but it does affect particle carryover from the bed. The tests were run at nominal full-scale flow per unit area so that the gas velocity was much higher than at full-scale. Therefore, larger particles were carried out of the test beds. Condensation in the bed occurs in the high pressure TES of the adiabatic CAES cycle (Ref. 2), but for thermomechanical screening it is sufficient to run a dry test. And since the test bed is much shorter than a full-scale bed, the dead wieght effect was simulated by applying a load to the top of the bed.

The test heater consists of an externally insulated steel vessel in 0.9m (3 ft) in diameter and is 6m (20 ft) high (Fig. 1). It will accommodate a 5m (16 ft) high bed and flanged sections can be rearranged for shorter beds. Upper and lower stainless steel grate-and-screen assemblies confine the matrix within the vessel. The upper grate is connected to a hydraulically driven load simulator that can apply a 450 KN (100,000 lb) force to the top of the bed. This mechanism also provided a means of measuring the subsidence of the beds during the tests.

Instrumentation was provided to continuously monitor operation during thermal cycling and to detect changes during a test. Vessel temperature, bed temperature and gas pressure were measured at approximately 30cm (1 ft) intervals along the height of the bed. The velocity distribution across the top of the bed was measured before and after each test to detect nonuniformities in flow distribution.

Operation of the facility is shown in Figure 2. The charging cycle simulates the full-scale plant where not air from the compressor flows downward through the heater, heating the bed, and then into the air storage chamber. The discharge cycle simulates the air from storage being heated by flowing upward through the bed and then to

the gas turbine. A complete charge-discharge cycle required about 4 hours. The system operated completely automatically, with cycle changes initiated by temperatures at the top and bottom of the bed.

The entering air was filtered to eliminate pickup of extraneous dust and the flow rate was measured during both cycles. Particle carryover from both the top and the bottom of the bed was measured. in addition, the size distribution of the particle carryover from the top of the bed was measured because this is the flow that could cause erosion in the turbine and other components.

Each batch of pebbles was visually inspected during installation and removal and photographs of the bed were taken at various levels (Figs. 3 and 4). Bulk density measurements were made and the results are presented in Table 1.

Two quality control tests used in the production of iron ore pebbles were used to give a relative ranking of the different materials and of the relative effects of thermal cycling. These were the ASTM E279 Tumble Test and E382 Compression Strength Test.

Each of the four bed materials was tested under similar conditions (Table 2). Typical bed temperature distributions are shown in Figure 5, in this case for basalt. The temperature profile moves up and down the bed as it is heated and cooled. The profiles shown are at the limits of this movement. Thus, during hot flow (downward), the profile moves from right to left on Figure 5, and the reverse during cold air flow. The flow rates were selected to provide a rate of heat transfer equal to full-scale conditions, and therefore the rate of movement of the temperature profile equals that for full-scale. The center region of the bed experiences the largest temperature variation and the upper region is exposed to the highest mechanical loads (from the hydraulic load system).

Pressure distribution was measured at one foot intervals along the height of the bed to determine whether detectable bed plugging occurred. In every case the pressure distributions were smooth and did not change shape during the runs, indicated no bed plugging. The bed height was also monitored during the runs. Each bed lost a small amount of height as follows: Denstone 0.6 in., iron ore 2.1 in., basalt 1.8 in., and cast iron 0.7 in. The duration of the tests was not sufficient to determine whether an asymtotic limit had been reached. Because of the low rate of particle carryover (Figure 7) these height reductions must have resulted from rearrangement of the pebbles to a tighter packing rather than loss of bed material.

The pressure drop across each bed was measured before and after each test. These measurements were made with the entire bed at room temperature. The results are shown in Fig. 6. The purpose was to determine whether detectable changes in bed pressure loss characteristic occurred. In every case the flow resistance increased slightly, but not by an amount that would have any significant effect on the CAES cycle.

The results of the particle carryover measurements are presented in Figure 7. The envelopes enclose the individual measurements taken with each bed material. These include carryover out both the top and the bottom of the bed (Fig. 2). The total number of measurements were: Denstone 21, iron ore 29, basalt 24, and cast iron 9. No significant difference was found between upward and downward flow. The scatter in the data was most likely caused by the very small samples that were collected.

The data can be used to make a crude estimate of loss of bed material in a CAES plant. Very roughly, the full range shown of 0.01 to 1 PPM corresponds to a bed loss of 0.05 to 5% over a 30 year plant life. A downward trend in particle carryover is indicated for the three nonmetallic materials. Thus the projected bed loss is well within tolerable bounds. Also, the dust loading in parts per million is well below the tolerable limits for gas turbines (4,5,6).

Erosion can be caused if particles are large enough, about 5 to 10 microns (7). The particle size distributions are shown in Figure 8. No data is shown for cast iron because the particle catch in the impactor was below the detectable limit. Denstone produced the fewest large particles, only about 2% above 3 microns and none above 6 microns. The curves for basalt and iron ore terminate at the upper size limit for the impactor. The basalt results show about 10% of the particles above 3 microns size. The iron ore bed gave the largest particles, about 70% above 3 microns and 40% above 5 microns. The rate and size data are combined and contracted to turbine limit data suggested by General Electric (6). These results indicate all of the materials except, perhaps, iron ore are acceptable with regard to corrosion. The iron ore may be acceptable only for CAES systems that use heavy duty expansion turbines or systems that employ particle filtration.

Crushing strength of the Densone and iron ore was measured before and after the tests by the ASTM E382 method. (The strength of basalt and cast iron exceeded the limits of the apparatus.) The cycling tests affected both materials. For Denstone, there was no change at the top of the bed, but for the remainder the strength decreased progressively to the bottom of the bed, where the loss of strength was about 30%. This loss may have been caused by thermal stress cycling. On the other hand, the strength of the iron ore improved throughout the bed by about 30%. The cause for this change is not known.

The tumbling test, ASTM E279, gives a measure of the resistance of handling. The measure is the change in the fraction of particles below a specified size. In all cases the as-received materials had less than 0.05% below the specified size of 1/4 or 3/8 inch. As-received samples and post-test samples from the top, middle, and bottom of the bed were tumbled (except cast iron). None of the materials were affected by bed location. The Denstone was not affected by thermal cycling. The affect of thermal cycling on iron ore was to triple the fraction less than 1/4 inch (from 0.8 to 2.4%). The effect on basalt was to double the fraction less than 3/8 inch (from 0.7 to 1.5%). Thus none of the materials were substantially affected by 100 temperature cycles.

Visible observations of each material are summarized as follows. There were a few broken Denstone pebbles in each layer in the region from one foot to four feet below the top of the bed. These were adjacent to the wall and showed rub marks. About half as many broken iron ore pebbles were found in the same location and no broken rock or cast iron pebbles were found. The cast iron pebbles with 8, 12, and 21% chrome were rusty; the 27 and 32% chrome pebbles were not.

There was very slight dustiness noted in handling all materials, before and after cycling, except for the iron ore. The iron ore was very dusty, more so after the test, and handling required the use of face masks.

Conclusion

Tests of 100 temperature cycles did not cause any significant deterioration of the four pebble beds. No bed plugging occurred and their performance as heat exchangers was not affected. Only a few of the Denstone and iron ore pebbles were broken, no damage was found with the basalt and cast iron beds. The rate of dust carryover was low, in the range of 0.01 to 1 PPM, which is well below the tolerable amount for gas turbines. Significant differences were found in the size of the particles carried out of the beds. Iron ore particles were the largest, with about 40% over 5 microns, which could cause erosion. The other materials appear satisfactory.

The very good performance of the basalt rock was the most significant result of the test program. This rock is readily available in large quantities at very low cost and has high volumetric specific heat. Its use for TES in advanced CAES systems would provide a storage media having a hearly insignificant fraction of plant costs. Additional longer term testing of 1000-2000 cycles will be needed to provide the data base to support construction of a commercial CAES TES. There is, however, sufficient data to prepare and evaluate a design using Dresser basalt or any other of the tested materials.

Since Dresser basalt is so inexpensive and performed so well, it should be considered for general use as a low cost thermal energy storage material. Its melting point is approximately 1480K (2200F), and it is reasonable to expect that it could be used for applications up to 1100K (1500F). This is the approximate operating temperature that has been considered for residential, commercial, and industrial thermal energy storage applications (8).

Acknowledgements

Funds for this program were provided by the Department of Energy (DOE), and the Electric Power Research Institute. Assistance and support by the DOE MHD program, the Bureau of Mines, and the previously noted suppliers and agencies is gratefully appreciated.

References

1. I. Glendenning, et al, "Technical and Economic Assessment of Advanced Compressed Air Storage (ACAS) Concepts," EPRI EM1289, 1979.

2. M.J. Hobson, et al, "Conceptual Design of Adiabatic CAES in Hard Rock," Proceedings of the International Conference on Seasonal Thermal Energy Storage and Compressed Air Energy Storage, DOE-CONF-811066 Vol. 2, Seattle, 1981.

3. D.C. James and P.E. Chew, "Thermal Energy Storage for Adiabatic CAES," Proceedings of the International Conference on Seasonal Thermal Energy Storage and Compressed Air Energy Storage, DOE-CONF-811066 Vol. 2, Seattle, 1981 (685-699).

4. D.L. Keairns, et al, "Design of Pressurized Fluid-Bed Combustor/ Particulate Control System for Reliable Turbine Operation," ASME 79-GT-190, 1979.

5. S. Moskowitz, "Pressurized Fluidized Bed Pilot Electric Plant - A Technology Status," ASME 79-GT-193, 1979.

6. R.R. Boericke, et al, "Assessment of Gas Turbine Erosion by PFB Combustion Products," Proceedings of the Sixth International Conference on Fluidized Bed Combustion, DOE-CONF-800428, Volume II, 1980.

7. J. Stringer, "Assessment of Hot Gas Clean-up Systems and Turbine Erosion/Corosion Problems in PFBC Combined Cycle Systems," ASME 79-GT-195, 1979.

8. M. MacDonald and D. Goldenberg, "Alternatives to Ceramic Bricks and Ceramic Brick Systems," Proceedings of the Sixth Annual Thermal and Chemical Storage Contractors' Review Meeting, DOE-CONF-810940, 1981.

TABLE 1. BED MATERIALS

	DENSTONE	IRON ORE	BASALT	CAST IRON
SIZE, IN.	0.4-0.5	0.4-0.6	0.5-2.0	1.0
DENSITY, LB/FT^2	150	218	185	480
BULK DENSITY, LB/FT^3	92	130	113	281
SPECIFIC HEAT, B/LB F	0.23	0.21	0.25	0.155
VOLUME SP. HT, B/FT^3 F	21	27	28	44
CURRENT COST, $/T	600	50	10	1000
PROJECTED COST, $/T	500	50	10	800

TABLE 2. TEST CONDITIONS

	DENSTONE	IRON ORE	DRESSER BASALT	CAST IRON
BED HEIGHT, FT.	16.3	15	15.5	10.0
GAS INLET TEMP., F	840	900	900	860
AIR INLET TEMP., F	100	105	105	105
GAS FLOW, LB/HR	3300	3800	4000	4300
AIR FLOW, LB/HR	3300	3350	3950	4300
PRESSURE LEVEL	ATMOS.	ATMOS.	ATMOS.	ATMOS.
DURATION, CYCLES	116	103	104	101
DURATION, HOURS	420	480	530	416

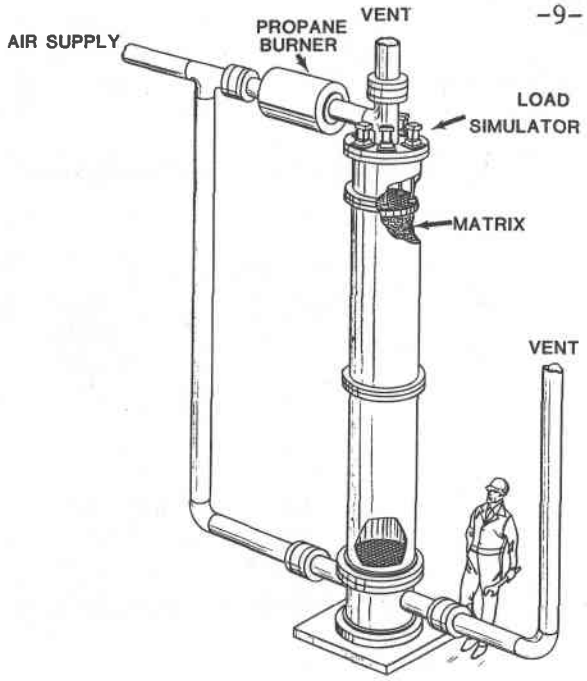

FIGURE 1. TEST HEATER

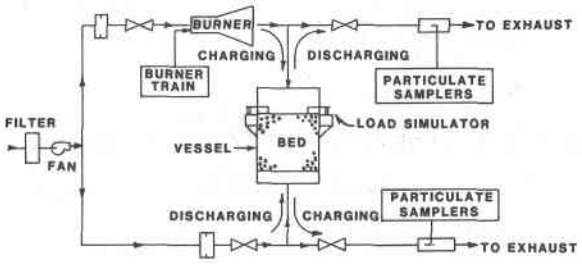

FIGURE 2. PROCESS SCHEMATIC

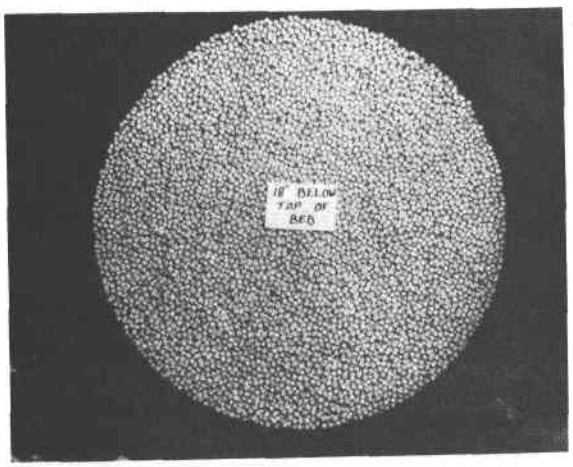

FIGURE 3. DENSTONE BED

FIGURE 4. BASALT BED

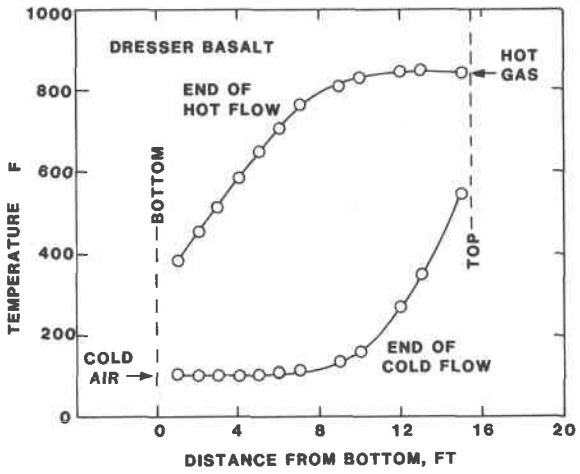

FIGURE 5. BED TEMPERATURE PROFILE

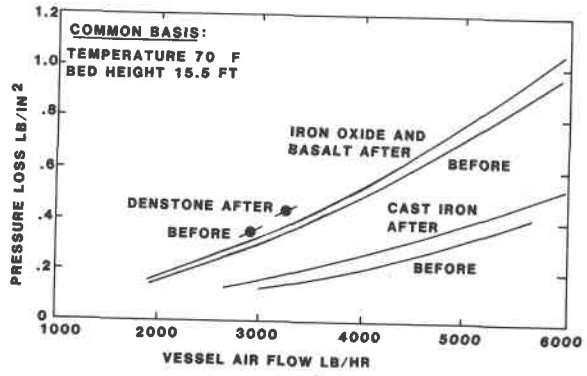

FIGURE 6. ISOTHERMAL PRESSURE DROP

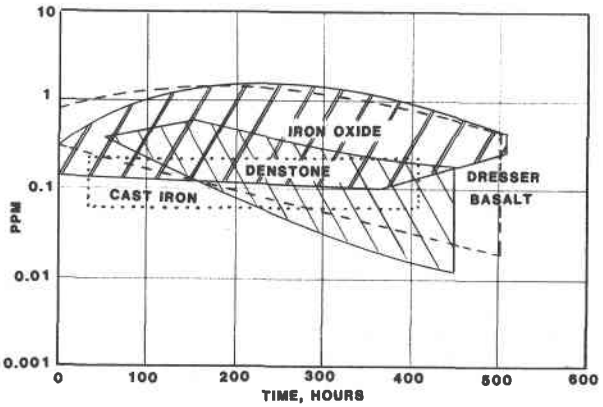

FIG.7. PARTICLE CARRYOVER FROM BED

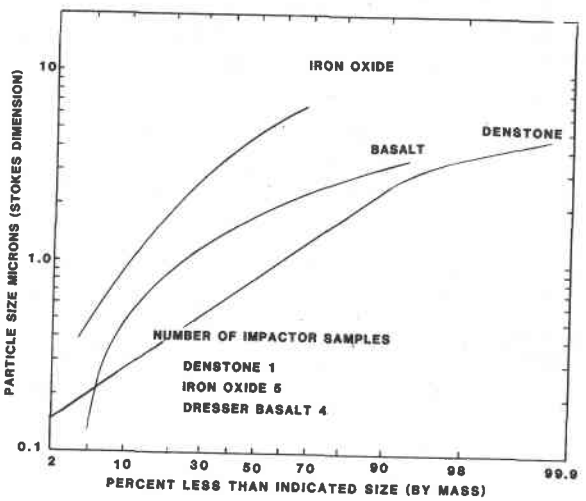

FIGURE 8. AERODYNAMIC PARTICLE SIZE

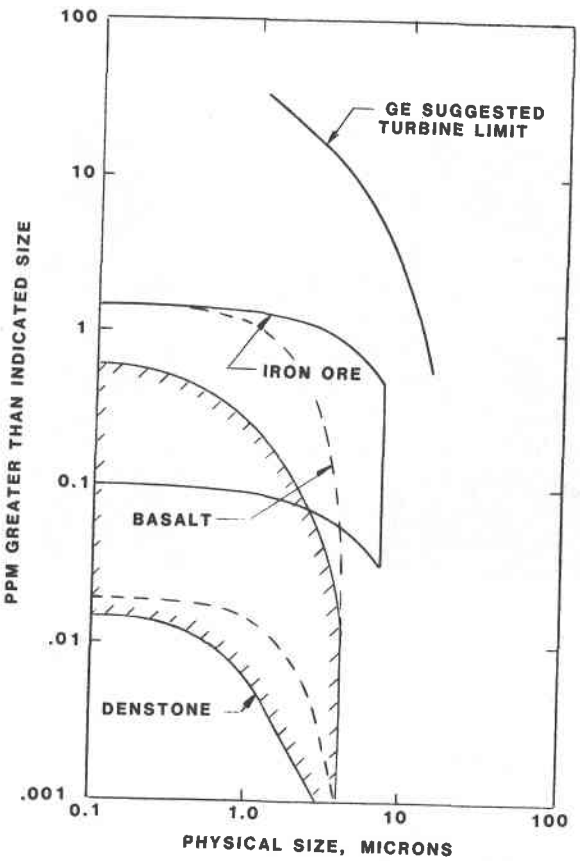

FIGURE 9. MEASURED PARTICULATE COMPARED TO ALLOWABLE IN A GAS TURBINE

TECHNICAL AND ECONOMIC ANALYSIS OF ENERGY STORAGE

J. Asbury, R. Giese, R. Mueller, A. Valentino, and W. Walsh
Argonne National Laboratory
Argonne, Illinois 60439

ABSTRACT

Progress is reported on several technical and economic analysis projects.

The Assessment of Cool Storage project, completed during 1982, evaluated the performance and cost of chilled water and ice storage systems in commercial building applications. Paybacks of less than four years were estimated under rate schedules currently in force in many parts of the country.

A project to evaluate new concepts for energy storage and transport identified three concepts that merit consideration for R&D support: multicomponent slurries for enhanced heat transfer, transport, and storage; superconducting magnetic energy storage for fusion reactor applications; and polymer materials for thermal storage (especially seasonal) applications.

Other projects, not reported here, include an analysis of the economic benefits of improved storage efficiency and a review of the findings of previous storage assessment studies.

COOL STORAGE IN COMMERCIAL BUILDINGS

Previous Argonne studies evaluated customer-owned storage for electric load leveling in residential applications.[1-4] These studies concluded that electric storage heating and cooling represented cost-effective methods of load management in service areas supplied by winter- and summer-peaking electric utilities, respectively, but that it would be difficult to design and implement electric rate schedules that would encourage adoption of residential cool storage systems.[3,4] A number of considerations favor commercial over residential buildings for the early application of cool storage technology. These include: the benefits of returns to scale, shorter building occupancy periods, the greater prevalence of demand charges, and better control of the operation of cool storage equipment.

Here we summarize several case-study analyses of the application of cool storage in commercial buildings. More detailed descriptions of cool storage and chiller system performance characteristics and costs are reported elsewhere.[5]

Conventional cool storage systems are based on either ice-making (latent heat) or chilled water (sensible heat) storage. The basic principle of operation is to shift a substantial part of the electrical requirement for building space cooling from the utility's peak to its off-peak period. A key consideration, affecting the sizing and operation of the storage and chiller components is choice between a full or partial storage mode of operation.

Under the full storage, or off-peak, mode of operation, the chiller is switched off during the peak period. Storage capacity must be adequate to meet the time-integrated building load during the peak period plus the thermal losses from storage on the design day. Under the partial storage, or load-leveling, mode of operation, the storage and chiller capacities are set by the criterion that the design-day load be met by continuous operation of the chiller at rated output. This mode of operation minimizes the chiller capacity requirement.

Case Studies

Detailed evaluations of the application of cool storage in four representative office buildings were performed;[5] two are reported here.

Building A is a large, seven-story masonry building located in a Mid-Atlantic service area. The building is typical of older GSA buildings employing large granite block construction. The building covers an entire square block and contains approximately 650,000 ft^2 of floor space. The HVAC system operates from 6 AM to 5 PM.

Building B is a large shopping mall located in a Midwestern service area. The mall is a two-story building containing a number of small and medium sized ships, but no large "anchor" stores. Total floorspace is approximately 750,000 ft^2. The HVAC system operates from 7 AM to 9 PM.

Two techniques were used to estimate building HVAC system loads. Actual building electric loads, measured at 15-minute intervals, were available for Building A and were used to estimate loads. For Building B, the DOE-2 computer code[6] was used to simulate building electric loads over a full annual cycle; estimated monthly loads were then calibrated on values from monthly electric bills.

System Costs

Component sizes and costs for the different cooling system alternatives under the partial and full storage modes of operation were estimated. The capital costs of the cooling system incorporating partial storage ranged from 15% to 65% higher than those for the conventional cooling system, the added costs of storage being partly offset by the chiller capacity savings. The capital costs of full storage systems are substantially greater than those for the partial storage system.

Customer Payback Analysis

Simple paybacks on investment in the alternative storage system were calculated from the estimated bill savings and system costs. The results are presented in Tables 1 and 2. For both buildings, simple paybacks of approximately three years are realized for chilled water systems designed for the partial storage mode of operation. As seen from the tables, both storage applications provide comparable percentage reductions in demand charges, approximately 50% for partial storage and 100% for full storage.

Table 1 Annual Cooling Loads, Bill Values, and Paybacks Building A

System	Cooling Load		Annual Bill			Bill	Incremental Investment ($10^3$$)		Payback (yrs)	
	Peak (kw)	Energy (MHW)	Demand ($10^3$$)	Energy ($10^3$$)	Total ($10^3$$)	Savings ($10^3$$)	New	Retrofit	New	Retrofit
Conventional	1250	1721	91.0	53.3	144.3					
Chilled Water										
Partial Storage	555	1680	40.5	51.2	91.7	52.6	160.7	292.8	3.1	5.6
Full Storage	0	1540	0.	41.4	41.4	102.6	331.9	513.7	3.2	5.0
Ice-Building										
Partial Storage	665	2024	48.5	61.5	110.0	34.3	152.1	152.1	4.4	4.4
Full Storage	0	2060	0.	55.3	55.3	89.0	380.4	380.4	4.3	4.3

Table 2 Annual Cooling Loads, Bill Values, and Paybacks Building B

System	Cooling Load		Annual Bill			Bill	Incremental Investment ($10^3$$)		Payback (yrs)	
	Peak (kw)	Energy (MHW)	Demand ($10^3$$)	Energy ($10^3$$)	Total ($10^3$$)	Savings ($10^3$$)	New	Retrofit	New	Retrofit
Conventional	3285	1712	74.9	41.0	115.9					
Chilled Water										
Partial Storage	1550	1629	35.3	35.7	71.0	44.9	122.7	374.4	2.7	8.3
Full Storage	0	1514	0.	27.1	27.1	88.8	1409.9	1985.5	15.6	22.4
Ice-Building										
Partial Storage	1860	1906	42.4	41.8	84.2	31.7	118.1	118.1	3.7	3.7
Full Storage	495	2200	4.9	42.4	47.3	68.6	1213.0	1213.0	17.7	17.7

It is instructive to examine the dependence of the calculated paybacks on the system costs and the demand charge values assumed in the analyses. Figures 1, 2 show that payback is most sensitive to the cost of storage under both modes of operation. For the full storage mode, the payback on investment is approximately independent of the cost of chiller capacity because of the small change in capacity relative to that required with the conventional cooling system.

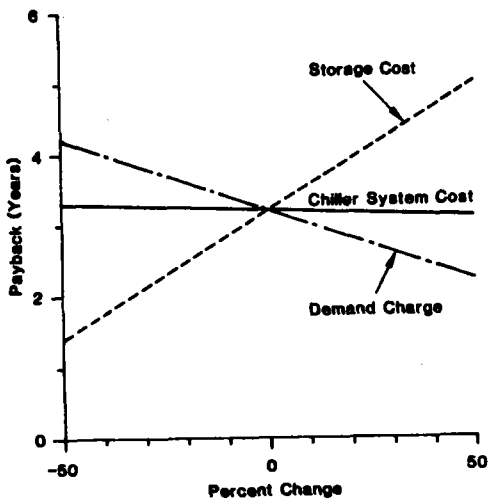

Fig. 1 Payback, Building A, Partial Storage

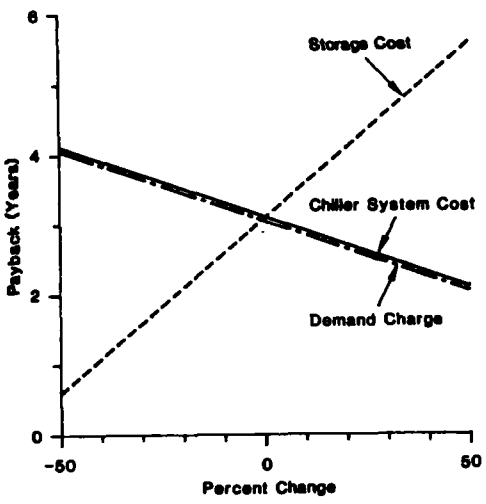

Fig. 2 Payback, Building A, Full Storage

Conclusions

Several conclusions can be drawn from the analysis of cool storage applications in commercial buildings.

- Cool storage is an effective load management technology for reducing commercial building peak demands.
- Chilled water systems consume less energy than ice systems and may actually consume less than conventional cooling systems.
- Partial storage systems, because of their smaller compressor capacity requirements, involve substantially lower capital outlays than do full storage systems; partial storage also offers faster payback.
- Storage is more economical in buildings with short daily occupancy periods and narrow cooling loads.
- Payback depends sensitively on the design of the electric rate schedule; large on-peak demand charges combined with long ratchets offer the best opportunities for cool storage.

Research and Development Needs

The analysis of cool storage described above is based on adoption of commercially available equipment components. Manufacturers of tanks, ice builders, and other devices are improving their products and marketing approaches. More rapid technology development will require public-sector support because of the non-appropriability (non-patentability) of research findings and technology improvements. Several problems and R&D needs have been identified for DOE consideration.

- Development of improved latent heat storage media;
- Heat recovery during storage charging;
- Chiller improvement especially at the lower temperature regimes encountered in ice-building applications;
- Evaluation and modelling of sensible heat stratification techniques;
- Parasitic reduction in ice building systems;
- Exploitation of economies of scale in chilled water systems.

These recommendations are discussed in more detail elsewhere.[5]

NEW CONCEPTS FOR ENERGY STORAGE AND TRANSPORT

The objective of this project was to identify new concepts for the storage and transport of energy and to define associated R&D needs. Emphasis was on the definition of generic approaches to the

solution of technical problems and to the meeting of application needs.

Two working groups -- one composed of individuals outside Argonne, the other drawn from Argonne staff -- were formed to identify and evaluate storage concepts. After reviewing a large number of concepts, these groups prepared brief descriptions of fifteen concepts, a subset of which were subjected to peer review by experts at other laboratories, universities, and industry. Out of this process, three concepts emerged meriting consideration for federal R&D support.

- Multicomponent slurries for enhanced heat transfer, transport, and storage;
- Superconducting magnetic energy storage (SMES) for fusion reactors; and
- Polymer materials for thermal storage systems.

Multicomponent slurries. The use of phase change materials (PCM) to increase the specific energy of storage devices can be extended to the entire heat transfer, transport, and storage system by creating a multicomponent working fluid or slurry. This could be achieved by mixing a PCM with a carrier heat transfer fluid in which it is insoluble and immiscible. The PCM might be solid-liquid or solid-solid.

Benefits of multicomponent slurries include: (i) reduced heat transfer areas because of particle-surface interaction and turbulence at the surface, (ii) a smaller temperature difference between the heat source and sink (or storage reservoir), (iii) reduced mass flow rates enabling the use of smaller pumps and piping, and (iv) reduced equipment and operating costs.

Although there have been a few studies of the benefits of slurries for energy transport,[7,8] these studies apparently did not recognize or take advantage of the enhanced heat transfer available through the use of slurry systems.

SMES for fusion reactors. The TOKAMAK magnetic confinement concept is the leading fusion power technology. Because TOKAMAK reactors require pulsed fields and transient power for plasma heating at the startup of the burn cycle, energy storage is needed as a buffer between the utility grid and the pulsed load to prevent power disruption during the startup period.[9,10] In current TOKAMAK conceptual designs, up to 15% of the capital cost is associated with energy storage. Superconducting magnetic energy storage, because of its rapid cycling and load following capabilities and its high turn-around efficiency, appears to be uniquely suited to fusion reactor applications.

Polymer materials. Recent advances in polymer technology have made possible large, lightweight, strong, and low cost materials. These extraordinary strength-to-weight ratio materials can be the basis for coverings and structures necessary for energy collection, storage, and utilization. In many thermal storage concepts, liners

and covers represent the most significant cost items. New polymer materials have the potential to significantly reduce the cost of such liners and covers.

Base technolgy research and design engineering is needed to support the development of low cost, high-strength polymer films for use in thermal storage systems. Films with appropriate mechanical and optical properties could enable the development of a host of cost-effective thermal storage systems, including solar ponds, thermal storage ponds, seasonal ice storage, and large thermal envelopes for building and city spaces.

REFERENCES

1. *Residential Electric Heating and Cooling: Total Cost of Service*, J.G. Asbury, R.F. Giese, R.O. Mueller, Proceedings, New Modes of Heating, Ventilation, and Air Conditioning, Residential HVAC Workshop, Jan. 1979, EPRI Report EA-2060 (Oct. 1981).

2. *Electric Storage Heating in New England: Field Test and Assessment*, H. Hersh, S. Nelson, J. Asbury, Proc. of the American Power Conference, (April, 1980).

3. *Heating with Electricity: The Right Price at the Right Time*, J.G. Asbury, R.F. Giese, and R.O. Mueller, article in Technology Review, (Dec./Jan. 1980).

4. *Assessment of Energy Storage Technologies and Systems, Phase I: Electric Storage Heating, Storage Air Conditioning, and Storage Hot Water Heating*, J. Asbury, R. Giese, S. Nelson, L. Akridge, P. Graf, and K. Heitner, ANL/ES-54, (Oct. 1976).

5. *Assessment of Cool Storage in Commercial Building Applications*, J. Asbury, R. Giese, and J. Calm, draft final report submitted to DOE (July 1982).

6. *DOE-2 Users Guide*, Building Energy Analysis Group, Lawrence Berkeley Laboratory.

7. *High Temperature Integrated Thermal Storage for Solar Thermal Applications*, A.P. Bruckner and A. Herzberg, DOE Thermal and Chemical Storage Annual Contractors Review, Washington, D.C., (1981).

8. *Fusible Pellet Transport and Storage of Heat*, P.A. Bahrami, ASME, Heat Transfer Division, Paper No. 82-HT-32, June 1982

9. *Power Supply Requirements for a Tokamak Fusion Reactor*, J.N. Brooks and R.L. Kustom, Nuclear Technology, Vol. 46, (Nov. 1979).

10. *Superconducting Magnetic Energy Storage for Electric Utilities and Fusion Systems*, J.D. Rogers, et al., LANL Report LA-UR-78-1213, (1978).

30 MJ SUPERCONDUCTING MAGNETIC ENERGY STORAGE FOR BPA TRANSMISSION LINE STABILIZER

John D. Rogers
Los Alamos National Laboratory
University of California
Los Alamos, NM 87545

ABSTRACT

The Bonneville Power Administration (BPA) operates the electric transmission system that connects the Pacific Northwest and southern California. A 30 MJ (8.4 kWh) Superconducting Magnetic Energy Storage (SMES) unit with a 10 MW converter is to provide system damping for low frequency oscillations. Installation of the SMES unit in the BPA Tacoma Substation is underway and should be in experimental operation by November 1982. Full utility operation is scheduled for March 1983. Progress during FY 82 is described and plans for FY 83 are given. The seismic mounting of the 30 MJ coil to the dewar lid is complete. Computer operation of the heat rejection trailer, high pressure gas recovery trailer, and converter has been accomplished. The converter has been operated with an inductive load with energy discharge through the protective dump circuit. Partial computer operation of the refrigerator has been performed. A refrigerator test with full load is to be made. Integrated operation of the entire system will be at the Tacoma Substation. The nonconducting dewar has been built and tested.

INTRODUCTION

The Pacific Northwest and southern California are part of the Western U.S. Power System and are connected by two 500 kV, ac-power transmission lines, collectively referred to as the Pacific AC Intertie and one ± 400 kV dc-transmission line, the Pacific HVDC Intertie, all are operated by the BPA.

The stability of the Western Power System is affected by the relative weakness of the tie provided by the 905 mile long Pacific AC Intertie. In 1974 negatively damped oscillations with a frequency of 21 cpm (0.35 Hz) were observed on the AC Intertie. BPA installed equipment on the HVDC Intertie to modulate power flow between the interties, damping the oscillations, and increasing the stability limit of the Pacific AC Intertie from about 2100 MW to 2500 MW, when the HVDC Intertie operates. The availability of the HVDC Intertie is 89.5%, and the southern terminal was down for six months at one time as a result of earthquake damage. In 1975 representatives of BPA and the Los Alamos National Laboratory developed the concept of installing a small back up SMES unit to provide system damping. The design parameters of the unit are listed in Table I.

Several descriptions of the project have appeared previously (1,2,3,4,5,6,7). This report concentrates on the FYs 82 and 83 work.

TABLE I
DESIGN PARAMETERS OF THE 30-MJ SYSTEM STABILIZING SMES UNIT

Maximum power capability, MW	10
Operating frequency, Hz	0.35
Energy interchange, MJ	9.1
Maximum stored energy, MJ	30.0
Coil current at full charge, kA	4.9
Maximum coil terminal voltage, kV	2.18
Coil operating temperature, K	4.5
Coil lifetime, cycles	$>10^7$
Heat load at 4.5 K, W	<150
Coil diameter, m	3.0

SITE PREPARATION

Detailed information--weights, sizes, locations--on trailer, converter, and transformer footings has been supplied to BPA. Power requirements for all the SMES components have been specified and transmitted. An aggressive interactive dialogue with BPA counterparts on the Tacoma Substation facility and SMES system utility control is underway. The Tacoma Substation site preparation is underway. The BPA activity is reported in two companion papers at this meeting.

30 MJ COIL AND ITS SEISMIC MOUNTING

At Tacoma, WA, the SMES system will be installed in a Zone C seismic region, with design accelerations of 0.24 g horizontal and 0.16 g vertical. A stiff support system was designed to suspend the coil freely within an open mouth helium vessel. The coil with two of the four trapezoidal shear panels and vertical axial load strut sets readily visible is shown in Fig. 1. The horizontal discs are thermal radiation shields. The slightly angled micarta blocks to the right of center on the coil are supports for the joints between conductor of the pancake coil pairs. Nineteen support block, joints are located around the coil. The vapor cooled leads, not shown, were shipped separately to BPA. The 30 MJ coil and the nonconducting dewar were shipped to the Covington Substation for assembly together in an enclosed building and then moved 17 miles to the Tacoma Substation. The vapor cooled leads are permanently mounted at that time.

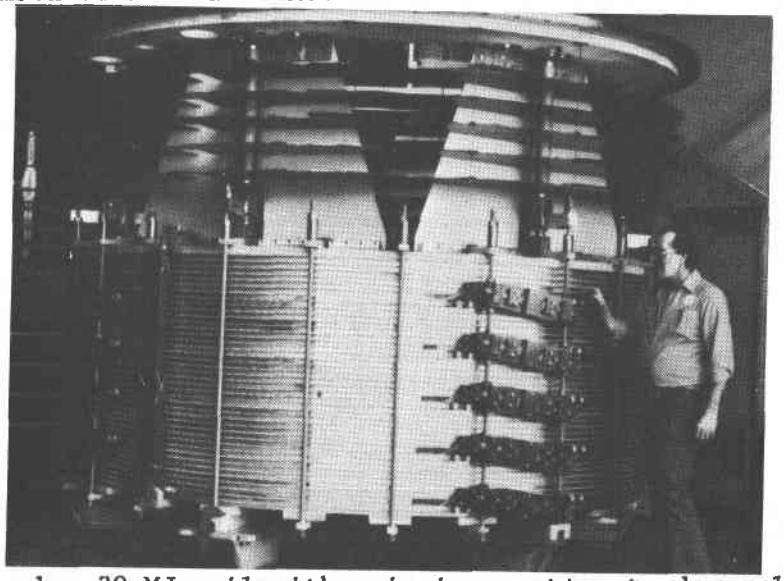

Fig. 1. 30 MJ coil with seismic mounting to dewar lid.

VAPOR COOLED LEADS

Each of the ten subcables of the 5 kA superconducting cable must carry equal currents of 500 A. The series resistance of the subcables varies because of the interpancake coil joints and superconducting strand cold welds. The leads were designed with ten separate vapor cooled sections. These connect individually to the subcables to provide series resistances to balance the currents. The leads were successfully tested at 5.5 kA with 80% of rated flow without overheating and at 13 kV withstand voltage, substantially above the expected maximum of 5 kV.

NONCONDUCTING DEWAR

The nonconducting dewar contract was placed in November 1981. Unusual delays occurred because California rains washed mud into the dewar assembly building. The dewar shells, epoxy fiberglass inner and polyester fiberglass outer, were made by wet layup techniques. One hundred layers of striped aluminized Mylar superinsulation, interleaved with Nexus cloth, were placed in the vacuum space for radiation shielding. A special aluminum lid was obtained for a flange bolt hole locating drill pattern and to test the dewar. The cryogenic test of the dewar was performed near the manufacturer's plant at the University of California, Berkeley, CA. Figures 2 and 3 show, respectively, the inner dewar shell with superinsulation in place and the outer shell being lowered into place over the inner shell.

ELECTRICAL SYSTEM

Load testing of the converter with ohmic and inductive loads was completed. Over five kilo ampere currents were interrupted with the protective dump circuit discharged into a resistive load. The converter SCR bridges were monitored and corrected for proper current sharing. The converter has been operated under computer control.

Fig. 2. Epoxy fiberglass inner dewar shell with 100 layers superinsulation.

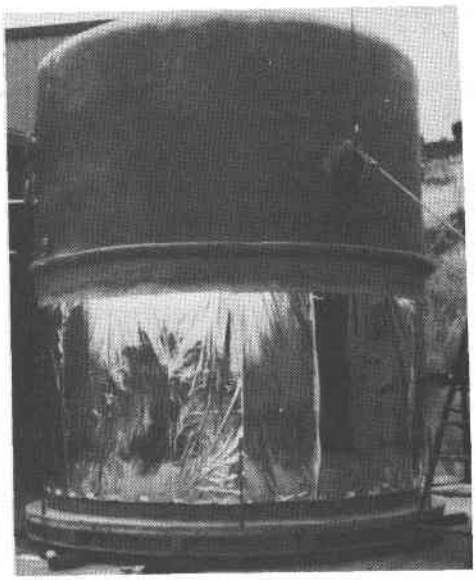

Fig. 3. Polyester fiberglass outer shell being lowered into place over inner shell prior to making joint between shells.

CRYOGENIC SYSTEM

The cryogenic system is composed of the heat rejection trailer, which has operated satisfactorily with computer inerfacing; the high pressure gas recovery trailer, which has operated with computer interfacing; a liquid nitrogen supply tank trailer; a helium gas supply, a railway tank car on a siding at the Tacoma Substation; and the Koch Model 2800 helium refrigerator.

The refrigerator has been run several times. It will only run with computer control of its ancillary systems. The main gas bearing turbine control is an internal refrigerator closed loop subsystem. The refrigerator, as supplied, was in very poor condition. The compressor aftercoolers were plugged, now cleaned and replaced; the computer instrumentation and control circuits were totally inadequate, now replaced; and the refrigeration capacity has not met performance specifications.

INSTALLATION AND OPERATION AT TACOMA SUBSTATION

The 30 MJ SMES system installation at the Tacoma Substation is in process. All equipment is either moved or in some phase of transit. The system, except the dewar, coil, transfer lines from the refrigerator to the dewar, and the dewar vacuum system, was preassembled and operated at Los Alamos. Full integration of the system is to occur at Tacoma, WA. The schedule for installation and operation is as follows.

Install at Tacoma Substation	8/1-10/1/82
Initiate 30 MJ coil cooldown	9/15/82
Charge coil to 5 kA	10/1/82
Experimental SMES operation	10/1-3/1/83
Initiate full utility operation	3/1/83
BPA decision to retain SMES	9/15/83

REFERENCES

1. H. J. Boenig, J. C. Bronson, D. B. Colyer, W. V. Hassenzahl, J. D. Rogers, and R. I. Schermer, June 1978, "A Proposed 30-MJ Superconducting Magnetic Energy Storage Unit for Stabilizing an Electric Transmission System," Los Alamos Sci. Lab. report LA-7312P.
2. J. D. Rogers, H. J. Boenig, J. C. Bronson, D. B. Colyer, W. V. Hassenzahl, R. D. Turner, and R. I. Schermer, "30-MJ SMES Unit for Stabilizing an Electric Transmission System," IEEE Trans. on Magnetics, Vol. MAG-15, Jan. 1979, pp. 820-823.
3. R. I. Schermer, "The Stabilization Unit for Bonneville Power Administration," Proc. 1979 Mech. and Magnetic Energy Storage Contractors' Rev., CONF-790854.
4. R. I. Schermer, "30-MJ Superconducting Magnetic Energy Storage for BPA Transmission Line Stabilizer," Proc. 1980 Mech. and Magnetics Energy Storage Contractors' Rev., CONF-801128.
5. R. I. Schermer, "30 MJ Superconducting Magnetic Energy Storage for BPA Transmission Line Stabilizer," Proc. Mech., Magnetic and Underground Energy Storage 1981 Annual Contractors' Rev., Conf-810833.
6. J. R. Purcell, S. C. Burnett, R. I. Schermer, "Design and Fabrication of the Bonneville Power Administration's 30-MJ Superconducting Energy Storage Coil for Long-Distance Transmission Line Stabilization," Proc. Mech. Magnetic, and Underground Energy Storage 1981 Annual Contractors' Rev., Conf-810833.
7. A. S. Criscuolo, "Computer Automated Controls for Superconducting Magnetic Energy Storage," Proc. Mech. Magnetic, and Underground Energy Storage 1981 Annual Contractors' Review Meeting, Conf-810833.

30 MJ SMES BPA'S TACOMA SUBSTATION ENGINEERING

Barry L. Miller
Bonneville Power Administration
P.O. Box 3621
Portland, Oregon 97208

Abstract

The on-site installation of the SMES unit developed by LANL to provide system stability/testing is being accomplished by BPA forces at Tacoma Substation in the Puget Sound Area of Washington state. Outdoor site preparation is nearly complete with the majority of LANL supplied equipment/trailers installed. Full system testing is anticipated by November, 1982 without modulation control. Full operation is expected by April 1, 1983.

Introduction

Tacoma Substation is a 500/230/13.8-kV substation supplying an adjacent aluminum reduction plant and various loads in the Tacoma industrial/commercial/residential area. The area of the station to be used for the SMES system was formerly a 115-kV switchyard. Abandoned tower footings and cable manholes, handholes, and concrete encased duct systems had to be removed to enable new footings to be poured and to remove steel rebar from the area immediately adjacent to the coil/dewar assembly.

Site Testing

Soil bearing properties were determined for the site, as well as mean depth to water level. Electrical parameters of the substation were also determined (i.e., fault magnitudes of 13.8-kV bus and ground mat resistivity/condition).

Equipment Layout

The SMES equipment location in the existing substation was based on several factors:

1. Maintaining the existing level of entry into and operation of the substation.

2. Providing an efficient and accessible area for LANL equipment.

3. Safety of personnel.

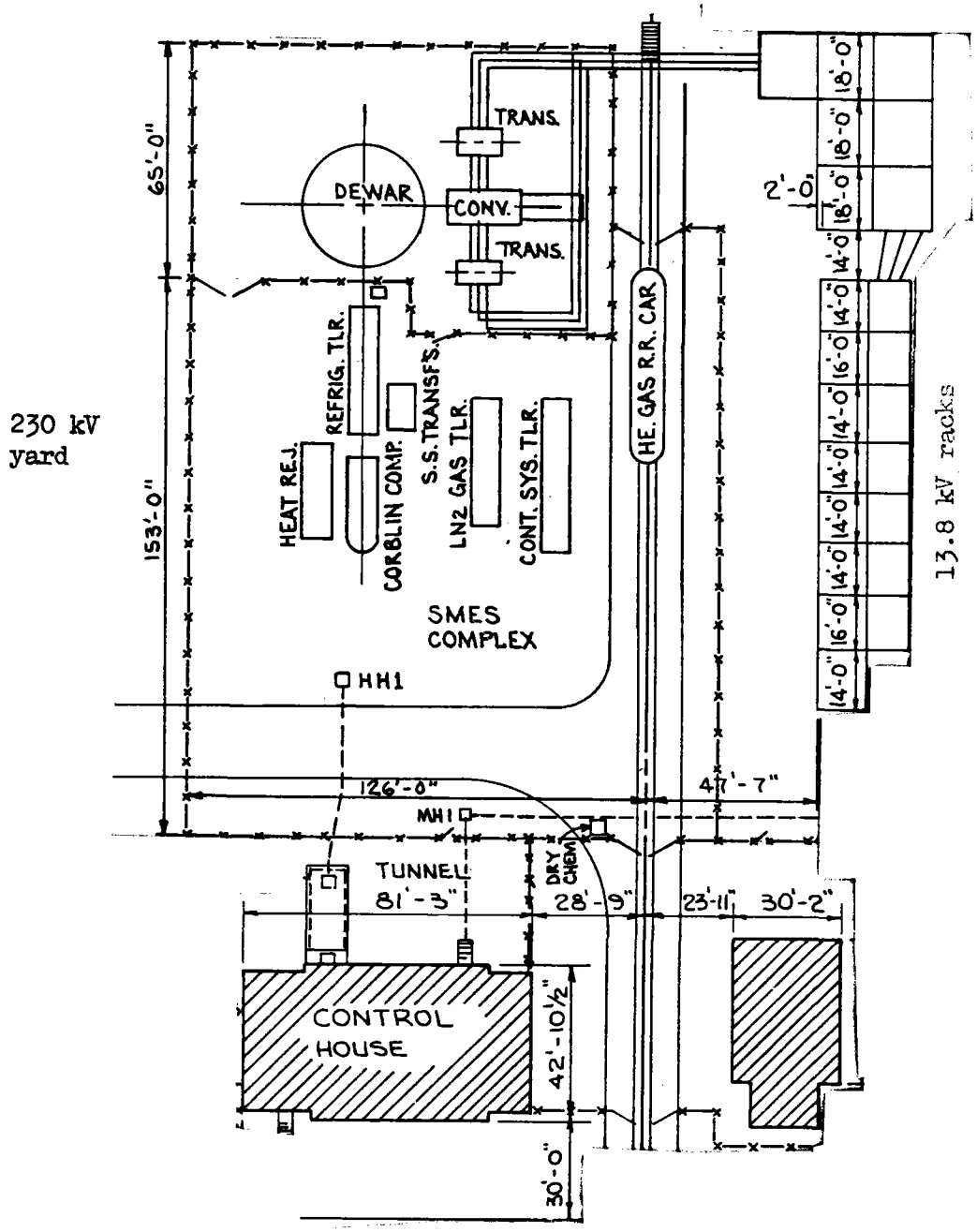

FIGURE 1

SMES PORTION OF BPA's TACOMA SUBSTATION

The layout is shown in Figure 1. Note that 7-foot chain link fence was used to segregate the entire SMES from the existing switchyard. A secondary four-foot fence was installed to separate the potentially hazardous dewar/coil assembly and electrical buswork from the trailer mounted equipment.

Footings

Soil testing and previous construction at the site indicated that pilings would be required below the dewar footing. Six sixty-foot wood pilings were driven in July. They were driven to a depth of approximately 30 feet. These pilings were cut off and the remaining portions also driven. Footings within a fifty-foot radius of the pilings were poured after the pilings had been driven to prevent any movement. The dewar and adjacent D.C. bus support footings use non-magnetic rebar to prevent coil losses. Fiberglass rebar and smooth 1" stainless rod were obtained. This reinforcement was held in place with nylon ties in lieu of the conventional steel wire method. The method of mounting the seismic designed dewar/coil assembly required a jig to hold the anchor bolts in $\pm$1/8 inch tolerance during the concrete pouring. Concrete pads were installed as foundations for the trailer mounted equipment. They were used to stabilize and prevent settling due to equipment vibration. Footings for this project were designed for BPA seismic zone "C." This is comparable to the Uniform Building Code Zone 3.

Grounding

With the presence of 500-kV and 230-kV lines, and high magnitude fault currents in the existing substation, equipment grounding is critical. All equipment has redundant bonds to the 4/0 copper mat. Existing ground mat loops within the vicinity of the superconducting coil were severed to prevent loop currents, and new grounding circuits were laid in a radial configuration relative to the coil/dewar assembly.

Cable Trenches/Conduct

The cable trench was to originally contain all power, control, and indication cables and the fiber optic control links. At the request of LANL the power cables were routed in underground conduits or in a segregated section of the trench. The high pressure helium line from the railroad helium tank car was located in the trench also for safety and ease of visual checking.

The trench design used for this project enables simple on-site manufacturing-the sides are made of railroad ties with a plywood lid.

Electrical Connection to BPA's Substation

The SMES system is connected to BPA's 13.8-kV bus by two methods:

1. The 30MJ coil via the converter and two 6 MVA pulse transformers is connected through a power circuit breaker with isolation switches. The buswork is all aluminum due to adjacent reduction plant fumes.

2. The station service transformers are connected to the 13.8-kV bus through resistored power fuses, thus maintaining continuous station service power when SMES is interrupted from the power grid. The new S.S. transformers were required due to the large connected load (500 kVA) and uncertain duty factors.

The Uninterruptable Power Supply for the computer in the control trailer is to be fed by a 70 amp hour 120-Volt battery added to the control house battery room. The battery will be on continual float charge with redundant power sources.

Operational Control

Control of the use of the SMES unit on the BPA power grid must be by BPA's power schedulers. The control of the 13.8-kV breaker which ultimately determines whether SMES is on or off system will be controlled manually from the control house by a BPA operator, by remote control from Dittmer control, or by protection relays. The SMES unit can also enable a disconnect from the power grid. Delayed system disconnecting will be used for non-emergency tripping to prevent energy dumping.

Integrating an R&D Project into an Operating Substation

BPA engineering, construction and operation personnel have attempted to install the SMES unit the most cost effectively possible while maintaining the operation standards of our Tacoma Substation.

The design used enables a complete isolation of the SMES unit from the power grid when necessary, and enables the SMES unit to fully integrate into the system for system stabilization and system testing.

UTILITY CONTROLS FOR BPA 30-MJ SMES SYSTEM

J. F. Hauer
THE BONNEVILLE POWER ADMINISTRATION
Portland, Oregon

A 10-MW, 30-MJ Superconducting Magnetic Energy Storage (SMES) unit is presently being installed at the BPA Tacoma substation, in a DOE project involving both the Los Alamos National Laboratory (LANL) and BPA. Signals provided by BPA will modulate the SMES unit setpoint in a manner designed to assure adequate damping of particular swing modes on the Western Power System, primarily the north-south mode that occurs at frequencies near 0.35 Hz [1]. The unit will thus provide an alternate means for augmenting dynamic stability of the power system when HVDC Modulation is unavailable. This occurs during periods of maintenance or hardware failure, when HVDC Intertie current is below 300 amperes, or when either the HVDC Intertie or the Pacific AC Intertie is importing power into the BPA system.

Modulation of the Tacoma SMES unit addresses control objectives [1] similar to those of HVDC Modulation at the Celilo converter station but its capabilities and operating environment are substantially different. The SMES unit is sized for small-signal use and the modulation signal is a random one with time-variable statistics, so management of stored control energy reserves and effects of sustained operation near the device limits must both be considered in overall controller design. A key element in this is the relative sensitivity of power system dynamic response to real and reactive components $\Delta P, \Delta Q$ of complex power modulation ΔS at Tacoma. Close estimates for the associated response functions will require direct measurement of system response to test signals injected

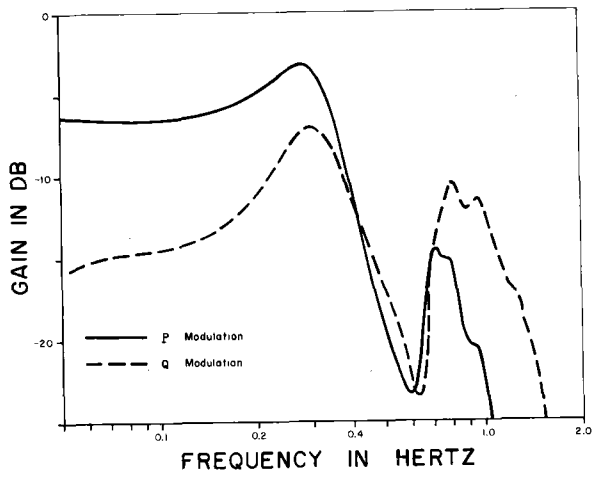

Fig. 1 Response of Pacific AC Intertie power to complex power modulation at Tacoma

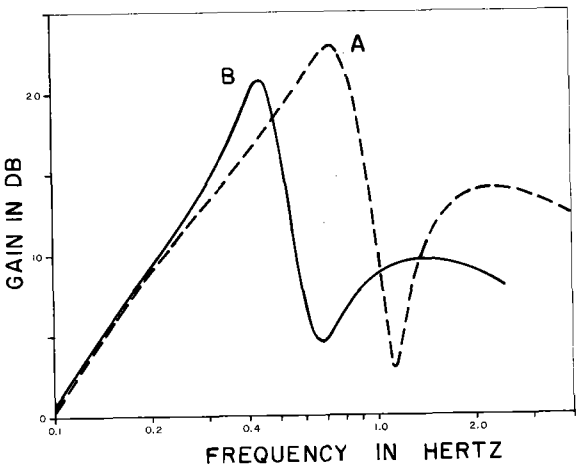

Fig. 2 Response for prototype SMES modulation systems

by the SMES unit itself, augmented by extended monitoring of its on-line performance. Preliminary estimates, typified by the curves in Figure 1, have been derived from computer swing simulations and agree generally with field tests [2]. These have been used to develop a series of prototype modulation systems, such as those shown in Figure 2. They also indicate that power system response to changes in SMES unit Q demand is strong enough that means should be provided for moderating the effects of P/Q interactions associated with the unit.

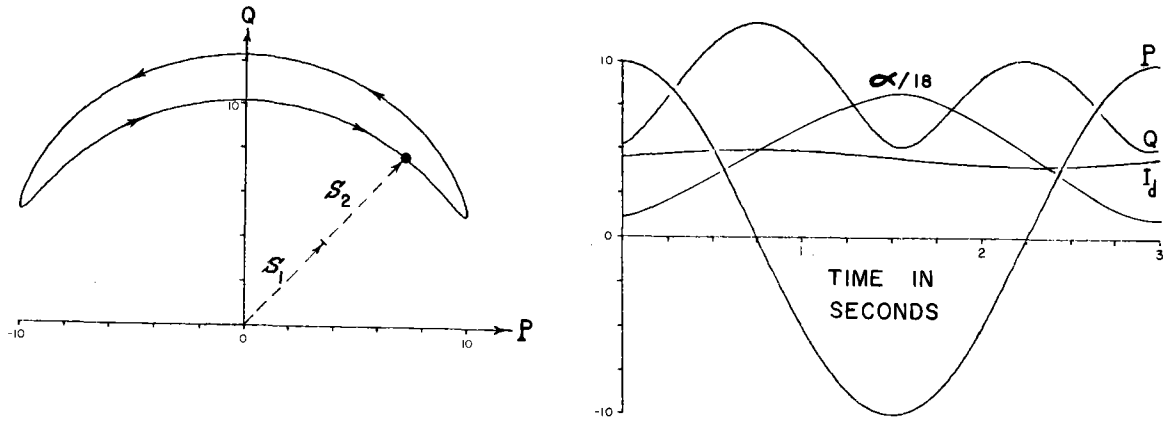

Fig. 3 SMES unit response to 1Ø MW sinusoidal demand, using parallel bridge controls ($\alpha_1 = \alpha_2$). Current in kA

Each of the two SMES converter bridges presents a somewhat variable complex load S_i to the AC system, and the power factor for each S_i can be set via an associated firing angle α_i. Figure 3 shows SMES unit response for a ±1Ø MW sinusoidal demand and parallel control of the converter bridges (which assigns each bridge the same nominal firing angle and orients the S_i in pure boost). As indicated by the P/Q locus, this operating mode produces a spurious $\Delta Q(t)$ signal that varies nonlinearly with P(t) and that contains several significant harmonics of the modulation frequency. It is not likely that this would raise serious difficulties during normal unit operation; the expected level of P modulation and hence the associated $\Delta Q(t)$ signal is then much smaller, and $\Delta Q(t)$ acts mainly as an unwanted noise injection peaking at twice the AC Intertie swing frequency (i.e., near Ø.7 Hz). High signal levels are required during system response tests, however, since ambient noise on the AC Interie can approach 1Ø MW rms and the gain presented to test inputs is quite low at some frequencies. The nonlinear P/Q interaction then handicaps an already sensitive measurement process that is central to good identification of the system dynamics under control.

Model studies indicate that operation of the SMES unit according to the buck/boost logic of Figure 4 permits Q(t) to be held at 8 MVAR for P demands up to about ±8 MW. Beyond this the limit logic sacrifices Q tracking in favor of P, as

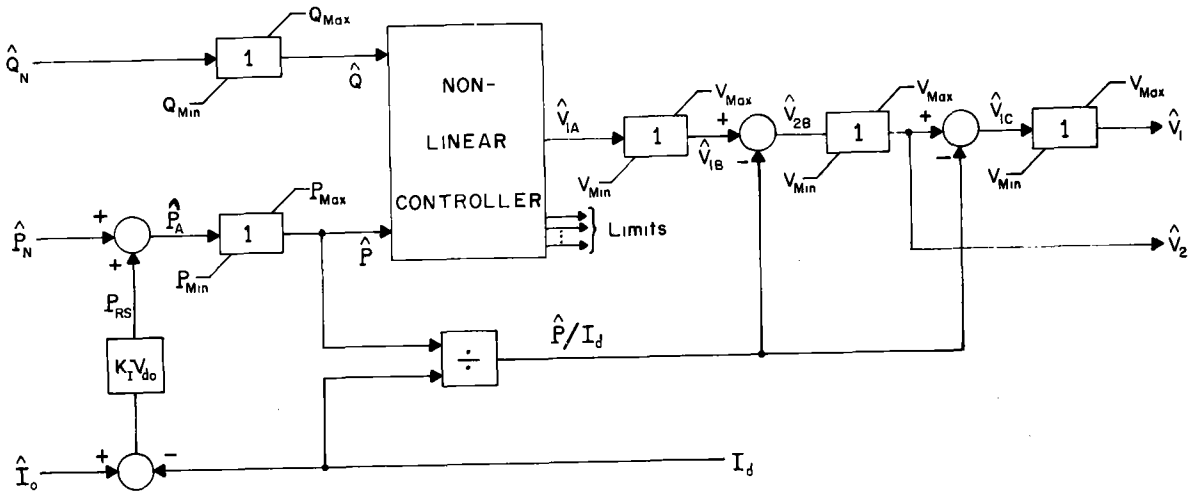

Relations Used:

$$\hat{S} = \sqrt{\hat{P}^2 + \hat{Q}^2} \qquad P_{Max} = 2\,\bar{V}_{Max}\,I_d$$

$$S_{Max} = 2\,V_{do}\,I_d \qquad P_{Min} = 2\,V_{Min}\,I_d$$

$$V_{Max} = V_{do}\cos(\alpha_{Min}) - R_c I_d \qquad Q_{Max} = \sqrt{S_{Max}^2 - \hat{P}^2}$$

$$V_{Min} = V_d \cos(\alpha_{Max}) - R_c I_d \qquad \hat{V}_{1A} = \frac{V_{do}}{S_{Max}}\left(\hat{P} - \hat{Q}\sqrt{\left(\frac{S_{Max}}{\hat{S}}\right)^2 - 1}\right)$$

Fig. 4 Prototype PQI controller for SMES unit

illustrated in Figure 5. The model also provides resetting of coil current I_d toward assigned value $\hat{I}_o$, a feature not used for the results shown here. Performance of this setpoint following logic was also examined for the modulation functions of Figure 2, using input signals extracted from AC Intertie power records (taken with HVDC Modulation in service) and with the SMES modulation system initially quiescent. While not final, the gains and filter settings used are regarded as representative. Current and Q(t) histories appear satisfactory in both cases, but P(t) indicates a considerable reduction in nonproductive high-frequency activity for prototype B. This is beneficial from a hardware standpoint, and is one of several reasons for preferring modulation functions that have minimal bandwidth.

Hardware for the modulation function will be located at the John Day substation and use either 24-bit or 32-bit signal processors (both are in standard use at BPA). AC Intertie current rather than power will be used as the input signal; the incremental response of these two quantities is identical within a scale factor, but that for current is less variable with changes in operating conditions [1]. The calculated setpoint for P will be transmitted to Tacoma via microwave, where setpoint follower controls provided by LANL translate it to voltage targets for the two converter bridges. Initial logic for this operates the unit in boost mode and is being extended

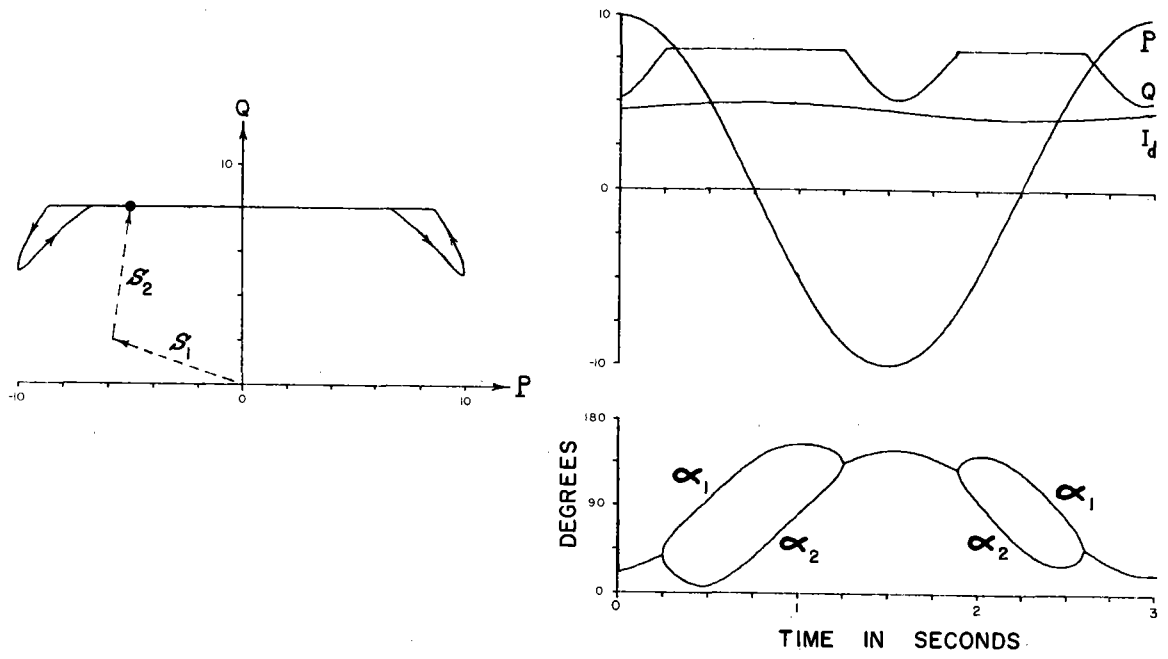

Fig. 5 SMES unit response to 1Ø MW sinusoidal demand, using PQI controller of Figure 4 and Q setpoint of 8 MVAR

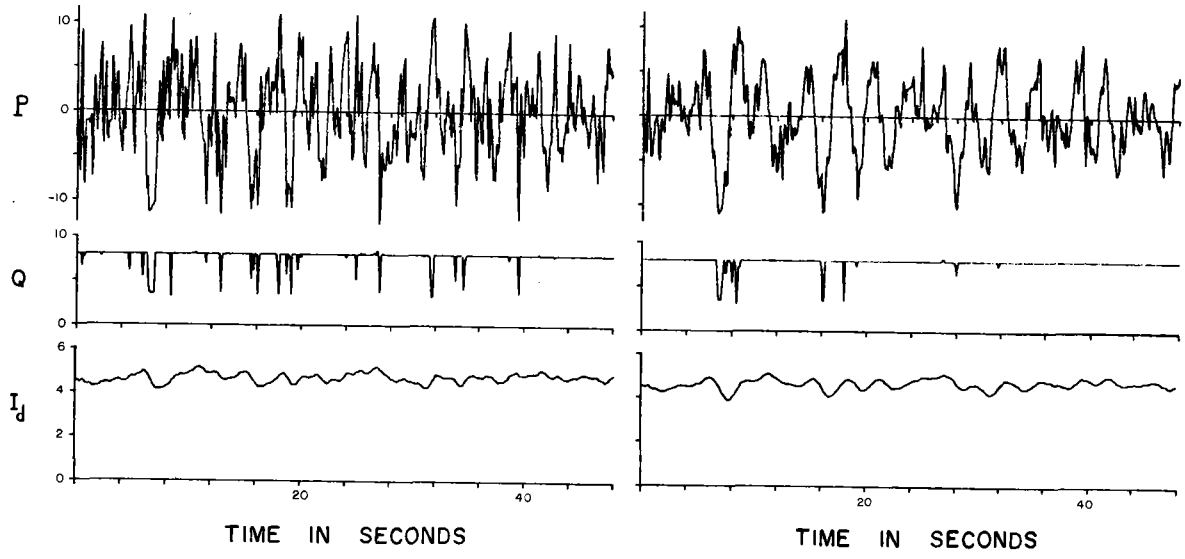

Fig. 6 SMES modulation startup for prototype modulation functions of Figure 2

for optional buck/boost operation along the lines of Figure 4 and analogous Q-dominant schemes. Setpoints for Q and I_d will be generated locally, as the range of feasible Q is too narrow to warrant Q modulation for other than experimental purposes. Tuning and evaluation of setpoint follower logic will be coordinated with that of the modulation system itself, in a BPA/LANL joint effort directed toward effective utilization of the SMES unit and toward related project objectives.

REFERENCES

[1] R. L. Cresap and J. F. Hauer,"Power System Stability Using Superconducting Magnetic Energy Storage - Dynamic Characteristics of the BPA System", Proceedings of the 1978 Mechanical and Magnetic Energy Storage Contractors' Review Meeting, pp. 254-262.

[2] J. F. Hauer,"Power System Identification by Fitting Structured Models to Measured Frequency Response," IEEE Trans. PAS, pp. 915-923, April 1982.

FLYWHEEL ROTOR AND CONTAINMENT TECHNOLOGY DEVELOPMENT - FY 1982*

Satish V. Kulkarni
University of California, Lawrence Livermore National Laboratory
Livermore, CA 94550

ABSTRACT

The status of the flywheel rotor and containment technology development program during FY 1982 is reviewed in this paper. The specific objectives of the different activities are delineated, and progress during the present reporting period is described briefly.

INTRODUCTION

The present emphasis on energy conservation and fuel economy has stimulated the development of energy-storage devices such as flywheels. Incorporating a flywheel (for engine load leveling and regenerative braking) into an internal-combustion engine vehicle that operates mainly on city streets could result in significant fuel savings. Using a flywheel in a battery-powered electric vehicle could also improve the vehicle performance and battery life. Additionally, flywheels have potential energy-storage applications in devices as diverse as wind- and solar-energy generators, cranes and fork lifts, and space vehicles.

Flywheels fabricated from fiber-reinforced composite materials offer significant advantages over metallic flywheels. These composite materials possess high specific stiffness and specific strength. With high specific strength, fiber-reinforced composite rotors can store more energy per kilogram and offer better long-term performance than metallic rotors. In addition, composites tend to break up into small pieces when they fail, making it easier to contain the fragments. Fiber-reinforced flywheel systems also have the potential, with further development, for lower manufacturing costs.

The U.S. Department of Energy has had a broad-based program to develop the technologies of electric and hybrid vehicles. LLNL has been assigned the responsibility to direct and coordinate the composite-materials flywheel research and development effort.

The two primary objectives of this effort are:

- To develop an efficient, economical, and practical composite flywheel having an energy density of 88 Wh/kg (40 Wh/lb) at failure, with an operational range of 44 to 55 Wh/kg (20 to 25 Wh/lb) and an energy-storage capacity of approximately 1 kWh.

- To develop a fail-safe, lightweight, and low-cost composite containment for the flywheel.

---

*This work was performed under the auspices of the U.S. Department of Energy by the Lawrence Livermore National Laboratory under contract No. W-7405-Eng-48.

The strategy being followed to achieve the objectives is outlined below:

- Design, develop, fabricate, and test the most promising generic rotor and containment concepts.
- Use existing technologies wherever applicable.
- Seek active participation by industry, national laboratories, and universities to (1) use expertise in an optimum fashion, (2) promote cross-fertilization of ideas, and (3) create a competitive environment.

The highlights of the accomplishments for this task during FY 1982 are:

- Completed the evaluation of the GE and Avco containment designs, and selected the GE design for prototype fabrication and testing (Task Milestone).
- Demonstrated and evaluated flywheel rotor cyclic test capability at the Oak Ridge Flywheel Evaluation Laboratory (Task Milestone).
- Initiated the design/fabrication of the thirty (30) second-generation composite flywheels (Garrett, GE, and Avco). A plan to test and evaluate these flywheels has been prepared, incorporating both pre- and post-test analyses.
- Initiated a study of composite flywheel performance projection using new, higher strength Kevlar and graphite fibers.
- Tested and evaluated LLNL designed, Owens-Corning and Lord Corporation fabricated molded SMC disk/ring hybrid flywheels. These flywheels have the lowest cost, moderate energy density and have the most predictable performance characteristics.
- Discussions were initiated with various industrial organizations (e.g. Owens-Corning, Borg-Warner, GM, University of Wisconsin, and others) to encourage them to build a passenger vehicle utilizing DOE developed mechanical energy storage technology. A follow-up meeting was held at Battelle Columbus Laboratories and requests for proposals were handed out to potential industrial participants.
- Technology transfer to Beckman Instruments has allowed them to build graphite/epoxy ring centrifuges in order to be competitive with foreign manufacturers.
- Volvo Bus Corporation of Sweden has demonstrated interest in the use of the Garrett flywheel and GE containment design in a project to build a diesel engine/flywheel hybrid bus.
- Testing at LLNL of the elastomer bond between the rotor and hub has been nearly completed. The data indicate that the bond strength exceeds the minimum torque requirements for automobile applications.

Specific objectives and the status of different activities are discussed subsequently.

OBJECTIVES AND STATUS OF VARIOUS ACTIVITIES

The work breakdown structure of this task consists of nine (9) major subtasks and several activity areas under each subtask. Progress in the areas of fiber composite materials technology, flywheel cost analysis, and the GE rotor and containment development is reported separately at this meeting.

Technical Management and Documentation, Lawrence Livermore National Laboratory (LLNL): Technical management activities play a crucial role because of the various industry and university subcontracts and the multidisciplinary nature of this task.

Objectives:

- o Identify activities and projected costs consistent with the task goals and the availability of funding.
- o Prepare invitations for proposal and evaluate responses.
- o Evaluate performance, track schedules, and milestones.
- o Prepare monthly and annual reports as well as a topical report projecting future flywheel characteristics, and documenting the utility of flywheel for various applications.
- o Promote technology transfer, and disseminate information to industry.

Status:

- o Planned, coordinated, and directed approximately ten (10) activities at LLNL, other national labroatories, industry, and universities
- o Completed the evaluation of the GE and Avco containment designs, and selected the GE design (Figure 1) for prototype fabrication and testing (Task Milestone).
- o Demonstrated and evaluated flywheel cyclic test capability ar ORFEL (Task Milestone).
- o Initiated the design and fabrication of thirty (30) second generation composite flywheels (Garrett, GE, Avco).
- o Discussions were initiated with various industrial organizations (e.g. Owens-Corning, Borg-Warner, GM, University of Wisconsin, and others) to encourage them to build a passenger vehicle using DOE developed mechanical energy storage technology. A follow-up meeting was held at Battelle Columbus Laboratories and requests for proposals were handed to various potential participants. The proposed effort is a joint DOE/LLNL/ORNL/Industry program with no DOE funding.
- o Technology transfer to Beckman Instruments has allowed them to build graphite/epoxy ring centrifuges in order to remain competitive with foreign manufacturers.
- o A report documenting the utility of flywheels for various energy storage applications is being prepared.

Rotor Technology Development - LLNL:

Objectives:
- o Generate design data for the rotor/hub elastomeric bond.
- o Develop a rotor cyclic test plan.
- o Evaluate ORFEL/APL rotor spin test data.
- o Develop a biaxial stress test fixture.

Status:
- o Static torsion tests for the rotor/hub elastomeric bond have been completed. Torque capability of a 3-inch diameter bond is 4000 in-lb which is in excess of vehicular requirements (20-50 ft-lb). Torsional fatigue test have also been conducted for "deep" cycles (400-2800 in-lb) with no failures occurring to 10,000 cycles. Also, some cyclic tests have been performed for a torque range of 1400-2800 in-lb.
- o An update of the preliminary cyclic test plan developed earlier is being prepared. (S.V. Kulkarni, K.L. Reifsnider, D.M. Boyd, "Composite Flywheel Durability and Life Expectancy: Test Program", UCRL-86450, July, 1981).
- o Spin test data of the LLNL/Owens-Corning/Lord Molded SMC disc/ring hybrid rotors (Figure 2) were evaluated (see Table 1). These rotors have the lowest cost, moderate energy density, and the most predictable performance characteristics.
- o A modified servo-controlled loading system has been designed for the biaxial test fixture.

Bidirectional Weave (BDW) Composite Material Flywheel Development - Avco, Systems Division:

Objectives:
- o Design, fabricate, and deliver three (3) BDW composite material disk rotors.

Status:
- o Difficulties have been experienced in the design of the hub and the molding of the BDW disks. The original polvarylate molded hub design was changed to Nylon II because of the need to avoid resonance during spin testing. Nylon II is linear to 10% strain and consequently its modulus is higher at higher stress levels than polyarylate. During molding of the BDW discs, which are bonded together three at a time to form a disc (Figure 3), full resin impregnation was not achieved initially. The problem has been resolved by modifying molding parameter. Consequently, this task has been delayed.

Advanced, 1 kWh Prototype "State-of-the-Art" Rotor Development - Garrett AiResearch:

Objectives:
- o Design, fabricate, and deliver ten (10) multi-material, multi-ring prototype rotors having an energy capacity of up to 1 kWh, a maximum energy density of 40 Wh/lb at burst, and an operational energy density of 20-25 Wh/lb.

Status:

- The design parameters for the ten (10) rotors (Figure 4) are given in Table 2. The graphite/epoxy struts for the new hub design were compression molded by Ewald Associates and met all Garrett specifications (dimensional tolerances and interlaminar shear strength). The adhesive bonding of these struts to the aluminum parts was successfully achieved after some initial difficulties.
- One prototype is being fatigue-tested at ORFEL.

Prototype Rotor Development for Vehicular Applications - General Electric, Space Division:

Objectives:

- Design, fabricate, and deliver nineteen (19) laminated disc/filament-wound-rim hybrid prototype rotors having performance goals consistent with vehicular application requirements.

Status:

- The status of this activity is being reported separately at this review meeting. See "Composite Flywheel Rotor Design Optimization and Fabrication," by A. P. Coppa. The design parameters for the nineteen (19) rotors (Figure 5) are given in Table 3.
- One S2-glass/epoxy disk has been burst-tested at ORFEL, and one disk/ring hybrid rotor is undergoing cyclic tests.

Composite Rotor and Containment Cost Analysis - Battelle Columbus Laboratories:

Objectives:

- Develop a costing methodology to establish the cost range of rotor/containment as a function of design, materials, manufacturing process, and production quantities.

Status:

- The status of this activity is being reported separately at this review meeting. See "Manufacturing Cost/Design Trade-Studies for Flywheels," by B. R. Noton.

Evaluation of Future Composite Flywheel Capabilities - Lawrence Livermore National Laboratory:

Objectives:

- Project possible improvements in composite flywheel performance through continued research and development.

Status:

- At the present time, a study is underway to screen and evaluate new, higher strength Kevlar and graphite fibers (see "Fiber Composite Materials Technology for Flywheel Energy Storage," by T. T. Chiao — to be presented at this review meeting.) Based upon the preliminary data for these fibers, which show a 15-30% increase in strength, projections are being made about the performance characteristics of the GE and Garrett designs. It appears that a straightforward translation of this strength increase to flywheel performance is not possible because of the need to consider matrix dominated failure modes. In fact, utilization of higher strain-to-failure resins such as urethanes could also improve flywheel performance, especially that of rim-type designs.

Fabrication of Prototype Containment Housings — General Electric, Space Division:

Objective: o Design and fabricate three (3) containment prototypes for the Garrett, GE, and Avco rotor designs having energy capacities ranging from 0.25 to 1 kWh at burst.

Status: o Technical and cost proposals have been received from GE. This effort will be initiated during the current fiscal year.

CONCULSIONS

In summary, an overview of the flywheel rotor and containment technology development effort during FY 1982 has been presented. That this effort encompasses a broad spectrum of technologies is obvious. Every effort is being made to use state-of-the-art techniques and advance them, if necessary, to accomplish the task objectives. The assessment is that significant progress has been made during the present reporting period in the area of second generation composite flywheel fabrication, and that it is indeed feasible to employ the rotor and containment designs for various energy storage applications.

ACKNOWLEDGEMENTS

The author would like to acknowledge the contributions and support of L. G. O'Connell and D. D. Davis of the Transportation Systems Research, LLNL, and J. Martin of the Oak Ridge National Laboratory.

Table 1

SPIN TEST DATA FOR LLNL/OWENS-CORNING/LORD S-2 GLASS SMC MOLDED DISK FILAMENT WOUND GR/EP RING "HYBRID" FLYWHEELS

Rotor Identification	Ring O.D.[a], in.	Ring Thickness, in.	Weight, lbs	Speed at Failure, rpm (Predicted speed)[d]	Energy, kWh	Energy Density Wh/lb
C-1a[b]	24.00	1.1	28.4	19,980 (21,660)	0.358	12.6
C-1b[c]	24.00	1.1	28.5	21,620 (21,660)	0.419	14.7
C-2a[b]	22.0	1.1	24.15	21,120 (21,440)	0.278	11.5
C-3a[b]	24.0	1.1-2.2 (trapezoidal with 20-degree taper)	32.21	22,020 (21,850)	0.534	16.6

[a]All disks have an O.D. of 21 in. (same as ring I.D.) and are 1 in. thick.
[b]Tested at Oak Ridge Flywheel Evaluation Laboratory.
[c]Tested at Applied Physics Laboratory.
[d]Based on disk burst ($\sigma_{rr} = \sigma_{\theta\theta} = 40$ ksi).

Table 2

GARRETT MULTI-MATERIAL
(S2-GLASS/KEVLAR-29/KEVLAR-49/EPOXY)
MULTI-RING RIMS WITH GRAPHITE/EPOXY-AL HUBS

ROTOR	NO. OF CYCLES	MAX. SPEED, fps	MAX. RIM STRESS, ksi	SPECIFIC ENERGY, Wh/lb	REMARKS
1	1	3350	225.0	40.0	15 Ring Rim, Burst Test
2	1	3350	225.0	40.0	15 Ring Rim, Burst Test
3	1	3350	225.0	40.0	15 Ring Rim, Burst Test
4	10^5	2500	124.5	23.0	9 Ring Rim, Initial Integrity Check, Long-Term Cyclic Test
5	1000	2650	140.0	25.0	9 Ring Rim, Short-Term Cyclic Test
6	1000	2650	140.0	25.0	9 Ring Rim, Short-Term Cyclic Test
7	5000	2700	145.0	26.0	9 Ring Rim, Short-Term Cyclic Test
8	5000	2700	145.0	26.0	9 Ring Rim, Short-Term Cyclic Test
9	2500	2720	147.0	26.4	9 Ring Rim, Short-Term Cyclic Test
10	2500	2720	147.0	26.4	9 Ring Rim, Short-Term Cyclic Test

Table 3

GE S2-GLASS/EPOXY DISK - GRAPHITE/EPOXY RING "HYBRID" AND S2-GLASS/EPOXY DISK ROTORS

		Rotor Type		
		Disk/Ring "Hybrid" (Prototype) Quantity: 14	Disk	
			Thick Quantity: 2	Thin Quantity: 3
Rotor OD,	in.	16.00	15.86	15.86
Ring ID,	in.	12.80	------	-------
Ring Thickness,	in.	1.74	------	-------
Disk Thickness,	in.	1.70	1.70	0.85
Rotor Weight,	lb.	22.33	23.44	12.30
Rotor Weight, less Hub	lb.	21.22	22.33	11.18
Polar Moment of Inertia	$lb.in.sec^2$	1.687	1.819	0.908
Burst Design Parameters				
Energy,	Wh	480	472	236
Speed,	rpm	40660	38880	38880
Energy Density,	Wh/lb	22.6	21.1	21.1
Cyclic Design Parameters (10^5 cycles)				
Energy,	Wh	293	189	95
Speed,	rpm	31770	24600	24600
Energy Density,	Wh/lb	13.8	8.5	8.5

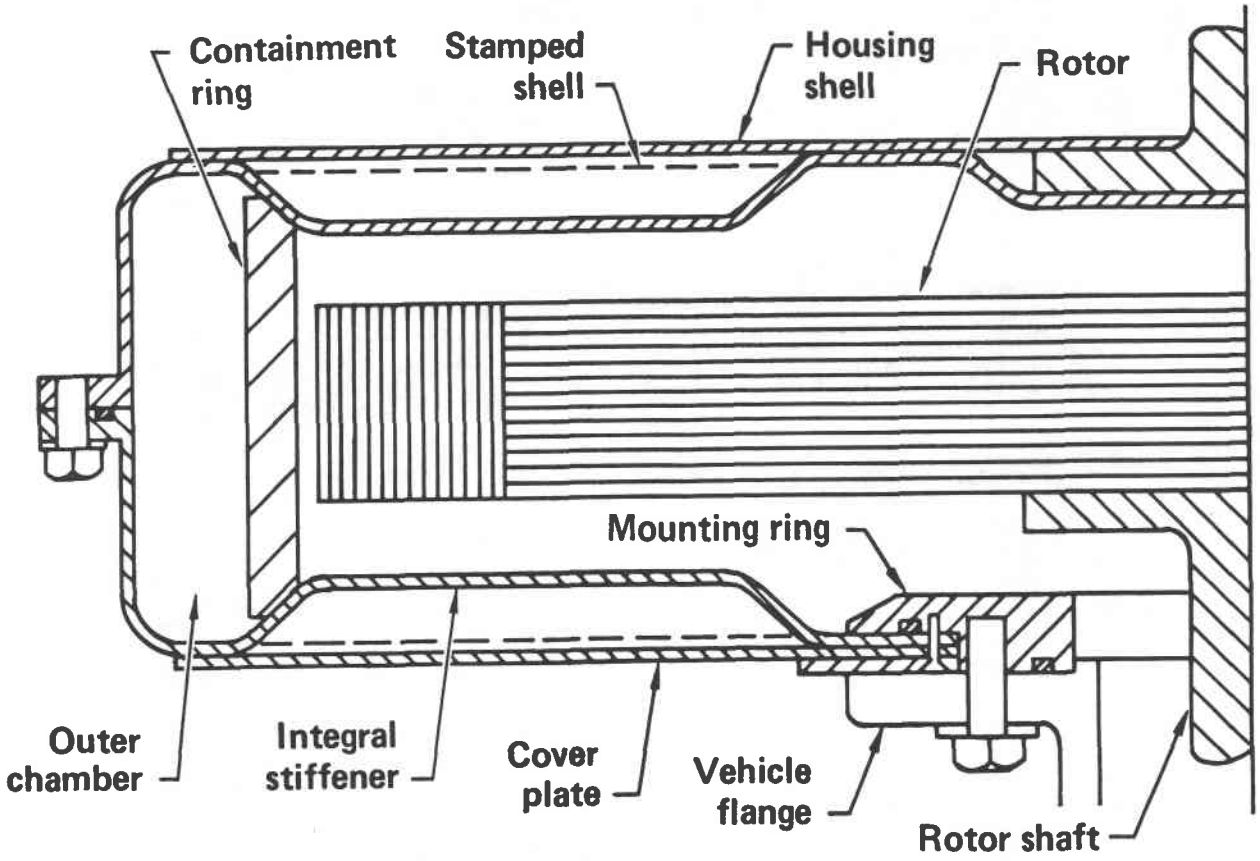

Fig. 1: General Electric "Floating-Ring" Containment Design

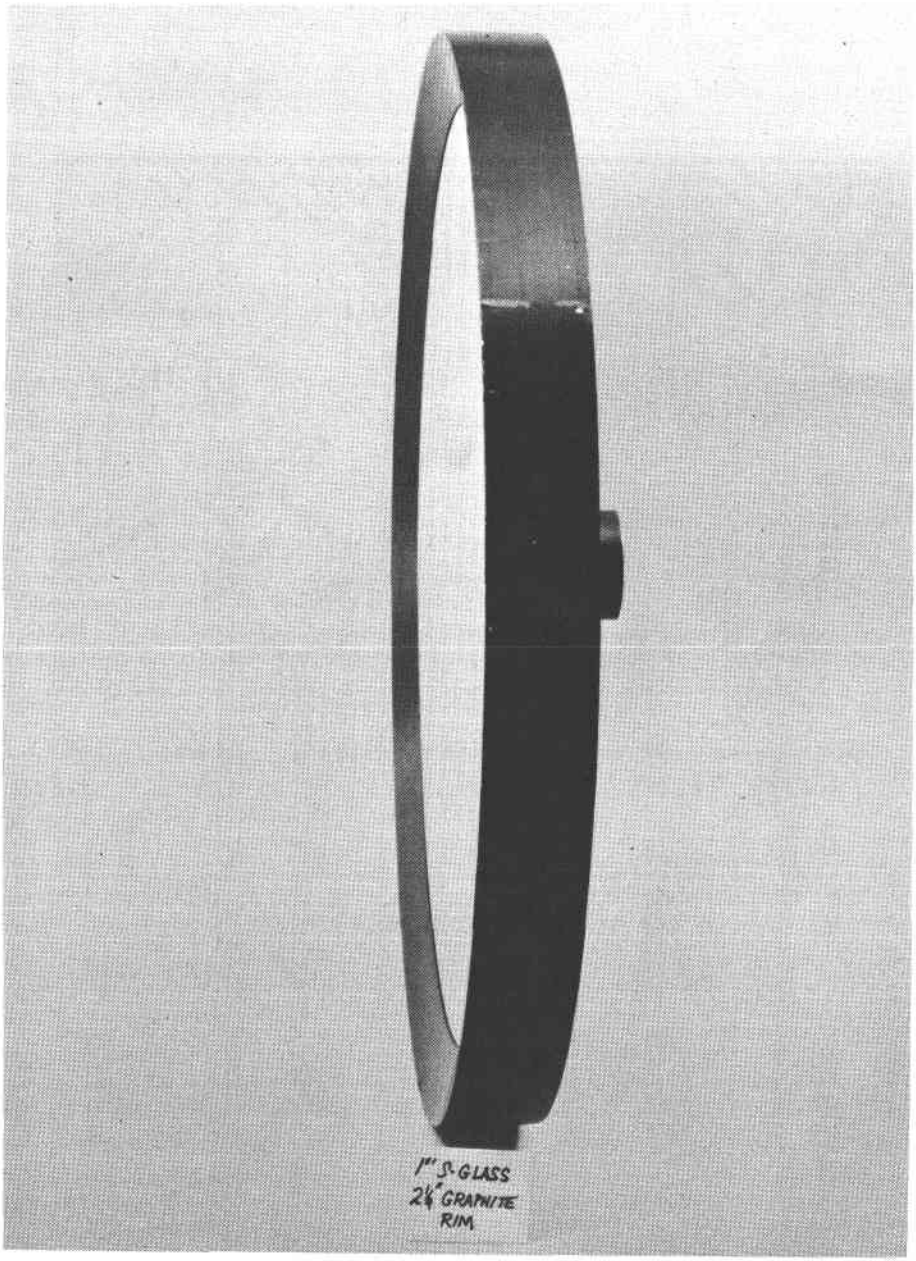

Fig. 2: LLNL/Owens-Corning/Lord Chopped S2-Glass/Polyester SMC Molded Disk with Filament-Wound Graphite/Epoxy Tapered Ring

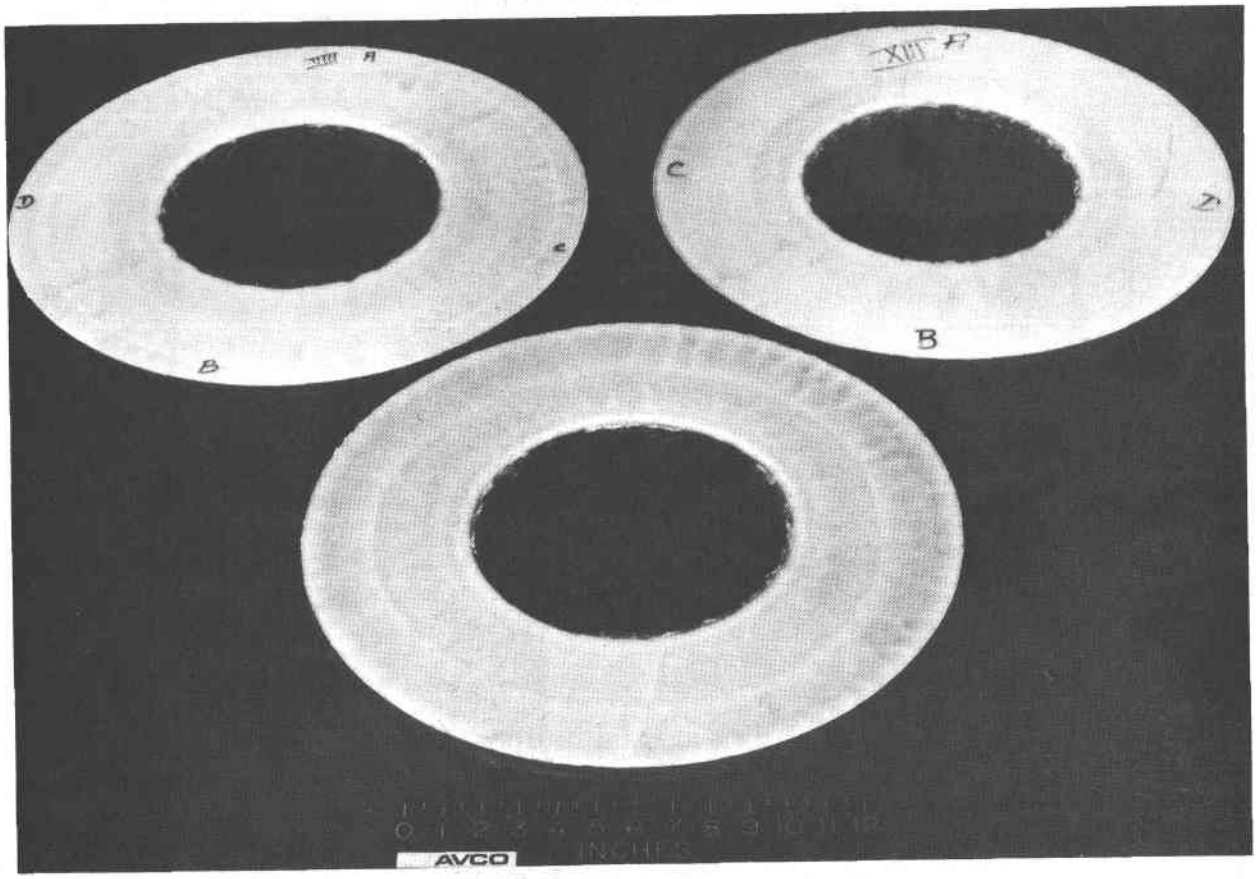

Fig. 3: Avco Bidirectionally Woven S2-Glass Cloth/Epoxy Molded Disks

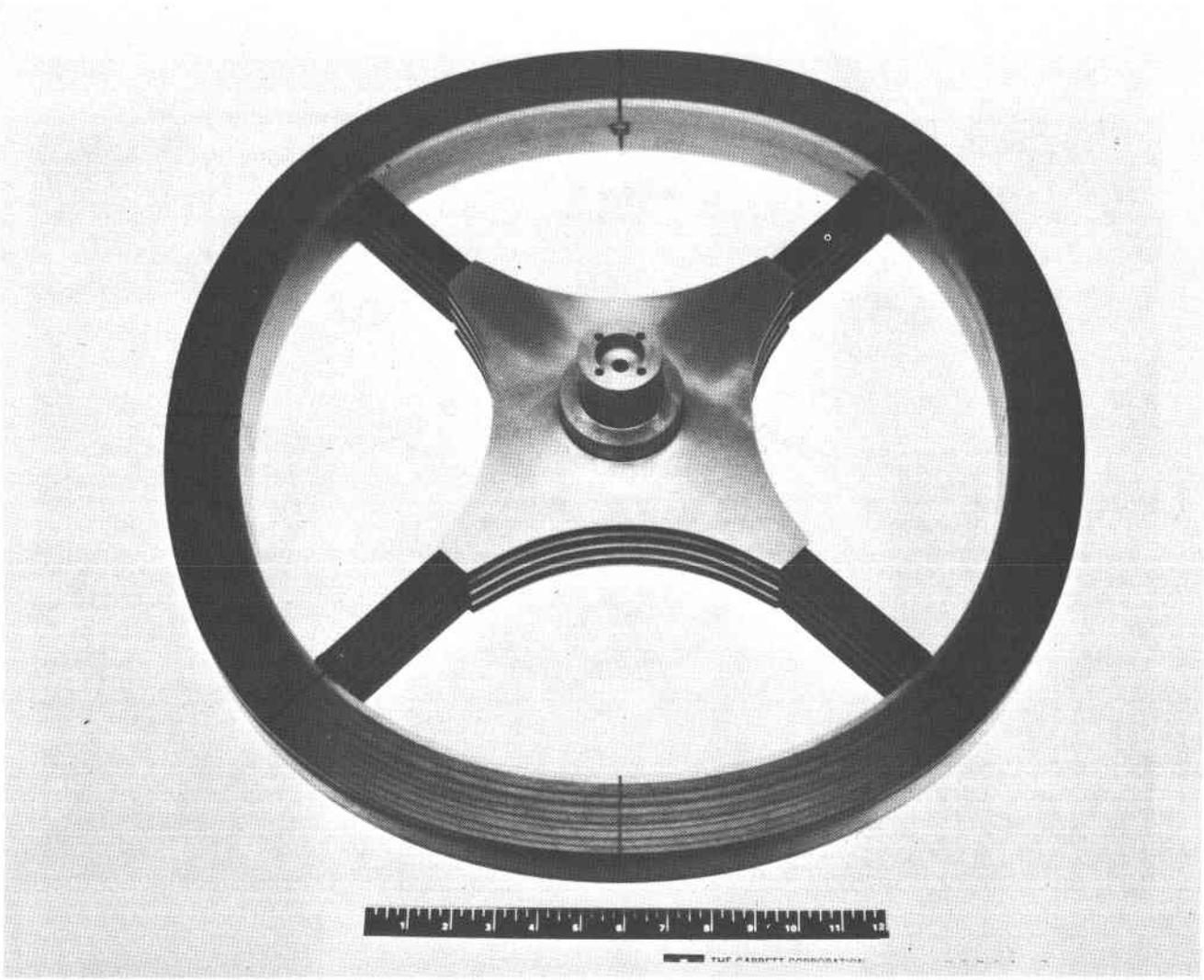

Fig. 4: Garrett Multi-Material Multi-Ring Rim Rotor with Graphite/Epoxy - Aluminum Hub

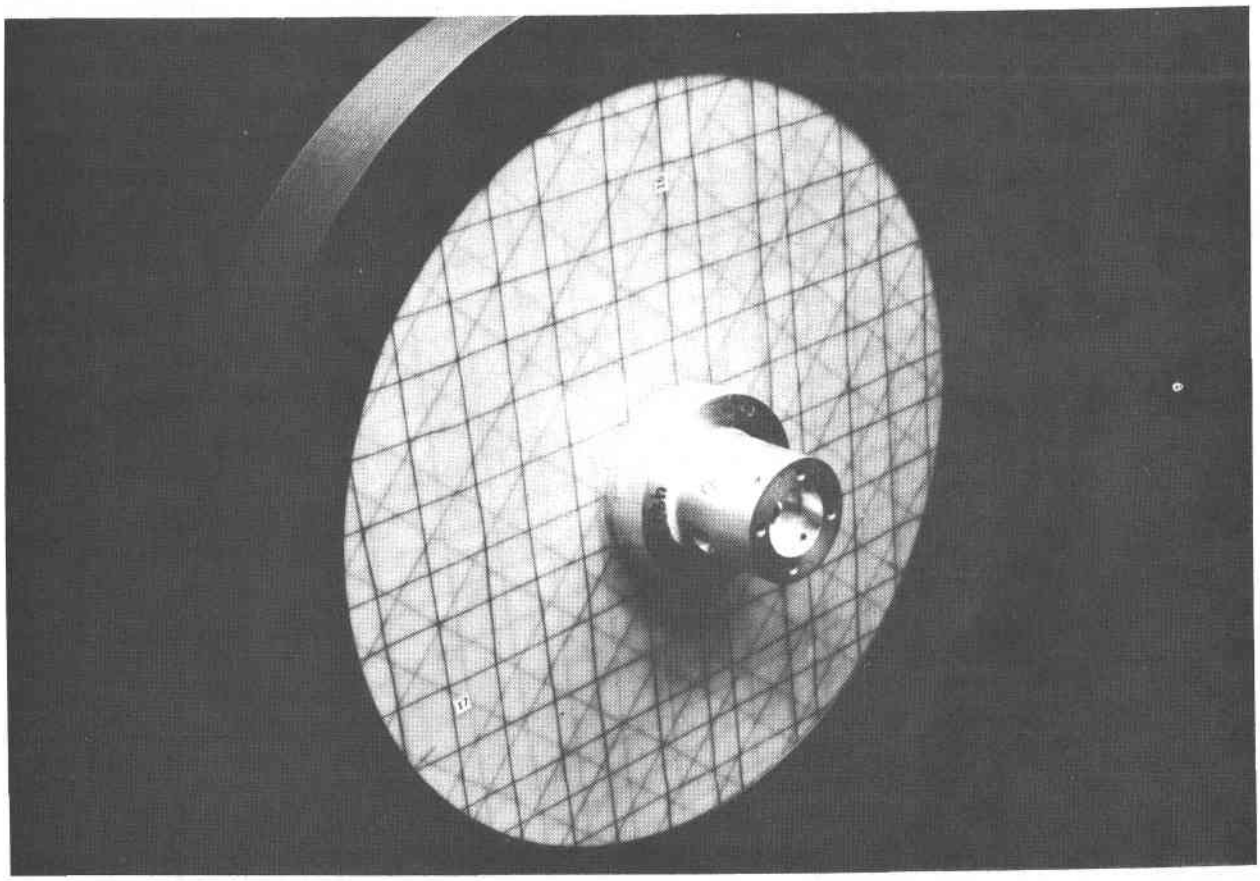

Fig. 5: General Electric S2-Glass/Epoxy Disk - Graphite/Epoxy Ring Hybrid Rotor

FLYWHEEL TESTING AND EVALUATION*

R. S. Steele
Oak Ridge National Laboratory**
Oak Ridge, Tennessee 37830

ABSTRACT

During the past several years, the DOE Mechanical Energy Storage program has supported spin testing of high performance composite flywheels to verify analytical predictions, identify unknown parameters, and understand the factors influencing flywheel reliability. In general, the results have supported the early predictions of flywheel performance; but certain real world factor evaluations now require further investigation. This paper discusses six general statements regarding the state-of-the-art in composite flywheels technology and presents the supporting data. (1) Composite flywheel performance is superior to that of metallic flywheels, while (2) presenting less severe containment requirements. (3) Composite flywheel fatigue life exceeds 1000 cycles. (4) Thermal considerations dictate a low pressure environment. (5) Balance characteristics of composite flywheels require special suspension provisions. And finally, (6) analytical models predict performance with increasing confidence and are thus becoming more useful in establishing the reliability of the rotor. Testing efforts must now address questions relating to lifetime, reliability, system design, and cost.

Introduction

Verification of analytical predictions, identification of unknown parameters, and the need to understand the factors influencing reliability of composite flywheels require comprehensive evaluation of prototype candidates. During the past several years, testing of this type has given much useful information regarding the performance characteristics of the designs developed under the DOE Mechanical Energy Storage Program. Strong statements regarding the performance and reliability of composite flywheels will need much more data than currently exists, but general trends are identifiable. These trends generally confirm the expectations of the early proponents, who now find credible support in the available data.

The data presented in this paper draw largely from the testing done at the Oak Ridge Flywheel Evaluation Laboratory (ORFEL) and the Applied Physics Laboratory (APL). Additional data come from tests at Garrett AiResearch, Rockwell Rocketdyne, and others.

*Research sponsored by the Division of Thermal and Mechanical Energy Storage Systems, U.S. Department of Energy, under contract W-7405-eng-26 with the Union Carbide Corporation - Nuclear Division.

** Current address Oak Ridge Y-12 Plant

These data lead to the following statements regarding the performance characteristics of composite flywheels:

a. Energy density performance exceeds metallic flywheels performance.
b. Containment requirements are less severe.
c. Fatigue life typically exceeds 1000 cycles.
d. Thermal considerations dictate low pressure environments.
e. Suspension system design must consider balance changes with speed.
f. Analytical models of the flywheels can be used with increased confidence.

The remainder of this paper will discuss each of these topics and present its supporting evidence.

Performance of Composite Flywheels

The past year's activities added several more points to the list of flywheel energy storage achievements. Figure 1 shows the learning curve for energy density since 1973 for composite flywheels storing greater than 0.250 Wh. The trend seen resulted from experience gained by the flywheel designers under the continuing support of the DOE. The current performance leaders are Garrett's high energy density flywheel at 80 Wh/kg and their high capacity DOT bus flywheel. A single section of this latter rotor has stored 3 kWh, and a stack of six of these rotors will soon store 16 kWh.

Efficient use of material is another category for consideration, since it relates so closely to rotor cost. This factor of merit resembles the shape factor used in the early selection of rotor designs but includes the real effects of actual design and fabrication performance. One calculates the design factor by dividing the energy density achieved in tests by the weighted average strength to density ratio of the material used. Table 1 gives the design factor for a number of rotors evaluated during the past several years. Owens Corning Fiberglass has the current best design factor with their chopped glass SMC disk with graphite support ring.

Containment Requirements

Composite flywheels have less severe containment requirements than metallic rotors for two reasons: designed-in benign failure modes and/or crushable fragments. The Garrett sub-circular rim demonstrated a benign failure mode when its ultimate speed was found to be limited by dynamic instability associated with rim circularity. Figure 2 shows the increasing circularity of this flywheel as the speed increased. The experience with the thick-ring designs of Union Carbide Corporation, Hercules, and others demonstrates another well-known type of benign failure. These circumferentially wound cylinders experience circumferential cracking resulting in pressure increases and minor balance changes. Either may be used as a noncatastrophic damage warning.

Containment requirements are also less severe, since catastrophic failures produce either stringy masses or crushable fragments. This is a direct consequence of the low transverse strength in the composites, as has been shown sufficiently in previous papers [1, 2, 3].

Adequate containment has now been shown to require more than prevention of simple penetration. Tests to date show the need to consider torque [4] as a major design factor and, in addition, explosions resulting from gas released by the decomposing composite during failure or by dust ignition should oxygen, entering the cavity during the failure, mate with the heat and ground fibers. The containment design [5] currently pursued by the Mechanical Energy Storage Project and scheduled for testing in FY 1983 addresses each of these items as a direct result of the observations made during the flywheel burst tests.

Fatigue Life of Composite Flywheel

Successful application of a composite flywheel assumes an adequate cyclic fatigue life. Only three fatigue tests involving composite flywheels provide directly applicable data. This year an alpha-ply disk with a graphite rim was cycled 1,454 times until failure, not believed associated with the composite, terminated the test. Previously, Garrett cycled their NTEV-2 composite rim with an aluminum hub to 106% of the operating speed 1,000 times as a proof test. They have also performed a similar test on a 3 kWh module of their DOT bus flywheel for 638 cycles. Neither flywheel failed.

The use of composite materials is in its early development. Thus, the necessary understanding needed to extrapolate accelerated or proof testing to estimates of life at the intended operating condition has low statistical confidence and is subject to considerable controversy. Thus, this year's activities include cycle testing of a GE disk rotor and a Garrett sub-circular rim rotor at near-operating conditions until a failure results. These tests will demonstrate whether adequate cycle life is available as well as start a data base for developing the analytical model needed for extrapolation.

Thermal Management and Pressure Requirements

The predictions of pressure requirements need definitive experiments for verification. The prediction by M. R. Baer [6] indicates maintenance of less than 66 C will demand a cavity pressure of less than 1 millitorr. The Rockwell Rocketdyne flywheel test experience illustrates the problem. This rotor was spun for approximately 2h at peripheral speeds up to 732 m/s and pressures up to 10 millitorr; the maximum temperature reached only 25 C. The same flywheel, tested in similar manner but at a chamber pressure of 1000 millitorr, reached a temperature in excess of 120 C at the time a portion of the rim was slung off.

Definitive experiments are needed and will require that a flywheel spin at a constant speed long enough, possibly over 10 hours, to reach thermal equilibrium at different pressures. The goal will be to verify the analytical models and to provide input as to any detrimental affects thermal energy produce.

Rotor Balance Experience

Muske and Flores [7] found in their survey of industrial balancing practice that items in the composite flywheel class are typically balanced to a mass eccentricity of less than 7.5 micrometers. Table 2 gives a summary of our balance experience in ORFEL and shows that the as-received flywheels would all require additional balancing to meet this specification. Thus, any cost analysis must include the expensive process of close tolerance balancing.

Whether or not balancing was possible did not concern rim type flywheel developers since the inside diameter of the rim provided a natural place for the balance weight. Disk type flywheel developers were less certain, since weights could not be bonded with confidence to the planer surfaces and the consequences of drilling holes near the outside diameter was unknown. Tests this year have now shown that the use of balance holes in both the SMC molded disk and the alpha-ply layup disk flywheels do not reduce performance. Figure 3 shows flywheel OCLB after balancing with this method.

Composite flywheels' tendency to change their balance as the spin speed and gyroscopic stresses change causes more concern. Table 2 shows the differing degrees at which various flywheels are affected. The phenomena appears worse in spoke-supported rims than in disk types; but even in the disk types, the design of the suspension system must consider the phenomena.

Increased Confidence in Performance Predictions

Confidence in performance predictions has increased significantly in the last several years. It results from improved fabrication of composite material, a growing maturity in the analysis of and for the failure mode, and an improved ability to test for a particular failure mode. The best example of this is given in Figure 4 showing the predicted and actual performance achievements of the Owens Corning SMC disk with several different supporting rings.

Conclusions

The testing to date supports the early proponents' predictions of composite flywheels' applicability. However, the data also show that the risk of using this new technology may still be high. Composite flywheels

have now demonstrated energy density and total energy capacity sufficient to accomplish the automotive energy storage requirements. We must now address questions relating to lifetime, reliability, system design and cost.

References

1. R. S. Steele and E. F. Babelay Jr., "Flywheel Tests at the Oak Ridge Flywheel Evaluation Laboratory," in Proceedings of the Mechanical, Magnetic, and Underground Energy Storage 1980 Annual Contractors Review, pp. 445-457, CONF-801128, November 1980.

2. R. S. Steele and E. F. Babelay Jr., "Rotor Testing in FY 1981", in Proceedings of the Mechanical, Magnetic, and Underground Energy Storage 1981 Annual Contractors Review, pp. 329-336, CONF-810833, August, 1981.

3. Anthony P. Coppa and Carl H. Zweben, "Flywheel Containment Technology Assessment", in Proceedings of the Mechanical, Magnetic, and Underground Energy Storage 1980 Annual Contractors Review, pp. 419-427, CONF-801128, November, 1980.

4. R. S. Steele and E. F. Babelay, Jr., "Data Analysis Techniques Used at the Oak Ridge Y-12 Plant Flywheel Evaluation Laboratory," Proceedings of the 1980 Flywheel Technology Symposium, Scottsdale, Arizona, October, 1980, pp. 423-434, CONF-801022.

5. A. Coppa, "Flywheel Housing Design-Concept Development," in Proceedings of the Mechanical, Magnetic, and Underground Energy Storage 1980 Annual Contractors Review, pp. 359-368, CONF-81033, August, 1981.

6. Melvin R. Baer, "Aerodynamic Heating of High-Speed Flywheels in Low Density Environment," CONF 781046, October 1978.

7. Muske and Flores, "Balancing Criteria and Their Relation to Current American Practice," Journal of Engineering for Industry, pp. 1035-1046, November, 1969.

Table 1. Design factors for rotors tested for ultimate storage capacity

Manufacturer	Wheel Type	Material[a]	Burst energy[b] (wh/kg)	σ/ρ (wh/kg)	Closest Rotor K factor	Design Factor (K´)
Brobeck	Rim	SG/K49	63.7	340.2[d]	0.44	0.20
Garrett/ AiResearch	Rim	K49/K29/SG	79.5	317.4[d]	0.44	0.23
Rocketdyne	Overwrap rim	G	36.1	274.2	0.44	0.13
APL-metglass	Rim	M	24.4	91.2	0.44	0.27
Hurcules	Contoured pierced disk	G	37.4	274.2	0.47	0.14
AVCO	Pierced disk	SG	44.0	262.6	0.35	0.17
LLNL	Tapered disk	G	62.6	274.2	0.80	0.23
LLNL	Flat disk	SG	67.1	262.6	0.61	0.26
GE	Solid disk	SG/G	55.1	263.7[e]	0.61	0.21
Owens/Lord	Disk	SMC/G	27.8	95.0[e]	0.61	0.29
		SMC/G	36.6	115.0[e]	0.61	0.32
		SMC/G	25.0	62.71[e]	0.61	0.39
		SMC	17.5	43.8[e]	0.61	0.40

[a]Material legend is: SG = S Glass; K49 = Kevlar 49; K29 = Kevlar 29; G = Graphite; M = Metglass; SMC = S-glass sheet molding compound

[b]Burst tests results as reported by DOE Mechanical Energy Storage Technology Program

[c]Calculated as follows: $K' = BE/(\sigma/\rho)$.

[d]Assumes higher σ/ρ material at outer part of rim is limiting factor.

[e]Proportioned by weight.

Table 2. Summary of balance data taken from tests performed at ORFEL

Rotor	Mass (Kg)	OD (m)	Mass Eccentricity at 200 H_z (μm)	Mass Shift		Out-of Plane Angle (μrad)	Hub Attachment Type
				Speed Range (Hz)	Distance (μm)		
UCCND-2	11.15	0.508	13[2]			636	Spokes
-3	7.17	0.467	53	200 to 400	129	694	Spokes
-4	7.17	0.467	25			1631	Spokes
-5	7.17	0.467	--[3]			500	Spokes
SLA	10.70	0.508	178[3]			1069	Spokes
WMB-1	11.79	0.350	46	200 to 500	45	844	Spokes
G-1[1]	15.55	0.584	23	200 to 400	46	-3	Spokes
H-1[1]	22.67	0.589	83	100 to 300	15	148	Disk
R-1	53.74	0.305	11	100 to 300	12	-3	Disk
LLNL-1[1]	5.88	0.610	121	200 to 500	3[4]	233	Disk
GE-1[1]	10.88	0.450	180	100 to 500	3[4]	879	Disk
LLNL-2	-3	-3	103			-3	Disk
OCLA	12.91	0.616	3148			485	Disk
OCLB	10.95	0.560	881	100 to 300	58	144	Disk
OCLC	14.59	0.614	868	100 to 300	218	500	Disk
OCLD	9.90	0.534	513	100 to 300	172	1160	Disk
GEB	10.08	0.450	200	100 to 400	75	498	Disk
GEC	10.35	0.400	278	100 to 500	51	896	Disk

[1]Rotors were not balanced. [2]Rotor was dynamically balanced prior to receipt. [3]Measure is unavailable. [4]Disk only, does not include shift due to elastomerically bonded hub. [5]Maximum speed not limited by material.

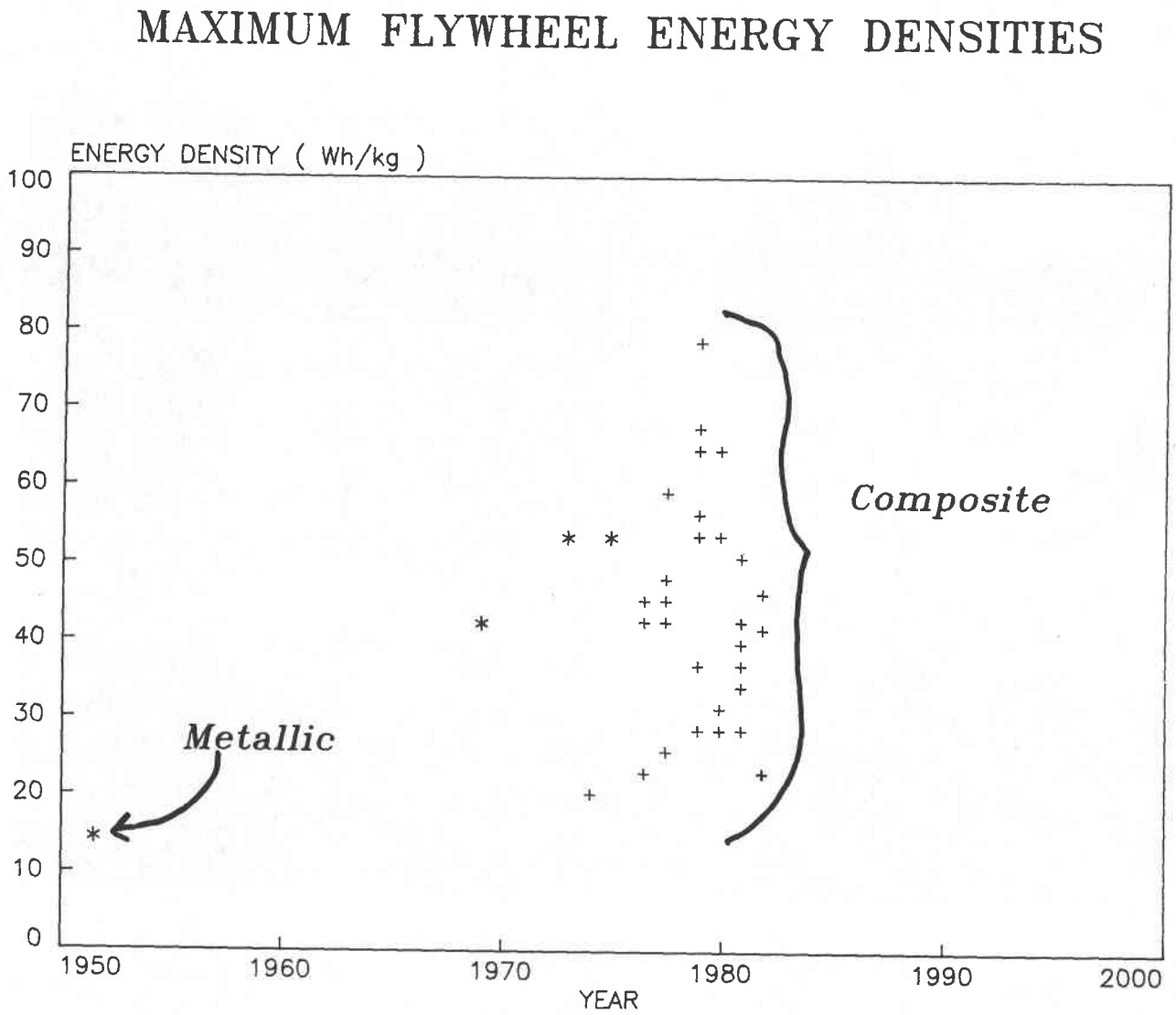

Figure 1. Maximum energy density achieved at ultimate speed with composite flywheels storing greater than 0.250 kWh exceeds the best metallic flywheel performance.

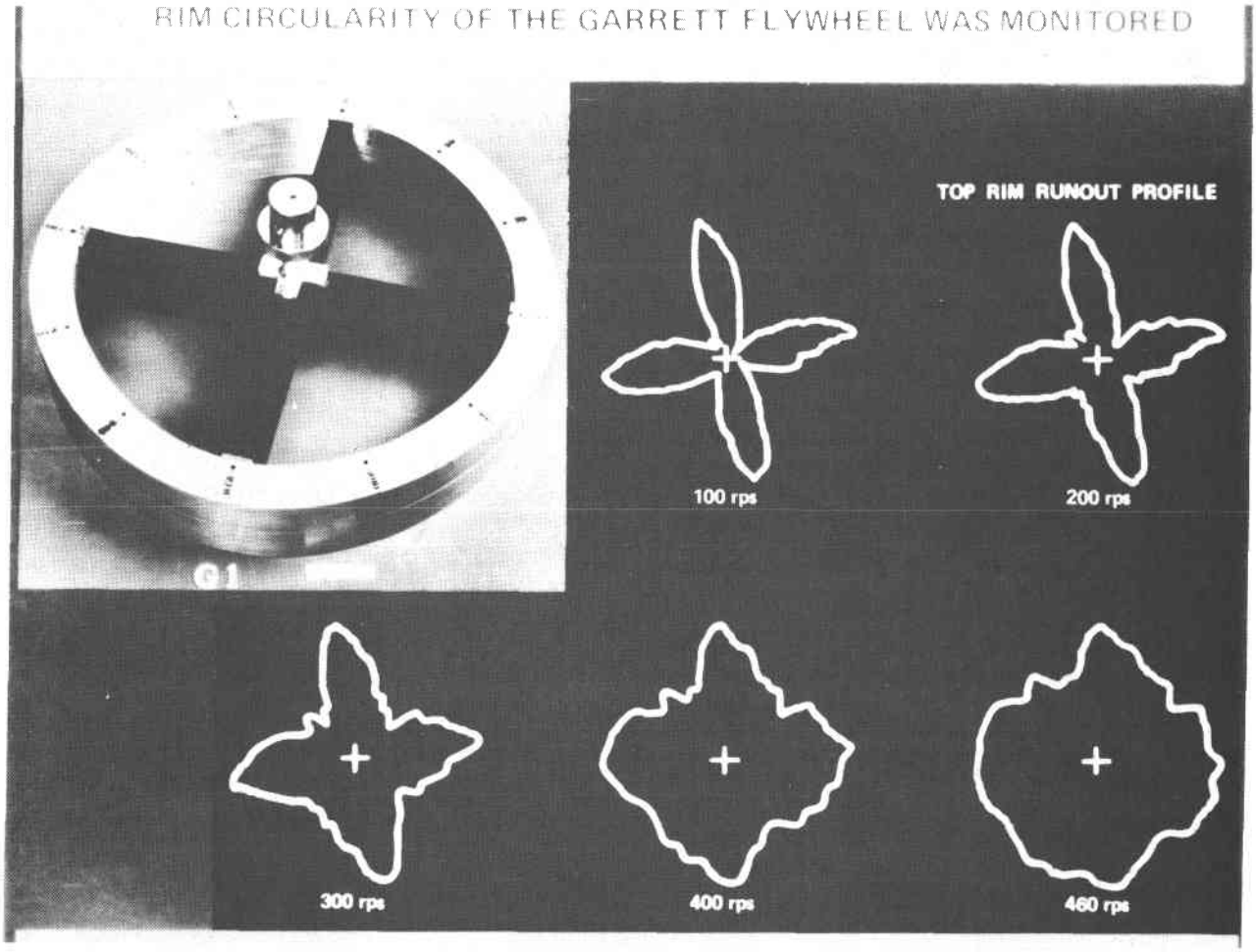

Figure 2. Garrett sub-circular rim has four distinct lobes. Ultimate speed is determined when rim becomes circular.

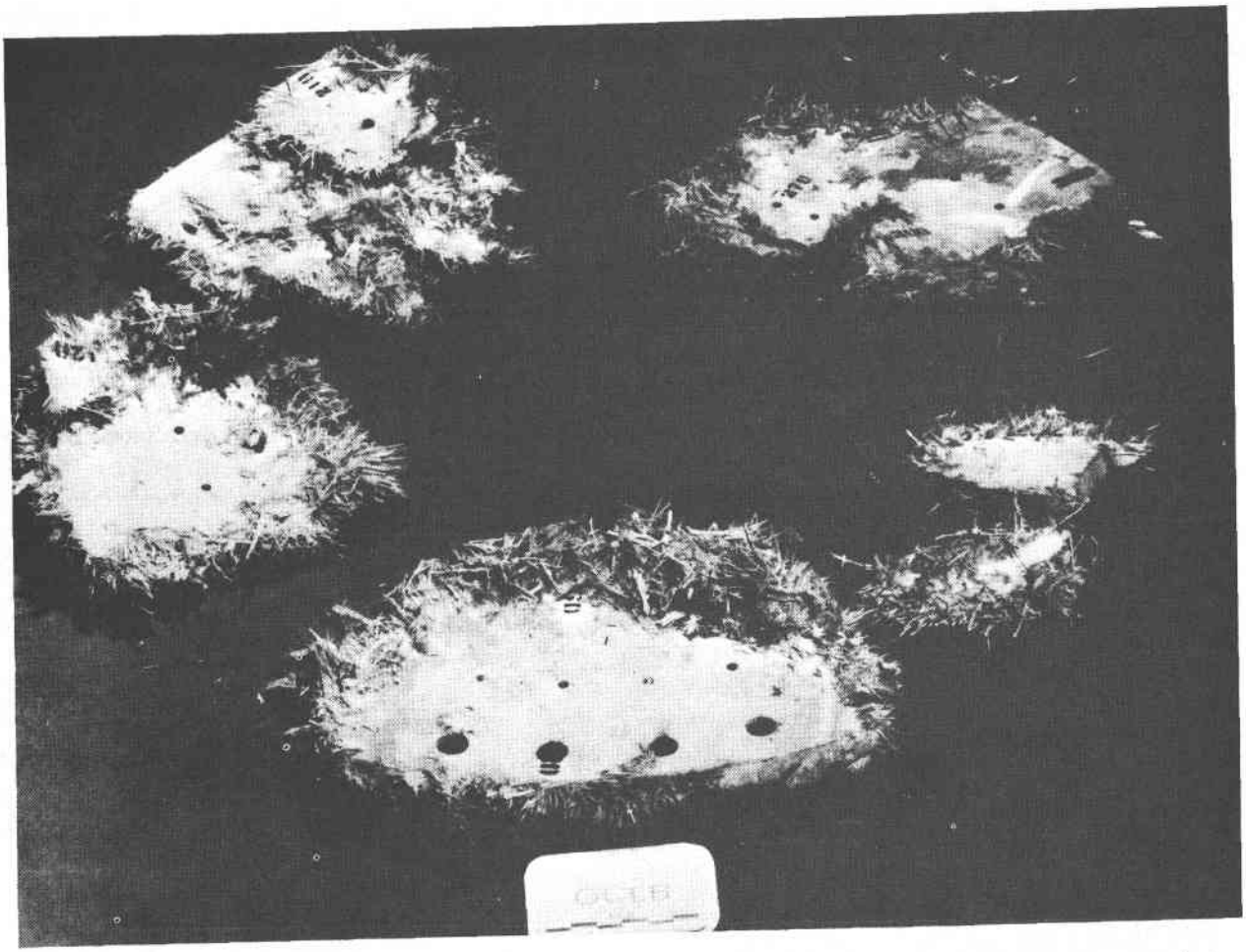

Figure 3. Balance holes found in wreck debris of OCLB do not appear to have influenced the failure mode.

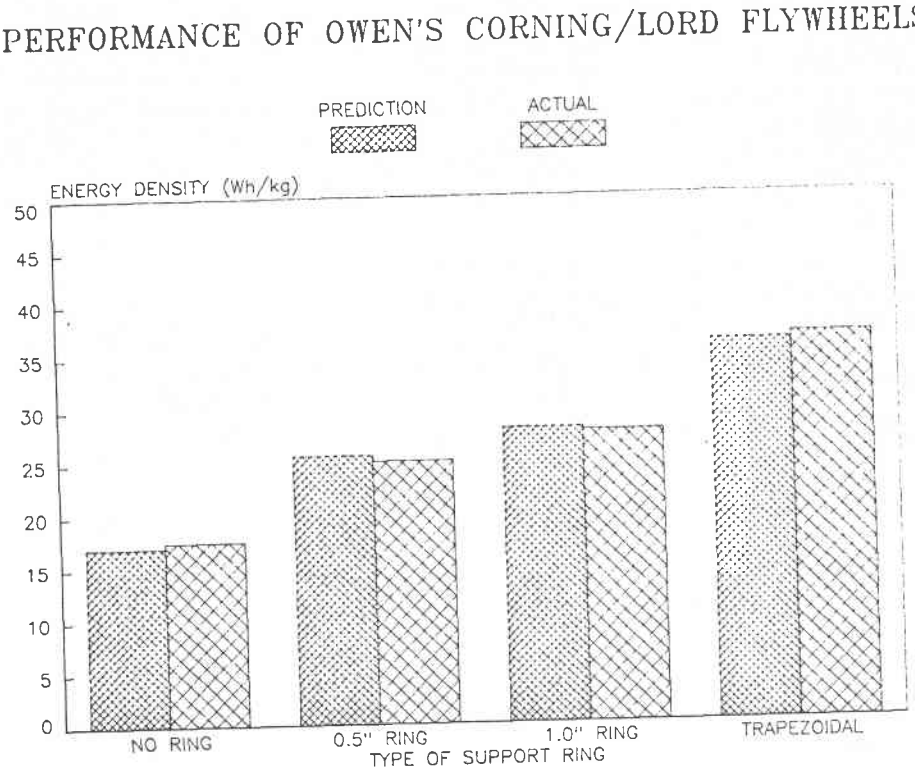

Figure 4. The ability to predict the performance of composite flywheels was demonstrated in the OCL series of flywheel evaluations.

MANUFACTURING COST/DESIGN TRADE-STUDIES FOR FLYWHEELS

Bryan R. Noton
Battelle's Columbus Laboratories
505 King Avenue
Columbus, Ohio

ABSTRACT

The primary objective of this program is to develop a procedure to enable comparisons to be made of different flywheel designs, based on both performance ratings, manufacturing and inspection cost. Development of the methodology, discussed at the 1981 meeting, requires identification of all steps in the manufacture and inspection of each design, cost-drivers and, ground rules and, providing a man-hour summary. The approach to determine the recurring and nonrecurring manufacturing man-hours is presented. The methodology is being applied to flywheel designs developed by Garrett, General Electric and AVCO. Cost-drivers in composite manufacture are discussed, the approach to assess cost-driver data from industry and some indications to reduce cost are also included.

INTRODUCTION

Promising designs of flywheels for both automotive and stationary applications are in various stages of development. The designs utilize widely differing configurations and material combinations, including hybrids. Cost is among the basic criteria for materials and concept selection. It is therefore necessary to conduct trade-studies between flywheel performance, e.g., energy per unit weight and volume, and acquisition cost. The ultimate objective is to compare the performance of selected flywheels, i.e., flywheel and containment, with the manufacturing cost.

The initial task of this program was to develop a method which not only enables credible manufacturing and inspection costs to be determined in person-hours or dollars, but also, by means of designer-oriented formats displaying cost-drivers, to provide guidance to conceptual and detail designers to achieve lowest cost. To realize this objective, interaction with industry is important and therefore advance information on the program has been submitted to designers and manufacturers of flywheels for critical review.

PRINCIPAL TASKS OF PROGRAM

1) To identify cost-driving designer-influenced cost elements (DICE), manufacturing and test, inspection and evaluation (TI&E) operational sequences for flywheels, including the hub and containment.

2) Project cost-effectiveness criteria for flywheel systems from literature sources.

3) To develop manufacturing cost/performance trade-study methodology for flywheel/containment systems.

4) To develop a worksheet for systems assessment and rating.

5) To provide illustrations to qualitatively indicate cost-drivers in design, manufacturing and TI&E for flywheels, including hub and containment.

6) To conduct cost-analysis of selected flywheel systems to demonstrate applicability of cost/performance trade-study methodology.

The experimental nature of the composite flywheel system projects creates problems for manufacturers as, for example, the tooling utilized may not lend itself to the automated production methods eventually required. The manufacturers may not therefore have adequate knowledge of the costs of producing even experimental hardware and the production mode is considerably more complex.

GROUND RULES FOR FLYWHEEL COMPOSITES

It is necessary to develop general and detailed ground rules when comparing designs of any engineering system. Ground rules provide a common base to achieve understanding, consistency, uniformity and accuracy in developing the manufacturing recurring and nonrecurring man-hours. Ground rules therefore promote confidence in the results of trade-studies. General and detailed ground rules are required for the following examples of categories.

General	Detailed
(a) Composite Material Types	(a) Material Specifications
(b) Manufacturing Method	(b) Material Cost Trends
(c) Facilities	(c) Flywheel Engineering Drawings
(d) Data Generation - Recurring Costs - Nonrecurring Costs	(d) Manufacturing Tolerances
(e) Support Function Modifiers	(e) Manufacturing Cost Methodology

PROPRIETARY DATA

The manufacturers of experimental flywheels have provided information on both the manufacturing operational sequences, e.g., for adhesive-bonding and also cost-estimates for various quantities of flywheel production. This information must be considered proprietary and therefore cannot be discussed in a conference paper.

MATERIAL COST

Until 1987, the major market for PAN-based graphite fibers will continue to be in the aerospace industry. The sports and automobile market for this type of material will represent 25 percent of the market. With respect to availability of fibers, ample suppliers can provide the response capability adequate for expanded use. The following table provides an approximate assessment of composite materials typical of those used in flywheel design.

TABLE 1.

APPROXIMATE PROJECTED COST OF VARIOUS COMPOSITE MATERIALS - $/LB.*
(1982 Dollars)

Fiber Type	YEAR			
	1982	1985	1990	2000
S2: Fiberglass	2.37	2.75	2.80	2.90
Kevlar-29	10.60	11.00	11.00	11.50
Kevlar-49	9.00	9.35	9.35	9.75
Graphite: AS-4	19.00	17.00	16.00	15.00
Graphite: P-55	18.00	14.00	13.00	12.00
Graphite: T300	19.00	17.00	16.00	15.00
G/E Prepreg	50.78	44.00	42.00	38.00
G/Polysulfone (P 1700)	42.00	32.00	28.00	27.00
S2 Fiberglass Prepreg	13.37	15.50	15.80	16.36
SMC	1.00	1.05	1.10	1.20

*Prices for the fibers are for the lowest cost form of the material.

MANUFACTURING TECHNOLOGY DEVELOPMENT

The composite manufacturing technology currently available was developed by the interaction between the materials and process engineering, manufacturing technology and tooling engineers, and also material suppliers.

A scientific approach is now required to improve the consistency and effectiveness of composites processing, to reduce costs, to widen the spectrum of materials that are routinely processed in production, and to increase the usage of composites to enhance the performance of engineering systems in both defense and commercial markets.

Advanced composites technology has experienced a transition from the early stages which were characterized by high materials cost, direct substitution in design, manual labor-intensive operations, limited material forms, limited application to structures, weight savings, and cost savings seldom achieved.

Today it is characterized by material prices in the $30-50/lb. range (for graphite/epoxy unidirectional tape); innovative design configurations, innovative manufacturing technology approaches, trend toward automated manufacturing processes, variety of material forms available, application to secondary and primary structures, and weight and cost-savings achieved.

A number of manufacturing processes have been developed to fabricate composite structures but problems still exist with some of these methods.

The state-of-the-art manufacturing methods are:

- Autoclave processing
- Oven/vacuum bag
- Injection molding
- Matched die molding
- Filament winding (fiberglass and Kevlar)
- Compression molding
- Automated tape-wrapping/laving
- Braiding (nongraphite)
- Automated ply cutting/trimming
- Drum-wound broadgood sheets
- Integrally-heated tools.

Manufacturing methods expected to enter production in the near future are listed below.

Accepted for production hardware within 3 years:

- Filament winding (graphite prepegs and wet-winding)
- Compression molding with continuous fiber prepegs (SMC)
- Thermoplastic matrix structural composites - continuous roll forming, vacuum forming, extrusion, press-molding
- Pultrusion
- Simplified automated-ply placement
- Multidimensional oriented fabrics
- Unitized construction.

Accepted for production hardware in 3- to 10-years:

- Rapid curing resins and prepegs
- Advanced automated ply placement
- CAM-operated processing steps
- Rapid, more efficient, automated nondestructive evaluation
- Computer collection and analysis of nondestructive investigation (NDI) data
- Tailored matrix and fiber properties within a single component
- More durable nonmetallic tooling
- Transfer molding of graphite fiber composite components.

Tooling for Composites

Research needs require the development of: integral tools that use novel techniques to apply heat and pressure; analytical techniques for designing better nonmetallic tools; improved plating, electroforming, plasma spraying, or other processes to make a contoured surface from a model without machining; better elastomeric materials for tools that retain their shape, e.g., do not suffer from compression set; metal alloys that can be more easily machined and with higher expansion coefficients for internal molding thereby facilitating removal; and finite element heat transfer analysis of materials and molds for uniform cure.

The interface with autoclave and presses causes facility problems due to size restrictions, high energy costs, and investments. Steel and aluminum tools pose problems such as excessive weight, uneven heat transfer, being costly to machine, and requiring long lead-times. Plastic tools have durability and material variability problems as well as poor heat trasnfer rates and uniformity. And rubber tools have poor dimensional stability, uneven pressure distribution, and poor heat transfer rates and uniformity.

Thick Laminate Processing

Important here is the development of material form for net resin/tight tolerance prepreg (approximately 1 percent on resin), and of cure cycle control with uniformity throughout with a possible need for integrally heated tooling. This could present a special problem for parts of variable thickness. Throughout the thickness, thermal gradients and gel transients must be eliminated, and porosity and ply compaction/thickness controlled. In addition, ply waviness must be eliminated.

COST-DRIVERS WHEN EMPLOYING COMPOSITE MATERIALS

A number of significant costs need to be considered by decision makers when making commitments to the production of products designed and manufactured in composite materials. These cost-drivers must be evaluated when commiting to a system as the manufacturing costs developed are based on the individual operational sequences. These cost-drivers include:

- OSHA requirements
- Waste disposal of liquids/solids
- 100 percent inspection frequently is conducted, in part to provide historical background
- Mixing of material types, e.g., in hybrids, due to tracking of these materials and user testing
- Lack of adequate standards for some applications of composites
- Finishing requirements
- Turn-over of composite factory people.

An integrated factory systems approach, employing robotics extensively, must be utilized to address the cost-drivers in flywheel manufacture so that a cost-effective and cost-competitive system evolves. Examples of the cost-drivers are as follows:

- Material
- Tolerances
- Handling
- Tooling
- Winding
- Processing (labor)
- Curing
- Facilities/Equipment
- Inspection

COMPOSITE COST REDUCTION OPPORTUNITIES

A number of opportunities need to be pursued to reduce the cost of composite flywheels which include:

- Reduce the number of product forms, while evaluating total systems cost
- Reduce supplier and user testing of composites
- Reduce inventory requirements of limited shelf-life materials
- Develop self-contained autoclaves and continuously operating ovens
- Reduce number of different materials used so that "dedicated" autoclaves (one-cycle) can be utilized
- Reduce manufacturing energy requirements
- Develop automated (computer-aided) non-destructive inspection equipment
- Reduce capital costs and include and evaluate optimum operating rates.

DESIGN/MANUFACTURING INTERACTION

Few of the flywheel designs have been designed with respect to high-volume production applications in regard to the tooling, manufacturing, and facility requirements. To achieve high-volume production, a manufacturing/design interaction program is important. It is not unusual that a subsystem approach is taken to a systems problem.

Factors to be Considered When Analyzing Cost Data Based on Experimental Flywheel Design

- Although detailed cost data may not be available, comparison of prototype cost data can indicate the relative cost of each flywheel.
- A major benefit of reviewing prototype cost data is the highlighting of "cost-drivers" which are the indicators of potentially high-cost flywheels.
- The closer the flywheels are manufactured to a production environment, the better the chances are for projecting the "in-production" costs.
- Companies that practice the principle of engineering design/manufacturing interaction will generally be the low-cost competitive manufacturers.

Characteristics of a Low-Cost Flywheel

- Design provides a flywheel that is fairly easy to balance
- Design is within the "state-of-the-art," i.e., the manufacturing "know-how" is available
- Reflects considerable manufacturing input to the engineering design
- Has been carefully reviewed by a design-to-cost study and a comprehensive trade-study evaluation.

Characteristics of a High-Cost Flywheel

- Design of the flywheel makes it difficult to balance
- Design requires the development of new and emerging manufacturing technology
- Engineering design reflects little or no input of manufacturing influence
- Lacks the input of design-to-cost and trade-study results.

Examples of opportunities to reduce the manufacturing cost of flywheel component parts follow. It will be noted that these recommendations apply to the Garrett AiResearch design. However, other recommendations have been formulated for other design concepts.

FLYWHEEL RIM COST REDUCTION

The total time to fabricate a flywheel rim can be reduced to 4-5 minutes. The mandrel and rim are removed from the filament winding machine, lowered in the die, and cured. It is important to design the die, so that no machining with the exception of cleaning up the flash, is required. The time required to remove the mandrel is approximately 3 minutes. The fiber types must not only be selected with respect to structural systems performance, but also concerning the most beneficial curing procedure. When possible, RF curing should be used due to the problems of curing thick laminates. RF curing is instantaneous, minimizes thermal gradients and hence, cracking.

SPOKE COST REDUCTION

A thrust in this study has been to identify methods of reducing the costs in manufacturing the discrete parts utilized in the flywheel/system. On experimental flywheels with spokes, matched-metal dies, most appropriate for prototype systems, have been used. Such dies are not suitable for the production environment and all hand lay-up operations must be avoided. Spokes can be economically produced utilizing the pultrusion process. Single or multiple streams and induction heating can be employed with the pultrusion process. The rate of production for slats/systems with single die is approximately 3 feet per minute. The costs of the facilities are as follows:

- Cost of pultrusion die = $2,500
- Cost of pultrusion machine (turn-key) = $185,000.

The economics are more attractive than hand layup and the pultrusion process lends itself to this type of product.

HUB COST REDUCTION

Hubs of flywheels may be manufactured from machined aluminum blocker forgings. The utilization ratio of the material (forging to final machined part/weight) is low. Furthermore, the lead-time presents a problem with respect to developing a precision forging to alleviate the machining. An alternative design concept is therefore recommended for flywheels where metallic hubs represent the optimum design. The concept has been used extensively for aircraft spars, e.g., the Dutch F-27 civil aircraft and consists of an adhesive-bonded laminate of aluminum sheets. A 3-inch thick hub would be manufactured from a series of thin gauge sheets (0.064 in.). The following are advantages of the approach:

- The forging lead-time problem is circumvented
- Negligible machining required
- Can be tailored from outset to respond to design requirements
- Conventional sheet-metal facilities can be utilized
- Utilizes conventional adhesive-bonded technology
- Avoids stress concentrations and deficiencies introduced during the manufacturing process
- Provides built-in crack stoppers.

CONCLUSIONS

- Material costs will not change significantly from the estimates used by companies. However, because of changes in the resin cost, the price could increase slightly.
- Where the fiber types permit, the use of RF curing and pultrusion will lead to significant labor cost reductions (of the order of 2/3).
- Tooling costs can also be reduced significantly (by 2/3).
- Tooling costs for slats or spokes can be significantly reduced by utilizing pultrusion.
- Inspection costs, which can equal the manufacturing labor costs today, need to be reduced utilizing computer-aided inspection.
- The low material utilization rate and extensive machining for hub forgings can be avoided by incorporating fracture tolerant concepts such as adhesive-bonded laminated aluminum sheet and cured in a single cycle.
- Balancing of the flywheel assemblies is a cost-driver and the degree of precision and potential requirements, need need study to justify possible relaxing balancing tolerances.
- Effects of manufacturing deficiencies during the winding process needs to be determined in order to relax inspection requirements.
- As manufacturing technology affects performance, design for production must be borne in mind from the outset due to the high cost and time involved in re-testing and certifying flywheels.

REFERENCE

1. Kulkarni, S. V., Composite Material Flywheels in Containment Systems, Energy and Technology Review, March 1982.

TABLE 2.

ASSESSMENT OF MAN-HOUR DISTRIBUTION FOR FILAMENT WINDING MANUFACTURING PROCESS

DIRECT OPERATIONS	% TOTAL LABOR
1. Clean Mandrel	3
2. Apply Mold Release	1
3. Load Mandrel	1
4. Wind	58
5. Unload & Remove Excess Resin	2
6. Oven Cure	11
7. Extract Mandrel	4
8. Finish Trim	5
9. Deburr & Clean Up Flash	2
10. Inspect	2
11. Identify	4
12. Package or Store	2
	95%

INDIRECT OPERATIONS	% TOTAL LABOR
1. Incoming Material Inspection	1
2. Creel Loading	1
3. Resin Mixing	2
	4%

NONRECURRING OPERATIONS	% TOTAL LABOR
1. Thread Up	1/2
2. Machine Setup	1/2
	1%

TABLE 3.

EXAMPLE OF QUESTIONS FOR INDUSTRY DISCUSSIONS ON FLYWHEEL MANUFACTURING DATA

1. What do you consider the major deterrents to wider acceptance of composite flywheels (Please rate on scale of 1 to 10, 10 being high disadvantage, 1 being minor disadvantage)

☐ Cost ☐ Size

☐ Present Specifications Too Stringent ☐ Low Volume Production

☐ Delamination ☐ High Rejection Rate

☐ Balancing ☐ Containment Problems

☐ Inadequate Inspection Equipment & Acceptance Criteria

☐ Corrosion Problems, e.g., Aluminum & Graphite/Epoxy

☐ Service Life ☐ Reliability

Other: _____

2. What production lot-size(s) do you consider to be economically feasible for the manufacture of composite flywheels:

☐ 5 ☐ 50

☐ 10 ☐ 100

☐ 25 ☐ Over 100

Minimum Total Quantity: ☐

3. Do you agree that the following tolerances are economically feasible?

	Yes	Recommend
A. Base Part Configuration ± 0.03 in. lineal dimensions ± 0.00025 in. on thickness per ply	☐	_____
B. Cocured Assembly ± 0.06 in. on part location	☐	_____
C. Fit-up Maximum Tolerance for Cured Details 0.03 in. Gap for "Mechanically Fastened Assemblies" and 0.15 in. for "Bonding"	☐	_____

NONDESTRUCTIVE TECHNIQUES FOR FATIGUE DAMAGE DETECTION*

W. A. Simpson, Jr. and R. W. McClung
Metals and Ceramics Division
Oak Ridge National Laboratory
Oak Ridge, TN 37830

Abstract

The ultrasonic properties of an S-2 glass-epoxy composite are being studied in an attempt to determine whether changes in these properties might serve as predictors of incipient failure and/or the extent of fatigue damage. The variables under consideration are the longitudinal and transverse wave velocities, the attenuation, and the backscattering characteristics. A material transfer function giving the attenuation as a continuous function of frequency is also obtained and monitored.

These properties are being studied as a function of strain history on tensile specimens and on actual spin-tested flywheels.

Introduction

The use of advanced composite materials in the design of variable-demand energy storage systems has provided strength-to-weight ratios not possible with more traditional structural materials. The lack of understanding of the basic failure mechanisms for such composites, however, has made the assessment of remaining life or the prediction of incipient failure much more difficult than for such materials as steels, where well-developed fatigue damage models exist. The use of a broad spectrum of nondestructive testing techniques, particularly those that are sensitive to the fiber-matrix bonding and microcracking within the matrix, would appear to be one of the more fruitful approaches in defining and quantifying failure mechanisms in advanced composites. This paper describes work at Oak Ridge National Laboratory in applying ultrasonic techniques to the determination of the properties and changes in properties of such materials in the expectation that some of these parameters might serve as predictors of incipient failure in finished flywheels.

It is reasonable to expect that one or more or the acoustic properties of fiber-reinforced composites would reflect the strain history of the specimen. For example, the elastic moduli, and hence the ultrasonic velocities, of the epoxy matrix might logically vary with stress, but changes in the fiber-matrix bonding or microcracking within

*Operated by Union Carbide Corporation under Contract W-7405-eng-26 with the U.S. Department of Energy.

the matrix would probably affect the attenuation of ultrasonic waves. In either event, the accumulation of stress-induced damage should lead to progressive changes in the ultrasonically determined properties.

Material Characterization Study

For the present study, two S-2 glass-epoxy composite flywheel materials in an alpha ply layup were available from two separate manufacturers. This is a lamination of layers with the reinforcing fibers in various orientations. A large (66-cm-square) piece of one material was obtained, and sections were cut at appropriate angles for velocity measurements. Ultrasonic velocities (both transverse and longitudinal) were first measured along the direction corresponding to a flywheel axis (perpendicular to the laminations). As expected from the configuration of the plies in this specimen, the axial transverse wave velocity was independent of polarization. The velocities were next measured for several directions in the plane of the wheel. In this case, the in-plane velocities (both transverse and longitudinal) were found to be independent of direction, but the transverse velocities did depend on polarization. Finally, the velocities along a direction inclined 45° to the wheel axis (ply normal) were measured. In this case, a pure-mode transverse and two mixed-mode waves were found.

From these measurements, one can immediately deduce that the composite exhibits a macroscopic symmetry belonging to the hexagonal or, perhaps more appropriately in a non-crystalline material, transversely isotropic system. Thus the elastic behavior may be described by five constants; namely, the elastic stiffness constants, C_{ij} (or, equivalently, their inverse — the elastic compliance constants). From the measured velocities and the density of the composite, these constants may be calculated. The matrix of computed stiffness values for the samples is

$$\begin{pmatrix} 31.2 & 14.6 & 8.33 & 0 & 0 & 0 \\ 14.6 & 31.2 & 8.33 & 0 & 0 & 0 \\ 8.33 & 8.33 & 20.4 & 0 & 0 & 0 \\ 0 & 0 & 0 & 5.73 & 0 & 0 \\ 0 & 0 & 0 & 0 & 5.73 & 0 \\ 0 & 0 & 0 & 0 & 0 & 8.28 \end{pmatrix},$$

where the C_{ij} are in gigapascals. For this symmetry $C_{66} = (C_{11} - C_{12})/2$, so only five constants are independent. Table 1 shows the measured velocities at both 1 and 2.25 MHz (the former were used in computing the elastic constants).

TABLE 1

MEASURED ULTRASOUND VELOCITIES

Directions[a]	Velocity (km/s)	
	1 MHz	2.25 MHz
V_{11}	4.193	
V_{22}	4.193	
V_{33}	3.369	
$V_{12} = V_{21}$	2.145	
$V_{13} = V_{31}$	1.784	1.778
$V_{23} = V_{32}$	1.784	1.776
Propagating 45° to axis		
Longitudinal wave	3.655	3.676
Shear wave polarized in 2-direction	2.010	2.002
Shear wave polarized normal to 2-direction	2.232	2.269

[a]The 3-axis is parallel to the flywheel axis, and the 1 and 2 axes are in the plane of the flywheel (laminations). The first subscript indicates the direction of propagation and the second the direction of polarization.

In characterizing the composite material, the ultrasonic attenuation as a function of frequency is also of great interest. That the flywheel material is highly attenuative was one of the first observations noted. Figure 1 shows the frequency response of a broadband transducer used to characterize the composite, and Fig. 2 shows the spectral content of the ultrasonic wave after propagating through the sample. These are normalized spectra; the absolute amplitude of Fig. 2 is considerably less than that of Fig. 1. Note that virtually none of the incident energy above 2 MHz survives.

The differences in Figs. 1 and 2 may be attributed to losses in the composite material itself and to geometrical and physical factors such as beam spread (diffraction) losses and losses at the entry and exit surfaces. In principle, the latter effects are known and hence may be removed. What remains is the material-dependent, length-independent attenuation alone. The process of obtaining this information is a straightforward application of deconvolution and yields a "transfer function," or attenuation versus frequency response for the composite. This process was applied to the above data by use of computer programs developed for use on linear isotropic media. Although the corrections for anisotropy are known, they were not found to be necessary, presumably because we compute the transfer

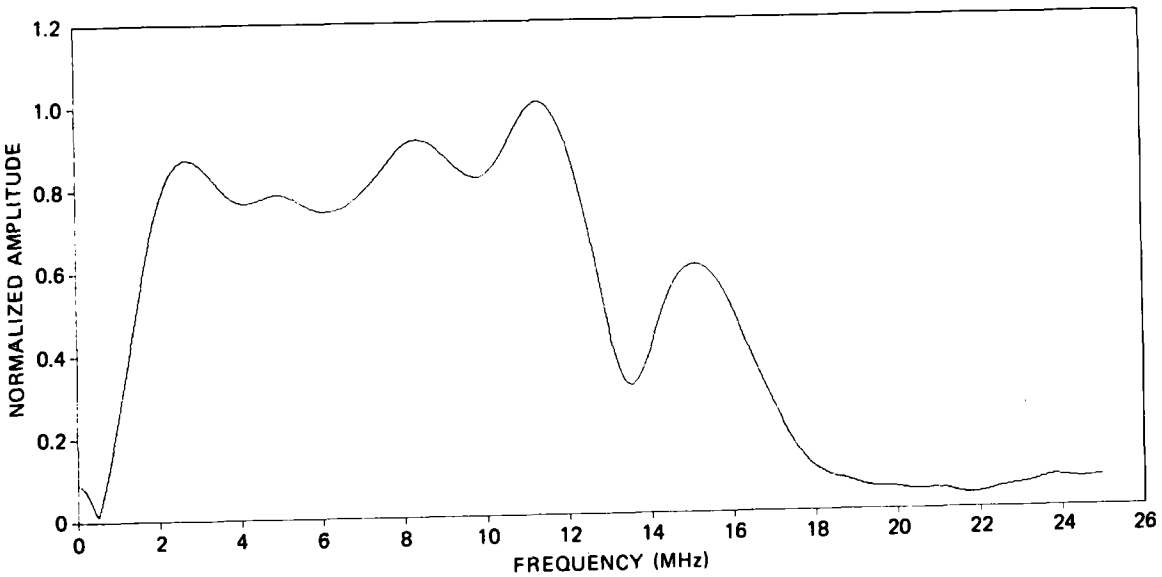

FIGURE 1

BROADBAND SPECTRAL RESPONSE OF ULTRASONIC TRANSDUCER USED TO CHARACTERIZE COMPOSITE

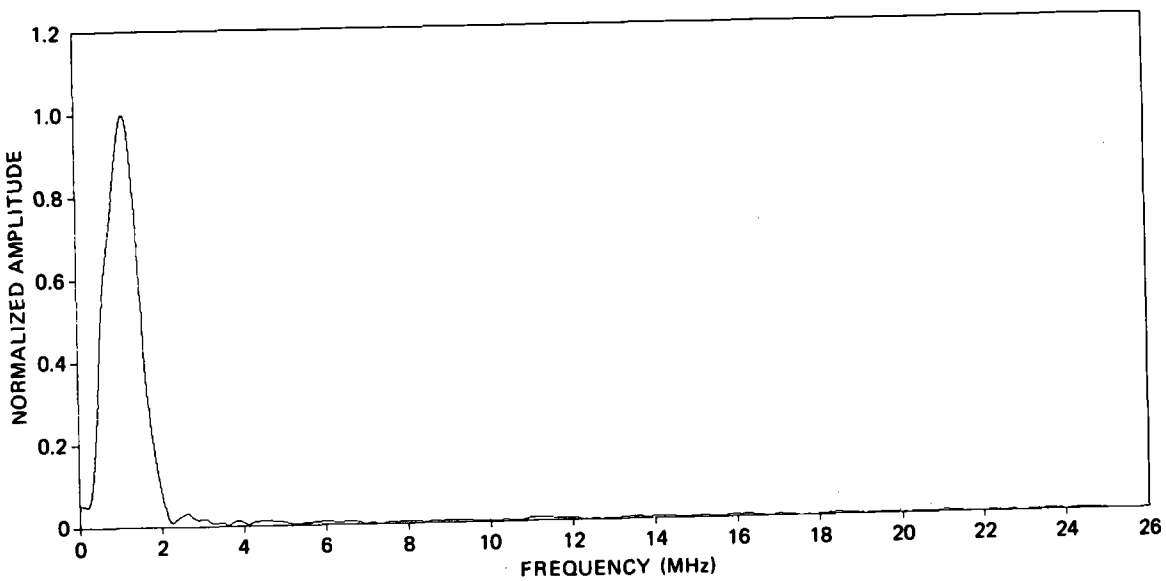

FIGURE 2

SPECTRAL RESPONSE OF ULTRASONIC ENERGY AFTER PROPAGATING THROUGH GLASS-EPOXY COMPOSITE

curve for longitudinal waves only, and then only for propagation along the pure-mode directions and for small beam spread angles about these axes.

The advantage in studying the transfer curve is that the attenuation at all frequencies within a band is determined in one measurement. Discrete frequency measurements could be made within the band, of course, but would be considerably more time-consuming.

Figure 3 shows the transfer curve obtained for propagation along the flywheel axis and in the plane of the flywheel. The calculations do not extend below 1 MHz, where the transducer has little energy (see Fig. 1), or above that frequency for which the attenuation exceeds 550 dB/m. Both limitations are related to the amplitude resolution of our analog to digital (A/D) converter. Note that the in-plane attenuation is considerably greater than the axial attenuation.

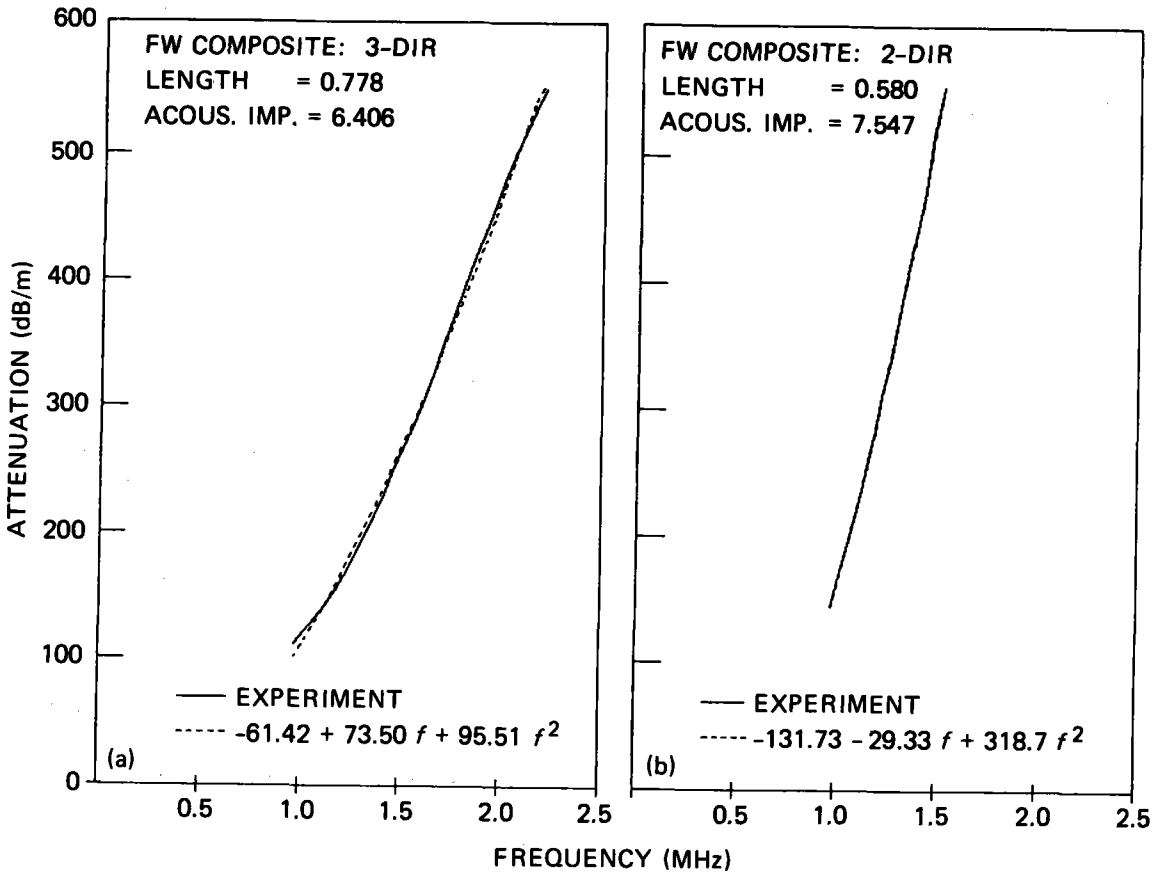

FIGURE 3

TRANSFER CURVES OF GLASS-EPOXY COMPOSITE

(a) Axial direction. (b) In plane of flywheel.

Property Variation with Strain History

After having studied the properties of the unstressed composite, we next prepared tensile specimens for which the properties could be monitored as a function of strain history. The specimens were square rods approximately 30 cm long with a cross-sectional area of about 4 cm^2. A uniaxial load was applied along the specimen (in-plane direction), and the axial ultrasonic properties were monitored. The properties chosen were the velocities (longitudinal and transverse) and the attenuation. The last was determined both by discrete-frequency (2 MHz) measurement and by the

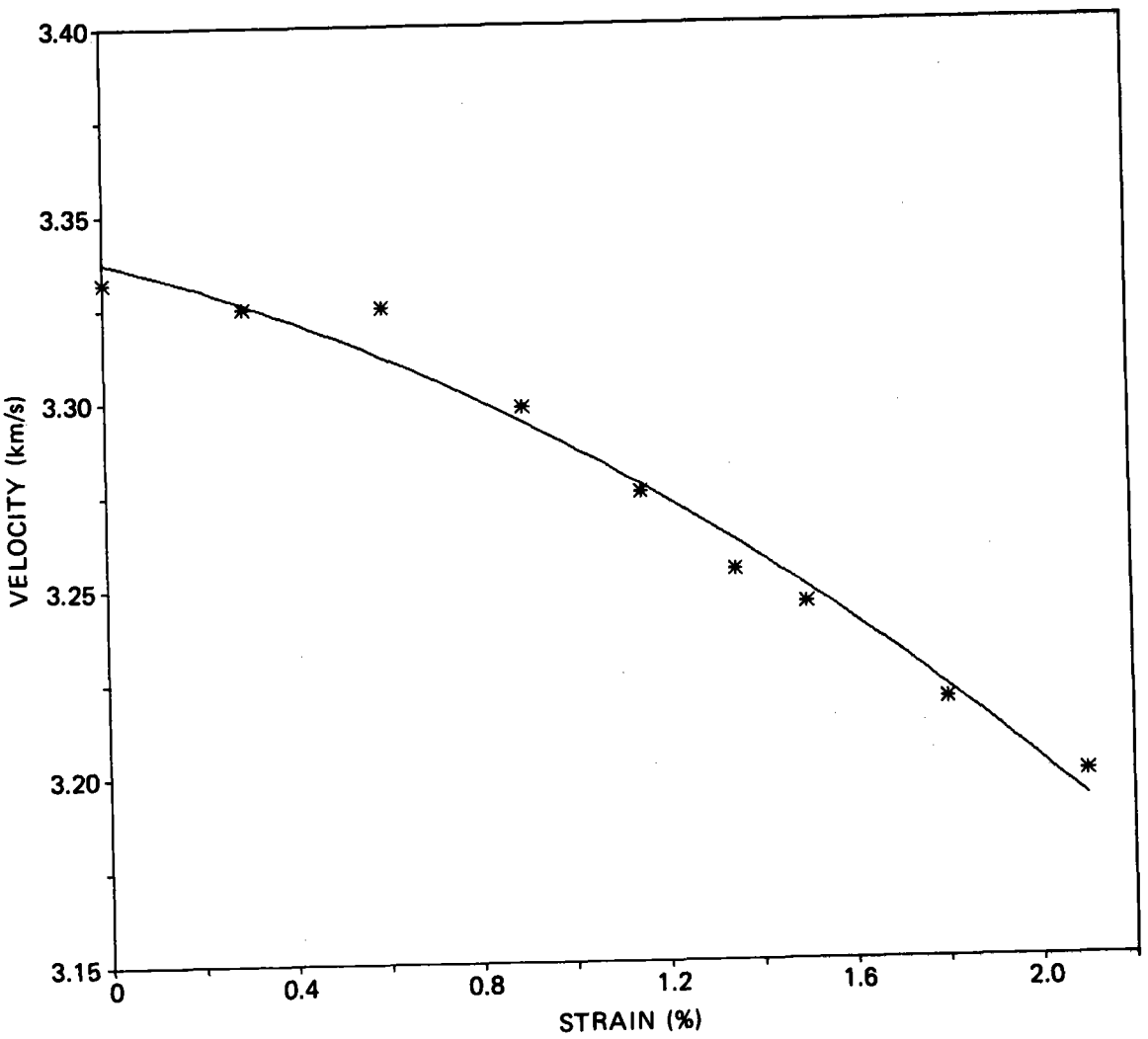

FIGURE 4

VARIATION OF AXIAL ULTRASONIC LONGITUDINAL VELOCITY WITH STRAIN

transfer curve approach. The data were first collected before the load was applied. The sample was then loaded to a strain of 0.3% (as measured with an extensometer), the strain was removed, and the data were retaken. This cycle was repeated for strains of 0.6%, 0.9%, etc. to failure, which occurred at a strain of 2.3% by delamination of the plies; the sample did not break.

Figures 4, 5, and 6 show the variation with strain of the longitudinal velocity, the transverse velocity, and the discrete-frequency (uncorrected) attenuation. The transfer curve was also computed at each strain level, and Fig. 7

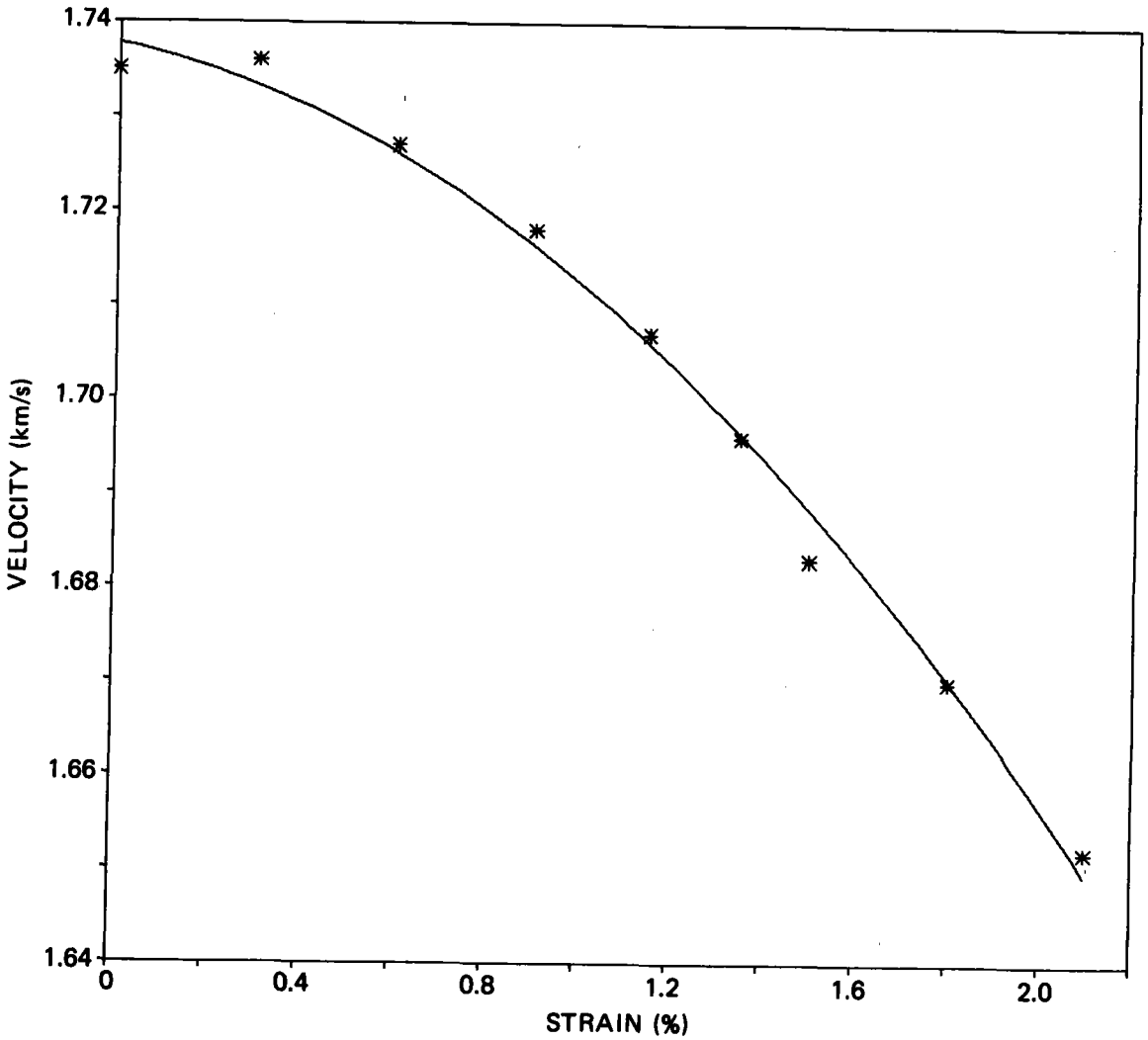

FIGURE 5

VARIATION OF AXIAL ULTRASONIC TRANSVERSE

VELOCITY WITH STRAIN

shows the least-squares fit data for the unstressed condition and after a strain of 2.1%. The slope of the transfer curve increased monotonically with strain from zero to the maximum strain. The crossing of these curves near the low frequency end is probably due to experimental error.

Examination of Fig. 6 shows that, except for the first two points, the discrete-frequency attenuation is not far from a linear function of strain. This can be corroborated from the transfer curve data, which provide an independent check on the attenuation. Taking the values at 2 MHz from these curves and removing the correction factors, the results obtained agree with the values of Fig. 6 within ±0.5 dB, except for the first two points. These points were corrected upward to lie on the same line that closely fits the last seven points, thus strengthening the conclusion that the attenuation is a linear function of strain history.

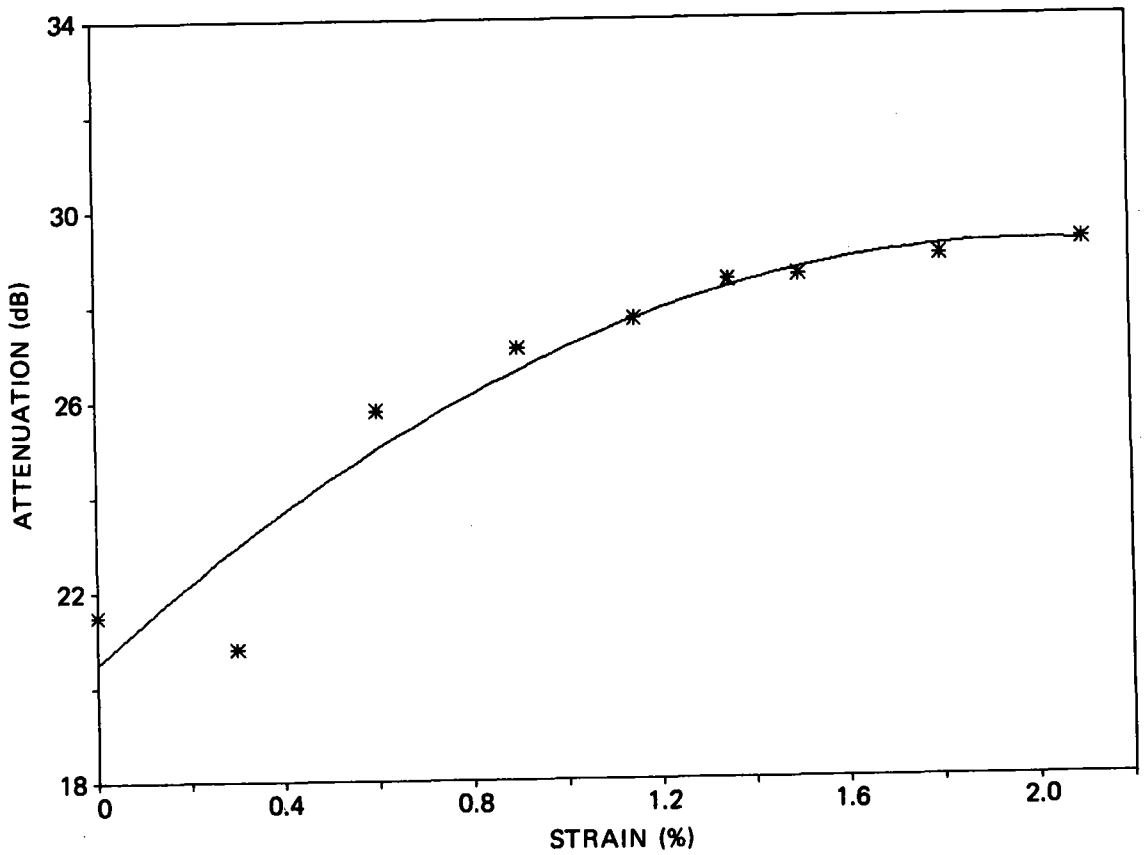

FIGURE 6

VARIATION OF ULTRASONIC ATTENUATION

WITH STRAIN

Figures 4 through 7 indicate that the ultrasonic properties of the glass-epoxy composite are indeed functions of the strain history. However, although the percentage change from the unstressed values may serve to predict the remaining service life, additional work on a considerable number of samples would be necessary to establish this. Additionally, the properties studied thus far are not critically sensitive to strain history, nor do they contain any *a priori* indication of incipient failure. Accordingly, additional properties that might be expected to be highly dependent on microstructure (e.g. backscattering) are being added to the studies.

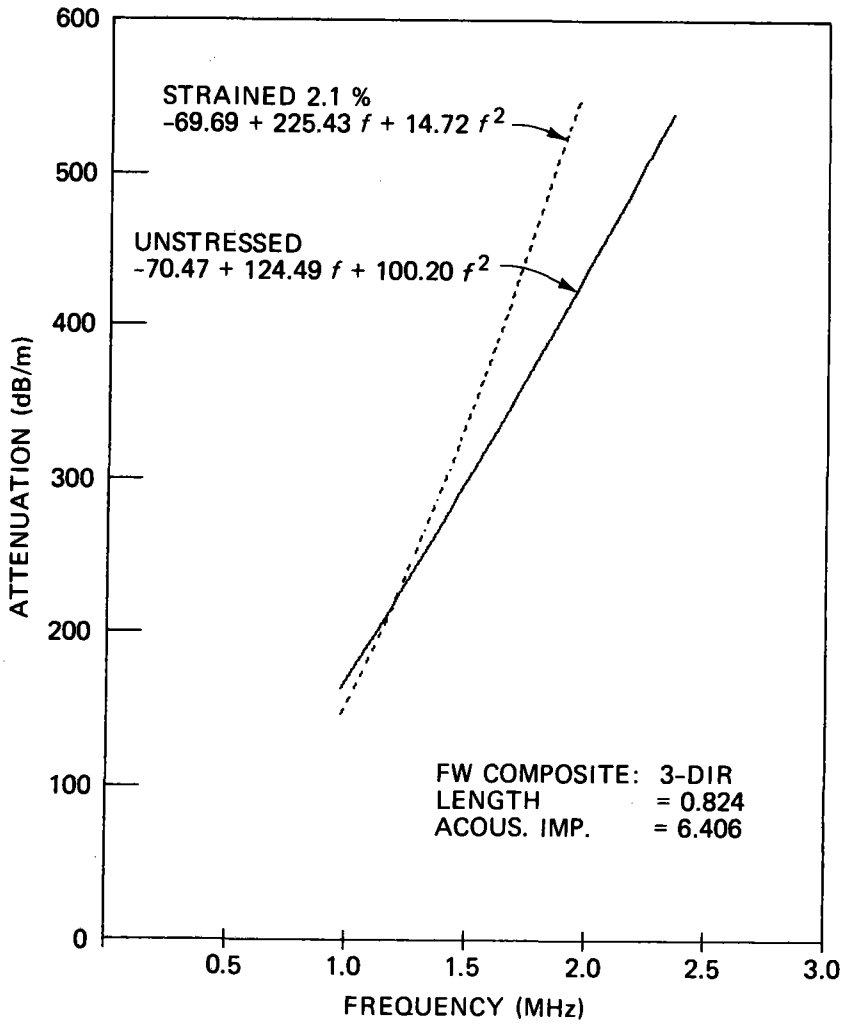

FIGURE 7

TRANSFER CURVE OF GLASS-EPOXY COMPOSITE BEFORE STRAINING AND AFTER A STRAIN OF 2.1%

Flywheel Specimens

At the time this work was performed, no actual flywheel was available for study. Subsequently we received two wheels, which were to be spin tested at the Oak Ridge Flywheel Evaluation Laboratory (ORFEL). Both were fabricated of S-2 glass-epoxy in an alpha ply layup. One of the wheels has a 41-mm-wide (1 5/8-in.) graphite ring around the periphery; the other has none. Initial (unstressed) measurements have been completed on the sample without a ring, and the wheel has been returned to ORFEL. The properties measured were the axial velocities, attenuation, and backscattering characteristics. Also, C-scan recordings were made to locate any laminations or voids. The results were similar to those obtained on the first specimen, except that the velocities were slightly lower (3.106 and 1.635 km/s) and the attenuation slightly higher. After each spin test the wheel will be returned to us for ultrasonic inspection.

Summary

Changes in the ultrasonic axial longitudinal and transverse wave velocities and attenuation have been found to correlate with the strain history of specimens of S-2 glass-epoxy composite. Additional parameters, particularly those that would depend strongly on microstructure, such as backscattering, are being added to the list of properties being studied. Ultrasonic testing has also begun on actual flywheels being evaluated in ORFEL.

FIBER COMPOSITE MATERIALS TECHNOLOGY FOR FLYWHEEL ENERGY STORAGE

T. T. Chiao and R. L. Moore
Lawrence Livermore National Laboratory
Livermore, CA 94550

Introduction

High performance flywheels are almost exclusively made from composite materials today. This is because fiber composites have very high tensile strength to density ratio, which is the key factor controlling the performance of a flywheel. The field of composite materials is very dynamic. New materials are constantly being introduced to the market. During the past years in our materials effort, we have provided the industry with much basic information. For FY1982 our objectives are:

1) Screen and evaluate new and high performance composite materials which are applicable to future flywheels.

2) Continue to generate engineering data on composites for flywheel design.

3) Disseminate material information to industry by quickly publishing them in Composites Technology Review.

The new materials evaluation work was done at the Lawrence Livermore National Laboratory (LLNL). Engineering data on composites were subcontracted to several universities: Washington University with Professor T. H. Kahn on materials database; Purdue University with Professor C. T. Sun on frequency effect on fatigue on S-2 glass composite; and Virginia Polytechnic Institute and State University with Professor J. Duke on spectrum loading damage and service potential. Composites Technology Review was edited at LLNL with additional publication support provided by ASTM and Publication Art Network.

Accomplishments

1) New fibers. We followed the development of four new fibers, and then narrowed down to two which showed promise for flywheel applications. One fiber is an improved organic which is not yet commercially available; the other is a graphite tow which is in pilot production. Data on 1140 denier strands for the organic and 6k filament tow of graphite impregnated with an epoxy (Dow 332/Jeffamine T-403, 100/45) are summarized in Table 1.

TABLE 1. Preliminary strength properties of new fibers.

Fiber/Epoxy Strand	Fiber Strength Ksi	MPa	Coefficient Of Variation	Number of Specimens
Organic (55-60% by vol.)	582	4014	1.5%	20
Graphite (high strain)	614	4234	3.5%	23

These fibers represent an improvement of 15-30% higher strength to density ratio over the comparable commercial fibers. Our evaluations are continuing on composite rings and structures.

2) Design Data for an S-2 Glass/Epoxy Composite. The S-2 glass flat composite specimens made from filament winding using a high temperature epoxy (Dow DER 332/Menthane Diamine, 100/24.5, Tg = 153°C) were tested for static and fatigue properties. Some data were obtained at different environments: room temperature (RT); elevated temperature (ET); elevated temperature in vacuum (ETV); and elevated temperature preconditioning (EVP, 100°C in vacuum). The static tension properties are shown in Table 2. Figure 1 shows the weight loss of the composite speciments during preconditioning. Fatigue data on fiber-controlled specimens at various conditions are plotted in Fig. 2. Generally, a frequency of 4 H_z was used except for load levels above 60%, when 2 H_z was sometimes used. During the fatigue tests, 10 specimens were evaluated at each stress level.

TABLE 2. Longitudinal tension properties of S-2 Glass/Epoxy Composite.

Days of preconditioning (vacuum at 100°C)	0	35-42	0
Test temperature, °C	RT	100	100
Fiber volume content, %	65	65	65
Failure stress			
Average, MPa (no. of specimens)	1983(14)	1782(10)	1788(10)
Coefficient of variation, %	6.16	6.50	5.40
Failure strain			
Average, % (no. of specimens)	3.96(4)	3.86(4)	--
Coefficient of variation, %	2.75	8.55	--
Modulus			
Average, GPa (no. of specimens)	56.41(5)	55.65(5)	--
Coefficient of variation, %	3.40	3.40	--
Poisson's ratio			
Average (no. of specimens)	0.242(4)	0.241(5)	--
Coefficient of variation, %	1.77	2.23	--

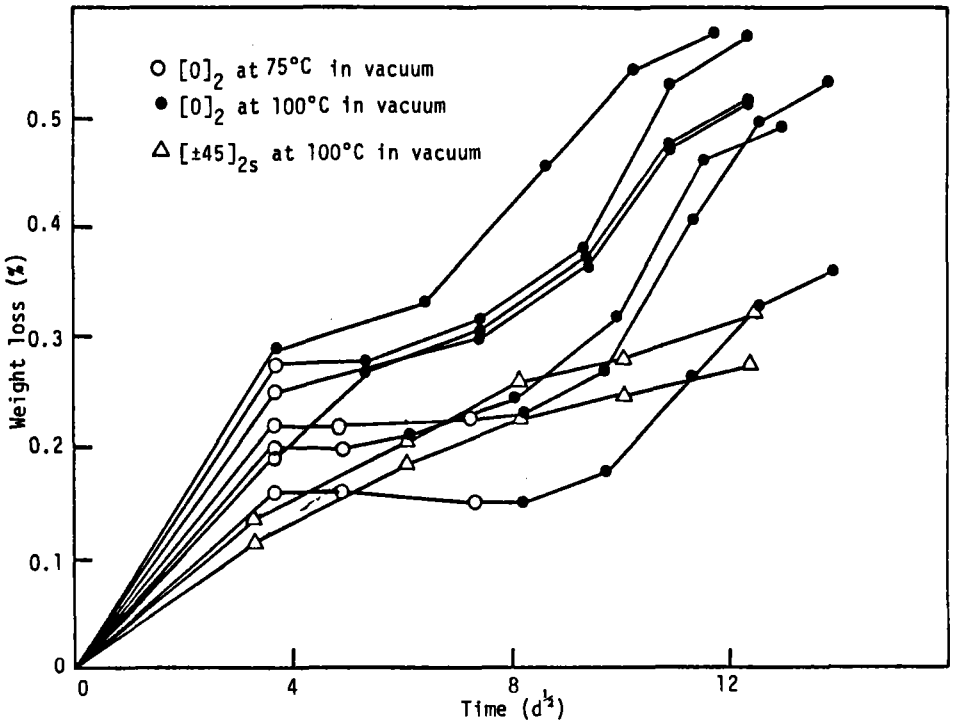

FIG. 1. Weight losses during preconditioning of S-2 glass/epoxy composite.

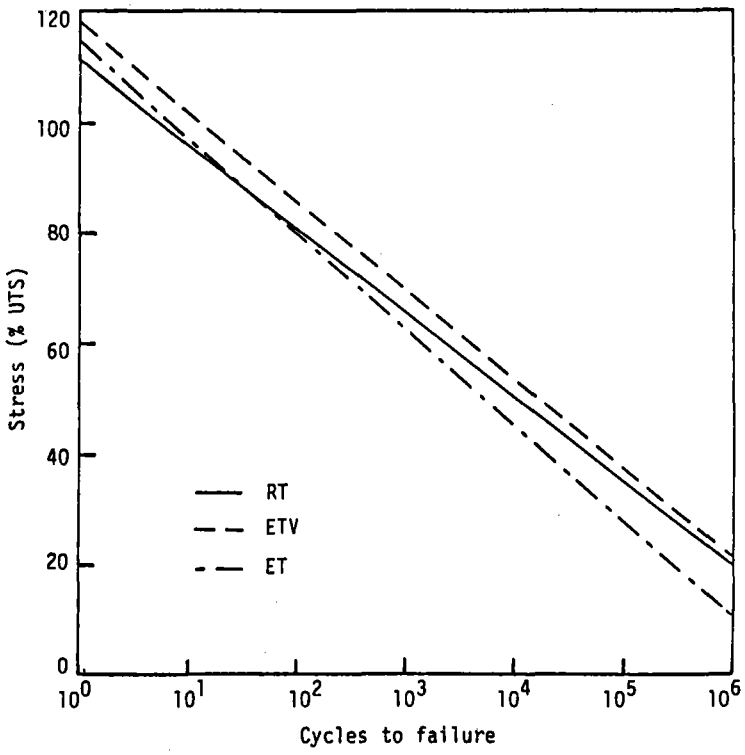

FIG. 2. Comparison of S-N relations at different environments for S-2 glass/epoxy composite.

Fatigue results for epoxy-controlled specimens, such as ± 45 in shear, are plotted in Fig. 3. Frequency dependency is clearly very strong in the range of 0.4 to 4 H_z. For fiber-controlled fatigue one would expect the frequency effect to be less pronounced than for the matrix controlled fatigue.

The trend on spectrum loading effect on fatigue of S-2 glass composite is not very clear at the present time.

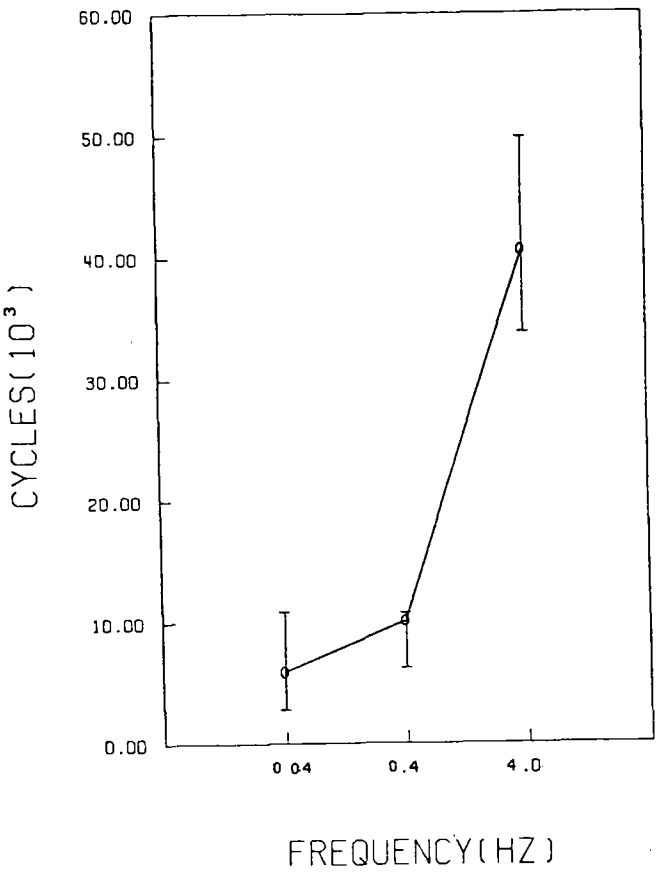

FIG. 3. Fatigue life in shear as a function of frequency for S-2 glass/epoxy ± 45° specimens.

3) Interaction with industry. In addition to the normal communication channels with industry such as telephone discussions and formal technical reports, we also published four issues of Composites Technology Review this year. Since this magazine is jointly sponsored by ASTM, it enjoys wide circulation in the industry.

Summary Remarks

1) The high-performance fibers evaluated look very promising for future flywheel use. Further studies using specimens more closely related to structures are continuing.

2) Activities on engineering data for design and the support of Composites Technology Review magazine have been regrettably closed out due to the lack of funding.

br/4737c

COMPOSITE HYBRID FLYWHEEL ROTOR DESIGN OPTIMIZATION AND FABRICATION

Anthony P. Coppa
General Electric Company
Space Systems Division
P.O. Box 8555, Philadelphia, PA 19101

ABSTRACT

This paper summarizes progress made during the past year in the further development of the General Electric composite hybrid flywheel rotor. A prototype design having an operational energy capacity of 0.25 kwh and a projected lifetime of 10^5 acceleration/deceleration cycles has been developed. Rotors based on this design have been fabricated and delivered for spin test evaluation at designated flywheel test centers.

INTRODUCTION

Previous to the present program, the General Electric Company pursued the development of the 'hybrid' flywheel rotor at its Corporate Research and Development Center (1,2,3). Major progress made by Nimmer, et.al. (3) led to fabrication and spin evaluation testing of several hybrid rotors which exhibited energy/weight and energy/volume ratios as high as 26 wh/lb (57 wh/kg) and 2600 wh/ft^3 respectively.

For the past year further development of the hybrid rotor has been performed at the General Electric Space Systems Division which has also been developing flywheel containment technology under DOE/LLNL sponsorship. The objects of the present program are (a) to refine the hybrid design in light of the latest material properties and spin test data and better understanding of rotor failure modes and related containment requirements; and (b) to fabricate a specified number of rotors for test evaluation. Under this program, 14 prototype hybrid rotors and five simple disk rotors are being furnished. The hybrid rotors have a nominal storage capacity of 250 wh at maximum operational speed and are designed to operate for 10^5 idealized acceleration/deceleration cycles as described in (4). The disk rotors are intended to provide valuable data about the short-time and fatigue strength and failure behavior of the glass/epoxy laminate under spin conditions.

The program was sponsored by the U.S. Department of Energy through the Lawrence Livermore National Laboratory; Dr. S. V. Kulkarni was the LLNL Project Engineer.

PROGRAM TASKS AND APPROACH

The program has been conducted according to the following major tasks: Task 1. Definition of design and Fabrication Requirements; Task 2. Design Optimization; Task 3. Rotor Design; Task 4. Rotor Fabrication; Task 5. Cost Analysis.

In implementing these tasks, an awareness of flywheel systems requirements that impact the rotor design itself was maintained. Such constraints, for example, as rotor operating temperature, which is related to housing

vacuum level, weight and packaging efficiency of the housing, which is strongly associated with the rotor diameter/axial thickness proportions, and containment weight, which is determined by the governing rotor failure mode or modes and rotor/housing weight entered into the selection of materials and dimension for the prototype rotor components. Also available design properties of rotor component materials and spin test data for hybrid and related disk rotors were studied and applied to the prototype design.

This result of this appraoch was to use the following materials for the rotor components:

Disk (19 rotors): Laminated S23 glass/Sp250 epoxy constructed in a repetitive [0,90,±45°] balanced layup of unidirectional plies (50% fiber volume). The laminates were made by the 3M Company, St. Paul, MN.

Outer Ring (14 rotors): Filament-wound Thornel 300, 15,000 filament graphite fiber in the following resins (60% fiber volume): Epon 826 (250°F) epoxy (10 rotors), Ciba-Geigy CY-179 (350°F) epoxy (two rotors), and Lord flexible polyurethane (two rotors). The Lord Corp., Erie, PA, fabricated the rings as well as an additional ring in the three different resins that were used for physical tests and to determine residual stress levels.

Hub (19 rotors): 6061-T6 aluminum alloy bonded to the disk with a polyurethane elastomer. The hubs and hub bonding were also fabricated by the Lord Corporation.

The choice of the above materials and fabricators was based on proven past performance. For instance, laminates of the above described material and produced by the 3M Company exhibited excellent performance in spin tests. Also, the T-300 Gr/Epon 826 system was chosen to represent previous hybrid rotor hardware and therefore to utilize a proven fabrication process and to build upon the existing spin test data base. The CY-179 epoxy resin system was used to permit spin test evaluation of hybrid rotors within higher pressure (1 Torr) environments in which rim temperatures of about 300°F might be attained. The T300 Gr/polyurethane system was selected to evaluate the effectiveness of the flexible resin to avoid transverse, (radial) ring failure, which is the limiting failure mode for radially thick outer rings.

DESIGN OPTIMIZATION

Rotor designs were studied by using a computer program furnished by Nimmer (5) which calculates the stresses in an orthotropic ring that is fitted to an isotropic disk with a radial interference, δ. The stresses are calculated in terms of three quantities, namely V, the peripheral speed at the rotor outside radius, b, the radius ratio $\beta = a/b$, where a is the inside radius of the ring, and $\bar{\delta} = \delta/b$. The energy density, E_w is also expressed in these same quantiites. Hence, given the ultimate and fatigue strengths of the rotor components, a maximum value of V and hence E_w corresponding to them is determined for given values of β and $\bar{\delta}$. Four modes of failure are defined, as follows: CRF, circumferential (hoop) ring failure, RRF, radial (transverse) ring failure; DF, disk

failure (determined at the disk center).; and S, ring/disk separation threshold. A plot of E_w vs. β for the failure modes displays their envelopes and aids identification of a value of β for which the E_w is optimum for a given value of $\bar{\delta}$. Such a plot may be called a Nimmer plot.

Early in the program, calculations were made for various values of $\bar{\delta}$, based on the material properties listed in Table 1. Upon consideration of corresponding Nimmer plots, values of $\bar{\delta}$ = .002 and β = 0.8 were selected for the rotor design. This particular plot is shown in Figure 1, in which the solid curves refer to short-time ultimate failure and the dashed curves to the 10^5 cycle fatigue limit.

A meaningful interpretation of a Nimmer plot requires careful consideration of ring/disk loading interactions in the light of uncertainties in governing material property values. These uncertainties are due to (1) limited available standard specimen data, (2) fabrication process dependency, (3) size effects, and (4) variation of certain properties with load and time. For example, one of the more uncertain properties is the transverse tensile strength σ_{RRU} of the graphite/epoxy ring. In addition, as can be seen in Figure 1, E_w is most sensitive to variations in σ_{RRU}.

Nimmer made an extensive effort (3) to determine a value of σ_{RRU}: Measurements of test coupons made from filament wound panels and ring sections showed (tensile test) strengths ranging from 2.28 to 3.45 (2.98 ksi avg.) and 2.10 to 3.99 (3.23 ksi avg.) respectively and three-point bend strengths ranging from 6.30 to 7.39 (7.16 ksi avg.). Based on these data, a value of σ_{RRU} = 1.59 ksi which accounts for test specimen/ring size effect was calculated. Additional data were obtained fortuitously from spin tests of two hybrid rotors (6). These tests rather conclusively indicated the rotor speed at which RRF occurred. As a result, values of σ_{RRU} = 2.0 and 3.5 ksi were derived analytically. From this data base, a design value of σ_{RRU} = 2.0 ksi was assumed to be reasonable for optimization purposes. RRF envelopes for the two spin-test values of σ_{RRU} are shown plotted in Figure 1.

Referring to Figure 1, the ultimate energy density, E_w = 22.6 wh/lb (49.8 wh/kg) and is limited by CRF. Confidence in this result is somewhat strengthened by a value of σ_{CRU} (circumferential ring tensile strength) that was deduced from another hybrid rotor spin test (6). The cause for this value being lower than the CRF curve (see Figure 1) is attributed to a value of $\bar{\delta} > .002$. With respect to 10^5 cycle fatigue, E_w = 12.5 wh/lb (27.6 wh/kg) and is limited by CRF and DF. Hence, the energy density ratio between ultimate failure and fatigue failure is 1.81, which is considered desirable. Rotor designs incorporating radially thicker rings (say β = .785 or less) would not be desirable at present because of excessive sensitivity of E_w to σ_{RRU}.

It was desirable to fix the value of β early in the program in order to provide sufficient lead time to meet the testing schedule. Despite this, considerable design flexibility was retained because of the freedom to alter the value of $\bar{\delta}$ later. Such a move was, in fact, made after greater understanding of hybrid rotor behavior had been obtained.

Once values of β and the required energy stroage are specified, a variety of rotor designs is defined, each of which has a particular combination of outside radius and axial thickness, h. Several designs are listed in

Table 2, in which N_{OP} is the maximum operating speed, corresponding to .25 kwh storage, N_U, the ultimate speed, W_R, W_C, and W_H are weights of the rotor, containment ring, and housing respectively, and E_{W_R} and E_{W_S} the operational energy densities of the rotor and combined system respectively. The system energy density, E_{W_S} = 3.4 wh/lb (7.50 wh/kg) which includes the weights W_R, W_C, and W_H, is considered acceptable for an efficient flywheel/heat engine hybrid vehicle application.

Selection of the actual rotor design was based on considerations of running speed, rotor vibration frequency, system energy density and housing packaging efficiency. The b = 8 in. design was selected as having a desirable combination of these quantities. Figure 2 is a photograph of the first prototype rotor produced under this program. Its final design properties are as follows (units are in., lb., sec.):

Rotor OD = 16.00, ring ID = 12.80, ring axial thickness = 1.74, disk axial thickness = 1.69, rotor weight = 22.33, of which the ring, disk, and hub/bond weights are 6.79, 14.43, and 1.11 respectively, total mass moment of inertia (excluding hub/bond) = 1.687, and energy storage = 480 wh (ultimate) and 293 wh (operational).

Further optimization was done on this particular design to define the desirable value of the interference fit, δ. This task was addressed after component hardware had been completely fabricated and test data obtained from specimens cut from fabricated parts. The test data indicated that the ringproperties of Table 1 are appropriate but that an elastic modulus, E = 2.90 msi applies to the laminate. Figure 3 shows governing failure envelopes for the β = .80 design, with E_W plotted against $\bar{\delta}$. Two envelopes for ultimate failure are shown in solid lines for disk moduli of 3.3 and 2.9 msi. Two additional envelopes, in dashed lines, are also shown for 10^5 cycle life, based on two different values of disk fatigue strength, namely 25 and 31 ski. The latter value is based on a spin test of one of the simple disk rotors produced under this program, from which a laminate strength of at least 75 ksi has been inferred. It is seen that optimum values of E_W both for ultimate and 10^5 cycle life occur near a value of $\bar{\delta}$ = .001. Within the range .0010 $\leq \bar{\delta} \leq$ .0015, the median values are E_W = 22.6 and 13.8 wh/lb (49.8 and 30.4 wh/kg) for the two operational conditions respectively. On such a basis the value of interference fit was established in the optimum range noted above. A value of $\bar{\delta}$ = .0011, for example was obtained in the first hybrid rotor.

In the preferred range of $\bar{\delta}$, CRF is the limiting mode for both ultimate and fatigue. The containment ring required to sustain an outer ring burst is estimated to be 25% ligher than that required to sustain a complete rotor burst. Hence the system energy density, E_{W_S} for the prototype design will be greater than the value given in Table 2.

CONCLUSIONS

Through a process of optimization relative to the radius ratio, β and C interference-fit, $\bar{\delta}$, rotor energy densities of about 23 and 14 wh/lb (51 and 31 wh/kg) corresponding to ultimate and 10^5 cycle life respectively have been obtained for the hybrid rotor and about 3.6 wh/lb (7.9 wh/kg) for the rotor, containment ring, and housing system opera-

tional energy density. These values pertain to present best estimates of the mechanical properties of rotor components. It is expected that the energy performance of the hybrid rotor will tend to increase with further development. This is based on the following: (a) Use of new, high strength graphite fibers, producing greater circumferential ring strength, (b) use of tougher resins, particularly in the ring, thereby increasing radial failure resistance, and (c) realizing the potential in biaxial strength levels that has been indicated in several spin tests of glass/epoxy laminated disks.

Even without such possible improvement the hybrid rotor flywheel design offers an attractive set of advantages, namely, good energy density with outstanding compactness, excellent ruggedness, and constructional simplicity that suggests low hardware cost in large quantity production.

Acknowledgement

The author is grateful to Dr. S.V. Kulkarni, LLNL for general guidance, to Drs. C.H. Zweben and B.T. Rodini, General Electric Co. for consultation on composite materials, to Mr. A.J. Hannibal of the Lord Corp., who directed ring fabrication and hub bonding operations, to Mr. J.W. Davis of 3M Co., who directed laminate fabrication, to Mr. W.R. Lowrie of Red Seal Electric Co. for laminate machining, and to Dr. R.S. Steele of Union Carbide Corp., Oak Ridge National Laboratory for hub design assistance.

References

1. Nimmer, R.P., "Parametric Design Analysis of a Hybrid Composite Flywheel Using a Laminated Composite Disk and a Filament-wound Outer Ring", General Electric Comapny TIS Report No. 80CRD038, March, 1980.

2. Nimmer, R.P., "Progressive Matrix Damage in Laminated Fiber - Epoxy Flywheel Discs," General Electric Co. TIS Report No. 80CRD263, December, 1980.

3. Nimmer, R.P., Torossian, K., Hickey, J., "Laminated Composite Disk Flywheel Development," Report No. UCRL-15301, Third Interim Report, Subcontract No. 2479309 by General Electric Company, February, 1980.

4. Reifsnider, K.L., Kulkarni, S.V., and Boyd, D.M., "Composite Flywheel Durability and Life Expectancy: Test Program", Proceedings of the Mechanical, Magnetic, and Underground Energy Storage 1981 Annual Contractors' Review, Report No. Conf-810833, February, 1982.

5. Nimmer, R.P., General Electric Company Corporate R&D Center, private communication, 16 July 1981.

6. Rabenhorst, D.W. and Wilkinson, W.O., "Prototype Flywheel Spin Testing Program", Johns Hopkins University, Applied Physics Laboratory Report No. SDO 5988, also UCRL-15381, Lawrence Livermore National Laboratory, April, 1981.

Table 1. Properties of Rotor Materials:
Disk (S-2 Glass/SP250 Epoxy);
Ring (T-300 Graphite/Epon 826 Epoxy)
Poisson's Ratio = .3

	Disk			Ring				
	E	σ	ρ	E_θ	E_R	σ_θ	σ_R	ρ
	msi	ksi	lb/in^3	msi	msi	ksi	ksi	lb/in^3
Ultimate	3.3	60	.066	18.8	1.40	170	2.0-3.5	.0531
10^5 Cycles	2.55	25	.066	18.8	1.40	110	1.2	.0531

Table 2. .25 kwh Hybrid Rotor Designs Based on $\beta = 0.80$ and $\bar{\delta} = .002$

b	h	N_{OP}	N_U	W_R	W_C	W_H	E_{W_R}	E_{W_S}
in.	in.	rpm	rpm	lb.	lb.	lb.	wh/lb	wh/lb
7	2.118	34670	46520	20	15.9	31.9	12.5	3.7
8	1.621	30340	40700	20	15.8	37.5	12.5	3.4
9	1.281	26970	36180	20	15.4	44.0	12.5	3.2

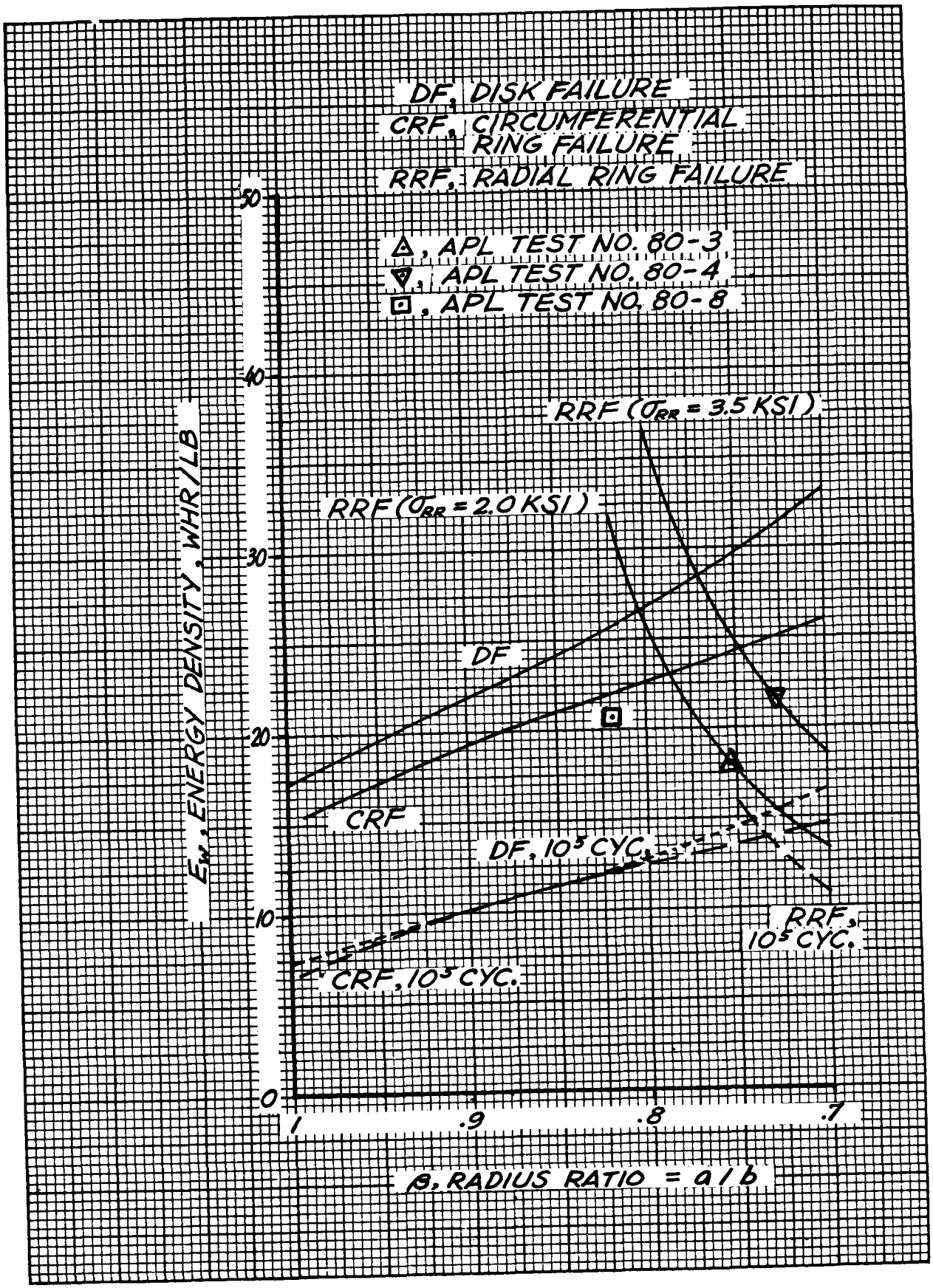

Figure 1. Hybrid Rotor Density vs. Radius Ratio for Governing Failure Modes ($\bar{\delta}$ = .002).

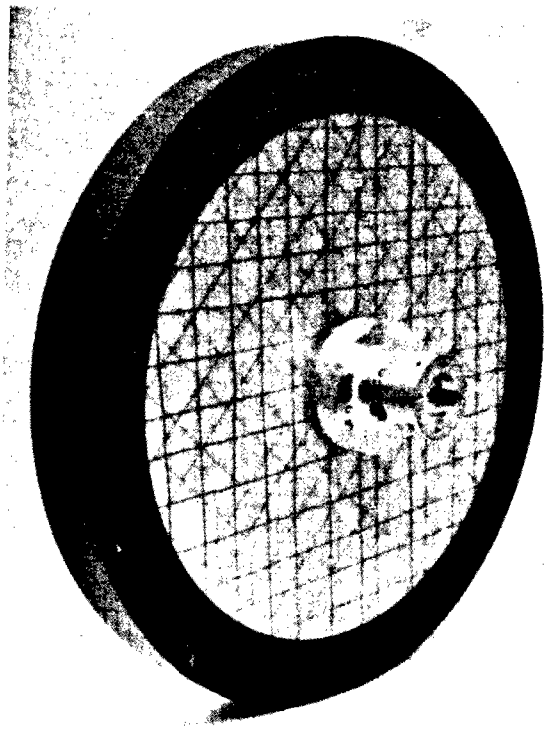

Figure 2. Composite Hybrid Rotors, 0.25 kw Operational Energy Storage, Showing Graphite/Epoxy Outer Ring, Laminated Glass/Epoxy Disk, and Elastomerically Bonded Aluminum Hub (β = 0.8).

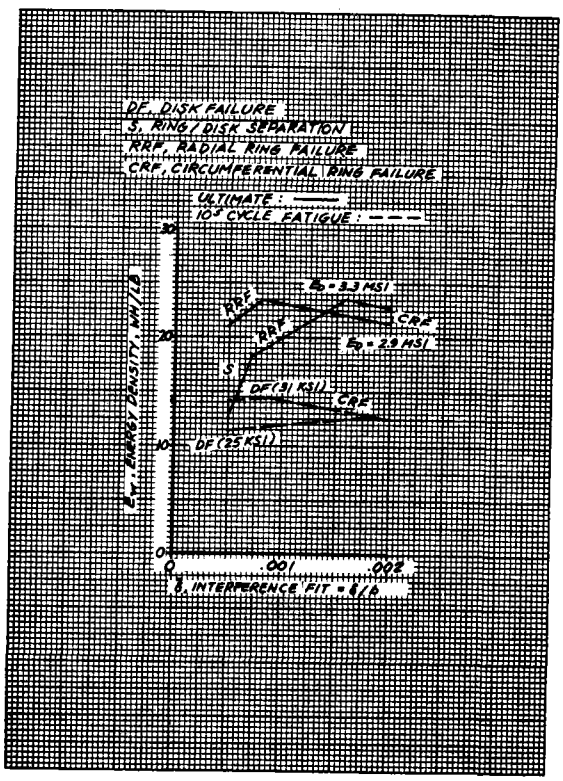

Figure 3. Energy Density of Prototype Hybrid Rotor Design (β = 0.8) vs. Interference Fit.

ASSESSMENT OF FLYWHEEL SYSTEM BENEFITS IN SELECTED VEHICLE APPLICATIONS

L. Forrest
The Aerospace Corporation
El Segundo, California

DISCUSSION

This study focused on two specific automotive applications in which the capabilities of flywheel-equipped vehicles were compared to their non-flywheel counterparts: a four-passenger commuter vehicle with electric drive (range extension application of the flywheel system) and a six-passenger family car with conventional heat engine drive (fuel conservation application of the flywheel system). The six-passenger vehicle was also examined with respect to its use in urban taxi service.

The study first characterized both metal and fiber composite flywheel systems in terms of size, speed, energy capacity, weight, and volume. Next, an operational analysis was performed to determine flywheel system loss characteristics for several basic flywheel system designs. In a third step, candidate propulsion powertrain configurations were selected for detailed examination and the driveline components in these configurations were characterized as to efficiency, size, and weight. In a final step, the defined vehicle/propulsion systems were analyzed by use of a computer simulation program to determine range extension and energy conservation effects as a function of vehicle driving cycle, vehicle use mode, battery type (range extension application), and flywheel system design. These analyses focused on the flywheel subsystem and its specific contribution to energy conservation.

A number of baseline vehicles were used as references in determining the energy benefits of the flywheel system. Sample characteristics of the principal baseline vehicle types are shown in Table 1. The intermediate class vehicle is a front-wheel-drive (FWD) configuration that generally conforms to GM projections for the 1982 downsized A-body vehicle (present Malibu, etc.). The electric vehicle generally reflects the dimensional characteristics of current FWD subcompact vehicles, but the values exhibited are those for the Department of Energy (DOE) near-term electric vehicle, ETV-1.

The principal flywheel systems examined are shown schematically in Figures 1 and 2. Figure 1 depicts a heat engine/flywheel powertrain with components arranged in a series power flow arrangement. The heat engine and flywheel are linked by a speed reduction gear of fixed ratio, and the flywheel is linked to the wheels through a continuously variable transmission (CVT) which operates to match flywheel rotational speed to the road speed requirement. The flywheel subsystem here is a through-shaft configuration, reflecting technology employed in the DOE ETV-2 vehicle design. In this powertrain arrangement, the flywheel (effectively) drives the vehicle, while the heat engine operates in an on-off mode to maintain flywheel speed above a controlled lower limit (a study variable). When on, the engine operates at near wide-open-throttle, minimum BSFC (brake specific fuel consumption) conditions for maximum efficiency. Vehicle kinetic energy during deceleration is recovered by using the forward motion of the vehicle to spin up the flywheel.

A second flywheel drivetrain examined is shown in Figure 2. The prime propulsion unit is a battery-powered separately excited DC motor mechanically linked to the vehicle wheels through an (optional) two- or three-speed transmission. The flywheel unit outputs electrical energy to augment the battery source as needed to meet peak road power demands. In this manner, the flywheel acts to load-level the battery, thereby increasing its energy capacity so as to extend vehicle range.

The essence of this project was a case study of the vehicle systems and missions described above, in which flywheel-equipped vehicles were compared with their non-flywheel counterparts (baseline systems) on the basis of energy utilization. To accomplish this, a computer-based vehicle simulation program was developed. This program determines the propulsion power required to negotiate each element of the driving cycle, and apportions this power between prime mover and storage device according to one or more selected operating strategies. The state of flywheel (and/or battery) charge is continuously tracked, along with the consumption of fuel or dissipation of battery energy. Energy flows associated with all major component processes are accounted for.

RESULTS

Heat Engine/Flywheel Powertrain. Results of the vehicle simulation/energy analysis effort are provided here for the series configuration heat engine/flywheel powertrain. Examples of the output for this element of the study are presented in Figures 3 through 7, showing flywheel vehicle fuel economy benefits expressed as a percentage improvement over baseline vehicle performance. All data except for Figure 7 are ideal quantities in that flywheel final spindown losses are neglected. Figure 7 addresses the influence of spindown loss effect.

Figure 3 shows the flywheel vehicle fuel economy improvement as influenced by driving cycle and by flywheel rotor energy storage capacity (heat engine size is fixed at 90 HP rated). The improvement is highly variable with driving cycle. It is a negative quantity for the highway cycle, where flywheel system losses constitute an energy liability, and it is greatest (approaching 150 percent) for the taxi cycle, where the potential for braking energy recovery by the flywheel is a maximum.

The improvement characteristic is shown to be relatively insensitive to rotor energy storage capacity. This is the net result of the following disparate effects which occur as rotor energy storage capacity is increased: (1) vehicle weight increases, (2) the frequency of heat engine starts (and associated fuel consumption) decreases, (3) braking energy recovery increases, and (4) flywheel system loss increases. In general, the curves decay at the low end of the capacity range, reflecting regenerative braking saturation effects in the smallest capacity wheels investigated.

Accessory loads can reduce the fuel economy benefits of flywheel vehicles substantially, as indicated in Figure 4. Here shown is a 500 Whr flywheel system operating with air conditioning, power steering, power brakes, and radio (air conditioning is the significant load element). With this equipment, the percent improvement for the taxi cycle is reduced from 146 to 70 percent.

The effect of possible technological improvements which could reduce flywheel system parasitic losses (windage, bearing friction, etc.) relative to the values employed in this analysis is illustrated in Figure 5. As indicated, the influence on fuel economy improvement is negligible for all but the taxi cycle, where the benefits are significant only for highly optimistic levels of loss reduction.

A reduction of heat engine size (rated power) has the principal effect of reducing engine (and vehicle) weight, but does not significantly improve BSFC for the series configuration heat engine/flywheel vehicle, since the engine already operates in an optimum efficiency mode. To maintain performance equivalent to the baseline vehicle for road acceleration maneuvers, it may be necessary to increase the minimum storage capacity of the flywheel system, either by increasing rotor size or by operating the flywheel at higher average speed to ensure a reserve capacity. Figure 6 disregards the road performance requirement and therefore displays the best fuel economy improvement that can be expected in the series heat engine/flywheel vehicle by means of engine downsizing. As indicated, the improvements related to engine downsizing are modest, suggesting that the full size engine may be the preferred choice for this drivetrain design.

The effect of flywheel spindown loss is incorporated in the fuel economy results presented in Figure 7, showing flywheel vehicle fuel economy improvement under urban cycle driving conditions, plotted as a function of trip length for two flywheel capacities. The data reflect a net flywheel loss defined by the energy required to spin up the flywheel from a condition of rest to its kinetic state at trip end. Two extreme end conditions are considered for a given trip: one in which the flywheel is at the low end of its operating speed range (minimum spindown loss) and one in which the flywheel is at the high end of its operating speed range (maximum spindown loss). Actual flywheel speed at trip end will fall randomly between these limits, as represented by the shaded bands in the figure.

Figure 7 demonstrates that the true fuel economy benefit of the flywheel vehicle will vary significantly with trip length. The improvement is poor for short trips because the rotor spindown loss constitutes a large fraction of trip energy expenditure. At the limits defined by the break-even trip distance plateau, the flywheel vehicle provides no fuel economy advantage over the baseline conventional vehicle and is less fuel-efficient at distances below these values. The smaller-capacity flywheel is seen to be distinctly superior with respect to the spindown loss effect. Therefore it appears that the smallest wheel meeting the power requirements of the driving cycle and capable of absorbing cycle-available braking energy without saturation would be an ideal selection for the implementation of a practical vehicle system.

Battery/Flywheel Powertrain. The mechanisms by which vehicle range may be extended by the addition of a flywheel to an electric powertrain are (1) the recovery of vehicle kinetic energy by regenerative braking and (2) the leveling of battery power drain by operating the flywheel to supply peak road power demands. If the electric vehicle is already designed to recover braking energy, as assumed in this analysis, then the benefits of mechanism (1) will disappear, except to the extent that the flywheel powertrain can perform the braking energy recovery function more efficiently than the all-electric design. Factors that can operate to reduce the energy benefit potential of the flywheel system are (1) the

greater weight of the vehicle, (2) the parasitic losses associated with flywheel operation, and (3) the losses associated with the transfer of energy to and from the flywheel system. If these opposing positive and negative influences balance, then the flywheel vehicle will provide no range advantage over an all-electric vehicle design.

The study examined a flywheel powertrain consisting of a battery-powered DC drive motor and a hermetically sealed flywheel/generator that outputs electrical energy to augment the battery source. The transfer of flywheel energy by electrical means, as embodied in this scheme, may be slightly less efficient than a mechanical power transfer path (e.g., CVT), but it exemplifies the design approach used in both the GE and AiResearch new-technology energy storage unit developments for DOE, and therefore it was of special interest to the present investigation.

The optimum operational configuration examined is equipped with a 250 Whr composite flywheel and operates with a controlled battery output power targeted to 8.5 kW. In one aspect of the analysis, the flywheel vehicle battery pack, which is volumetrically identical to that of the all-electric baseline vehicle, was taken to consist of conventional Pb-acid or Ni-Zn batteries designed for electric vehicle traction service. In another element of the analysis, the battery systems were conceptually redesigned to trade off power for increased energy capacity, and the utility of the flywheel was reexamined under these conditions.

Sample results of the analysis are given in Figures 8 through 10, showing battery/flywheel vehicle range benefits expressed as a percentage improvement over baseline vehicle range at 80 percent battery energy depletion. The vehicles represented in these plots are (1) an all-electric four-passenger compact vehicle (baseline) equipped and configured similar to ETV-1 (Table 1), and (2) a class-equivalent flywheel vehicle, stretched to accommodate the packaged density of the flywheel powertrain. Thus burdened, the flywheel vehicle is about 350 lb heavier than the all-electric vehicle.

Figure 8 is representative of results obtained for flywheel vehicles equipped with either Pb-acid or Ni-Zn batteries as conventionally designed for traction service. At optimum conditions (8.5 kW battery power setting and 250 Whr flywheel storage capacity), the flywheel vehicle barely exceeds the range of the baseline all-electric vehicle. It thus appears that, in this propulsion scheme, the energy conserved by the mechanism of load-leveling is insufficient to appreciably outweigh the negative influences of increased system weight and loss.

Given the power potential of the flywheel system, it is not unreasonable to expect that the range capabilities of the battery/flywheel vehicle could be extended if the battery system were redesigned so as to trade off power for increased energy capacity. When this was done (using battery redesign relationships developed by Lawrence Livermore Laboratory), it was indeed found that the range improved considerably and became much greater than the all-electric vehicle, which relies solely on the battery system as a source of both power and energy.

Flywheel vehicle range extension effects related to battery redesign are displayed in Figure 9 for the case of Pb-acid batteries. Here, however, the tradeoff in battery power impacts the ability of the vehicle to satisfactorily perform sustained-duration maneuvers such as hill climbing,

as shown on the right-hand vertical scale. Accordingly, this approach is not viable for an automobile intended to have full performance capability.

Results for the case of the nickel-zinc battery/flywheel vehicle, shown in Figure 10, are of somewhat greater interest, since this battery has significantly greater specific power than lead-acid, and therefore may be more suitable in terms of performance as redesigned for improved range capability. In reference first to the curve labeled battery/flywheel vehicle, Figure 10 indicates that the Ni-Zn battery system could be redesigned to a peak specific power as low as 72 W/kg (equal to EV2-13 Pb-acid) and still provide the flywheel vehicle with sufficient power to achieve a 50 mph speed on a 5 percent grade. At this redesign condition, the system would provide a range benefit of 43 percent relative to an all-electric vehicle with conventional battery design. On the other hand, the second curve drawn on Figure 10 indicates that if the same redesigned batteries were used in an all-electric vehicle design its range would improve by 58 percent, while its road performance would still be as good as the Pb-acid all-electric baseline vehicle.

CONCLUSIONS

Heat Engine/Flywheel. The series heat engine/flywheel automobile provides substantial fuel economy benefits for driving duty cycles in which the potential for braking energy recovery is large (e.g., taxi, urban cycles). The benefits appear to be essentially constant over a wide range of rotor energy storage capacities and start to decay only when wheel capacity is reduced to the magnitude of the cycle-average recoverable energy level. Accessory loads have a much larger fuel efficiency impact on flywheel vehicles than on conventional vehicles for reasons cited in the analysis; a full accessory load including air conditioning reduces the fuel economy benefit of the flywheel vehicle by a factor of about one half.

For the ETV-2 flywheel system examined, parasitic losses constitute a relatively small part of total powertrain losses; therefore, technological advances in flywheel design alone do not appear to offer significant benefits in overall vehicle fuel economy improvement. Heat engine downsizing appears to have little effect on flywheel vehicle performance for the series configuration drivetrain. Flywheel spindown loss can have a significant effect on flywheel vehicle short trip energy efficiency. The smaller rotors are best in this regard, as shown by the concept of break-even trip distance.

Battery/Flywheel. The analysis shows that battery/flywheel vehicle designs incorporating new technology flywheel systems (hermetically sealed flywheel generators) do not provide measurable benefits in range relative to all-electric vehicles equipped with the same battery pack. Redesign of the flywheel battery system so as to trade off power for increased energy capacity substantially increases range beyond the capability of the all-electric vehicle equipped with conventional traction batteries. At comparable battery redesign conditions, the flywheel vehicle provides no range advantage over the all-electric vehicle. Properly configured, however, the flywheel system will provide improved performance in the execution of short-duration road maneuvers such as standing-start acceleration, merging, and passing.

The present study has compared battery/flywheel vehicles with all-electric vehicles at acceleration-performance design conditions consistent with electric and hybrid technology goals for the near term. For the case in which vehicle performance specifications for short-duration maneuvers are set at extremely high levels, it can be shown that the range capability of the all-electric vehicle will deteriorate significantly, while the range of the flywheel vehicle will be virtually unaffected. Under these conditions, the flywheel vehicle could demonstrate superior range capabilities, particularly through the utilization of the energy/power tradeoff potential provided by such batteries as the nickel-zinc system.

Table 1. Baseline Vehicle Characteristics

VEHICLE	ICE PASSENGER CAR AND URBAN TAXI (Intermediate)	ELECTRIC COMMUTER CAR (Subcompact ~ ETV-1)
PASSENGER CAPACITY	5	4
VEHICLE LENGTH, ft	15.3	14.1
CURB WEIGHT, lb	2780	3320
ENGINE/MOTOR PEAK RATED POWER, hp	90	41
CONSTRUCTION	CONVENTIONAL	ALUMINIZED
RANGE, mi	350	51
TOP SPEED, mph	95+	60
SUSTAINED SPEED ON 5% GRADE, mph	70	55
ACCELERATION TIME, sec		
0-30 mph	4	9.0
25-55 mph		17

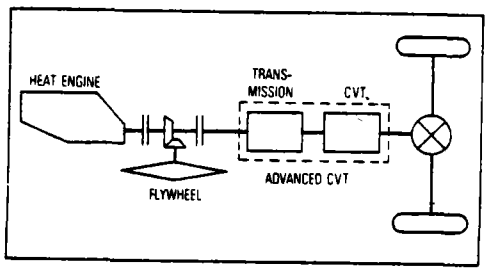

Figure 1. Heat Engine/Flywheel Drivetrain

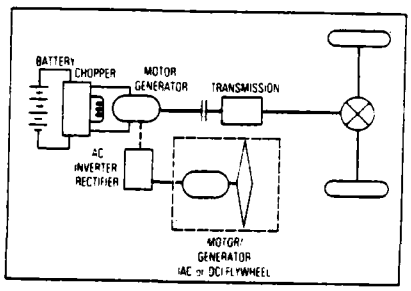

Figure 2. Battery/Flywheel Drivetrain

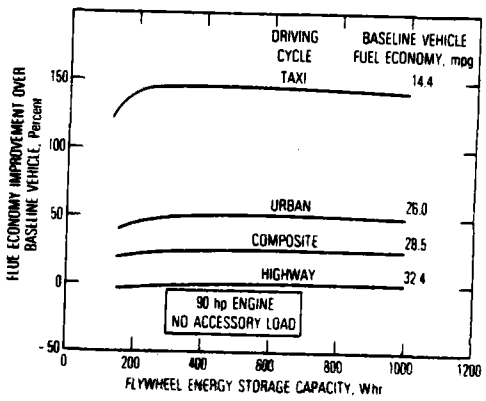

Figure 3. Driving Cycle and Storage Capacity Effects on Flywheel Vehicle Fuel Economy Benefits

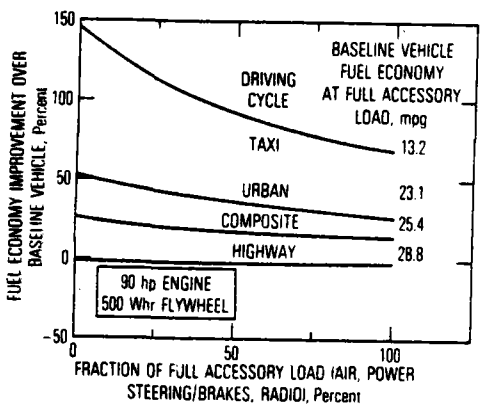

Figure 4. Accessory Load Effects on Flywheel Vehicle Fuel Economy Benefits

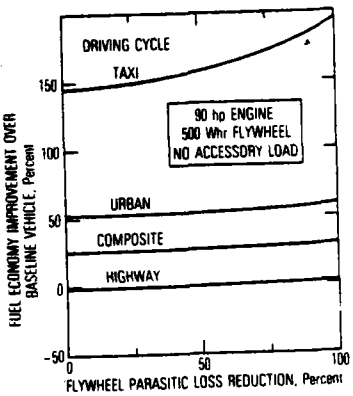

Figure 5. Flywheel Parasitic Loss Effects on Flywheel Vehicle Fuel Economy Benefits

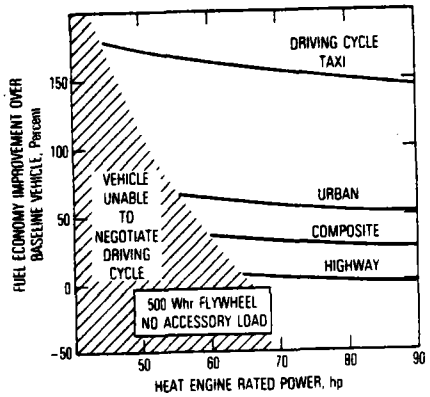

Figure 6. Heat Engine Size Effects on Flywheel Vehicle Fuel Economy Benefits

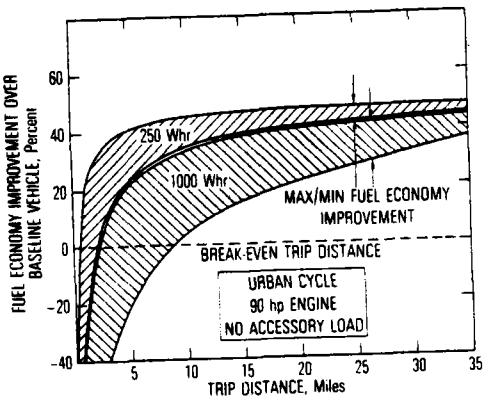

Figure 7. Rotor Spindown Loss Effects on Flywheel Vehicle Fuel Economy Benefits

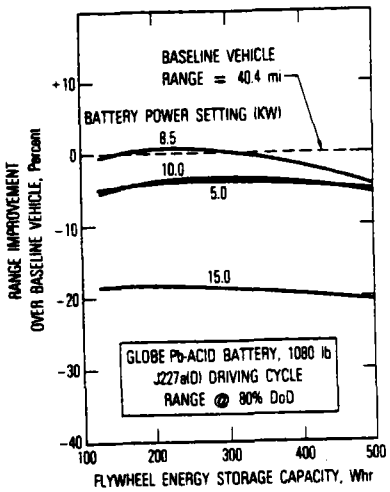

Figure 8. Battery Power Setting and Rotor Storage Capacity Effects on Flywheel Vehicle Range Benefits

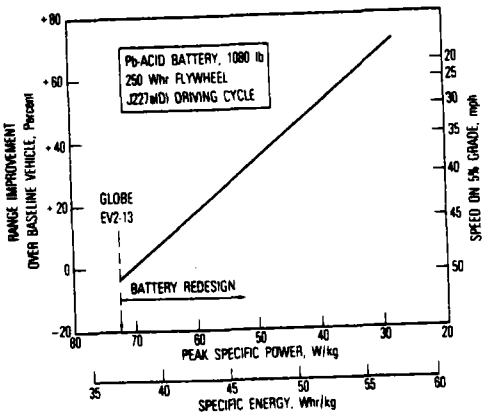

Figure 9. Battery Optimization Effects on Flywheel Vehicle Range Benefits: Lead-Acid Battery

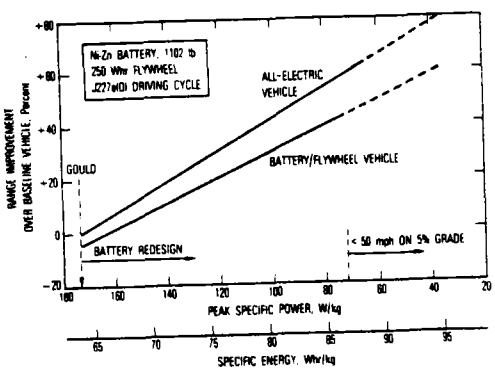

Figure 10. Battery Optimization Effects on Flywheel Vehicle Range Benefits: Nickel-Zinc Battery

ROTOR TESTING IN FY 1982*

E. F. Babelay, Jr.
Union Carbide Corporation, Nuclear Division
Oak Ridge, Tennessee 37830

ABSTRACT

This paper summarizes the results and observations of flywheel spin tests conducted in the Oak Ridge Flywheel Evaluation Laboratory for the Mechanical Energy Storage Program at the Oak Ridge National Laboratory. Test results include the completed cyclic fatigue test of a flywheel designed and fabricated by General Electric. This test was started during FY 1981 and some results were reported at the 1981 Annual Contractors' Review. Ultimate speed evaluations for a modified General Electric rotor and three low cost flywheels built by Owens-Corning Fiberglass and Lord Kinematic Corporation are also reported.

INTRODUCTION

The Oak Ridge Flywheel Evaluation Laboratory (ORFEL), located at the Oak Ridge Y-12 Plant, was established to comprehensively evaluate high performance composite flywheels for the Department of Energy's Mechanical Energy Storage Program. It is operated under an interdivisional work order from the Mechanical Energy Storage Program at the Oak Ridge National Laboratory (ORNL).

Many factors affect the ultimate performance of composite flywheels; thus, flywheel evaluations at ORFEL include measurements other than the maximum speed or number of cycles until failure. Flywheels typically receive a pretest dimensional and radiographic inspection, and the flexural resonant frequencies and mode shapes are determined. During the actual spin testing other parameters such as balance condition, rotor temperature, and test chamber pressure are characterized. The data analysis and spin testing techniques used at ORFEL have been reported in other papers (1); thus, the discussion in this paper has been limited to only those data which bear directly upon the final conclusions regarding the performance of individual flywheels.

---

*Research sponsored by the Division of Thermal and Mechanical Energy Storage Systems, U.S. Department of Energy, under contract W-7405-eng-26 with the Union Carbide Corporation — Nuclear Division.

ALPHA-PLY LAYUP/GRAPHITE RING FLYWHEEL EVALUATION

FLYWHEEL GEB

General Electric designed and fabricated flywheel GEB (2) as a constant thickness, solid, circular disk of laminated, uniaxial S-glass composite sheets in an alpha-ply layup. The central disk was surrounded by a circumferentially wound graphite ring. The flywheel was 35 mm (1.4 in.) thick, had a diameter of 450 mm (17.7 in.), and weighed 10 kg (22 lb). An aluminum arbor was bonded to the center of the disk with an elastomer over a 152 mm (6 in.)-diameter bond area.

The purpose of the cyclic fatigue test of GEB was primarily to check out the facility. It consisted of shuttling the flywheel between a high speed point of 417 rev/s (25,000 rpm), and a low speed of 140 rev/s (8,400 rpm). A 4-in. air turbine accelerated and decelerated the rotor at an overall average power of 4.7 kW (6.4 hp). Approximately 8 min were required to complete one cycle. The cycle test was stopped at scheduled intervals to allow visual, dimensional, and ultrasonic inspection of the flywheel. Except for minor epoxy crazing of the S-glass disk, no major defects or trends were detected during these inspections. Figure 1 shows GEB after it had completed 1000 cycles.

The failure of GEB occurred after 1454 cycles. The rotor was decelerating from the high speed point when a dynamic instability developed and failure of the flywheel occurred within ~1 s. Analysis of the runout signals and flywheel debris indicate the aluminum arbor fractured as its runout exceeded the turbine limit. The fractured arbor allowed the disk to drop and the graphite ring was destroyed as the flywheel spun to rest on the bottom of the spin pit. The S-glass disk sustained little damage as is seen in Fig. 2. The cause of the dynamic instability was uncertain, although more recent experience with rotors of this type indicates the instability can result from the failure of the elastomeric bond. The maximum energy stored at 417 rev/s (25,000 rpm) was 0.218 kWh with an energy density of 22.3 Wh/kg.

FLYWHEEL GEC

An ultimate speed evaluation was performed on a modified flywheel designed and fabricated by General Electric. Flywheel GEC consisted of an alpha-ply, S-glass layup disk, similar to GEB, except GEC did not utilize a graphite ring. The disk was 398 mm (15.7 in.) in diameter, had a thickness of 43 mm (1.7 in.), and weighed 10.5 kg (23.1 lb). The aluminum arbor was bonded to the disk over a 76 mm (3 in.) area. Since the flywheel

balancing performed in FY 1981 before starting the high speed evaluation and spin tests demonstrated that the drilling of holes near the outer diameter of a disk type composite flywheel did not appear to affect its ultimate speed capability, the technique was used to balance GEC. Approximately 20 gm of composite were removed. Figure 3 shows GEC and the locations of the balancing holes.

The flywheel demonstrated little shift in balance and no dynamic stability problems when tested to its operating speed. During the final test run of the rotor, as it reached a speed of 653 rev/s (39,180 rpm), the spin pit vacuum rose above the 10 microns test limit and the test operator decelerated the flywheel. By the time the flywheel had slowed to 618 rev/s (37,080 rpm), the pit pressure had reduced to less than 10 microns; and the drive air was applied to the turbine. Upon accelerating the rotor, the arbor runout reached 0.5 mm (0.020 in.) and the brake air was applied to the turbine to decelerate the flywheel. During this braking, low frequency whirl caused the arbor to repeatably make contact with the arbor constraint at a rate of once every 2 to 5 s. When the flywheel had slowed to ~550 rev/s (33,000 rpm), the disk fell from the arbor to the bottom of the tank.

Debris analysis reveals that the elastomeric interface between the arbor and disk became unbonded from both surfaces. The composite disk lost about 5 mm (0.2 in.) thickness but was otherwise intact. At its maximum speed of 653 rev/s (39,180 rpm), flywheel GEC stored 0.46 kWh with an energy density of 43.9 Wh/kg.

SMC/GRAPHITE RING FLYWHEEL EVALUATION

FLYWHEEL OCLB

Three composite flywheels fabricated by Owens-Corning Fiberglas (3) and Lord Kinematic Corporation were evaluated for ultimate speed at ORFEL during FY 1982. This completed the series that began with flywheel OCLA tested in FY 1981. All rotors consisted of a 25.4 mm (1.0 in.) constant thickness S-glass disk made from sheet molding compound (SMC). Two of the rotors tested this year were surrounded by a circumferentially wound graphite ring. Flywheel OCLB was 560 mm (22.0 in.) in diameter, weighed 10.9 kg (24 lb), and had a 12.5 mm (0.5 in.) thick graphite ring. An aluminum arbor with a 150 mm (6 in.) diameter flange was bonded to the SMC disk using an elastomer. Final machining of the spindle hole in the arbor was performed at ORFEL. The lack of an accurate machining datum resulted

in a rotor still requiring balance. Balancing of OCLB was accomplished by drilling holes near the outer diameter of the SMC disk. Figure 4 is a photograph of the rotor.

The arbor of OCLB exhibited a shift with speed similar to that reported in other flywheels that utilize the elastomeric bond to attach the arbor. This shift is a relative displacement between the arbor and disk that grows with increasing speed and can be detected by comparing the runouts of the arbor and disk at a given speed. Runout data for OCLB shows a shift of 0.085 mm (0.0033 in.) when the rotor speed was increased from 100 to 270 rev/s. In order to evaluate the effect of bond area on this phenomenon, the arbor was machined to reduce the bond area from the original 150 mm (6 in.) to 89 mm (3.5 in.) in diameter. Figure 5 is a photograph of the modified arbor. Evaluating the modified flywheel over the same speed range showed that the shift between the disk and arbor was reduced by approximately one-third.

After characterizing the performance of the elastomeric bond, the flywheel was tested to failure. The failure of OCLB was catastrophic, instantaneous, and was obviously the result of rotor overstress. At the ultimate speed of 352 rev/s (21,120 rpm), the rotor stored 0.278 kWh with an energy density of 25 Wh/kg. Figure 6 is a photograph of the rotor debris and is typical of a flywheel fabricated from SMC.

FLYWHEELS OCLC AND OCLD

Construction of flywheel OCLC was similar to OCLB with the exception of the design of the graphite ring. The ring had a trapezodial cross-section which was 25 mm (1 in.) thick at the diameter of the SMC disk and increased to a 50 mm (2 in.) thickness at its own outer diameter. The ring had a radial thickness of 37 mm (1.5 in.). The arbor was machined to an 89 mm (3.5 in.) diameter, and the rotor balanced in a manner similar to OCLB. The ultimate speed of OCLC was 367 rev/s (22,020 rpm). Failure of the rotor was likewise instanteous and catastrophic. At failure, flywheel OCLC stored 0.53 kWh at an energy density of 36.6 Wh/kg.

Flywheel OCLD was the final SMC type rotor tested during FY 1982. The rotor had the same SMC construction as OCLB and OCLD; however, no graphite support ring was used. The arbor was machined and the flywheel balanced as the previous OCL flywheels. The ultimate speed was 306 rev/s (18,360 rpm) with a total energy storage of 0.17 kWh at 17.5 Wh/kg. Failure of OCLD was identical in nature to the other OCL flywheels tested. Table 1 summarizes the performance data of Owens-Corning/Lord flywheels.

Table 1. Performance summary for Owens-Corning Fiberglass/Lord flywheels

Flywheel ID	Weight (kg)	Diameter (m)	Rim thickness (mm)	Maximum speed (rpm)	Maximum energy (kWh)	Energy density (Wh/kg)
OCLA	12.9	0.615	25.4	19,980	0.360	27.7
OCLB	10.9	0.560	12.7	21,120	0.278	25.0
OCLC	14.6	0.614	38.1	22,020	0.534	36.6
OCLD	9.9	0.534	0	18,360	0.173	17.5

MISCELLANEOUS FINDINGS

A number of ongoing investigations must be updated. One is the search for resonant vibrations excited in a spinning disk. The at rest flexural natural frequencies of all flywheels tested have been measured. To date, none have exhibited behaviors in spin tests attributable to this phenomena.

Another continuing investigation attempts to measure the accoustical attenuation through the composite thickness at various stages throughout a fatigue test. The correlation of attenuation with cycles should be indicative of internal damage. The correlation with flywheel GEB was not statistically significant. This supports, weakly, the contention that the failure in that test was not initiated in the composite.

Containment aspects of the two disk type flywheels evaluated this year are quite different. Both rotors use a circumferentally wound graphite rim; and in both designs, first failure occurs in the rim. But, in the GE flywheel, the alpha-ply disk will typically remain intact; since it does not rely upon the rim for support. The opposite is true in the OCL type flywheels, since the disk requires the rim for radial restraint and without the rim it fractures immediately in the fashion shown in Fig. 6.

The remainder of the year's activity will involve the balancing and testing of flywheels fabricated by General Electric and Garrett-AiResearch for ultimate energy storage and fatigue life. Also, studies of flywheel temperature and drag resulting from casing pressure will be pursued. Studies designed to measure strain in the rotor at speed are expected to begin in September.

REFERENCES

1. R. S. Steele, Jr., E. F. Babelay, Jr., "Data Analysis Techniques Used at the Oak Ridge Y-12 Plant Flywheel Evaluation Laboratory," 1980 Flywheel Symposium, October 1980, CONF-801022.

2. R. P. Nimmer, "The Alpha-Ply Laminated-Disk Flywheel Rotor," Proceedings of Mechanical, and Underground Energy Storage 1980 Annual Contractors' Review, CONF-81128, Washington, D.C.

3. J. F. Kay, "Low-Cost Compression Molded Fiber Reinforced Flywheels," Proceedings of Mechanical, and Underground Energy Storage 1980 Annual Contractors' Review, CONF-81128, Washington, D.C.

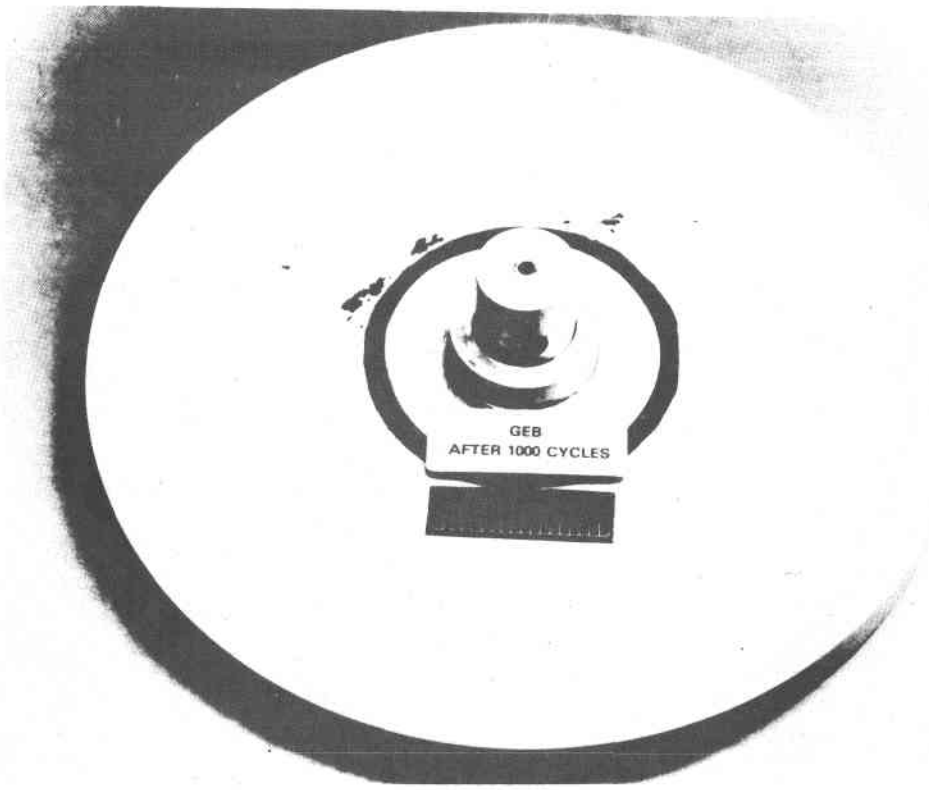

Fig. 1. The General Electric flywheel evaluated at ORFEL. Top and OD surfaces have been painted white.

Fig. 2. Flywheel debris of GEB.

Fig. 3. Flywheel GEC shown after balancing.

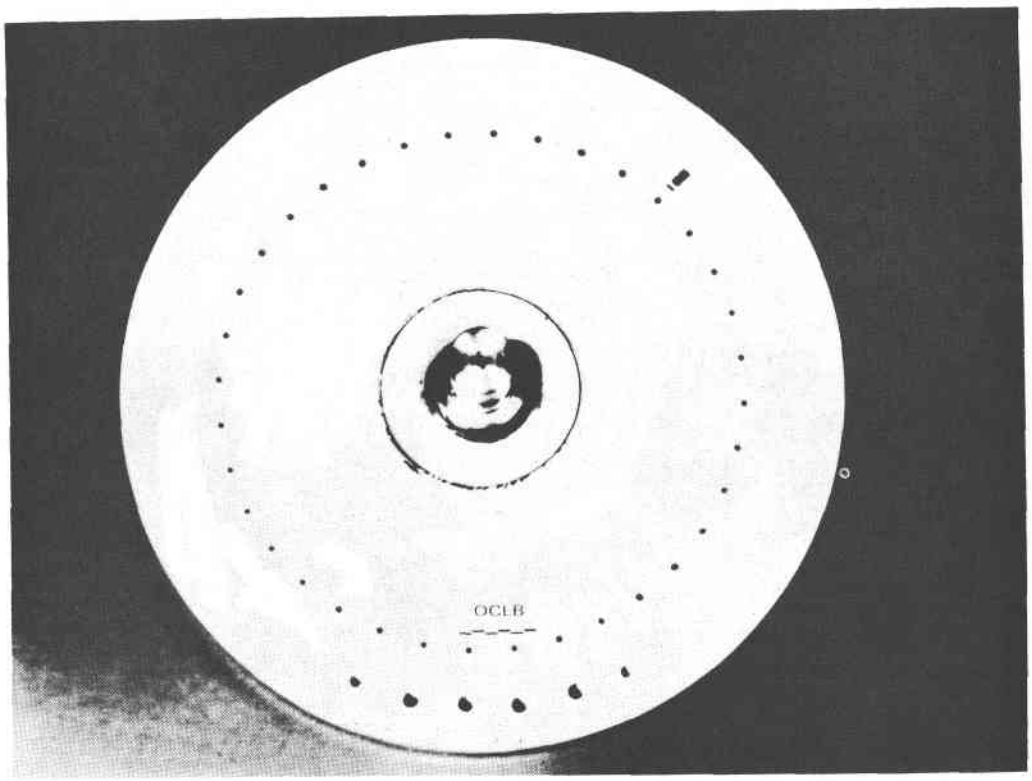

Fig. 4. Flywheel fabricated by Owens-Corning Fiberglass and Lord Kinematic Corporation. Top and OD surfaces have been painted white.

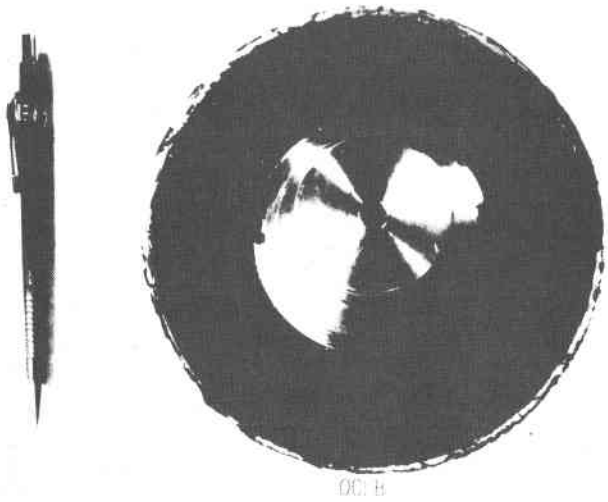

Fig. 5. Arbor of flywheel OCLB shown after removing flange.

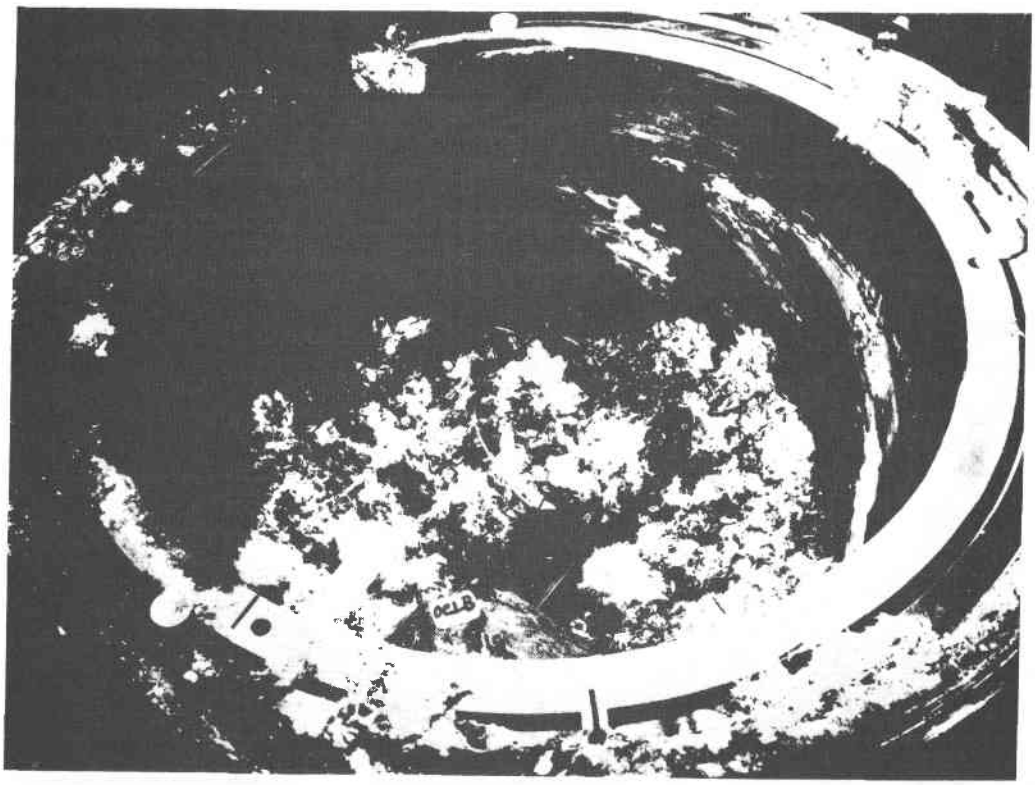

Fig. 6. Debris of flywheel OCLB.

REGENERATIVE BRAKING THROUGH ELASTOMERIC ENERGY STORAGE

L. O. Hoppie, J. H. McNinch, and G. C. Nowell
Eaton Corporation
26201 Northwestern Highway
P. O. Box 766
Southfield, MI 48037

INTRODUCTION

At the previous STOR meeting, it was reported (1) that a full-size elastomeric energy storage unit showed a round-trip energy transfer efficiency of 96 percent, a fatigue life of 170,000 cycles, and an energy density of about 1 J/cm^3. When the energy density of a second unit was increased to 2.5 J/cm^3 by increasing the axial pre-load, the efficiency remained high (95 percent), but the fatigue life fell to about 1,000 cycles. A project aimed at retaining high efficiency and fatigue life at the higher energy density was subsequently proposed and is described in this paper.

Also referenced last year were efforts aimed at devising a compact method of mechanical attachment. The work aimed at evaluating the preferred method in full-size units is also described in this paper.

ELASTOMERIC MATERIALS RESEARCH

Several suppliers of elastomeric material have attempted to achieve an energy density higher than that of the previous preferred material, i.e., a natural rubber compound formulated by the Hygenic Corporation. The most promising results are shown in Figure 1, where the stress-strain curve to failure of a sample of the Hygenic Corporation compound is compared with that of a new compound formulated by the General Tire and Rubber Company. Other data for these samples show that the hysteresis loss is nearly the same, and that the fatigue lives can be expected to be comparable. Consequently, full-size units fabricated with the GT and R compound will be evaluated during this project.

FABRICATION RESEARCH

Figure 2(a) shows an end view of a full-size unit after fatigue failure. The rings which can be seen correspond to the growth (from one cycle to the next) of a crack as it propagates across the cross-section of the unit. The origin of the failure can be traced to the origin of the rings, and as shown in Figure 2(b), the origin was at a surface flaw introduced during the molding of the unit.

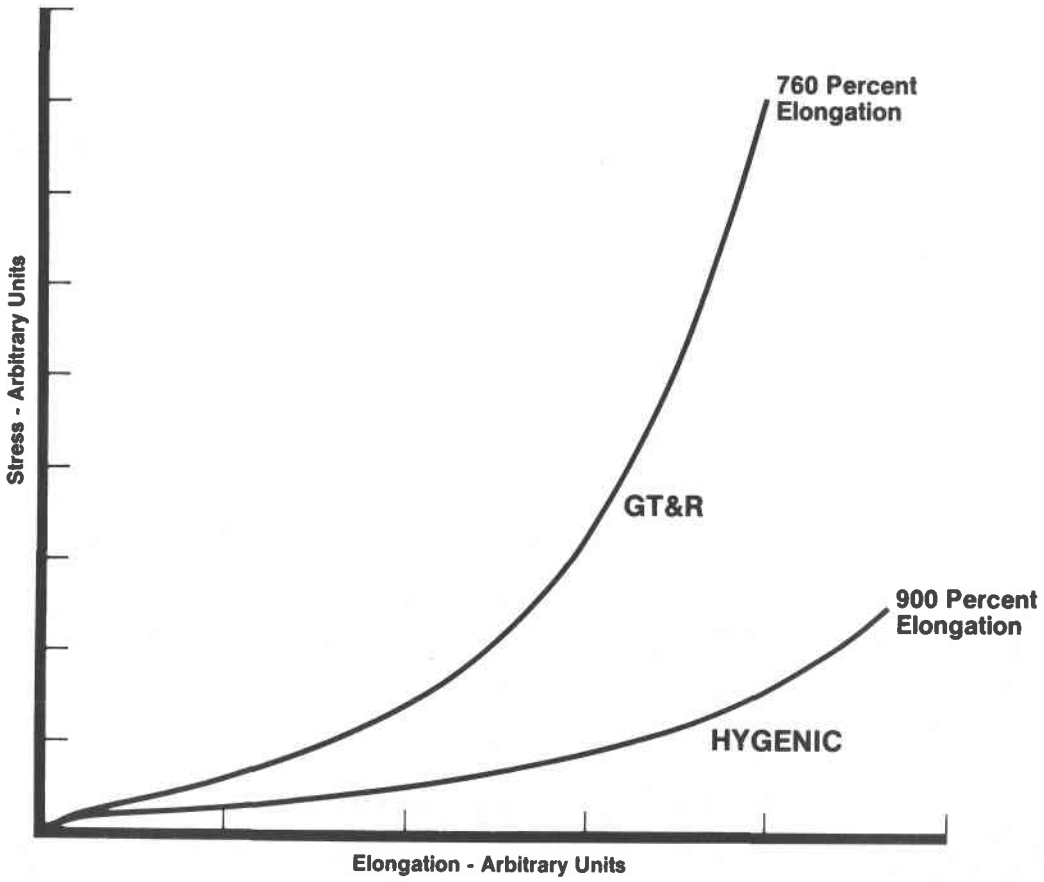

Figure 1 Stress vs Elongation to Failure for Two Natural Rubber Compounds

It is felt that surface flaws can be eliminated if a compression mold having neither parting lines nor air vents is employed. Consequently, such a mold for full-size units will be built by GT and R, and units fabricated in this mold will be evaluated.

MECHANICAL ATTACHMENT

In the torsionally induced tension scheme of stressing elastomers, an elastomeric rod is first elongated to typically 400 percent of its original length, and consequently, the diameter is reduced by 50 percent. If flat circular plates are initially bonded onto the rod, the space requirements of the ends are larger than desired since the plates will not shrink as the unit is stretched.

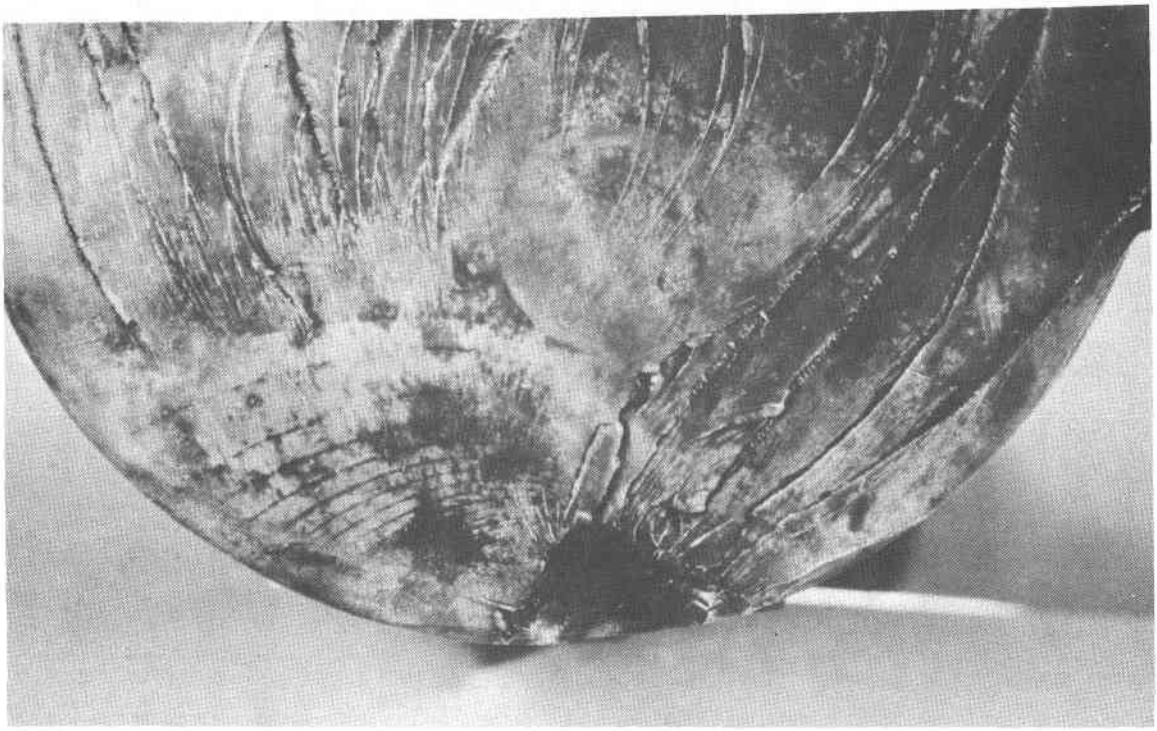

(a) End View of Origin of Failure

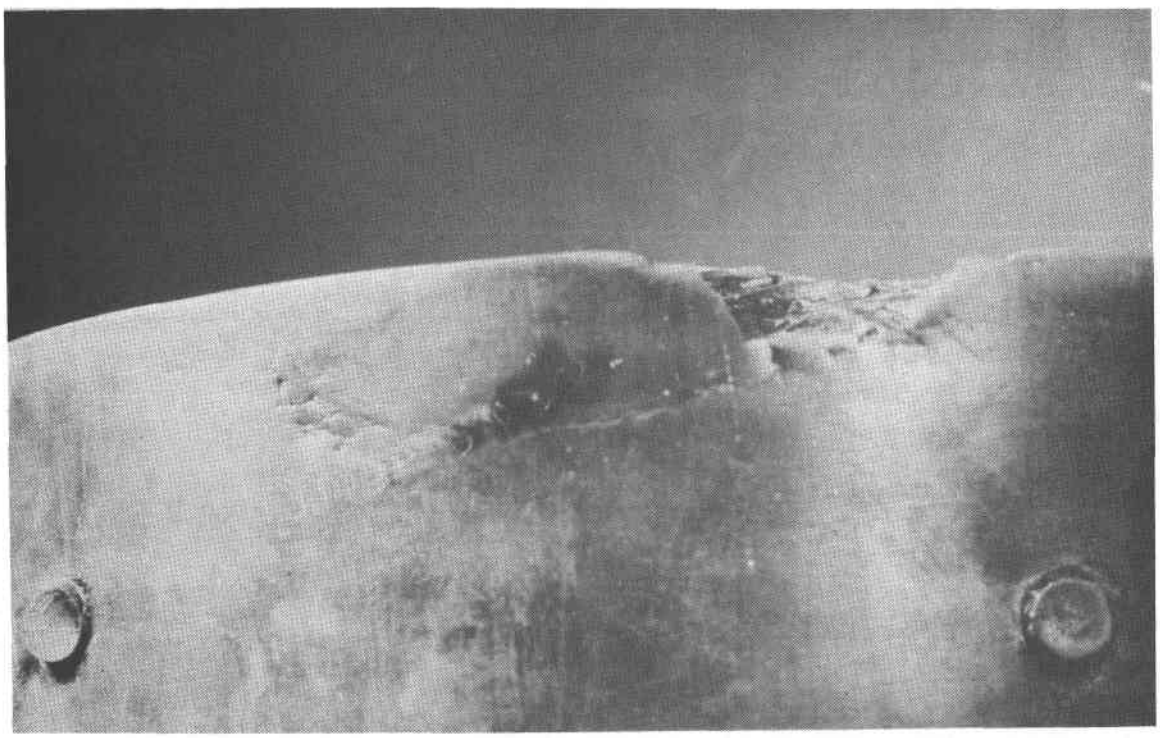

(b) Side View of Origin of Failure

Figure 2 Views of Full-Size Unit After Failure

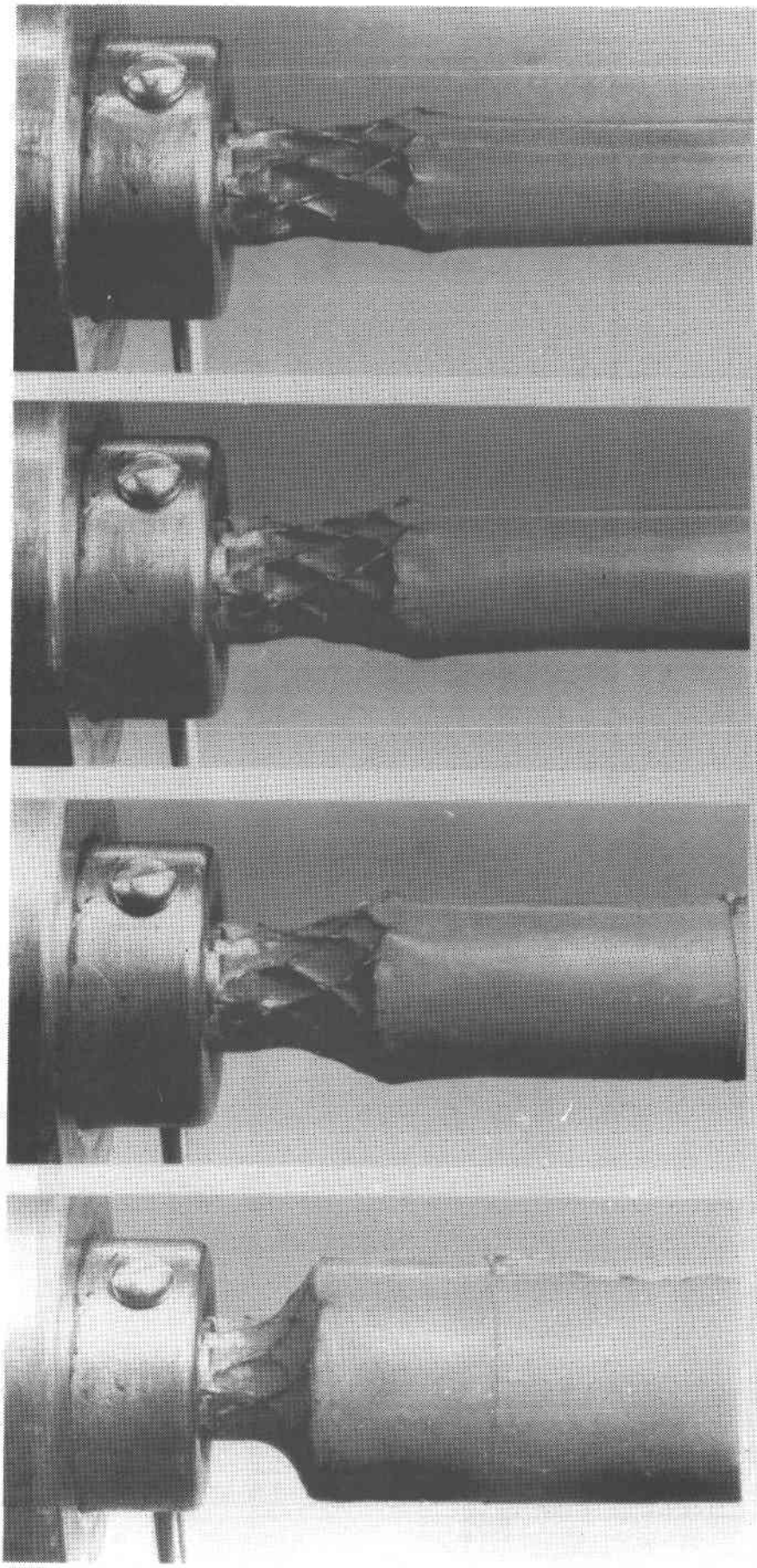

Figure 3 Attachment Scheme Incorporating Wire Braid Reinforcement at Various Axial Elongations.

Several concepts for minimizing the space requirement of the attachments have been considered, and small-scale samples of some of these concepts have been fabricated and evaluated. The most promising scheme consists of a custom transition region profile reinforced with wire braid. As shown in Figure 3, this concept does provide the desired result, namely, the diameter of the mechanical attachment itself is not larger than that of the elastomeric rod after the rod is elongated. Such attachments will be incorporated into full-size units for subsequent test and evaluation during this project.

REFERENCES

1. L. O. Hoppie and G. C. Nowell, "Regenerative Braking Through Elastomeric Engery Storage Systems," Conf-810833, pp.256-265.

ELECTRIC HYBRID VEHICLE SIMULATION

Dan C. Pasma
Eaton Corporation
Engineering & Research Center
26201 Northwestern Highway
P. O. Box 766
Southfield, MI 48037

ABSTRACT

The simulation of electric hybrid vehicles is to be performed using experimental data to model propulsion system components. The performance of an existing ac propulsion system will be used as the baseline for comparative purposes. Hybrid components to be evaluated include electrically and mechanically driven flywheels, and an elastomeric regenerative braking system.

INTRODUCTION

Conceptualizations of electric hybrid vehicles using secondary energy sources to load level the batteries for improvements in range and performance have been proposed by industry and government. Computer simulations and prototype development of such hybrid components have been performed with varying results. A quantitative comparison of independently developed system simulations and prototypes is difficult since detailed assumptions of component models is often unknown, control schemes vary, and evaluations are made using different or unrealistic driving cycles.

This program effort is directed toward the comparison of various electric hybrid vehicle propulsion schemes. Each is to be evaluated on the same driving cycle, and using experimentally obtained data to model drive system components to ensure the accuracy of the analysis as it applies to near term hybrid vehicles incorporating currently available components.

DISCUSSION

The program plan outlines six electric hybrid vehicle configurations to be evaluated as listed below:

1. Baseline electrical vehicle.

2. Electric vehicle (EV) with an electrically-controlled flywheel (Electric CVT).

3. EV with a mechanical non-recirculating continuously variable transmission (CVT).

4. EV with an electric CVT where the flywheel is used for regenerative braking only.

5. EV with a mechanical CVT where the flywheel is used for regenerative braking only.

6. EV with an elastomeric regenerative braking system.

The current plan calls for the use of the HEAVY computer program as the basis for the vehicle system simulations.(1)

The HEAVY program uses a modular, building block approach for the simulation of electric hybrid vehicles. Standard modules (e.g., battery model, induction machine model, etc.) are available within the program which can be connected together in various schemes to evaluate hybrid vehicle configurations. As long as library models of the components of interest exist, the simulations require no mathematical development or computer programming. In this program effort, those components in the HEAVY program that can accommodate the available experimental data will be used as is. Other components will be modified and developed as required.

The use of experimentally obtained data to model propulsion system components will ensure the accuracy of the overall system models. The use of the HEAVY program permits all simulations to be formed from the same basis. That is, components which are common to the varying schemes such as the electric propulsion system, clutches, and transmissions, are all modeled using the same respective modules.

The use of the HEAVY program also presents a unique opportunity for others interested in hybrid vehicle simulations. Simulations in the past have often involved the development of custom computer software to model the various systems. There being no mathematical standards for models of hybrid vehicle components, models have been developed which reflect the level of detail desired by the particular analyst. Outsiders, having further interest in published results of such work have no recourse to determine the detailed assumptions incorporated in the models, or to extend the work to include a particular area of interest of their own. Since the HEAVY program is generally accessible, interested parties may make additional modifications to particular vehicle components, or rerun a vehicle simulation over an alternative driving cycle, without having to develop a simulation capability of their own.

CURRENT PROGRAM STATUS

A block diagram of the electric vehicle propulsion system to be used as the basis for comparison is shown in Figure 1.

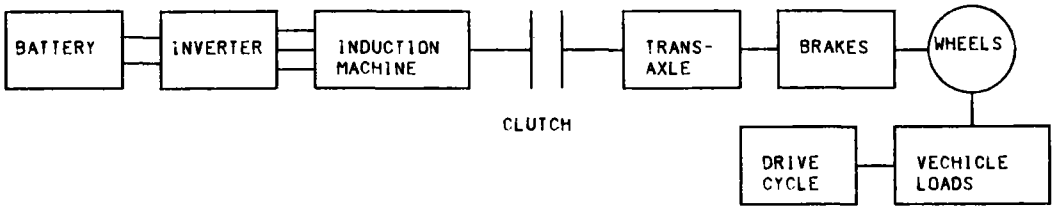

FIGURE 1
BASELINE ELECTRIC VEHICLE PROPULSION SYSTEM

Work has been initiated to modify and convert existing computer code developed at Eaton Corporation into the HEAVY program format. The components available within HEAVY are also being evaluated to ensure they can properly manage the experimental data which will be input. In addition to the components noted in the schematic of Figure 1, mechanically and electrically driven flywheels, CVT, and elastomeric regenerative braking system (ERBS) components are required, along with the control schemes required to direct power flow through the various components.

The following section gives a list of the required components with their current status and availability

Component	Status/Comments
Battery	Previous electric vehicle simulations have indicated the HEAVY battery model to be adequate and it will be used without modification (2).
Inverter and Induction Machine	A redevelopment of these HEAVY components is currently being considered. Experimental data from Phase II of reference 2 will be used provided it is available in time.
Mechanical Clutch	Conversion of a clutch model developed at Eaton into HEAVY format has been initiated (3).
CVT	Conversion of a CVT model developed at Eaton into HEAVY format has been initiated (3).

Transaxle	An Eaton transmission model will be converted into HEAVY format (3).
Flywheel	The flywheel simulations performed by the Aerospace Corporation are being reviewed. The best of the HEAVY, Aerospace, and Eaton models will be used (4).
Brakes	The HEAVY vehicle brake component will be used. A clutch/brake combination required for the ERBS will be developed.
ERBS	A HEAVY component for the elastomeric regenerative braking system has been developed (5).
Vehicle Loads	Standard HEAVY component.
Controllers	Various control schemes will be developed and evaluated to optimize the performance of the particular electric hybrid vehicle configuration under investigation.

FUTURE WORK

The development of the component models should be basically complete by the end of August, 1982. Development of vehicle system models will commence in September, 1982.

REFERENCES

1. R. A. Hammond and R. K. McGehee, "Final Report - Hybrid and Electric Advanced Vehicle Systems (HEAVY) Simulation," NASA CR-165536, November, 1981.

2. S. Geppert, ed., "AC Propulsion System for an Electric Vehicle: Phase I Final Report," DOE/NASA/0125-1, August, 1981.

3. I. Kalns, "Heat Engine/Flywheel Vehicle Drive Design Results and Analysis, Phase I," Proceedings of the Mechanical, Magnetic and Underground Energy Storage 1981 Annual Contractors' Review, August, 1981.

4. L. Forrest and L. H. Kubo, "Assessment of Flywheel System Benefits in Selected Vehicle Applications," Proceedings of the Mechanical, Magnetic and Underground Energy Storage 1981 Annual Contractors' Review, August, 1981.

5. L. O. Hoppie and G. C. Nowell, "Regenerative Braking Through Elastomeric Energy Storage," Proceedings of the Mechanical, Magnetic and Underground Energy Storage 1981 Annual Contractors' Review, August, 1981.

THE SERI SOLAR ENERGY STORAGE PROGRAM IN FY 1982

Werner Luft
Solar Energy Research Institute
1617 Cole Boulevard
Golden, Colorado 80401

ABSTRACT

The SERI solar energy storage program in FY 1982 is summarized against the background of earlier years and the broader program of the DOE Division of Energy Storage Technology. The program provides research, systems analyses, and assessments of thermal and thermochemical storage and transport, primarily in support of the DOE joint development plan for thermal energy storage for solar thermal applications (TESSTA). Current activities include recommendations for the development of promising storage concepts for specified solar thermal power and process heat systems, in-house and subcontracted explorations of advanced concepts, and assessments of long distance solar thermal energy transport concepts.

INTRODUCTION

Within the thermal energy storage program of the DOE Division of Energy Storage Technology, certain laboratories are assigned lead responsibilities in identified application areas. The SERI assignment is to conduct systems analyses, assessments, and research in thermal and thermochemical storage and transport for solar thermal power and process heat applications. Its primary objectives are improved understanding of storage and transport technologies for solar thermal systems, selection and recommendation of promising technologies for specified systems, and exploration of advanced concepts.

In pursuit of these objectives the main emphasis in FY 1982 continues to be support of the joint plan of the DOE Division of Solar Thermal Energy Systems and the Division of Energy Storage Technology for developing thermal energy storage for solar thermal applications (the TESSTA program, described in Ref. 1). Relatively minor efforts continue on long distance thermal energy transport, low-temperature direct-contact heat exchange, and subcontracted work on photochemical hydrogen production.

Activities this year are discussed briefly in the following narrative under four general headings, with broad program background where appropriate. Several areas of activity and subcontracted investigations are presented in more detail by others at this meeting.

TESSTA PROGRAM DECISION POINT SUPPORT

In FY 1982 SERI completed systems analyses that have been conducted since FY 1979 in support of the TESSTA program focused development phases. The analyses were intended to identify for development thermal storage concepts that show promise of meeting the program cost goals and of being significantly more cost effective than first generation concepts defined in the program. This overview summarizes the FY 1982

activities, which are reported more fully by R. Copeland at this meeting, in the overall context of the completed effort.

Originally, SERI was to have provided guidance for decision points on the development of storage concepts for specified solar thermal systems with five different types of central receivers: water/steam, organic fluid, gas cooled, liquid metal, molten draw salt; and for focally mounted receivers on parabolic dishes. Preliminary analysis of the molten draw salt central receiver system showed that the first generation storage concept (molten salt in two tanks) would meet the cost goals, therefore further analysis of draw salt receiver systems was assigned a low priority and later cancelled for budgetary reasons. Budgetary constraints also dictated cancellation of planned analyses of storage for focally mounted receivers. For the remaining four systems, Stearns-Roger Corp. was subcontracted to integrate the design of first generation (as reference) and selected alternative storage concepts, and to estimate storage cost and performance on a consistent basis. SERI then analyzed Stearns-Roger's findings and ranked the storage concepts on the basis of delivered energy cost and cost/value comparisons. Conclusions for water/steam, organic fluid, and gas (air) cooled receiver systems were summarized at this meeting last year [2]. Systems analyses of the liquid metal (sodium) receiver system were completed this year and are reported at this meeting by R. Copeland.

Table 1 lists the essential findings in FY 1982 along with those previously reported, characterizing the solar thermal systems to which they apply and the corresponding first generation reference storage concepts. Significantly improved storage for the solar thermal systems considered appears possible only with water/steam and liquid sodium receivers, and only with relatively long-duration storage in the case of power systems. Suitability of the underground pressurized water alternative is limited to regions with favorable geology.

Table 1. Analysis Results

	Receiver Fluid					
	Water/Steam		Organic Fluid		Gas (Air)	Liquid Sodium
Use:	Power	Process Steam	Total Energy	Process Steam	Power	Power
Cycle	Rankine		Rankine		Brayton	Rankine
Capacity (MW electric)	100		400		150	100
Use temperature (°C)[a]	510	288	382	172	816	538
First-Generation Storage Concepts:						
• Oil/rock thermocline	X[b]	X		X		
• Molten draw salt, 2-tank	X[c]					
• Sylltherm/taconite trickle			X			
• Air/alumina brick					X	
• Liquid sodium, 2-tank						X
Promising Second-Generation Storage Concepts:						
• Underground pressurized water	X[b,e]	X[f]				
• Latent heat tube intensive	X[b,e]	X[e]				
• Latent heat direct contact	X[d,e]					
• Molten draw salt, 2-tank						X[e]
• Air/rock						X[e]

[a]Maximum temperature of end use medium; the storage and transport fluid temperatures are higher.

[b]To vaporize the water working fluid.

[c]To superheat the generated steam.

[d]To evaporate (by phase change) and superheat (by sensible heat) using the latent heat storage medium.

[e]Superior only for storage durations in excess of approximately six hours.

[f]Superior only for storage durations in excess of approximately three hours.

EXPLORATION OF ADVANCED STORAGE CONCEPTS

SERI also has a continuing charter under the TESSTA program to explore advanced storage concepts that are not necessarily tied to the solar thermal systems identified in the focused development program phases of the program plan. This is being pursued through in-house analyses and experiments and by subcontracted investigations. Current activities in this area are listed in Table 2 and briefly discussed below.

The work at the University of Washington, subcontracted in FY 1981 and reported by A. Bruckner at this meeting, investigates the feasibility of the storage and stored heat delivery elements of a very high temperature molten glass (slag) central receiver system. Emphasis of the investigation has shifted from a 100-MWe to a 10-MWe system because of uncertainties in the structural design of large storage vessels for molten slag.

Systems analyses at SERI show that high temperature molten salts such as sodium hydroxide are potentially attractive both as receiver coolants and as storage media, but at high temperatures they may require direct heat exchange and new kinds of storage tank insulation and thermocline maintenance [3]. These analyses, and small-scale experiments with water using a raft for thermocline maintenance, are reported at this meeting by R. Copeland.

The subcontracted investigations at the Institute of Gas Technology (IGT) began in FY 1981 with the objective of exploring the feasibility for solar applications of a concept using phase-change salts contained within a ceramic matrix and using direct contact heat exchange with a gas. A related investigation by IGT of the same concept applied to other high temperature processes was subcontracted in FY 1981 by the Oak Ridge

Table 2. Exploration of Advanced Storage Concepts

Concept	Storage Temp. (°C)	Heat Exchange	Applications	Investigating Organization	Activities
Slag, latent heat	To 1450	Direct solid/liquid-gas	Closed cycle Brayton power	Univ. of Wash.	Heat exchange experiments
High temperature molten salt	To 1100	Direct liquid-air	Combined cycle power	SERI	Analysis and experiments
High temperature molten salt	To 800	Indirect	Thermochemical hydrogen production	SERI	Analysis
Salt and ceramic	To 800	Direct solid/liquid-gas	Various	IGT	Materials testing
Molten draw salt to air/rocks	To 550	Direct liquid-air	High solar thermal capacity factor process heat	SERI	Analysis [5] and heat exchange experiment
Salt to metal	385	Direct liquid-solid/liquid and indirect tube and shell	Rankine power	Grumman	Subscale system experiments with mixed chlorides and Pb-Bi
Salt hydrate latent heat	115	Direct liquid-solid/liquid and indirect tube and shell	Absorption cooling with parabolic troughs	SERI	Analysis of double effect system with magnesium chloride hydrate and oil [7]
Salt hydrate latent heat	60	Direct liquid-solid/liquid and indirect tube and shell	Space heating	SERI	Analysis and experiments with salt hydrate and oil [6]

National Laboratory (ORNL). The two subcontracted activities, jointly reported by T. Claar at this meeting, are being consolidated, and any subsequent work on this concept will be sponsored only by ORNL.

As indicated previously, there is relatively little incentive to explore improved diurnal storage technologies for solar thermal systems with molten draw salt receivers since storage of the molten salt in two tanks has been shown to be quite cost effective. However, systems analyses at SERI suggest that supplementary air/rock storage with direct heat exchange between molten salt and air may be justified in process heat applications that call for long storage durations. Results to date of these analyses are reported at this meeting by R. Copeland.

A molten salt test loop is being assembled because of the potential attractiveness of direct-contact molten-salt-to-air heat exchange and the scarcity of validated performance data in operating regimes of interest. Design point experiments are scheduled for completion by the end of FY 1982. The experimental program is described at this meeting by J. Wright.

Direct-contact heat exchange between latent heat (solid-liquid phase change) storage materials and immiscible liquids avoids the heat transfer degradation caused by tube surface encrustation, thereby offering opportunities for cost reduction. This general approach is being explored in three separate activities. The subcontracted experiments by the Grumman Aerospace Corporation continue work originally supported by the NASA Lewis Research Center and are reported at this meeting by J. Alario. The Grumman work is also intended to validate the latent-heat direct-contact storage concept identified in Table 1. Analysis at SERI of a lower temperature application, using oil and a salt hydrate in a double-effect solar-powered absorption chiller, is reported at this meeting by R. Copeland. The final phases of an analytical and experimental program at SERI on the basic mechanisms of oil-salt hydrate interactions are reported by J. Wright.

THERMOCHEMICAL ENERGY STORAGE AND TRANSPORT (TEST)

Since FY 1980 SERI has been exploring possibilities of storing and transporting solar heat through the use of reversible chemical reactions rather than in sensible or latent heat. The main incentives for doing so are increased energy storage density and the ability to store and transport thermal energy at near-ambient temperatures. However, analyses at SERI have tended to confirm the conclusion by other investigators that thermochemical storage is not cost effective for solar thermal power systems of the types defined in the TESSTA program focused development plan. Accordingly, recent emphasis has been on solar process heat applications that combine storage and thermal energy transport.

In FY 1982 a feasibility study of thermochemical energy storage and transport for a large heat utility was completed and the preliminary report underwent peer review. A study of thermochemical transport in a smaller distributed dish collector system for process heat was also completed this year. Laboratory work has been deemphasized, with experiments performed only as needed to resolve uncertainties in the systems analyses. Work has also continued on a general technical review of thermochemical reactions, new system definitions and screening criteria, and a search for more cost-effective applications that may merit future scrutiny. These and other thermochemical energy storage and transport activities are reported at this meeting by G. Nix.

OTHER ACTIVITIES

In addition to the studies of thermochemical heat transport, SERI has been examining new approaches to long distance heat transport by steam and hot water. One such approach is to use internal rather than external pipe insulation to protect the pressure wall from corrosion and high temperatures thereby permitting the use of less expensive materials and fewer expansion bends. In FY 1981 Eureka Laboratories was subcontracted to examine the technical and economic feasibility of this approach. The work was completed this year and the results are reported at this meeting by S. Leung.

Subcontracted work completed in FY 1982 also includes an experimental investigation of catalyst synthesis at Rensselaer Polytechnic Institute for photochemical generation of hydrogen from water. The objective was to develop new organometallic complexes (bipyridyl derivatives) obtained by organic synthesis. The work is reported at this meeting by K. Potts.

REFERENCES

1. "Thermal Energy Storage Technology Development for Solar Thermal Power Systems: Multiyear Program Plan," Draft, U.S. Department of Energy, Div. of Energy Storage Technology, Washington, D.C., 13 March 1979.

2. "Proceeding of the Sixth Annual Thermal and Chemical Storage Contractors' Review Meeting," DOE report CONF-810940, Feb. 1982.

3. R. J. Copeland et al. High Temperature Molten Salt Thermal Systems, presented at the 17th Intersociety Energy Conversion Engineering Conference, Los Angeles, 8-12 August 1982.

4. R. J. Copeland, F. W. Leach, and C. Stern, High Temperature Molten Salt Solar Thermal Systems, presented at the 17th Intersociety Energy Conversion Engineering Conference, Los Angeles, 8-12 August 1982.

5. J. Wright and C. d'Agincourt, Direct-Contact Air/Molten Salt Heat Exchange for Solar Thermal Systems, presented at the 17th Intersociety Energy Conversion Engineering Conference, Los Angeles, 8-12 August 1982.

6. J. Wright, M. Bohn, and R. Barlow, Oil/Salt Hydrate Direct-Contact Heat Exchange Experiments, SERI/TR-252-1614, Golden, CO: Solar Energy Research Institute, June 1982.

7. J. R. Parsons and R. J. Copeland, Use of Parabolic Trough Collectors for Residential/Light Commercial Solar Cooling Systems, presented at the 17th Intersociety Energy Conversion Engineering Conference, Los Angeles, 8-12 August 1982.

ANALYSES OF THERMAL STORAGE SYSTEMS

Dr. R.J. Copeland
Solar Energy Research Institute
Golden, Colorado

ABSTRACT

During FY 1982, thermal storage systems were analyzed for solar thermal applications. Promising thermal storage concepts were identified for a liquid metal receiver in an electric power application. We assessed both an advanced, high-temperature (1100°C maximum) molten salt system and a double-effect solar cooling system. Both systems with associated thermal storage were promising. Currently, we are assessing a long duration storage system with a molten nitrate salt central receiver.

INTRODUCTION

Thermal storage systems are being analyzed to identify promising thermal storage concepts for further development. The criteria to be met in this process are

- The attainable cost must be less than or equal to program cost goals.
- The concept must be more cost-effective than alternative thermal storage technologies.

The program cost goals are being established to assure a marketplace for each developed technology. To develop cost goals, certain elements of potential marketplaces must be defined: the size of each market, the locations, user economic criteria, and alternative energy systems. From this knowledge, the cost of the most attractive alternative energy system is employed as a measure of what the user will pay for a new energy system--that is, the system's value. The value of thermal storage is that part of the system value which is due to storage or which can be allocated to storage. The program cost goals for thermal storage are established based on the value of thermal storage.

The second criterion requires a direct comparison of the various thermal storage concepts. This analysis must be conducted with a similar cost data base and for a specified application. Furthermore, to assure a fair comparison each technology must perform the same mission. The storage concepts are not required to have the same efficiency, but there must be a way of accounting for differences. A ranking methodology for conducting the comparisons has been developed by SERI (1), and SERI is using that methodology to analyze the thermal storage concepts.

In FY 1982 this effort focused on thermal storage for solar thermal applications. Cost and performance trade-off analyses were conducted for thermal storage in a liquid metal receiver. Two advanced technology studies were completed, and an assessment of long duration storage for a molten nitrate salt receiver is being conducted.

THERMAL STORAGE FOR LIQUID METAL SOLAR THERMAL RECEIVERS

During FY 1981, a study was initiated to evaluate thermal storage in liquid metal solar thermal receivers. Stearns-Roger Services, Inc., (under subcontract to SERI) evaluated the cost and performance of several thermal storage concepts. On 6 August 1981, a review/workshop was held to present the results of this effort. Nine concepts were defined and costed for this review. Several concepts were selected for continued evaluation at 1, 6, and 15 h of thermal storage capacity.

The final data were presented at a review/workshop held 11 November 1981. Comments from the reviewers, including those comments of developers of the thermal storage concepts, were integrated into Stearns-Roger's final report (2); descriptions of each concept are also presented in that report.

SERI analyzed the impact of each concept on the whole solar thermal system. Both concept cost, operation and maintenance (O&M), and efficiency are included in the analysis. Figure 1 presents the data as the ratio of the solar thermal plant busbar energy cost (BBEC) of one of the alternative thermal storage concepts to the BBEC of the reference thermal storage concept (sodium two-tank). The collector area and cost are included, and the optimum collector area for each storage capacity is employed in the analysis. Air/rock and draw salt (two versions of each) are the most promising thermal storage concepts.

SERI determined the sensitivity of these results to the various uncertainties in the analyses, including costing methodology, O&M uncertainty, storage use scenario for varying locations and user load profiles, and relative cost uncertainty. The first three did not have significant effects. Relative cost uncertainty had the largest effect. For example, at 6 h of storage capacity, the uncertainties are larger than the cost differences in the concepts.

Figure 2 presents the effect of the cost uncertainty at 15 h of storage. Since the concepts are still being researched these costs may or may not be accurate. The relative cost uncertainty was estimated at ±20% (note the absolute uncertainty is much higher). The data in Fig. 2 indicates that air/rock thermal storage is clearly the most cost-effective concept. The only overlap is in the lower cost estimate for draw salt and the higher cost estimates for air/rock. There is little doubt that air/rock storage offers a substantial improvement over other types of thermal storage.

ADVANCED THERMAL STORAGE

Very High-Temperature Molten Salt Storage for a Central Receiver

Solar thermal applications include fuel and chemical production, process heat, and electric power. These users sometimes require heat up to 1100°C (2000°F). Currently, molten nitrate salt storage receivers are among the most attractive solar thermal central receivers (3) but are temperature limited to 566°C (1050°F). This study investigated the use of carbonates, chlorides, and sodium hydroxide for a molten salt receiver and storage for a high-temperature application--thermochemically generated hydrogen.

Reference 5 presents the results of the analysis. Substantial cost reductions are present for thermal storage costs less than $\$20/kWh_t$. Costs for molten sodium hydroxide thermal storage were estimated as less than $\$5/kWh_t$. Due to this high potential, SERI initiated research in advanced, high-temperature molten salt storage. This work is described in another paper to be presented at this meeting (4) and in another recent paper (5).

Thermal Storage for an Absorption Air Conditioning Cycle

Parabolic troughs and some other high-temperature solar collectors should become cost-competitive with flat-plate collectors in the next decade. In this study, the potential for using these collectors as residential/light commercial solar cooling devices was considered. The absorption cycle, the desiccant cycle, and the heat-engine-driven vapor compression cycle were studied. Coefficients of performance (COP) over 1.0 are possible with all three types of cycles driven by parabolic troughs. A double-effect absorption machine was chosen to represent these advanced concept devices, and a seasonal performance comparison was made with a flat-plate-driven absorption cycle.

Seasonal performance was estimated for both a single-effect absorption cycle with a flat-plate collector and the double-effect absorption cycle with a parabolic-trough collector. Both winter heating and cooling loads for a typical residential building were included. Nashville, Tenn., and Fort Worth, Tex., were selected as typical sites with significant cooling loads. At both sites the collector area was smaller with the double-effect system, but essential equivalent annual performance was obtained.

Table 1 presents a comparison of the double-effect cycle system with a parabolic trough to a single-effect cooler with a flat-plate collector. (The temperature required by double-effect chillers is too great for a flat-plate collector.) The cost estimates are for a 1990 system application and are given in 1980$. Reductions from current collector prices are anticipated for both flat plates and parabolic troughs, and projections of the attainable installed cost for both are employed. Although flat plates are less expensive than troughs per unit area, the smaller

TABLE 1
COMPARISON OF DOUBLE-EFFECT CYCLE SYSTEM PARAMETERS

Item	Flat-Plate	Trough	Comments
Collector area (m^2)	32	20.5	Fort Worth, Tex.
$/$m^2$	99	129	
Cost ($)	3168	2645	
Absorption cycle (3 t)($)	3360	4032	SAI cost data for single effect, double effect, assumed at 40% increase over single-effect machine.
Thermal storage	Assumed equal		
Backup energy (natural gas) ($)	3200	1356	Levelized for 1990s and capitalized; assumed as one-half total load
TOTAL ($)	9728+	8033+	Biggest gain is reduced backup and collector area

area required gives a lower collector cost. The double-effect absorption unit requires an additional condenser and heat exchanger, but the evaporator, absorber, regenerative heat exchanger, and generator are the same size. A 40% cost increase was estimated for the double-effect chiller compared to a single-effect system. Backup fuel costs were estimated assuming natural gas. Because natural gas can provide 200°C heat to the generator, and thus can effectively employ the double effect, there is a substantial reduction in the back-up energy requirement. Thermal storage costs were not estimated, but were assumed to be equal for flat-plate and parabolic-trough systems. The data indicates a good potential for the double-effect absorption cycle. [A more detailed analysis is presented in a recent paper (6).] Additional study to evaluate latent heat and sensible heat storage for this system was recommended and was planned. That study was not conducted due to lack of funding.

WORK IN PROGRESS

1400°C Thermal Storage

A thermal storage concept was identified that provides energy storage for solar thermal industrial process heat applications that require up to 1400°C (2550°F). A preliminary assessment indicates that potential costs are less than the value. Research will be initiated when FY 1983 funds are available.

Long Duration Thermal Storage with a Molten Nitrate Salt Receiver

Long duration thermal storage (40 to 100 h) can increase fuel savings with a solar thermal collector. An industrial process heat application providing 68 atm (1000 psi) saturated steam is being studied. A molten nitrate salt receiver with both molten nitrate salt storage (for diurnal use) and air/rock (for long duration) comprise the system. The potential economic merits of this system will be assessed.

REFERENCES

1. R. J. Copeland, "Preliminary Requirements for Thermal Storage Subsystems in Solar Thermal Applications," SERI/RR-731-364, April 1980.

2. L. J. Dubberly et al., "Cost and Performance of Thermal Storage Concepts in Solar Thermal Systems, Phase 2: Liquid Metal Receiver," Stearns-Roger Services, Inc., Denver, Colo. SERI/TR-XP-9001-1-B, Dec 1981.

3. K. W. Battleson, P. DeLaquil, J. D. Fish, H. F. Norris, Jr., J. J. Iannucci, "1980 Solar Central Receiver Technology Evaluation," SAND 80-8235, 1980.

4. Robert J. Copeland, "Advanced, High-Temperature Molten Salt Storage," presented at the Energy Storage Contractors' Review Meeting, Washington, D.C., 23-26 Aug 1982.

5. Robert J. Copeland, James W. Leach, Curtis Stern, "High-Temperature Molten Salt Solar Thermal Systems," presented at the 17th Intersociety Energy Conversion Engineering Conference, Westin Bonaventure, Los Angeles, Calif., 8-12 Aug 1982.

6. Robert J. Copeland, J. Roger Parsons, "Use of Parabolic Trough Collectors for Residential/Light Commercial Solar Cooling Systems," presented at the 17th Intersociety Energy Conversion Engineering Conference, Westin Bonaventure, Los Angeles, Calif., 8-12 Aug 1982.

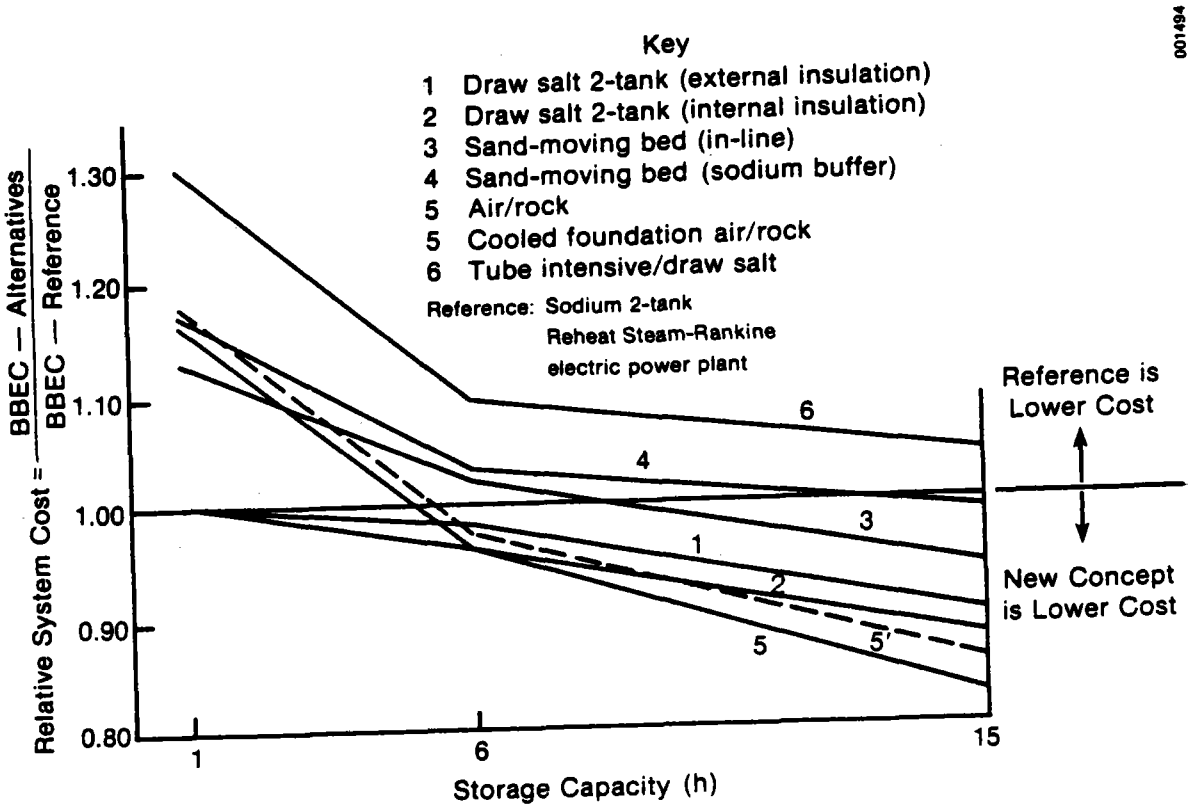

FIGURE 1
RELATIVE SYSTEM COSTS OF LIQUID METAL RECEIVERS

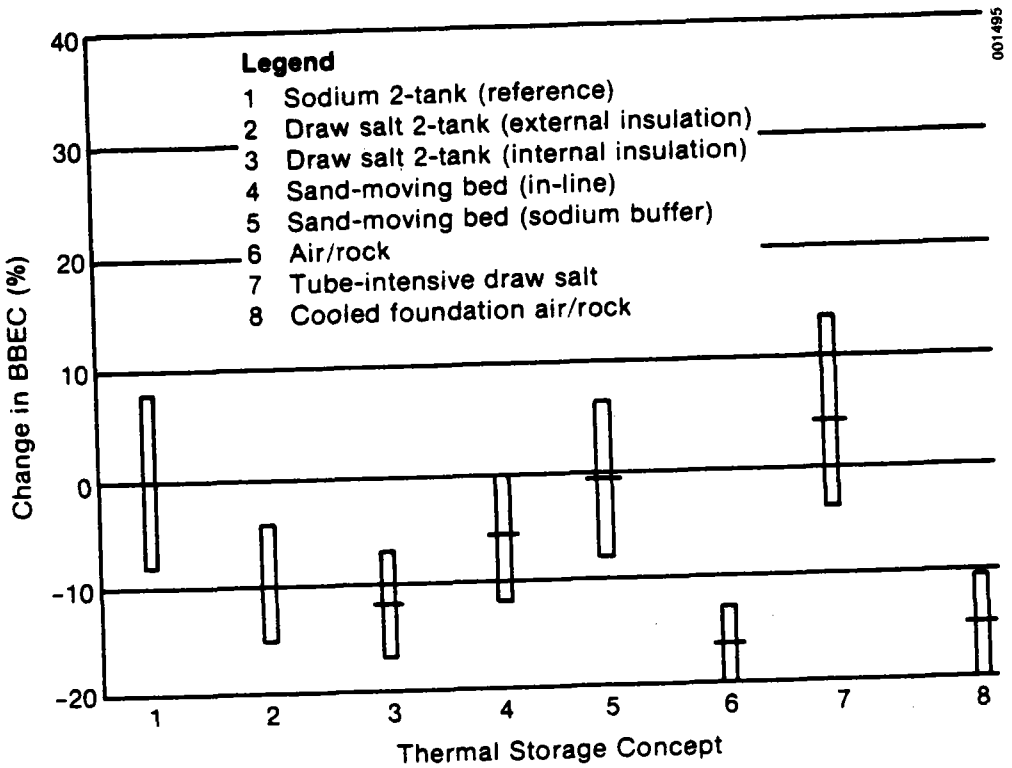

FIGURE 2
COST UNCERTAINTY RESULTS OF LIQUID METAL RECEIVERS (±20%)

ADVANCED, HIGH-TEMPERATURE MOLTEN SALT STORAGE

Robert J. Copeland
Solar Energy Research Institute
Golden, Colorado

ABSTRACT

Advanced molten salts (hydroxides, carbonates, and chlorides) are being researched for solar thermal applications. These salts may be used in both the receiver working fluid and in thermal energy storage. Potential applications include electric power production, fuel and chemical production, and high-temperature process heat. Molten salts can store sensible heat at temperatures up to 1100°C in a thermocline system with a unique insulating platform (raft) that floats between the hot and cold molten salts.

This paper describes overall solar thermal and thermal storage systems, and also assesses the economic potential of the systems. In current research, we are testing the performance of insulating raft thermocline and studying materials compatibility.

INTRODUCTION

During systems analysis at the Solar Energy Research Institute (SERI) (1), researchers found that high-temperature, molten salt storage had a high potential for solar thermal applications. The initial assessment was conducted in a solar thermal plant producing hydrogen via a sulfur cycle thermochemical process. The key technical issues in an advanced high-temperature molten salt storage system are feasibility of raft thermocline; materials compatibility, including insulation and structure; wetted internal insulation; heat exchange; piping; and pumps. A research program is underway to resolve these key issues. In the first phase, the feasibility of a raft thermocline and materials compatibility are being researched. The results of the work in progress as well as the evaluation of the electric power application are discussed in this paper.

ELECTRIC POWER GENERATION

Figure 1 presents an advanced, high-temperature, molten salt system for generating electric power. An advanced, molten salt receiver collects solar thermal energy at temperatures as high as 1100°C. Thermal energy is stored in an internally insulated tank with a thermocline in the molten salt. An insulating platform (raft) reduces radiative heat transfer from the hot to the cold salt. A combined cycle (Brayton/Steam-Rankine) generates the electric power. Heat is transferred to pressurized air in a direct-contact heat exchanger.

Receiver

Computations were made to evaluate improvement in collector efficiency made possible by two design modifications proposed by SERI. The first modification employs a secondary reflector adjacent to the receiver cavity. In the second proposed modification the transport fluid would flow as a film over the walls of the receiver cavity and be heated directly by radiation. The vapor pressures of several salts are low enough that the vapor could be contained within the receiver cavity with minimal losses. Computations were made to determine how the receiver efficiency is improved by direct radiative heating of the transport fluid. Reference 2 presents results from two types of direct film heating receivers.

Thermal Storage

Figure 2 is a schematic of a conceptual tank design for storage at 1100°C. The concept uses the salt itself as insulation. Although the conductivity of the salt is low, a rigid internal structure is needed to prevent natural convection. Calculations based on correlations from Refs. 3 and 4 indicate that an enclosure size of approximately 0.63 cm (0.25 in.) is required. Therefore, costs for stainless steel honeycomb with cell dimensions of approximately this size were assumed when computing the tank costs.

The liquid level in Fig. 2 must be maintained at a near constant level to prevent 1100°C salt from flowing into the honeycomb and contacting the carbon steel structure. Therefore, a thermocline tank design is most appropriate. The radiation exchange between the hot and cold layers of the thermocline can be significant, so the raft (shown in the figure) is included to reduce heat transfer in the vertical direction.

Several salts have been identified that can be used as the thermal storage media and also as the receiver working fluid. Sodium hydroxide (NaOH), carbonates, and chlorides are all inexpensive and stable up to 1100°C. The costs of all three media are about the same, although NaOH is the cheapest. All three media are less than molten nitrate salt storage. Table 1 presents the estimated capital investment required for storage as two temperatures.

ECONOMIC ASSESSMENT

Researchers also compared high-temperature molten salt storage to other central receiver power generation systems. Figure 3 presents the results. The data for all but the high-temperature molten salt system were received from Sandia (6). The same costing data base was employed for the high-temperature molten salt system and other systems. Although these results are obviously preliminary, the advanced molten salt system shows a high potential.

TABLE 1
CAPITAL INVESTMENT FOR NaOH STORAGE SUBSYSTEM

Temperature Limits (°C)	Storage Configuration	Materials Cost (at 3360 MWh)		Capital Investment [a,b] ($/kWh)
		Tank Materials (10^6)	Media (10^6)	
350-1100	Thermocline	2.24	4.07	4.74
600-1100	Thermocline	3.75	5.82	7.29

SOURCE: Reference 5.

[a] CI = 1.95 (1.8 x Tank Materials + Media).

[b] By comparison the same capacity of thermal energy stored in molten nitrate salts costs $14.63/kWh (at 600°C max).

WORK IN PROGRESS

Raft Experiments

The raft in the thermal storage tank must follow the interface of the hot and cold fluids at all states of charge and discharge. Such a device has not previously been demonstrated in practice. Stability is the fundamental problem in the raft, and two mechanisms are present which could make it unstable: hydrodynamic forces and manufacturing tolerances.

Experiments are being conducted to evaluate these effects. Water was used as the medium for the first experiments to minimize cost. Later in the program, a molten salt raft will be tested. The water-only thermocline apparatus has been designed and is being assembled. A static verification of the raft density control was performed. The first experimental raft was floated between 40°C hot water and 25°C cold water. Dynamic testing has not been performed to date.

Materials Compatibility

Structural and insulating materials must be compatible with molten salts. Currently literature reviews, equilibrium calculations, and vendor contacts are being performed. Three mechanisms can cause incompatibility: chemical reactions, corrosion, and solution. The rate at which these influences can occur has a strong influence on the compatibility. Due to the need for a long life and minimal replacement costs, very low rates are required.

Available literature indicates that the carbonate salts are the most benign, then NaOH, and finally chlorides are the most corrosive. Materials containing SiO_2 are incompatible with all of the salts. Some metallic and ceramic materials can be used in both high- and low-temperature applications. Some of these materials have been identified; preliminary results are presented in Table 2. Additional work is underway to test compatible materials. Some experiments will be necessary to investigate materials and salts where there is no data.

TABLE 2.
MATERIALS POTENTIALLY COMPATIBLE WITH MOLTEN SALTS

Material	High Temperature ≈1000°C			Low Temperature ≈370°C		
	NaOH	CO_3=	Cl-	NaOH	CO_3=	Cl-
Stainless steel	X	X	ND	C	C	C
Carbon steel	X	X	X	C	X	X
Nickel	C	C	ND	C	C	C
Al_2O_3	ND	C	ND	ND	C	ND
MgO	ND	C	ND	ND	C	ND
Bison fireclay	ND	C (to 1200°C)	ND	ND	C	ND
Varnon BF	ND	C (to 1200°C)	ND	ND	C	ND
SiC	ND	ND	ND	ND	ND	ND

X - Not compatible
C - Compatible
ND - No data

CO_3 = : Na,Li,K Carbonate
Cl- = : Mg,Na,K Chloride

REFERENCES

1. R. J. Copeland, "Systems Analysis of Thermal Storage," to be presented at the Energy Storage Contractors' Review Meeting, Washington, D.C., 23-26 Aug 1982.

2. R. J. Copeland; J. W. Leach; J. Ullman; "Ground-Mounted Thermal Storage of the Parabolic Dish Solar Collector/Stirling Engine System," Proceedings of 16th Intersociety Energy Conversion Engineering Conference, Atlanta, Ga., Aug 1981.

3. "Conceptual Design of Advanced Central Receiver Power Systems," Report No. DOE/ET/20314, Denver, Colo., Martin Marietta Corp., Sept 1980.

4. M. Jacob, Heat Transfer, Vol. 1, New York: John Wiley & Sons, Inc., 1949.

5. Dubberly, L. J., et al., "Cost and Performance of Thermal Storage Concepts in Solar Thermal Systems, Final Report." Contract XP-0-9001-1a. Denver, Colo., Stearns-Roger Services, Inc., Nov 1981.

6. Battleson, K. W., et al., "1980 Solar Central Receiver Technology Evaluation," SAND/80-8235, May 1980.

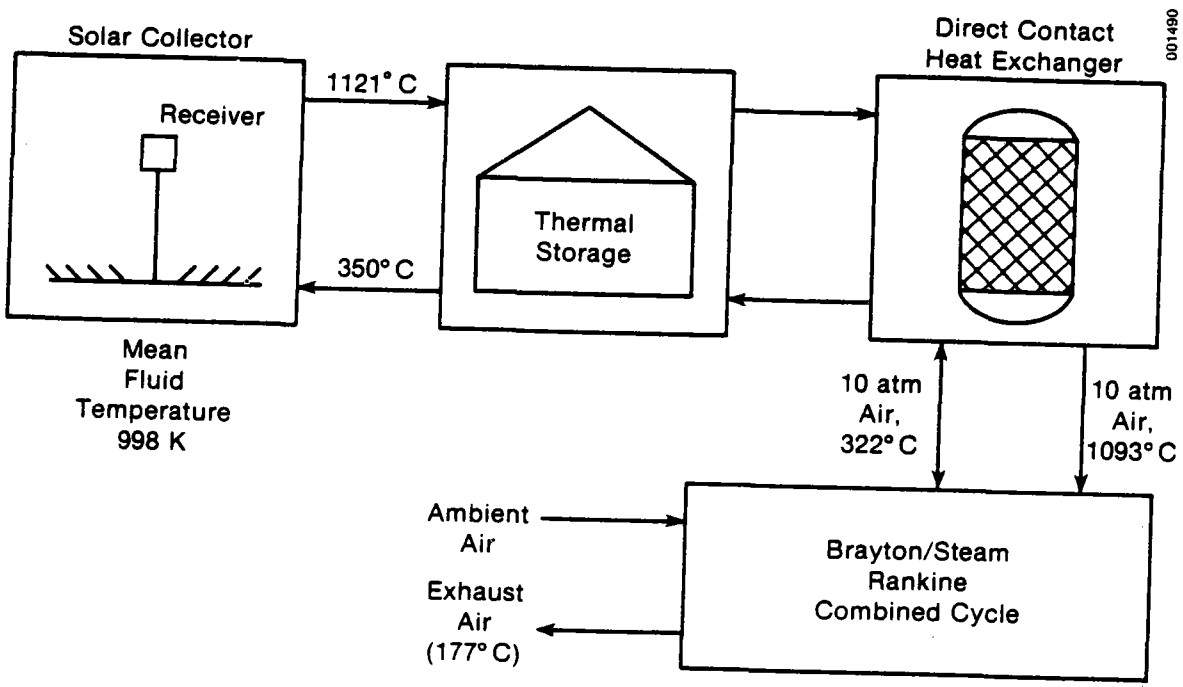

Figure 1
Electric Power Generation System with High-Temperature Molten NaOH

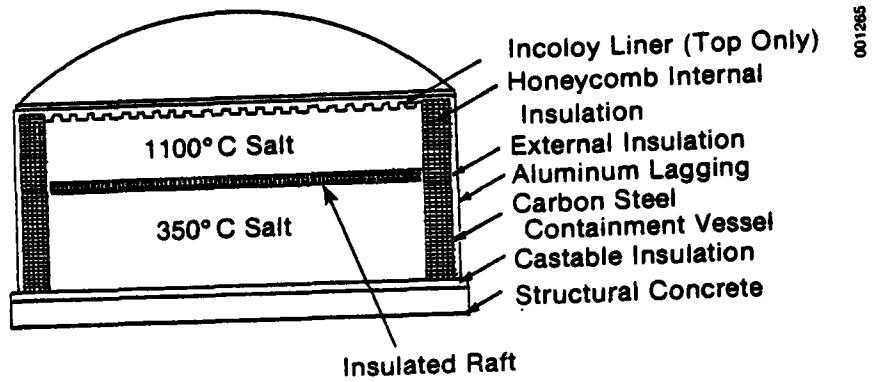

Figure 2
1100°C Tank Design

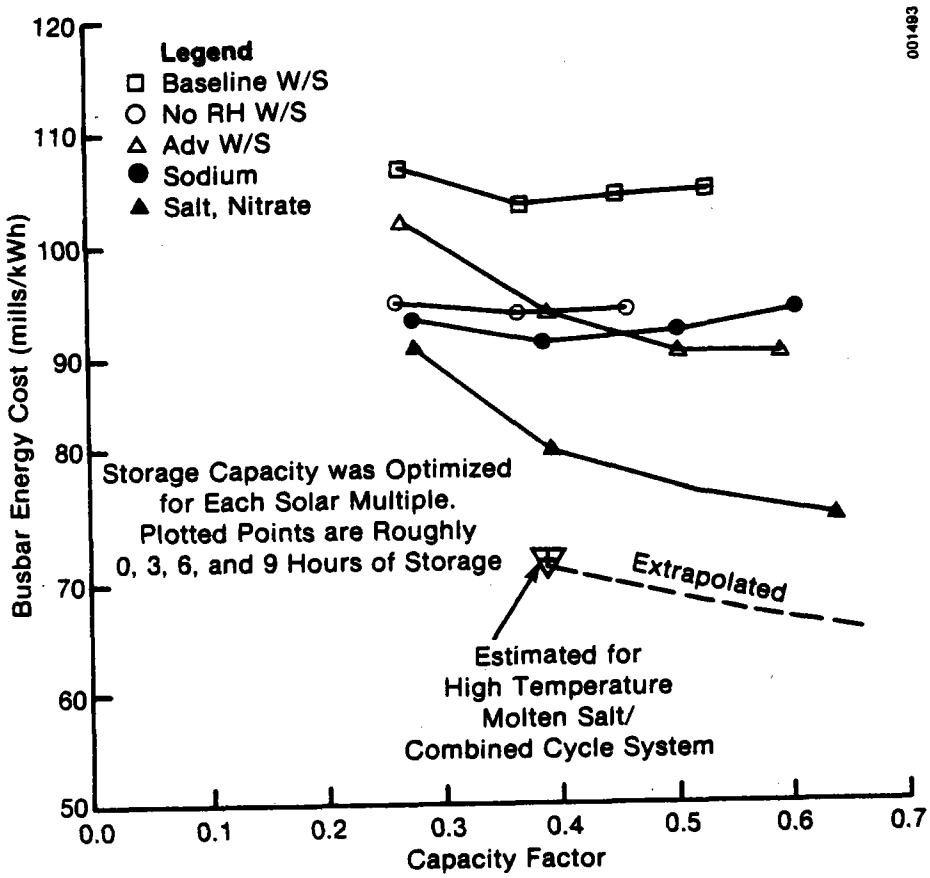

Figure 3
Solar Central Receiver Busbar Electricity Cost as a Function of Capacity Factor

THERMOCHEMICAL ENERGY STORAGE AND TRANSPORT

R. Gerald Nix
Solar Energy Research Institute
1617 Cole Boulevard, Golden, CO 80401

ABSTRACT

This paper describes feasibility studies performed by SERI of thermochemical energy storage and transport (TEST). Cases studied include a large central receiver heat utility and a small industrial process heat application with distributed parabolic dish solar collectors. TEST does not appear to be generally cost-effective; however, there are special cases of cost-effectiveness. The overall recommendation is that research on thermochemical processes should emphasize the manufacture of renewable fuels using solar energy and the search for more cost-effective TEST systems.

INTRODUCTION

This paper describes feasibility studies of thermochemical energy storage and transport (TEST). TEST involves the capture of thermal energy as near-ambient-temperature, chemical bond energy through use of a reversible chemical reaction. The chemicals are not consumed, merely acting as energy carriers in this cyclic process. The primary motivation for studying TEST is the potential for efficient long-term energy storage and efficient long-distance energy transport because both are possible at near-ambient temperatures. This study is to determine the technical and economic feasibility of TEST and make recommendations for future thermochemical energy research. This paper describes the results of studies for a large-scale heat utility (Case A) and a small-scale industrial process heat application (Case B).

CASE A: LARGE-SCALE HEAT UTILITY

System Definition. A large-scale heat utility (Fig. 1) was studied. From the single central receiver heat source, 10 equally sized heat users each receive 26.2 MW_t (89.5×10^6 Btu/h) as 4.14 MPa (600 psig), 400°C (750°F) superheated steam. The energy transport and storage system is thermally decoupled from the solar energy collection system through use of a working fluid system which contains an independent diurnal storage system. The source and users are connected by pipelines, and the users are grouped together in an industrial park. Each user is sold the product steam since the utility owns all equipment. The analysis is structured so that the storage capacity and the transport distance can be varied.

The objective met by TEST can also be met through use of sensible thermal energy storage and transport. Therefore, for comparison, a molten draw salt system (60% $NaNO_3$, 40% KNO_3) was studied with storage provided by multiple insulated tanks as proposed by Martin-Marietta (1). Another standard for comparison is steam generated by fossil-fuel-fired boilers at a central site and transported to the individual users.

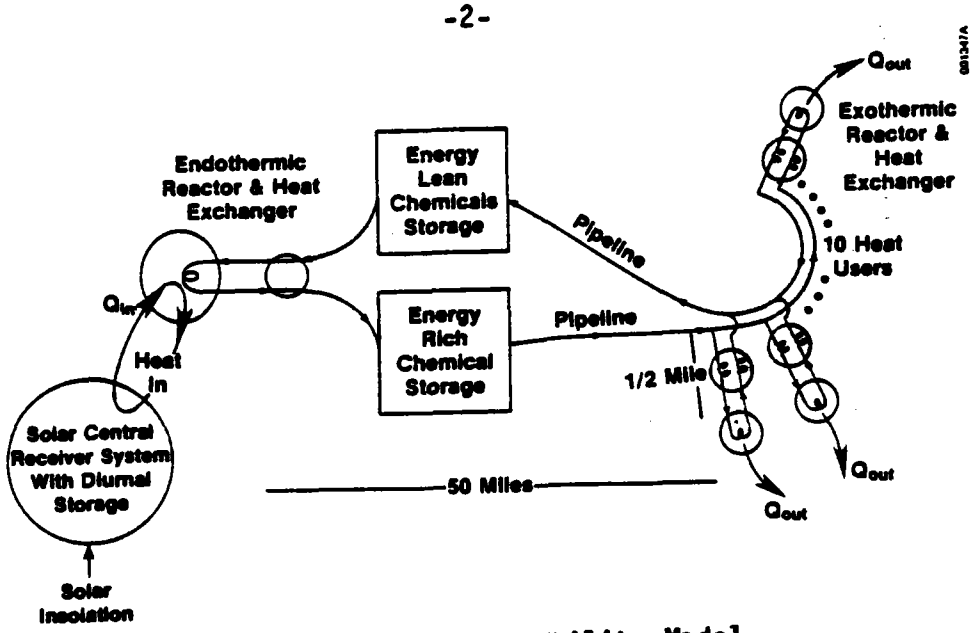

Figure 1. Heat Utility Model

Economic Model. The economic model described in the EPRI "Technical Assessment Guide" (2) is appropriate for a heat utility. The levelized revenue requirement is the appropriate criterion because alternatives can be compared by single numbers that characterize the cost of each alternative.

Calculations were based on a 30-yr life from 1990 to 2020, with tax credits, a 0.65 capacity factor for energy transmission without long-duration storage, and a 0.90 capacity factor for systems with long-duration storage. The fuel prices listed in Ref. 3 are used.

Process Definition. The reactions appearing most promising for near-term application and chosen for the feasibility study are

$$\text{heat} + CH_4 + H_2O = CO + 3H_2,$$
$$\text{heat} + CH_4 + CO_2 = 2CO + 2H_2,$$
$$\text{heat} + Ca(OH)_2 = CaO + H_2O,$$
$$\text{heat} + 2NH_3 = N_2 + 3H_2, \text{ and}$$
$$\text{heat} + 2SO_3 = 2SO_2 + O_2.$$

Results. The SO_3 system does not appear to be feasible for this application.

Figures 2 and 3 present some of the results. Details are listed in a report by Nix and Bergeron (3). A recent report by Sandia (4) indicates a base solar energy of $6.63/GJ ($7/MBtu) is possible.

Conclusions. The major conclusions for a large-scale heat utility are as follows:

- The draw salt system has the greatest economic potential for 100-350 h storage capacity.

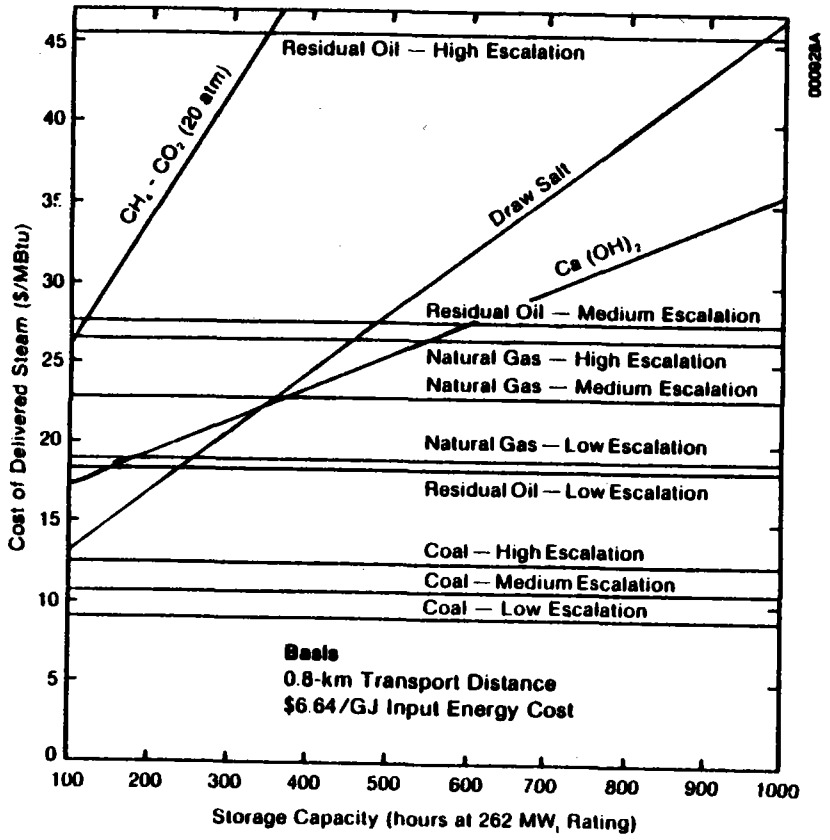

Figure 2. Effect of Storage Capacity on Delivered Energy Cost

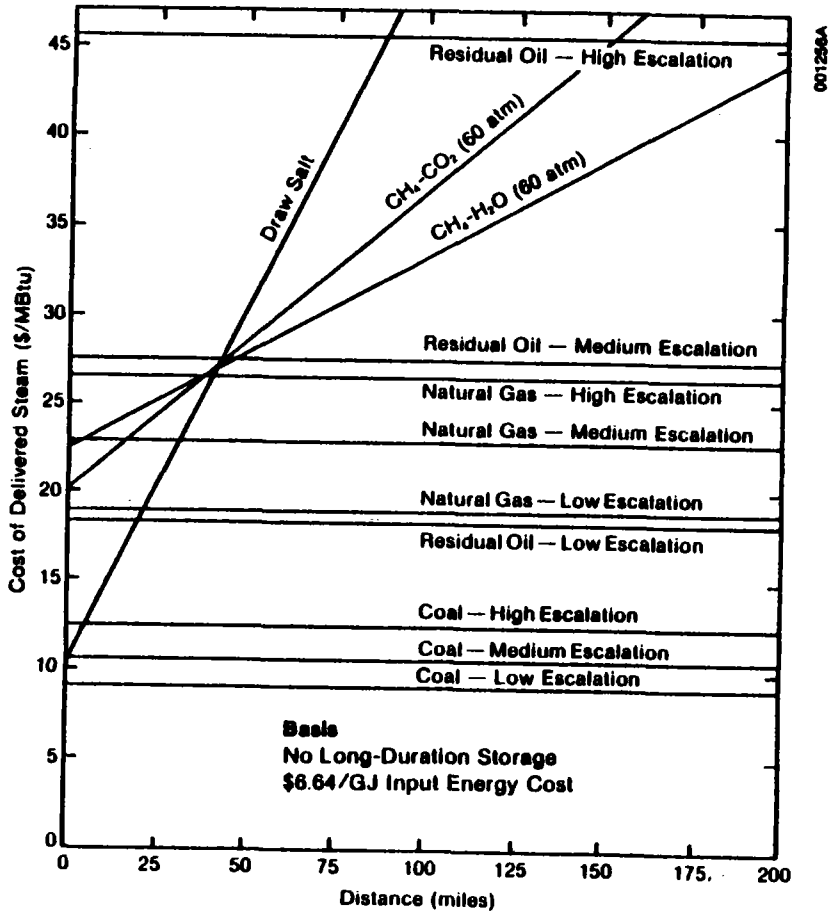

Figure 3. Effect of Transport Distance on Delivered Energy Cost

- The $Ca(OH)_2$ energy storage system has the most economic potential for >350 h of storage capacity.
- Central receiver thermal systems with $Ca(OH)_2$ long-duration storage subsystems can compete with oil or natural gas-fired boilers.
- The CO_2-CH_4 long-duration energy storage system does not appear cost-effective.
- No central receiver thermal system with the long-duration storage subsystems studied is competitive with coal-fired boilers.
- Transport of sensible energy by molten draw salt appears more favorable than the CH_4 thermochemical energy transport systems for distances up to 65 to 80 km.
- Beyond 80 km, either CH_4 thermochemical energy transport system is more cost-effective than a molten draw salt system.
- For transport distances greater than 80 km, a solar thermal system with a CH_4 thermochemical energy transport subsystem is competitive only with oil-fired boilers at a high oil price escalation rate.

CASE B: SMALL-SCALE INDUSTRIAL PROCESS HEAT APPLICATION

System Definition. An industrial process heat system with parabolic dish solar collectors (Fig. 4) is to deliver 1 MW_t (3.41×10^6 Btu/h) as 4.14 MPa, 400°C superheated steam. A field of parabolic dishes, each 11 m in diameter, collects the solar energy. The study is not site specific. Both molten draw salt storage and nonstorage situations were considered. The dish field and the steam user are separated by 0.4 km (0.25 mile) with energy transport by either thermochemical reactions or sensible energy. The industrial user owns all of the equipment. Neither the transport distance (0.4 km) nor the amount of storage (0 or 24 h) varies in this study. Fossil fuel backup systems are not included since transport alternatives are compared at equal capacity factors. Standards of comparison are a solar thermal system with molten draw salt transport and storage, or a fossil-fuel-fired boiler to generate steam at the user site.

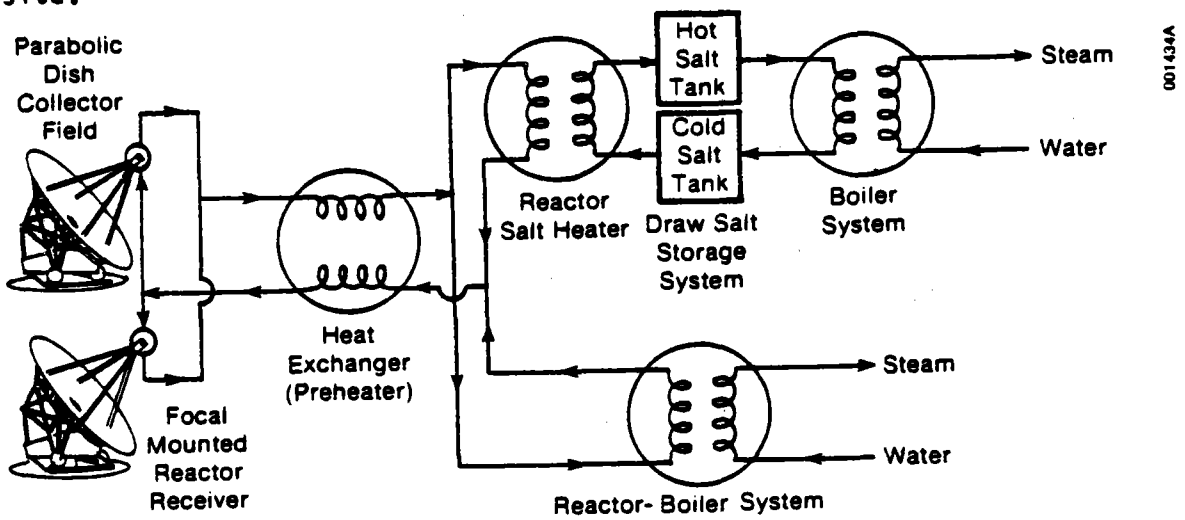

Figure 4. Distributed Dish IPH System: 24-Hour Storage

Economic Model. The economic model and parameters used for Case A are appropriate for Case B. The fixed charge rate is 0.25 and the levelizing factor is 1.886 to reflect the industrial financing situation.

Process Definition. The reactions chosen for thermochemical energy transport are

$$\text{heat} + CH_4 + CO_2 = 2CO + 2H_2 \quad \text{and}$$
$$\text{heat} + 2SO_3 = 2SO_2 + O_2.$$

Results. The dish IPH solar system can produce steam for \$74/GJ using molten salt transport, for \$78/GJ using CH_4 thermochemical transport, and for \$194/GJ using SO_3 thermochemical transport (no storage). Corresponding costs are \$34-\$41/GJ for natural gas boilers and \$33-\$59/GJ for residual oil boilers. Within the error bounds of this study, the draw salt and CH_4 thermochemical transport system costs are equal. When 24 h draw salt storage is included, draw salt transport results in a delivered energy cost of \$82/GJ, whereas the CH_4 thermochemical transport system results in \$133/GJ, and the SO_3 system costs are even higher. The costs of installed dishes and thermal receivers were taken from Ref. 5. The cost of the thermochemical receivers is the approximate cost of construction materials. Details and additional results are in Ref. 3.

Conclusions. The major conclusions are as follows:

- The CO_2-CH_4 system transports energy at a lower cost than the SO_3 system.
- The CH_4-CO_2 thermochemical system is not cost-effective relative to molten draw salt energy transport, particularly when storage is included.
- Natural gas- or oil-fired boilers will produce energy at a lower cost than the distributed dish system.

GENERAL DISCUSSION OF TEST

For both the large-scale heat utility and the small-scale IPH application, TEST has failed to show economic potential superior to sensible heat transport and storage in molten draw salt.

Why was TEST not particularly cost-effective? The primary reasons are the high investment for chemical reaction systems and the low efficiency of the thermochemical system. These factors are the result of both the choice and process definition for the thermochemical systems. It is difficult to envision any innovations sufficient to change the conclusions of this study.

Are there other thermochemical energy systems that might be cost-effective? Thermochemical energy studies should not yet be terminated. The ultimate application of thermochemical energy is manufacture of a renewable, synthetic fuel. Such renewable fuels are generated from combustion products by the absorption of energy from either solar or nuclear sources. In the hydrogen program, for example, combustion product H_2O is converted back to H_2 fuel. A process that has not been

sufficiently evaluated is generation of fuels via the analogous carbon dioxide reactions. Combustion product CO_2 is converted back to CO: heat + CO_2 → CO + 1/2 O_2. However, this direct reaction is not favored thermodynamically so it must be coupled with another reaction (e.g., an oxide cycle) to drive it. Once CO is obtained, it can be used to produce H_2. H_2 and CO can be reacted to produce liquid fuels. Thus, a high-energy liquid fuel can be produced using energy from a stationary source such as a central receiver solar system or a nuclear reactor and waste flue gas containing CO_2. Fuel generation via thermochemical reactions should be thoroughly investigated to define the economic potential and research opportunities.

More efficient, less costly TEST systems should be defined and researched. Specific efforts should be to find liquid systems in which the high energy density will result in lower investment and to make use of heat pumping to maximize efficiency and cost-effectiveness.

RECOMMENDATION

The recommendation is that the thermochemical energy portion of the SERI Energy Storage program should emphasize thermochemical fuel generation and the search for more cost-effective TEST systems. The program should be continued through FY 1983, and if justified, through FY 1984 to thoroughly define the potential of thermochemical energy systems.

REFERENCES

1. Martin-Marietta Corporation, "Conceptual Design of Advanced Central Receiver Power System," DOE/ET/20314-1/2, 1978.

2. Electric Power Research Institute, "Technical Assessment Guide," EPRI PS-1201-SR, 1979.

3. R. G. Nix and P. W. Bergeron, "Feasibility of Thermochemical Energy Storage and Transport," SERI/TR-234-1655, in press.

4. K. W. Battleson, "Solar Power Tower Design Article: Solar Thermal Central Receiver Power Systems--A Source of Electric and/or Process Heat," SAND 81-8005, 1981.

5. J. P. Thornton, Kenneth C. Brown, Joseph G. Finegold, James B. Gresham, F. Ann Herlevich, and Thomas A. Kriz, "Final Report: Comparative Ranking of 0.1-10 MW_e Solar Thermal Electric Power Systems," Vol. II: Supporting Data," SERI/TR-351-461, 1980.

DIRECT-CONTACT THERMAL STORAGE RESEARCH

John D. Wright, Mark S. Bohn
Solar Energy Research Institute
Golden, CO 80401

ABSTRACT

The objective of the direct-contact thermal storage research task is to reduce the heat-transfer-related costs of thermal energy storage systems by performing research on direct-contact heat transfer. Research is presently focused on direct contact between air and molten nitrate salts. These devices have cost advantages over conventional fin-tube indirect heat exchangers and would be used to couple short-term molten salt storage to longer term air/rock storage to obtain long duration storage. These devices would also be used in very high-temperature systems that employ molten carbonates or sodium hydroxide. An experimental loop is being constructed to develop and to test methods for predicting the performance of such devices, and to test new packing designs.

Work using direct-contact heat exchange on low-temperature latent heat storage in salt hydrates was concluded in FY 1982. Heat transfer was adequate, but some practical operating problems remained. The problem of oil distribution was resolved, but no solution was found for the problem of salt hydrate carryover. Because of the carryover problem, because latent heat storage in direct-contact salt hydrate systems offers only small reductions in storage volume, and because there is little potential for cost reduction compared to water storage, further research on such systems is not recommended.

HIGH-TEMPERATURE, LIQUID-TO-GAS, DIRECT-CONTACT HEAT EXCHANGE FOR THERMAL STORAGE

Direct-contact heat exchangers can provide potentially large cost reductions in solar thermal storage systems where one of the working fluids is a gas because these exchangers offer an inexpensive method of providing large heat-transfer areas made necessary by the poor heat-transfer properties of gases.

Air/rock storage systems have been identified as a promising high-capacity factor storage alternative for molten nitrate salt receivers. A large component of the cost is the heat exchanger needed to transfer energy to and from the air. The cost of these heat exchangers can be reduced by approximately 2/3 if they are replaced with packed columns in which air and molten salt are in direct contact (1,2).

A second possible use for such exchangers would be in very high-temperature (400°-1100°C) molten salt receiver/storage systems using molten NaOH and/or carbonate salts. Analyses have shown that these systems can produce electricity for 12% less than nitrate salt systems. At these

temperatures, the direct-contact exchangers would compete even more favorably with conventional heat exchangers because conventional exchangers need ceramic tubes, which are expensive and difficult to fabricate. The cost differences are so great that they have a direct bearing on the system practicality.

Several potential designs have been identified for air/salt direct-contact heat exchangers. The turbulent flow, packed tower design is frequently used in the chemical industry for mass transfer operations. A packed column is filled with a loose, open, random packing fabricated from either metal or ceramic, through which the salt trickles down. The packing slows the progress of the salt through the column. As the salt flows over the packing, a large and inexpensive heat-transfer area between the gas and salt is provided. Heat is transferred between the air and the packing not covered with flowing salt, as well as between the packing and the salt; thus, the packing acts as a fin. Additionally, direct-contact devices are advantageous because they are not subject to fouling.

Preliminary designs of direct-contact heat exchanger design may be obtained with existing correlations. A correlation by Eckert (3) provides an accurate method for determining the cross-sectional area of the column. A correlation by Fair (4) roughly estimates the volumetric heat-transfer coefficients within the column. However, the correlation is based on mass-transfer data obtained at room temperature. Heat-transfer predictions are obtained by using the mass-heat transfer analogies. At best, these analyses will predict only the direct contact contribution between the air and salt. The packing contribution, performing as a fin, is unmodeled because it does not have a mass-transfer analog. Therefore, this correlation will probably underpredict the volumetric heat-transfer coefficient.

While turbulent flow packed columns are widely used in the chemical industry, the capitalized pumping costs for the air stream are similar to the capital costs. Therefore, it may be desirable to use laminar flow devices. The salt would flow down the packing as a film, exchanging heat with the air both by direct contact and by conduction through the metal. Laminar flow is achieved by utilizing very small spacings in the packing. By forcing laminar flow, pressure drops per unit length are reduced by an order of magnitude. Also, because lower velocities are used, the columns become short and fat instead of tall and thin, which further reduces the pressure drop. Finally, air-side heat-transfer coefficients are inversely proportional to the plate spacing. Therefore, the rate-limiting resistance is reduced.

To provide a basis for equipment design, we need to determine heat-transfer coefficients and to develop a fundamental understanding of these coefficients for high-temperature, direct-contact heat exchange. Secondly, we need to identify and resolve operational problems. To accomplish this, a bench-scale, air/molten salt, direct-contact heat-exchange experiment is being constructed (Fig. 1).

Measurement of the air and salt inlet and outlet temperatures and flow rates will allow determination of the heat load, mean temperature difference, and therefore overall volumetric heat-transfer coefficient U_v as a function of the flow rates. These data will then be compared with values of U_v predicted from existing correlations for low-temperature packed columns. If the comparison is not favorable, new correlations will be derived for the air/molten salt system. Heat-transfer phenomena will be investigated to determine the source of discrepancies. A better understanding of the heat-transfer mechanisms will allow more accurate correlations.

LATENT HEAT, DIRECT-CONTACT STORAGE IN SALT HYDRATES

SERI conducted a research program on direct-contact heat exchange in FY 1980 and FY 1981 to better understand the operation of latent heat, salt hydrate storage systems. The salt hydrate storage medium (simply a salt-water solution when melted) is stored in a tank. To add thermal energy, hot oil is bubbled through the tank, transferring heat directly to the salt solution. After rising through the storage medium, the oil drops coalesce. The oil is then pumped to the heat source (collector) and recycled through the storage tank. To discharge the unit, drops of cold oil introduced at the bottom of the tank absorb heat as they rise through the salt solution. When they reach the top of the tank they coalesce; the oil is pumped to the load to deliver heat and is returned to storage. As heat is extracted, flakes of solid salt hydrate form, grow, and settle to the bottom of the tank.

Simulations of solar heating applications have shown that active latent heat storage in salt hydrates offers no performance advantages over sensible heat storage and that the volume savings realized are only 50% when compared to water storage (5). Although the user may be willing to pay a small premium for the space saved by latent heat storage the cost of latent heat storage must be generally no higher than the sensible heat alternative (6).

The two major problems are oil distribution in the salt hydrate, and salt hydrate carryover in the oil stream. Proper oil distribution is required to ensure flow regardless of the state of the salt (molten liquid, partially frozen solid, or completely frozen solid), adequate surface area available for efficient heat transfer, and prevention of salt phase segregation. Salt carryover must be minimized because salt carried with the oil can freeze on cold surfaces of the heat exchanger, and plug the flow or foul the heat exchanger.

Experimental work to address the key operating problems of fluid distribution and carryover was performed on a multidrop column. This column is essentially a pilot-scale, direct-contact storage system, which may be cycled at will through the charge and discharge cycles (Fig. 2).

Oil Distribution

Several different distributor configurations were tried to achieve reliable operation. The original distributors were perforated metal plates at the bottom of the column. Oil pumped through the holes would rise through the column. During cooling cycle operation, crystals form and grow in the bulk continuous phase. The crystals grow into flat flakes of approximately 1-2 mm. They then settle out and form a loosely packed layer on the bottom. Oil drops easily tunnel through the loosely packed bed. If cooling is continued until the salt hydrate is completely frozen, the unit may be turned off, left indefinitely, and started at will. However, if the salt is only partially frozen when flow is stopped, crystallization will continue as heat is lost. A layer of salt hydrate continues to grow at the boundary between the settled bed and the remaining molten salt hydrate. The salt layer built up during the no-flow condition consists of nearly solid, nonporous crystals.

If the solid layer grows to more than 1 or 2 in. thick, it may block or drastically reduce the flow rate through the column. Additionally, perforated plate distributors had problems with salt freezing in the perforations and blocking the flow.To avoid flow blockage, multistage distributors were utilized. The first design was the "Christmas Tree." The Tree uses multiple arms or "branches" to achieve good dispersion. Each level of the branches is separated by a pressure relief valve (lower relief valves are set to lower pressures). When the salt is molten, oil sprays out of the bottom branches. As salt builds up on the bottom or the holes plug with salt, the pressure in the bottom branches of the tree rises, opening the relief valve and spraying the oil from the next set of branches. As the solid layer grows, successive levels of branches become involved.

Experience with this design revealed three major problems. Pressure drop across the relief valves is excessive. Second, salt can be sucked into jets on nonoperational branches because oil flows past the shutoff branches at high velocity in the main distribution line, creating a low pressure in the branch. Finally, the distribution system is complex and costly relative to the rest of the system.

Further work on the Christmas Tree design was abandoned in favor of the inverted serrated cone. Because the oil passes through an opening of several centimeters instead of fractions of a centimeter, it is difficult for salt to totally block the oil flow path. In addition, the large area allows a low oil pressure to force frozen salt away from the cone opening. Since a cone placed near the bottom may become locked in a relatively deep layer of frozen salt, it will be desirable to use two or three cones per column. The cones can be built inexpensively so cost is not a disadvantage. Serrations on the lower edge of the cone create oil droplets to ensure good heat transfer. No operational problems were found with this method of oil distribution.

Phase Separation

The amount of salt hydrate entrained in the oil phase has a major effect on the design of a direct-contact storage unit. Large amounts of carryover could require the use of an indirect heat-exchange loop to prevent fouling or plugging in the collectors or load-side heat exchangers.

An understanding of the drop coalescence mechanism suggests methods of reducing salt hydrate entrainment. Phase separation is a two-step process. In the first step, oil drops coalesce as they reach the oil-salt hydrate interface where they pack together in a layer, separated from each other and from the upper oil layer by thin skins of the aqueous phase. The rate-limiting coalescence step is the point where the film separates from the drops and drains away. In the second step, the minute aqueous drops formed when the oil drops coalesce are removed from the oil layer. When the skin around the drop ruptures, the skin material contracts into many small droplets, with diameters of a few microns. These droplets are entrained in the oil layer. Since the settling velocity of such drops is on the order of 0.1 to 0.01 mm/s, the majority of aqueous drops will not settle out but will be carried off with the oil. Although both steps in the phase separation process are important, the second step is rate limiting.

The first goal in a phase-separation scheme is to encourage coalescence of rising oil droplets. This is accomplished by a screen or perforated plate which is preferentially wet by the oil phase. Such devices are commonly used in liquid-liquid extraction columns; a metal screen is currently being used in the multidrop apparatus.

Screens are useful for several reasons. Most simply, they fix the level of the oil/water interface, preventing the interface from rising up into the second stage of the phase separator, which would not be able to handle the large amount of the salt solution trapped between the bubbles. Secondly, several researchers have reported the formation of an emulsion of oil and water at the interface. If such a layer is permitted to grow to the level of the outlet, massive carryover may result. Through use of screens, we have avoided such emulsion problems.

While screens generally do well at promoting coalescence, they do little to remove the secondary aqueous drops formed when the aqueous film ruptures. Since such small drops will not settle out in a reasonable time, it is necessary to catch them and promote interdrop coalescence until the they grow large enough to settle out from gravity. To catch the drops, packings of fibrous materials wetted by the secondary drops may be used. Fiberglass is a good material for separating water from oil because it is preferentially wet by the water and not attacked by the oil.

We developed a spectrophotometric technique for measuring the concentration of salt in oil to determine how effective a secondary filter was in reducing salt carryover. The test loop was designed so that oil samples could be taken before and after the secondary filter. Tests were

to be carried out using several filter materials over a wide range of operating conditions. However, due to a programmatic decision, we discontinued the experiment after only a few data points were gathered from a stainless steel mesh filter.

The system was operated at a temperature well above the phase change temperature and allowed to reach steady state before samples were taken. Drop size was varied by using two distributors: an orifice plate, which produced 2-4 mm diameter drops; and an inverted cone, which produced 4-7 mm diameter drops. Oil flow rate was also varied.

The data showed that the stainless steel mesh does not reduce carryover at higher flow rates. The filter reduces carryover at low flow rates, but the net carryover is still greater than at the high flow rates. This data suggests that this type of filter does not substantially reduce salt carryover.

REFERENCES

1. J. D. Wright, C. d'Agincourt, "Direct Contact Air/Molten Salt Heat Exchanger for Solar Thermal Systems," presented at the 1982 IECEC, Los Angeles, Calif., 8-12 Aug 1982.

2. J. D. Wright, R. J. Copeland, "Technical and Economic Evaluation of a Brayton-Rankine Combined-Cycle Solar Thermal Power Plant," SERI/TP-631-1154, presented at the American Section Annual Conference, International Solar Energy Society, Philadelphia, Penn., 26-30 May 1981. Available from NTIS, Springfield, Va. 22161.

3. J. S. Eckert, E. H. Foote, L. F. Walter, "What Affects Packing Performance," Chemical Engineering Progress, Vol. 62, No. 1, p. 59, Jan 1966.

4. J. R. Fair, "Designing Direct-Contact Coolers/Condensers," Chemical Engineering, pp. 91-100, 12 June 1972.

5. D. J. Morrison, "Performance of Solar Heating Systems Utilizing Phase Change Energy Storage," M. S. Thesis, Madison, Wis., University of Wisconsin, p. 103, 1976.

6. J. D. Wright, "The Design and Economics of Direct Contact Salt Hydrate Storage Systems," presented at the Second World Congress of Chemical Engineering, Montreal, Canada, 4-9 Oct 1981, SERI/TP-631-1163, Golden, Colo., Solar Energy Research Institute. Available from NTIS, Springfield, Va.

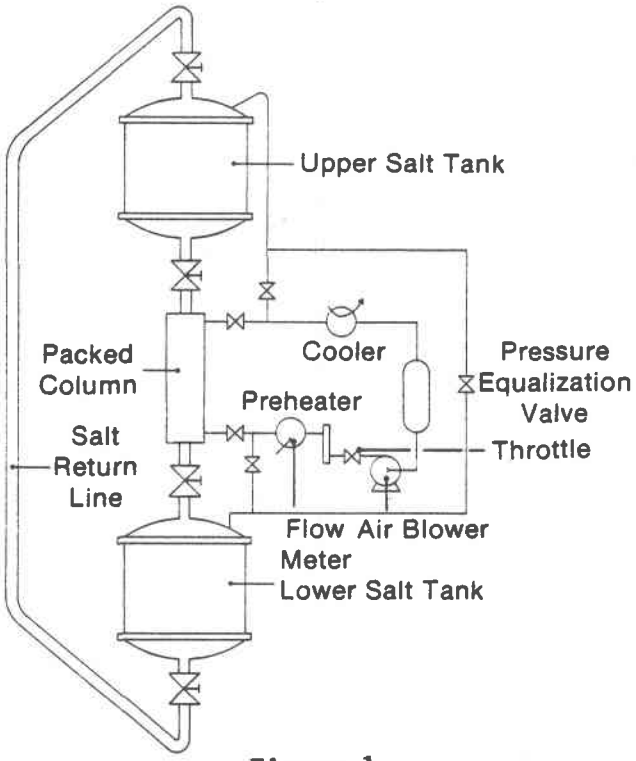

Figure 1

Air/Molten Salt Direct-Contact Heat Exchange Experiment

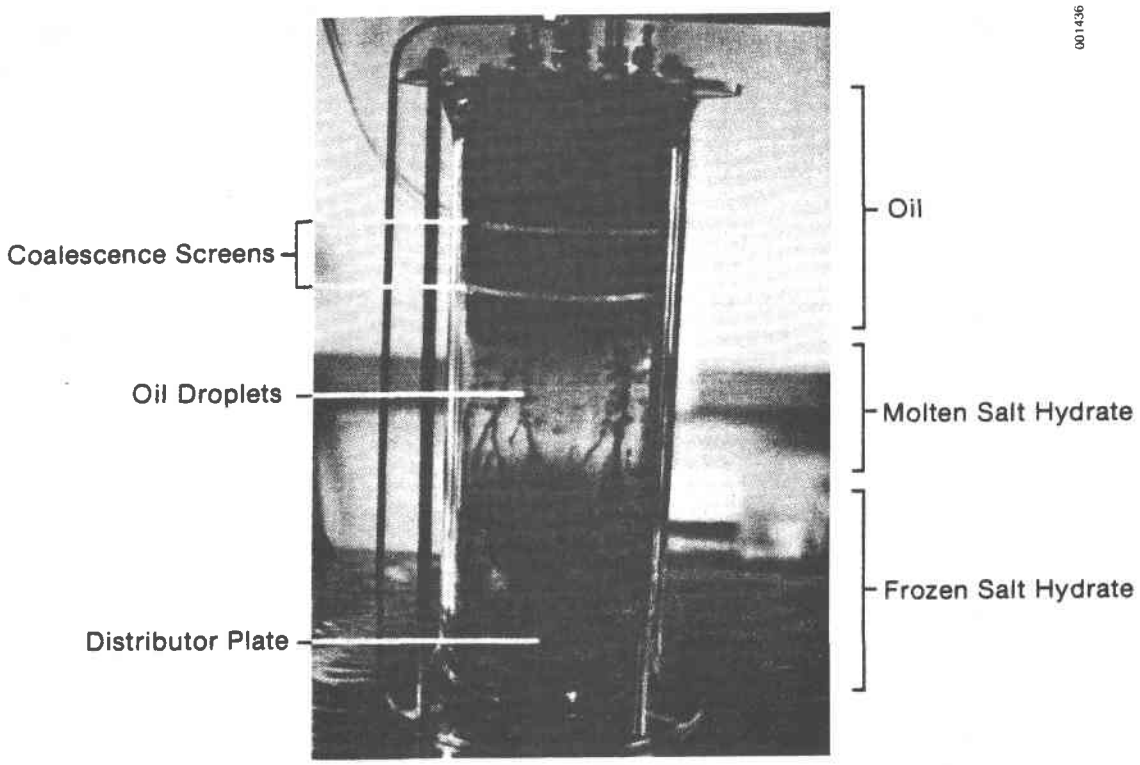

Figure 2

Multidrop Column

A RELATIVE ECONOMIC ASSESSMENT OF INTERNALLY INSULATED PIPE SYSTEMS

S. K. Leung, T. F. Tanton, W. Hausz
W. Reed and B. Bolden
Eureka Laboratories, Inc.
215 - 26th Street
Sacramento, CA 95816

This paper presents the results of a study conducted by Eureka Laboratories, Inc. (ELI) for the Solar Energy Research Institute (SERI). The purpose of the study was to evaluate the relative feasibility of internally insulating pipe systems used for the transport of thermal energy. The specific objectives were to screen technologically feasible concepts of internal insulation and to determine the relative cost of transport for steam or high temperature water (HTW) using internally applied insulation compared to conventional external insulation.

In order to achieve these objectives, the following tasks were performed:

- o Identify technically feasible options for internal insulation of pipelines, using simplified computerized stress analysis;
- o Conduct economic comparison of the transportation of heat by internally insulated pipes with the transportation costs by conventional externally insulated pipes.

Whenever an analysis like this is done, there is a natural tendency to focus on the technical aspects or on the economic aspects. The primary emphasis in this project was on the economic feasibility of internally insulated pipe relative to conventional pipe with external insulation, because of the unavailability of direct mechanical data for several insulation materials' properties. Several aspects of the technical feasibility were analyzed using a boundary approach, in order to evaluate the economics.

Steam and HTW were the assumed thermal transport media. The nominal flow diameters considered in the analysis range from 8 inches to 48 inches for steam and up to 60 inches for HTW, with temperature ranges of 600° to 1000°F for steam and 250° to 450°F for HTW. The pressure range used in the analysis of steam is 600 to 1800 psi. The economic methodology used to compare internal with external insulation was based on the following equation:

$$C.O.E. = \left[\frac{C.\ I.\ x\ F.C.R.}{L.F.\ x\ 8760\ x\ D.E.}\right] + \left[\frac{C.O.H.\ x\ S.E.}{D.E.}\right]$$

where
- C.O.E. = Cost of delivered energy: $\$/10^6$ Btu
- C.I. = Capital investment; $
- F.C.R. = Fixed charge rate = 0.18 (assumed)
- L.F. = Load factor = 0.75 (assumed)
- C.O.H. = Cost of supply heat; taken as $\$2.63/10^6$ Btu
- D.E. = Delivered energy: 10^6 Btu/hour
- S.E. = Initial supplied energy: 10^6 Btu/hour.

It should be noted that the use of this equation provides results which are very sensitive to the assumed cost of supply energy; a fact which must be taken into account when comparing our results with those

of other analyses of the cost to transport thermal energy by pipeline.

Because this was a comparative economic analysis, and not an absolute feasibility study, some cost parameters normally included in pipeline systems were included while others were not. Table 1 lists those parameters included, and those parameters explicitly excluded.

TABLE 1

PARAMETERS INCLUDED AND EXCLUDED IN ECONOMIC ANALYSIS

Cost Parameters Included	Cost Parameters Excluded
Capital Investment	Cost of Pump Stations
o Pipe material cost	Cost of Pumping Energy
o Point-to-point multiplier	Cost of Trenching
o Insulation material cost	Cost of Hydrostatic Membrane
o Insulation installation cost	Terrain Effects
Heat Lost Per Foot	Underground Hazards
Cost of Energy Supplied	
Financial Parameters Included	
o Fixed charge rate	
o Rate of inflation	
o Energy escalation	

The cost parameters included are all self-explanatory except perhaps the "point-to-point multiplier". The "point-to-point multiplier" is used to convert straight pipeline distance to actual feet of pipe used, to allow for expansion loops, fittings, etc. Certain factors were excluded because they would be the same for both externally and internally applied insulation; the flow diameters and mass flow rates were held constant between cases.

In order to estimate the capital costs for the insulated pipe, ELI developed nominal systems, within the ranges of parameters considered. The nominal system analyzed are summarized in Table 2, for both steam and HTW transport. The nominal systems were developed maintaining similar values between external and internal insulation cases for as many parameters as possible, to avoid complicating the economics. Of course, the systems analyzed are reasonable compromise rather than optimal for those systems. For example, thicker internal insulation could be used, trading-off either increased pipe diameter or pumping requirements, or both to optimise the internal concept. This was not done, except on a preliminary basis. This simplifying assumption was used since the purpose was to compare the internal with external application of insulation.

TABLE 2

INSULATION CONCEPTS ECONOMICALLY ANALYZED FOR STEAM AND HTW

Concepts		Pipe Size (Inches)	Insulation Thickness (Inches)
STEAM			
External Insulation			
Conventional	o Calcium silicate o Carbon steel/chrome molybdenum or stainless pressure boundary (depends on temperature)	8-16 30	2.0 2.5
Evacuated Superinsulation (ESI)	o ESI applied externally; pressure boundary as above (1.0 inch thick insulation)	36-48	3.0
Internal Insulation			
Concept I	o ESI o Carbon steel pressure boundary	8-48	1.0
Concept II	o Calcium silicate with 0.05 inch stainless steel liner o Carbon steel pressure boundary	8-16 30 36-48	2.0 2.5 3.0
HTW			
External Insulation			
Conventional	o Calcium silicate o Carbon steel pressure boundary	8-16	1.5
ESI	o ESI applied externally, pressure boundary as above (1.0 inch thick insulation)	36-60	2.0
Internal Insulation			
Concept I	o ESI o Plastic pipe pressure boundary	8-60	1.0
Concept II	o Calcium silicate with 0.05 inch stainless steel liner o Plastic pipe pressure boundary	8-16 36-48	1.5 2.0

Results

Tables 3 and 4 summarize the comparisons of delivered energy cost for the external insulation case and internal insulation case, for steam and HTW respectively.

TABLE 3

BREAK EVEN POINTS* FOR STEAM TRANSPORT @ 600 PSI

Fluid Temperature	Break Even Flow Diameter (In.)	
	ESI	Concept II
600°F	8	30-36
700°F	8	16-30
800°F	8	8-12
900°F	8	< 8
1000°F	8	< 8

* The flow diameter at which cost is equal for both external and internal cases.

TABLE 4

BREAK EVEN POINTS* FOR HTW TRANSPORT

Fluid Temperature	Break Even Flow Diameter (In.)	
	ESI	Concept II
250°F	12-16	36
350°F	12	16
450°F	8	12-16

* The flow diameter at which cost is equal for both external and internal cases.

Conclusions

(1) Based on the comparative cost analysis done, internal insulation is in many cases more attractive than conventional external insulation for the long distance transportation of thermal energy by steam in the range of 600°-1000°F and power levels up to 1500 MWt. For HTW in the range of 250° to 450°F supply temperature, and up to 4000 MWt power levels, internal insulation is marginally cost effective depending on the maintenance cost benefits associated with plastic pipe.

(2) The transport cost is most sensitive to the load factor and to the ratio of capital cost to the value of heat lost. The evacuated superinsulation is the most economically attractive because of its high thermal resistance, and relatively constant cost compared to other insulation concepts. Even with a doubling of evacuated system cost, the concept would still be preferred for steam transport. The second preferred concept, based on cost, involves non-evacuated rigid internal insulation with a thin (0.05 inch) stainless steel liner.

(3) The actual installed cost of the insulation concepts is very insensitive to whether or not the insulation is evacuated. Because of the much lower amount of lost heat and the value associated with it, the evacuated system prevails. For non-evacuated insulation applied internally, the major component of cost is the liner, which varies linearly with its assumed thickness.

(4) The lower pressure boundary temperature with less resultant pipe strength derating, and less expansion requirements with resultant material reduction and heat loss reduction provided by internal insulation provide the potential for sufficient economic benefits that further technical and economic analysis and concept development should be undertaken. In cases that the delivered cost increases with increase in temperature, the cost increases less rapidly with internal insulation than with external insulation.

HIGH TEMPERATURE INTEGRATED THERMAL STORAGE FOR SOLAR THERMAL APPLICATIONS

Adam P. Bruckner and A. Hertzberg
Aerospace and Energetics Research Program
University of Washington
Seattle, WA 98195

and

Robert T. Taussig
Mathematical Sciences Northwest, Inc.
2755 Northup Way, Bellevue, WA 98004

INTRODUCTION

The objective of this program is to investigate the technical and economic feasibility of a unique approach to TES in which thermal storage and heat transfer are accomplished at the same high thermodynamic potential at which the solar radiation is absorbed in the solar collector. Our approach involves a phase conversion of a glass-like silicate slag, which is very stable at high temperatures, to a liquid in a solar-heated furnace. This TES material is a very cheap substance, widely available and benign in its contact with the environment. A schematic of a proposed 10 MW solar power pilot plant which utilizes the novel heat exchanger and storage system appears in Fig. 1. The working material is delivered to the top of the solar receiver tower as a uniform aggregate of small beads, which are melted by a combination of direct solar radiation and reradiation from the cavity walls. The resulting liquid is delivered to the storage vessel and thence to the heat exchanger. The molten material is injected into the heat exchanger under pressure as small diameter streams, which break up into drops. The drops fall through a counter-flowing high pressure working gas, giving up their heat by convection and changing phase into the solid bead state in the process. The solidified droplets are collected at the bottom of the heat exchanger as an aggregate and delivered directly back to the furnace. The heated gas is removed at the top of the heat exchanger and employed by a regenerative Brayton cycle.

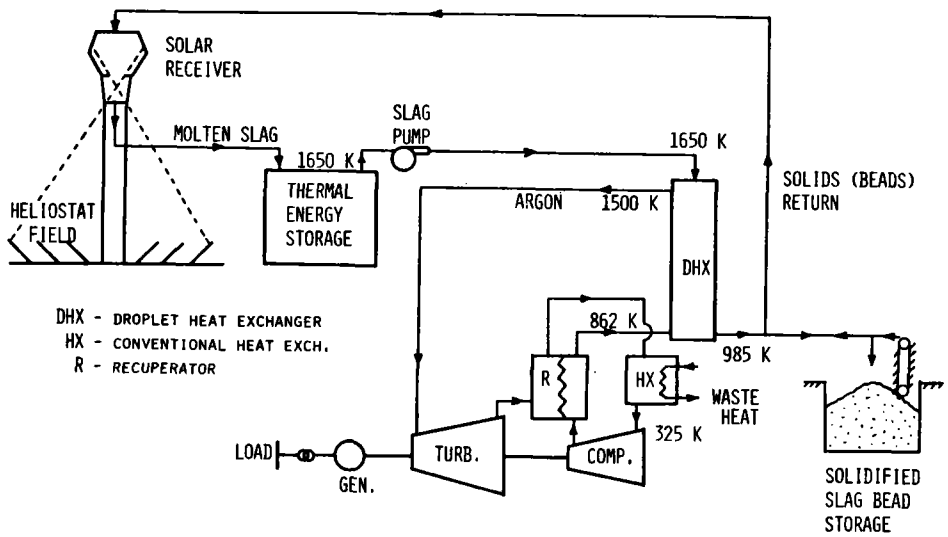

Fig.1 High temperature solar thermal power plant using molten slag TES and direct contact heat exchange.

THE HIGH TEMPERATURE TES MATERIAL

The choice of a suitable TES material for the proposed system is limited by considerations which are fairly unique to high temperature materials science. The material must have a melting point in the range desired for an operating temperature (~1650-1750°K) and should also exhibit relatively low viscosity and high surface tension to facilitate droplet formation in the droplet heat exchanger (DHX). Furthermore, the material should have low vapor pressure to avoid loss of material and contamination of the working gas in the DHX. Since the material is exposed to air in the solar receiver, it should be stable at high temperatures under oxidizing conditions. Finally, it should be low in cost.

A number of pure metal oxides exhibit viscosities of under 1 poise in the molten state and have other desirable properties (1). However, their melting points tend to be too high to be of interest. Common glass formers on the other hand, such as silicates, have low melting temperatures but very high viscosities. The addition of alkali oxides and basic oxides can decrease viscosity values by many orders of magnitude (2). The system SiO_2-CaO-MgO-Al_2O_3, which is similar to metallurgical slags, appears particularly attractive, not only from the point of view of low viscosity (3), but also because of the very low vapor pressure and high chemical stability of its components (4).

We have carried out high temperature experiments with various slags of this type to study the droplet formation characteristics of thin jets of these materials. Small quantities of slag mixtures have been melted in a molybdenum cup heated in an RF induction furnace. The cup is equipped with a removable molybdenum nozzle through which the melt is allowed to flow in response to a one atmosphere pressure differential. Slag droplets in the 1-3 mm range have been successfully generated.

The slag composition which appears to be most attractive as a TES material is 50% SiO_2, 30% CaO and 20% MgO, by weight. The viscosity of this slag varies from ~7 poise at 1650°K to ~2.5 poise at 1750°K (3). Its liquidus temperature is 1630°K. The density of the slag in the molten state is 2.9 g/cm^3, as calculated from the measured density of the solid and assuming a 10% increase in specific volume on melting. The specific heat of this slag at 1650°K is 0.292 cal/gm/°K (5) and its surface tension is 420 dyne/cm (6). Its vapor pressure is very low, even at the high temperatures considered. Evaporation occurs through dissociation of its constituent oxides, primarily that of SiO_2 into SiO and O_2 (2). At 1650°K the partial pressures of SiO and O_2 in a neutral atmosphere are 3.45×10^{-8}atm and 1.73×10^{-8}atm, respectively.

THE ENERGY STORAGE SYSTEM

The capability of storing energy at the same high thermodynamic potential at which it is collected in the solar central receiver is a unique feature of the integrated system proposed here. Absorbing energy directly into the heat storage material in the solar central receiver leads to a storage method that is very easily integrated with the power cycle. Energy storage is accomplished by piping the molten slag to a large storage vessel. The material fills the vessel, whence it is pumped to the droplet heat exchanger. Thus, a reserve of high temperature molten slag is available at all times.

The energy storage vessel, which in the point design being considered is located at ground level directly beneath the solar collecting tower, is a relatively large, unpressurized container, insulated on the inside, similar in design to modern glass-melting tanks. The power plant represented in Fig. 1 has a 10 MW net electrical output and requires 23 MW circulating power with the 43% efficient regenerative argon Brayton cycle illustrated. Storage capacity of 1104 MW-hr would supply the power generation cycle for 48 hours. For a temperature drop of 670°K through the droplet heat exchanger this results in a storage mass of 4.96×10^6 kg and thus a storage volume of 1710 m^3. To minimize the hydrostatic pressure head of the molten slag the inside diameter of the tank has been chosen to be approximately three times its height, i.e., dia = 18.4 m, height = 6.5 m.

The storage container is designed with due regard for the physical and chemical compatibility of the molten slag with the container material. Studies of the corrosion of refractories by slags of various compositions have indicated that the corrosiveness of such media increases rapidly with increasing basicity and that the corrosion resistance of the refractories relates to their alumina-silica ratios, i.e., the refractories with the highest alumina contents possess the greatest resistance to slag corrosion (7). The AZS refractories widely used in the glass industry are prone to severe corrosion by basic slags due to their relatively high silica content. Fused-cast alpha alumina (99.3% Al_2O_3) has the highest corrosion resistance to basic slags.

Fused-cast alumina also exhibits high density, low porosity and high strength (4). Its thermal shock resistance is not as good as that of refractories containing silica but is nevertheless adequate. Before filling, the storage tank would be preheated to approximately 1500°K to minimize thermal shock gradients and avoid freeze-up of the incoming slag. This preheat would utilize a natural gas heating system with inlet burners in the roof of the tank. The off-gas would exit through the slag inlet conduit, preheating it also in the process.

STORAGE COSTS

The cost of the storage vessel and associated equipment has been calculated based on the volumes and masses of liner, insulation, structural (steel) and slag materials required for storage of 1104 MW-hr for the baseline 10 MW_e power system. The costs include construction materials, labor, overhead for engineering design, and utilities needed during construction. Auxiliary storage of the warm, solidified glass beads has been estimated roughly as being less than or equal in cost to the high temperature storage vessel. The cost of pumps, valves, and piping and conveyor systems to and from the storage units has also been included.

The costs of the storage vessel were modeled by assuming that structure, foundation, and refractory liner costs are fixed and that the heat transfer material costs will vary according to the materials used and the sensible heat available from those materials. This model was used to compare molten salt storage costs (heat of fusion) to slag storage costs (sensible heat). Specifically, the capacity costs associated with molten salt (e.g., 33% LiF/65% KF) are \$15.53/kW-hr(th), and the capacity costs of the slag storage are \$0.15/kW-hr(th) [= (\$0.035/kg) ÷ $(C_p \Delta T)_{slag}$ where ΔT = 670°K] where only the storage

material costs (e.g, salt or slag) are used. Hence, if the total material costs for the slag vessel are multiplied by (15.53/0.15) and added to the fixed costs of the structures, foundation, and refractory liners, the resulting total capacity cost rises to $23/kW-hr for a salt storage vessel. This compares very favorably to the costs of $27/kW-hr quoted in the earlier draft of the Copeland report (8) and gives considerable confidence to the costing for the slag thermal storage system, i.e., $6/kW-hr. This figure does not include the cost of carrying the capital during the construction period.

THE DROPLET HEAT EXCHANGER

The ability of the droplet heat exchanger to transfer heat between the TES material and a working gas in direct contact at high temperature circumvents many of the material limitations of conventional tube-type heat exchangers and does away with complicated plumbing systems and their potential for catastrophic single point failure.

The droplet heat exchanger consists of a single, large, insulated cylindrical pressure vessel. A pressurized gas pumping system is used to force molten slag from the storage chamber through an insulated refractory pipe. The molten slag is injected into the heat exchanger through a suitable refractory metal nozzle plate pierced with a multitude of small holes. The resulting thin streams break up quickly into a series of uniform drops (9), which fall through the heat exchanger giving up their heat to an inert working gas capable of running a high temperature heat engine.

The heat exchanger has been modeled as a simple one-dimensional two-phase flow problem, including radiative effects. The heat exchanger is assumed to be a cylindrical chamber with an adiabatic side wall. The droplets are injected axially at the top of the chamber, are of uniform diameter and are uniformly distributed across the flow area. The counter-flowing gas, which enters at the bottom and leaves at the top, is assumed to have a uniform radial velocity profile.

A slag inlet temperature of 1650°K and gas inlet and exit temperatures of 862°K and 1500°K were respectively chosen for our baseline system. The mass flow rates of the two media were adjusted to match their thermal capacities, although any suitable mass flow ratio may be chosen to tailor the temperature profiles or heat exchanger effectiveness to specific needs.

For the baseline design a regenerative argon Brayton cycle with an inlet temperature of 1500°K at 20 atm and a pressure ratio of 5 was assumed (Fig. 1). For compressor and turbine efficiencies of 0.85 and 0.88, respectively, and a recuperator effectiveness of 0.95 the cycle efficiency is 43%. Assuming no electric generation losses, a pilot plant of 10 MW_e output would require 23 MW of thermal power to be delivered to the turbine inlet and would require an argon mass flow of 2.6×10^5kg/hr and a mass flow of slag of 1.03×10^5kg/hr.

Utilizing slag droplets of 1.0 mm dia. injected at their terminal velocity in the gas, transfer of the required 23 MW_{th} is accomplished in a heat exchanger 6.5 m high and 3.0 m dia. The pressure drop in the gas is less than 0.1% of the inlet pressure due to the low particle loading

fraction and the low gas velocity. Although the droplets solidify during their transit (their exit temperature is 985°K), there is no release of heat of fusion due to the amorphous nature of the slag.

The vaporization of the slag in the heat exchanger has been calculated to be only 4.3×10^{-4}kg/hr. Compared to the argon mass flow rate of 2.6×10^{5}kg/hr, the contamination of the gas is negligible (~2 parts per billion). The loss of argon resulting from removal of the solid bead aggregate at the bottom of the heat exchanger is estimated to be only ~0.05% of the mass flow of the gas.

The interaction of the flow with the walls, turbulence and end effects will cause deviations from the simple one-dimensional flow assumed here. These phenomena are the subject of ongoing investigations by the authors.

REFERENCES

1. J.L. Bates, C.E. McNeilly and J.J. Rasmussen, "Properties of Molten Ceramics," in Materials Sciences Research, Vol. 5, W.W. Kriegel, ed., Plenum, New York, 1971.

2. W.D. Kingery, H.K. Bowen and D.R. Uhlman, Introduction to Ceramics, 2nd ed., John Wiley & Sons, 1976.

3. E.T. Turkdogan and P.M. Bills, "A Critical Review of Viscosity of CaO-MgO-Al_2O_3-SiO_2 Melts," Ceramic Bull. 39, 682, 1960.

4. "Engineering Property Data on Selected Ceramics: Volume III, Single Oxides," Report No. MC1C-HB-07-Vol. III, Metals and Ceramics Information Center, Battelle, Columbus Laboratories, Columbus, OH, 1981.

5. E.F. Foerster and P.L. Weston, Jr., "Heat Content of Some Blast-Furnace and Synthetic Slags," Report No. 6886, U.S. Department of the Interior, Bureau of Mines, 1967.

6. K.C. Lyon, "Calculation of the Surface Tensions of Glasses," J. Am. Ceram. Soc. 27, 186, 1944.

7. W.A. Miller and W.L. Shott, "Corrosion of Refractories by Blast Furnace Slags," Am. Ceram. Soc. Bull. 47, 648, 1968.

8. R.J. Copeland, "Preliminary Requirements for Thermal Storage Subsystems in Solar Thermal Applications," SERI/RR-731-364, Solar Energy Research Institute, Golden, CO, 1980.

9. J.P. Anno, The Mechanics of Liquid Jets, D.C. Heath & Co., Lexington, MA, 1977.

SYNTHESIS AND CHARACTERIZATION OF NEW BIPYRIDINYL LIGANDS

K. T. Potts, A. Ruffini and P. Winslow
Department of Chemistry
Rensselaer Polytechnic Institute
Troy, New York 12181

tris (2,2'-Bipyridinyl) ruthenium (II) cation, $Ru(bpy)_3^{2+}$ (1) and its derivatives have attracted considerable interest (1) as the excited state of this complex can serve either as an electron donor or an electron acceptor and photoinduced electron transfer from it to an electrode has been demonstrated. The ruthenium complex absorbs light over an appreciable portion of the visible spectrum and,as its excited state is relatively long-lived and possesses in principle sufficient energy to produce hydrogen from water, considerable effort has been expended on this application. Many of the systems studied using this complex as photosensitizer require the presence of heterogeneous catalysts (e.g., Pt or Au) and very few homogeneous systems have been reported. In some instances, photoinduced electron transfer reactions have given high energy products with good efficiency but it is generally found that rapid back-reaction occurs, degrading the stored energy. Surfactant ruthenium complexes have been utilized (2) in these studies but in monolayer assemblies hydrolysis of the long-chain ester group occurs and on prolonged photolysis non-hydrolytic degradation of the complex was observed.

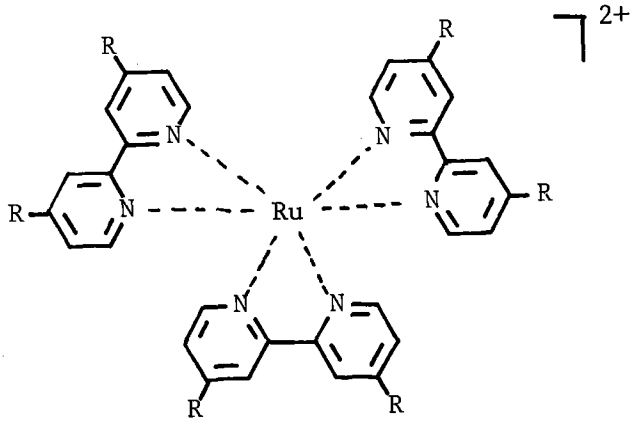

1

R = H, $COOR^1$ where R^1 = Et or $C_{18}H_{37}$

This research program has focused on the synthesis of 4,4'-disubstituted-2,2'-bipyridinyl systems in which the 4,4'-substituents are alkylthio, long chain alkoxy, and long chain dialkylamino groups for complexation with ruthenium salts to yield the tris(bipyridinyl)ruthenium complexes analogous to (1). These newly developed ligands would have the advantage of remaining inert towards substitution and dissociation during continuous irradiation and cyclic redox processes, and the character of the long chain alkyl substituents (e.g., dodecyl) would influence hydrophobic interactions.

2,2'-Bipyridinyl (2; R = H) is commercially available and its 4,4'-dimethyl and 4,4'-bis(alkoxycarbonyl) derivatives (2; R = CH_3 and COOR', respectively) are readily synthesized by straight-forward procedures from the appropriately substituted pyridines, either using copper-catalyzed coupling reactions (3) or pyridyl lithium reactions (4). The synthesis of 2,2'-bipyridinyls with 4,4'-substituents containing electron donating groups such as alkoxy, alkylthio and dialkylamino, however, is not straight-forward and requires the development of new synthetic approaches. From a conceptual point of view, the most direct route to such a ring system could involve: (1) the nucleophilic displacement of the group R in 1 with an anion such as RO^- or RS^-, or a nucleophile such as R_2NH; (2) Fabrication of the pyridinyl nuclei in such a way that the synthetic procedure incorporates the desired substituent in place; or (3) Structural modification of the group R to give the desired 4,4'-substituents. Our study has involved methods (1) and (2) which were considered to be the most direct procedures to obtain the required bipyridinyl derivatives.

Syntheses Leading to 4,4'-Bis(disubstitutedamino)-2,2'-bipyridinyls. The required intermediate for this synthetic route was 4,4-dichloro-2,2'-bipyridinyl (5). This intermediate has been prepared in moderate yield, with variation of the reaction conditions resulting in higher yields of the various intermediates. Thus, use of 50% hydrogen peroxide in the conversion of 2 to 3 resulted in a 98% yield of 3 (increased from 74% using 30% H_2O_2). Nitration of 3 to give 4 resulted in 41% yield, comparable with that reported in the literature (5). This reaction is extremely sensitive to reaction conditions, the optimum conditions being conc. nitric acid and fuming sulfuric acid (65% oleum) for 5 hours at 100-110°C. Higher reaction temperatures and diminished or longer reaction times resulted in a drastic reduction in yield of the dinitro compound 4. The best yields were obtained using a 5.0 g quantity of 3. When the reaction was carried out on a larger scale, reduced yields of 4 were obtained. This reaction constitutes a serious bottle-neck to this synthetic route and a detailed study of this nitration procedure will be required to increase the efficiency of this process.

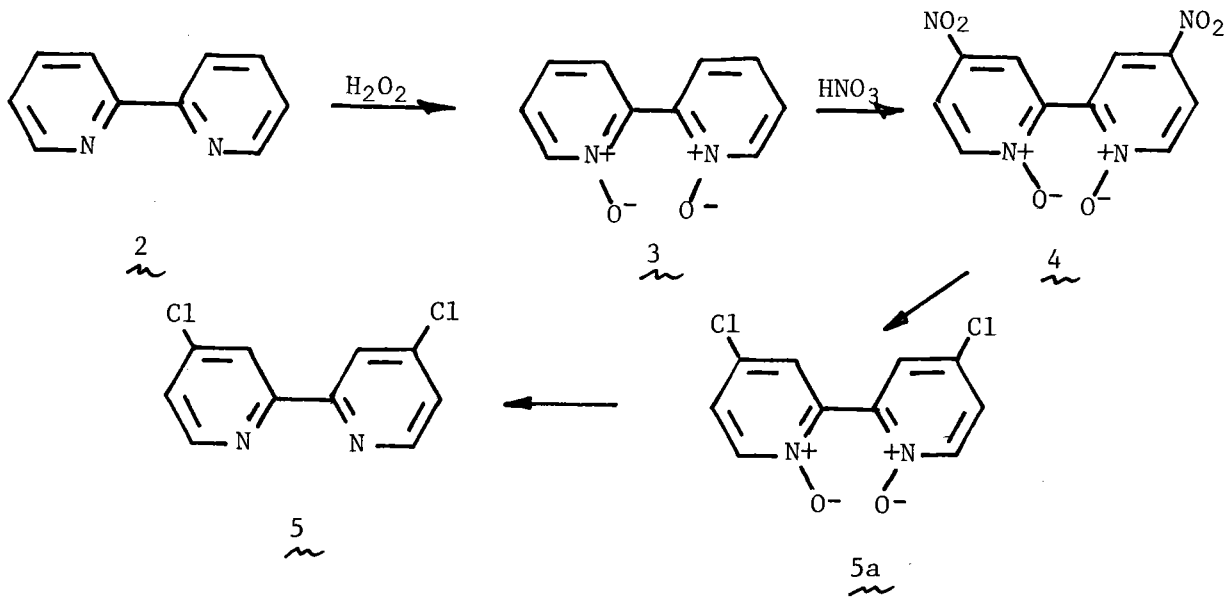

Conversion of 4,4'-dinitro-2,2'-bipyridyl-1,1'-dioxide (4) into 5 was carried out using a two-step reaction sequence. Reaction of 4 with acetyl chloride in acetic acid resulted (6) in a clean conversion of 4 into 5a in 85% yield. Deoxygenation of 5a to 5 occurred in 70% yield using phosphorus trichloride in anhydrous chloroform (7).

The 4,4-dichloro compound 5 failed to undergo reaction with a variety of nucleophiles, including didodecylamine and potassium pentadecanoxide but it did react with sodium ethanethiolate to give the corresponding 4,4'-bis(ethylthio)-2,2'-bipyridinyl, a desired target compound.

This lack of nucleophilic character of the secondary amine in this reaction may be rationalized in terms of the long chain alkyl groups preventing access of the nitrogen atoms lone pair of electrons to the electron-deficient 4,4'-positions of the bipyridinyl system. In support of this idea, we found that morpholine readily displaced the 4-chloro group in 4-chloropyridine-1-oxide.

The lack of success with this synthetic approach suggested a route with the basic nitrogen atom already introduced at the 4,4'-positions. Reduction of 4 with iron and acetic acid resulted in a simultaneous reduction of the nitro group and deoxygenation, giving the 4,4'-diamino-2,2'-bipyridinyl (6) in 43% yield. Condensation of 6 with myristoyl chloride (7) in THF solution readily gave 8 in 32% yield. The structure of this product was evident from analytical and spectral data, especially $\underline{M}^+$ 606 (87%), ν_{CO} 1660 cm^{-1}; ν_{NH} 3280 cm^{-1}. Reduction of 8 with lithium aluminum hydride gave 4,4'-bis(tetradecylamino)-2,2'-bipyridinyl (9) in 52% yield.

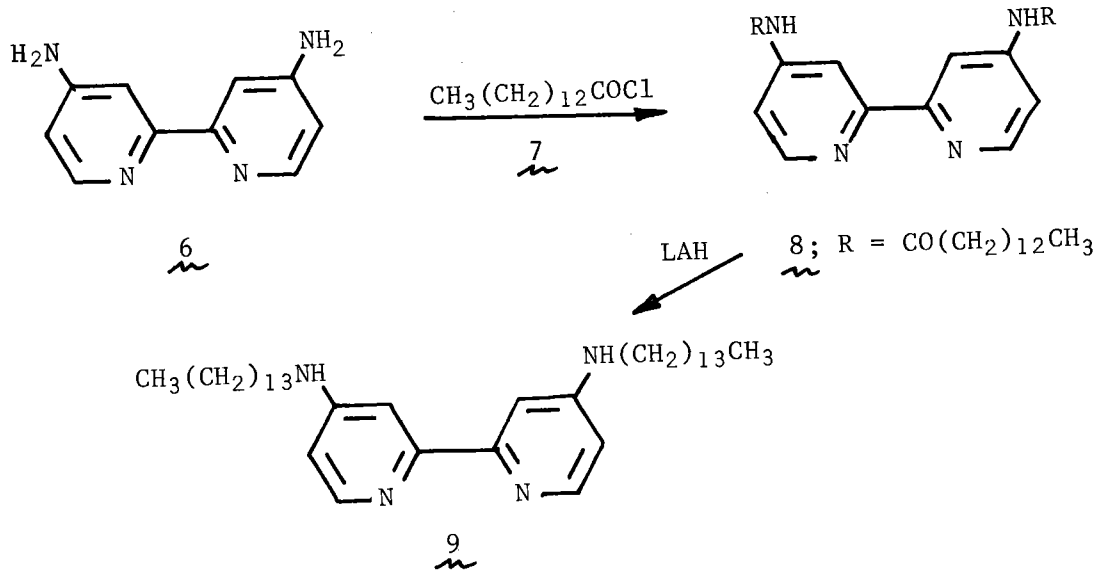

9

Reactions currently under way involve conversion of 8 into 10 by an intial generation of the anion with NaH/DMF and acylation of the anion with myristoyl chloride. Subsequent reduction of 10 with lithium aluminum hydride will give 11, a desired target compound.

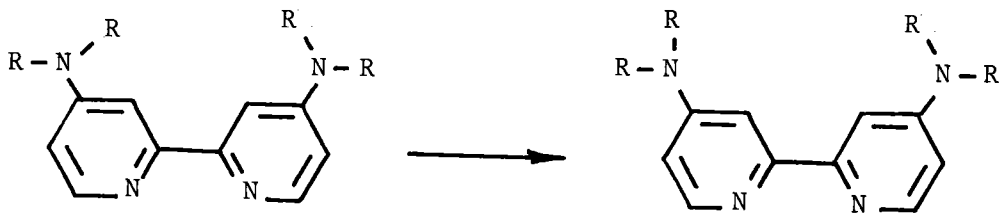

10; R = $CO(CH_2)_{12}CH_3$ 11; R = $(CH_2)_{13}CH_3$

An alternative approach to these bipyridinyl systems using ketene dithioacetal methodology was also studied. Retrosynthetic analysis indicates that 2 (R = SEt) should be synthesized by reaction of the ketene dithioacetal derivative 12 with the bis-anion of biacetyl as shown below. This would be an extremely direct and versatile synthesis and required the prior development of a practical route to 12, formally the

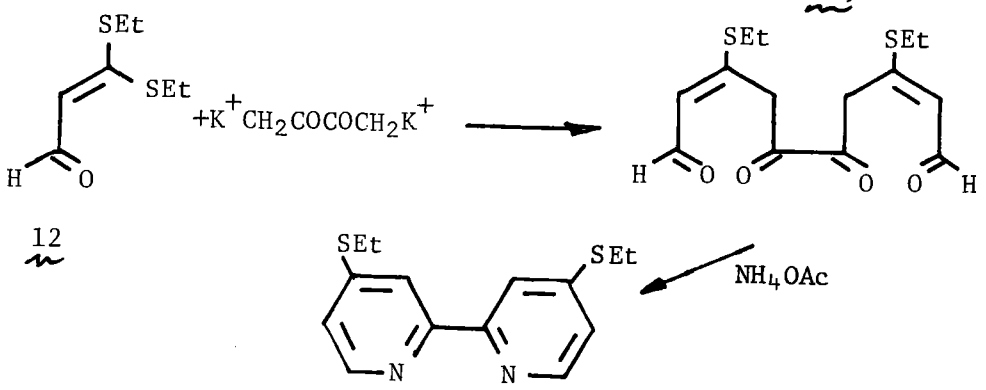

12

ketene dithioacetal derived from acetaldehyde. The preparation of this potentially versatile synthon has now been accomplished via the sequence of reactions show below.

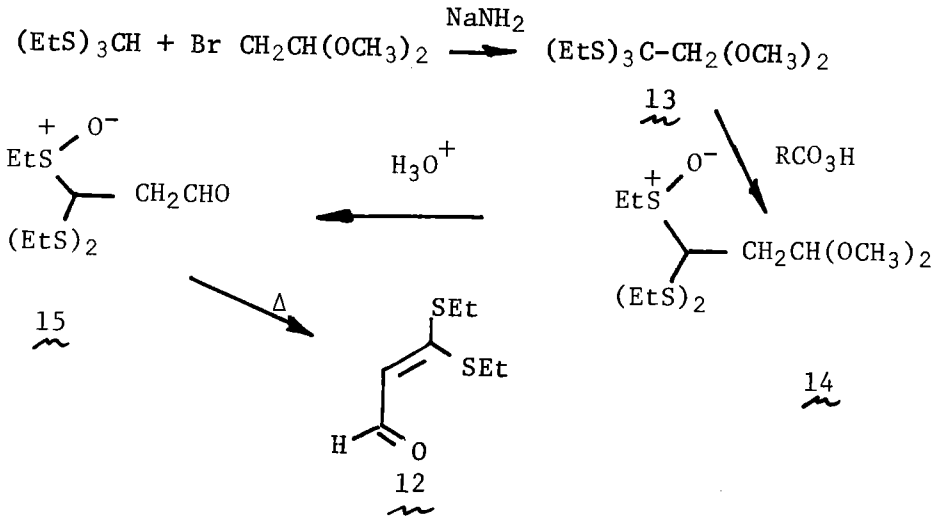

1,1,1-Tris(ethylthio)-3,3-dimethoxypropane (13) was prepared (8) in 84% yield by reaction of ethyl orthothioformate with bromoacetaldehyde diethyl acetal. Sulfoxide formation by reaction of 13 with m-chloroperbenzoic acid (one equivalent) occurred readily, the formation of 14 being apparent by the downfield NMR shift of an S-ethyl group. Hydrolysis of 14 to 15 occurred readily with dilute HCl and the isolated aldehyde was then heated at 116-129°C/4 mm. This resulted in the formation of 12 as a pale yellow oil whose structure was established by the analytical and spectral data.

Preliminary experiments on the condensation of 12 with the bis-anion of biacetyl indicate that reaction does occur and ring closure to the pyridine with NH_4OAc and hot acetic acid results in a small yield of nitrogenous base. These experimental conditions are currently being modified to improve the yield of 2 (R = SEt).

Introduction of only one alkylthio group into 2,2'-bipyridinyl was also of interest and the ketene dithioacetal route provided ready access to this system. Reaction of 3,3-bis(methylthio)-1-(2-pyridinyl)propen-1-one (9) with the potassium enolate of acetone and subsequent condensation of the intermediate 1,5-enedione 17 with ammonium acetate gave the bipyridinyl 18 in 72% yield. Oxidation of the methyl group with potassium permangante and subsequent decarboxylation to give 19 was unsatis-

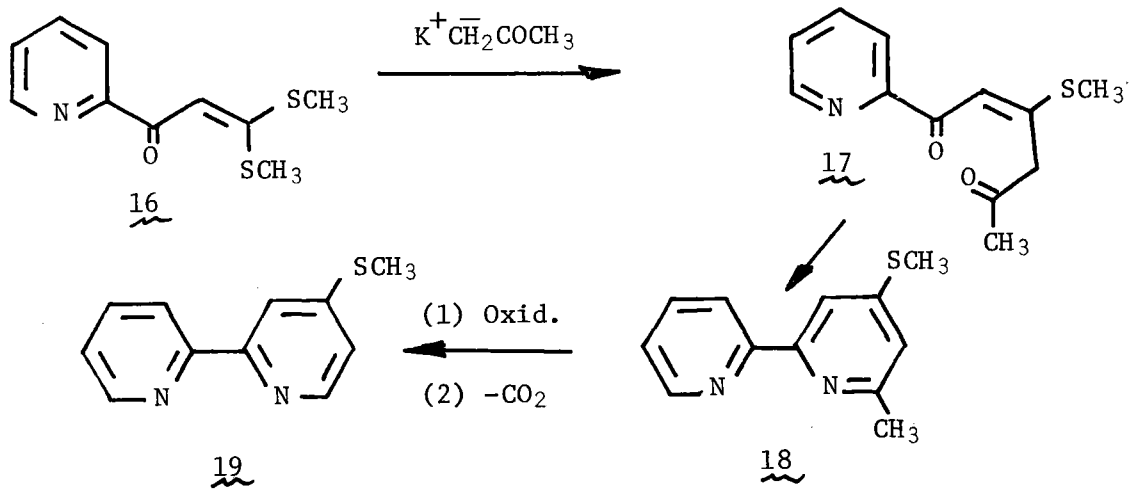

factory, the corresponding sulfone being formed. An alternative procedure using O_2/potassium tert-butoxide is now being studied and appears to have promise.

References

1. For compilations of references dealing with this topic see: C. V. Krishnan and N. Sutin, J. Am. Chem. Soc., 103, 2141 (1981); A. Harriman, G. Porter and P. Walters, J. Chem. Soc. Faraday Trans. 2, 77, 2373 (1981).

2. G. Sprintschnik, H. W. Sprintschnik, P. P. Kirsch and D. G. Whitten, J. Amer. Chem. Soc., 98, 2337 (1976); S. J. Valenty and G. L. Gaines, J. Amer. Chem. Soc., 99, 1285 (1977); G. Sprintschnik, H. W. Sprintschnik, P. P. Kirsch and D. G. Whitten, ibid., 99, 4947 (1977); G. Sprintschnik, H. W. Sprintschnik, P. P. Kirsch and D. G. Whitten, J. Amer. Chem. Soc., 99, 4947 (1977); O. Johansen, C. Kowla, A. W. H. Man and W. H. F. Sasse, Aust. J. Chem., 98, 4853 (1976; G. L. Gaines, P. E. Behnken and S. J. Valenty, J. Amer. Chem. Soc., 100, 6549 (1978); S. J. Valenty, D. E. Behnken and G. L. Gaines, Inorg. Chem., 18, 2160 (1979).
3. J. P. Wibaut and J. Overhoff, Rec. Trav. Chim. Pays-Bas, 47, 761 (1928).
4. T. Kauffmann, J. König and A. Woltermann, Chem. Ber., 109, 3864 (1976).
5. J. Haginiwa, J. Pharm. Soc. Japan, 75, 731 (1955).
6. G. Maerker and F. H. Case, J. Am. Chem. Soc., 80, 2745 (1958).
7. H. Hamana, J. Pharm. Soc. Japan, 71, 263 (1951).
8. A. Froling and J. F. Arens, Rec. Trav. Chim. Pays-Bas, 81, 1009 (1962).
9. K. T. Potts, M. J. Cupullo, P. Ralli and G. Theodoridis, J. Am. Chem. Soc., 103, 3584, 3585 (1981); J. Org. Chem., in press.

HIGH TEMPERATURE ACTIVE HEAT EXCHANGER RESEARCH FOR LATENT HEAT STORAGE

J. Alario, R. Haslett, and R. Brown
Grumman Aerospace Corp.
Bethpage, N.Y. 11714

ABSTRACT

The objective of this research program is to develop a high-temperature direct-contact latent heat exchange thermal energy storage system by demonstration and test evaluation of a 10 kW-hr scale model. This work entails the completion of an experimental program, begun under a previous DOE contract, which was interrupted due to excessive corrosion and subsequent equipment damage.

The current follow-on project is a three-phase program including inspection and redesign of the existing equipment (Phase I), fabrication/assembly and checkout (Phase II), and experimentation (Phase III). Phase I has been completed and the assembly and instrumentation tasks of Phase II are currently underway.

The major system modifications are as follows: installation of all new tanks and plumbing; substitution of a lower melting point salt; elimination of immersion heaters; improved trace heating including automatic control of all heater circuits; upgraded liquid metal pump, and replacement of the salt pump with a pressurized gas feed.

INTRODUCTION

The potential benefit of the direct contact concept is smaller, less costly heat exchangers resulting from greatly improved heat exchange efficiency during extraction of the latent heat of fusion from thermal storage media. This is accomplished by reducing the thermal resistance of the solid phase through the transfer of heat across the phase boundaries of two well-mixed immiscible fluids. In our system, molten droplets of salt, which serves as the TES medium, are injected at the bottom of a column of liquid metal carrier fluid. As the lighter weight molten salt droplets rise through the cooler column of liquid metal, they release their heat of fusion and solidify individually.

This research effort will modify the existing hardware and perform necessary testing to: (1) evaluate the overall effectiveness of the direct contact heat exchange system in extracting the latent heat of fusion from the salt storage media; and (2) model the heat transfer mechanism between the dispersed (salt) and continuous (metal) fluid streams within the heat exhange tower.

A work flow plan which summarizes the major technical tasks and indicates primary SERI decision points is shown in Fig. 1. The program consists of three phases, each preceded by a go/no-go decision point. In Phase I, the existing hardware was partially disassembled and examined to determine the state of media contamination, material corrosion, and hardware serviceability. Grumman's chemical and metallurgical laboratories supported the evaluation. On the basis of these findings, the design was modified to eliminate previous deficiencies. A test plan was also prepared which contains detailed information about instrumentation (type and location), measured parameters, and equipment operating procedures. Phase II, which is now proceeding, encompasses component procurement and fabrication, system assembly, instrumentation, and a checkout run. The system will be ready for a detailed test evaluation at the end of Phase II. The Phase III effort will involve extensive testing and data analysis in accordance with stated objectives. If warranted, specific recommendations and plans for additional development and demonstration programs will be submitted to SERI. The program will conclude with a final report to document the entire technical effort, including design, test results, and recommendations.

DISCUSSION

Results of Inspection

The significant findings of the physical inspection are summarized below:

- The immersion heaters in the salt module leaked salt vapor through the tapered threads, which eventually corroded the heater terminals and the external surfaces of the tank. There was a large salt leak at the rear of the tank

- The internal surfaces of the salt tank showed no signs of corrosion and the solidified chloride salt was pure white in appearance, showing no evidence of moisture absorption. A nitrogen gas blanket was maintained during system operation but had not been replenished for over three months while the tank was dormant

- There was no evidence of salt in the discharge plumbing, indicating that there was a local "cold spot" (possibly at the impeller) which prevented pumping

- Liquid metal had been pumped into the heat exchange tower and was encrusted around the salt injector plate. Some liquid metal had overflowed the tower and was solidified at the bottom of the heat exchange tank, within the volume set aside for the storage of solidfied salt

- The appearance of the liquid metal and heat exchange modules was acceptable, but each would require significant refurbishment to remove the immersion heaters

- Tanks and lines showed charring due to over-temperature of the external band and line heaters

- Melting point measurements of the media showed no change in the lead bismuth metal eutectic (124°C), but the chloride salt melt range (328-429°C) exceeded the spec value (385-393°C)

- Most of the thermocouple instrumentation was unusable, but the two flowmeters (metal and salt) and the liquid level indicators in the heat exchange tower were salvageable.

System Modification

A schematic diagram of the revised system is shown in Fig. 2. The following list summarizes the major system modifications:

- New tanks (mild steel) were fabricated for all three modules (salt, metal, and heat exchange) which eliminated all immersion heaters and any penetration beneath the liquid levels

- The liquid metal pump was upgraded to increase lift capability and improve seal design. The new centrifugal pump can provide a 12-foot lift and comes attached to the cover lid as a complete assembly. It is powered by a 2 hp electric motor instead of the 1 hp air-driven motor previously used

- In view of the batch-type discharge cycle, the salt pump was replaced by a pressurized nitrogen gas pumping system

- The salt medium was changed from the chloride eutectic (20.5 KCl, 24.5 NaCl, 55.0 $MgCl_2$) to draw salt (46 $NaNO_3$, 54 KNO_3) because of the latter's widespread use in sensible heat storage systems. Thus, latent storage test data would be of more immediate use in augmenting these existing sensible systems. Also, the lower melting point of the draw salt (222°C) would simplify operation of this demonstration system since it would be easier to preheat tanks and lines and to control temperature

- All heater circuits will be equipped with proportional controllers to achieve accurate temperature regulation. The tanks will use external band heaters while the plumbing, valves, and fittings will be traced with adhesive backed heater tape (serviceable up to 316°C)

- The filling system for both the molten salt and liquid metal tanks was changed from one that used an underneath canister containing liquified material which was then pressurized to a system using an access port in the lid through which solid material is introduced. The new method is simpler for a one-time evaluation and also permits mixing and processing of materials in place

- The length of the heat exchange tower was increased by 15 inches (to 30 inches) to accommodate uncertainties in the reported value for thermal conductivity of the solidified salt. The modified design is suited for values of salt conductivity as low as 0.35 Btu/hr-ft-°F (0.60 W/mK)

- An access port was included in the top cover of the heat exchange module to permit sampling of the solidified salt droplets for subsequent measurement and analysis.

Current Status

As of July 26, 1982 all purchased items had been received except for the liquid metal pump and the refurbished flowmeters. These items should arrive by August 30 and will not impact system assembly. All internal tank module thermocouples (Type K) have been installed and the new tanks are in process of being mounted to the test stand. Final assembly is well underway.

A problem occurred with the initial batch of commercial grade draw salt (Partherm 430), purchased from Park Chemical Co. Various samples were prepared for analysis by a differential scanning calorimeter (DSC). Traces were run both with material in the "as-received" condition and after preprocessing by melting, mixing, and drying. All results differed from published data and indicated a melting point of 290°C compared with the specified 222°C (430°F). Similar samples made from available laboratory chemicals gave much better results, melting uniformly at 222°C.

A theoretical thermodynamic analysis of the draw salt/lead bismuth system indicated a possible reaction, with the formation of lead oxide. Laboratory tests were run for confirmation and to determine the rate of reaction. The as-received draw salt showed evidence of chemical incompatibility when a brownish orange residue appeared within hours after melted salt and liquid metal were mixed together. However, the same tests were negative when run with a laboratory salt mix that had been previously dried at 150°C for 24 hours and kept in an inert nitrogen gas atmosphere.

We are now conducting tests to confirm that the draw salt/liquid metal combination is acceptable when the salt is properly dried and an inert nitrogen cover gas is present . In the event of negative results, the original choloride ternary eutectic salt will be substituted if an alternate salt cannot be found quickly.

Future Effort

The program will be completed before the next reporting period. This includes the following remaining tasks:

- Select a compatible salt suitable for this demonstration
- Complete hardware assembly and system checkout
- Conduct the test evaluation
- Document all program results.

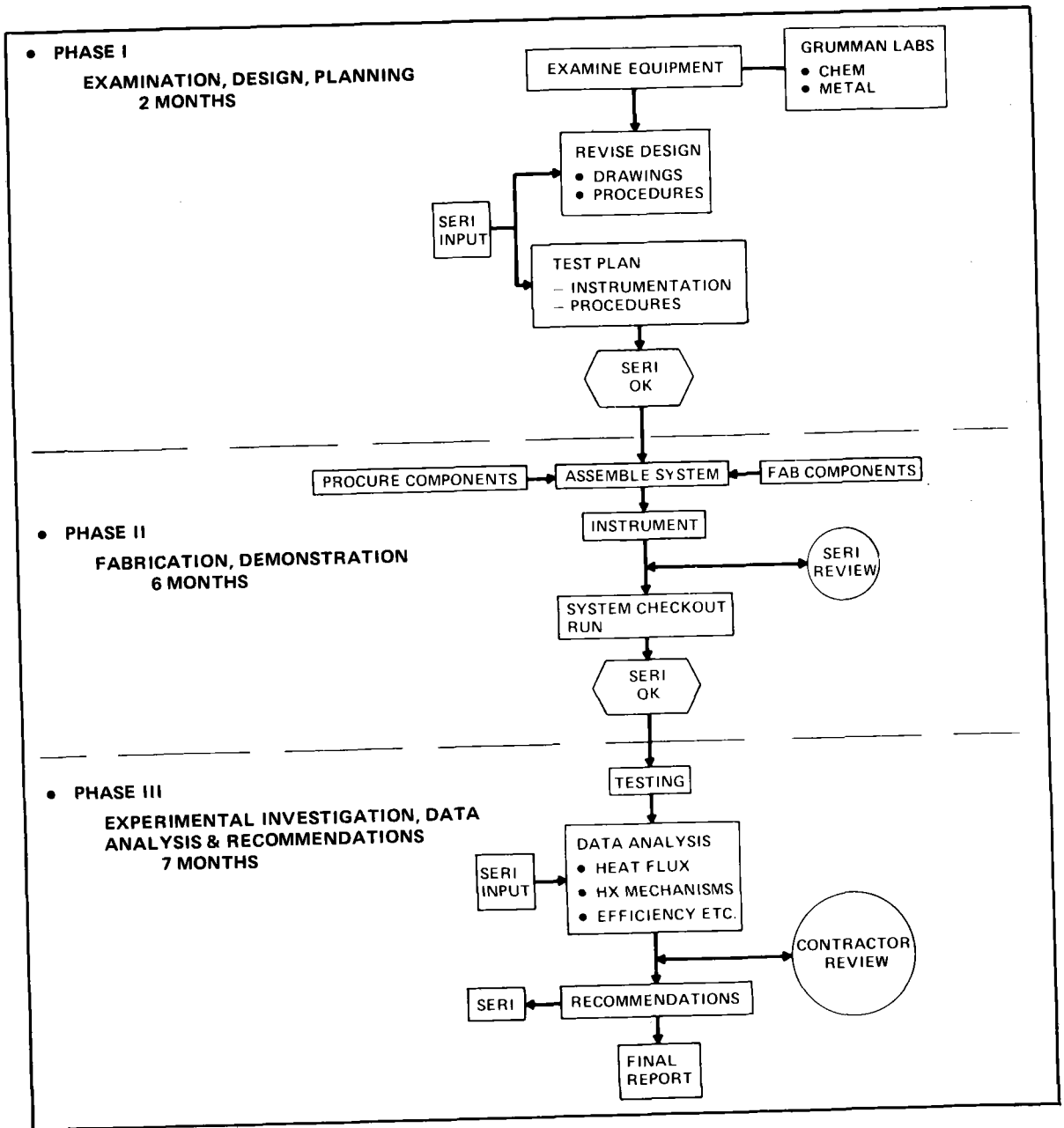

Fig. 1 Follow - On Program Work Flow Plan

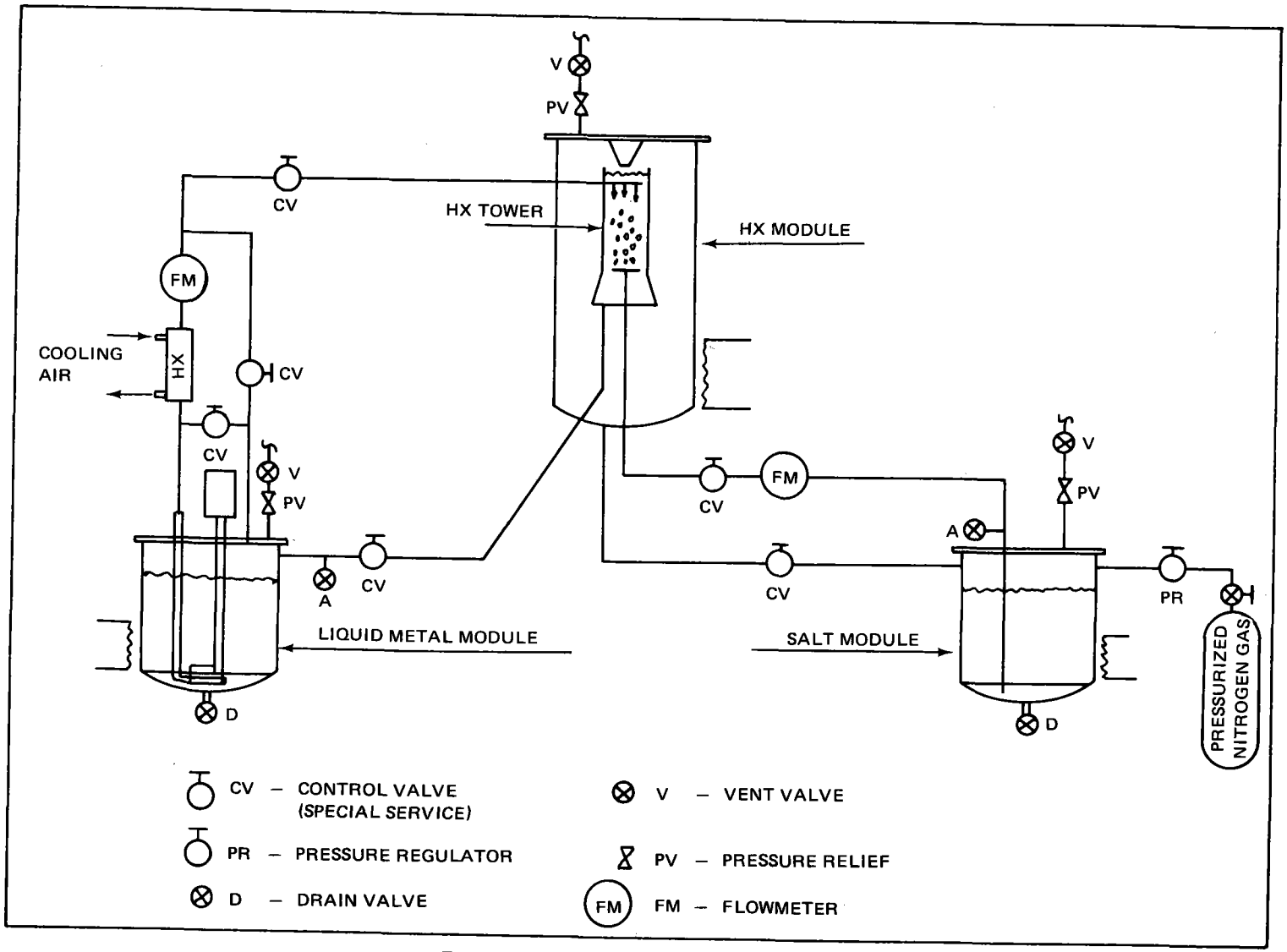

Fig. 2 System Schematic (Hybrid Pumping)

SOLAR THERMAL STORAGE APPLICATIONS PROGRAM
SANDIA NATIONAL LABORATORIES

W. C. Peila
Sandia National Laboratories
Livermore, California

The Sandia National Laboratories Storage Application Program concentrated much of its efforts into two related areas - investigation of storage media and evaluation of storage methods. The resulting matrix included oils, molten nitrate salts, and liquid sodium as storage media candidates (for near-term applications); and single-tank thermocline and dual-tank (hot, cold) storage as method options. Prior to their consideration for solar storage applications, the heat transfer oils and sodium had been quite well characterized as regards their containment, and chemical and physical properties. The nitrate salt data base, however, was considerably leaner when salts emerged as a promising contender for storage applications. To increase this data base, Sandia embarked, in 1978, upon an extensive effort - funded by both the central receiver and storage programs - which included several major experimental and analytical investigations. The program culminated with three major efforts: 1) single-tank oil thermocline storage experiment; 2) a dual-tank molten salt storage experiment; and 3) a detailed study concerning the manufacturing and handling of the large amounts of salts required for a full-scale storage system. All but a few of the salt containment and chemistry experiments are complete, and the salt materials program can be summarized as follows:

1. Nitrate salt degradation is not a problem for solar applications up to 1100°F.

2. An adequate selection of satisfactory containment materials is available.

3. Although all the studies are not complete, we see no major obstacles to solar applications of nitrate salts.

The molten salt storage experiment, shown in Fig. 1, was the culmination of work done during the Molten Salt Storage Program. Conducted over the past three years, this program had dual objectives - to minimize the cost of a molten salt, sensible heat Thermal Energy Storage (TES) system and to resolve the uncertanties associated with the design, fabrication, operation, and performance of a salt TES system.

To meet these objectives, two major work tasks were defined: 1) the preliminary design, including costing and assessment, of a 1200MW_{th} system; and 2) the design, construction, operation, and evaluation of a Subsystem Research Experiment (SRE), which utilized the same design as the TES system.

Following a competitive solicitation, Martin Marietta Corporation (MMC) was selected to carry out this program. Martin's general design approach included:

a. A dual tank sensible heat TES - 550°F cold, 1050°F hot.

b. Hot Tank - internally insulated; leak tight, flexible internal metallic liner; carbon steel shell; water-cooled, concrete foundation.

c. Cold tank - externally insulated, carbon steel shell, water-cooled concrete foundation.

d. Capacity - $7MW_{th}$.

The internal insulation was designed to reduce the tank shell temperatures to a level (550°F) which would allow the use of carbon steel for construction rather than the more expensive stainless or chrome-nickle alloys required for 1050°F use, thus realizing a substantial materials cost savings. The metallic liner prohibited contact of the molten salt with the interal insulation to insure insulating qualities as well as adequate lifetime. The liner, in turn, was required to distribute the hydrostatic loads to the tank shell and accomodate the thermally-induced dimensional changes. This liner then was a critical component; and the design selected by MMC was a patented one from Technigaz of France, who developed and has used it extensively for LNG storage applications. Since all previous experience with the liner was at ambient to cryogenic temperature with little pressure cycling, a small-scale (1 cubic meter) tank was constructed and evaluated by Technigaz, which reproduced all critical design features proposed for hot salt use. Evaluation included tens of thousands of pressure cycles with 1050°F salt, posttest examination of the liner and internal insulation and demonstration of repairability. All phases of the test were successful. Figure 2 is a cutaway view of the SRE hot tank showing how the liner was utilized. The external insulation is not shown.

Specific objectives of the SRE included:

- establishment of tank design criteria
- demonstration of tank fabrication with liner and insulation
- demonstration and evaluation of system operation
- verification and "fine tuning" of performance models
- resolution of uncertainties associated with fabrication, operation, and performance of a full-scale system

The SRE was constructed at the Central Receiver Test Facility (CRTF) in Albuquerque, New Mexico. Figure 3 is an overhead photo of the CRTF showing the 220 sun-tracking heliostats and the 200-foot tall test tower. The SRE was erected just behind and to the left of the tower. Figure 4 is a view of the hot tank, showing the internal liner. Figure 5 is a photo of the completed SRE taken from the top of the tower, and figure 6 is a schematic of

the SRE system. The propane heater simulates a solar receiver and the heat exchanger replaces a turbine. The MMC test activities were completed in April, 1982, and Sandia is continuing to conduct additional performance tests. Data is still being taken and analyzed, but some preliminary conclusions are:

1. A satisfactory design was achieved for the liner and its attachment, and fabrication techniques were developed utilizing existing commercial materials.

2. The hot tank performed close to pretest predictions, and no leaks were encountered.

3. The liner fatigue strength margin seems adequate, but predictions of creep effects have not been accomplished because of the complexity of the liner geometry.

4. Accurate detection and location of liner leaks remains an open issue.

5. Based upon SRE results, MMC projects storage efficiencies for the 1200 MW_th TES systems at >97%, with an estimated cost of \$10 per KW_th.

6. Sandia is presently updating the economics of more conventional stainless steel hot tank designs for comparison with the internally insulated tank. Although a final assessment is not yet available, results to date suggest that potential costs arising from conservatism in design (resulting from the uncertainties of 3 and 4 above), coupled with the skilled labor intensiveness of the MMC hot tank fabrication, may offset the material savings gained by utilizing a carbon steel shell. The Martin Marietta final report on this effort will be published in September, 1982 (SAND80-8192).

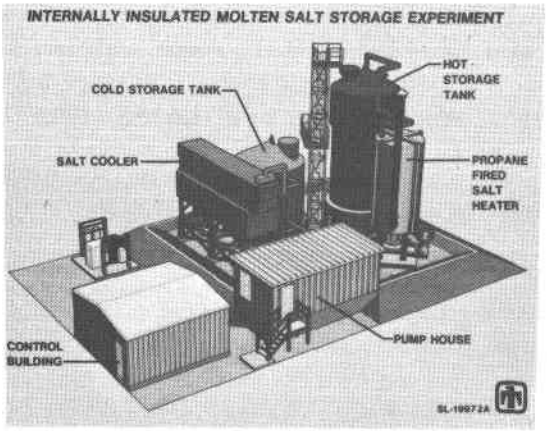

Figure 1

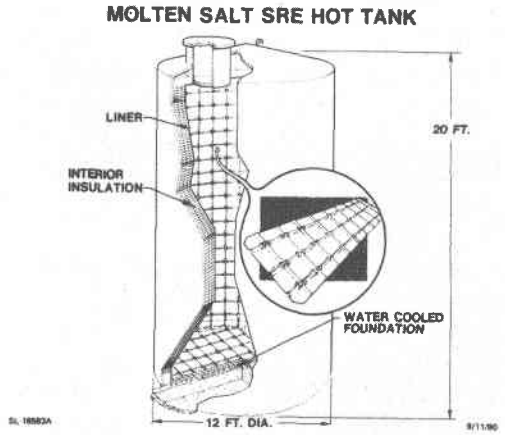

Figure 2

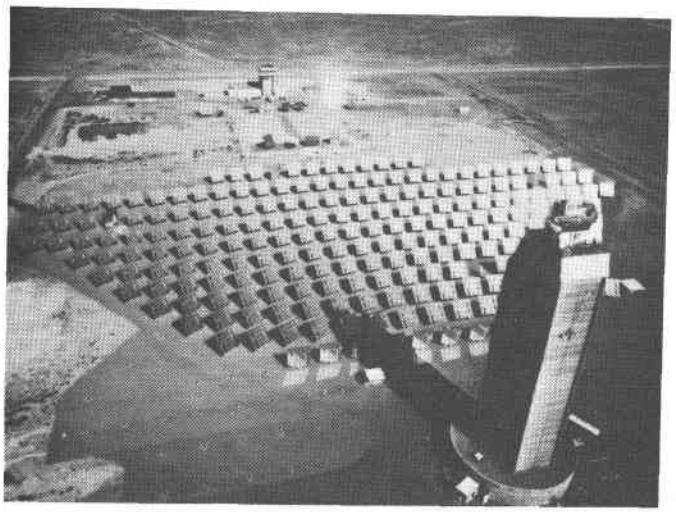

Figure 3 Central Receiver Test Facility

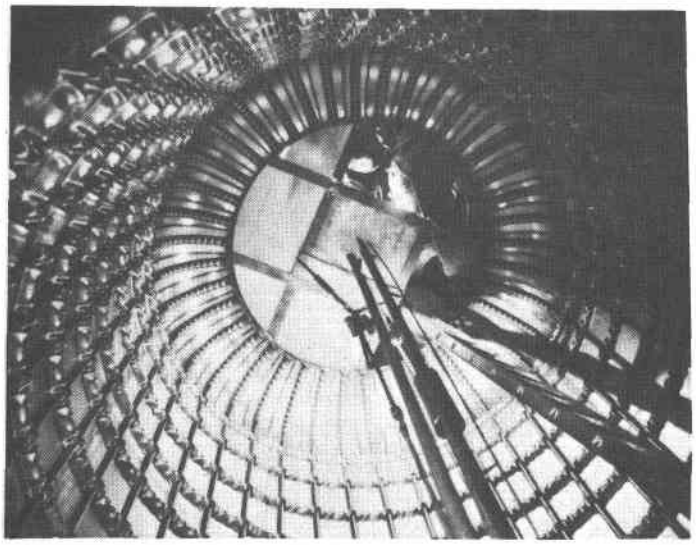

Figure 4 Hot Tank Interior

Figure 5 Molten Salt SRE

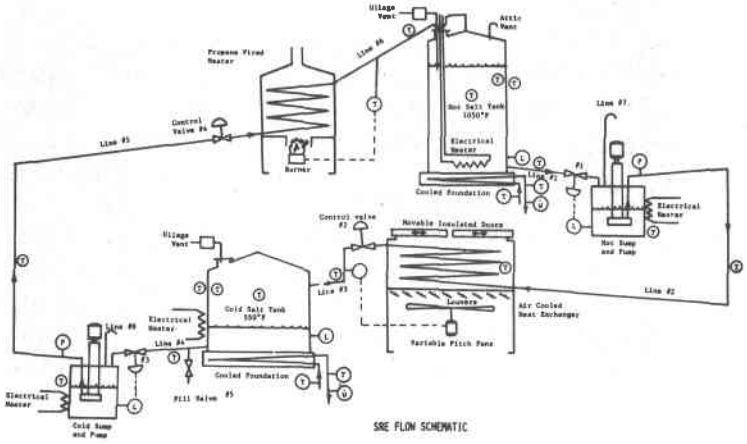

Figure 6

SUMMARY REPORT OF THE STUDY OF SINGLE MEDIUM THERMOCLINE THERMAL ENERGY STORAGE

R. J. Gross
Sandia National Laboratories
Albuquerque, New Mexico 87185

ABSTRACT

Experiments conducted on the 4.54 m^3 (1200 gal) engineering prototype thermocline tank at Sandia National Laboratories, Albuquerque (SNLA) are described. Heat loss tests showed that the maximum heat loss could be limited to 4.8% a day. An effective flow diffuser is presented in conjunction with an accurate method for predicting its pressure drop. Charge and discharge tests yielded sharp thermoclines over a broad flow rate range. The one-dimensional measured temperature distributions led to a one-dimensional predictive model which agreed well with static (no flow) thermocline degradation tests.

INTRODUCTION

Thermal energy storage (TES) can affect the economics either of thermal power systems by load-leveling or of industrial and residential process heat systems by providing thermal energy when a thermal source is not available. Since the thermocline TES concept consists of a single tank storing sensible energy in a fluid, it is one of the simplest of the many thermal storage concepts now available. This simplicity makes the Thermocline Thermal Energy Storage concept attractive as it implies low capital, operating and maintenance costs.

In thermocline TES, hot fluid from the thermal source and cold fluid from the thermal load are both stored in a single tank with natural buoyancy forces acting to keep the two layers separated. However, the attractiveness of thermocline TES hinges on the assumption that the losses which may degrade the energy in the hot upper layer can be minimized. Five loss mechanisms which can decrease the efficiency of thermocline storage, illustrated in Figure 1, are: 1) heat loss to ambient, 2) convective motion induced by heat transfer from the hot layer to the cold layer via the highly conductive tank walls, 3) mixing during charge or discharge when the thermocline region is near the inlet or outlet, 4) thermosiphoning loops in the inlet and outlet manifolds when the tank is in a "static" condition, i.e., no flow, and 5) thermal diffusion from the hot layer to the cold layer. Experiments were conducted at SNLA on an engineering prototype thermocline tank to investigate these loss mechanisms. The tank has a 4.54m^3 (1200 gal) capacity and is instrumented with 384 thermocouples. Therminol-66 is the working fluid. During testing the high temperature (inlet) was nominally 316°C and the low temperature was

nominally 204°C. Figure 2 shows an internal view of the tank and much of the thermocouple placement. Reference [1] contains a more detailed description of the facility.

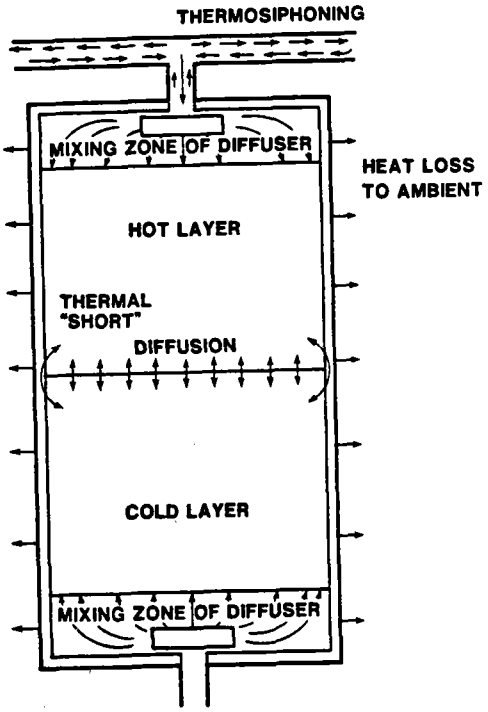

FIGURE 1

The five heat loss mechanisms which decrease the efficiency of a thermocline thermal energy storage system

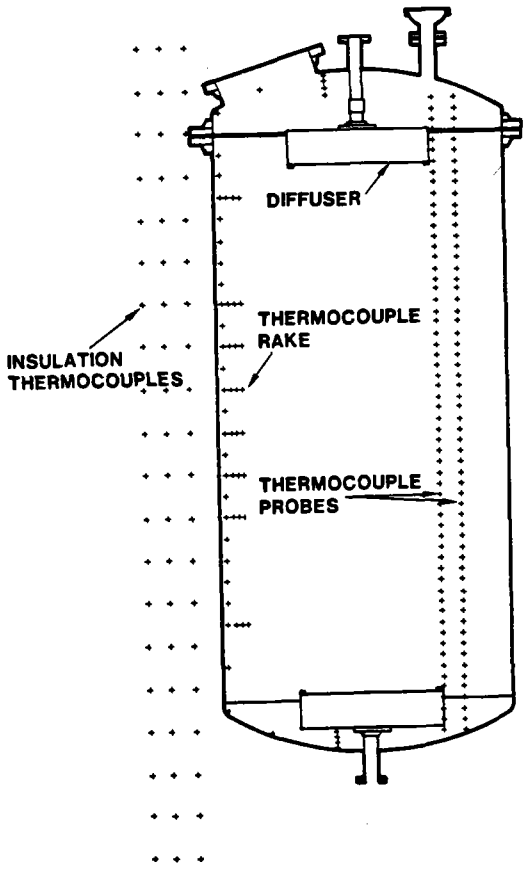

FIGURE 2

An internal view of the large-scale SNLA thermocline tank showing diffuser, internal thermocouples and insulation thermocouples

HEAT LOSS TESTS

Heat loss tests are reported in detail in Reference [2] but are mentioned briefly here for completeness. These tests were performed to determine the overall heat loss of the storage tank to ambient and to verify that the losses were not significantly different than predicted. Previous TES systems tested by SNLA have lost from three to ten times the energy anticipated resulting in lower than expected overall system efficiencies. For this system it was found that the total heat loss could be accurately represented by the simple expression

$$Q_{loss} = Q_{initial}\, e^{-0.00215\ t}$$

where t is time in hours and $Q_{initial}$ is the energy originally available in the tank, given by

$$Q_{initial} = \rho V C_p (T-T_{amb}) \quad ,$$

where ρ is fluid density V is fluid volume and C_p is specific heat of the fluid.

STATIC THERMOCLINE DEGRADATION TESTS

Static thermocline degradation tests were conducted to determine the effect of the 0.48 cm conducting tank wall (carbon steel), thermosiphoning, and diffusion between the hot and cold layers on an in situ static thermocline. A thermocline was developed in the tank by either a charge or discharge flow test. Then flow was shut off and the change of the thermocline (temperature profile) with time was observed. The hot layer was nominally at 316°C and the cold layer at 204°C so that the ΔT between the layers was approximately 112°C in each test.

Figure 3 depicts the initial axial temperature profiles for a case which included thermosiphoning. The horizontal lines crossing the graph near the top and bottom denote the location of the top and bottom diffusers. Experimental points in the figure are spaced 10 cm apart; the line drawn between points is merely to improve readability. Different symbols represent temperatures of the axial probe, inside wall and outside wall thermocouples. The tank was not

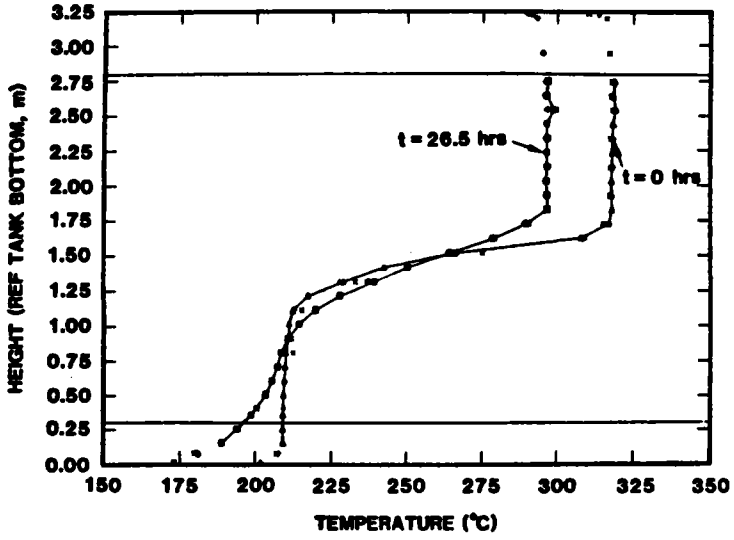

FIGURE 3

Thermocline temperature profiles in the large-scale SNLA thermocline tank initially and 26.5 hours into a static test. Thermosiphoning was present. First curve: Δ, axial probe; +, 0.62 cm from inside wall; x, outside wall. Second curve: ◊, axial probe; ▽, 0.62 cm from inside wall; ☒, outside wall.

fully filled, and thermocouples in the nitrogen ullage space above the fluid level were slightly cooler than the fluid. Figure 3 also shows the temperature profile 26.5 hours after the start of the test. The hot charged upper layer has cooled approximately 17°C and the thermocline region has remained essentially unchanged. The cold uncharged bottom layer has lost comparatively little energy and developed a non-uniform temperature profile characteristic of a diffusion process. Figure 3 is representative of the results obtained from each static thermocline degradation test.

An early hypothesis was that thermosiphoning in the tank's upper manifold was increasing the heat loss in the upper layer and leading to the observed stratification of the lower layer. However, although this process could account for some of the phenomena noted above, there were two discrepancies. First, the cold fluid, by dropping from the manifold, down through the hot layer, to its equilibrium buoyancy position, should stratify the upper layer. Second, the flow rate induced by thermosiphoning was insufficient to cause the magnitude of observed heat loss in the upper layer. In addition, the static thermocline degradation tests were repeated with the upper manifold drained, thus effectively eliminating the thermosiphoning phenomenon. The temperature distributions did not change significantly as compared to the tests with thermosiphoning present. Thus, thermosiphoning was not a major cause of the observed cool-down behavior. In any event, thermosiphoning was minimized in the SNLA thermocline system by insulating the manifold and placing valves near the inlet manifold thus resulting in a short (small heat transfer area) thermosiphon loop.

Another possible explanation for the observed behavior is large-scale natural convection induced by heat loss to ambient and the wall thermal-shorting phenomenon. If this occurred, significant radial thermal gradients in the tank would be observed. Figure 4 shows the radial temperature profiles from 38.1 cm off the tank centerline to a location in the insulation 10.2 cm from outside ambient conditions. Radial profiles at twelve axial locations within the system, ranging from a tank height of 50.8 cm to 274.3 cm, are shown. The curves show an insignificant temperature dependence on the radial coordinate inside the tank. This observation held true for the entire duration of every static test. Therefore, large-scale natural convection was not observed in the SNLA thermocline tank and did not appear to be an important loss mechanism.

The diffusion of heat from the hot layer to the cold layer was reasonable and predictable. This loss mechanism has been amply investigated elsewhere [3] and will not be discussed here.

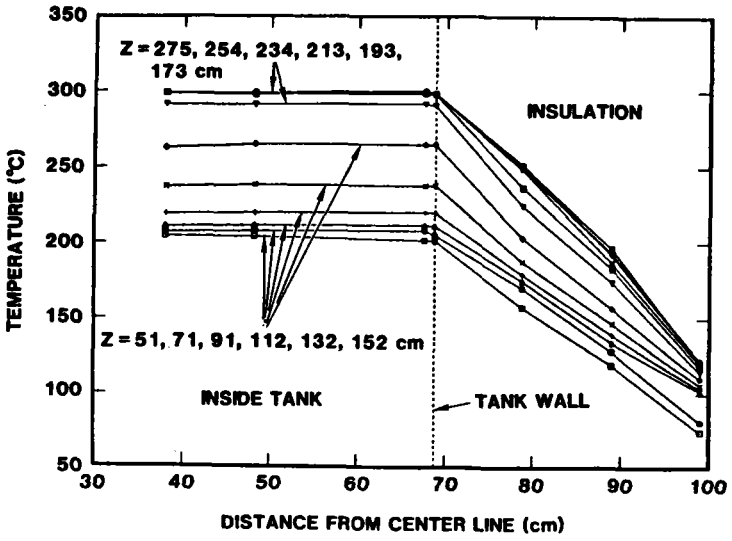

FIGURE 4

Radial temperature profiles in the large-scale SNLA thermocline tank

THE FLOW DIFFUSER

To limit the initial mixing between the incoming hot fluid and cold fluid in the tank, a flow diffuser can be placed in the path of the inlet jet. This device "diffuses" the momentum of the jet and, in the ideal case, changes the high velocity turbulent jet into a slug-like laminar flow over the entire tank cross-section. The diffuser's function, then, is to lay the incoming hot fluid on the cold layer with minimal disturbance. Because significant mixing will occur inside the diffuser, the diffuser volume is the minimum possible volume for the thermocline, thus establishing the minimum thermocline width which can be achieved. Therefore, the diffuser should have a large area ratio (tank area/inlet pipe area) and the shortest possible axial length. It is also necessary that the diffuser operate satisfactorily over a broad range of temperatures and flow rates, be compatible with Therminol-66, and experience a small pressure drop.

A laboratory-scale effort was initiated to investigate various design ideas, test them, choose the best candidate and then optimize the chosen design within the available time frame. A scale model of the final diffuser design placed in the engineering prototype thermocline tank is shown in Figure 5. A detailed description of the device may be found in Reference [2].

An important component of the diffuser design is the perforated plate, which transforms the single high velocity jet entering the tank from the manifold into many small

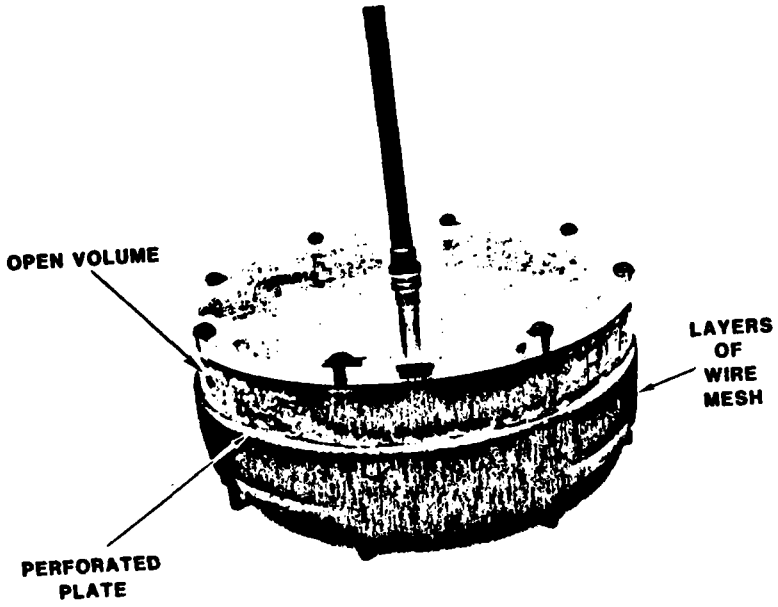

FIGURE 5

Laboratory-scale prototype of the diffuser employed in the large-scale SNLA thermocline tank

jets which are distributed evenly over the diffuser's cross-sectional area. The critical design parameter of the perforated plate is the porosity, which determines the number of distribution points and the pressure drop across the diffuser. The need to have as many holes (high porosity) in the plate as possible to achieve the uniform slug-like flow must be traded off with the need for a relatively low porosity to achieve sufficient pressure drop to force the inlet jet to spread across the entire diffuser diameter. It was necessary, therefore, to know the dependence of the pressure drop on plate porosity, flow rate and fluid viscosity.

The standard equation to compute pressure drop across a perforated plate is

$$\Delta p = \frac{\frac{1}{2}\rho U_o^2}{C_o^2}\left[\frac{1}{\alpha^2} - 1\right] \qquad (1)$$

where Δp is the pressure drop, ρ is the fluid density, U_o is the bulk averaged approach velocity, C_D is discharge coefficient and α is the plate porosity. Usually, all of the necessary flow parameters are known except C_D, which accounts for frictional and other irreversible effects and must be determined empirically.

Guidance for the evaluation of C_D for flow through perforated plates may be found in [4] and [5]. However, the effective range of the published C_D correlation is

limited to a hole-pitch to hole-diameter ratio of five and a diffuser diameter of 38.1 cm. Both of these limits were exceeded in the 66 cm diameter diffuser placed in the engineering prototype tank, where the pitch-to-hole diameter ratio was 24 with a hole diameter of 0.16 cm. Additionally, the experiments in [4] and [5] were performed in air and the resulting correlations showed a weak dependence on viscosity. Since the viscosity of Therminol-66 varies from below 0.4 centipoise at operating temperatures to more than 40 centipoise at start-up temperature, there was concern that the pressure drop in the situation of current interest might be more highly dependent on viscosity.

Pressure-versus-flow tests were conducted on the diffuser placed in the engineering prototype tank. A test series was conducted at 38°C and 204°C to determine the effect of viscosity. Figures 6 and 7 depict the experimental results and also show the curves resulting from Equation 1 where C_D is determined from [4] and [5]. The agreement is excellent, implying that the limitations placed on the C_D correlation of [4] and [5] were too strict, and that no modification of the correlation was necessary for the diffuser porosity, flow rate and fluid viscosity ranges of present interest. Because the pressure drop varies with the square of the flow rate, a compromise must usually be made between the desired flow rate range and the desired pressure drop of the plate. From Reference [8] and our laboratory-scale experiments it appears that a pressure drop of 0.5 to 1.0 psi is necessary to achieve complete spreading of the entering jet to the full diffuser diameter. However, porosities on the order of 0.001 are necessary to obtain even this small pressure drop.

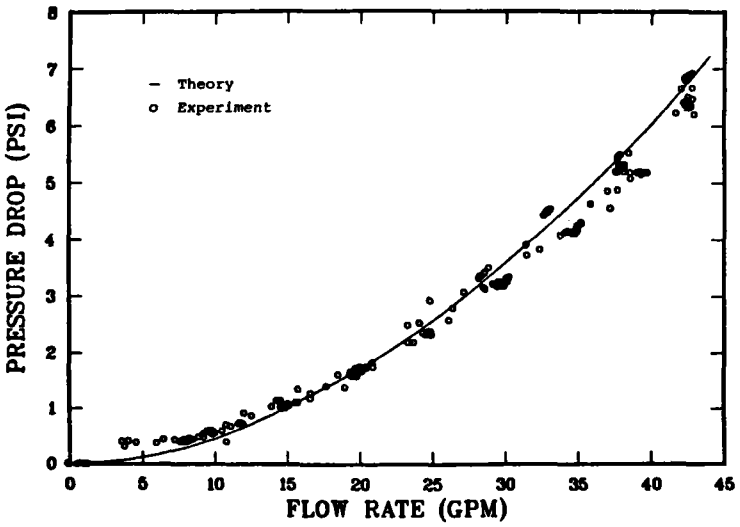

FIGURE 6

Comparison of theory to experimental pressure drop data in the diffuser of the large-scale SNLA thermocline tank, T = 38°C

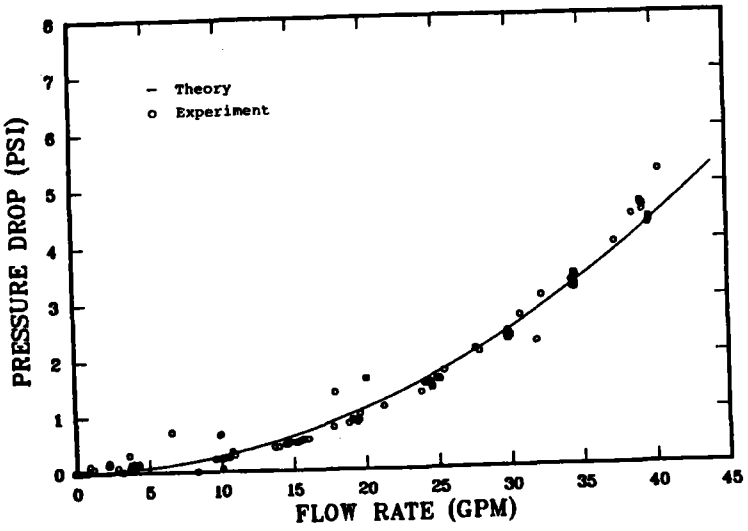

FIGURE 7

Comparison of theory to experimental pressure drop data at 316°C in the diffuser of the large scale SNLA thermocline tank

CHARGE TEST

Two series of charge tests were performed to determine the effectiveness of the diffuser in preventing mixing in the tank, i.e., to establish how "sharp" a thermocline could initially be placed in the engineering prototype tank. On the first test series no diffuser was present while in the second test series a diffuser of the type shown in Figure 5 was used.

The large-scale diffuser used in the second test series was 66 cm in diameter, about half the tank diameter. Although a diffuser which covers the full tank diameter would be the most desirable, considerations such as instrumentation which limited accessibility to certain areas, the difficulty of welding and assembly inside the tank, and size of the access port made the full-diameter diffuser impractical in this system.

For each test, the initial fluid temperature in the tank was a nominal 204°C. Hot fluid at 317°C was then pumped into the tank. The fluid level in the tank, the flow rate and the inlet temperature were held as constant as practical operation of such a large facility allowed. The test procedures called for preheating of the piping loop in order to heat the fluid in the loop, the pipes and the piping insulation to the charging temperature prior to the test. However, the pipe network would always cool down somewhat before charging began.

The fluid level relative to the location of the top diffuser was an important consideration. If the fluid level was such that cold fluid was above the location of hot fluid injection into the system, an unstable situation existed which encouraged mixing, broadened the thermocline region and lowered the efficiency of the system. Thus, comparisons of test results are made only between runs in which the fluid level was comparable.

Substantial mixing occurred in the tests with no diffuser. A typical axial temperature profile for a charge test at 315.5 cm^3/sec (5 gpm) is shown in Figure 8, in which the initial fluid level was 20.3 cm above the inlet level. If the flow rate was kept low and the initial fluid level was near the inlet level, then sharper thermocline profiles were obtained, also shown in Figure 8, in which the thermocline region is about 30.8 cm thick. Distinctly narrower thermocline profiles were obtained from discharge tests than charge tests at the same flow rate, as Figure 9 indicates. Figure 9 also shows that fairly sharp thermocline profiles were obtained at higher discharge flow rates (10 gpm). However, charge tests without a diffuser when the flow rate was 631.0 cm^3/sec (10 gpm) or higher resulted in a thermocline region occupying an unacceptably high percentage of tank volume -- 25% or greater.

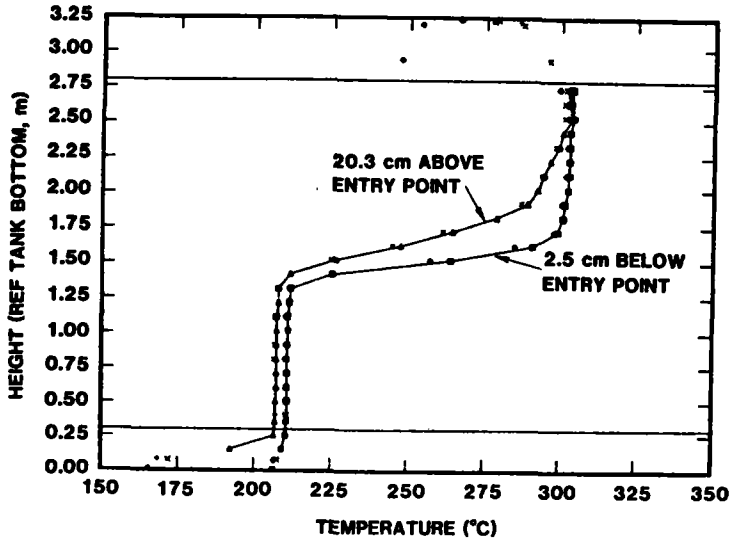

FIGURE 8

Thermocline temperature profiles obtained from 315 cm^3/sec (5 gpm) charge tests at varying fluid levels without a diffuser

Tests conducted with the diffuser in the tank indicated that it was very effective in reducing mixing of the hot and cold layers. However, when the initial cold fluid level was significantly above the diffuser, mixing due to the resulting buoyancy instability was excessive. For example, in a 315 cm^3/sec (5 gpm) charge test in which the

initial cold fluid level was 35.6 cm above the upper diffuser, the thermocline region occupied 187 cm or about 45% of the tank volume.

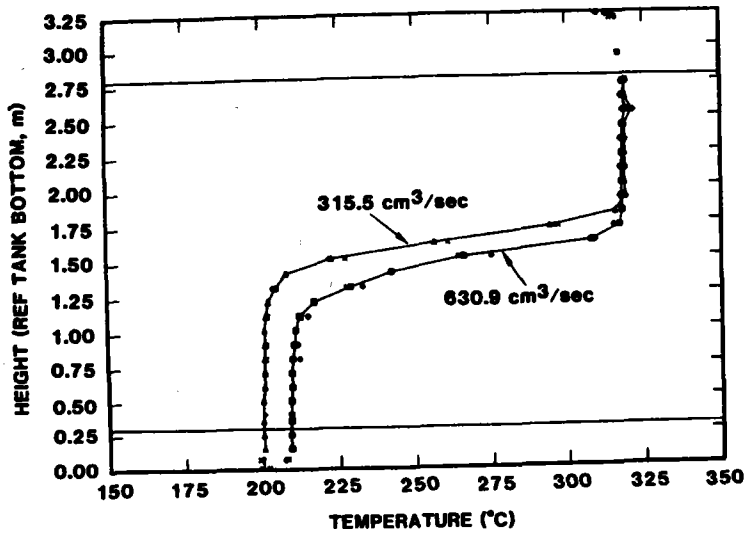

FIGURE 9

Thermocline temperature profiles obtained from discharge test with no diffuser. Fluid level has no influence on discharge test results

On the other hand, when the fluid level was lowered to the level of the diffuser bottom, the temperature profile indicated by the 315.5 cm^3/sec (5 gpm) curve in Figure 10

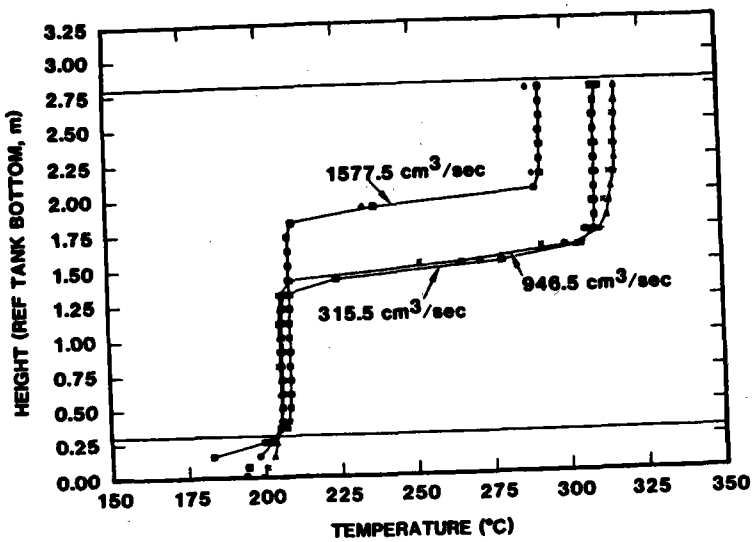

FIGURE 10

Thermocline temperature profiles at varying flow rate obtained from charge tests with a diffuser

was obtained. The thermocline region of this test was 30.5 cm wide. A comparison of this curve in Figure 10 to the comparable curve in Figure 8 reveals that the diffuser made a difference in the initial thermocline thickness, even at low flow rates. However, the difference was more readily apparent at higher flow rate. Figure 10 also shows charge test results with a diffuser at 946.5 cm^3/sec (15 gpm) and 1577.5 cm^3/sec (25 gpm). The thermocline width was almost independent of the flow rate when the diffuser was used.

ONE-DIMENSIONAL MODELING

As mentioned earlier, the static tests showed that thermocline degradation was not explained by thermosiphoning or large-scale natural convection. The radial temperatures were quite uniform from the centerline to 0.64 cm from the inside wall. It then is reasonable to assume that heat transfer through the conducting steel wall and external insulation to ambient is relatively small and, therefore, that the thermal boundary layer is thin. An approach developed by Rahm and Walin (6,7,9) provides a simple one-dimensional analysis of the stratification induced by natural convective flow in a thermocline TES system. The thin boundary layer assumption is incorporated into their analysis. Additionally, the radial heat flux leaving (or entering) the side walls of the specified geometry must be small. The model requires a knowledge of a modified heat transfer coefficient along the side walls of the tank and assumes that the top and bottom are perfectly insulated.

For a cylinder, combining the continuity, momentum and energy equations together with the above assumptions leads to

$$\frac{\partial T}{\partial t} + \frac{2\,\alpha\,S_o}{R}\,(T-\hat{T}) = \alpha\,\frac{\partial^2 T}{\partial z^2} \qquad (2)$$

where T is temperature, $\hat{T}$ is ambient temperature, α is the thermal diffusivity of the fluid, R is the cylinder radius, t is time and z is the axial coordinate. S_o is the modified heat transfer coefficient which represents the ratio of convective heat transfer to conductive heat transfer at the vertical walls of the cylinder. The above equation was solved using an implicit finite-difference technique.

The model was compared with results from the large-scale static tests. Figure 11 shows the measured temperature profile at the beginning of a static test in which thermosiphoning occurred. Also shown is the curve fit to the data used as an initial spatial temperature condition in the model. Figure 11 also shows the experimental and one-dimensional model temperature profiles 22.6 hours later. The model's agreement with the data in the upper hot layer is excellent. However, the cold bottom layer experiences

substantially more diffusion than the model predicts. The modified heat transfer coefficient, s_o, was set to 0.05 cm^{-1} in the simulation to match the overall measured energy loss.

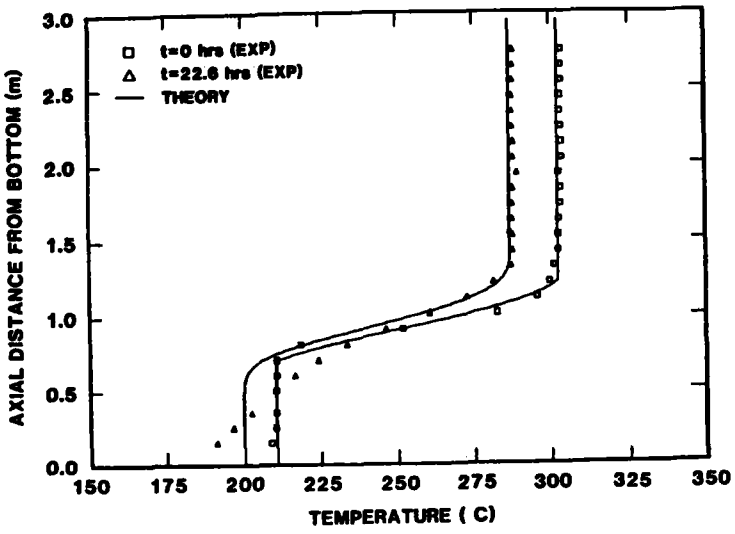

FIGURE 11

Comparison of the 1-D model to experiment at the initiation and 22.6 hours into a thermocline cool down test in the large-scale SNLA thermocline tank. Thermosiphoning was present.

SUMMARY

The heat loss tests demonstrated that the total heat loss from the SNLA large-scale thermocline tank was within acceptable limits for its size. If the entire tank contained fluid at 316°C, 4.8% of the total energy in the tank would be lost in the first day. Thermocline degradation tests demonstrated that the temperature distribution in the tank when in a static (no flow) condition is one-dimensional, implying that large-scale natural convection did not occur. Thus, the effect of the highly conducting walls must be confined to a thin boundary layer near the wall. Since the pipe manifolds in the SNLA system were either drained or valved off such that the length of pipe for the thermosiphon loop was short, thermosiphoning was not an important contributor to heat loss.

A diffuser was developed which prevented mixing between the hot and cold layers during the charge or discharge operation. A relatively simple method of predicting the pressure drop across a performated plate as a function of flow rate and porosity was demonstrated. The method of [4] and [5] was shown to be accurate for evaluation of the discharge coefficient.

Charge tests demonstrated that the point of entry of the hot fluid relative to the fluid level in the tank is

as important as the suppression of mixing in initially establishing a sharp thermocline. The observation of Lavan and Thompson [10] that the thermocline thickness becomes almost independent of the flow rate with a well-designed diffuser in the system was confirmed in a much larger system and for much higher flow rates. A comparison of discharge tests with charge tests showed that without a flow diffuser much less mixing occurs when the jet is opposed by the gravity force vector than when both are acting in the same direction. The radial temperature profile data revealed that the temperature distribution in the tank was essentially one-dimensional. This led to the development of a one-dimensional heat loss and thermocline degradation model using the approach of Rahm and Walin. The comparison of theory to experiment showed good agreement in the hot layer and in the thermocline region.

More thermal diffusion occurred in the bottom layer than the one-dimensional model could predict. Large-scale natural convection and thermosiphoning were unable to account for this effect. We conjecture that a thermal short from the tank bottom to ambient caused excess heat loss from the bottom of the tank, leading to the observed diffusion and stratification. This postulate is supported by the fact that insulating the bottom of the tank proved to be a difficult task, resulting in the greatest nonuniformity and uncertainty in insulation value. Additional information will become available when the facility is dismantled.

With the exception of the unexplained diffusion in the bottom layer, these experiments have quantified the important loss mechanisms in the SNLA large-scale thermocline storage system. In conclusion, it appears that a full-size single-medium thermocline TES system can be an efficient TES concept if sufficient consideration is given to minimizing the five thermal loss mechanisms.

RECOMMENDATIONS

The construction and operation of the SNLA large-scale thermocline facility has not only provided a "proof-of-concept" demonstration of thermocline technology, but also resulted in a considerable experience base. The insight gained from this experience should be useful for future-generation thermocline TES systems. With this in mind the following recommendations and suggestions for future thermocline systems are made.

1. The insulation process must be thorough and meticulous, with as few penetrations into the system as possible. In addition to external insulation, internal insulation such as that in LNG tankers is highly recommended. Internal insulation should be effective in minimizing the thermal short at the tank walls.

2. An effective diffuser which covers the entire tank diameter is desirable. Fluid velocities and pressure drop in the diffuser can be properly scaled such that the same 0.3 m thermocline that occupied approximately 10% of the volume in the SNLA tank would occupy only 2% of the volume of a 15 m high commercial tank. Some provision should be made to keep the top diffuser outlet at the fluid level. Two possible methods of accomplishing this are a level indicator coupled to a motor which can mechanically raise or lower the diffuser or a diffuser designed to float on the fluid surface.

3. Thermosiphoning can and should be eliminated or minimized by placing a valve as close as possible to the tank, building U-type thermosiphoning "traps" in the entry lines, or draining the upper manifold when the storage system is placed in a static condition for any length of time.

4. It may be possible to considerably reduce the diffusion of heat from the hot layer to the cold by the inclusion of a floating, insulating piston. The buoyancy of the piston would be fixed such that it always remains in the thermocline region separating the two layers.

If the above items were incorporated into a thermocline TES system and proved effective, all of the known loss mechanisms associated with thermocline TES would have been eliminated or reduced to a small quantity. In this case, thermocline thermal storage would be a most efficient means of storing thermal energy. In essence, the thermal storage subsystem would consist of a single tank containing two isolated, well insulated compartments whose variable displacement could meet the transient needs of a thermal system.

REFERENCES

1. R. J. Gross, "An experimental Study of Single Medium Thermocline Thermal Energy Storage", presented at the AIAA/ASME Fluids, Plasma, Thermophysics and Heat Transfer Conference, St. Louis, MO, June 7-11, 1982.

2. R. J. Gross, "Single-Media Thermocline Thermal Energy Storage", DOE Thermal and Chemical Storage Annual Contractor's Review Meeting, McLean, VA, September 14-16, 1981.

3. T. Brumleve, "Sensible Heat Storage in Liquids", Sandia National Laboratories, Report No. SLL-73-0263.

4. P. Smith and M. VanWinkle, "Discharge Coefficients Through Perforated Plates at Reynolds Numbers of 400 to 3000", Amer. Inst. of Chemical Engineers Journal, 4 (1958) pp. 266-268.

5. P. Kolodzie and M. VanWinkle, "Discharge Coefficients Through Perforated Plates", Amer. Inst. of Chemical Engineers Journal, 3 (1957) pp. 305-312.

6. L. Rahm, G. Walin, "Theory and Experiment on the Control of the Stratification in Almost Enclosed Containers", J. Fluid Mech., 90 (1979) pp. 315-325.

7. L. Rahm, G. Walin, "On Thermal Convection in Stratified Fluid", Geophys. Astrophys. Fluid Dynamics, 13 (1979) pp. 51-65.

8. G. Walin, "Contained Non-Homogeneous Flow Under Gravity or How to Stratify a Fluid in the Laboratory", J. Fluid Mech., 48 (1971) p. 647-672.

9. Z. Lavan and J. Thompson, "Experimental Study of Thermally Stratified Hot Water Storage Tanks", Solar Energy, 19 (1977) pp. 519-524.

MANUFACTURE, DISTRIBUTION AND HANDLING OF NITRATE SALTS FOR SOLAR THERMAL APPLICATIONS

L. C. Fiorucci, S. L. Goldstein
Olin Corporation
Chemicals Group
275 Winchester Avenue
New Haven, Ct. 06511

Based on their low cost and attractive physical properties, molten sodium/potassium nitrate salts have been shown to be one of the most cost-effective fluids for heat absorption and thermal energy storage in Solar Central Receiver (SCR) systems.

This report is intended to provide the potential user of sodium/potassium nitrates with information relevant to the availability, transport, handling, and utilization of these salts for commercial-size SCR applications. It provides an overview of existing manufacturing processes for natural and synthetic nitrates; the up-stream availability of raw materials; downstream existing and projected demand for these products in other sectors of the economy; and relevant handling and distribution technologies. Also reviewed are safety considerations and issues more directly related to the SCR facility, such as initial system charging, salt maintenance and regeneration, and disposal. Options for supply, surge storage, and initial charging are discussed for the 1 MWt to 300 MWe range of solar plant sizes. (1)

A. Salt Availability

The Chilean sodium nitrate is refined from crude ore deposits and is produced in large quantities. Similarly, the Chilean nitrate mixture of $NaNO_3$ and KNO_3 is produced in large quantities by upgrading the crude sodium nitrate with potassium chloride, thus producing a fertilizer grade of nitrates.(2) Ore reserves are expected to be adequate to meet volumes of salt required by solar plant construction.

However, salt purity in Chilean products may pose a problem for SCR use. Work by Martin Mairetta shows that chloride and hydroxide impurities in the salt can reduce the corrosion resistance of containment alloys in nitrate salts. They conclude that nitrate products should have chloride levels below 0.5% (preferably below 0.25%) and hydroxide levels at or below 0.5%. (3) A survey of Chilean products, revealed that chloride levels for both agricultural and industrial grades exceed the recommended 0.25%. The values are 0.72% and 0.64% respectively. Similarly, the Chilean mixed product of $NaNO_3/KNO_3$ contains chloride as high as 1.0%. These products may not be good candidates as for Solar Thermal Power Plants.

Synthetic sodium nitrate produced by Olin Corporation in Louisiana is a high purity material having 99.4% $NaNO_3$ and a maximum of 0.25% chloride. The capacity of this production facility is currently limited to solar by the demand of other markets. The owner/operator of a new Solar Central Receiver Plant would be able to receive sodium nitrate from Olin in required quantities if advance notice is given. If in the future, a large demand develops for nitrate salts for Solar Receiver Plants, Olin would consider expanding capacity to more easily

meet these needs. Raw material availability is not a concern. The recommended specifications are given in Table I. (4)

TABLE I

Nitrate Salt Specifications

Component	Limits, %
KNO_3	39.2 ± 0.5%
$NaNO_3$	59.6 ± 0.5%
Cℓ	0.30
SO_4	0.23
CO_3	0.11
Alkali	0.10
OH	0.21
H_2O	0.50
Al_2O_3	0.03
Ca	0.03
SiO_2	0.02
Fe	0.01
Insoluble	0.10

In addition to producing sodium nitrate, Olin Corporation has developed processes and products which provide both sodium and potassium nitrates in the ratio (60% $NaNO_3$/40% KNO_3 by weight) required by SCR plants. The product has trace amounts of impurities and is identified as Olin Solar Nitrate Salt.

Synthetic potassium nitrate is produced by Vertac Chemical in Mississippi and is available in several grades. (5) Vertac, like Olin has limited capacity due to developed markets which are already being served. However, the raw materials and energy required for production of synthetic KNO_3 are adequate for anticipated initial demands placed by solar applications. The product quality ranges from 96.7 to 99.4% KNO_3, with different levels of $NaNO_3$ and sulfate. The chloride levels may vary for all synthetic grades. High purity technical crystal product (99.4%) is currently recommended because the levels of impurities are very low. The standard agricultural grade (96.7%) may be acceptable for solar use: the principal "impurity" in agricultural grade KNO_3 is sodium nitrate (up to 2.7%) which is of no consequence when it is used in a mixture of $NaNO_3$ and KNO_3, but the impurity levels may be higher than those recommended by corrosion rate test work. Vertac would not guarantee the assay for agricultural or industrial products beyond the K_2O and nitrogen contents, and that the agricultural grade is not available to industrial markets.

In general, as raw material, energy, and manufacturing costs rise, the prices of the nitrate salt products are expected to rise slightly. It is somewhat difficult to predict price increases in a variable economy.

B. Safety

Although nitrate products are oxidizers and can be found in explosive formulations, they are safe if handled and used properly. In considering their use in Solar Central Receiver Plants, they pose no major problems in either dry or molten form. Any concern about them can be removed by proper safety awareness in storage, handling, transportation, and end use. The practices currently used to store, handle, and transport dry nitrate salts provide adequate safety to the environment and personnel using them. If an emergency should arise involving nitrate salts, established procedures are implemented and the problem placed under control.

There is extensive user experience with molten nitrate and nitrite salts both in heat treating and process applications. Both good engineering design and product use awareness minimizes any danger from use of a high temperature fluid. The operating and safety records of both industries are very good.

C. Handling

The standard practice used in the chemical industry to handle, store, load, transport, and unload bulk chemicals are well suited for the quantities needed for Solar Central Receiver Power Plants. Although options exist for handling large quantities of salt, mechanical conveying systems serve best. The product is moved at high speed, completely protected from contamination, and experiences the least damage.

The shipment of dry nitrate salts is done in closed containers-bags or drums for small quantities, and covered hopper cars or tank trucks for large bulk quantities. These means are adequate for the wide range of quantities required by different size Solar Plants.

While shipment of molten nitrate salt in tank car containers is possible, it may not be economical due to the extra cost of special tank cars for high temperature service. Another problem exists with the chance that en-route delay of the car may cause the contents to solidify before arriving at the solar site.

D. Charging

Any large quantity of nitrate salt scheduled for Central Receiver Service should be ordered well in advance, and the product

stored for charging. The storage of product at the user's site provides protection for the salt quality and physical form; it also provides adequate charging inventory and protection against transportation strikes. If a Solar Plant has an adequate charging inventory (30 days minimum), outside problems should pose little threat to the charging operation. Planning is important.

Over the past 30 years, many process plants using molten nitrate salts for heat transfer have been charged by conventional procedures. These procedures include direct melting of crystalline salt, or the use of a water dilution technique. (6) Both systems work well, although the water dilution system has served best for small plants. The quantity of nitrate salts used for large (e.g., 300 MWe) Solar Thermal Power Plant would require considerable energy to melt. As an alternate to using a fossil-fueled melter, solar-assisted can be used for charging a Solar Central Receiver Plant once a suitable starting inventory has been established with conventional fossil units. The use of solar heating to charge the balance of a Solar Plant may result in a saving of both charging time and energy costs.

E. Plant Operation

Process plants utilizing nitrate salt mixtures have used standard industrial practices to prevent freezing of salt in line and storage vessels. These practices include electric or steam heat tracing of piping, exchangers, and storage tanks. Also vital to heat tracing is the use of insulation to reduce heat loss from the traced equipment. During brief shutdowns, molten salt may be left in lines or components which have adequate heat tracing, or drained back to storage. Salt would normally be drained to storage during more extended shutdowns or certain types of emergency transient conditions.

Another option during extended shutdowns is to reduce the salt freezing point using water dilution methods.

Upon start-up, the plant piping and components would be preheated by steam or electric tracing to a temperature well above the melting point of the salt mixture (typically 550°F for a 60/40 salt mixture with a melting point of 435°F). Then the "cold" (e.g., 550°F) salt would be pumped through the loop to maintain the minimum temperature. Solar heating of the salt would then be applied slowly, raising the "hot" salt output temperature to its design level. If small quantities of salt should freeze in the lines, the heat tracing system can slowly melt the salt or other external sources of heat can be applied. A major concern with thawing of salt plugs is thermal expansion of the melt phase, which may cause undue stress and busting of components. During melting, caution should be taken to allow the

melt to flow away from the solid mass. Water and/or steam applied directly to the salt involved in a major pipe line plug will dissolve the salt easily. Water can be evaporated and the salt reused.

Over the years, some industrial users of molten nitrate salts have experienced problems when the salts are exposed to carbon dioxide and water. These problems may develop when a cover gas is not used to protect the salt. The formation of hydroxides may change the melting points of the process salts. Carbonates may precipitate out onto heat exchanger surfaces, reducing heat transfer characteristics. Hydroxides may cause increased corrosion of the containment material. If such species should develop in the molten salt, technologies exist today to treat contaminants and make the salt more suitable for the process. (7) These technologies include additions of nitric acid, nitrogen dioxide, or calcium nitrate. The products of these reactions involve nitrate salts, carbon dioxide, water, calcium hydroxide, which usually leave the system by gas evolution or precipitation.

If the salt should leak from the molten circulating system, an analysis of contaminants should be made. From this analysis, a decision can be made for disposal: i.e., direct disposal in landfill: re-use in the Solar Plant, or in metal heat treating, or as a fertilizer; or heavy metal removal; and disposal. If the salt is contaminated with hexavalent chromium, it must be treated before being disposed of as fertilizer. A process exists to reduce hexavalent chromium to trivalent, and remove it from the salt.

Finally, after a 30 year operating life, a SCR Plant may be decommissioned, and it would be advantageous to recover some value from inventory of molten salt. Options include treatment for heavy metal removal, re-sale to the fertilizer market, landfilling, or reprocessing into a transportable form for shipment to another Solar Plant. (8)

References

1. L.C. Fiorucci, S. L. Goldstein, "Manufacture Distribution and Handling of Nitrate Salts for Solar Thermal Applications", SAND 81-8186, June 1982.

2. R. D. Crozier, "Chilean Nitrate Mining", Mining Magazine, Mining Journal Publishing Co., September 1981.

3. Martin Marietta Corporation, "Alternate Central Receiver Power System, Phase II," Vol. III, Sandia Contract No. 18-6879C, March 1981.

4. Martin Mairetta Corporation, Request for Quotation December 1981.

5. M. L. Spealman, "New Route to Chlorine & Saltpeter", Chemical Engineering Reprint, McGraw Hill, New York,1965.

6. American Hydrotherm Corporation, New York, N.Y., Process Data Sheet No. 16, October 1967.

7. Olin Corporation, Chemicals Group, Private Communication, 1981.

8. Olin Corporation, Chemicals Group, Private Communication, 1981.

OAK RIDGE NATIONAL LABORATORY THERMAL ENERGY STORAGE PROGRAM OVERVIEW*

James F. Martin
Engineering Technology Division
P.O. Box Y, Bldg. 9204-1, MS-3
Oak Ridge, Tennessee 37830

ABSTRACT

Oak Ridge National Laboratory is the Lead Technical Laboratory for DOE in the areas of thermal energy storage technology development for building heating and cooling and industrial applications. The program of technical assessment and research and development is carried out in support of the national objective of energy conservation and development of new energy sources. The activities supported by this program in FY 1982 are described. The major thrust of next year's program is given.

INTRODUCTION

The Oak Ridge National Laboratory (ORNL) acts for the Department of Energy (DOE) Office of Energy Systems Research, Division of Energy Storage, as Lead Technical Laboratory in prescribed areas of Thermal Energy Storage (TES) technology development. The ORNL program is structured to fully support the national objectives of energy conservation and development of new energy sources through development of TES technology. The two program major thrusts are building heating and cooling and industrial applications. The objective of the program is to conduct the research and development which is required to establish a base technology for reliable, low cost, high performance TES systems. Such systems make feasible the use of thermal energy sources whose times of availability are significantly disparate with their times of use, thereby greatly increasing the opportunities for national energy conservation. This objective is pursued in a number of generic research and development and technical assessment areas which are chosen on a priority basis from the structure illustrated in Figure 1.

This matrix of project areas provides for selection of specific projects which support the most promising technology areas. The selection is made with further restrictions of keeping within budget constraints and maintaining program continuity. During FY 1982, twenty-six projects were supported, these are listed in Table I. The majority of these projects are reported in the proceedings of this conference.

*Research sponsored by the Division of Physical and Chemical Energy Storage Systems, U.S. Department of Energy contract W-7405-eng-26 with the Union Carbide Corporation - Nuclear Division.

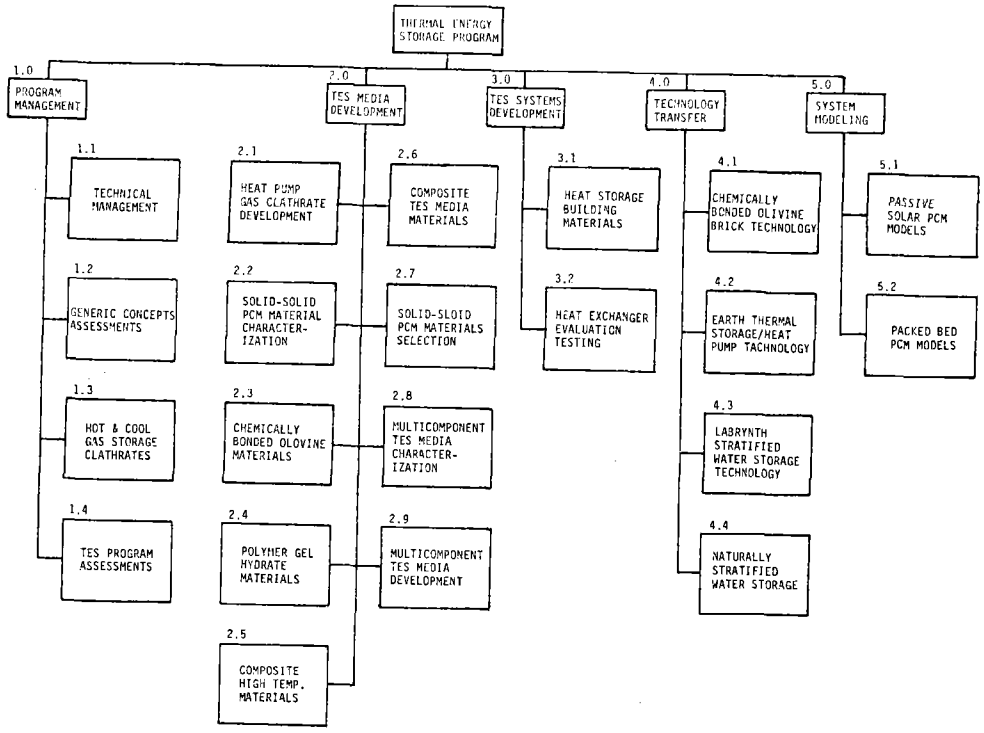

Figure 1. Thermal Energy Storage Program Work Breakdown Structure

TECHNOLOGY ASSESSMENTS

Seven projects may be characterized as technology assessments. They comprise activities which provide inputs to program planning and direction through definition of storage concepts and identification of promising areas of research. An important goal of assessment activity is the definition of the state-of-the-art of storage technology, thus enabling evaluation of proposed research from a proper perspective.

The several projects which address the state-of-the-art of TES are:

A critical review of the state of salt hydrates has been completed by the ORNL Chemistry Division. A report of the study discusses the nature of non-ideal behavior of salt hydrates and reviews the literature of R&D in application of salt hydrates to thermal energy storage. It is concluded that further research is needed in the areas of basic kinetics of crystal growth, prediction of phase behavior in ternary systems, and the influence of non-equilibrium temperature gradients on composition gradients.

ANL has completed an analysis of field test data on the use of electric furnaces with thermal storage for off-peak charging. The study examines the performance and cost effectiveness of such units under residential

heating service in Maine and Vermont. The general conclusion is that home owners were pleased with the units' adequacy in heating the houses but that a price in energy usage must be paid for shifting the utility load to off-peak times.

Franklin Research Center completed a survey of operational, non-solar TES systems in commercial buildings in the U.S. and Canada. Descriptive information on 201 installations has been assembled in a report which will be issued by ASHRAE this year. The survey found general satisfaction with the systems. The majority of responses showed a lack of quantitative data to determine the performance and the economic benefits of the installations.

Decision Research Group is engaged in a study of generic TES applications in the industrial sector. The objectives are the definition of system performance requirements in terms of total energy stored, heat rates, storage temperatures and efficiencies, and identification of economic constraints imposed by the values assigned to the particular usage of the recovered energy.

New York State ERDA has completed the test of storage CHUBS used as cool storage for residential air conditioning. A final report is in the publication process. The question of partial storage wherein an undersized air conditioner is supplemented by off-peak charged storage drying high cooling requirement, on-peak times, is addressed. The economics of such a system in a high rate differential area are found to be marginally attractive.

Other assessment activities are aimed at assigning technical goals to candidate storage systems through analysis and computer modeling.

Mathematical modeling is an important prerequisite to development of a TES system. It allows one to identify the relative value of the physical parameters and provides input to the process of setting system performance goals. A passive solar room computer code has been developed at ORNL for the purpose of identifying the value of incorporation of PCMs into building materials. Various configurations of PCM-enhanced building materials were studied by applying an equivalent room comfort temperature criteria to the daily performance of the sytem. Preliminary results indicate that room temperature fluctuations are reduced and that the benefits of massive heat storage systems can be achieved with the much smaller volumes associated with PCM storage. Parameters of importance were identified as the placement of the building material in the room, the placement of the PCM in the material, the PCM thickness, and its melting temperature. While additional questions need to be addressed, the basic guidelines developed for PCM incorporation in a passive solar room indicate the feasibility of this concept.

Mathematical modeling also serves the function of extending the range of applicability of experimental results beyond the immediate experiment. Work has continued on a model of heat transfer to and from the earth for the purpose of predicting the value of earth storage assisted heat pumps. Simulations of steady state air flow conditions have been validated by experimental data. The incorporation of variable conditions representing heat pump cycling in the model is now being addressed.

Experimental studies of the moving boundary problem were continued both at Kalamazoo College and the University of Tennessee. The experiments at Kalamazoo consist of laboratory scale tests of the transport processes at the melting/freezing boundary. A laser beam deflection technique of measuring thermal gradients has been developed to study the contribution of thermal gradients in the liquid phase to the melting process. The experiments by the University of Tennessee are aimed at measurements of thermal convection effects on the freeze/melt boundary when the plane of the heat source is oriented vertically.

RESEARCH AND DEVELOPMENT

Five major areas of TES research and development were pursued this year. The first is R&D in phase change storage materials.

Three projects addressed basic research in PCM storage materials. One effort by Pennwalt Corporation was directed towards development of a process of pelletization and roll-encapsulation of phase change materials. Four PCMs were successfully encapsulated in 1.27 cm pellets and withstood thermal cycling equivalent to a 10-20 year operational life.

Calmac Corporation completed an experimental study of the effects of additives to hypo and a Glauber salt eutectic. Calor gel showed promising results in mitigating the incongruent melting problem of Glauber salt. Ethylene glycol and glycerine were effective in depressing the melting temperatures of the salt hydrates, thereby providing a means of tailoring the phase change temperature for a specific application. An unfavorable decrease in the heat of fusion also results from adding either of these two materials, however.

The ORNL Chemistry Division has conducted exploratory studies of possible new materials for thermal storage. There are a vast number of chemical systems which have properties with a strong dependence on temperature. Although the associated transitions do not necessarily involve large enthalpies, their existence implies that substantially enhanced heat capacities on a volume basis may be involved. Systems which have, or which chemically similar analogs have, such behavior are being experimentally surveyed by differential scanning calorimetry. Initially, systems which remain in a single liquid phase at all temperatures were looked at because of avoidance of phase transition problems and of a more favorable heat transfer environment. The investigation has been widened to solid-liquid and solid-solid transitions.

Lockheed Missiles and Space Co. is conducting an experimental program to develop a wallboard material containing PCM for passive solar buildings. Channeled polypropylene boards filled with calcium chloride hexahydrate have been initially selected for laboratory testing. Thermal cycling and vapor transmission tests are being conducted. Tests will also be conducted on polycarbonate panels and with lithium nitrate trihydrate PCM. Techniques for heat sealing the panel channels are being investigated by several plastics manufacturing companies. Two other tasks are also included. An applications

analysis to identify specific passive solar building industry opportunities will be conducted, and an economic model will be developed to assess the wallboard system in comparison with conventional sensible heat storage systems.

A second R&D area is the development of high temperture storage materials for industrial applications. An ongoing project to develop a high temperature storage media is being conducted by the Institute of Gas Technology. A survey and assessment of the potential for TES in brick/ceramic industries (SIC-32) has led to an estimated 50% fuel savings over current sensible heat recovery practices. The objective is to develop a material suitable for storing the heat contained in 700 to 900°C flue gases from periodic kilns. Development is directed at a composite carbonate salt/ceramic containment material which will allow direct contact heat transfer from the hot gas to the storage material. The PCM is supported and immobilized within the submicron sized capillary structure of the particulate ceramic matrix. A 50-50 weight percent mixture of sodium carbonate - barium carbonate, which has a melting temperature of 710°C, has been selected as the PCM. The ceramic matrix is magnesium oxide. Pellets are made by compression and sintering of spray-dried powders of the constituents. They have shown compression strengths of 300 psi and liquid retention on thermal cycling of less than 1.5%. The research is generic in nature in that it is applicable to a number of other carbonate salts forming storage materials with a range of transition temperatures of 400 to 900°C. The technology will, therefore, be applicable to a broad range of high-temperature, industrial applications in the metallurgical ceramic and refractories industries.

The third R&D area of the program is development of advanced sensible heat storage technology. Four projects were active in the solid sensible heat area. All were concerned with development of heat storage bricks for electric storage furnaces. This area of storage technology has given sufficiently promising results that the private sector has shown a strong interest in its application.

The University of Washington has developed a successful method of making friction ram-pressed, cement-bonded bricks of Washington State olivine. The process requires only low temperature brick curing, thereby reducing the manufacturing energy requirements greatly from that of presently used ceramic heat storage bricks. Material Consultants Associates is midway through a companion project of developing low-cost bricks from North Carolina State olivine. The vibratory-assisted casting manufacturing process differs from the University of Washington project as does the range of binding materials being investigated. The addition of high heat capacity aggregates to increase volumetric heat capacity and the casting of resistance heating elements into the brick itself are now being studied.

The University of North Carolina completed an experimental program of cycling high quality ceramic bricks manufactured by the University using North Carolina State olivine. Extensive data were taken on temperature distributions within the furnace and in individual bricks. The mechanical properties of these bricks were shown to compare favorably with those of European manufacture. Testing of commercial storage furnaces for efficiency and of bricks in storage furnace use was continued throughout this year at Purdue University. The extensive results of this program, both in the area of testing technology and in brick performance, are incorporated in a final report which is under preparation.

Stratification of hot and cool water to allow energy storage in a single tank with maximum useful heat extraction is the subject of four projects. A theoretical study of stratification has been completed by Argonne National Laboratory. A critical Richardson number affecting interface stability was identified and confirmed by laboratory tests. The University of New Mexico is conducting tests of use of a labyrinth in storage tanks to restrict interface mixing. Tests of a membrane separation system in a public school building installation by the University of Tennessee were only partially successful due to severe design deficiencies in the heating/cooling system in which the thermal storage is incorporated. Finally, tests of a multiple level inlet/outlet storage tank system are being conducted in a public school building by Research Triangle Institute in a cooperative DOE/North Carolina Alternate Energy Corporation program.

Three projects address heat pump storage systems. Research Triangle Institute (RTI) has completed an economic and technical assessment of a wide range of heat pump/phase change thermal storage systems in residential heating and cooling applications. The thirteen most promising configurations were modeled and their cost, performance, and load factors determined for three climate conditions. Optimum systems based upon a life cycle cost analysis were identified for various utility time-of-day rate structures. The study shows that storage heat pump systems can reduce both on-peak and total energy use. Cost and system design factors that require development to make storage heat pumps economically competitive with conventional systems were identified.

In-house research has been conducted on the use of gas clathrates as storage media for cool-side heat pump storage. Clathrates formed with water and the heat pump refrigerant provide one solution to the direct contact heat exchange problem, thus allowing storage without the heat pump working fluid temperature penalty imposed by a storage heat exchanger. Freon clathrates can be formed in the ideal cool storage temperature range around 7°C, thereby providing a second benefit to the heat pump system. Preliminary experiments have resulted in formation of clathrates and provided encouragement for more detailed studies of a practical heat pump cool storage system.

A program conducted by Carrier Corporation was terminated after the initial tasks of survey of cool storage experiments conducted in the U.S. and the identification and classification of technical problems with equipment and operational strategy. A report summarizing the survey conclusions and the preliminary control strategy developed for establishing the proper daily ice inventory required was issued.

The earth thermal storage project has confirmed, via tests of two configurations of the crawl space heat pump against a control house, that seasonal performance of a heat pump is increased in the heating mode. Summer data are being taken to complete the overall assessment of this convenient form of thermal storage.

Two district heating projects were carried out by Rocket Research Company. They are performing a technical and economic assessment of thermal energy storage opportunities for one site among the series of district heating sites which are included in the HUD district heating program.

The other project is an experimental evaluation of a subscale heat exchanger installed in the Intalco Aluminum Plant. This test will be concluded at the end of this fiscal year. This also represents the conclusion of federal support to the Bellingham District Heating Program.

FUTURE PROGRAM THRUST

The purpose of the TES program is to perform research and development (R&D) in critical high risk technology areas and to transfer the results of the R&D to the private sector such that advanced high performance TES system products may be developed and marketed for specific applications. It is the economics of using TES systems that drives research into higher performance TES media and associated TES system components. Attaining the improved economics and system performance characteristics requires the FY 1983 R&D program to address the following problem areas:

- Resolution of the heat transfer problems associated with charging and discharging TES systems.
- Resolution of the thermal problems associated with attaining appropriate TES storage temperatures.
- Resolution of the thermodynamic problems associated with attaining appropriate TES system storage densities and discharge temperature qualities.

The use of TES media materials which undergo a change of state (such as change of phase, structure, or chemical composition) at the desired discharge temperature are fundamental to obtaining the required heat storage densities and discharge temperature qualities. Ongoing R&D has indicated that the following types of materials may be used to address the storage temperature and heat transfer requirements:

- Clathrates (gas hydrates) for storage temperatures (7°C and 49°C) suitable for hot and cold storage/heat pump applications.
- Phase transition materials for passive solar applications (21 to 27°C).
- Multi-component, high-temperature phase change materials for use in direct, as well as indirect, contact storage systems for industrial applications (200 to 800°C).

The FY 1983 program will see initiation of projects aimed at developing both these materials and the TES systems which make use of their storage potential. Besides emphasizing R&D in these areas, tasks will be pursued in the three support areas of System Development, System Modeling, and Technology Transfer.

In the later area, four prospective opportunities for implementation of technology developed under the DOE program are being pursued. TPI Corporation, a manufacturer of thermal storage bricks and Olivine Corporation

of Bellingham, WA, a manufacturer of industrial incinerator lining material, are looking seriously at the new low energy fabrication processes for olivine bricks being developed by the University of Washington and Materials Consultants Associates under the TES program. Discussions have been initiated with American Electric Power for incorporation of sample bricks supplied by the TES program into their ongoing field experiment of off-peak electric storage furnaces.

Interest in the PCM pelletization process and in making use of a product resulting from the technology has been evidenced by the Concrete and Masonry Association for application to enhancement of concrete storage capacity and by several manufacturers of commercial solar storage components for buildings.

EPRI has proposed a follow-on effort to the TES program sponsored by the University of New Mexico experiment in water stratification which will be completed this winter. The work contemplated will extend the experimental study of the effectiveness of the various engineering methods of maintaining stratification in both hot and cool water storage.

Table I

TES Programs Active in FY 1982

Project Category	Subcontractor	Title of Project
3.3.2	University of New Mexico	Performance of a Labyrinth - Stratified Water Storage System
3.3.1	University of Washington	Development of Unfired Olivine Heat Storage Bricks
3.3.1	Materials Consultants Associates	Development of Castable Olivine Heat Storage Bricks
3.3.1	Purdue University	Standard Testing Procedures for Electrically Heated Storage Furnaces
3.4.1	ORNL	Freon Clathrate Cool Storage Research
3.3.2	Argonne National Laboratory	Natural Thermal Stratification Technology
3.1.2	Lockheed Missiles and Space Co.	Passive Solar Building Materials
3.1.1	Calmac Manufacturing Corporation	Evaluation of Additives to PCM
3.4.2	ORNL	Evaluation of Earth Storage-Assisted Heat Pump
3.2.1	Institute of Gas Technology	Development of Composite Sensible Latent High Temperature Heat Storage Media
3.5	Rocket Research Corp.	Heat Exchanger Technology for Industrial Waste Gas Steam
2.1.2	Decision Research Group	Study of Generic Industrial TES Requirements
3.3.2	Research Triangle Institute	Performance of Naturally Stratified Water Storage Systems
3.3.2	University of Tennessee	Performance of Membrane Stratified Water Storage System

Table I cont'd

Project Category	Subcontractor	Title of Project
3.1.1	ORNL	Basic Chemical Studies Related to Low Temperature TES
2.1.3	Kalamazoo College	Experimental and Analytical Studies of Moving Boundary Problem With Convection
2.0	ORNL	Critical Review of the State of the Art of Salt Hydrates
2.1.3	ORNL	Analytical and Computer Modeling Support of TES Program
3.1.1	Argonne National Laboratory	Pelletization and Encapsulation of Phase Change Materials
2.2	New York State ERDA	Evaluation of Storage CHUBS in Residential Cooling
2.0	Franklin Research Center	Survey of Non-Solar TES Installations in Commercial Buildings in the U.S. and Canada
3.3.1	North Carolina State University	Evaluation of Olivine Refractories for Electric Storage Furnaces
2.1.2	Argonne National Laboratory	Analysis of Residential Thermal Storage Field Experiment Data
3.4.1	Research Triangle Institute	Simulation and Evaluation of Heat Pump/TES Configuration
3.5	Rocket Research Company	Site-Specific District Heating TES Assessments
3. .1	Carrier Corporation	Development of Residential AC Ice Storage System

PERFORMANCE OF LABYRINTH-STRATIFIED WATER STORAGE TANKS FOR HEATING AND COOLING

M. W. Wildin
Department of Mechanical Engineering
The University of New Mexico
Albuquerque, New Mexico

ABSTRACT

The feasibility of storing heating or cooling capacity in thermally-stratified water contained in rectangular concrete tanks has been demonstrated in this project. For the approximately cubical tanks and for the flow rates employed, thermoclines about three feet thick were routinely established during charging and discharging phases of an operating cycle. Initially, vertical internal partitions were installed in the tanks during construction to prevent direct streaming from inlet to outlet and to maximize the active fraction of storage volume. However, it was found that these partitions were unnecessary, and, furthermore, they leaked water, so they were eventually removed. Also, the original blunt inlet/outlets were replaced with linear diffusers designed to introduce water into the tanks and remove it at low velocity and with a relatively uniform distribution. These diffusers were located at diagonally opposite horizontal corners of a tank.

Tank performance was evaluated in terms of the ratio of integrated capacity delivered by storage during discharging to that supplied to storage during charging. This ratio was termed thermal efficiency and was evaluated for periods long enough that changes in internal energy of storage could be neglected relative to total energy flow to and from storage. The efficiency realized from cooled storage was in the range from 80 to 90 percent, while that for heated storage was in the range from 65 to 84 percent with the most frequent value being near 70 percent. The higher efficiency of cooled storage is due to several factors, including lower temperature differences to produce energy flow across the boundaries. Evaluation of the performance of cooled storage using tanks with no internal partitions is being performed in the 1982 summer cooling season.

INTRODUCTION

The previous report on this project identified the importance of stratification in liquid thermal storage, the nature of the storage system being monitored, the heating and cooling system which it serves, the monitoring system used to collect data and some promising results obtained after modifying the internal components of one of the tanks (Reference 1). To summarize this report briefly, thermal storage in this system was accomplished by use of up to eight poured, reinforced concrete tanks which are approximately cubical, i.e., 3.6 m (11.8 ft) by 4.2 m (13.6 ft) in cross section and 4.6 m (15 ft) in depth. Energy recovered from the building at the cooling coils during one day was retained in cooled storage until early the following day, when it was transferred to heated storage by means of water-to-water heat pump/chillers. The heat pump/chillers are of the reciprocating type with electric motor drive. They were operated only during the off-peak

hours of the electric utility system. Also, any excess solar energy collected one day was stored overnight for use the next day. Thus, use of thermal storage in the heating season accomplished two functions, energy conservation through heat recovery and electric load management. In the 1981 cooling season, up to six tanks were charged with cooled water during off-peak hours to accomplish load management.

Relatively continuous results were obtained from the computer-based monitoring system starting in January 1981 and continuous data on electrical energy use were obtained by an independent recording system with battery back-up starting in February 1981. The first data on behavior of thermal storage were obtained in the fall of 1980, when the storage was cooled. These data indicated that chilled water introduced through the low inlet at the bottom of the right-hand compartment was leaking through the internal partitions into the bottoms of the other two compartments (Figure 1). This early observation of water leakage was confirmed by subsequent data on both heated and cooled storage. It was found that such leakage had a more deleterious effect on the performance of heated storage than that of cooled storage (Reference 1). It was concluded during the first half of 1981 that the direction change passages should be redesigned to eliminate water leaks, to reduce heat transfer through the walls of these passages and to increase the velocity of flow through the passages. These measures were employed to increase the Reynolds number and to decrease the Grashof number, so that forced convection, rather than mixed forced and free convection, dominated the heat transfer process in the passages. A prototype of the redesigned direct change passage was installed in the summer of 1981 between the middle and right-hand compartments of one of our tanks, designated Tank No. 6, which was heavily instrumented and used as an experimental tank. Also, a linear inlet/outlet diffuser designed to produce uniform emission or withdrawal of water at a low velocity near the bottom of the tank was fabricated and installed in the right-hand compartment. Initial operation of this tank as a cooled tank indicated that the thermocline moved through the direction change passage with only modest distortion. These early results are illustrated by the plots in Figure 2, which are reproduced from Reference 1. Due to the presence of the original partitions and direction change passage between the middle and left-hand compartments during the first year of this project it was not possible to quantitatively evaluate the effects of the design changes on tank performance during that period.

EVOLUTION OF TANK STRATIFICATION SYSTEM

Because of the promise indicated by the temperature distributions displayed in Figure 2, the other half of Tank No. 6 was modified in essentially the same way early in the second year of the project. A test run on November 20, 1981 using Tank No. 6 with all modifications in place indicated that the thermocline in a heated tank during charging was preserved, even after moving through two compartments and two direction change passages (Figure 3), although some broadening occurred. This tank was operated as the sole heated tank throughout December, 1981 with an unusually high monthly thermal efficiency of 84

percent. Additional detailed observation of thermocline behavior occurred in early January; the results from a charging-discharging cycle on January 3 are shown in Figures 4 and 5. In this test, the heat pump charged storage for 3 hours (Figure 4); and this was immediately followed by discharging for about 6-1/2 hours (Figure 5). Discharging was discontinued early, since the test was performed on a Sunday. Two major features of the data in Figure 4 are noteworthy. One is that a thermocline about three feet thick formed in the left-hand compartment and moved into the middle compartment with little distortion. Charging ceased before the thermocline moved into the right-hand compartment, so the effects of the second direction change passage cannot be determined. The second feature is that warm water leaked from the top of the middle compartment into the top of the right-hand compartment, as indicated by higher temperatures at the top of one compartment and lower temperatures at the top of the other compartment. The plots in Figure 5 also have two major features. One is that the thermocline broadens a great deal during its passage back into the left-hand compartment (right side of plot). The second is that another thermocline forms in the right-hand compartment due to return water from the heating coil being cooler than the water initially in this compartment. The second thermocline involves a temperature difference of only about 7°C, but the Richardson number for this thermocline is 16.2, corresponding to stable stratification, as indicated by the shape of the thermocline (2).

A second tank, designated Tank No. 5, was modified by installing the new linear inlet/outlet diffusers and a new direction change passage of the same design as used in Tank 6; but only one direction change passage was used in this tank. One of the original pairs of internal partitions was removed to produce one narrower and one wider compartment (Figure 6). This was done to help determine whether a larger distance between the inlet and outlet would produce poorer thermoclines than a shorter distance. Tank 5 was initially charged on January 5, 1982 and was operated as the only heated tank throughout the rest of January and for the first 17 days of February. This period included the coldest weather experienced during the past two heating seasons; yet a single tank sufficed to heat the building. The results obtained from operation of Tank 5 were generally favorable. As shown in Figure 7, it was possible to produce and maintain a narrow thermocline during charging. The width of the thermocline is indicated by the data for positions 1 through 14, which are located in the larger compartment on the right side of Figure 6. (The absence of evenly-spaced temperature sensors near the bottom of the smaller left-hand compartment produces the deceptive appearance of a broad thermocline in this compartment.) The thermocline continued to be relatively narrow during the early portion of discharge, as indicated in Figure 8 for the period 06:00 through 08:00. It is not possible to determine the distortion produced by movement of the thermocline back through the direction-change passage, due to the lack of temperature sensors near the bottom of the left-hand compartment, but it appears that some spreading occurred. The results for performance of Tank 5 in terms of thermal effciency were less favorable than those in terms of

temperature distribution. The thermal efficiency of Tank 5 for the 27 days of January in which it functioned was 69 percent, and for the first 17 days of February the efficiency was 75 percent. These values would be higher if such a large fraction of solar energy collection had not occurred on weekends. In January this fraction was 43 percent and in February it was 40 percent. The longer residence time in storage of solar energy collected on weekends increases losses from storage and reduces its thermal efficiency. If solar energy collected on Saturdays were neglected, for example, the two efficiency values given above would both increase about 10 percent. This illustrates the very important point that the thermal efficiency of storage depends strongly on the operating pattern used to charge and discharge storage as well as the behavior of the flow through storage and the insulation of the storage envelope. It should be evident that the longer the residence time of capacity in storage, the larger are the storage losses.

It was decided to remove both sets of internal partitions from Tank No. 6 prior to further testing, for two reasons. One was the good results for thermocline shape obtained in Tank No. 5. The other was the fact that the modified partitions had developed leaks, as noted above. It was reasoned that if good stratification could be obtained in a tank with no partitions, this would simplify the modifications to be performed to our remaining tanks in preparing them for the 1982 cooling season. It was thought that if the behavior of the thermocline with no partitions was not satisfactory, it would be possible to produce suitable behavior by installing a single partition in the middle of the tank. So Tank No. 6 was modified by removing the partitions while retaining the linear inlet/outlet diffusers. Initial operation of this configuration of Tank No. 6 occurred on February 18, when it was charged with hot water at a relatively high flow rate of 100 gpm over a period of only three hours, but with an unusually large temperature difference across storage of 19°C. The corresponding Richardson number was 23.6. It may be observed from Figure 9 that a thermocline thickness of about 3 feet was realized throughout the charging period. It is not evident from the data presented, but there was no evidence of hot water breaking through the thermocline or streaming toward the low outlet until the leading edge of the thermocline was within 15 inches of this outlet. The exact location of the thermocline relative to the outlet when streaming began cannot be obtained from our data, but within 15 minutes after streaming began, the only significant horizontal temperature gradient evident in the tank was at the six inch level. Thus there was little unused tank volume or "dead space".

Due to the good thermocline behavior exhibited in the heating test, it was decided to check the behavior of Tank 6 with no internal partitions for chilled water storage. The initial test of Tank 6 as a cooled tank was performed on March 18. The Richardson number was 12.9, corresponding to a flow rate of 66 gallons per minute. A thermocline thickness of about two feet was observed in this test, but the temperature of the coldest water below the thermocline remained significantly above the temperature of the inlet water. The water below the thermocline gradually mixed with incoming water and its temperature dropped

nearly uniformly and steadily from 8°C to 5.5°C. The latter temperature was about 1.5°C above the inlet temperature at the end of the test. Subsequent tests have confirmed that good stratification occurs in a chilled water tank during both charging and discharging, and that the difference between the temperature of the inlet water and that of the coldest water in the tank decreases as the flow rate through storage decreases. For flow rates of about 30 gallons per minute or less, this temperature difference drops to about 0.5°C. For the unusually high flow rate of 131 gallons per minute, corresponding to a Richardson number of 4.8, which occurred during a test of Tank No. 6 on June 19, 1982, a sharp, stable thermocline formed as shown in Figure 10, but its formation occurred further into the tank than for lower flow rates, resulting in a larger mixed region near the inlet. This is consistent with Sliwinski's results (2) and with results obtained from scale models, reported recently by Baines (3).

CONCLUSIONS

Satisfactory thermocline behavior can be obtained in our water tanks with no internal partitions and with linear inlet/outlet diffusers which introduce or withdraw water at low velocity and relatively uniformly across a tank. Overall Richardson numbers corresponding to stable thermocline formation can be realized for storage of both heating and cooling capacity, for flow rates through storage consistent with charging periods of as low as two hours. However, for chilled water storage, the higher the flow rate the greater is the temperature difference between inlet water and water below the thermocline. A similar phenomenon does not occur during charging with hot water, apparently due to greater buoyancy forces. Our results appear to be consistent with those of others, and the principles our results illustrate should be applicable to other sizes and configurations of storage tanks.

REFERENCES

1. M. W. Wildin, "Performance of Labyrinth-Stratified Water Storage System for Heating and Cooling," Proceedings of the Thermal and Chemical Energy Storage 1981 Annual Contractor's Review, U.S. Department of Energy, Washington, DC, September 14-16, 1981.

2. B. J. Sliwinski, A. R. Mech and T. S. Shih, "Stratification in Thermal Storage During Charging," International Heat Transfer Conference, Toronto, 1978.

3. W. D. Baines, W. W. Martin and L. A. Sinclair, "On the Design of Stratified Thermal Storage Tanks," Technical Paper No. 2728, presented at ASHRAE Annual Meeting, June 30, 1982, Toronto, Ontario.

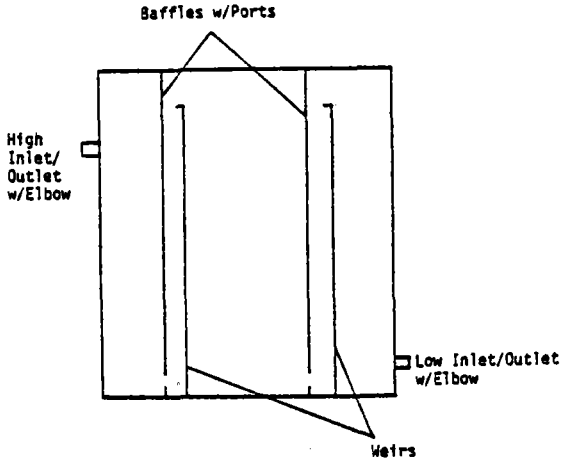

Figure 1. Section of Typical Storage Tank Showing Original Internal Partitions.

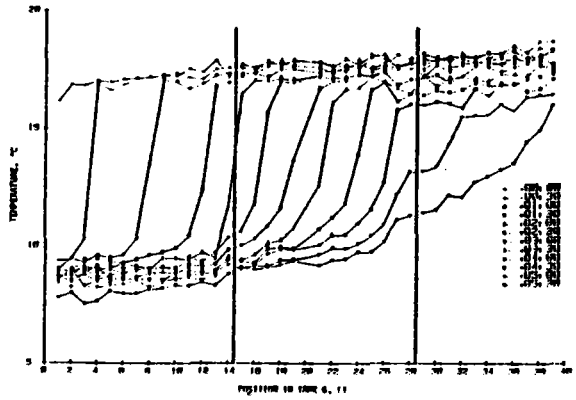

Figure 2. Temperature Distributions in Tank 6 During Charging with Chilled Water, 20 July 1981.

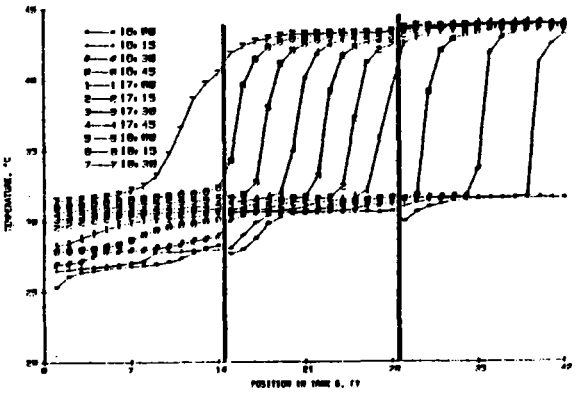

Figure 3. Temperature Distributions in Tank 6 with Redesigned Inlet/Outlets and Direction Change Passages During Charging with Hot Water, 20 November 1981 (95.1 gpm).

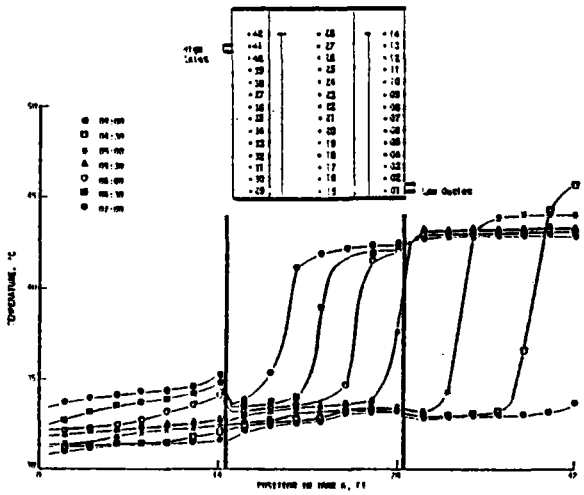

Figure 4. Temperature Distributions in Tank 6 During Charging with Heat Pump, 3 January 1982 (61.1 gpm).

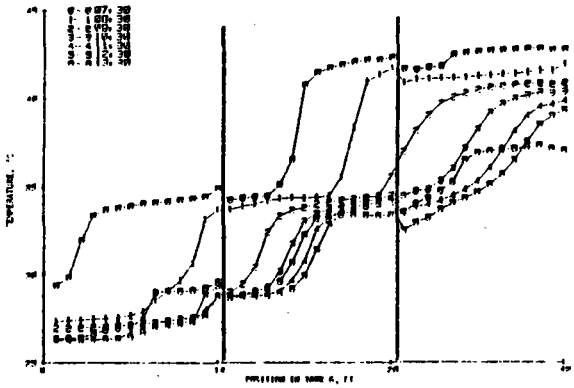

Figure 5. Temperature Distributions in Tank 6 During Discharging to Heating Load, 3 January 1982.

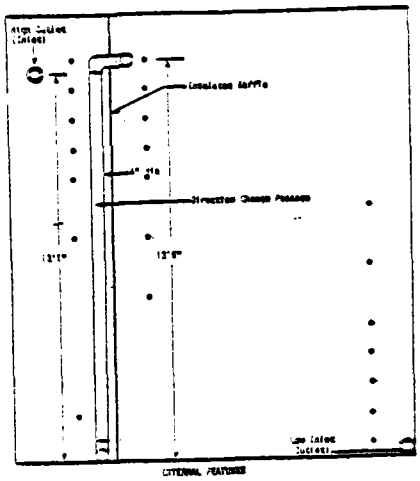

Figure 6. Section of Tank 5 with One Partition and Redesigned Inlet/Outlets and Direction Change Passages, Showing Temperature Sensor Locations.

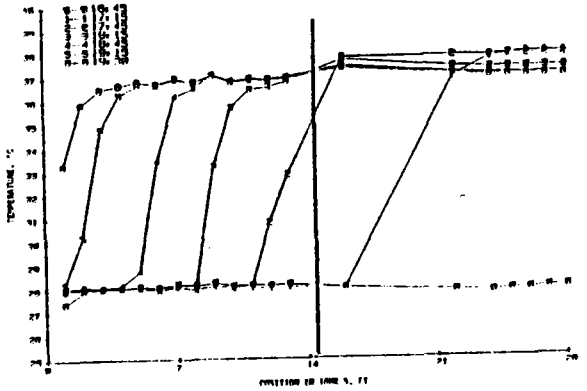

Figure 7. Temperature Distributions in Tank 5 During Charging with Hot Water, 14 January 1982 (100 gpm).

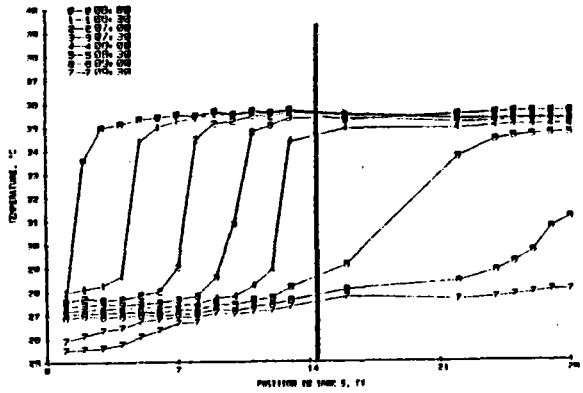

Figure 8. Temperature Distributions in Tank 5 During Discharging, 15 January 1982 (86.1 gpm).

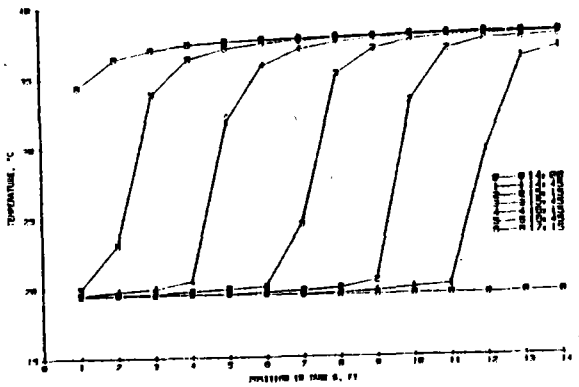

Figure 9. Temperature Distributions in Tank 6 with No Partitions During Charging with Hot Water, 18 February 1982 (100 gpm).

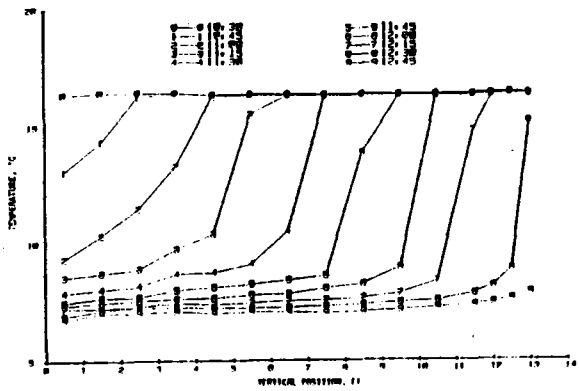

Figure 10. Temperature Distributions in Tank 6 with No Partitions During Rapid Charging with Chilled Water, 19 June 1982 (131 gpm).

UNFIRED OLIVINE BRICKS FOR TES

O. J. Whittemore
Ceramic Engineering, FB-10
University of Washington
Seattle, WA 98195

Introduction

Olivine is a ferromagnesium silicate mineral occurring in a number of locations in the world. Commercial deposits are being mined in Norway, North Carolina and in Washington where the Twin Sisters mountain range (southwest of Mt. Baker) consists principally of olivine (1). Olivine bricks for thermal energy storage (TES) are being produced in Germany, Great Britain and in Tennessee.

Olivine is particularly useful for TES because of the following reasons:

(1) Low cost. The mineral requires only mining and crushing and little beneficiation before processing into TES brick.

(2) High heat storage capacity. Only magnesia refractories have slightly higher volumetric heat storage capacity. However, magnesia refractories are either made from sea-water magnesia or from magnesite ($MgCO_3$) either of which require high temperature calcining before processing into brick. Large magnesite deposits occur in Washington (2) and Nevada but are not now mined because the refractories produced from them are not suitable for the high temperature now used in steel production.

(3) No crystallographic inversions. Some refractories, e.g. silica, experience large volume changes during heating and cooling due to inversions which would cause destruction during TES cycles.

(4) Refractoriness. Olivine refractories are capable of use above 1400°C.

Olivine TES brick are now being produced by adding small amounts of clay, compacting into bricks and firing at 1200°C or higher (3). The purpose of this project was to develop an olivine composition which could be compacted into dense bricks, and simply dried or cured at low temperatures to obviate the expensive firing process.

Experimental Procedures

Compositions were studied by mixing solids in a laboratory mixer, adding in water, then pressing into 6 x 1 x 1 inch test bars in a hydraulic press at 52 MPa (7500 psi). After curing at some desired temperature, the bars were broken in a 3-point beam test and moduli of rupture calculated. Densities were measured from volumes determined by linear measurements and weights. Strengths (moduli of rupture) and densities were the criteria for the development and will be stated in MPa and g/cm^3 respectively.

Olivine Sizing

Olivine used (Olivine Corp., Bellingham, WA) was blasted from bedrock and crushed to desired sizes. Several lots were obtained, crushed to pass 6-mesh, 4-mesh, or 1/2 inch. In addition, olivine fines, 180-mesh and finer, were obtained which are a by-product from foundry sand production, the principal present use of olivine.

Several compositions of varied mixed sizes were studied, including "gap-graded" mixtures. However, the densities obtained from 65 to 80% of run-of-mill olivine crushed through 6-mesh or 4-mesh with 20 to 35% of olivine fines were found to be equivalent and should be less costly. A mixture of 80% of 6-mesh and finer olivine with 20% of olivine fines was used through most of the development. The sizing of 6-mesh olivine was:

Screens	Weight %	Screens	Weight %
-6+8	4.8	-50+70	6.9
-8+10	16.9	-70+100	4.2
-10+14	16.3	-100+140	1.2
-14+20	15.3	-140+200	1.1
-20+30	13.0	-200+270	0.9
-30+40	8.7	-270	3.0
-40+50	7.7		

The amount coarser than 20 mesh is 53%. Other lots used had up to 80% coarser than 20-mesh but this resulted in little change in brick density.

The sizing of the olivine fines was determined by sedimentation to be: 85% finer than 60 μm, 50% finer than 34 μm, 20% finer than 19 μm and 10% finer than 9 μm.

Bonds and Formulations

A number of bonding agents was studied but certain sodium phosphates were found to be superior early in the work as will be noted in Table 1. Phosphoric acid was not studied because of concern for acid fumes which might evolve in use and corrosion of production equipment. Magnesium oxychloride was not studied because earlier work showed very low strengths after heating to the TES range. Compositions listed in Table 1 are of 80% olivine, 6-mesh and finer and 20% olivine fines to which the bond shown together with water was added. Properties are after 300°C curing.

Table 1. Comparison of Bonds Used for Olivine

Bond	Amount, %	Strength MPa (psi)	Density g/cm^3
Sodium tripolyphosphate (STP-Monsanto)	6	4.1(600)	2.63
Sodium polyphosphate (Agilu 70-Giulini)	3	7.9(1150)	2.66
" " " "	2	5.4(760)	2.60
" " " "	1	2.6(370)	2.56
Sodium hexametaphosphate (SHMP-Monsanto)	3	7.7(1110)	2.71
" " " "	2	4.9(710)	2.65
" " " "	1	2.3(330)	2.61
" " " "	3		
+ hydrated lime	1	3.2(462)	2.69
STP and aluminum sulfate	2,1	2.7(390)	2.60
High Alumina portland cement	10	2.0(294)	2.48
Calcium aluminate cement	5	0.4(56)	2.38
Sodium silicate solution (N-Phila. Quartz)	5	10.3(1490)	2.58

The strengths obtained with 3% of either Agilu or SHMP were thought desirable and production of TES brick was made from that amount of bond. However, an English brick (density 2.42) and a North Carolina brick (density 2.60) were obtained later. Test bars, 6 x 1 x 1 inch, were sawed out of these bricks and also from Washington brick (density 2.82). Moduli of rupture were determined as: English - 2.2 MPa (314 psi); North Carolina - 2.2 MPa (325 psi); and Washington 10.6 MPa (1540 psi). For equivalent strengths, one percent of Agilu or SHMP would thus be adequate.

Heat Treatment

TES brick will be used to 800°C so deterioration in strength up to 800°C would be undesirable. A composition with 3% sodium polyphosphate (Agilu) was heated at various temperatures and strengths determined, as follows: 100°C - 12.7 MPa (1840 psi); 300°C - 9.3 MPa (1340 psi); 500°C - 8.8 MPa (1280 psi); 725°C - 9.1 MPa (1320 psi); 1400°C - 11.3 MPa (1640 psi). No serious deterioration in strength thus occurs.

Later, a similar series of heatings were performed on a composition with sodium hexametaphosphate (SHMP) with strengths resulting, as follows: 110°C - 10.5 MPa (1520 psi); 300°C - 7.7 MPa (1110 psi); 800°C - 7.1 MPa (1030 psi); 1400°C - 11.4 MPa (1660 psi).

The above compositions were found to adsorb some water if allowed to stand after heating to 110°C. Some loss in strength was also noted if samples were not tested immediately after heating at 110°C. Also, the water slaking resistance was found to improve greatly when compositions were heated at 260 to 300°C.

No objectionable fumes have been noted in heating brick made with either Agilu or SHMP binder. However, acrid fumes evolved from bricks made with sodium tripolyphosphate.

Production

A two day brick molding campaign was conducted at the North American Refractories Co. plant in Renton, WA. A mold had been constructed to produce the T.P.I. Corp. brick shape for TES. This brick has grooves on the face and ends to accomodate heating elements and recessed sides to permit air flow. Outer dimensions are 9-3/8 by 6-9/16 by 3-7/16 inches.

Three and one-half tons of the composition of 80% 6-mesh olivine and 20% olivine fines were prepared using 3% of sodium polyphosphate (Agilu) binder and 1.8% water. Slightly higher water contents (2.2%) caused sticking. One ton lots were mixed in a muller-type mixer.

Bricks were molded in a heavy-duty refractories friction press using 3 "bumps" per brick. After molding, the bricks had a density of 2.9 to 2.95 g/cm^3. The bricks were heated to 260°C and then had densities of 2.8 to 2.83 g/cm^3, weighing about 18-1/2 lbs. each. A load for a commercial size off-peak heater, comprising 160 bricks and 12 half-bricks, was shipped to Purdue University for testing.

A significantly higher density was obtained with the friction press as compared with test bar densities (2.8 as compared with 2.7). The repetitive impact loading of the friction press gives more uniform density particularly in the unusual TES brick shapes.

Properties

As noted, densities of full size bricks were 2.8 g/cm^3, and by water absorption a porosity of 14% and an apparent density of 3.27 g/cm^3 were measured. Moduli of rupture of 6 x 1 x 1 inch bars cut from a brick were 10.6 MPa (1540 psi). Other properties determined were:

Coefficient of thermal expansion: 7.2×10^{-6}/°C to 800°C determined by dilatometry on samples heated to 100, 260, 500 or 1400°C.

Thermal conductivity: 6.4×10^{-3} cal cm/cm^2 sec °C determined by Mr. Richard Stone by a flash technique.

Thermal shock: Test bars were heated in an electric furnace to 800°C in 45 minutes, soaked at 800°C for 20 min., and then cooled with a fan to 100°C in 80 min. From a control set strength of 7.9 MPa, the strength dropped to 5.2 MPa after 20 cycles, to 4.8 MPa after 40 cycles, and 3.8 MPa after 80 cycles.

To simulate service, a stack of 8 TES bricks, 4 high x 2 wide, was constructed with nichrome heating elements in the grooves. The stack was insulated with insulating fire brick. When 3200 watts was applied for 6-1/2 hours, the stack interior reached 800°C and then was cooled to room temperature by forced air in 12 hours. After 10 cycles all 4 interior bricks cracked along the heating grooves. However, an English and a North Carolina brick were placed in the stack and they also cracked. It is thought that both tests described were too severe. No dusting was observed in the Washington bricks after 69 cycles and no additional damage was noted after the initial cracking observed. It

should be noted that the power applied per brick was about twice that of a commercial unit.

Conclusions

TES olivine brick can be produced without firing by utilizing from 1 to 3% of either of two sodium phosphate binders. Utilizing run-of-mill Washington olivine and molding in a friction press, denser brick can be produced than those now being used.

Acknowledgments

This project was supported by contract No. W7405-eng-26 (ORNL/sub. 9063) from Union Carbide Corp., Nuclear Division for the Dept. of Energy. The original concept came on a "mini-project" from the Washington Mining and Mineral Resources Research Institute. Most of the work described was performed by Mr. Mel Eng, Ceramic Engineer. Two companies cooperated: Olivine Corp., Bellingham, WA in supplying olivine and the North American Refractories Co., Renton, WA who constructed a mold and formed and dried bricks.

References

1. U.S. Bureau of Mines, "Mineral Commodity Summaries, 1982".
2. Division of Mines and Geology, State of Washington, "Mineral and Water Resources of Washington", 1966.
3. H. Palmour III, B. M. Gay, I. H. Redeker, "Ceramics for Energy Storage Units: Bricks from North Caolina Olivine for Heat Storage Furnaces", in Energy and Ceramics, Elsevier, 1979.

DEVELOPMENT OF CHEMICALLY BONDED CERAMIC MATERIALS FOR USE IN THERMAL ENERGY STORAGE DEVICES

D. A. BROSNAN
MATERIALS CONSULTANT ASSOCIATES, INC. (MCA)
PELL CITY, AL 35125

Chemically bonded ceramic materials offer potential advantages in thermal energy storage (TES) devices because they can be fabricated without the energy intensive firing step used with conventional refractory bricks. Chemically bonded "castable" materials can be used to fabricate complex shapes without powder pressing techniques. These advantages facilitate the production of TES shapes by small business concerns since large capital investments are unnecessary. The goal of this project is to combine the advantages of castable refractories cited above with domestically available olivine minerals to produce compositions suitable for TES devices.

Conventionally fired olivine bricks have been known since the 1930's based on work by Goldschmidt (1). Fired olivine bricks based on N.C. olivine were produced in the 1950's but are no longer available. Palmour (2) has shown that fired bricks based on N.C. olivine have adequate properties for use in TES devices. Some early work by Greaves-Walker (3) demonstrated that chemically bonding olivine was possible, but products of that time (ca. 1943) were intended for use in the steel industry and were not commercialized. Recent work by Whittemore (4) has shown that phosphate bonded Washington state olivine bricks have potential for TES. Similar work with N.C. olivine has not been previously reported.

The N.C. olivines occur both as massive rock formations and as weathered sandstone minerals. By contrast the Washington state olivines occur primarily as the massive rock formations.The geologic variations in the N.C. olivines produce important physio-chemical variations which affect the ability to chemically bond these materials.

Chemical analyses of N.C. olivines is shown in Table 1. The magnesium oxide (MgO) content is shown to vary appreciably from mine to mine with the impurity content (Fe_2O_3) exhibiting large differences in shipments from the same mine. Two important consequences were found as follows:

1. The content of undesirable accessory minerals such as serpentines and vermiculite varies both by source and as a consequence of beneficiation technique. These minerals are the primary contributor to the loss on ignition of the material. Lowest possible loss on ignition is desirable for TES materials.

2. The MgO to SiO_2 ratio shows significant variation. This influences the pH or "acidity" of water slurries of castable materials and has influence on binder-aggregate reactions.

Olivine compositions and physical properties are shown in Table 2. The calcium aluminate cement bonded compositions such as C-1 exhibited normal setting (hardening) characteristics as are typical of alumina - silica refractory concretes. After high temperature exposure, these compositions showed the typical loss in strength of refractory concretes due to dehydration of the cement hydrate phases prior to the onset of ceramic sintering reactions. Significantly, the shrinkage (linear change) was very small indicating that these compositions can be used in TES

devices to 1200°C. Phase diagrams suggest significant deformations for these compositions at temperatures of 1260-1300°C (5).

It was found necessary to add basic (high MgO) materials to phosphate bonded castables to produce the highest density and strength specimens. The most effective basic addition as found to be refractory grade magnesite (calcined MgO at 87% MgO content). The properties of composition P-18 in Table 1 show that phosphate bonded N.C. olivine castables gain strength with high temperature exposure. This implies that phosphate bonded compositions offer advantages over cement bonded compositions which lost strength with the same thermal exposure.

Firing tests indicate that the chemically bonded olivine castables retain good strength properties on thermal cycling if heating and cooling rates do not exceed 140°C/hr. Further test work is underway with special "gap-graded" compositions which are expected to have improved thermal shock resistance over those compositions developed to date (6).

One potential weakness of castable olivine materials is their lower density than conventionally pressed and fired olivine bricks. Lower density implies that the volumetric heat capacity would also be low for olivine castables. For example, commercial olivine bricks typically exhibit densities of 2.56 g/cm^3 (160 lb/ft^3) whereas the olivine castables have densities in the range of 2.20-2.40 g/cm^3 (137-150 lb/ft^3). For this reason olivine castables were formulated with iron oxide bearing minerals in the composition. These compositions such as C-11 in Table 2 show cured densities comparable to that of fired olivine brick. Due to the higher iron oxide content than fired brick, it is possible that the volumetric head capacity of these high iron olivine castables may exceed that of the fired brick.

In conclusion, experimental activities with N.C. olivine castable compositions to date have shown the following:

1. Olivine raw material variability with N.C. material is an important factor influencing the properties of candidate TES materials.

2. Both calcium aluminate cement and phosphate bonded castables appear to have adequate properties for use in TES devices. Compositional design as through using "gap-graded" sizing will affect the maximum safe heating and cooling rates for olivine castables.

3. Additions of iron oxide bearing minerals to olivine castables has prodiced densities comparable to those of fired olivine.

References:

1. V. M. Goldschmidt, U.S. Patents 1,926,094; 2,105,943; and 2,516,249.
2. H. Palmour, "Ceramics For Energy Storage Units: Bricks From North Carolina Olivine For Heat Storage Furnaces," presented at CIMTEC IV, Energy and Ceramics (1979).
3. A. F. Greaves-Walker and R. L. Stone, "The Production of Unfired and Fired Forsterite Refractories From North Carolina Dunites," Bulletin Number 16, Engineering Experiment Station, N.C. State University (1943).
4. O. J. Whittemore, personal communication.
5. "Phase Diagrams For Ceramists," The American Ceramic Society (1964).
6. J. Homeny, Ph.D. Dissertation, Penn State University (1980).

TABLE 1

RAW MATERIALS CHARACTERIZATION - N.C. OLIVINE

Chemical Analysis:	Addie Olivine First Shipment	Addie Olivine Second Shipment	Green Mountain Olivine First Shipment	Dillsboro Olivine First Shipment
MgO	22.9	29.8	43.1	45.0
SiO_2	55.8	28.9	47.1	39.9
Al_2O_3	0.4	2.8	0.1	0.9
Fe_2O_3	7.0	29.2	7.0	12.3
Na_2O	0.1	0.5	0.1	0.1
K_2O	0.1	0.3	0.1	0.1
Loss on ignition, %	4.8	1.7	1.7	1.7
Moisture, %	0.9	1.1	0.4	1.1
Specific Gravity (ASTM C-357)	2.67	2.70	-	3.07
Thermogravimetric Analysis				
Weight loss after 150°C	-0.70		-0.23	
260°C	-0.76		-0.26	
540°C	-1.59		-0.62	
810°C	-4.67		-1.71	
1100°C	-5.18		-1.79	

TABLE 2

SAMPLE COMPOSITIONS AND PHYSICAL PROPERTIES

Composition, Weight %	C-1 Cement Bonded	P-18 Phosphate Bonded	P-25 Phos-Gap Size	C-11 Cement-Fe_2O_3
Olivine	75.0	68.2	67.0	45.8
Magnesite	-	22.7	22.3	-
Iron rich minerals	-	-	-	30.8
Calcium aluminate	25.0	-	-	23.4
Na-polyphosphate	-	9.1	10.7	-
Physical Properties:				
Bulk density after 110°C, g/cm^3	2.30	2.20	2.35	2.58
Cold crushing strength after 110°C, kPa	19065	10208	-	-
Modulus of Rupture after 110°C, kPa	5499	5155	-	-
Properties After Firing:				
Bulk density after 927°C, g/cm^3	2.10	2.12	-	-
Linear change after 927°C, %	-0.09	+0.35	-	-
Cold crushing strength after 927°C, kPa	12434	11972	-	-
Bulk density after 1204°C, g/cm^3	2.08	2.27	(In Progress)	(In Progress)
Linear change after 1204°C, %	-0.19	-1.00	-	-
Cold crushing strength after 1204°C, kPa	5872	15974	-	-

THERMAL ENERGY STORAGE TESTING FACILITY*

R.J. Schoenhals, W.R. Laster and M.R. Elter
Ray W. Herrick Laboratories, School of Mechanical Engineering
Purdue University, West Lafayette, IN 47907

INTRODUCTION

This project was associated with a parallel effort by the American Society of Heating, Refrigerating, and Air-Conditioning Engineers (ASHRAE) to establish a standard for performance evaluation of electrically heated TES units. This has recently been issued as ASHRAE Standard 94.2 [1]. In assessing and validating the quality of the procedures specified by the Standard, a 30 kW central TES unit and eight smaller individual room-size units were tested. Recent project activities have concentrated on evaluation of performance of commercially available TES units when incorporating different energy storage materials. Brief descriptions of technical progress were presented during the course of the project [2-4]. Activities pursued and results obtained throughout the project have been summarized in more detail recently [5-7]. Additional information is available in a number of project reports which are cited in References [5]-[7].

CENTRAL TES UNITS

All experimental work in regard to testing of central TES devices was performed with a single 30 kW unit. ASHRAE Standard 94.2 specifies three types of tests for central TES units: (1) Initial Charge Test, (2) Maximum Standby Emission Test, and (3) Discharge Test.

In the Initial Charge Test the TES unit is at room temperature at the start, and is then fully charged. Figure 1 shows typical test results from an Initial Charge Test and a following Discharge Test in which the device was alternately discharged and re-charged. In this particular case the Initial Charge Test yields E_1 = 236.38 kWh and τ_1 = 9.25 h. In the Discharge Test the energy delivered to the duct during the second discharge is called the discharge capacity (Q_d = 155.77 kWh). The effectiveness, η, is defined as the percent of the electrical input during a complete cycle which is delivered to the duct. The thermal energy remaining in the storage core at the end of discharge is called the residual capacity (Q_R = 44.09 kWh). η and Q_R can be calculated from the experimentally determined values of E_1, E_4, E_5, E_6 and Q_d. For the test depicted in Fig. 1, η = 79%. The remaining portion of the electrical input (21% in this case) is balanced by heat transfer from the cabinet of the TES unit to its surroundings. In the Maximum Standby Emission Test the TES unit is maintained essentially at the full charge condition by the internal control system for an extended period of time (τ_2). The electrical input energy (E_2) is measured. The ratio represents the average heat transfer rate from the cabinet for this condition. A typical test yielded $q_{e,max} = E_2/\tau_2$ = 42.075 kWh/8.790 h = 4.787 kW.

* This project was supported initially by Argonne National Laboratory under ANL Contract No. 31-109-38-4666, and was supported more recently by Union Carbide Corporation, Nuclear Division, Oak Ridge National Laboratory, under Contract No. W-7405-eng-26 (ORNL/Sub-7961).

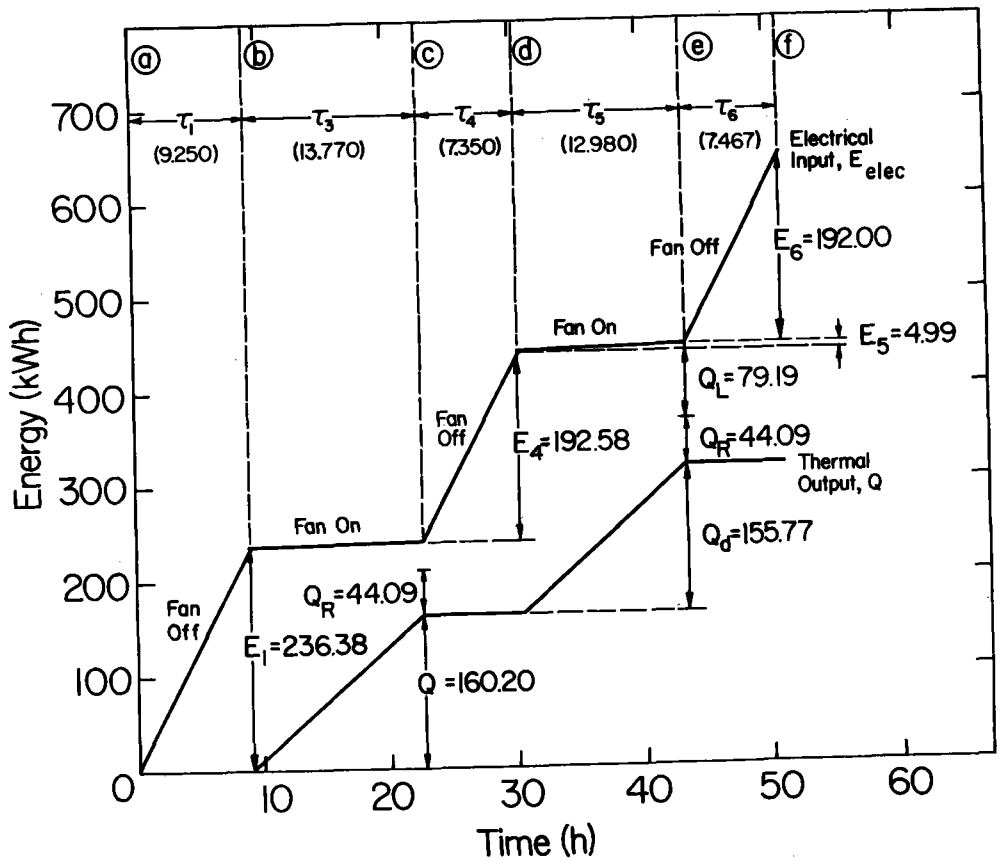

Fig. 1 Results from an Initial Charge Test (a to b) followed by a Discharge Test (maximum fan speed, set-point temperature = 54.4°C)

Tests were conducted at various ambient temperatures and, in addition, Discharge Tests were conducted at different fan speeds and set-point temperatures. Variations in ambient temperature were found to have a negligible effect on results from Initial Charge Tests and Maximum Standby Emission Tests, and to have relatively little effect on Q_d for Discharge Tests conducted at constant fan speed and set point temperature. No definite trend was apparent in regard to η. However, Q_R was found to be significantly affected by changes in ambient temperature. Humidity variations were found to affect Discharge Test Results to an extent no larger than 1/2%.

The energy storage bricks supplied with the 30 kW central unit were fabricated from olivine and were manufactured in England. Domestic supplies of olivine are available in North Carolina, Georgia and Washington. Several tests were performed employing bricks fabricated from North Carolina olivine [8], and the test results were compared with those obtained for the originally supplied English-manufactured olivine. Differences in performance were judged to be minimal. A second set of domestic olivine bricks is currently being tested. These were fabricated from olivine, obtained from deposits in the State of Washington, employing an unfired process. Characteristics of these bricks are described in Reference [9]. The first Initial Charge Test yielded τ_1 = 9.67 h and E_1 = 275.42 kWh, approximately 15% higher than obtained with the two types of olivine bricks previously tested.

ROOM-SIZE TES UNITS

ASHRAE Standard 94.2 specifies that a calibrated calorimeter be used for testing of room size units. In the Static Discharge Test the unit is fully charged, and then allowed to transfer heat with its internal fan off. In the Dynamic Discharge Test the the internal fan is turned on at the conclusion of the charging process. Figure 2 contains results from a typical Dynamic Discharge Test. Notice that the thermal energy output of the TES unit at the conclusion of the test is essentially equal to the total electrical energy input, as expected. In the many tests conducted with eight different TES units, the deviation between these two experimentally-determined quantities typically did not exceed 2%, thus providing confidence in the calibrated calorimeter method.

A comparison with test results obtained independently at another laboratory was performed. Two identical 4 kW TES units were provided. One was tested in this work and the other was tested at a laboratory in Stuttgart, West Germany [10] in accordance with a German Standard, DIN 44572 [11]. Figure 3 contains plotted results from Dynamic Discharge Tests. The comparison is quite favorable, lending additional support to the validity of the calibrated calorimeter method. Since the tests performed in Stuttgart could not be expected to exactly duplicate test conditions existing in this work (calorimeter airflow rate, calorimeter dimensions and detailed features, laboratory ambient temperature and humidity), it appears that the test results are not strongly affected by these parameters. The deviation observed in Fig. 3 appears to be primarily due to differences in total charge, as a result of differences in action of the internal control systems which terminate the charge, and perhaps also due to a small difference in supply voltage. It was found that the former deviation can be partially removed by normalizing the ordinate. This is demonstrated in Fig. 4, which contains a comparison of the Static Discharge Test results when plotted in this manner.

Normalization of the ordinate, as described above, also makes it possible to make meaningful comparisons among various TES units of different sizes. Figure 5 shows results obtained from Static Discharge Tests. Curves (a) and (b) reveal that results from two tests of a 2 kW unit deviate somewhat, even after normalization of the ordinate. Curves (c) and (d) show the same behavior for a 4 kW unit. Curve (e) was

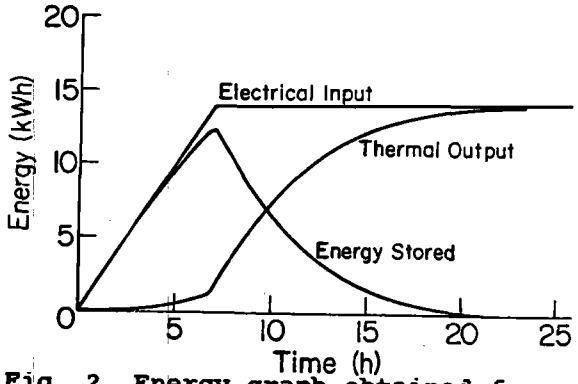

Fig. 2 Energy graph obtained from a Dynamic Discharge Test conducted with a 2kW TES unit (calorimeter blower speed = 1700 rpm)

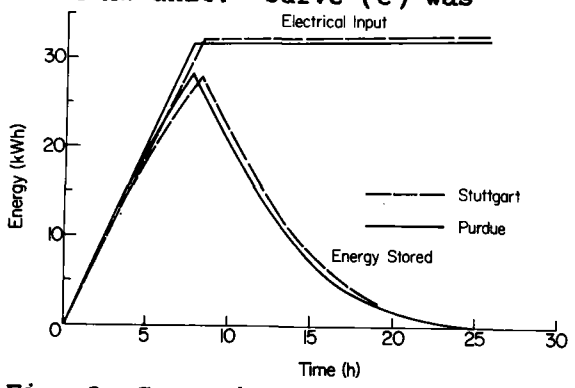

Fig. 3 Comparison of results obtained from Dynamic Discharge Tests conducted for a 4kW model at different laboratories (two identical TES units)

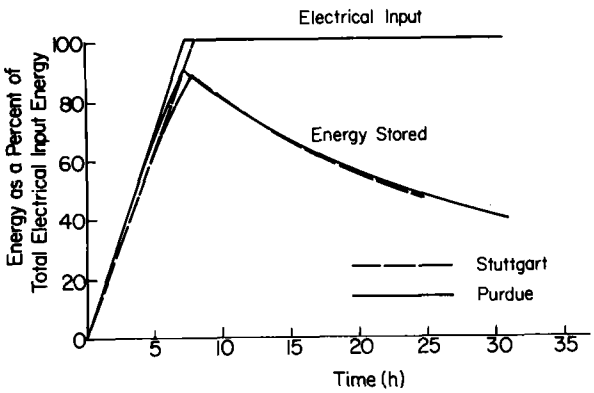

Fig. 4 Comparison of results obtained from Static Discharge Tests conducted for a 4 kW model at different laboratories (curves plotted with the ordinate normalized)

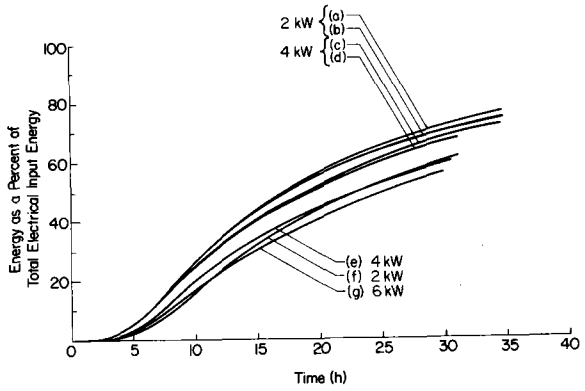

Fig. 5 Results obtained from Static Discharge Tests conducted with several TES units (curves plotted with the ordinate normalized)

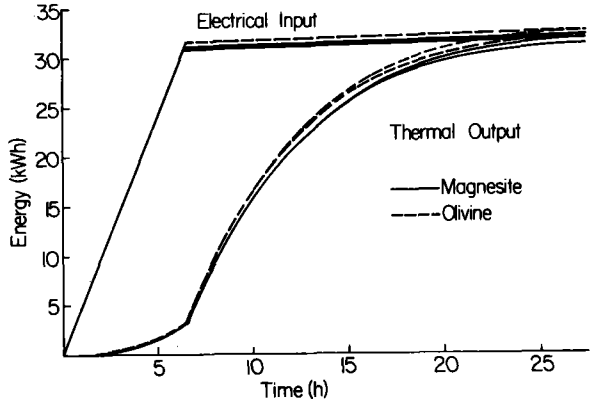

Fig. 6 Comparison of results obtained from Dynamic Discharge Tests conducted with a 4kW TES unit (two tests for each type of storage brick)

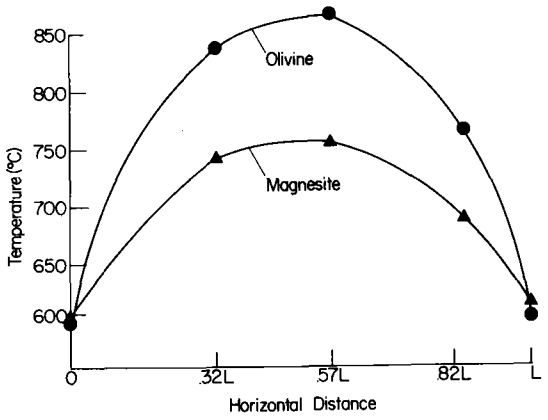

Fig. 7 Core temperature profiles in the central vertical plane midway between the top and center heating elements at charge termination (storage core length L = 0.76m)

obtained employing a second 4 kW unit [different from that used to obtain curves (c) and (d)], and curve (f) was obtained employing a second 2 kW unit. Curve (g) was obtained employing a 6 kW TES unit.

In addition to assessing and improving the test apparatus and procedures, tests were performed with two different TES units (a 2 kW unit and a 4 kW unit) when containing the European magnesite storage bricks supplied with these devices and also when containing domestic olivine bricks fabricated from North Carolina olivine [8]. A typical comparison is given in Fig. 6. In all cases the performance of the domestic olivine equaled, or sightly surpassed, the performance of European magnesite in tests specified by ASHRAE Standard 94.2. This was surprising initially, since magnesite has the higher specific heat. The fact that the olivine stored as much, or slightly more, thermal energy (see Fig. 6) was traced to the fact that the internal control system allowed the olivine material to achieve higher temperatures in the interior, primarily as a result of the lower thermal conductivity of the olivine.

Figure 7 contains plots of experimentally determined temperature profiles existing in the two cores at charge termination for the 4 kW TES unit. By studying the various experimentally determined temperature profiles, it was determined that the maximum temperature was higher by roughly 200°C and the average temperature was approximately 35°C higher for the olivine at charge cut-off, thus offsetting the higher specific heat of the magnesite.

REFERENCES

1. ASHRAE Standard 94.2, "Methods of Testing Thermal Storage Devices with Electrical Input and Thermal Output Based on Thermal Performance," Atlanta, 1981.
2. R.J. Schoenhals, H.F. Kuehlert, and C.P. Lin, "Thermal Energy Storage Testing Facility," Thermal Energy Storage, Fourth Annual Review Meeting, NASA Conference Publication 2125, DOE Publication CONF-791232, Tysons Corner, Virginia, December 3-4, 1979, pp. 223-231.
3. R.J. Schoenhals, C.P. Lin, H.F. Kuehlert and S.H. Anderson, "Thermal Energy Storage Testing Facility," Proceedings of the DOE Thermal and Chemical Storage Annual Contractor's Review Meeting, CONF-801055, McLean, Virginia, October 14-16, 1980, pp. 33-36.
4. R.J. Schoenhals, S.H. Anderson, L.W. Stevens, W.R. Laster, and M.R. Elter, "Thermal Energy Storage Testing Facility," Proceedings of the Sixth Annual Thermal and Chemical Storage Contractors' Review Meeting, CONF-810940, Washington, D.C., September 14-16, 1981, pp. 155-160.
5. M.R. Elter, C.P. Lin, and R.J. Schoenhals, "An Evaluation of ASHRAE Standard 94.2 for Testing Electrically Charged Thermal Energy Storage Central Units," Symposium TO-82-3, Paper No. 1, 1982 ASHRAE Annual Meeting, Toronto, June 27-30, 1982, to be published in ASHRAE Transactions, Vol. 88, Part 2, 1983.
6. H.F. Kuehlert, S.H. Anderson, W.R. Laster, L.W. Stevens, R.J. Schoenhals and H. Hersh, "An Evaluation of ASHRAE Standard 94.2 for Testing Electrically Charged Thermal Energy Storage Room-Size Units," Symposium TO-82-3, Paper No. 2, 1982 ASHRAE Annual Meeting, Toronto, June 27-30, 1982, to be published in ASHRAE Transactions, Vol. 88, Part 2, 1983.
7. W.R. Laster, B.M. Gay, R.J. Schoenhals, and H. Palmour, III, "Comparison of Domestic Olivine and European Magnesite for Thermal Energy Storage," Symposium TO-82-3, Paper No. 3, 1982 ASHRAE Annual Meeting, Toronto, June 27-30, 1982, to be published in ASHRAE Transactions, Vol. 88, Part 2, 1983.
8. The special bricks fabricated from North Carolina olivine were supplied by B.M. Gay, North Carolina State University, Raleigh, NC.
9. O.J. Whittemore, "Unfired Olivine Bricks for Thermal Energy Storage," Proceedings of the Seventh Annual Thermal and Chemical Storage Contractors' Review Meeting, Washington, D.C., August 23-26, 1982.
10. The tests were conducted at G. Bauknecht, Engineering Laboratories, Stuttgart, West Germany.
11. DIN 44572, "Electrical Space Heating Appliances, Storage Heaters with Controlled Heat Output," Part 5, (German Standard, Jan. 1972, English Translation).

HEAT PUMP COOL STORAGE IN A CLATHRATE OF FREON *

J. J. Tomlinson

Oak Ridge National Laboratory
Oak Ridge, Tennessee 37830

Abstract

This paper presents the analytical description and assessment of a unique heat pump/storage system in which the conventional evaporator of the vapor compression cycle is replaced by a highly efficient direct contact crystallizer. The thermal storage technique requires the formation of a refrigerant gas hydrate (a clathrate) and exploits an enthalpy of reaction comparable to the heat of fusion of ice. Additional system operational benefits include cool storage at the favorable temperatures of 4-7°C (40-45°F), and highly efficient heat transfer rates afforded by the direct contact mechanism. In addition, the experimental approach underway at ORNL to study such a system is discussed.

Introduction

Distributed cool storage systems which can be "charged" in the evening during offpeak hours and "discharged" the following day with little onpeak purchased electricity can reduce the utility peak load and improve the daily load factor. A key element of a cool storage system is the creation of a heat sink to which thermal energy removed from a conditioned space can be transferred. This heat sink is conventionally ice or chilled water and is generated by the evaporator in a vapor compression cycle. Residential ice storage systems have been extensively studied by many utilities through private and government-sponsored field tests and demonstrations (1, 2). These studies have shown that while ice storage systems can effectively shift a cooling load to an offpeak period, the economics provided by existing equipment are unfavorable due to increased system capital costs and extra purchased energy requirements. Ice manufacture for cool storage usually imposes severe operational penalties which can be traced to two sources: (A) the decrease in condensing unit efficiencies with decreasing evaporator temperatures, and (B) use of a storage material (ice) with a melt temperature substantially lower than that required to meet the load. As ice builds on the evaporator surface, the overall heat transfer coefficient between the refrigerant and the freeze front decreases, resulting in progressively lower evaporating temperatures and reduced system thermodynamic efficiencies. Periodic ice removal from the evaporator surface raises the heat transfer coefficient but also requires an additional expenditure of energy. These problems serve to underscore the effects of heat transfer limitations caused by ice buildup. Although the heat of fusion of ice is high (80 Kcal/Kg = 144 Btu/lb) so that an ice storage tank can be small in volume, the low storage temperature of 0°C (32°F) promotes heat gains through the storage tank walls. A storage medium with a higher melt temperature would be advantageous in minimizing uncontrolled heat gains.

From a thermodynamic viewpoint the "ideal" cool storage medium would have the following attributes:

1. A melt temperature of 4-7°C (40-45°F) low enough to provide sufficient dehumidification of the building supply air,

2. A high volumetric storage density which has the three-fold benefit of reduced tank size, cost, and heat losses,

3. High heat transfer coefficients and attendant low temperature differences between the storage medium and the charge/discharge fluid resulting in a minimum of purchased energy during system charging and discharging.

Clearly, ice is not the ideal cool storage medium. Due to the low melting temperature and heat transfer limitations, existing residential-scale ice storage systems have been shown to exact a toll in extra energy consumption of 40-50% (1). Eutectics of hydrated salts which melt at the appropriate temperature have been used in cool storage demonstrations, but low heat transfer rates within the salt have required that the storage capacity be oversized, sometimes by as much as a factor of three (3). Based on the above attributes of an ideal cool storage medium, the choice may be a type of clathrate called a gas hydrate.

Clathrates

A clathrate is a compound formed by the inclusion of molecules of one kind in cavities of the crystal lattice of another. Gas hydrates form a class of clathrates or inclusion compounds in which the host lattice is composed of water molecules held together by hydrogen bonding which enclose a guest molecule of gas similar to that which is shown in Figure 1. Although the water molecules are bound together by primary forces, the gas molecule is constrained by weak Van der Waal forces of attraction between itself and the surrounding water molecules. These weak forces are sufficient to cause the hydrate crystal to form at a higher temperature than pure ice.

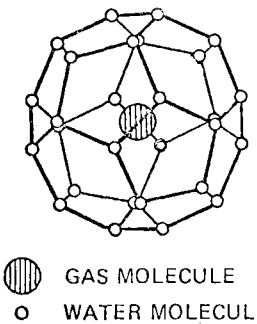

Figure 1. Gas Hydrate

Although gas hydrates were first discovered in 1810, they remained a laboratory curiosity until the early 1960's when their elevated formation temperature was exploited in a unique freeze desalination process (4, 5). In this process, heat is removed from salt water by evaporation of a refrigerant gas intimately mixed with it to produce a hydrate free of salt. The hydrate is then separated from the brine and melted using

the heat of condensation from the compressed refrigerant. The key advantage of this technique lies in freeze desalination at temperatures higher than 0°C (32°F) with attendant higher system thermodynamic efficiencies. Of the many gas hydrates studied, it has been determined that a large quantity of energy must be removed from the water/gas mixture to form the hydrate crystal. This heat of formation varies between 72-111 Kcal/Kg (130-200 Btu/lb) of solidified water and, thus, can be greater than the heat of formation of ice. Although this high heat of formation is of no particular benefit in freeze desalination, it is precisely this characteristic that make gas hydrates interesting as cool storage media.

There are two basic crystalline structures of gas hydrate molecules. Structure I consists of a 12Å unit cell containing 46 water molecules and 8 cages which can contain guest molecules. Structure II is more complex consisting of a 17.2Å unit cell containing 136 water molecules arranged to form 24 guest molecule cages. In general the size of the guest molecule is the single most significant determinant of whether structure I or II is formed. It appears that structure I is formed exclusively by gas molecules less than 5.3Å in diameter, and structure II by molecules 5.6 to 6.6Å in diameter. With this criterion, there are many gases which can form hydrates including the noble gases, halogens, straight-chain hydrocarbons and, of particular interest in the cool storage application, halogenated hydrocarbons or common refrigerants used in vapor compression cycles. Dichlorodifluoromethane (R-12) is an excellent example of a substance which forms a Structure II clathrate at favorably low pressures. The experimentally-determined phase diagram for R-12/H_2O is shown in Figure 2.

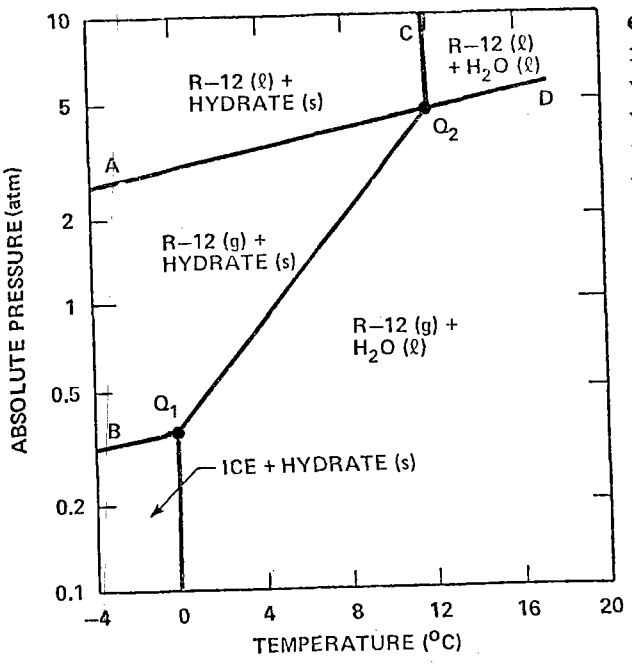

Figure 2. Phase Diagram for R-12/H_2O Mixture

Since R-12, like many refrigerants is only slightly soluble in water, curve A-Q_2 and beyond very closely approximates the vapor pressure-temperature relation of R-12 alone. When the mixture R-12/H_2O is present, additional regions appear on the phase diagram as indicated. Points Q_1 and Q_2 are quadruple or invariant points where four phases exist in equilibrium. The gas hydrate R-12·15.6 H_2O can exist in equilibrium in the region to the left of curve Q_1-Q_2-C. If a mixture of R-12(g) and H_2O(ℓ) exists at 12°C (54°F) and 2.0 atm, a decrease in temperature along a constant pressure line would result in the formation of a hydrate at approximately 8°C (46°F). The

position of the initial starting point is purely arbitrary, and it is obvious that the temperature at which hydrates are formed is a function of operating pressure. If we assume that R-12(g) is an ideal gas and further that the volume ν'' of the R-12(g) is much larger than the volume of the resulting hydrate ν', we may apply the Clausius-Clapeyron equation:

$$\left(\frac{dP}{dT}\right)_{sat} = \frac{h'' - h'}{T(\nu''-\nu')} ,$$

to closely approximate the heats of reaction for transitions across lines A-Q_2, Q_1-Q_2, and B-Q_1 in Figure 2. In the particular case of the transition across Q_1-Q_2, the heat of reaction ΔH is found to be:

$$\Delta H = 75.6 \text{ Kcal/Kg hydrate} = 108.3 \text{ Kcal/Kg } H_2O$$
$$= 136 \text{ Btu/lb hydrate} = 195 \text{ Btu/lb } H_2O$$

That is, at a phase change temperature of 8°C,

$$\text{R-12(g)} + 15.6\ H_2O \rightarrow \text{R-12}\cdot 15.6\ H_2O + 75.6 \text{ Kcal/Kg hydrate.}$$

This large heat of reaction is available over any temperature range covered by the line between the invariant points Q_1 and Q_2. Fixing the operating pressure of a cool storage unit employing the R-12/H_2O mixture establishes the phase change temperature.

System Description

The proposed heat pump/storage system shown in Figure 3, is one in which the storage component is coupled directly into the vapor compression cycle through direct replacement of the conventional evaporator by an evaporator/storage tank in which R-12 gas hydrate is formed and stored. The refrigerant state conditions entering and leaving the storage tank during the hydrate-building process are similar to those found across a conventional evaporator coil so that the impact of conventional evaporator replacement on the remainder of the vapor compression loop will be minimal. The expansion device is a thermostatic expansion valve which controls the flow rate of subcooled R-12(ℓ) entering the storage tank so that it corresponds to the rate at which the refrigerant can be completely vaporized by the absorption of heat.

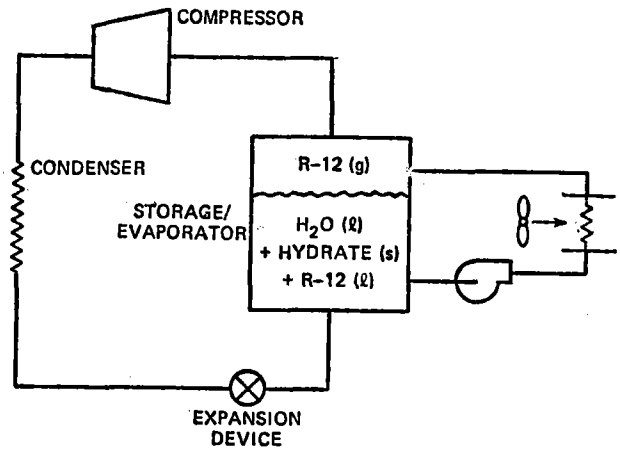

Figure 3. Heat Pump/Storage System

absorption of heat. The thermostatic expansion valve is controlled by the temperature of the superheated R-12 leaving the storage tank. At the beginning of the charging period, the tank contains $H_2O(\ell)$ and R-12(ℓ). During charging, liquid R-12 entering the storage tank is sparged into the warmer water, vaporizes and rises upward through the cooled R-12/H_2O mixture. When the mixture reaches the temperature corresponding to the Q_1-Q_2 line in Figure 2; hydrate formation is possible. Clearly the hydrate formation temperature is the storage temperature and is dependent on the storage system pressure. As the system is discharged, the operating pressure is limited by the R-12 vaporization curve A - Q_2 - D in Figure 2; and as the storage system gains heat from the building load, the operating point Q_2 is reached and maintained as the hydrate dissolution progresses, returning finally to the uncharged condition defined by the presence of $H_2O(\ell)$, R-12(ℓ) and R-12(g).

Experimental Approach

Development of a heat pump/cool storage clathrate system requires that the functional dependence of clathrate formation and dissolution rates on system operating temperatures, pressures, refrigerant flow rates, and agitation rates be determined. An experimental loop shown in Figure 4 has been designed to study these relationships. The refrigerant used in the loop is R-12 and is injected with zero quality into the bottom of the storage/ evaporator. The condenser, chiller, associated pump, and valve arrangement are used simply to establish the desired thermodynamic state of the entering R-12. The storage evaporator section can be operated as a constant temperature bath. Thermal energy can be delivered to the section via an electric heater, or removed from the section by a chilled water coil. In both cases, the heat added or removed is measured, so that a quantitative clathrate determination can be made. A preliminary test run of the loop has resulted in clathrate crystal formation in the 7-10°C (45-50°F) range. Further tests are currently underway.

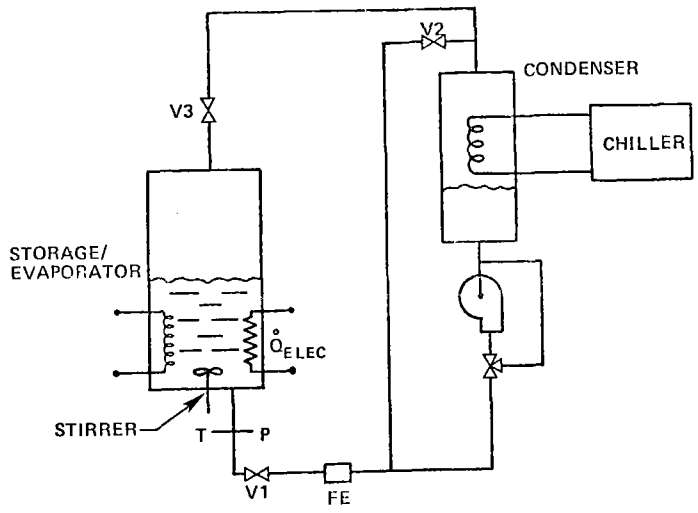

Figure 4. Experimental Loop Design

* Research sponsored by the Division of Thermal and Mechanical Energy Storage Systems, U. S. Department of Energy, under contract W-7405-eng-26 with the Union Carbide Corporation - Nuclear Division.

References

1. Wroblewski, D. E., "Residential Thermal Cool Storage System Development - Assessment of prior Experience Report," Carrier Corporation, Syracuse, NY, prepared for Oak Ridge National Laboratory, January 1982.

2. Reedy, W., Bullock, C. E., "Residential Cool Storage Implementation Handbook, EPRI EM-2054," prepared for The Electric Power Research Institute, Palo Alto, CA, September 1981.

3. Rizzuto, J. E. Avril, F., Irvine, T., "Design and Demonstration of a Storage Assisted Air Conditioning System," draft final report, prepared for New York State ERDA and Oak Ridge National Laboratory, March 1982.

4. Barduhn, A. J., et al., "The Properties of Some New Gas Hydrates and Their Use in Demineralizing Sea Water," A. I. Ch. E. Journal, May 1962.

5. Barduhn, A. J., "Desalination by Crystallization Process," Chemical Engineering Progress, Vol. 63, No. 1, January 1967.

STRATIFIED STORAGE MEASUREMENT AND ANALYSIS

Roger L. Cole
Argonne National Laboratory
9700 South Cass Avenue
Argonne, IL 60439

INTRODUCTION

This paper is a summary of a completed project. Details of the work can be found in reference [1]. The work applies only to hot tanks. Water tanks operated at low temperatures (0-15°C) will be more difficult to stratify because water's coefficient of thermal expansion β is small in that temperature range and it changes sign at 4°C.

European research has shown that stratification can improve the performance of solar systems by as much as 20%.[2] Other researchers have shown that the Richardson number $Ri = g\beta L\Delta T/u^2$ is the most important parameter governing thermal stratification.[3-5] For Richardson numbers less than the critical value of 0.25 mixing occurs, but for Richardson number greater than 0.25 stratification is possible.

ANALYTICAL MODEL

Effect of Solar Collector Strategy

The conventional solar collection strategy specifies a constant collector flow rate of about 0.015 $\ell/s\cdot m^2$ which is equivalent to about 3-6 tank volumes per day.[6] The National Solar Data Network has monitored the operation of several systems, and a typical day of operation of one of them is shown in Figure 1.[7] The tank was initially stratified at the 09:11 startup. At that time the Richardson number calculated from data in reference [7] was 0.55.

Cold water was drawn from the bottom of the tank, heated slightly, and returned to the top of the tank. Since the returned water was denser than the water at the top of the tank, the returned water sinks with a negligible amount of mixing. The result of this process as shown in the 09:43 curve is an increased bottom temperature but little change in the upper temperature profile. The Richardson number at 09:43 decreased to 0.28 because of the decrease in top-to-bottom ΔT.

At 10:10 the Richardson number decreased to 0.22 which was less than the critical value, and the tank began to mix. By 11:09 the tank was completely mixed and remained mixed for the rest of the day.

Any solar collection strategy must avoid a decreasing Richardson number if stratification is to be maintained. Therefore, a new 3-point strategy was developed and is summarized here:

1. Decrease the collector and collector heat exchanger flow rates so that no more than one tank volume passes through the collector heat exchanger per day.

2. Vary the flow rate through the collector and collector heat exchanger so the temperature of the water returned to the top of the tank is constant.

3. Adjust the temperature of the water returned to the tank to equal the minimum temperature necessary to satisfy the load.

Summary of One-Dimensional Theory

A one-dimensional analytical theory giving the water temperature T as a function of elevation x and time t was developed in reference [1]. The temperature is normalized by its initial temperature T_s and its inlet temperature T_{in}. The normalized temperature consists of a component θ which derives from the heat originally contained in the water and a component Δ which derives from the heat originally contained in the tank wall.

$$\frac{T - T_{in}}{T_s - T_{in}} = \theta + \Delta \qquad (1)$$

$$\theta = \frac{1}{2}\left[1 + \operatorname{erf}\left(\frac{\frac{x}{L} - \frac{at}{t^*}}{2\sqrt{Fo}\sqrt{\frac{at}{t^*} + c}}\right)\right] \qquad (2)$$

$$\Delta = \frac{1}{2}H\left(\frac{a-1}{a}\right)\left\{e^{\frac{\left(\frac{HC^2}{2a}\right)^2 + \frac{2x}{L}\left(\frac{HC^2}{2a}\right)}{C^2} - \frac{Ht}{t^*}}\left(\frac{x}{L} + \frac{HC^2}{2a}\right)\left[\operatorname{erf}\left(\frac{\frac{x}{L} + \frac{HC^2}{2a}}{C}\right) - \operatorname{erf}\left(\frac{\frac{x}{L} + \frac{HC^2}{2a} - \frac{at}{t^*}}{C}\right)\right]\right.$$

$$\left. + \frac{C}{\sqrt{\pi}}\left[e^{-\left(\frac{x^2}{L^2C^2} + \frac{HT}{t^*}\right)} - e^{-\left(\frac{\frac{x}{L} - \frac{at}{t^*}}{C}\right)^2}\right]\right\} \qquad (3)$$

where L is the water depth. The heat capacity ratio a, the time constant t*, and the Fourier number Fo are defined in reference [1]. The mixing parameter c and normalized film coefficient H are empirical constants determined by experiment.

EXPERIMENTAL RESULTS

Details of the experimental apparatus can be found in reference [1]. Results are summarized below.

Figure 2 shows that dip tubes and vertical baffles degrade stratification. The slope of the lines between normalized time 0.4 and 0.9 is indicative of heat transfer between the cold water in the dip tube and

the hot water at the top of the tank. The worst performance was shown by the dual concentric baffles, which had the largest area for heat transfer, but even the uninsulated dip tube configuration did not perform as well as the tank without diffusers or baffles (side inlet and outlet).

Figure 3 shows that the best performance was obtained for a tank having dual radial-flow diffusers. The radial-flow diffusers, which are simple to construct, reduce the inlet velocity and inject the water horizontally near the top and bottom.

The mixing parameter c and the normalized film coefficient H determined from experimental measurements were correlated with the Fourier number Fo and the Richardson number Ri. The approximate values (valid for $1 \leq Ri \leq 500$) are

$$c = 2.44 \times 10^{-5}\, Fo^{-1.5} \exp(-0.6134 Ri) \quad (4)$$

$$H = 7.7 \quad (5)$$

Figure 4 shows that equations 1-5 give a good estimate of tank temperatures in the interior as well as at the outlet.

Figure 5 compares the theoretical outlet temperature for tanks having light and massive wall. The heat originally contained in the wall can enter the water only after the thermocline has passed. When the heat finally enters the water its temperature is too low to be useful.

CONCLUSIONS

1. The new collection strategy is necessary to maintain stratification.
2. Dip tubes and vertical baffles degrade stratification.
3. Simple diffusers at the inlet and outlet give the best performance.
4. Although thermal diffusion broadens the thermocline, the rate of diffusion is sufficiently slow that most tanks can remain stratified in diurnal cycling.
5. The one-dimensional theory gives a good representation of the temperatures within the tank as well as at the outlet.
6. Thermally massive tank walls degrade stratification.
7. Conditions that improve stratification are (1) low inlet velocity, (2) large top-to-bottom temperature difference, and (3) ratio of water depth to tank diameter of about 4.

8. Additional work is necessary to develop methods of stratifying cold water storage tanks reliably.

REFERENCES

1. R. L. Cole and F. O. Bellinger, "Natural Stratification in Tanks: Phase I Final Report," Argonne National Laboratory Report ANL-82-5, February 1982.

2. W. B. Veltkamp, "Thermal Stratification in Heat Storages," Thermal Storage of Solar Energy, C. den Ouden, ed., p. 48, Martinus Nijhoff Publishers, The Hague, Netherlands, 1981.

3. J. S. Turner, "Internal Mixing Processes," Buoyancy Effects in Fluids, p 313-337, Cambridge University Press, 1973.

4. S. Chandrasekhar, "The Stability of Superposed Fluids: The Kelvin-Helmholtz Instability", Hydrodynamic and Hydromagnetic Stability, p 383-427, Oxford University Press, London, 1961.

5. B. J. Sliwinski, A. R. Mech, and T. S. Shih, "Stratification in Thermal Storage During Charging," Sixth International Heat Transfer Conference, p 149-154, Hemisphere Publishing, Washington, 1978.

6. W. A. Beckman, S. A. Klein, and J. A. Duffie, Solar Heating Design, p 7, John Wiley and Sons, New York, 1977.

7. M. J. Kennedy, S. J. Sersen, and S. M. Rossi, Vitro Laboratories, Silver Springs, MD, "Comparison of Liquid Solar Thermal Storage Subsystems in the National Solar Data Network," p 7, ASME Paper Number 80/WA/SOL-36, November 1980.

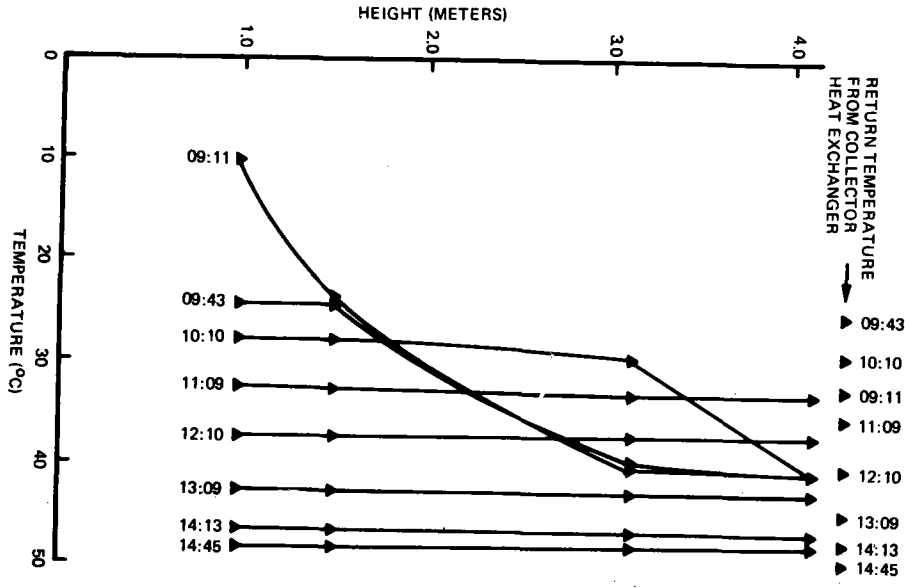

Figure 1. Temperature profile measurements as a function of time. Reproduced with permission from reference [7].

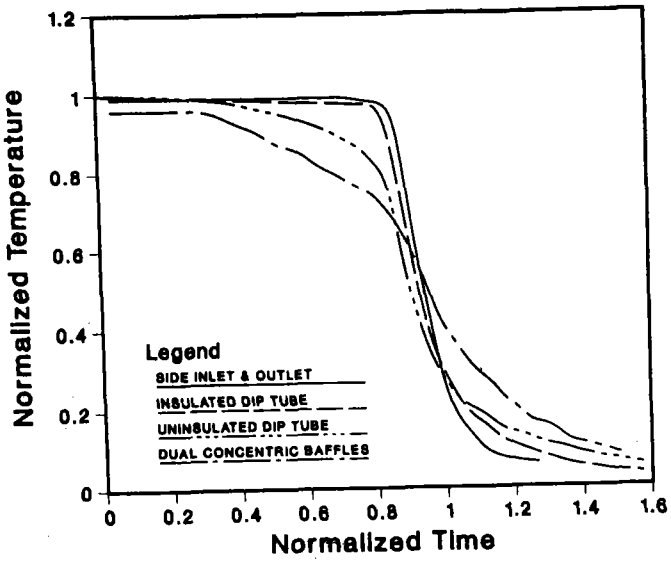

Figure 2. Discharge tests of 190-ℓ tank at 7.5 ℓ/min. ΔT = 40°C.

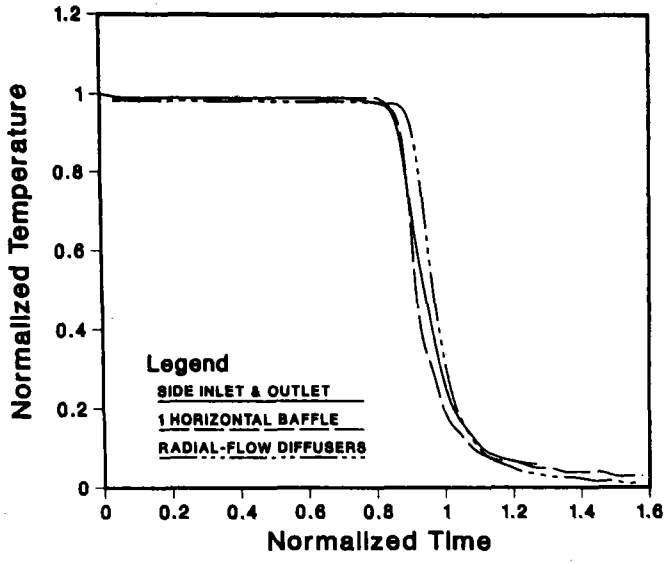

Figure 3. 7.5 ℓ/min discharge tests of three 190-ℓ tank configurations. ΔT = 40°C

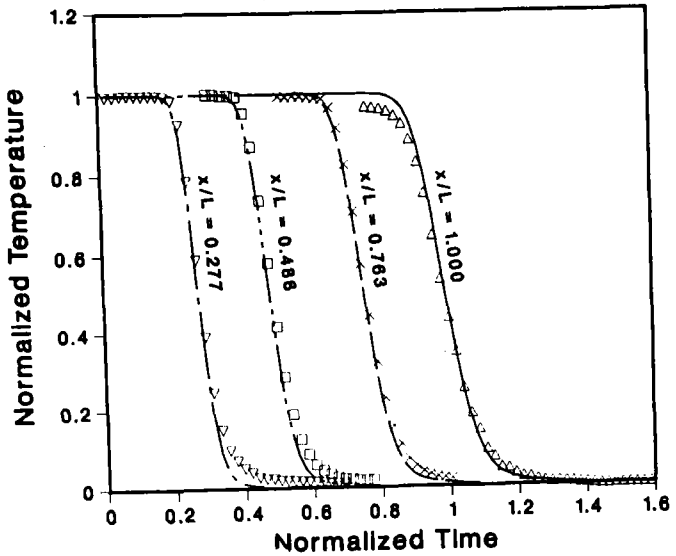

Figure 4. Comparison of analytical model (Equations 1-5) with November 3, 1981 experiment.

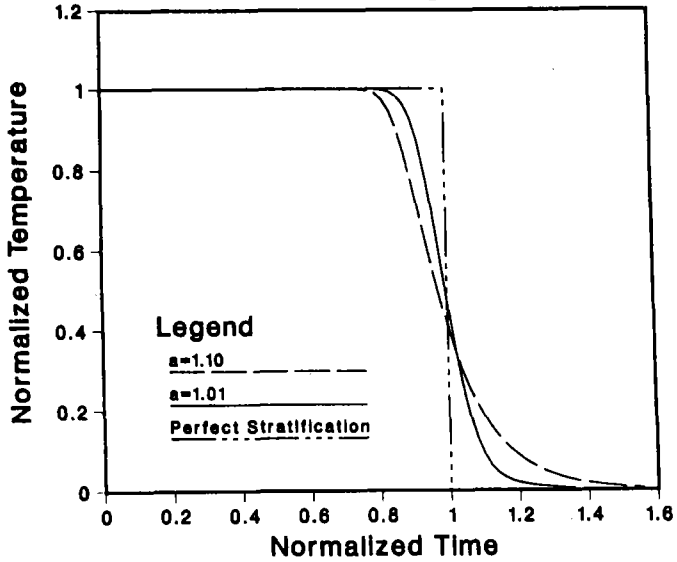

Figure 5. Comparison of tanks having light and massive walls.

HEAT STORAGE BUILDING MATERIALS FOR PASSIVE SOLAR APPLICATIONS

J.W. Fletcher and P.G. Grodzka
Lockheed Missiles & Space Co., Inc.
Huntsville, Alabama 35805

INTRODUCTION

Thermal storage in building materials for passive solar homes has generated considerable interest and research in recent years because of rapidly escalating fuel costs and the desire to reduce dependence on fossil fuels. The use of masonry walls and floors for thermal storage of solar energy has been successfully demonstrated and gained some acceptance by the public. However, the large volume and weight requirements for such systems work against their use in multi-story structures, manufactured homes and retrofitted applications. Furthermore, the non-traditional architectural design often meets with customer resistance among the more conservative community (Ref. 1). The concept of incorporation of phase change material (PCM) into building materials has received some attention recently and provides an attractive alternative to the use of aggregate construction for addition of thermal mass. The PCM concept lends itself to lightweight, low volume construction techniques, more closely related to standard building practices. PCM research has revealed several problem areas that must be addressed before successful incorporation into building materials: (1) incongruent melting of PCM; (2) nucleation requirements, (3) vapor transmission through container, and (4) corrosiveness of PCM.

The Lockheed approach to heat storage building materials involves incorporation of PCM into double-walled, hollow-channeled plastic panels of approximately 1/4 in. thickness. In this concept these PCM-filled panels would replace the interior walls and ceiling of the dwelling. The use of these wall and ceiling panels for thermal mass lends itself well to almost any passive solar concept since heating of the dwelling during the day is the only mechanism needed to store energy. In addition, the PCM-filled panels should moderate the interior temperature swing during the spring and fall, improving comfort and saving both heating and cooling costs.

This study is not intended to be a PCM study, but rather an engineering study of the overall concept. Therefore, only well characterized PCMs were considered for this study: Calcium chloride hexahydrate ($CaCl_2 \cdot 6H_2O$), Glauber's salt ($Na_2SO_4 \cdot 10\ H_2O$), and lithium nitrate trihydrate ($LiNO_3 \cdot 3H_2O$). Since development and testing of candidate building materials (panels) containing well characterized and "behaved" PCMs is of major importance in this study, Lockheed has obtained the services of Winston Industries, Inc., a fabricator of manufactured homes, to provide valuable building trade information, to ensure adherance to building codes and to ensure customer acceptance of the developed product.

PROJECT DESCRIPTION

Lockheed's approach to encapsulation of PCM in wallboard and ceiling tiles is not totally unique. A prior MIT study (Refs. 2 and 3) encapsulated PCM in specially developed polyester concrete ceiling tiles. Lockheed has tentatively chosen a corrugated plastic wallboard material that is commonly used in a number of applications. The corrugated polypropylene boards, 4' x 8' x 1/4 in.; are available in a variety of colors and cost about $0.10 to $0.23 per square foot. Filled with $Na_2SO_4 \cdot 10\ H_2O$ or $CaCl_2 \cdot 6\ H_2O$ the material cost of the PCM paneling is between $0.21 and $0.33 per square foot. Decorative vinyl and foil-backed films are presently available to allow a liberal selection of patterned wall or ceiling coverings. With reasonable manufacturing techniques the panels should be cost effective as a replacement material for wallborad and ceiling tiles.

This study will address the technical concerns and cost aspects of developing these heat storage wall/ceiling panels for use in passive solar heated structures. The PCM wall and ceiling panels will be developed and tested for applications where the charge mechanisms are free and forced air convection and direct irradiation of the panel by the sun. The discharge mechanism will involve both convection and radiation heat transfer to the room from the PCM wall and ceiling panels. Structured in this way, this panel development program is responsive to the needs of structures which utilize attic air collectors and interior storage as well as direct-gain structures. Specifically, the following tasks are included in this study.

Laboratory Development and Testing

The objective of this task is to perform the technical development, testing, parameter selection, and demonstration of the long-term reliability of the PCM-filled panel concept using laboratory-scale samples. The major thrust of this activity is to integrate current technologies of hollow extruded plastic panels along with a technically and economically acceptable PCM into an acceptable building material.

The technical concerns with regard to the panels are compatibility with the chosen PCM, filling the small channels (1/4 in. x 1/4 in.), sealing the panel edges, attaching panels to walls and ceilings, providing cut-outs for wall sockets and light swiches, sealing these cut-outs, and thermal and structural characteristics of the panels.

Each of the tests to be performed is discussed as follows:

PCM Screening Tests: Minor laboratory testing of various PCM formulations are to be performed prior to PCM selection. Aspects such as nucleation catalyst effectiveness, melting and freezing temperatures as a function of water content (for $CaCl_2 \cdot 6H_2O$ and $LiNO_3 \cdot 3H_2O$), and realizable heats of fusion are to be determined. A differential thermal analysis (DTA) will be used to determine relative magnitudes of realizable heats of fusion and to adjust transition temperature range.

Container Material Properties: Physical and chemical properties of the plastic panels will be determined. Water vapor transmission tests (ASTM E-96) will be performed for the various plastic panels and panels with decorative vinyl and foiled-backed films attached. Thermal expansion and specific heat tests for finished panels are also to be performed as part of this task.

Thermal Cycling Tests: Small samples of PCM-filled panels will be subjected to various thermal cycles, i.e., fast heating and cooling, slow heating and cooling, and expected temperature extremes. The effect of such cycling on PCM performance will then be checked by subjecting withdrawn samples of PCM to a simple DTA. The realizable heat of fusion of the small PCM-panel samples after thermal cycling will be determined by a water calorimeter. These preliminary thermal cycling tests will provide data for subsequent final PCM-panel design.

Dynamic Performance Tests: A test stand suitable for a full-sized panel will be constructed such that the panels will be faced with insulation on one side in a typical installed configuration. The PCM test panels will be instrumented with thermocouples at various exterior and interior locations to monitor heat flows and PCM state. The test stand will be capable of subjecting the panels to various heating and cooling environments. These environments will include forced and natural convection heat transfer using air as the heat transfer fluid. A separate outside test chamber will be designed and constructed for direct-gain performance testing.

Accelerated Life Tests: In these tests the panels used in the preceding dynamic performance tests will be subjected to an accelerated program of thermal cycling in the test chamber. A heater and an air-conditioner will provide the alternate heating-cooling requirements. The realizable heat of fusion of the small test panels after the accelerated thermal cycling will be determined. The performance of the larger panels will be checked after accelerated thermal cycling, by determining the dynamic thermal response.

Materials compatibility Tests: The compatibility of PCM and panel materials will be determined by keeping samples of PCM-filled panel at high (136°F) temperatures for prolonged periods of time. Signs of attack by the PCM on the plastic will be ascertained by examining the interior surfaces.

Durability Tests: Simple tests involving applied vibrations will be conducted on the full-scale panels. An apparatus that provides a vibration of about 0.3 mm amplitude and a frequency of 12 cycles/sec will be devised. The performance and the physical integrity of the panels after being subjected to such a vibration will then be checked.

Drop tests will be conducted. Panels in different orientations will be dropped one meter ten times. The performance and physical integrity of the panels after subjection to such drops will then be checked. Structural integrity of the panels (particularly regarding the attachment point stresses) will be evaluated.

Application Analysis

Based on the performance of the wall/cycling panels specific passive solar applications will be investigated and the one best suited to this concept will be identified. This system will be thermally modeled so that appropriate design parameters can be selected, thermal performance estimated, and required control mechanisms and strategy determined. The issue of thermal comfort will also be addressed for the system and compared to available heat systems.

The compatibility of the concept with all codes and construction practice will be ensured. Where necessary, new construction techniques will be invented. The effect of PCM leakage and other factors that may affect customer acceptance more than thermal performance will also be evaluated.

Concept Evaluation

A conceptual design of a passive solar residence located in Albuquerque, New Mexico will be prepared. The design will be of sufficient flexibility to allow comparison of a passive system with sensible heat storage to that utilizing the proposed PCM concept. For both systems, installed costs, annual energy requirements for space conditioning, and solar fractions will be determined. The life cycle cost of the PCM building materials system will also be determined.

PROJECT STATUS

As of this writing, five months of the 15-month study have been completed, and considerable progress has been made toward the successful completion of the primary task, Laboratory Development and Testing. Achievements within this task are summarized in the following subsections.

PCM Screening Tests: Laboratory screening of the three PCM candidates ($CaCl_2 \cdot 6\ H_2O$, $Na_2SO_4 \cdot 10\ H_2O$, $LiNO_3 \cdot 3\ H_2O$) is essentially completed. Various properties of the PCMs have been established and the effectiveness of their respective nucleating agents observed. The Dow Chemical formulation of $CaCl_2 \cdot 6\ H_2O$ (Thermol 81) and $LiNO_3 \cdot 3H_2O$ have performed very well in the sample plastic panels. Performance of $CaCl_2 \cdot 6H_2O$ and $LiNO_3 \cdot 3H_2O$ have also been monitored as a function of water content, and show some promise for alteration of the freezing/melting points. Glauber's salt has not behaved as well as the other two and is still considered only because of its low cost.

Filling and Sealing: Considerable time and effort has been spent on determination of adequate filling and sealing techniques. Prevention of air entrapment (bubbles) in the PCM has been a problem, primarily due to the long, narrow channels to be filled. All methods tested have proven to be very time consuming, including the presently used method. Hot PCM is pumped into an inclined panel, with one end sealed, through a long tube (with specially designed nozzle to allow trapped air to escape) which is injected into the channel and extracted slowly as the channel is filled. More efficient methods are under investigation.

Samples of plastic panels have been sent to numerous companies that manufacture apparatuses for sealing plastics. Techniques investigated to date include hot melt glue, ultrasonic, electromagnetic and pressure-heat. Although none of these have been eliminated for sealing during manufacture of PCM-filled panels, only the pressure-heat seal has been successful for laboratory sealing of 4 x 8 ft panels. Control of temperature during this procedure is critical (as is channel dryness) and thus sealing of all channels is difficult to obtain. Efforts will continue to determine a reliable sealing technique.

Container Material Properties: Water vapor transmission tests (ASTM E-96) were begun in April on various plastic panels at 20 mm Hg vapor pressure differential. These tests will continue through the contract period of performance and tests on other samples will be added as necessary to develop a successful container system. Should these tests prove that water vapor transmission over the expected life would be enough to affect performance, decorative vinyl and foil-backed films are being considered as vapor barriers. Thermal expansion and specific heat of finished panels have not yet been determined.

Thermal Cycling Tests: Preliminary thermal cycling tests have been performed on laboratory scale PCM-filled panels, simply to observe the affect on PCM performance. Samples of the PCM have been drawn from the panels and stored for later DTA tests. These samples will be subjected to DTA prior to the dynamic performance tests to be conducted in the full-scale test chamber. Orientation proved to be a factor in the small samples during these preliminary tests, with performance degradation noted for the vertical channel orientation. It appears incongruent melting is overcome, however, by the horizontal channels.

Test Chamber Construction: Design, construction and check-out of the test chamber, along with instrumentation, controls and data acquisition system, have been completed. Full-scale panels are under preparation for testing within the chamber in three orientations: wall-mounted with horizontal channels, wall-mounted with vertical channels and ceiling-mounted. Dynamic performance tests are to begin in early August with accelerated life tests to follow. Design of the direct-gain test chamber has been completed and construction should begin in August.

REFERENCES

1. E. Holland, "Albuquerque Backs Low-Cost Homes," Solar Age, Vol. 6, 1981, p. 57.

2. T.E. Johnson, "Lightweight Thermal Storage for Solar Heated Buildings," Solar Energy, Vol. 29, 1977, pp. 669-675.

3. T.E. Johnson, "Preliminary Performance of the MIT Solar Building 5," ERDA Report, March 1978, (No other identification available).

EFFECTS OF ADDITIVES ON PERFORMANCE OF HYDRATED TES SYSTEMS

Calvin D. MacCracken
Calmac Manufacturing Corporation
Englewood, NJ 07631

INTRODUCTION

Elimination of stratification in many phase change materials is paramount in achieving a useful thermal storage medium. Successful attempts to solve the problems of stratification include use of a pump (Calmac 1980) and various suspension media. The stirring pump works well in Calmac's bulk storage tank, but is limited to congruently melting PCMs. Suspension media presently marketed are frequently limited to use in systems of shallow depth (i.e. 1") and some require that 20% or more thickener be added to the PCM.

A suspension medium comprising a minor proportion of the whole PCM and exhibiting long-term stability in a bulk system has obvious advantages over present systems.

Kent and Page (1981) of CALOR Group Limited patented a hydrogel consisting of a water-soluble synthetic polymer and a crosslinking agent. They cycled a number of PCMs with gel over 500 times in container 4½ cm diameter and 10 cm high resulting in reproducible thermal behavior and no segregation.

The 45F salt hydrate is a eutectic combination of three salts: sodium sulfate, ammonium chloride and potassium chloride. A thickening agent is required to prevent stratification. A previously tested clay-type thickener was inadequate for bulk storage purposes because of a 30% decline in 60 cycles with stratification of both large crystals of anhydrous sodium thiosulfate and saturated sodium sulfate solution. See Bulk Storage of PCM, NTIS DE 8 1023402,Fig.43. Successful elimination of the stratification problem would result in a PCM appropriate for coolness storage during periods of reduced electrical rates.

The 115F PCM is sodium thiosulfate pentahydrate (STP). The actual melting point of STP is 118F. For storage purposes, however, a less expensive, slightly impure material that has a lower melting point has been proposed. Thus originated the 115F PCM using a stirring pump to prevent stratification of the dihydrate crystal.. Use of a thickening agent would have the advantage of expanding usage to include passive appications. Additives to control crystal growth rate and size were sought for the stirring pump systems so as to allow a reduction in HP required and to minimize disruption of the internal heat exchanger by dihydrate crystals should pump and heater fail to function, as in the case of electrical power outage. In addition fusion point depression by the additives would allow pinpointing of the most appropriate temperature for various applications. Adjustment of pH was investigated in an attempt to reduce subcooling.

Primary Activities

A confidentiality agreement was concluded with the CALOR Group in Slough, England providing CALMAC with all information for the mixing and testing of their hydrogel with PCMs used by CALMAC in a previous Argonne contract. Over 1000 melt-freeze cycles were performed with variations of gel formula, ethylene glycol and glycerine additives, pH of the solution, rate of heat transfer, and PCM formulation. Nearly 750 calorimetric measurements were taken in small and large samples with good accuracy and consistency.

General Laboratory Procedure

All formulations were initally tested as approximately ½ pound samples in 4 oz. polyethylene bottles for evaluation of thermal behavior. 45F PCM mixtures were cycled in refrigerator air for cooling and room air for heating. 115F PCM mixtures were cycled usually in room air for cooling and in a water bath for heating. Nucleating behavior and some fusion point data were obtained from this cycling.

After preliminary assessment of characteristics, calorimetric tests were performed. Samples were about ½ pound each, contained in two 2 oz. polyethylene bottles.

Promising mixtures were then tested in 2 gallon polycarbonate tanks for long term stability/cycling behavior. Stability of the 45F PCM was also evaluated in 3 foot high tubes.

As a result of exemplary performance in all small scale tests, a 45F mixture was tested in a 90 gallon tank (875 pound PCM) with Calmac's internal heat exchange coil.

Effect of Varying Gel Percentages

In the 45F PCM, a formulation containing 37.8% water, 29.5% Na_2SO_4, 22.4% NH_4Cl, 3.9% KCl, 3% Borax, gel and sometimes Formalin or Glyoxal as a crosslinking agent, as little as 3% gel with crosslinking and 4% gel without crosslinking was sufficient for stabilization.

Often vertical height makes a difference in PCM performance. Whether in vertical rods or trays or tanks this condition is likely to be encountered. The tests at 4 ft. height showed both in rods and a tank that the 3% crosslinked and the 4% non-crosslinked CALOR gel resists that effect in repeated cycling. Figure 1 shows the stable results of the 45F PCM in 37 cycles compared to 30% reduction in thermal storage when clay-type thickness were used (Calmac 1980).

115F PCM with Gel

STP samples with gel were alternatively heated and cooled, during which no stratification was observed. After a week or more at room temperature a bulging, lighter colored layer of

crystals, presumed to be partially dihydrate crystal, appeared at the bottom of each sample except 59.5 parts. The height of this layer was proportional to the salt content.

A mix with 63.5 parts salt: 36.5 parts water with CALOR gel provided optimum performance in terms of both supercooling and heat storage capacity. Some stratification occurred but did not have detrimental effect on performance.

Ethylene Glycol and Glycerine as Additives

Extensive work was done showing the effect on both 45F and 115F PCM's of above additives. Curves are given in the Final Report showing the decrease in fusion temperature, heat of fusion, and effect on rate and size of crystal growth. These additives soften the drystals to eliminate the effect on stirring pump impellers or sihydrate bulging noted in previous work (Calmac 1980).

A wide range of pH values in the 115F PCM showed that varying the standard 8.7 value supplied by the manufacturer caused supercooling problems.

CONCLUSIONS

1. The CALOR gel reliably eliminates stratification in sodium sulfate decahydrate and its eutectics stabilizing at a heat of fusion of 72 to 77 Btu/lb for the 89F salt and 52 to 55 Btu/lb for the 45F eutectic, as shown in repeated cycling teats in samples up to 4 foot vertical height; mixed gel costs add about 5 to 10 cents/lb.

2. The present CALOR gel is a decided improvement in stabilizing raw unstirred 115F PCM but still shows some separation and discoloration upon repeated cycling; in active systems a stirring pump is deemed preferable but in passive encapsulations of 115F PCM the gel may be useable although expensive; recent further improvements are reported.

3. The CALOR gel when mixed with both PCMs in recommended percentages is pumpable provided the crosslinking agent is added only at the time of final filling; barrels of the gel/PCM can be shipped to a fill site and pumped in as needed with strap-around electric barrel heaters to keep the PCM melted.

4. Ethylene glycol and glycerine were equally effective in lowering the fusion point and reducing crystal size but at a penalty in heat of fusion; a 1 to 2% addition of glycol in the 115F PCM is effective in eliminating oversized crystals with only minor effects in fusion point and heat of fusion; this protects container or heat exchanger from damage.

5. No real effect of pH on subcooling of the 115F PCM was found; pH must be kept slightly basic to prevent free sulfur formation; the most effective way to prevent subcooling of this salt is to limit its temperature above the melting point.

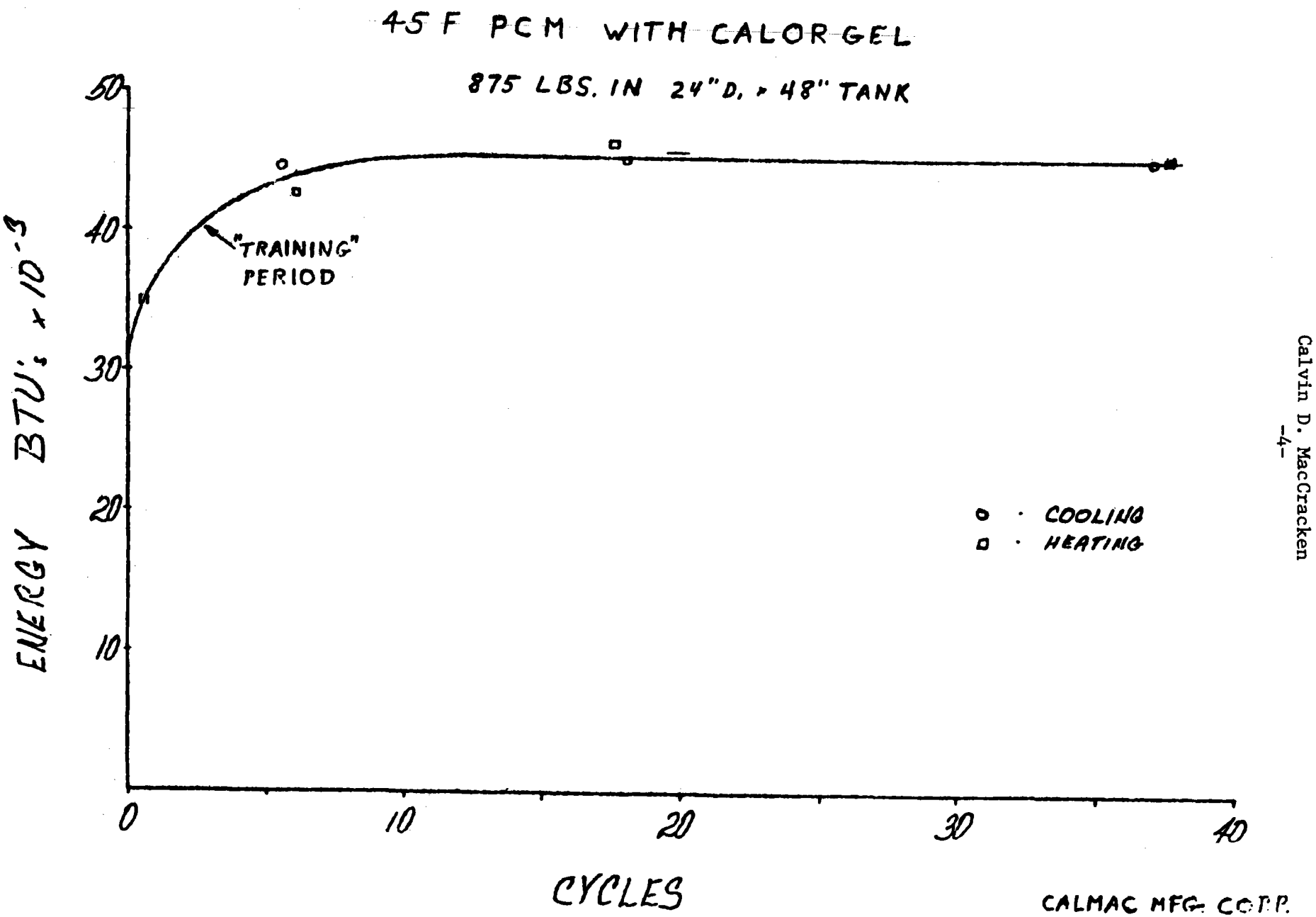
45 F PCM WITH CALOR GEL
875 LBS. IN 24" D. x 48" TANK
ENERGY BTU's x 10⁻³
50
40
30
20
10
0
10
20
30
40
CYCLES
"TRAINING" PERIOD
o · COOLING
□ · HEATING
CALMAC MFG. CORP.
MAR. '82

FIGURE 1

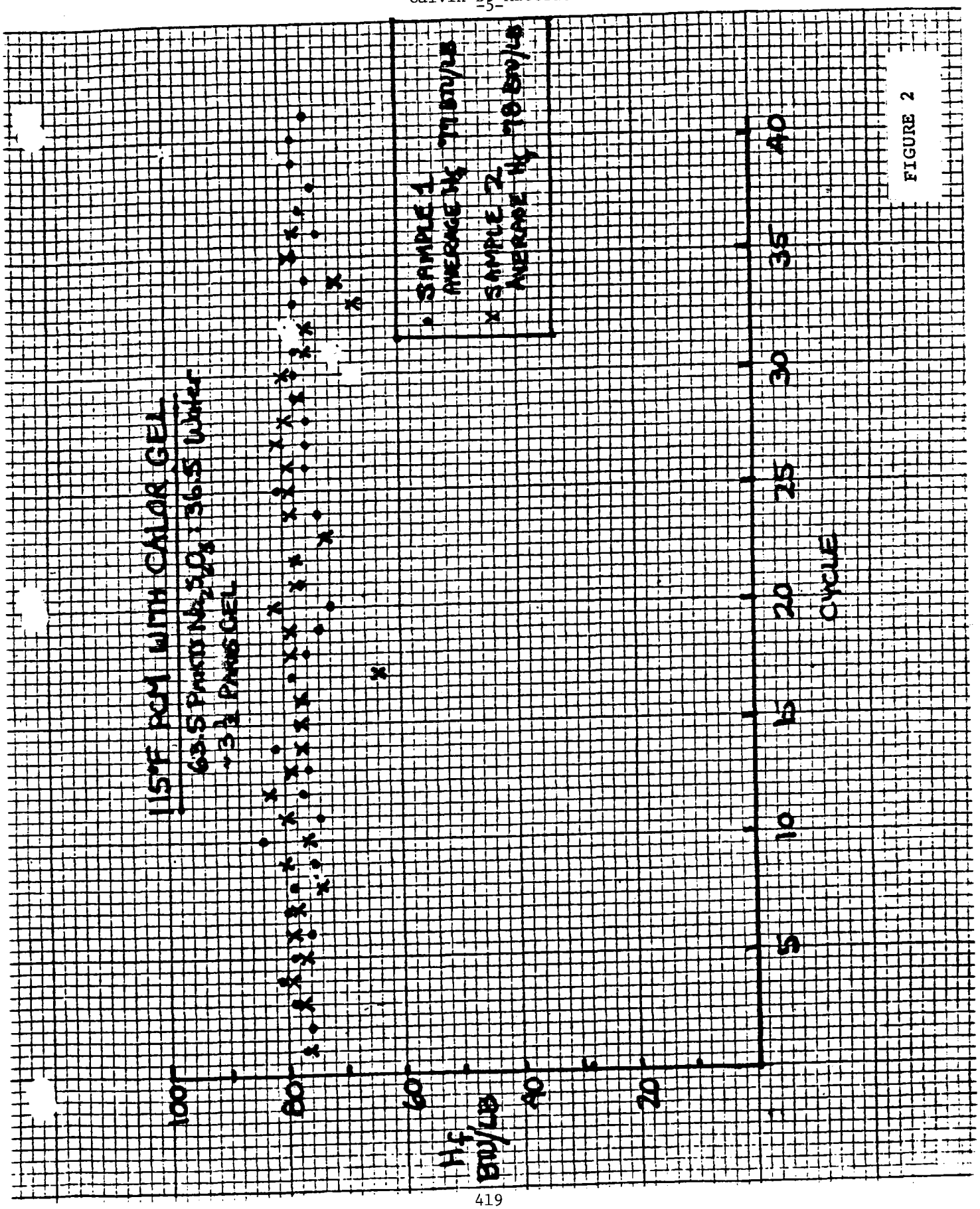
ISF RUN WITH CALGON GEL
63.5 Parts Na2SO4 in 365 Parts Water
+3.5 Parts Gel
• SAMPLE 1
AVERAGE Hf 77 BTU/LB
x SAMPLE 2
AVERAGE Hf 78 BTU/LB
Btu/lb
Hf
100
90
80
70
5
10
15
20
25
30
35
40
CYCLE

FIGURE 2

EARTH THERMAL STORAGE-ASSISTED HEAT PUMP*

M. P. Ternes
Engineering Technology Division
Oak Ridge National Laboratory
Oak Ridge, Tennessee 37830

ABSTRACT

The earth under a house with a crawl space may be used to thermally condition the source air of an air-to-air heat pump during the winter as well as the summer. This allows the heat pump to operate in a temperature climate more favorable than ambient and, thus, at a higher efficiency. During this reporting period, a comprehensive, comparative test involving three unoccupied houses was begun to determine the net benefit of this concept. Results from the experiment for the past winter showed that dramatic improvements in the heat pump performance were obtained during midwinter conditions. Definitive conclusions cannot be made, however, because of the anomalies which were encountered. Summer data collection is currently underway, and no results are available at this time.

Introduction

Heat or "cool" stored naturally in the earth under a house with a crawl space might be used to temper the source air temperature of an air-to-air heat pump throughout the year and, thereby, bring about improved heat pump performance. The source air is conditioned by drawing it through the crawl space where it exchanges heat with the warmer or cooler earth. The improved performance would result because the heat pump would operate in a more favorable temperature climate than ambient. The seasonal performance factor (SPFH for heating or SPEC for cooling - the ratio of the amount of heat or cool delivered by the heat pump system to the amount of electricity used by the system) represents the efficiency of the total heat pump system and, thus, provides a measure of performance. An increase in the SPFH during the winter would be expected because: (1) the steady-state coefficient of performance (COP) of the heat pump would be higher for a given outdoor temperature, (2) the steady-state capacity of the heat pump would be higher for a given outdoor temperature resulting in a decreased need for supplemental resistance heat, and (3) the need for defrosting would be decreased since the source air would be at a higher temperature. The SPFC would be expected to increase during the summer because, again, the steady-state cooling COP of the heat pump would be higher for a given outdoor temperature.

*Research sponsored by the Division of Thermal and Mechanical Energy Storage Systems, U.S. Department of Energy, under contract W-7405-eng-26 with the Union Carbide Corporation - Nuclear Division.

Houses making use of the crawl space concept would have lower than average crawl space temperatures in the winter and higher than average temperatures in the summer, resulting in an increased house heating and cooling load. Furthermore, the heat pump might cycle more frequently since it would effectively be "oversized" for the milder conditions in which it would operate. This increase in cycling could increase the magnitude of the cycling losses causing a decrease in the heat pump's performance. Both of these effects, the increased cycling losses and the increased loads, if significant, could negate the benefits obtained from the improved heat pump performance.

Tests were performed during 1979 and 1980 to determine whether the concept was feasible, and, if so, in which direction further work should proceed. These tests have been discussed previously by this author [1, 2] and McGill [3]. Based on the conclusions of these studies, the concept looked promising, and a more definitive test was begun this fiscal year to: (1) determine the net energy savings which could be realized over an entire year, (2) evaluate the impact of the altered crawl space conditions on the heating and cooling requirements of the house, and (3) obtain detailed heat pump performance data to quantify the improved performance as well as the effect of cycling losses.

Current Experiment

It was felt that a controlled test involving several structures with identical heating and cooling loads would be required to study this concept further because of the uncertainties involved in using heat pump calculational models alone. Definitive conclusions on the merits of this concept could then be drawn for the climatic region of this test. Therefore, three "identical" houses, located in relatively close proximity to the Oak Ridge National Laboratory (East Tennessee), were leased. The houses have a floor area of 1200 ft^2 and are unoccupied. Two of the houses are configured to use the crawl space preheating concept, one each for the single pass and total recycle modes. In the single pass mode, outdoor air is drawn through the crawl space, passed over the outside coil of the heat pump, and finally discharged to the atmosphere. In the total recycle mode, air discharged from the heat pump is recirculated through the crawl space and then returned to the outside coil. A conventional heat pump installation in the third house serves as the control for the experiment. The houses are insulated according to recommendations provided by the Knoxville Utilities Board, the local utility for the Knoxville, Tennessee area: R-11 in the walls, R-19 in the floor, and R-30 in the ceiling. Each house is equipped with the same make and model two-ton single package residential heat pump with all duct work located in the crawl space and initially insulated to R-3.8.

Winter data collection began in the middle of December 1981 and continued until the middle of April 1982. Summer data collection will begin in mid-May 1982 and will be terminated around the end of the fiscal year. The results to be discussed in the next section are concerned only with the winter data.

Results

Ideally, three "identically" built houses, all unoccupied, would have the same heating loads allowing data from the houses to be compared on a one-to-one basis. If the heating loads are not the same, then the difference must be taken into account in the analyses. The loads were checked by heating the houses using resistance heat only for two one-week periods during the winter. The loads obtained in this manner will be referred to as the base heating loads. Note that in heating with resistance heat only, outside air is not drawn through the crawl spaces of the earth storage houses. Consequently, the crawl space temperatures were nearly the same in all three houses. The results obtained from the two weeks of data indicated that the control house and the single pass house had similar base heating loads and, thus, further results from these two houses can be compared directly. However, the data also indicated that the base heating load of the total recycle house was 6% less than that of the control house for reasons as yet unresolved. Results from the total recycle installation will be modified when appropriate to take this difference into account.

The three houses were heated by their respective heat pump heating systems for a 27-day period starting December 22, 1981. As in the base heating load test, the inside temperature was maintained at approximately 70°F. Results from this period are shown in Table 1. (In this table, as in the table to follow, the normalized results are the ratios of the actual data to the control house data.) The total recycle data was modified by increasing the measured house heating load by 6% (based on the base heating load data), and by assuming that 75% of this increased heating load had to be met by supplemental resistance heat and that the remaining increased heating load was met by the heat pump operating at the same average efficiency determined for the period. The amount of electricity used for supplemental resistance heat and defrost decreased, as expected, for both of the earth storage systems. In fact, the electricity required for defrosting in the single pass system was

Table 1

27 Day Heat Pump Results

	Control house		Single pass house		Total recycle house			
	Measured	Normalized	Measured	Normalized	Measured	Normalized	Modified	Normalized
Seasonal performance factor	1.74		2.03		2.22		2.11	
Electricity used for defrost, kWh	108.3	1.00	48.9	0.45	28.5	0.26	30.2	0.28
Electricity used for supplemental resistance heat, kWh	140.7	1.00	126.9	0.90	29.4	0.21	111.9	0.80
Heat pump efficiency neglecting resistance heat	1.98		2.25		2.31		2.31	
House heating load, kWh	1,612	1.00	1,974	1.22	1,780	1.10	1,887	1.16
Total electricity used for heating, kWh	927.3	1.00	971.5	1.05	800.7	0.86	889.3	0.96

Total hours covered: 556

Degree days for the period: 741

Time period involved: December 22, 1981 – January 18, 1982

reduced by 55%, meaning that the need for defrosting was substantially reduced. The heat pump efficiencies for the earth storage systems were about 15% higher than the control because of the higher source air temperature attained with these systems. This heat pump efficiency is based on the heat output and electrical use of the heat pump itself and does not include the effects of resistance heat. Therefore, the increase in the SPFH for the earth storage systems results from a combination of the improvements just outlined. In summary, the data show that the performance of heat pump heating systems making use of crawl space preheating can be improved significantly.

The house heating loads and total heating electricity use for this period are also listed in Table 1. The data show that the heating loads for the earth storage houses are higher than that of the control house by 10 and 22%. But, the base heating load test discussed earlier indicated that the heating loads of the earth storage systems were the same or less than that of the control house when exposed to similar conditions. Thus, the increase in heating load for this period must have been due to the influence of the heat pump system on the crawl space which, in turn, affected the house heating loads. This increase in the house heating load was much larger than expected necessitating further studies.

Calculations showed that approximately one-third of the increased heating load in the single pass house could be attributed to increased heat loss through the floor because of the colder crawl space. Additionally, the remaining two-thirds of the increased heating load could be attributed to increased heat loss from the duct work located in the crawl space, again because of the colder crawl space. Thus, these two increased sources of heat loss, additional heat loss through the floor and the duct work, can account for the increased house heating loads found in Table 1. Tests proved that the increased loads were not due to exfiltration of warm air from the house to the crawl space. To reduce the heat loss, the ducts in the earth storage houses were reinsulated, raising the R value from 3.8 to 7.6.

Data were collected after the duct work was insulated for a four week period beginning February 12, 1982. These data are shown in Table 2. Modified total recycle house data are not shown because results obtained from a third base heating load test and analyses of house heating load profiles obtained from earlier data indicate that the base heating load of the total recycle house, although less than that of the control house at cold outdoor temperatures, may be higher for warm outdoor temperatures. Since this new data set was obtained at warmer outdoor temperatures, it is unclear how best to modify the data, if a modification is required at all.

The house heating loads for the earth storage houses were less than that of the control house after the extra insulation was added to the duct work. The amount of electricity used for supplemental resistance heat and defrost in the earth storage houses was also less than that of the control house. However, no significant increase was seen in the heat pump efficiencies of the earth storage systems. This is because the average outdoor temperature for this data gathering period was a

relatively mild 47°F, resulting in little heating of the source air by the earth. Consequently, no significant increases in the SPFH were observed, and the savings in the amount of electricity used to provide heat during this period was primarily due to the reduced duct heat losses.

Table 2

Results After Reinsulating the Duct Work

	Control house		Single pass house		Total recycle house	
	Measured	Normalized	Measured	Normalized	Measured	Normalized
Seasonal performance factor	2.23		2.26		2.34	
Electricity used for defrost, kWh	37.5	1.00	10.3	0.27	6.1	0.16
Electricity used for supplemental resistance heat, kWh	6.4	1.00	0.1	0.02	0.1	0.02
Heat pump efficiency neglecting resistance heat	2.33		2.28		2.36	
House heating load, kWh	1099	1.00	1001	0.91	1079	0.98
Total electricity used for heating, kWh	493.5	1.00	443.0	0.90	460.5	0.93

Total hours covered: 592

Degree days for the period: 506

Time period involved: February 12, 1982 – March 9, 1982

Summary and Conclusions

We have shown that dramatic improvements in heat pump performance during the winter are realizable by employing the crawl space preheating concept. The SPFH for a single pass mode installation in eastern Tennessee increased 17% based on data taken over a 27 day period in the middle of the winter. This increase in the SPFH was due to reductions in the amounts of electricity used for supplemental resistance heating and defrosting of 10 and 55%, respectively, and a 14% increase in the heat pump COP. A 21% increase in the SPFH was predicted for a total recycle mode installation based on modified data recorded over the same time period. This increase can be attributed to a 20 and 72% decrease in the amounts of electricity used for supplemental heating and defrosting, respectively, as well as a 17% increase in the heat pump COP.

An unexpected additional heat loss from the duct work and an inability to collect a sufficient amount of data during a representative winter period once the duct work was reinsulated have prevented us from drawing definitive conclusions as to the energy savings and heat pump improvement one could expect for an entire winter season. Summer data collection is currently underway and the results from this phase of the experiment are not known at this time. Some simple solutions to the problems which were encountered this winter are currently being studied, and if successful, a relatively inexpensive method of improving heat pump performance and possibly expanding its service area into colder climates will exist.

References

1. M. P. Ternes, Crawl Space-Assisted Heat Pump, DOE Publication Conf -791232, pp. 271-276, 1980.

2. M. P. Ternes, Crawl Space-Assisted Heat Pump, DOE Publication Conf - 801055, pp. 24-27, 1981.

3. R. N. McGill, Crawl Space-Assisted Heat Pumps, Heat Pump Contractors' Program Integration Meeting, June 2-4, 1981, DOE Publication CONF-810672.

DEVELOPMENT OF COMPOSITE TES MEDIA FOR HIGH-TEMPERATURE STORAGE APPLICATIONS

T. D. Claar, R. J. Petri, and E. T. Ong
Institute of Gas Technology
IIT Center
Chicago, Illinois 60616

ABSTRACT

A novel thermal energy storage (TES) media concept utilizing carbonate salts retained within the micro-porous structure of a ceramic matrix is being developed for such high temperature storage applications as industrial waste heat recovery/storage and solar thermal power systems. The composite carbonate salt/ceramic media can operate in direct contact with compatible working fluids, a feature which offers significant potential for cost reduction and improved heat exchange performance over previous shell-and-tube molten salt TES designs. Results of the generic composite media development efforts, materials stability testing, and TES performance evaluations are discussed.

BACKGROUND

Many opportunities exist for implementation of thermal energy storage in industrial, solar, utility, and commercial applications as a means of providing a better time match between heat availability and heat demand. Various materials have been proposed and developed as sensible- or latent-heat media, including water, rock, sand, organic oils and waxes, metals, inorganic salts, and ceramics. The preferred medium for a given application depends on various factors, including storage temperature and capacity requirements, charge/discharge rates, and allowable cost.

Numerous technology development and systems studies have been conducted on latent-heat storage using phase-change salts (e.g. carbonates, chlorides, fluorides, hydroxides, and nitrates). These studies have generally shown the advantages of latent-heat systems in providing high energy storage densities and availability of stored energy at nearly constant temperature. Most of these efforts have focused on containment of molten salts in passive shell-and-tube heat exchanger (HX) configurations, which have inherent heat transfer performance limitations caused by growth of solid salt layers on external HX tube surfaces during thermal discharge. Attempts to improve heat transfer through the use of high-conductivity extended surfaces, mechanical scrapers, and coatings to prevent solid salt from adhering to HX tubes have been only partially successful.

Work conducted at IGT under previous TES development programs has demonstrated the attractive properties and stability of alkali metal/alkaline earth metal carbonate salts as phase-change storage media.(1-4) Carbonate compositions with melting points covering the range from 397°C to 898°C have been evaluated for materials compatibility and TES performance as free melts in shell-and-tube HX designs utilizing austenitic stainless steel or nickel-base superalloy materials of construction. An engineering-scale TES module of 25,000 Btu thermal capacity (latent plus sensible heats) was designed, fabricated and tested with 130 lb of

$LiKCO_3$ salt, which melts congruently at 505°C with a heat-of-fusion of 148 Btu/lb. The TES module showed very stable thermal performance and excellent compatibility between the carbonate salt and the AISI 316 stainless steel containment and HX tube during 5650 hours of testing and 129 charge/discharge cycles over the temperature range 480° to 535°C. Although the 300-series austenitic stainless steels have been found to be generally compatible with molten carbonates at temperatures up to 700°C, superalloys or coatings are required for long-term operation in shell-and-tube configurations at higher temperatures, significantly increasing the cost of such a TES subsystem.

More recent R&D efforts at IGT have demonstrated the feasibility of an alternative approach to containing molten salts that offers the potential for elimination of HX tube configurations and operation in direct contact with compatible working fluids. The approach thus represents the possibility for significant cost reductions through elimination of HX tube materials and fabrication costs, as well as improved thermal performance via direct-contact operation.

COMPOSITE SALT/CERAMIC MEDIA CONCEPT

The composite TES media concept involves retention and immobilization of a phase-change salt (latent-heat phase) within the micro-porous structure of a particulate ceramic matrix or porous sintered ceramic body (sensible-heat phase).* The molten salt is retained within the micro-porosity defined by the ceramic network by capillary surface tension forces. The volume fraction of molten salt that can be retained is determined by the characteristics of the support material (e.g. particle size and shape, distribution and specific surface area), salt properties (e.g. surface tension and viscosity), and wetting behavior between the molten salt and ceramic phases. The feasibility of retaining 60 vol % of molten carbonates within a ceramic particle matrix at 800°C has been experimentally demonstrated. Retention of higher volume fractions of liquid is possible by optimization of ceramic support characteristics and media processing conditions.

The composite media may be fabricated into cylindrical pellets, briquettes, spheres, etc. and used in a packed bed arrangement. Alternatively, composites may be formed into brick shapes and stacked in a regular array, such as a brick checkerwork regenerator. Media shapes and sizes may be varied to provide the optimum heat transfer surface area/volume ratio and bed packing density.

The technical feasibility of this composite approach to high-temperature TES depends largely upon the behavior and stability of the media —

- Ability of the ceramic support to retain adequate amounts of molten salt by capillary action, with minimal chemical interaction between salt and ceramic. Creepage of molten salt from the porous shape must be minimal.

---

* IGT has filed a patent application on this concept.

- Ability of the salt/ceramic composite to be repeatedly thermal cycled (melting/solidification of the salt phase) with minimal cracking, spalling, or other structural damage.

- Chemical compatibility of the molten salts with TES charge/discharge fluids to minimize vaporization losses or changes in salt chemistry, melting behavior, surface tension, and other critical physical properties.

- Sufficient strength to maintain structural integrity under the stresses imposed by the system design.

COMPOSITE MEDIA DEVELOPMENT AND TESTING

Materials Selection

The phase-change salts are being selected from available alkali metal and alkaline earth metal carbonates and their mixtures, which are attractive for direct-contact utilization because of their superior high-temperature chemical stability in air and other oxidizing gases containing CO_2, O_2, and H_2O. Numerous congruently melting salt mixtures based on the alkali carbonates Li_2CO_3, Na_2CO_3, and K_2CO_3 are available with melting points covering the range 397°C (Li_2CO_3-Na_2CO_3-K_2CO_3 ternary eutectic) to 898°C (pure K_2CO_3), as summarized in Table 1. Candidate carbonates are being selected primarily on the basis of melting point, heat-of-fusion, cost, and thermochemical stability, although other properties such as density, volume change on fusion, heat capacity, thermal conductivity, viscosity, and surface tension are also being evaluated. Emphasis is being given to compositions based on Na_2CO_3 because of its attractive heat-of-fusion (114 Btu/lb), heat capacity (0.40 Btu/lb-°F) and low cost as a technical-grade salt ($0.03/lb). The congruently melting sodium carbonate-based compositions under consideration include Na_2CO_3-Li_2CO_3 (496°C m.p.), Na_2CO_3-K_2CO_3 (710°C m.p.), Na_2CO_3-$BaCO_3$ (715°C m.p.) and Na_2CO_3 (858°C m.p.). Incongruently melting compositions are also being considered in the Na_2CO_3-Li_2CO_3 and Na_2CO_3-K_2CO_3 systems as a means of "tailoring" thermal and physical characteristics.

The ceramic support materials are being selected primarily from metal oxides, aluminates, ferrites, titanates, or zirconates. The functions of the ceramic phase are to provide stable capillary forces for retention of the molten carbonate phase and to contribute sensible heat. The most critical property of the ceramic support material is expected to be its chemical stability in the high-temperature carbonate environment. Other selection criteria for the ceramic support materials include specific heat, cost, and ability to prepare as fine particulates or micro-porous bodies.

A medium consisting of 50 wt % of the carbonate salt of composition 48 wt % Na_2CO_3-52 wt % $BaCO_3$ (m.p. of 715°C) supported by 50 wt % submicron-sized MgO particles is being investigated as a model composite TES material.

Media Processing and Fabrication

Composite carbonate/ceramic powders are prepared from aqueous slurries using a spray drying process, which produces homogeneous, intimately dispersed powders with good flowability and forming characteristics. Spray-drying process procedures are being developed for preparation of ceramic supports and composite powders with controlled properties satisfying TES functional requirements. These materials are characterized with respect to critical properties such as chemical composition, specific surface area of support, particle size and shape distributions, flowability, and forming characteristics.

For laboratory testing purposes, composite powders are cold-pressed into cylindrical pellets at pressures of 10,000 to 30,000 psi and sintered to densities of 85 to 95% of the theoretical. Results of these compaction/densification studies are being utilized in the development of processes for cost-effective mass production of composite shapes. The feasibility of forming composite pellets by automatic dry pressing, extrusion, and molten salt impregnation of porous sintered ceramic shapes has been demonstrated. Development of appropriate fabrication process parameters is in progress, with emphasis on binder and lubricant selection and powder flowability for dry pressing, and on binder formulation, paste rheology, and binder burnout for extrusion.

Figure 1 shows composite Na_2CO_3-$BaCO_3$/MgO pellets fabricated by pressing and sintering of spray dried powders. Figure 2 is a scanning electron micrograph of a fracture surface of a typical composite pellet after sintering, revealing the morphology and distribution of carbonate and ceramic phases.

Media Behavior and Stability

Cylindrical pellets pressed from the model material Na_2CO_3-$BaCO_3$/MgO have shown excellent high-temperature stability in air at temperatures up to 850°C, and endurance to repeated thermal cycling. After 510 hours of testing at 800°C with 22 thermal cycles to ∿75°C, only minor weight loss (∿1%) and density change (∿1%) were observed. The pellets retained their initial shapes and no significant pellet cracking occurred.

The high-temperature mechanical behavior of TES pellets is being determined in compressive loading experiments. Pellets containing 60 vol % molten Na_2CO_3-$BaCO_3$ supported by MgO have exhibited compressive yield strengths exceeding 300 psi at 800°C. Elastic moduli of ∿1 x 10^6 psi at room temperature and ∿1 x 10^4 psi at 800°C have been measured on these pellets. Further mechanical property measurements (crushing strength at low temperature, creep rates at high temperature, and contact stress effects) are in progress to assure media structural integrity in packed-bed configurations.

A packed bed of Na_2CO_3-$BaCO_3$/MgO pellets (∿60% packing density) has been tested in a lab-scale TES unit for 17 thermal cycles from 815° to 615°C during 398 hours of operation. The bed was thermally discharged with ambient air after indirect charging by electrical clam-shell heaters. The high heat transfer rates (relative to previous tests on molten

Na_2CO_3-$BaCO_3$ with HX tube) and excellent media and bed stability observed in these tests have provided the initial verification of the feasibility of the direct-contact composite media approach.

A bench-scale TES unit (0.79 ft^3 bed volume) has been designed for a more quantitative evaluation of the charge/discharge performance of a packed bed of composite carbonate/ceramic media pellets. The TES unit will be adequately instrumented to provide reliable and detailed data for evaluating radial and axial temperature distributions, solid/gas heat-transfer coefficients, efficiency, flow rates of charge/discharge gases, flow distribution, and pressure drops through the media bed. The system will be charged using air heated by an electric heating element and discharged with ambient air.

THERMAL ENERGY STORAGE APPLICATIONS

This composite TES media concept is expected to be applicable to a broad range of intermediate- and high-temperature storage uses in industrial, solar, and utility systems. One proposed industrial TES application is in the SIC-32 industries (brick, ceramic, clay products, and refractories), which use periodic kilns that generally exhaust large quantities of waste heat in hot flue gases at temperatures of 250° to 1100°C. Approximately half of the firing kilns in SIC-32 industries are periodic in nature and well-suited to integration with thermal energy storage. It is estimated that implementation of TES could result in ~45% energy savings for a typical periodic kiln installation and a total annual SIC-32 industry energy savings of 0.2 quad. Potential applications also exist in the iron/steel and cement industries.

A possible solar application of the concept is in storage for solar Brayton central receiver power systems operating at 700° to 900°C with air or helium working fluids. Preliminary analyses indicate that a direct-contact TES subsystem containing composite carbonate/ceramic media shapes offers potentially significant reductions in system cost and size relative to proposed second-generation solar Brayton storage concepts utilizing MgO or Al_2O_3 refractory sensible-heat media.(5)

CONCLUSION

The composite salt/ceramic TES media under development offer the potential for a cost-effective and direct-contact approach to utilization of phase-change storage materials. By proper selection of salt and ceramic materials, these media can be designed for storage applications covering a broad range of use temperatures and working fluids. However, further efforts in the areas of composite processing, long-term stability testing, and TES system performance evaluation and scale-up are required before the technology can be implemented commercially.

ACKNOWLEDGMENT

This work was supported by the U.S. Department of Energy under Union Carbide/ORNL Subcontract No. 86X-95001C and SERI Subcontract No. XP-0-9371-2.

REFERENCES

1. Maru, H. C., Dullea, J. and Huang, V. M., "Molten Salt Thermal Energy Storage Systems: Salt Selection," COO-2888-1. Chicago: Institute of Gas Technology, August 1976.

2. Maru, H. C., et al., "Molten Salt Thermal Energy Storage Systems: System Design," COO-2888-2. Chicago: Institute of Gas Technology February 1977.

3. Maru, H. C., et al., "Molten Salt Thermal Energy Storage Systems," COO-2888-3. Chicago: Institute of Gas Technology (NASA-CR135419, 1978), March 1978.

4. Petri, R. J. et al., "High-Temperature Molten Salt Thermal Energy Storage Systems." Chicago: Institute of Gas Technology (NASA-CR159663), February 1980.

5. Boeing Engineering and Construction, "Advanced Thermal Energy Storage Concept Definition Study for Solar Brayton Power Plants, Vol. 1." Report prepared under Contract No. EY-76-C-03-1300 for the U.S. Department of Energy. Seattle, Wash., November 1977.

TABLE 1.

CONGRUENT MELTING CARBONATE COMPOSITIONS

Composition, wt %	m.p., °C (°F)	ΔH_f, Btu/lb	Cost, \$/lb*	Btu/\$**
$32Li_2CO_3$-$33Na_2CO_3$-$35K_2CO_3$	397 (747)	119	0.46	259
$46.6Li_2CO_3$-$53.4K_2CO_3$	488 (910)	168	0.67	251
$44.3Li_2CO_3$-$55.7Na_2CO_3$	496 (925)	169	0.55	307
$28.5Li_2CO_3$-$71.5K_2CO_3$	498 (928)	136	0.48	283
$35.0Li_2CO_3$-$65.0K_2CO_3$	505 (941)	148	0.55	269
$55.7Li_2CO_3$-$44.3CaCO_3$	662 (1224)	-	0.69	-
$50Na_2CO_3$-$50K_2CO_3$	710 (1310)	70	0.11	636
$47.8Na_2CO_3$-$52.2BaCO_3$	715 (1319)	80	0.11	673
Li_2CO_3	723 (1330)	261	1.21	216
Na_2CO_3	858 (1576)	114	0.03	3800
K_2CO_3	898 (1648)	86	0.19	453

* Costs from Chemical Marketing Reporter, June 16, 1980.

** Based on heat-of-fusion only; sensible heats neglected.

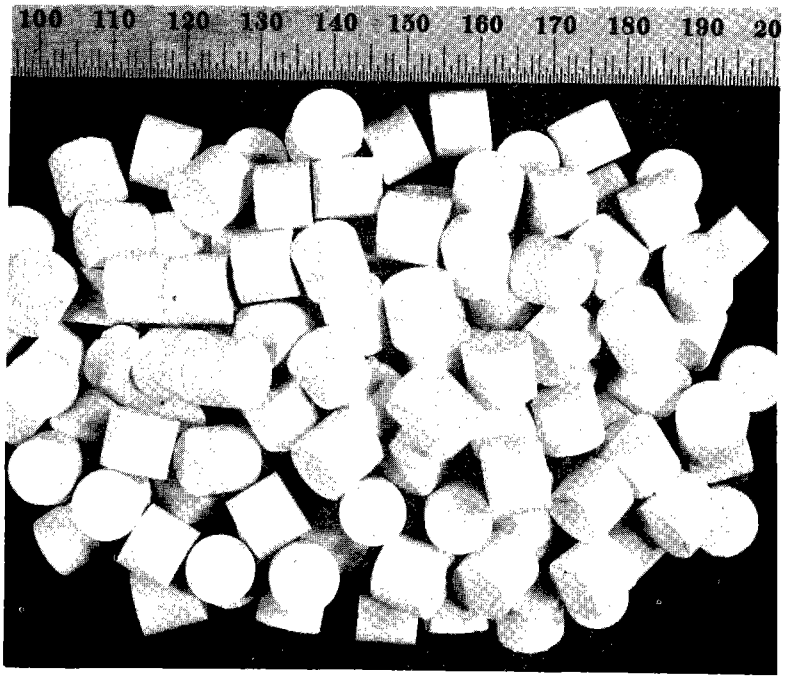

Figure 1. COMPOSITE Na_2CO_3-$BaCO_3$/MgO PELLETS FABRICATED BY COLD-PRESSING AND SINTERING OF SPRAY-DRIED POWDERS

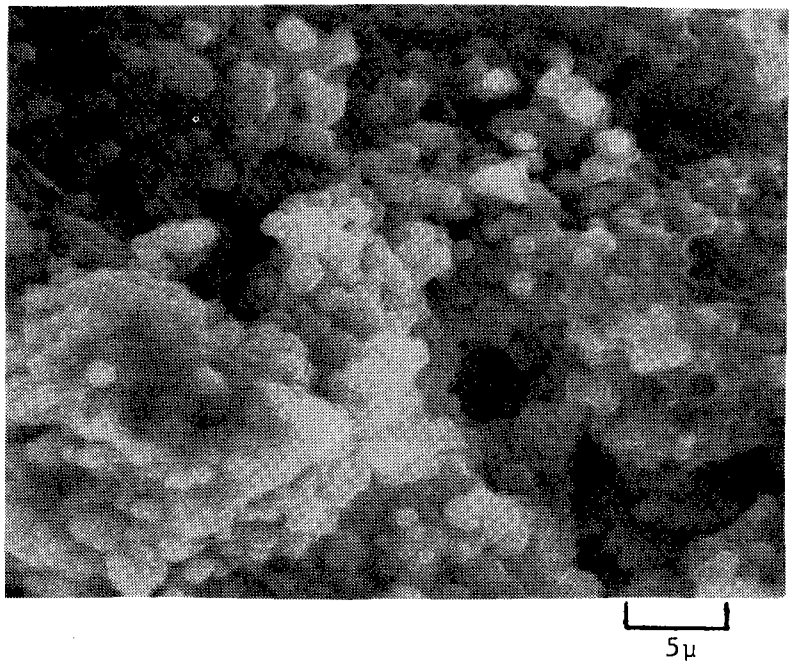

Figure 2. SCANNING ELECTRON MICROGRAPH OF FRACTURE SURFACE OF A COMPOSITE Na_2CO_3/MgO TES PELLET (SM45N-1A)

APPLICATION OF THERMAL ENERGY STORAGE TO PROCESS HEAT RECOVERY - PHASE III HEAT EXCHANGER TESTING IN DIRTY GAS ENVIRONMENT

L. B. Katter and D. J. Shaw
Rocket Research Company
York Center
Redmond, Washington 98052

INTRODUCTION

Under Department of Energy contract, Rocket Research Company, a Division of ROCKCOR, Inc., is investigating the use of thermal energy storage to improve the utilization of reject process heat as a source of energy for a district heating system. The specific energy source being studied is the aluminum reduction process. Energy supply in an aluminum plant is continous and constant 24 hours/day, 365 days/year. The energy demand in a district heating system is highly variable with diurnal, weekly and annual cycles. Thermal energy storage improves the cost-effectiveness of investments in energy recovery and distribution equipment and decreases the need for supplemental fuel for the district heating system.

During earlier project phases, the requirements for such a system were defined technically and economically and problem areas identified. Phase III, which is currently in progress, is directed towards developing data which will enable design of a heat exchanger suitable for continuous operation in the aluminum plant environment. Specifically, three areas are of concern. These are 1) corrosion or erosion of the heat exchanger by evolved cell gases, 2) surface fouling on the heat exchanger and 3) the possibility of decreased performance in the pollution control system due to lower temperature. A series of tests has been devised to accomplish this goal in a cost-effective manner. These tests are escalated gradually in scale in order to provide a maximum of information with minimum test investment. Intalco Aluminum Company has allowed these tests to be carried out at their plant in Ferndale, Washington.

First in the series were preliminary investigations aimed at characterizing the operating environment surrounding the aluminum reduction process. Included were collection and analysis of a series of gas and solid samples from the air pollution control ducts. A long term exposure corrosion test was undertaken to direct the selection of appropriate construction material for a heat exchanger. The second step in the series was a set of tests involving small probes, undertaken to investigate the fouling of heat exchange surfaces in the air pollution control ducts. The results of these preliminary tests indicated that a baseline heat exchanger design using finned tubing and carbon steel heat transfer surfaces was appropriate, both from the standpoint of fouling accumulation and corrosion.

The next step in this graduated series of tests was the fabrication and installation of a subscale heat exchanger. A test program was designed to determine the effects of corrosion and fouling on the design and operation of the heat recovery system under actual operating conditions in an aluminum reduction plant.

Based on the results of the preliminary tests, the experimental hardware for a subscale heat exchanger test facility was designed. The heat exchanger is rated at 850,000 Btu/hr and represents a 1/12 slice of a full scale heat exchanger. Auxiliary equipment includes a system to make use of the heat collected, a system to circulate water between the load and the heat exchanger and a data collection and instrumentation system. The heat exchanger test facility was built in September 1981 and put in service in January 1982. The operating experience gained during the past year is the subject of this report.

EXPERIMENTAL PROCEDURE

The heat exchanger and its auxiliary equipment are operated continously for extended periods of time in order to include a realistic range of process and ambient conditions. A total of 167 days of operating experience has been accumulated over the period of January 22 to July 31. The system is instrumented in order to record values of operating variables continuously during operation.

The system instrumentation schematic is presented in Figure 1. Water and gas temperatures at the inlet and outlet to the system circulating loop are measured with thermocouples. Pressure transducers are used to measure gas and water pressures and pressure drops. Water flow rates are measured with orifices with pressure transducers to transmit differential pressure. Gas flow rates are measured with a pitot tube with a pressure transducer to transmit velocity pressure. The data system scans the instruments at regular intervals, corrects the signals to digital format and stores the readings on magnetic tape for later analysis off-site.

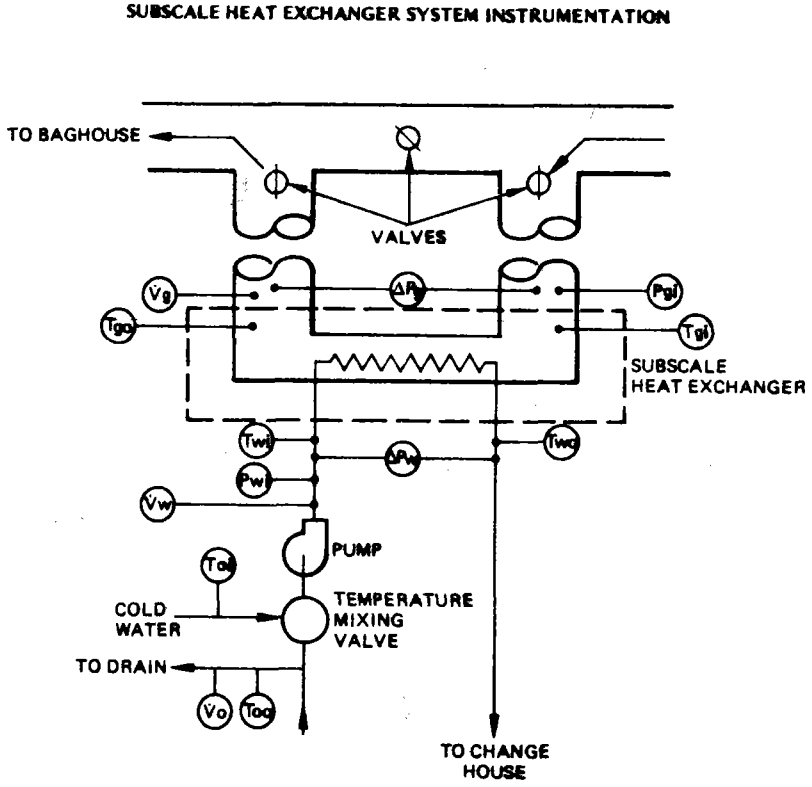

FIGURE 1

Analysis of the test system is based on the heat balance illustrated in Figure 2. Heat extracted from the gas in the heat exchanger is transferred to water with some loss through the heat exchanger walls. The water is pumped through pipes to the loads, incurring some heat loss enroute. The energy delivered to the useful load is limited by the instantaneous demand. Some energy is dumped to a dummy load to maintain a steady state in the heat exchanger.

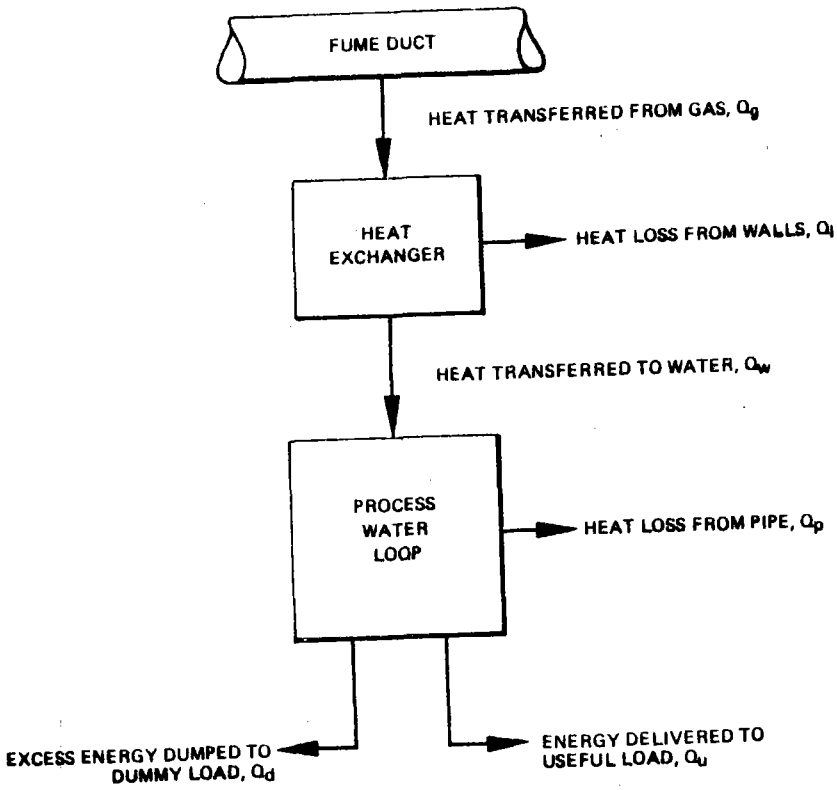

FIGURE 2

SUBSCALE HEAT EXCHANGER SYSTEM ENERGY BALANCE

The measured value of the overall heat transfer coefficient, U_{meas}, is calculated using:

$$Q_w = U_{meas} A\Delta T_m$$

where A is the heat transfer area from the manufacturer's data, ΔT_m is the logarithmic mean temperature difference (LMTD) between streams and

Q_w is the heat transferred to the water. The LMTD is given by:

$$\Delta T_m = \frac{(T_{gi} - T_{wo}) - (T_{go} - T_{wi})}{\ln \frac{T_{gi} - T_{wo}}{T_{go} - T_{wi}}}$$

All the temperatures involved are measured variables. The nomenclature is given in Figure 1.

The heat transferred can be calculated from the heat gained in the water stream:

$$Q_w = \rho_w \dot{V}_w C_w (T_{wo} - T_{wi})$$

The density, ρ_w, and specific heat, C_w are available in the literature. The inlet and outlet temperatures, T_{wi} and T_{wo}, respectively, and the flow rate, $\dot{V}_w$, are measured variables.

An overall predicted heat transfer coefficient, $U_{predict}$, was calculated, using gas and waterside film coefficients derived from correlations of the form:

$$Nu = f(Re, Pr)$$

This is the heat transfer rate that would be expected with no fouling accumulated on the core. An effective fouling factor was then calculated from:

$$F = \frac{1}{U_{meas}} - \frac{1}{U_{predict}}$$

The value indicates the amount of fouling present at a given time, independent of variations in flow rate of either fluid.

In practice, the gas flow measurement proved unreliable due to fouling of the pitot tube. A series of measurements taken when the pitot tube had been recently cleaned indicated that gas flow was quite stable. The waterside coefficient contributes only a small amount to overall resistance so $U_{predict}$ is relatively constant over the range of operating conditions. The measured value of conductance, U_{meas}, was then used directly as an indication of the amount of fouling present.

The fan power and pumping power is evaluated using:

$$P = \dot{V} \Delta P$$

Where P is the power, V the volume flow rate and ΔP the pressure drop across the device. $\dot{V}$ and ΔP are measured variables for both the gas and water streams.

The heat transferred from the gas, Q_g, can be calculated in a manner similar to the heat gained by the water. Thus,

$$Q_g = \rho_g \dot{V}_g C_g (T_{gi} - T_{go})$$

Similarly the heat dumped to the dummy load is:

$$Q_d = \rho_w \dot{V}_w C_w (T_{oo} - T_{oi})$$

A computer program was written to complete the analysis above for each point at which data were taken (typically 10-minute intervals).

In addition, an inspection was scheduled in which the system was shut down and the equipment opened up so that the internal condition of the heat exchanger could be observed. The internal inspection was carried out after 120 days of operation. Water inlet and outlet connections were removed and visual observations made of the condition of the water side of the tube. Access doors which opened into the core at one quarter and three quarters of the distance through the heat exchanger were removed. Inlet and outlet plenum sections were removed to allow access to the first and last rows of tube. Visual and photographic observations were made of the condition of the gas side of the tube at these locations.

Three methods of gas-side cleaning were investigated during the shutdown. First, an attempt to loosen the accumulation of dust with vibration was made by pounding on selected points in the tubing support structure. Second, some steel shot of the type used for shot blasting operations was acquired and cascaded through the heat exchanger. Third, a compressed air lance was made and used to manually blow the dust from the core.

RESULTS AND CONCLUSIONS

Testing with the heat exchanger facility commenced early in January 1982. At that time heat transfer performance was approximately 800,000 Btu/hr recovered from the waste gas stream. In the ensuing 8 months, performance has degraded due to internal and external fouling to a current value of approximately 600,000 Btu/hr. Both wet side and dry side surface fouling contribute to the overall decrease in performance.

Parasitic power is used by this example system in the fan which overcomes the gas side pressure drop of the core, the pump which overcomes the waterside pressure drop of the core and transmission system and the air compressor which provides air for the soot blowing system. These three components of parasitic power sum to slightly less than 12% of the energy being recovered from the gas stream.

Energy recovered by the heat exchanger is furnished to a large hot water heater used to supply hot water for personnel showers. This is furnished on demand through a double tube sheet, double tube, water-to-water heat exchanger located approximately 800 feet from the gas-to-water heat exchanger which is the subject of the study. When energy recovered is in excess of that which can be used by the hot water heater excess energy is dumped by rejecting heated water and blending cold industrial process water with the remaining stream to achieve 140° inlet temperature to the heat exchanger. At times as much as 40% of the heated water is rejected and is made up by cold process water in this manner.

Since the heat exchanger is located upstream of the air pollution control equipment which removes from the gas stream some potentially corrosive elements, it was considered to be a possibility that these corrosive elements would attack the heat exchanger core as the gas was cooled in passing through the heat exchanger. This does not appear to be a problem. Inspection of the steel surfaces in the heat exchanger during the scheduled shutdown period revealed that no attack had taken place. Surfaces were typically covered with a layer of dust of varying thickness. Under the dust accumulation, the steel surface was bright and clean with no evidence of corrosive attack. Inspection of the outlet plenum and fan on the cold side of the heat exchanger also revealed no evidence of corrosive attack. Analysis done under an earlier task in this phase indicated that the gas was extremely dry due to the adsorption of moisture on the alumina dust which the gas is carrying. The lack of moisture then reduced the corrosive action of the gas. This analysis has evidently been confirmed by the results of the experiment.

Conclusions regarding the effect of gas side fouling on heat exchanger performance are clouded due to variations in the operation of the heat exchanger as well as the effects of water side corrosion. Water side corrosion, due to dissolved oxygen in the cold process water added to the system, has a substantial effect on the heat transfer coefficient. The magnitude of the corrosion problem is an artifact of the experiment and would not be present in a full-scale system as the full-scale system would operate in the closed loop mode. The water would be maintained at a high level of purity, so that water side corrosion is not envisioned to be a problem with a full-scale heat exchanger.

The experimental system is subject to the variations and operating conditions caused by the maintenance operations of the line. Each few hours hoods must be opened and fresh ore added to the bath of molten salt in the cell. Additional disturbances to the cell gas balance occur when molten aluminum is withdrawn. During a cell - working cycle, for example, each time a hood is opened, variations in the gas inlet temperature to the heat exchanger on the order of 20°F occur in a few minutes. In addition, it takes approximately 5 minutes for an element of water to flow through the heat exchanger and approximately 10 minutes for it to complete its circuit to the shower house and return. It has been necessary to carefully choose data taken under relatively stable thermal condi-

tions in order to obtain results which fairly represent the performance of the heat exchanger. Figures 3 and 4 summarize the performance of the heat exchanger over a period of approximately 4 weeks. Figure 3 illustrates an experimental procedure in which the sootblowers were operated continuously for a period of about 4 hours. This procedure took place 2 weeks after a shutdown inspection during which the heat exchanger core was completely cleaned, both on the water side and the gas side. The heat exchanger performance, defined by the Stanton number-Prandtl number product as used by Kays and London, increases until sootblower operation is ceased at 240 minutes. Figure 4 illustrates the same procedure which was carried out approximately 4 weeks after the procedure illustrated in Figure 3. The heat exchanger performance exhibits approximately the same behavior. The overall level is somewhat lower since corrosion on the water side has progressed over the 4-week period. A continuous cycle where each sootblower is operated in turn a few minutes apart is the most effective schedule that has been tried to date. No work has been done with regard to rearranging or increasing the numbers of sootblowers.

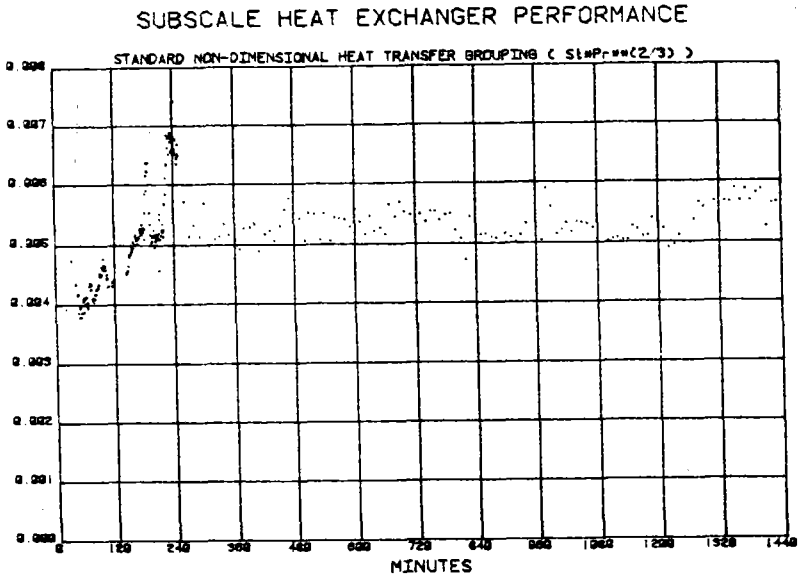

FIGURE 3

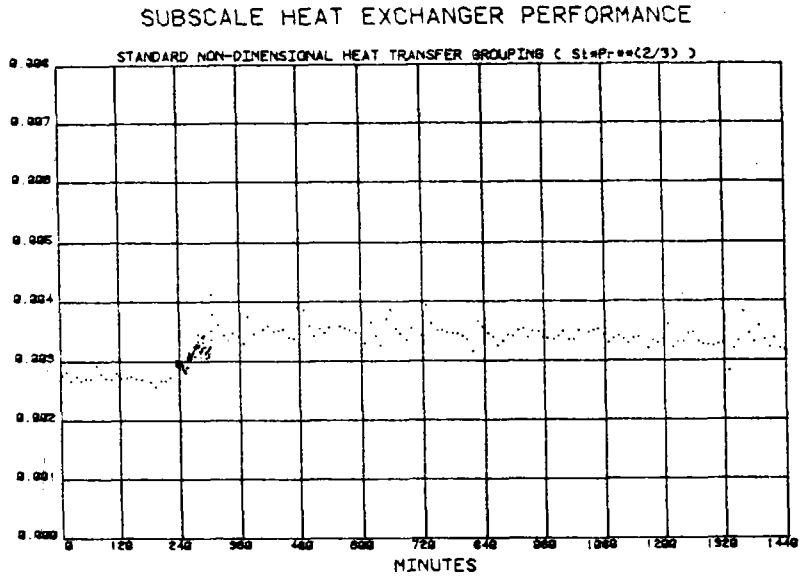

FIGURE 4

Continuous operation of the sootblowers would require a compressor load of 7-1/2 hp, which is approximately 2 percent of the rated capacity of this heat exchanger. Other components of the parasitic power requirements are the fan at 30 hp or approximately 9 percent of the rated capacity of the heat exchanger. Figure 5 illustrates the friction factor over the course of the sootblowing procedure described above. The friction factor, and therefore fan power, is relatively constant. The circulating pump on this system requires approximately half of one percent of the rated capacity of the heat exchanger. Total parasitic power is then 11-1/2 percent of heat exchanger capacity.

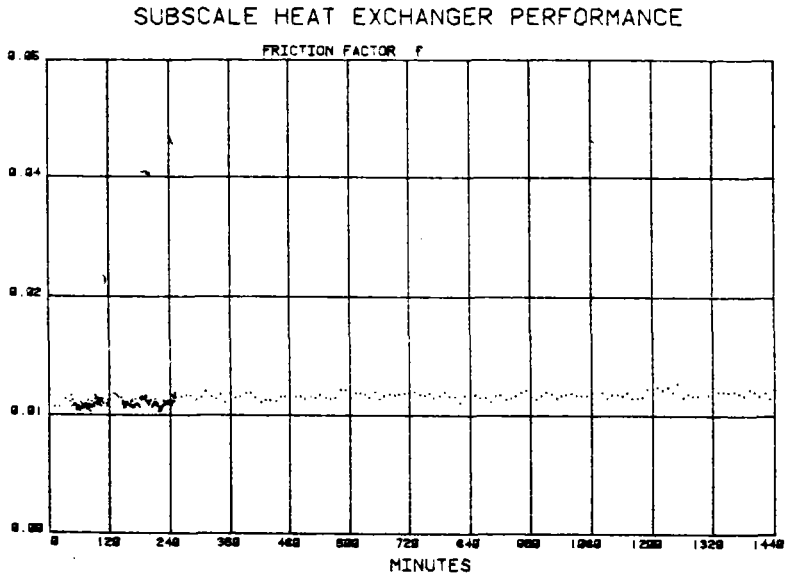

FIGURE 5

It has not been determined if the operation of the heat exchanger has any effect on the dry scrubbing process used for emission control at the Intalco smelter. The gas that has passed through the heat exchanger is diluted 12:1 by gas from the remainder of cells on the line before it reaches the dry scrubber system. Any changes in the concentration of contaminants in the gas stream after the dry scrubber due to operation of the heat exchanger would be very small. Since the contaminants are extremely active chemically, measurements must be made immediately after sampling. Instruments are not available which are both sufficiently sensitive to detect the level of changes expected and sufficiently portable to be used on-site in order to take immediate measurements. In order to determine if the cooling of the gas by the heat exchanger causes a change in the operation of the dry scrubber, two possibilities exist. The first is to construct and test a full-scale heat exchanger approximately 12 times the size of the present experiment. The second possibility is to construct a small-scale dry scrubber of a capacity to match the present experiment. Either would allow measuring changes in the operation of the dry scrubbing system in gases which have been undiluted by the effluent from pots which have not undergone cooling in the heat exchanger.

IDENTIFY GENERIC THERMAL ENERGY STORAGE NEEDS FOR INDUSTRIAL APPLICATIONS

D.R. Glenn and A.B. Uzowihe
The Decision Research Group, Inc.
Burke, VA 22015

It is commonly accepted that thermal energy storage (TES) systems will find applicability in industrial, utility and renewable energy processes as well as in limited residential settings. Starting in 1975, six studies were commissioned to evaluate thermal storage for the processes including brick/ceramics produced in periodic kilns, cement production in rotary kilns, steam swing demands in paper/pulp mills, heat recovery from aluminum plants and iron and steel furnaces(electric arc), and food process plants. These reports are tabulated below, in Figure 1. The study undertaken by Decision Research covers a indepth review of these six, and any other relevant TES applications

Application	Example Industry	Contractor	NTIS Report #/Date
Periodic Kilns	Brick/Refractory	General Electric	COO-2558-2 / 10/76
Rotary Kiln/Furnace	Cement	Martin-Marietta	CONS-5084-1/ 3/78
Electric Arc Furnace	Iron & Steel	Rocket Research	N79-11473/ 10/78
Heat Recovery from Process Waters	Food	Westinghouse	ORNL/SUB/ 79-4253 7/79
Steam Supply	Pulp-Paper	Boeing	CONS-5082-1/ 9/78
Heat Recovery from Process Gas	Aluminum	Rocket Research	CONS-5080-1/ 4/79

Figure 1. Source Reports for DRGI Study

efforts that have been reported in the literature since the original six were published. The work includes 1) Derive and tabulate a consistent series of storage-related performance requirements using the energy data presented in the six studies, 2) investigate for patterns of thermal energy parameters lending to a "standardized" set of temperature/heat rate/mass flows, 3) define a "best fit" set of TES requirements from the analysis and 4), conceptualize a off-the-shelf design capable of providing the capacity, thermal and mass flows with interfacing components, i.e. heat exchangers, blowers, etc., accounted for in the schematic in order to generate a set of baseline costs (using breakeven economic analysis).

Data Reconciliation

Each of the source reports were commissioned by ERDA/DOE during a particularly volatile period when there were no consistent groundrules for specifying TES-related performance specifications, energy price projections, or industrial use of energy forms, real time data or network analytical details, as would have likely occurred if this were an electrical circuit/network. Consequently, each contractor "did their own thing" and what results is a failure in each study (to a greater or lesser extent) to present a unambiguous, definitive set of reference process requirements allocated to the storage system. This could not be anticipated at the work beginnings because no previous attentions were given these contracts/reports until DRGI and ORNL initiated discussions for this study. The essence of the point made is illustrated by the broad view of the needed parameter definitions in the listing below, Figure 2. All of these are variable in any dynamic process, which underlies the TES opportunity in the first place. The six studies were analyzed to

derive the TES-associated factors (Figure 2), as a general guide for maintaining a consistent approach for all the studies. Unfortunately, this did not

	Input(charging)	Output(discharging)
Thermal Conditions		
Temperature(T)		
Heat Rate(Q)		
Specific Heat(C_p)		
Fluid Properties		
Density(ρ)		
Pressure(P)		
Volumetric Flow(v)		
Mass flow($\dot{m}$)		
Chemical Properties		
Pollutants		
pH		
Contaminants		
Process Conditions		
Thermal periodicity		
Heat duration		
Plant operating schedule(s)		
Plant capacity/output rate(s)		
Process energy flow timeline(s)		

Figure 2. TES Performance Criteria Guide

pan out. While the GE study came closest to covering the full scope of the requirements, no report met the mark. The project team synthesized the missing data wherever possible and with regard to minimizing unrealistic relationships from a thermodynamic point of view. The next illustration, Figure 3, presents the nominal conditions for the storage function in each application. Notice the higher degree of variation in heat flows while the mass flow range is basically within one order of magnitude. Temperature range deviations are expectedly wide and the specific discharge functions demand some control of temperature, mass and heat flows. For the TES-assigned possible functions-kiln preheat, combustion air preheat, and drying heat, temperature regulation /control is critical to required heat balance to avoid ware damage from diffusing moisture release, or imperfect combustion (air/fuel ratios) causing a explosive environment within the kiln.

For the Cement application, on-site generation is the assigned TES function. Here, the thermal condition (heat rate and mass flow) is important. It should be noted that this process operation is essentially steady-state although the contractor recognizes a varying plant power demand though the case of power variation is not clearly detailed. It is questionable as to whether a TES can provide a viable conservation benefit in cement plants. A further serious constraint is the high concentration of particulates, about 14%, in the exhaust gas streams at 1500 ^{o}F.

Industry	Waste Heat Energy Level			Application(s)
	Heat flow(BTU/hr)	Temp.(°F)	Mass flow(lb/hr)	
1 Brick/Ceramic	6.0×10^6	400-1000	3.0×10^4	Kiln preheat Combustion air preheat Dryer heat source
2 Cement	4.0×10^9	350-1500	1.72×10^5	Electricity
3 Iron/Steel	4.0×10^7	350-1300	1.37×10^5	Electricity
4 Food Processes	5.2×10^5	120-250	5508 (11gpm)	Hot water supply Cleaning Space heat
5 Paper/Pulp	4.5×10^8	360@600 psi	1.0×10^5	Make-up steam for load following
6 Primary Aluminum	3.13×10^8	70-270	6.8×10^6	Hot water supply distrt Comfort heating

Figure 3. Thermal Energy Demands (to Process)

The Steel application looks at the fume hood of an electric arc furnace, as a heat exchanger to recover and store the recovered heat, at 400 °F for use as feedwater heater into a turbine-generator to augment plant grid power demands. The thermal swings for an electric arc furnace operation appear to support a TES use as would a number a iron/steel manufacturing processes. The study doesn't even skim the surface of opportunities for storage uses within a integrated mill. Nevertheless, some useful energy flow data is provided for the arc furnace operation.

Although aluminum processing/manufacturing is at 1200-1800 °F, the contractor limits the scope of interest to a 260 °F stream related to fume exhaust ducts, because his contract limited their investigation to lower temperature sources, an indication of the confusion that reigned over the TES program at that time. The contractor cleverly related this heat source to a diurnal cycle for hot water distribution to a close, small municipality. A thorough loads analysis shows that, though lower in thermal potential, a hot water system could prove profitable in offsetting fossil fuel consumption. It should also be noted that primary aluminum manufacture is a steady-state process. Thus no in-plant TES application is apparent.

The remaining two industries, Food and Paper/Pulp, contain interesting operating characteristics well-suited to TES use. In the food processing industry, one and two shift operations dominate, with the off-shift for cleaning activities. Where the heating/cooking functions require large amounts of clean water, the "used" water rejected is at 150 °F. The portion of these wastewaters not able to be directly recovered to preheat process waters are used to heat third shift cleaning water, over an 8-hour period. In a second operational plant (for frozen foods), condenser coil heat from refrigeration machines, are recovered and applied to floor heater loops to minimize cooling losses through the earthen floors of the freezers.

The Paper/Pulp study points out the very commonly found need for large steam swings in industrial processes, one being the paper mill. The specific interest in this work, is to supplement the fossil-fired boiler with a increased hog fuel

boiler that is uprated to produce excess steam, to be stored in an accumulator, for those periods when the steam demands exceed the steady-state rating of the fossil-fired boiler. The steam storage(as pressurized water at 350-400 ^{o}F) is discharged at controlled rates to the high or low pressure headers augmenting the fossil boiler steam supply. Resultant response curves for the generator system, and boilers are significantly leveled allowing optimized design point conditions.

Both lower temperature schemes (food, pulp-paper) employ off-the-shelf, and standard engineering design. Since a substantial amount of attention has been devoted to low temperature storage, no additional use is planned for these levels of waste/reject heats, relative to the program evaluations remaining.

Effort Remaining

DRGI will be reviewing several additional applications studies located through a technical search, to add to the energy dynamic flow/real-time data base. This will add a measure of confidence to the "standard" design sizing of the industrial TES system/modules. A breakeven economic analysis of applications using projected energy costs, savings attributable to TES and nominal escalation rates will finalize this effort.

ANALYSIS OF THERMAL ENERGY STORAGE IN A PUBLIC SCHOOL FACILITY IN NORTH CAROLINA

by

Tony W. Sigmon
Research Triangle Institute
Research Triangle Park, North Carolina

1.0 INTRODUCTION

1.1 Background and Objectives

The trend over the past ten years has been to use electrical power for heating and cooling public school buildings in North Carolina. The growth of electrical power use has expanded to the point that approximately 20 percent of the public elementary and secondary schools within the State are "all-electric" schools. Many of these facilities employ electric chiller and boiler systems to supply the heating, cooling, and domestic hot water loads. The daily electrical load profile in these cases is characterized by a substantial electrical power demand for a short period of time during midday, while for the remainder of the day the electrical load is relatively constant at a substantially smaller fraction of this peak load.

The objective of the activities proposed is to provide an assessment of the viability of thermal energy storage (TES) through an analysis of the technical and economic performance of a working system. It is anticipated that the successful implementation of such a TES system will provide a basis for the extension of thermal energy storage, not only to similar boiler/chiller systems but also to other primary heating and cooling equipment such as heat pumps and solar thermal energy sources in public school facilities.

1.2 Scope of Work

The activities to be completed under the contract include:

- detailed definition of monitoring and evaluation goals and procedures,
- specification, installation, and check-out of data acquisition equipment,
- a computer-aided systems analysis of the interaction between the HVAC system and building thermal loads,
- development of data reduction and analysis software,
- system monitoring and performance evaluation, and
- documentation of findings.

2.0 DESCRIPTION OF TES FACILITY

The school building is a single-story brick building with approximately 74,000 square feet of conditioned classroom, administrative, gymnasium and cafeteria space. A 2,500 ft^2 room at the northwest wing of the school is dedicated to housing the TES system and associated equipment. The school is located in Mocksville, North Carolina.

The school's space heating and cooling load are met from the storage system except for three small zones which are met by three roof-top heat pumps. The TES system also provides preheated domestic hot water for eventual delivery to the cafeteria and gymnasium areas. The total HVAC system and associated equipment consists of the following primary components:

- TES subsystem T1 which is a rectangular above-ground reinforced concrete tank with a total storage volume of approximately 67,000 gallons,
- TES subsystem T2, which is similar to T1 in design but has a volumetric capacity of 20,000 gallons,
- a reciprocating electric chiller with a total capacity of 68.5 tons and matched cooling tower,
- three electric boilers rated at 240kW, 65kW, and 55kW peak capacity, and
- three roof-top air-to-air heat pumps.

The three heat pump systems meet the heating and cooling load of the administrative areas on demand without reference to the operation of the TES system. The TES system is intended to modify the electrical load profile of the school by utilizing the smaller tank T2 for storing preheated domestic hot water and tank T1 for storing heated or chilled water for meeting the space heating and cooling load. This heated/chilled water is then circulated through four parallel roof-top air handlers for distribution throughout the school. The preheated domestic hot water is circulated through the two smaller boilers for delivery to the shower and kitchen areas.

Tank T1 is coupled to the primary water circuits by means of four distributor manifolds installed at vertical increments internal to the tank. Water enters and exits the tank by means of orifices spaced at consistent intervals along the length of each manifold. Water enters and exits tank T2 in the same manner; however, only two manifolds have been installed within this smaller tank.

There are 16 modes of operation possible with the system.

Cooling Operation

Mode 1 - Cooling Charge of T1 with Chiller, Condenser Heat to T2
Mode 2 - Cooling Charge of T1 with Chiller, Condenser Heat to Cooling Tower

Mode 3 - Cooling Discharge of T1, Stage 1 } Discharge from
Mode 4 - Cooling Discharge of T1, Stage 2 } progressively
Mode 5 - Cooling Discharge of T1, Stage 3 } lower manifold
Mode 6 - Cooling Discharge of T1, Condenser Heat to T2
Mode 7 - Cooling Charge Discharge of T1, Condenser Heat to Cooling Tower

Heating Operation

Mode 8 - Heating Charge of T1 with Boiler
Mode 9 - Heating Charge of T2 with Boiler
Mode 10 - Heating Discharge of T1
Mode 11 - Boiler Assisted Discharge of T1

Mixed Heating and Cooling Operation

Mode 12 - Between Seasons Charge of T1 with Chiller, Condenser Heat to T1
Mode 13 - Between Seasons Charge of T1 with Chiller, Condenser Heat to T2
Mode 14 - Between Seasons Charging of T1 with Chiller, Condenser Heat to Tower
Mode 15 - Between Seasons Cooling Discharge of T1
Mode 16 - Between Seasons Heating Discharge of T1

3.0 SYSTEM MONITORING AND DATA ACQUISITION

The objective of the monitoring activities is to provide data that can be used to determine the degree of stratification attained within tank T1, compute energy flows into and out of each major system component, determine the distribution of electrical demand and consumption throughout the day, and compute component and system efficiencies.

3.1 Temperature Measurements

General purpose RTD's are used to measure the following system temperatures:

- 90 water temperatures inside main storage tank T1,
- water temperatures entering and leaving the HVAC boiler,
- water temperatures entering and leaving the chiller evaporator,
- water temperatures entering and leaving the chiller condenser,
- water temperatures entering and leaving the air handler system,
- 4 air temperatures inside TES building, and
- ambient temperature outside TES building.

3.2 Flow Measurements

Flow rate is measured with differential strain gauge pressure transducers at five locations.

- condenser inlet
- chiller inlet
- primary supply inlet
- boiler exit
- hot water coil exit

3.3 Power Measurements

Six electrical power loads are continuously monitored with in-line watt transducers. The loads monitored include:

- total school
- total TES system
- chiller
- each of the three boilers.

3.4 Valve and Pump Status

The on/off status of twenty-one valves and nine pumps is monitored with a parallel relay network interfaced to the data logger digital input.

4.0 DATA REDUCTION AND ANALYSIS METHODS

A software package has been developed and is being used for the purpose of determining the operational performance characteristics of the system and its impact upon the electrical use of the school as a whole. The software package has five output components which address component, system, and school energy use patterns. These incude:

(Component Energy Flow Analysis) - Computes energy use, peak demnd, time of peak demand, average demand, on-time, and thermal energy flows by mode for each of the primary system components. These computations are completed over any time interval requested.

(System Energy Flow Analysis) - Computes system peak demand and time of occurrence, school peak demand at time of system peak, average system demand, system energy use, thermal energy supplied to heating, cooling and domestic hot water loads. These computations are completed over any time interval requested.

(School Energy Flow Analysis) - Computes school peak demand and time of occurrence, system peak demand at time of school peak, average school demand and school energy use. The computations are completed over any time interval requested.

(System Variable Analysis) - Outputs all variables being monitored at up to 20 requested times.

(Tank 1 Thermal Stratification) - Outputs values for temperatures internal to T1 and state of charge at up to 20 requested times.

5.0 RESULTS

Figure 1 shows average water temperatures as a function of tank height for T1 and reflect the degree of stratification and level of charge during a weekday in January. The time clock on the boiler allows operation during non-school hours only. The level of charge is seen to increase from midnight to 6:00 a.m. while discharge takes place during the next six-hour period. The level of charge then increases over the next six hours as a result of the tank being charged during the latter portion of this period.

Table 1 shows various energy use characteristics of the TES system for the January-May period. Load factor is defined as average demand divided by peak demand for the period. This data reflects the decrease in load on the system during the latter months and the relatively poor load factors associated with the system. These load factors will be improved during the coming school year by operating the boiler at a lower capacity for the full day.

Table 1. TES System Performance Data

Month	Peak Demand (kW)	Average Demand (kW)	Load Factor	On-Time (% of Total)			
				Charge of T1	Dis-charge of T1	Combined Charge/ Discharge of T1	Off
January	248.8	108.7	0.44	10	35	50	5
February	251.1	115.3	0.46	21	39	30	10
March	256.9	62.5	0.24	12	42	11	35
April	248.5	6.1	0.02	3	29	0	68
May (Cooling Only)	69.0	19.7	0.29	40	12	0	48

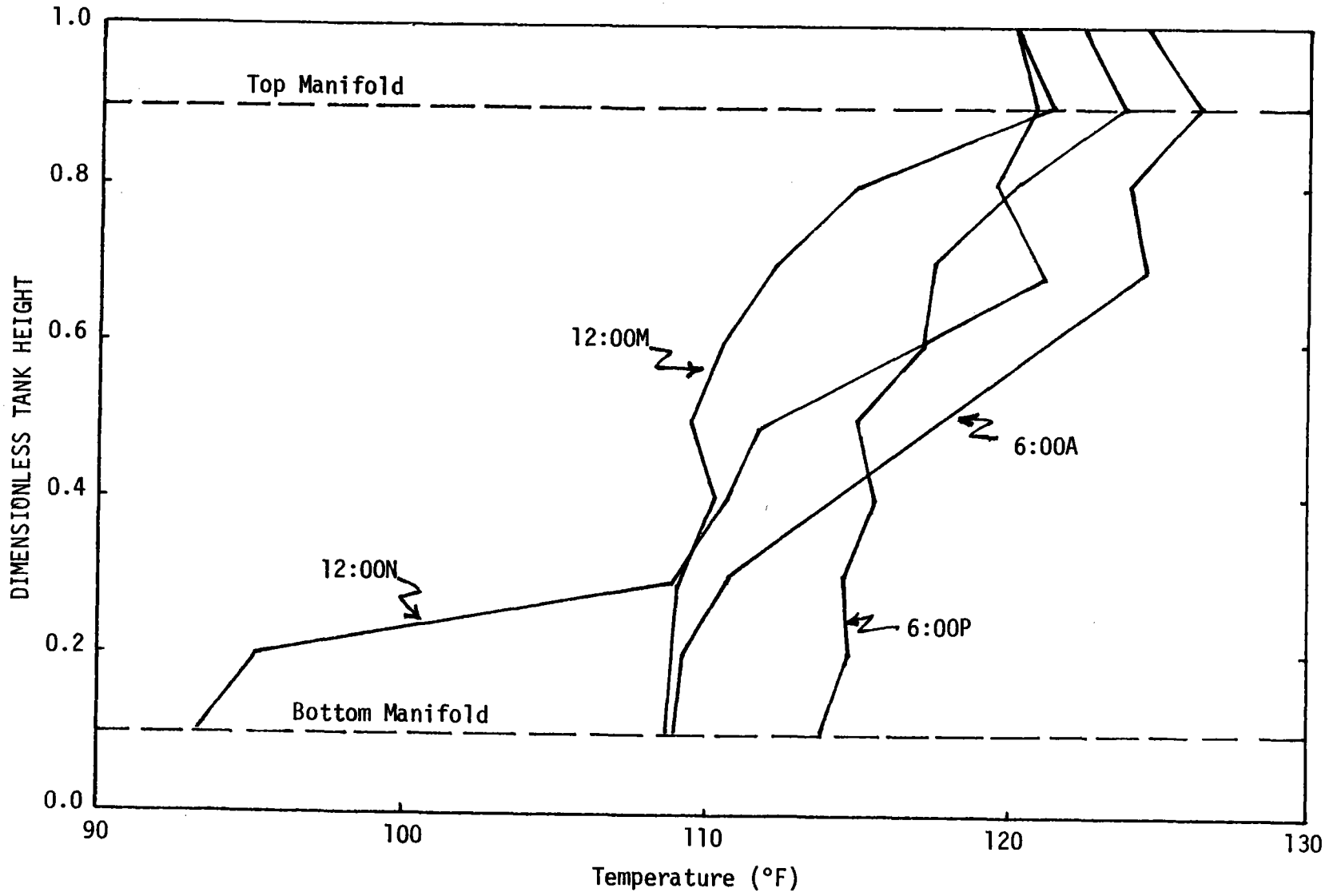

Figure 1. Tank T1 Temperature Profiles

PERFORMANCE OF STRATIFIED THERMAL STORAGE SYSTEM FOR OLIVER SPRINGS ELEMENTARY SCHOOL: PROGRESS REPORT

R. L. Reid
Mechanical and Aerospace Engineering Department
The University of Tennessee
Knoxville, Tennessee 37916

A. F. G. Bedinger
Energy, Environment, and Resources Center
The University of Tennessee
Knoxville, Tennessee 37916

DESCRIPTION OF SYSTEM

The Oliver Springs Elementary School has recently been constructed in Roane County, Tennessee. The school is approximately 68,117 square feet in conditioned floor area. The design cooling load is 1.32 X 10^6 BTUH and the design heating load is 1.14 X 10^6 BTUH. The HVAC system in the school consists of a double bundle heat recovery water chiller to enable simultaneous heating and cooling as required. There is also an oil fired hot water boiler for space heating when chiller heat rejection is insufficient to carry the load. Thermal storage in the form of 3 cast-in-place, concrete water storage tanks are utilized in conjunction with the chiller and boiler (Figure 1). The tanks are equal in size. Each tank is approximately 2,956 ft^3, thus the total storage capacity is approximately 64,400 gallons of water. The tank array is insulated on the top and sides with 3 inches of polystyrene and on the bottom with 3 1/2 inches of foamglass. Each storage tank uses a flexible membrane device to resist temperature blending (1, 2). The flexible membrane is constructed of coated fabric and fastened to the tank walls at mid-height. The membrane can float up and down to suit variable conditions. Water level sensing wells are located in two corners of each tank with appropriate controls to sense when the membrane is at the top or bottom of the tank (see Figure 2). A screen is positioned over the sensing well outlet hole to avoid trapping the membrane against the holes.

The two design goals of the heat recovery and TES for the Oliver Springs School are (1) to minimize the need to purchase energy for space heating, cooling, and water heating and (2) to minimize electrical demand. During periods of the year when there is a need for space heating and cooling the HVAC system can provide such services simultaneously. Through the use of TES the HVAC system can store unwanted refrigeration system heat for later use when the demand for space heating occurs. Additionally, the HVAC system is designed such that the heat recovery chiller can operate only during un-occupied periods at times of otherwise low electrical use thus potentially saving demand charges. Through such a strategy the chiller is selected slightly smaller than the design cooling load and will operate at favorable (night) condensing temperatures for the following days thus saving operating costs, energy, and installation costs.

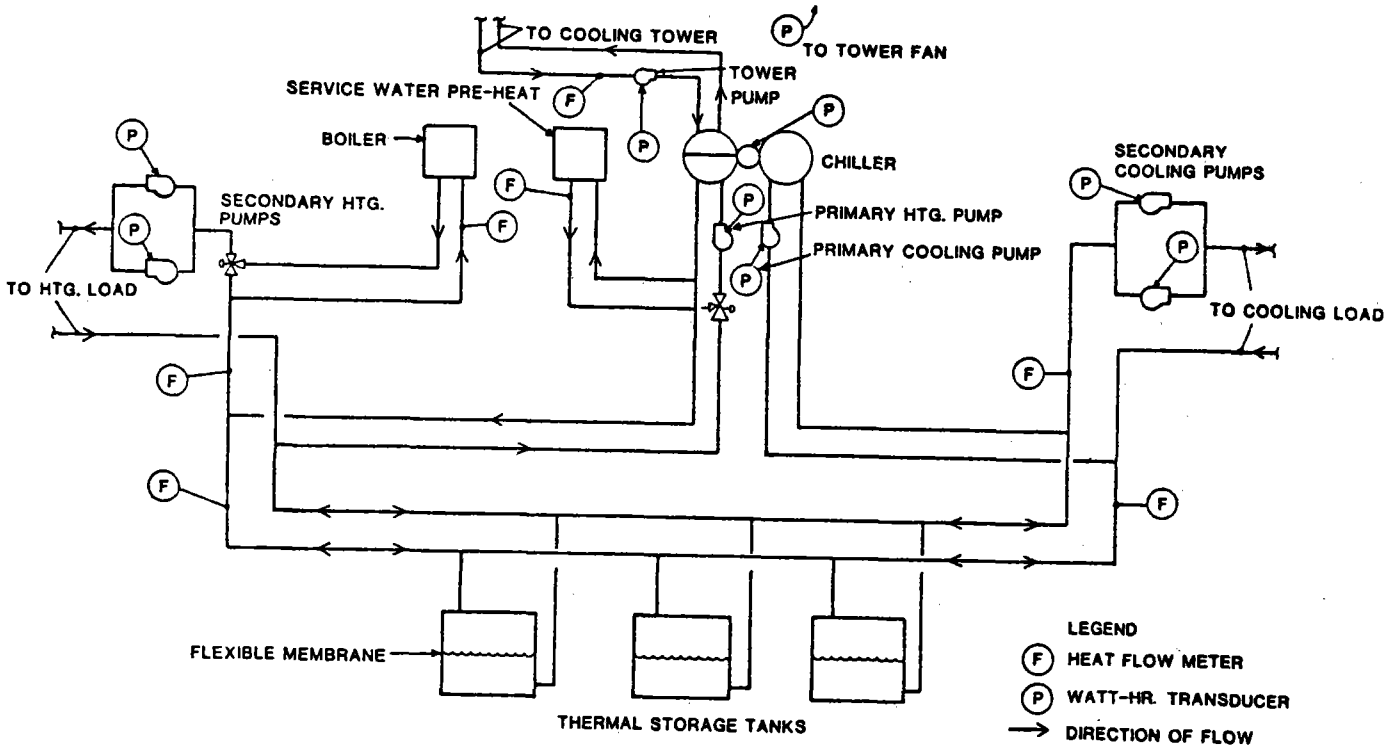

FIG. 1 HVAC SYSTEM SCHEMATIC SHOWING DATA ACQUISITION SYSTEM SENSOR LOCATION

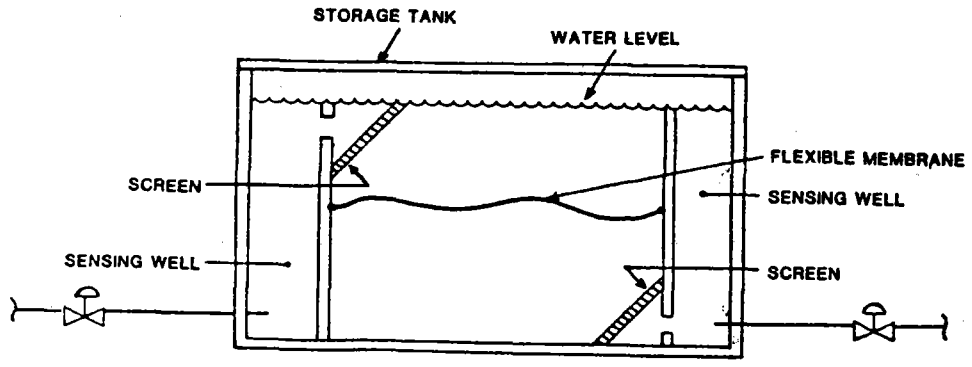

FIG. 2 SECTION OF THERMAL STORAGE TANK

HISTORY OF PROJECT

A membrane stratified thermal energy storage system (TES) has been installed in the Oliver Springs Elementary School in Roane County, Tennessee. Design of the school and TES was performed by a local architectural/engineering firm. Construction of the school was by a local general contractor. Funds for the design and construction of the school came entirely from the Roane County School System. The University of Tennessee and Union Carbide Corporation have assumed no responsibility for design, funding, or operation of the school and TES.

The Oliver Springs Elementary School was occupied in the spring of 1981. Fully one year later, the TES system has not performed as originally expected by any of the parties involved. Indeed, even though the basic concept is still thought to be valid, the entire HVAC system (including TES) has performed poorly and caused a great deal of discomfort and inconvenience for the Roane County School System. Since neither The University of Tennessee nor the Union Carbide Corporation had any involvement in the design and construction of the school, these parties can assume no responsibility for the problems.

The HVAC/TES system is more complex than a typical elementary school HVAC system. Also, the type of system installed is unique to designers and contractors in this geographic area. As such, start-up problems were expected. However, the system is still experiencing operational problems. Over the past twelve months the HVAC/TES system has gone through a day-night cycle only one or two consecutive days without requiring manual interaction. A short discussion of some of the problems is appropriate.

The storage tanks are open to the atmosphere. The air handling units served by the TES, chiller, and boiler are at a higher elevation than the TES. Thus, some means of maintaining water pressure in the air handling units is required. A check valve is located on the supply hot water and cold water piping to the air units. A pneumatically operated back-pressure valve is located in the return piping which is set to maintain 10 psi pressure in the water piping serving the air units. If either of these valves leak when the secondary heating or cooling pumps are off then the water in the air unit piping can drain back into the TES. The result of this is air binding in the water coils of the air handling units. Air binding has also been a problem in the primary heating pump which is located at about the water level of the TES. If the water level drops a few inches then this pump no longer has a flooded suction which results in zero or near zero pumping action. Additionally the suction line to the primary heating pump takes off the header on the top of the pipe. If any air is entrained in the piping it can accumulate in the top of the pipe causing loss of suction pressure to the pump. The secondary heating and cooling pumps

have repeatedly experienced air binding as well. The cause or causes for this are not entirely clear. One possibility is that the controls for the TES sensing wells do not valve off the tanks or stop the pumps fast enough to prevent the well from pumping dry and pulling air into the pumps. The water level in the tanks is somewhat critical in that too much water will prevent the charge cycle from terminating. The reason for this is that water will spill over the upper screen and prevent the sensing well from pumping down even though the membrane is at the top. One final hydronic problem worth mentioning is water leakage. There is no automatic water level control and perhaps it is best that there is none. However, if the water level is not watched daily, problems can arise. Each of the three tanks have experienced leakage problems. At the time of the writing of this report one of the tanks is losing water at the rate of approximately 1,200 gallons per day which requires constant supervision for refill.

Internal chiller controls have been a chronic problem for the past year. The most recent problem has been with the capacity controller. The chiller has six stages of cooling capacity from a high of approximately 100 tons to a minimum of 25 tons. The capacity controller was not staging the compression as the machine was loaded and unloaded. As the refrigeration load reduced the chiller would run fully loaded and the low water temperature safety control would de-energize the machine at its setting of 35°F. This control must be manually reset and if no one is attending the machine the charge cycle will not be successful.

There have been numerous control and electrical problems some of which include the blending valve on the chilled water side of the chiller. This valve is in the circuit to maintain a fixed chilled water temperature delivery to the TES. This valve typically will continually "hunt" for a stable position and in many cases short circuit the water to the chiller for too long a period of time and cause the low water temperature control to de-energize the chiller. The cooling tower pump has stopped due to an apparent electrical problem and without being manually reset the chiller will not restart resulting in an incomplete charge cycle. The cooling tower basin has been observed to have insufficient water to flood the cooling tower pump suction resulting in the chiller de-energizing due to high head conditions which must be manually reset.

Other problems and design considerations associated with thermal storage systems can be found in References 3, 4, and 5.

DATA ACQUISITION SYSTEM

An automatic data acquisition system is used for system performance data gathering. Four types of data sensors are used. Heat flow meters are installed in the HVAC system piping to measure heat flow from all heat sources and/or heat sinks (see Figure 1). The heat

flow meters consist of positive displacement turbine meters for the measurement of fluid flow rate and solid state temperature transducers for the temperature difference measurement across the appropriate heat source or heat sink. Heat flow integration circuitry is provided with the heat flow meter and a 5 VDC square wave output proportional to heat flow is fed into the on-site data logger for accumulation. Electric power to each of the motors comprising the HVAC system (exclusive of terminal units) and total building power is being measured using solid state watt-hour transducers. The output of each watt-hour transducer is again a 5 VDC square wave signal. High and low tank fluid temperature measurements are being made using solid state temperature transducers with milli-volt output. Weather data consisting of dew point temperature and wet bulb temperature is also being measured. An aspirated dew cell is used for the dew point temperature measurement and solid state temperature transducer for dry bulb temperature measurement.

The on-site data logger is capable of receiving the digital output from the heat flow meters and watt-hour transducers, totalizing these data, storing on magnetic tape and hard copy and resetting the counters to zero at the rate of once every hour. Instantaneous temperature measurements are made at the same scan interval and stored on magnetic tape and hard copy.

DATA ANALYSIS

The data collected from the heat flow meters and power consumption meters was fed into the ORNL computer in order to manipulate the data into an interpretable and useful form. A computer program was written to put the data into the useful form and extract weekly data summaries. The summaries consisted of nine (9) heat flow and eight (8) power consumption summations. These summations are listed when the TES is in the charge mode and discharge mode separately. Also, total heat flows and power consumptions are listed for each week. With these data, the purchased power consumption was to be estimated if the building had a more conventional HVAC system. Temperature data was also collected from each storage tank. These data in conjunction with TES heat flow data were to be used to determine temperature stratification and storage efficiency.

Since the HVAC/TES system has not operated properly, data collection on system performance has been seriously compromised. The data acquisition system has, with some minor problems, operated continuously, recording data hourly since Fall of 1982. However, since the HVAC/TES system has not operated properly, the detailed data taken on the system is of very little scientific benefit.

There are several portions of the original proposed work effort that can be accomplished since the HVAC/TES can be manually operated for tank charge and discharge cycles.

Temperature versus time profiles have been experimentally determined for a chilled water storage tank. Figure 3 is a representative plot of a recharge cycle for one chilled water tank. The plot shows that good temperature stratification was achieved for the first two hours of the recharge cycle. However, for the remaining hour of the cycle there is an indication of heat transfer across the membrane.

After a quiescent period of twelve hours the chilled water tank was discharged. Figure 4 shows the upper and lower tank temperature variations over the six hour discharge time period. The promotion of temperature stratification for the discharge cycle is less pronounced than for the recharge cycle. After about three hours, or one half of the discharge period, the lower tank temperature began increasing at a large rate. Indeed, for the last hour of the discharge period the chilled water being supplied to the air units was 65°F or higher which is insufficient for dehumidification at best. These data indicate significant heat transfer across the membrane.

Further tests are underway in order to better identify the source of the tank thermal losses both during the recharge and discharge cycles as well as the quiescent period.

REFERENCES

(1) Tamblyn, R. T., "Thermal Storage: A Sleeping Giant," ASHRAE Journal, June 1977, pp. 53-57.

(2) Tamblyn, R. T., "Thermal Storage: Resisting Temperature Blending," ASHRAE Journal, January 1980, pp. 65-70.

(3) Tamblyn, R. T., "Grappling with the Gremlins for Thermal Storage Applications," Thermal Energy Storage Cooling Commercial Buildings Using Off-Peak Energy, EPRI Report EM-2244, Project 2036-2, February, 1982, pp. 7.1 - 7.30.

(4) Tamblyn, R. T., "Thermal Storage Applications," Heating/Piping/Air Conditioning, January 1982, pp. 59-70.

(5) Water Storage for Energy Optimization in Buildings, published by Engineering Interface Limited, Willowdale, Ontario, May 1981.

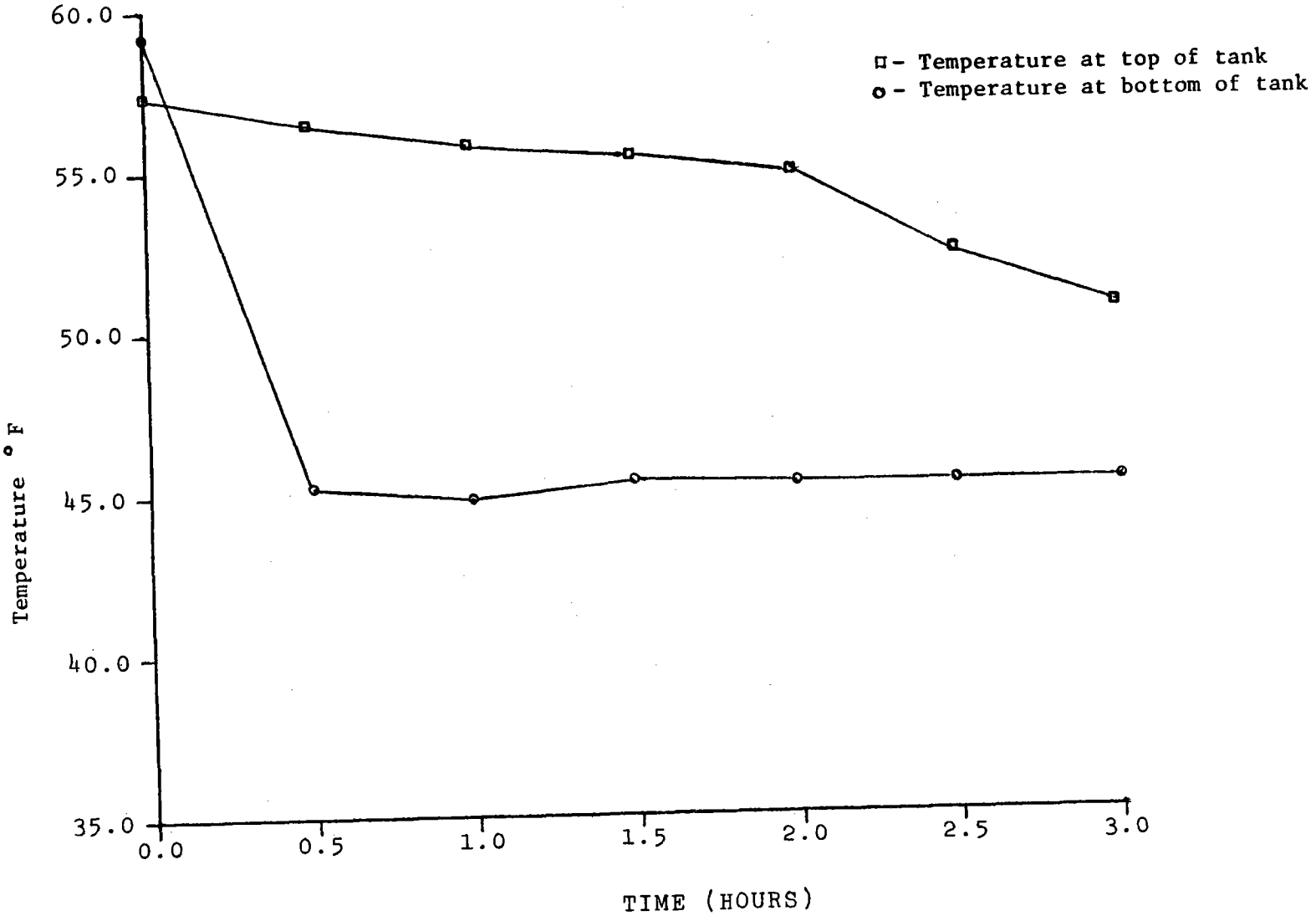

Figure 3. TES Recharge Cycle #1

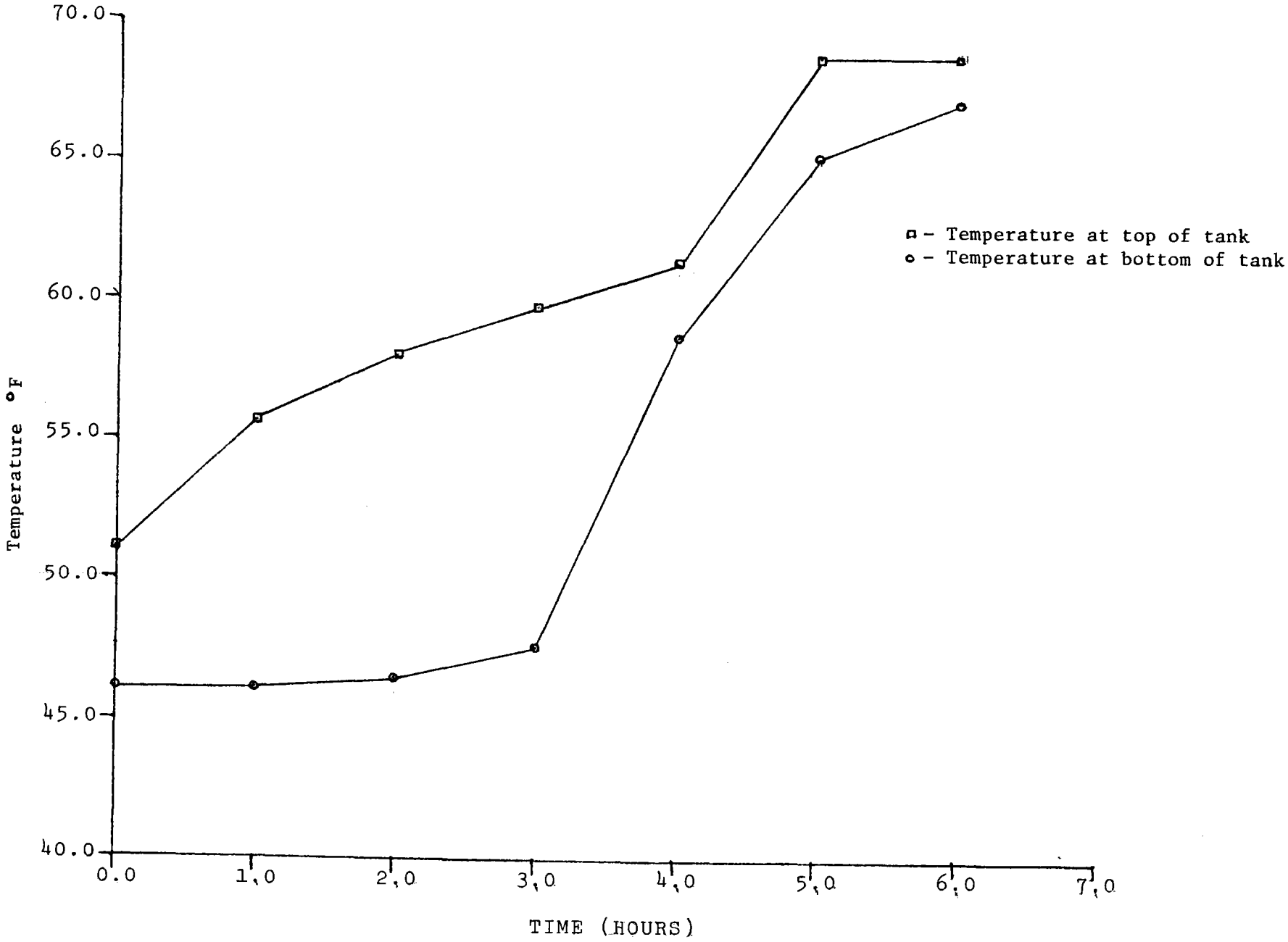

Figure 4. TES Discharge Cycle #1

MATHEMATICAL MODELING OF TES SUBSYSTEMS

A. D. Solomon
C. A. Serbin
J. J. Tomlinson
Union Carbide Corporation, Nuclear Division
Oak Ridge, Tennessee 37830

It is believed that the use of phase change materials (PCMs) levels the load and improves the comfort. This is because large amounts of heat can (in principle) be stored in the PCM at its phase change temperature. During the past year we have focused on the options available to us when PCM is put into the building structure using analytical and numerical studies, we have identified the optimal approaches to doing this. Among other questions, we looked at the efficacy of locating the PCM at the wall surface as opposed to internal storage, the necessity of exposing the PCM directly to beam radiation, and the optimal choice of the PCM. Many of our projections and recommendations spring from a one-room computer simulation of solar flux room thermal processes.

Introduction

The key to successful passive design is the successful incorporation of a thermal storage mechanism. Sensible heat storage requires the use of some "massive" storage medium--the archetype being the Trombe wall. The use of PCMs for thermal storage would appear to do away with the need for massive structures, because of the high latent heat of these materials. With this in mind PCM storage panels [2] and PCM Trombe walls [5] have been studied in the past. The basic suppositions have been that temperature fluctuations would be reduced and that benefits would be observed with small volumes of PCM. This year we have seen that this conjecture may indeed be correct. As seen in an earlier study [5] the most critical parameter is the melting or critical temperature, T_{cr}, of the PCM.

How do we incorporate PCM into the building structure to derive maximum benefits? We have seen that PCM placement at the wall/ceiling structure surface is preferable to its placement within the structure. On which surface do we put the PCM? We have seen that it must be placed on the surfaces most exposed to direct solar gain. Which PCM is best? We have seen that the optimal T_{cr} is determined by the desired interior temperature and the building configuration and location.

Our discussion opens in Part 1 with a sketch of the simulation program used. In Part 2 we present our main results. We close with some additional points.

Part 1. Simulation Program

When faced with the task of simulating a building structure, one naturally looks for building simulation packages already in existence. However, to our knowledge, no existing model contains an option for a PCM substructure. Attempts to incorporate the PCM effect via specific

heat enhancement must be regarded with suspicion because of the near-cyclic temperature variation. Indeed most existing models will not even permit the use of arbitrarily large specific heats. For this reason we have been drawn to the development of a simulation TES2 that permits the inclusion of PCM in the walls, ceilings, and/or floors of a passive solar building. TES2 directly incorporates building structure, beam and diffuse radiation, and cross radiation between walls. A "comfort" temperature is computed, and the state of the system is updated through discrete time increments.

Part 2. The Effect of PCM Incorporation

We will now present the results of our study thus far. We turn first, in section 2.1, to a typical simulation. In the next section we examine how the PCM should be incorporated. In section 2.3 we turn to the results of our simulation. Section 2.4 is concerned with the optimal thickness of the PCM layer. We close in section 2.6 with some general conclusions.

Section 2.1. A typical TES2 run.

Consider a "building" consisting of four walls, a ceiling, and a floor. The walls are of two types: panels and PCM. The ceiling and the panel walls are assumed to consist of the following layers, beginning with the room side: plasterboard, air gap, wood, and asbestos cement siding. The floor is stone. The PCM is to have the properties of $CaCl_2 \cdot 6H_2O$, except for the melt temperature, which we will vary. The remaining property values are representative for most PCMs. The PCM wall is taken to be of 1" thickness and insulated to the outside.

Each wall/floor/ceiling except for the window-wall is divided into four equal area subsections for which temperature and state are individually updated. The building dimensions are 20' × 18' × 12'. The front wall faces south and contains a large picture window. The outside air temperature is to be periodic over a 24-hour period with mean temperature 35°F and amplitude 14°F. The simulation is performed for Albuquerque, New Mexico, for February 14-17, from 5 a.m. to 5 a.m. The particular run we describe is for the choice T_{cr} = 70°F with PCM in the west wall. In all cases the behavior of the system is, for all intents and purposes, periodic with a 24-hour period over the three day simulation. We have found the dominant thermal driver to be the beam radiation into the structure, inducing high surface temperatures for those components on which it impinges.

In the desire to know how the PCM is performing, we may output all temperatures as well as the phase change structure of the PCM wall. In the simulation we do not utilize the entire 1" thickness of the PCM.

The key aim of PCM incorporation is to reduce the heating and cooling loads on the building. As measures of these loads (in Btus), we have found the total amount of supplemental energy needed to raise T_{eu} to 60°F(denoted by HEAT) and removed to lower T_{eu} to 80°F (denoted by COOL) after our three day runs. These are HEAT = 3.4×10^4 Btu and COOL = 3.2×10^4 Btu respectively.

Other information available from TES2 includes temperature profiles in structures, heat fluxes, and general heat balances.

Section 2.2. PCM incorporation.

The proper incorporation of the PCM is one of the keys to successfully utilizing the PCM concept. We have found that it is essential to have beam radiation impinging on the PCM surface and that the PCM not be separated from asy thermal exchange with other elements in the structure. The concept that appears to be most appealing is that of incorporation of the PCM into boards of corrugated plastic with small hollow channels. The plastic sheets could literally be glued onto the walls in some attractive manner. On the basis of our results, it would appear that a PCM layer thickness would be adequate for having the desired bahavior.

Section 2.3. Simulation results.

In this section we compare the results of a number of simulations, each one a variation of that described in section 2.1. What we wish to know is (a) For what choice of T_{cr} will T_{eu} be most in the comfort range $60° \leq T_{eu} \leq 80°F$? (b) Where should the PCM be placed? (c) Does the PCM offer any advantages over having nothing at all? (d) Does the PCM concept "perform" better than a one foot thick stone wall?

Question a: To address question a, we compare cases in which T_{cr} = 50°, 60°, 70°, 80°F, and the PCM is placed in the western side wall. We find that T_{eu} is best behaved for T_{cr} = 70°F, where the night temperature is greatest and the maximum day temperature is least. The total heating and cooling loads over the simulation duration are the following:

T_{cr}(°F)	HEAT (Btu)	COOL (Btu)
50	5.69×10^4	4.17×10^4
60	4.46×10^4	3.00×10^4
70	3.40×10^4	3.21×10^4
80	4.10×10^5	3.73×10^4

As we see the choice of T_{cr} = 70°F is again optimal.

Question b: To address the question of PCM placement, we have performed simulations with 70°F PCM on the rear wall, eastern side wall, and the floor of the building. We find that for the eastern wall the nighttime performance is substantially poorer; on the other hand, the PCM floor case is a considerable improvement for daytime use.

Question c: PCM vs. non-PCM Performance. We have compared the T_{eu} values for 70°F PCM in the western wall against the case of four paneled walls and found that the non-PCM case results in substantial overheating during daylight and cooling (via diffuse loss) at night.

Question d: What is the effect of a stone wall? We have compared the cases when the western wall is PCM at T_{cr} = 70°F, as against when it is a one foot thick stone wall. We find that the cooling load is diminished via the stone wall. On the other hand, the heating load is not.

Remark 1. On placing the PCM within a wall. It is interesting to consider placing the PCM behind the interior wallboard. We find that the PCM performance is degraded substantially by such a layer.

Remark 2. The use of other PCMs. No significant difference is noted between the results of choosing other PCMs, so long as the melt temperatures are the same.

Section 2.4. Thickness of the PCM layer.

Under realistic conditions, a PCM layer of 1" is adequate for the PCMs that we consider (e.g., hydrated salt and paraffin waxes).

Part 3. General Conclusions

Passive solar approaches contain some inherently difficult problems. From a thermal analysis point of view, the chief difficulties stem from the fact that while we wish to maximize the solar input into a structure (e.g., through direct gain into the room), the heat once in the room tends to make the room very uncomfortable unless thermal storage can be effected at a comfortable temperature. The principle way of doing this is, hitherto, via the use of massive masonry structures for storing the heat as sensible heat. The value of this has, of course, been seen in our simulation with a one foot thick western wall. The use of PCMs can, we believe, improve upon the results observed via sensible heat. This is not only due to the fact that the PCM can store heat in a manner that is more controllable than that of sensible heat storage. Thus in our comparison of PCM and wall storage, we found that the PCM could "buffer" extreme values of the temperature both during the daytime (e.g., lowering the cooling load) and during the night (by lowering the heating load), a feat which could not be achieved by the stone wall. For those who have lived in masonry passive dwellings in an arid zone environment, the early morning "chill" in the house may well not be a welcome event, and via PCM use, this might well be avoidable.

Generally speaking, successful PCM incorporation requires that the PCM be directly illuminated via beam radiation through window or other entrances. Indeed the air-to-wall convective heat transfer is essentially ignorable when compared to radiative heat transfer with direct gain. It is essential the PCM layer contain in itself, a phase change front at the time of thermal extremes. Thus if the PCM were not directly impinged upon by beam radiation, it would not be an active participant in the heat transfer process.

The second most critical factor in PCM incorporation is the choice of the optimal phase change temperature. While other thermophysical properties do not strongly affect PCM performance since they are about the same for most standard PCMs, the melt temperature constitutes the controlling "switch" which turns the latent heat storage process on or off. In our simulations we have found the optimum temperature to be about 70 degrees F, assuming that the indoor comfort range of from 60 to 80 degrees is desired. Whether this is generally true is a point that would require some further study. We would stress that our results are based only upon four-day-long simulations in Albuquerque. Longer term simulations of the order of a year or more are under preparation and will give us further necessary information regarding system performance and expected comfort conditions and annualized loads.

Do we place the PCM on a wall, floor or ceiling? Our results indicate that again, the most critical factor is knowing where the beam radiation reaches. If the floor is principally illuminated, then it is best that the PCM be placed on it simply due to the large detrimental effect on comfort that a hot floor can have. On the other hand, if the room is not too deep, from north to south, the rear wall should have a PCM layer for essentially the same reason. The ceiling would appear not to be the best choice because of poor heat transfer and comfort considerations.

Should the PCM be placed on the wall surface or deep within the wall in some type of container? Our results indicate that much of the positive effect of the PCM can be lost by placing a layer of material between it and the room air. We believe that any layer between PCM and room should be kept as thin as possible. For this reason, the concept of plastic wallboard incorporation would appear to be particularly attractive.

Generally speaking, our simulations lead us to believe that PCM incorporation in the manner described represents an effective way to make possible large-scale passive solar use. While additional questions must yet be addressed, we are convinced that the basic guidelines of PCM incorporation described above will place passive concepts within the domain of feasibility for building structures.

References

1. J. Duffie and W. Beckman, Solar Energy Thermal Processes, Wiley-Interscience, New York, 1974.

2. T. Johnson, "Lightweight Thermal Storage for Solar Heated Buildings," Solar Energy, 19, pp. 669-675, 1977.

3. W. Place, R. Kammerud, B. Anderson, B. Curtis, and W. Carroll, "Human Comfort and Auxiliary Control Considerations in Passive Solar Structures," Solar Energy Research Institute, Report No. SERI/TR-721-823, October, 1980.

4. A. Solomon and C. Serbin, "TES - A Program for Simulating Phase Change Processes," Union Carbide Corporation, Report No. ORNL/CSD-51, January, 1980.

5. A. Solomon, "Design Criteria in PCM Wall Thermal Storage," Energy 4, pp. 701-709, 1979.

6. A. Solomon, "Mathematical Modeling of Phase Change Processes for Latent Heat Thermal Energy Storage," Union Carbide Corporation, Report No. ORNL/CSD-39, August, 1979.

MEASURING THERMAL GRADIENTS IN A MELTING/FREEZING PCM WITH A LASER

Ralph M. Deal and Rene Papo
Chemistry Department
Kalamazoo College
Kalamazoo, MI 49007

ABSTRACT

A water loop was constructed and used to control the temperature on one face of a 4"x4"x4" cell containing PCM. Two faces were equipped with plate glass windows allowing a laser beam to pass through the cell and its net deflection to be measured. Thermal gradients in the liquid phase were compared with computer simulation of conduction in a PCM. Preliminary measurements with the current cell design show significant contributions to heat transfer in the PCM from convection despite attempts to limit heat transfer to conduction.

INTRODUCTION

In an extension of studies first initiated by R. M. Deal at the Oak Ridge National Laboratory, an experimental call was constructed to allow measurements of temperature gradients in a PCM undergoing melting/freezing due to heat being transferred through that PCM by conduction. The data is to be used to test the validity of computer simulations of that heat flow. The cell was designed to allow degassing of the PCM and to have a pair of walls allowing a laser beam to pass through the liquid portion of the PCM with minimal distortion due to the walls. A water loop with a controlled temperature bath is used to control the temperature of one face of the cell.

THE PCM CELL

Using a crude design tool written for the purpose in PASCAL on an Apple II microcomputer, plans were drawn up for a local machinist to construct a cell from aluminum and Plexiglas. The images produced are reproduced in Figure 1 and 2 to show the details of the cell design.

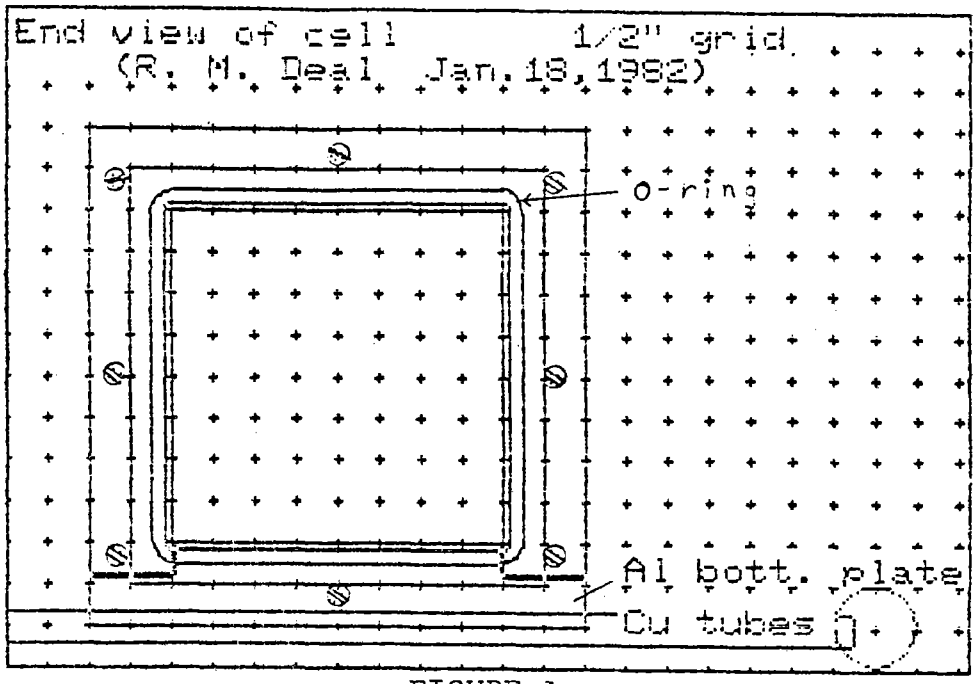

FIGURE 1
PCM - VIEW ALONG THE LASER BEAM

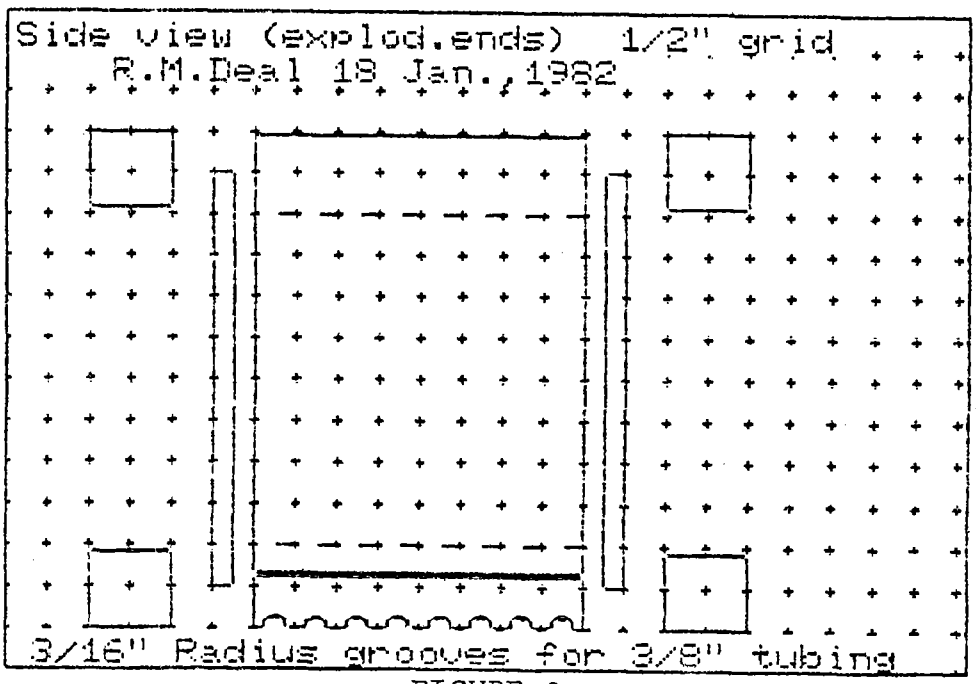

FIGURE 2
SIDE VIEW SHOWING GLASS END PLATES

The cell was designed to be evacuated to allow the pumping out of dissolved gases. Unfortunately, the current cell developed after a few cycles minute leaks at the corners where the aluminum face meets the Plexiglas walls. As a result the PCM, n-octadecane, a linear hydrocarbon (wax), shows the same production of bubbles at the freezing interface that had been noted as problem in the earlier studies at ORNL. Some of these bubbles are frozen into the solid wax layer, altering its thermal conductivity; others rise to the surface, producing some stirring of the liquid region. This stirring produces some heat transfer by convection and produces local distortions of the density profiles which in turn lead to distortions in the laser beam being directed through the wax parallel to the freezing interface.

THE OPTICAL BENCH

A 1/2 mw He-Ne laser was mounted on a 1 meter optical bench about 1 meter from the cell and the beam directed normal to one of the plate glass walls. The deflected beam emerging from the other plate glass wall travelled about 1 meter to a vertical target - a piece of white paper. A cathetometer situated off the optical path was used to measure precisely the height of the laser beam leaving the laser, entering the cell, and striking the target. Measurement of the net height of the laser beam relative to the Al face were also made. From the height measurements and distances of the laser from the cell and the cell from the target, the net angle of deflection could be measured. From this angle, the refractive index gradient could be calculated and therefrom the thermal gradient. Propagation of error analysis of the thermal gradient show an expected uncertainty of 6%. The major contributors to that uncertainty were the data collected in this project on the temperature dependence of the refractive index of n-octadecane and the measurement of the beam position at the target.

SHAPE OF THE DEFLECTED BEAM

The shape of the deflected beam at the target is not the sharp dot of about 1 mm diameter the undeflected laser will produce at that distance but a vertical streak with a sharp upper end and a gradually diminishing tail on the lower end. This shape seemed a natural result of the second derivative of the temperature with vertical position in the cell but the streaking was considerably larger than would be predicted from the second derivative. The explanation lies in multiple internal reflections within the PCM and plate glass walls. This can also be seen in the shape of the beam reflected back toward the laser. Unfortunately, the upper end of the streak seems to have made only one pass through the cell and so was used in measuring deflections.

THE LOOP

The initial design for the loop called for microcomputer control of the cycling of the PCM through various experiments as well as the collection and processing of data from those experiments. These were features of a loop constructed by R. M. Deal at ORNL using an LSI-11 microcomputer. Obtaining similar performance from an Apple II microcomputer proved considerably more difficult. A major problem was the interfacing of a Keithley 181 nanovoltmeter to the Apple. A commercial IEEE-488 interface (SSM) did not lead to smooth interaction with programs in PASCAL on the Apple. If further funding is available, this system will be equipped with one of several effective laboratory interfaces available commercially. The loop consists of two water baths, one being a Precision model #260 as a hot temperature bath, melting and stabilizing the PCM before dropping the temperature of the face. The other is a regulated water bath with a locally modified air conditioner as a cooler to produce 5 F water for the freezing. The Keithley was used to measure the temperature of the face and temperatures recorded in data files for subsequent plotting by the Apple.

The cell was filled by a PCM reservoir (a filter flask) and evacuated by an aspirator pump for degassing.

COMPARISONS WITH COMPUTER MODEL PREDICTIONS

Initial comparisons were made with an analytical model developed by Neumann (2). However, this solution is only valid for a semi-infinite slab, not the finite thickness slab corresponding to the PCM in the cell. The fit to the experiment was quite poor because in the cell, the temperature of the liquid portion drops considerably more rapidly in the finite case than the infinite slab case. The modelling is only valid as long as the temperature at the back side (top) of the PCM is still very near the initial temperature. That condition is only valid for a time during which only about 1/4" of the 3" PCM layer has frozen.

Subsequent comparisons with the TES model developed by A. D. Solomon at the ORNL (1) show considerable improvement in fit. The detailed analysis is still being completed but initial comparisons indicate that a larger thermal conductivity for the liquid than usual must be used to fit the results. There are two sources which can lead to apparently large thermal conductivities in the liquid. One is the gas bubble problem. The other is that the thermal conductivity of the Plexiglas walls is considerable. No material with thermal conductivity much less than that of the wax seems available. Because the PCM contains a moving heat source, namely the freezing surface, no single phase wall material can have the same thermal profile as the PCM unless its temperature is actively driven to match that of the PCM, a

difficult task at best. Because of this inevitable difference in the wall temperature at the same level as the PCM in the cell and the finite conductivity of the walls, some convection at the walls is inevitable. Just how important that is a question that is being considered through two-dimensional modelling of the cell (using a program developed by A. D. Solomon at ORNL).

EVALUATION OF THE LASER METHOD FOR MEASURING THERMAL GRADIENTS

While the final analysis has yet to be completed, it is clear that accurate information on the temperature gradient within the liquid region of a PCM can be obtained with this method as long as the thermal gradient is fairly constant along the laser beam path. The method can be used in the liquid regions through which heat is being transferred by convection as well as by conduction as long as the beam can be directed along a path of constant thermal gradient. While multiple parallel beams would yield more information in less time, the smearing effect noted above would make interpretation of overlapping patterns difficult. The simple single beam method used here is inexpensive and effective in measuring thermal gradients in liquid regions where the thermal gradient is constant along one direction. It provides a thermal probe that can be moved easily from one region to another by only shifting the position of the beam and does not interfere with the actual heat transfer process being studied.

REFERENCES

1. A. D. Solomon and C. E. Serbin, TES - A Program for Simulating Phase Change Processes, ORNL/CSD-31.

2. H. Carslaw and J. Jaeger, Conduction of Heat in Solids, Oxford at the Clarendon Press (1959).

THERMODYNAMIC PROPERTIES AND INTERACTIONS OF SALT HYDRATES USED AS PHASE CHANGE MATERIALS*

J. Braunstein
Chemistry Division, Oak Ridge National Laboratory
P. O. Box X, Oak Ridge, Tennessee 37830

The purpose of this task was to review the state-of-the-art of salt hydrates as phase change materials for low temperature thermal energy storage, with the objective of recommending research that would result in more practicable use of these materials. Areas for review included phase equilibria, nucleation behavior and melting kinetics of the commonly used hydrates.

A great deal of effort has been expended over the past thirty years towards the development of efficient, reliable inexpensive systems based on phase change materials, especially salt hydrates, for the storage (and retrieval) of thermal energy for residential heating. The pioneering work by Telkes stimulated, among her colleagues and in other groups, exhaustive searches of the literature and in the laboratory for compounds with phase change temperatures in an appropriate range and having high latent heats of transition, experimental investigation of properties, theoretical correlations for the estimation of unknown properties, and ingenious chemical, physical and mechanical solutions to the problems of assuring essentially reversible thermal behavior on long term cycling.[1] Although some commercial development is now occurring, the use of phase change material thermal energy storage systems is not yet widespread. The reasons for this are no doubt primarily economic. But a major contributing factor to the economics is that solution of the problem of long term reliability has been elusive.[2] Much of the development work has been of a short range nature, as required in the commercial sector. Relatively little effort of a basic nature has been made to answer continually recurring questions relating to nucleation, crystal growth, crystal melting kinetics, detailed thermodynamic analysis of phase equilibria in complex salt hydrate systems, analysis of nonequilibrium behavior in solution and other phenomena which bear on the effectiveness and therefore ultimately the economics of PCM-TES. Detailed basic studies that are needed of these phenomena are of a long range generic nature that might not justify short term commercial support, but they offer the possibility of greatly improved choice, modification and utilization of PCMs based in a better understanding of their behavior.

Based on literature studies, a list of recommendations of needed basic research has been prepared. The list is derived largely from generic problems which have recurred in the past thirty years. A prime example of these problems is the prevention of segregation, e.g., in Glauber's salt, by stirring, by container configurations designed to

---

*Research sponsored by the Division of Energy Storage Systems Research, U.S. Department of Energy under contract W-7405-eng-26 with the Union Carbide Corporation, Nuclear Division.

assure thin layers of salt hydrate rather than large masses, by encapsulation of the PCM or suspension. The areas of research may be characterized as related to the search for new PCMs, or to the search for improvements in performance of known PCMs. Common to all is the need for an increased knowledge of physical properties. The first three topics are considered to have the higher priority.

1. Crystallization and Melting (Kinetic and Structural Studies)

The usefulness and reliability of salt hydrate PCMs would be greatly enhanced by an improved understanding of crystal nucleation, growth and agglomeration (of salt hydrate crystals). A great deal of effort, much of it empirical, has been devoted to searches for suspension agents, salt crusts, and encapsulating media for, e.g., Glauber's salt to prevent segregation of the solid Na_2SO_4 formed during heating. The thermodynamics and kinetics of crystal growth with cycling needs to be better understood. A suspending agent may be effective for several cycles in partly suppressing segregation. But if the dynamics of crystallization favor growth and agglomeration of large crystals, even with a relatively small free energy advantage, the suspending agent will not provide long-term stable prevention of segregation, and other means (stirring or other salts) need to be considered to overcome the degradation of performance of PCM's. Work in this area should be aimed at an expanded understanding of the kinetics of crystal growth.[3] Modeling studies have contributed valuable insight into the process of melting of phase change materials via conductive or convective heat transfer.[4] The possibility should be investigated of extension of models from slabs and "mushy zones" to distributions of crystallite sizes. Testing of such extended models would require experimental data on the crystallite size distribution. In addition to physical studies of nucleus formation and growth, chemical studies of crystal modification would be useful. E.g., studies of the crystal structure and the possible incorporation of additives to form solid solutions or defects that would distort the crystal structure to make it less refractory. Incorporation of mobile species (e.g., protons) in a crystal might lead to more rapid reaction with water, by increased diffusion rates. Olmsted and Garrett have reported screening tests of a number of additives to Glauber's salt which modify its crystal habit by changes in the nucleation rate and growth rate.[5] Additives that showed some effect included magnesium nitrate, potassium chromate, and some surface active agents including dyes. As the authors pointed out, crystal habit modification is still an art. Additional systematic work is needed in this area.

The general area of crystal melting kinetics of salt hydrates has had little attention, although indications are that heat and mass transfer during the melting or peritectic decomposition process of Glauber's salt contribute to the irreversibility.

Physical-chemical means of altering nucleation and crystallization should be sought, e.g., via electrochemical means, to adjust compositions in the liquid phase and vary the degree of supersaturation.

2. Prediction of phase behavior in ternary systems (two salts plus water, two salt hydrates, or a salt hydrate and organic solvent)

This requires a study of solubilities and of activity coefficients for mixtures in which a second salt has been added to a salt hydrate system which undergoes peritectic decomposition on heating rather than melting. This would have as aim the development of theoretical and empirical correlations that would permit predictions of how a salt hydrate binary system with an incongruent or semicongruent compound could be converted into a ternary system in which the compound melts without forming a solid phase. (The reported "solubilization" of $CaCl_2 \cdot 4H_2O$ by $SrCl_2$ in the $CaCl_2 \cdot 6H_2O$ system was discovered almost accidentally.[6] Some modified salt hydrate compositions have been developed commercially and are in the patent process.) A thermodynamic investigation of such systems could lead to predictions of the kinds of additives that would be useful in such systems and with other hydrates. Both theoretical and experimental studies are needed. The theoretical part would involve a thermodynamic analysis of solubilities and of chemical potentials in solution for concentrated salt solutions at compositions in the vicinity of salt hydrate compositions and peritectic points. The effect of a third component on the chemical potential of the primary salt can be written in terms of interaction coefficients of the ions and water. Such an analysis would lead to criteria for the sign and magnitude of interaction coefficients which would be required to shift the composition (and temperature) at which a salt undergoes a peritectic reaction to a composition (and temperature) where the hydrate melts and freezes without decomposition. The theoretical study would include compilation of data in some known systems for phase equilibria, water activities, salt solubilities as a function of composition and temperature. Experiments needed would be measurements of solubilities or phase equilibria and the measurement of salt activities or chemical potentials. A convenient means for obtaining the latter would be from water activities determined, e.g., by isopiestic equilibration.

Modification of the thermodynamic properties by a suitable organic solvent also should be considered. For example, ethylene glycol has been reported as an additive to sodium thiosulfate pentahydrate to lower the fusion temperature of the hydrate.[7] An understanding of the interactions in such systems among the ions, water molecules and organic molecules, both in the liquid and solid phases should be helpful in predicting new useful systems.

The aim of the correlation would be to predict the kinds of additives that might be useful in converting an incongruently melting salt hydrate into a system which melted congruently, and to improve the performance of a system undergoing nonequilibrium phase transformations. In addition to helping to remove some of the empiricism of searches for such additives, the improved understanding would help to test consistency of data such as that which may be suspect.

3. Thermal diffusion-Soret effect

Significant temperature gradients are to be expected in unstirred systems. These can drive composition gradients, so that even a congruently melting compound or eutectic can develop into a system with nonuniform composition and which can cause solid phase segregation. This may be what happens in the $CaCl_2$ $6H_2O$ system, where the peritectic point has been reported shifted to coincide with the compound composition and melting point by addition of $SrCl_2$, but segregation is still reported to occur. Very little research effort appears to have been devoted to the area of the behavior of salt hydrate systems in thermal gradients.

The existence of a temperature gradient in a concentrated salt solution (or melted PCM) provides a driving force for denser (i.e., more concentrated) solution to accumulate at the bottom of a container under the influence of gravity, and therby to establish a concentration gradient. This tendency is opposed by convection, which is why unsaturated solar salt gradient ponds generally are not stable in the absence of barriers to convection. PCM-TES systems generally incorporate gels or suspending agents to reduce segregation. If the PCM-suspension agent is not in closed cells, convection would be reduced but mass transfer (diffusion) would still be possible. There would then be a mechanism to establish concentration gradients. This could lead to segregation of solid during repeated freeze-melt cycles, and may be a contributing factor in the degradation of some PCM systems. A study of the tendency toward segregation under the driving force of a thermal gradient should be part of the screening process of a PCM and, should be known in designing the containers and heat exchanger configurations of the system.

4. Physical Properties

Using some estimates, choices now are probably not restricted by lack of knowledge of heats of fusion. Small differences are washed out by differences in masses and thermal capacities of containers, suspension agents, and segregated materials. A consistent testing program would be desirable which includes DSC measurements of heats for small samples and calorimetric measurements for larger samples and containerized samples. Tests should incorporate cycles with slow and with fast heating and cooling rates as well as temperature gradients in order to ascertain nucleation and phase segregation behavior. In comparisons of TES systems, a more appropriate thermodynamic criterion is required, analogous to the exergy, to represent the quality of the heat in cycles which are clearly not isothermal.[8]

5. Literature search for new PCMs

This is probably approaching the law of diminishing returns in view of the number of independent extensive searches that have been carried out, e.g., by Lane, Telkes (1980), Kauffman (1973), Reiter (1979), Marcus (1980) and others. Establishment of a clearing house for compilation and systematization of phase data, phase diagrams, solubilities, and other thermodynamic properties would be useful.

References

1. M. Telkes, "Thermal Energy Storage in Salt Hydrates," Chapter 11 in Solar Materials Science, L. E. Murr, editor, Academic Press, NY (1980).

2. R. J. Borkowski, R. J. Kedl, T. K. Stovall and J. J. Tomlinson, "Energy Storage using Phase Change Materials for Active Solar Heating and Cooling: An Evaluation of Future Research and Development Directions," Oak Ridge National Laboratory Report, Report No. ORNL/TM-8098, April 1982, p. 180.

3. L. Christensen, N. Cho, G. Keyser, D. Lamb, F. Wedeum, and J. Hallett, "Studies of Nucleation and Growth of Hydrate Crystals with Application to Thermal Storage Systems, Final Report," Desert Research Institute, Reno, Nevada, Report No. NSF/RANN-AER-95-19601.

4. A. Solomon, "Some Aspects of the Computer Simulation of Conduction Heat Transfer and Phase Change Processes," Oak Ridge National Laboratory Report, ORNL/CSD-100, April 1982.

5. H. Olmsted and D. E. Garrett, "Solar Energy Storage Projects," DOE/SF/01964T1 (1980).

6. B. Carlsson H. Stymne and G., Wettermark, "Storage of Low-Temperature Heat in Salt-Hydrate Melts-Calcium Chloride Hexahydrate," Document D12:1978, Swedish Council for Building Research, Stockholm, Sweden, 1978.

7. D. C. MacCracken, "Effect of Additives on Performance of Hydrated Salt Systems," in Proc. of the Sixth Annual Thermal and Chemical Storage Contractors Review Meeting, Sept. 1981, Washington, D. C., USDOE Report CONF-810940, p. 186 (1982).

8. A. A. Bejan, "Second Law Analysis in Heat Transfer and Thermal Design," in Advances in Heat Transfer, 15, 1(1980), ed. J. P. Hartwell and T. F. Irvine, Jr., Academic Press, New York.

NEW PHYSICAL-CHEMICAL REACTIONS USEFUL FOR TES

James S. Johnson, Jr., and C. Gary Westmoreland
Oak Ridge National Laboratory
Oak Ridge, Tennessee 37830

Introduction

The objective is to evaluate novel potential systems for thermal energy storage. In most cases, these are to be classes not known to us to have been tested previously, although some variation of approaches under investigation previously are included. Initially, economics of specific materials tested is not a primary concern; consideration of practical embodiments is deferred.

The selection is based largely on equilibria which are reported to have high temperature coefficients, and evaluation is based on whether or not the enhanced enthalpies which might be expected to accompany these in the temperature range of interest are detected by differential scanning calorimetry (DSC). Although the systems investigated so far have not proved interesting, many of them have been looked at only in preliminary fashion, and we remain hopeful that new options may be uncovered.

Examples of Systems Tested

Poly(ethylene oxide-propylene oxide). Cross-linked polymers of these polyethers have been reported (1,2) to have rather remarkable ability to desalt brines in temperature cycles. Water is imbibed, at temperatures near ambient, and released by raising the temperature, the temperature depending on the composition and the degree of cross-linking. The changes in water solubility are sometimes substantial, the wet polymer containing 75% water at 0°C and 30% at 45°C in one case (2). High desalting reported, sometimes over 90% rejection from sea-water salinities (water uptake was less in these samples), indicate that there must be substantial chemical interactions between the polymer and water.

These properties have been correlated with phase behavior of aqueous solutions of uncrosslinked polymers, such as lower consolute temperatures of phase separation. So far, our evaluation has been limited to such aqueous solutions, in the hope that some of these transitions might result in enhancements of heat capacities. In a few cases, phase behavior was examined in a cursory way, and rather complex patterns of immiscibility were seen.

Polymers tested:

Carbowax 1000	polyethylene glycol of nominal molecular weight of 1000 (Union Carbide)
Methoxy PEG 750	molecular weight about 750
Polyglycol 15-750	polyethylene oxide-polypropylene oxide copolymer (presumably random) of molecular weight about 1465 (Dow)

Pluronic L62	Block copolymer of polyethylene oxide (about 20%)-polypropylene oxide, molecular weight about 2000 (Wyandotte Division, BASF)
P103	30% ethylene oxide, molecular weight about 4500
L92	20% ethylene oxide, molecular weight about 3300
L61	10% ethylene oxide, molecular weight about 2500
L101	10% ethylene oxide, molecular weight about 3600

Some of these were measured at several different concentrations, as weight percents in water, usually four compositions evenly spaced, as well as the pure polymer; some were tested only for 25% polymer-75% water. The heat absorbed over the range of 10° to 85° C did not appear in any cases to be substantially different than values on a straight line between values for pure polymer and pure water. A few tests at 2.5°/minute, rather than the 10°/minute rate usually used did not indicate that apparent heat capacities were affected by slow kinetics.

We are attempting to prepare crosslinked samples of polyglycol 15-750; DSC measurements were made on this material (2), but the results reported were too sparse for interpretation. We hope to be able to check the properties of crosslinked material before the end of the program.

Hydrolysis of metal ions. Enthalpies of the reaction of metal ions with water are positive and in many cases for the first hydrolysis step are close to the value for dissociation of water (13.4 kcal/mole) (3). Hydrolysis could therefore increase substantially the effective heat capacity of a solution, if the solution were concentrated, and there were a substantial change in the degree of hydrolysis over the temperature range of interest. The systems we are seeking should have fast kinetics, reversible reactions, and soluble hydrolyzed species. If these conditions were met, phase transition problems of many heat storage compounds might be deviated.

As a test case, we have selected Bi(III) perchlorate in water. The hydrolysis scheme is fairly well established (4,5,6), the main species being a hexamer of hydroxyl number 2, which can be written approximately as $[Bi(OH)_2]_6(ClO_4)_2^{4+}$; there is also a monomeric hydrolyzed species. Ultracentrifugation indicates a strong increase in hydrolysis between 15° and 35° C (7). Bismuth (III) is highly acidic, i.e., it hydrolyzes in the presence of excess $HClO_4$, so that the acid produced by increased hydrolysis as the temperature is raised will not altogether suppress further hydrolysis. The hexamer is very soluble; concentrations as high as 5.8 moles Bi(III)/liter can be attained at room temperature.

We have tested by DSC three solutions: one should have contained at 25°C essentially unhydrolyzed bismuth; one should have been predominantly the hexamer; and one at intermediate hydrolysis. None had enhanced heat capacity over that of water on a weight basis, although

they may have been greater per unit volume. We are formulating a computer program to allow predictions of observations and selection of optimal conditions.

Soluble fluorinated organic compounds. Some freons form clathrates or hydrates of melting points above ambient temperatures, of heats of fusion approaching that of ice. Use of these requires high pressures, however. If water-soluble fluorinated organics formed such complexes with water, low-pressure devices might be feasible. One available class are commercial fluorinated surfactants. These are clearly far too expensive for practical use, but we felt they might give an indication if the approach has any promise. Several Zonyl^{R} surfactants were tested by DSC in solutions or dispersions of 25 wgt% in water. These duPont products have an average of seven perfluorinated carbons and two to five protiated carbons. Samples with anionic, cationic, and neutral hydrophilic groups were tested. None showed any transitions indicating melting of hydrates from 7° to 87° C.

Organic compounds. These fall in classes already investigated for energy storage, and were tested largely to validate the performance of the calorimeter. However, some of them seemed of possible interest for energy storage, if the properties happened to be superior to the related paraffin hydrocarbons. These were ester waxes, obtained for the Amoco research laboratory in Napierville, a byproduct of motor lubricant production. Some results are summarized in Table I. Their heat of melting ranged from about a third to slightly less than a half of that of ice. One of them (R-35) was carried through several cycles. Supercooling was not great (measurements at 5°/min) and the area under the melting peaks was reasonably reproducible. Measurements of coconut oil and two other organic carbons are included for comparison. The waxes appear to have heats of fusion similar to those of paraffin. These materials are highly purified, to meet food-grade standards, and the cost, which varies from time to time, is usually in the range of $0.40-0.50 per pound. If crude material could be used, the cost might be about half this range. In either case, they appear to be of limited interest.

References

1. R. E. Anderson and G. D. Jones, "Desalination of Water with Thermally Reversible Water-Swellable Resins," U. S. Patent 3,438,893, 15 Apr 1969.

2. R. W. Lawrence and W. J. Schell, "Study of Crosslinked Polymers of Desalination," Office of Saline Water Report 996, PB236934.

3. C. F. Baes and R. E. Mesmer, "The Hydrolysis of Cations," John Wiley & Sons (1976).

4. A. Olin, *Acta Chem. Scand.*, 11, 1445 (1956).

5. J. S. Johnson, G. Scatchard, and K. A. Kraus, *J. Physical Chemistry*, 63, 787-793 (1959).

References (cont.)

6. H. A. Levy, M. D. Danford, and P. A. Agron, *J. Chem. Phys.*, 31, 1458-1461 (1959).

7. Chemistry Division Annual Report, period ending 20 June 1962, ORNL 3320, p. 67.

TABLE I

DIFFERENTIAL SCANNING CALORIMETER TESTS OF ORGANIC COMPOUNDS

Substance	Transition Range, °C	DSC, Squares/mg	Transition	DSC Area, Sample/H_2O	Literature, Heat of Fusion, Sample/H_2O
Waxes from Petroleum Sources (Amoco)					
R-25	45-57	35.9	Melting		
R-35	45-56	37.6	Melting		
R-40	50-60	35.6	Melting		
R-45	50-64	28.4	Melting		
LW-0676	42-54	32.8	Melting		
Cycles					
R-35	44-56	35.7	Melting		
	51-40	35.4	Freezing		
	44-56	38.7	Melting		
	51-40	35.7	Freezing		
	44-56	37.1	Melting		
	51-40	34.6	Freezing		
Coconut Oil					
	10-25	42	Melting		
Thymol	50-54	32.5	Melting	0.37	0.34
	12-10		Freezing		
n-lauric acid	44-48	41.4	Melting	0.47	0.54
	42-40		Freezing		
H_2O	1-7	87.6	Melting		
	-21 to -26		Freezing		

PROJECT SUMMARY

Project Title: Metal Hydride/Chemical Heat Pump Development Program

Principal Investigator: Samuel J. Cunningham

Organization: Southern California Gas Company
Box 3249, Terminal Annex
Los Angeles, CA 90051

Subcontractor

Solar Turbines Incorporated
P.O. Box 80966
San Diego, CA 92138

Project Goals: The main objective of this project is the development and testing of a heat/mass flow enhancement device for a metal hydride assembly.

Project Status: Phase I of the project was initiated in February 1981 and was completed in January 1982. The tasks of Phase I included the selection of the temperature upgrade heat pump cycle for design purposes, a decision on the appropriate hydride alloys, a filter design study, development of transient heat transfer models and comparisons with experiments, and the design of an advanced hydride heat exchanger.

Phase II plans call for the fabrication and testing of the hydride heat exchanger device. This phase began in March 1982. Accomplishments to date include the construction of the heat exchanger with initial testing in progress and characterization of the hydride alloys.

Contract Number: 534098-S

Contract Period: February 1981 - November 1982

Funding Level: $330,580

Funding Source: Brookhaven National Laboratory

PROJECT SUMMARY

Project Title: Sulfuric Acid and Water Chemical Heat Pump - FY'82 Program

Principal Investigator: E. Charles Clark

Organization: Rocket Research Company
York Center
Redmond, Washington 98052
(206)885-5000

Project Goals: The objective of this program is to determine the complete operational characteristics of the sulfuric acid and water verification test unit (VTU). The acquired information will provide data to assess the technical and economic merit of the industrial chemical heat pump operation. The four-task program is designed to conduct performance mapping tests at various source/sink temperature combinations for both single and dual source systems. The effects of overall system performance as a function of condenser temperature will also be measured. The test program will be completed by operating the VTU for an extended 100-hour test period at equilibrium. An additional program goal is the transfer of the R&D technology to the private sector by means of a Department of Energy-sponsored seminar.

Program Status: The current program is being managed by Brookhaven National Laboratories. Performance mapping has been completed with both single and dual source closed loop operation. Preparations are now under way to conduct the 100-hour extended test operation. A microprocessor system controller has been designed and built to provide control of fluid circuits, monitor instrumentation, and provide automatic system shutdown. All testing will be completed in September 1982. The CHP seminar is scheduled to be held September 29, 1982.

Contract Number: 568761-S

Contract Period: 15 March 1982 - 30 November 1982

Funding Level: $369,589

Funding Source: Department of Energy/Brookhaven National Laboratory

PROJECT SUMMARY

Project Title: Chemical Heat Pump Cost- and Energy-Effectiveness Evaluation

Principal Investigator: Warren R. Standley

Organization: TRW Energy and Environmental Division
8301 Greensboro Drive, McLean, VA 22102
(703) 734-6412

Project Goals: The objective of this project is to compare the cost- and energy-effectiveness of existing chemical heat pump (CHP) concepts with a baseline of conventional energy technologies and a group of near-term and emerging energy technologies with which CHPs are expected to compete.

Project Status: Under contract to Brookhaven National Laboratory, TRW conducted a cost-effectiveness and energy resource evaluation of two chemical heat pump (CHP) concepts: a sulfuric acid-water CHP and a methanol-calcium chloride CHP. The CHPs were compared to baseline and emerging competitive technologies for providing space conditioning services to residential and commercial buildings and for upgrading industrial process heat, using levelized annual cost as the measure of cost-effectiveness. An initial study concluded that CHPs could be cost-effective and conserve energy resources in applications for industrial process heat upgrading and, in specific applications, for residential heating and cooling. CHPs for commercial office building space conditioning are neither resource nor cost effective.

The initial CHP evaluation was expanded to develop a more detailed cost-effectiveness and energy-effectiveness evaluation of the sulfuric acid CHP in industrial applications for recovering and upgrading waste heat for process use. The recent technical iterature was thoroughly reviewed and candidate industrial heat pumping applications have been selected. The selection criteria were based on a desire to use technically-appropriate, industrial applications for the sulfuric acid CHP, those which would be familiar to a broad audience of potential industrial users of the CHP. The economic methodology for cost-effectiveness is based on discounted cash flow, and employs ROI, payback period, and equivalent cost of energy saved/displaced as the indicators. A data base of technical performance information and economic parameters has been assembled, and work is proceeding to complete the final analysis and present the cost/energy effectiveness comparisons.

Contract Number: 519403-S

Contract Period: June 1980 through September 1982

Funding Level: $158,391

Funding Source: Department of Energy

PROJECT SUMMARY

Project Title: The OHZ Hydrogen Process

Principal Investigator: C.C. Silverstein

Organization: CCS Associates
P.O. Box 563
Bethel Park, Pa. 15102
(412) 221-0999

Project Goals: The objectives of this program are 1) to assess the potential of the OHZ hydrogen process for further development, and 2) to identify process parameter goals which are necessary for commercial viability.

Project Status: A survey of the current state of knowledge of the OHZ process and of zeolites with potential for use in the OHZ process has been completed. Plant design studies have been carried out to determine: process materials requirements, process efficiency, and hydrogen cost. Process parameter goals for commercial viability have been identified. It has been concluded that the OHZ hydrogen process warrants further development.

Contract Number: BNL 567949-S

Contract Period: March 10, 1982 - September 30, 1982

Funding Level: $40,661

Funding Source: Brookhaven National Laboratory

PROJECT SUMMARY

Project Title: Thermochemical Water-Splitting Program

Principal Investigator: G. E. Besenbruch

Organization: General Atomic Company
General Programs Division
P. O. Box 81608
San Diego, California 92138
(714) 455-3079

Project Goals: This program involves experimental research and development of the sulfur/iodine thermochemical water-splitting cycle. Specific objectives include improvement of the critical chemistry aspects of the process, operation of a bench-scale unit which evaluates the major aspects of the cycle, and development of engineering flowsheets for estimation of process costs and efficiency. Funding on solar and fusion applications of the process is provided by the DOE Solar Thermal Power Office and the DOE Office of Fusion Energy.

Project Status: Operation of the bench-scale unit (Section III) resulted in modifications to the system. Portions of the iodine removal section were placed inside of a hot box to improve operability of this subunit. The design of a solar-powered water-splitting plant was completed and a cost estimate of the hydrogen production was made. Several process improvement concepts were investigated in greater detail. The use of HBr in place of H_3PO_4 as an agent to separate the H_2O-HI-I_2 product was studied. Also, the testing of a homogeneous liquid catalyst for HI decomposition showed that this enhanced concept is viable and practical.

Contract Number: DOE Contract DE-AC02-80ET26225
LLNL Subcontract 2198401
NUSCO/PSE&G/GA Joint Agreement

Contract Period: October 1981 - March 1982

Funding Level:

100,000	DOE STOR	(FY-1982)
75,000	DOE Fusion	(FY-1982)
40,000	NUSCO/PSE&G	(CY-1982)
50,000	GA Contribution	(CY-1982)

Funding Source: Department of Energy - STOR
Department of Energy - Office of Fusion Energy and Lawrence Livermore National Laboratory
Northeast Utilities Service Company and Public Service Electric and Gas
General Atomic Company

PROJECT SUMMARY

Project Title:	Hydrogen Recovery from Hydrogen Sulfide
Principal Investigator:	D. L. Hildenbrand
Project Leader:	G. N. Krishnan
Organization:	SRI International 333 Ravenswood Avenue Menlo Park, California 94025
Project Goals:	Perform bench scale experiments to obtain kinetics of reaction of hydrogen sulfide with liquid copper for the purpose of recovering hydrogen from hydrogen sulfide.
Project Status:	The project has been completed and a final report has been submitted.
Contract Number:	5232360-S
Contract Period:	January 15, 1981 through June 14,1982
Funding Level:	$105,651
Funding Source:	Brookhaven National Laboratory

PROJECT SUMMARY

Project Title:	Effect of Hydrogen on Low-Cycle Fatigue Life and Subcritical-Crack Growth in Pipeline Steels
Principal Investigator:	John H. Holbrook
Organization:	Battelle, Columbus Laboratories 505 King Avenue Columbus, Ohio 43201 (614) 424-4357
Project Goals:	The practicality of using hydrogen as a supplement or substitute for natural gas depends on whether hydrogen can be transported safely and efficiently in conventional steel pipelines. The objective of this program is to determine the influence of hydrogen on fatigue- and sustained-load crack growth in pipeline steels in order to help assess the feasibility of transporting hydrogen in present and future pipelines.
Project Status:	During the course of this program, it has been established that hydrogen gas at typical transport pressures increases the fatigue-crack-growth rate in pipeline steels by greater than an order of magnitude. It has also been found that the acceleration in fatigue-crack-growth rate is very sensitive to the purity of the hydrogen and the cyclic-stress-intensity during the crack growth. Some evidence has also been found for hydrogen-induced subcritical-crack growth under sustained loads in the heat-affected zones of pipe welds. However, critical-crack sizes required to observe subcritical-crack growth in hydrogen were only slightly less than the critical-crack size in nitrogen, an inert gas.
Contract Number:	BNL 550772-S
Contract Period:	June 1981 - September 1982
Funding Level:	$182,500
Funding Source:	Brookhaven National Laboratory (DOE)

PROJECT SUMMARY

Project Title: Photovoltaic Array/Advanced-Technology Electrolyzer Testing

Principal Investigator: G. Strickland

Organization: Brookhaven National Laboratory
Bldg. 120
Upton, New York 11973
(516)282-4091

Project Goals: Design and construct an integrated test bed as a technical illustration on coupling a state-of-the-art photovoltaic array (PVA) to an advanced-technology electrolyzer (ATE); test, demonstrate, and evaluate the system in several operating modes, especially under transient conditions.

Project Status: The final report on the design/planning activity was completed. The design calls for a nominal 15-kW ATE coupled to a 5-kW (peak) PVA via a power conditioner (PC-1) that will supply the balance of the power and provide an output simulating 100% solar supply. A programmable microprocessor controller (MPC) will govern the output of PC-1 and other operating modes such as 100% AC power, constant blended power, and decaying voltage output simulating a battery supply. Functional designs of PC-1 and the MPU were completed. When the project is implemented, design work will be completed to the point where a contractor can build the component; and BNL staff will manage the work. The schedule calls for all work leading up to the formal experimental program being completed in 12 months after implementation. The estimated capital and operating costs, which are about equal, total $700,000 for the first year's effort. Second- and third-year costs involving reduced manpower and nominal maintenance costs are about $200,000.

Problems/Issues: Use of a decommissioned PV array (5-kW peak) will depend on its condition and expected life. Purchase of a new PV array ($60K) may be warranted. After the planned test program is completed, a decision has to be made on converting the electrolyzer for use in a smaller stand-alone system.

Contract No.: DE-AC02-76CH00016

Contract Period: October 1, 1980 - TBD

Funding Level: $190,000

Funding Source: U.S. DOE via BNL C/HES

B94
PS 1

PROJECT SUMMARY

Project Title: C/HES Systems Analysis Program

Principal Investigator: Morris Beller

Organization: National Center for Analysis of Energy Systems
Brookhaven National Laboratory
Building 475
Upton, New York 11973
(516) 282-2041 (FTS) 666-2041

Project Goals: The objective of this program is to perform systems analyses of the major components in the portfolio of projects in the Chemical/Hydrogen Energy Systems Program for which Brookhaven National Laboratory provides management support and technical oversight.

Project Status:

1. Analyzed the SRI process for the decomposition of hydrogen sulfide to hydrogen and sulfur dioxide. Performed a market analysis for the products, and issued a final report.
2. Studied recovery of hydrogen from chemical and petroleum process streams using metal hydride systems. Concluded that alloy bed life is critical to the process economics, and that lifetimes of at least one year are necessary for successful processes.
3. Performed an analysis of the potential for photochemical production of hydrogen. Described the state-of-the-art of various photochemical concepts including heterogeneous and homogeneous systems, and organic and inorganic derivatives. Described advantages and disadvantages of various systems, and performed a breakeven cost analysis taking capital, operating, and power costs, as well as load factor, into account. Outlined a set of R&D criteria, and a set of cost goals.
4. Initiated an analysis of anode depolarization applied to electrolytic hydrogen production. Developed a set of criteria for depolarization media and their products. Applied depolarization potentials to the economics of an advanced electrolyzer system as a base case. Demonstrated quantitatively the potential savings to be gained in hydrogen production both as a function of power cost and future time frame.
5. Reviewed various proposals and reports in support of the Office of Energy Systems Research.

Contract Number: DE-AC02-76CH00016

Contract Period: October 1, 1981 - September 30, 1982

Funding Level: $90,000

Funding Source: U.S. Department of Energy

PROJECT SUMMARY

Project Title:	Advanced Concepts for Electrolytic Hydrogen Production
Organization:	Brookhaven National Laboratory
Project Goals:	Develop the base technology to reduce the electrical requirements for electrolytic hydrogen production.
Project Status:	Work in FY 1982 included investigations of the electrochemistry and materials science problems of high temperature solid oxide electrolyte electrolyzers and studies of carbonaceous anode depolarizers for aqueous electrolyte electrolyzers. Work on solid oxide electrolytes included development of techniques to investigate the initial stages of oxidation of metals at elevated temperatures and in situ surface science studies under conditions simulating actual operation of a high temperature solid oxide electrolyte electrolyzer. Work on anode deplolarizer included identification of an excellent electrocatalyst for formate oxidation and the development of simple chemical treatments to enhance the anode depolarization activity of coal.

PROJECT SUMMARY

Project Title: Static Feed Water Electrolysis for Large-Scale Hydrogen Generation

Principal Investigator: F. H. Schubert

Organzation: Life Systems, Inc.
24755 Highpoint Road
Cleveland, OH 44122
(216) 464-3291

Project Goals: The overall objective of this program is to demonstrate the inherent capability of the alkaline electrolyte, Static Feed Water Electroylsis System (SFWES) to generate low cost hydrogen for chemical storage/industrial chemical applications.

Reduction in capital and operation costs will be addressed through cell area scale-up demonstration (1.0 ft^2); operation at high current density (1,000 ASF); demonstration of low cell voltage (through high temperature and improved anode electrode); and testing with contaminated feed water, e.g., brackish water or sea water, to eliminate water treatment expendables and equipment.

Project Status: An initial four task program was completed during GFY 81. Major accomplishments of those four tasks were: (1) demonstration of a steady-state total cell voltage of 1.81 volts at 1,000 ASF and 180 F, (2) operation of a single cell for 1,150 hours using unpretreated brackish water, (3) scale-up of single cell hardware by a factor of ten (from 0.1 to 1.0 ft^2) and (5) definition of development sequences for future large scale hardware.

Added activities were funded for GFY 82 including: (1) testing of the Model I, 1.0 ft^2 single cell hardware, (2) cell hardware scale-up/test results analysis and investigation, (3) continuation of efforts to operate with impure water feed sources (both at the 0.1 ft^2 and 1.0 ft^2 levels) and (4) efforts to improve or maintain the same high performance while decreasing capital equipment costs and reducing parasitic power loads.

The following represents the current status of the new activities.

1. Performance/characterization testing of the Model I 1.0 ft^2 hardware has been completed.

-continued

2. Design of the Model II 1.0 ft^2 cell hardware and fabrication of test facilities for this hardware have been completed.

3. Testing with brackish water at elevated pressures has been started.

4. Cell hardware and test facilities have been readied to demonstrate increased performance at elevated temperature level (300 F goal).

5. A Final Report summarizing the activities through December 1981 has been

Contract Number: BNL-522723-S

Contract Period: October 1981 - September 1982

Funding Level: $275,830

Funding Source: Brookhaven National Laboratory/U.S. Department of Energy

PROJECT SUMMARY

Project Title: Advanced Alkaline Water Electrolysis; Development of Electrolysis Cell Separator for 125 C Operation

Principal Investigator: John N. Murray

Organization: Teledyne Energy Systems
110 West Timonium Road
Timonium, Maryland 21093

Project Goals: (Current) To verify advanced C-AN cathode with admixed 20 V/o PBI - 80 V/o K_2TiO_3 electrode separator is stable in operation at up to 125 C.

(Overall) The project is directed to identification of improved electrochemical cell components which exhibit stability at operating temperatures of 100 to 150 C, operating current densities of approximately 500 ma/cm^2 and attain an overall hydrogen production electrochemical process efficiency approaching 100%.

Project Status: The feasibility of operating cells at less than 1.65 V/cell, 500 ma/cm^2 (90% η_V) was demonstrated for operation of the cells at approximately 125 C. The conventional asbestos electrode separator is chemically unstable in this temperature range and in CY/GFY 1981 a six-month effort was undertaken to establish an acceptable electrode separator using polybenzimidazole (PBI) and potassium titanate (K_2TiO_3) for the porous separator materials. The final report covering that effort, released in December, 1981, showed an acceptable admixed 20 V/o PBI - 80 V/o K_2TiO_3 porous separator to have nearly all the equivalent characteristics of the porous asbestos separator. The present contracted effort involves testing the improved composites (i.e., the C-AN cathode electrocatalyst, the 20 V/o PBI - 80 V/o K_2TiO_3 separator and a non-catalyzed, porous nickel battery plaque anode) at up to 125 C in a two-cell, 300 cm^2 active area electrolysis module. The test fixture, dubbed ARIES, was modified by removing the electrolyte pump/filter elements so as to minimize problems encountered previously in the high temperature region. The ARIES Module No. 20 test was initiated in early-June. Data obtained to date show reasonably stable behavior and good performance with cell voltages at 500 ma/cm^2 of 1.85 at 75 C, 1.75 at 100 C recorded at approximately 650 hours of accumulated testing (6 July 1982).

Contract Number: BNL 545767-S

Contract Period: 1 April 1982 - 30 November 1982

Funding Level: $92,546

Funding Source: Brookhaven National Laboratory/U. S. Department of Energy

PROJECT SUMMARY

Project Title: Solid Polymer Electrolyte Water Electrolyzer Technology Development

Principal Investigator: J.F. McElroy

Organization: General Electric Company
Electrochemical Energy Conversion Programs
50 Fordham Road
Wilmington, Massachusetts 01887
(617) 657-5277

Project Goals: The overall objective of this program is to develop low-cost (< $150/kW) hydrogen generation plants (200 kW - 2 MW) for electric utility/industrial chemical applications using the solid polymer electrolyte technology. The goal is to generate hydrogen at high current densities (1000 ASF) at pressures in the range of 100 to 300 psig at an overall efficiency of 85-90%.

Project Status: A Techno-economic study was completed during the past year. The study quantified the cost of hydrogen from the current solid polymer electrolyte water electrolyzer design.

A spin-off product (SPE modules and systems utilizing 1 ft^2 cells) has entered the industrial/utility marketplace for production of on-site hydrogen for electric generator cooling and special applications. The Electric Power Research Institute (EPRI) and Public Service Electric and Gas (PSE&G) provided funding in support of this development.

For the balance of 1982 and 1983, it is planned to verify full scale hardware (2.5 ft^2 cells) in accelerated endurance testing and to establish the system configuration for a 500 kW field demonstration system. This effort is sponsored by Niagara Mohawk Power Corporation (NMPC) and the Empire State Electric Energy Research Corporation (ESEERCO) as well as by the Department of Energy.

Contract Number: DE-AC02-78ET26202

Contract Period: May, 1981 through January 1982

DOE Funding Level: $97,910 (GFY 81)

Funding Source: Department of Energy and Co-sponsors

PROJECT SUMMARY

Program Title: Underground Energy Storage Program

Program Manager: Landis D. Kannberg

Organization: Pacific Northwest Laboratory
P. O. Box 999
Richland, Washington 99352
Telephone: (509) 375-3919

Program Objectives: The objective of this program is to reduce technical and economic risks obstructing commercial development of underground energy storage concepts promising more effective and efficient utilization of energy resources. Primary concepts are Seasonal Thermal Energy Storage (STES) and Compressed Air Energy Storage (CAES).

STES objectives include characterization and mitigation of STES concept technical deficiencies and uncertainties and evaluation of economic features.

CAES objectives include development of stability criteria for CAES reservoirs and analysis and development of promising second-generation CAES systems.

Program Status: Characterization of the performance of TES systems at injection temperatures of less than 85°C is nearly complete. Field testing and numerical modeling of the Mobile Field Test Facility (FTF) will be completed in the first quarter of FY 1983. Studies of injection and storage at temperatures up to 150°C have been initiated and will be continued through FY 1983. These studies include the field testing at the St. Paul FTF, numerical modeling by the U.S. Geological Survey, and extensive laboratory studies at PNL.

Studies of nonaquifer STES systems including cavern and ice storage systems have been conducted and will continue in FY 1983. Additional studies of novel STES systems have been initiated and are planned for next year.

Stability criteria and guidelines documents have been published for salt and hard rock CAES reservoirs. All design and construction on the Pittsfield Aquifer Field Test will be completed by the end of FY 1982 and bubble development and air cycling will be conducted in the first six months of FY 1983.

A preliminary screening of materials for use in thermal storage units of adiabatic and hybrid CAES systems has been completed. Two materials, Denstone (a registered product of the Norton Company) and Dresser basalt, survived screening tests and are recommended for additional long term testing.

Contract Number: DE-AC06-76RLO 1830

Contract Period: FY 1982

Funding Level: $3900K BA/$4200K BO

Funding Source: U.S. Department of Energy, Office of Energy Systems Research, Division of Energy Storage Technology

PROJECT SUMMARY

Project Title:	Aquifer Thermal Energy Storage (ATES) Technology Studies
Principal Investigator:	John R. Raymond
Organization:	Pacific Northwest Laboratory P. O. Box 999 Richland, Washington 99352 (509) 375-3929
Project Goals:	The goals of the ATES Technology Studies are to develop technology for the economic storage and retrieval of thermal energy on a seasonal basis in aquifers, using heat or cold available from waste sources or other sources during a surplus period to reduce peak period demand, reduce electrical utilities peaking problems, and contribute to the establishment of favorable economics for district heating and cooling systems for commercialization of the technology.
Project Status:	Work continued during FY 1982 on ATES Technology Studies and Alternate STES Concepts. Planning was completed for conversion of the St. Paul, Minnesota ATES Demonstration Project to a high temperature field test facility (FTF). Closeout documentation was completed for the Stony Brook ATES Chill Demonstration project; but follow-on work was initiated to resolve the well-plugging problem which occurred at that site. Work continued at the Mobile, Alabama FTF with completion of the 2nd-cycle (82¼C) heat injection test and completion of the injection and storage phases of the 3rd-cycle (82¼C) heat injection test. Development continued on modeling technology, and simulation/prediction studies were made for the Mobile FTF tests. The Aquifer Properties Test Facility (APTF) and Field Injectivity Test Stand were completed and used for evaluation of tests for the St. Paul FTF.
Contract Number:	DE-AC06-76RLO 1830
Contract Period:	FY 1982
Funding Level:	$1452K
Funding Source:	U.S. Department of Energy, Office of Energy Systems Research

PROJECT SUMMARY

Project Title: Numerical Modeling

Principal Investigators: Charles T. Kincaid and Lance W. Vail

Organization: Pacific Northwest Laboratory
P. O. Box 999
Richland, Washington 99352
(509) 376-8325 (FTS: 444-8325) - Vail

Project Goals: The goal of the numerical modeling subtask is to provide and apply the simulation capabilities necessary for the evaluation of the subsurface performance of Aquifer Thermal Energy Storage (ATES) systems. During FY 1982 the goals of PNL activity were the development of a simplified analysis of areal ATES systems, publication of the Oregon State University (OSU) study on heat and mass transport in the vadose zone (PNL-4036), publication of the documentation for the CFEST code (Coupled Fluid, Energy, and Solute Transport; PNL-4260), and the administration of subcontractors.

Project Status: The underlying concepts of the Steady Flow Model (SFM; LBL-11029) have been extended to an areal domain. This analysis capability requires the coupling of a non-isothermal flow representative with the energy transport equation. An equal volume mesh enabling the simple convection of fluid during equal time steps has been generated from potential flow theory. This mesh includes the effects of ground-water gradient and multiple wells. A fundamental change in the SFM logic is the interpolation of node point values of temperature when the equal volume mesh is altered by changes in pumping and injection rates. In this initial analysis the explicit time step algorithm has been retained from the SFM; however, the small element volumes within areal domains are requiring uneconomically small time steps based upon explicit stability criteria. Future versions of the areal analysis will be converted to an implicit time step method.

During the fiscal year the previously developed CFEST code and its draft documentation have been revised. Quality assurance files have been established and the primary documentation has been published. The publication (PNL-4260)

presents the basic physics and numerical methodology, the input requirements, and the verification studies. The CFEST code has undergone extensive shakedown testing and is ready for hydrothermal computations in support of the Minnesota field test facility.

OSU's report on "Heat and Mass Transfer in Unsaturated Porous Media" was received late in FY 1981. This report (PNL-4036) published in FY 1982, provides the reader with an excellent review of the literature and the processes involved, and also presents several analyses describing the sensitivity of vadose zone energy transport to key parameters.

Contract Number: DE-AC06-76RLO 1830

Contract Period: FY 1982

Funding Level: $75,000

Funding Source: U.S. Department of Energy, Office of Energy Systems Research

PROJECT SUMMARY

Project Title:	Mathematical Studies in Aquifer Thermal Energy Storage
Principal Investigator:	Chin Fu Tsang
Organization:	Lawrence Berkeley Laboratory Berkeley, California 94720 (415) 486-4000 ext. 5782
Project Goals:	To perform ATES generic studies, improve modeling techniques, and carry out field-specific planning and simulation studies.
Project Status:	The three-cycle ATES field experiment in Mobile, Alabama, carried out by Auburn University has been successfully simulated by LBL numerical model PT. Prediction calculations were made on the first two cycles. With only the well-test data and injection-production schedule made known to LBL, calculations were done to predict experimental production temperatures and energy recovery factors. The results were then compared with field observations, with very good agreements. Design studies were carried out to help in the design of the third-cycle experiment. Various injection and production schemes were studied and an optimal method to maximize the recovery factor was suggested. Conclusions are (1) LBL method of prediction has proved to be successful for the Mobile site aquifer storage system. It is ready to be applied and tested on other sites, (2) it is demonstrated that numerical models can be used as a design tool for future field experiments. For the generic studies, a paper on the steady flow model with negligible buoyancy flow has been published. Detailed, graphic results applicable to all such systems are presented in this paper. The computer program of the steady flow model, SFM, is also prepared and is available to the public.
Contract Number:	
Contract Period:	1 October 1981 through 30 September 1982
Funding Level:	$90,000
Funding Source:	U. S. Department of Energy through Pacific Northwest Laboratory

PROJECT SUMMARY

Project Title: Laboratory and Field Studies of Aquifer Materials and Injection/Withdrawal Fluids from STES Field Test Facilities

Principal Investigator: Stephen C. Blair

Organization: Pacific Northwest Laboratory
P. O. Box 999
Richland, Washington 99352
Telephone: (509) 376-5960
FTS: 444-5960

Project Goals: Use laboratory scale and field test data to determine how the physical and chemical properties of an aquifer system may change under conditions imposed by a STES facility.

Project Status: The Aquifer Properties Test Facility (APTF), a laboratory apparatus for testing aquifer materials at elevated temperatures and pressures, was installed at PNL and a series of experiments designed to simulate the conditions imposed on the storage aquifer at the Field Test Facility (FTF) in St. Paul, Minnesota, are underway. Tests include measurement of permeability and creep/compaction on aquifer samples as well as chemical monitoring of pore fluid as it is formed at pressure, temperature, and flow conditions similar to conditions in the injection/withdrawal zone at the St. Paul FTF.

A portable Field Injectivity Test Stand (FITS) is presently in use at the St. Paul FTF. This apparatus provides a means of characterizing the injection and withdrawal streams at a STES facility and, since April, has been used extensively at the St. Paul site to monitor water quality and injectability characteristics of the injection stream.

A contract has been awarded to Terra Tek, Inc. to study the causes of injection impairment at the Stony Brook Field Test Facility. Most of the experimental data has been collected and preliminary analysis indicates that injection impairment was caused by mobilization of internal fines.

A geochemical model (MINTEQ) with ion speciation, solubility, and mass transfer

capabilities has been developed and is now operational on the Univac computer. This model has been used to simulate heating of ground water at the Minnesota FTF and to estimate the expected quantity of mineral precipitates in the injection stream at that site. In addition to its application at Field Test Facilities, this geochemical model will also be used in interpretation of the APTF experiments.

Draft papers have been completed on 1) guidelines for sampling and analyzing solutions from aquifer thermal energy storage systems, and 2) preliminary results of injectability studies at the St. Paul FTF.

Contract Number: DE-AC06-76RLO 1830

Contract Period: FY 1982

Funding Level: $116K

Funding Source: U.S. Department of Energy

PROJECT SUMMARY

Project Title: Field and Laboratory Studies of Subsurface Water Injection - Seasonal Thermal Energy Storage Program (STES)

Principal Investigators: S. C. Blair; L. B. Owen

Organization: Battelle, PNL, P.O. Box 999, Richland, WA 99352; Terra Tek Research, 420 Wakara Way, Salt Lake City, UT 84108

Project Goals: Design and implementation of a field and laboratory assessment of subsurface water injection. The major elements of the laboratory program involved a study of reservoir response to cyclical thermal stress, geochemical modeling of scale deposition from production and injection waters, water-rock interaction, water treatment procedures, and an evaluation of injection well impairment at the Stony Brook, New York STES site. A field evaluation of water injectability was also initiated at the STES site on the campus of the University of Minnesota, St. Paul, MN.

Project Status: A laboratory evaluation demonstrated that the most likely cause of injection well impairment at the Stony Brook STES site was due to formation fines migration caused by high fluid velocities in the injection interval. The field injectability evaluation at the University of Minnesota STES site confirmed chemical modeling that indicated carbonate precipitation at 18°C or higher could impair injection well performance. Experimental data also identified a potential bearing failure in an injection pump. Turbidity data from the Minnesota field site indicated the importance of flowing production wells to waste prior to initiation of subsurface injection. Laboratory studies to determine the effect of reservoir thermal cycling on production/injection well performance are in progress.

Contract Number: DE-AC06-76-RLO-1830

Contract Period: October, 1981 - September, 1982

Funding Level: $160,000

Funding Source: Department of Energy

PROJECT SUMMARY

Project Title: Monitoring and Analysis of a Chill Storage System

Principal Investigator: W. J. Schaetzle

Organization: W. J. Schaetzle & Associates, Inc.
P. O. Box 1523
Tuscaloosa, Alabama 35403
(205) 339-9587

Project Goals: The main objective of this program is to monitor, for a complete year of operation, a "Free Cooling System" which utilizes annual aquifer thermal energy storage. The system is installed in a major department store (Parisian, University Mall, Tuscaloosa, Alabama) containing over 60,000 ft^2 of floor area. Data being collected include water input and output temperatures and water flow to the cooling coils during air-conditioning and to the cooling tower during periods of winter water chilling. Power input is concurrently measured. Water level and inlet, outlet, and bottom temperatures are being monitored for the wells. The data will be analyzed and performance calculated.

Project Status: Approximately fifty percent of the monitoring equipment has been installed. The installation is expected to be complete in early August. Some data, including cooling coil and cooling tower data, has been taken since October 1981. Estimations of air-conditioning, water chilling and energy input are being made. More accurate calibrated instrumentation is beginning to produce more precise monitoring.

The tasks are to complete installation of the instrumentation, record the data, and analyze the results.

Contract No. DE-AC06-76RLO 1830
Subcontract No. B-B5232-A-0

Contract Period: May 1982 - April 1983

Funding Level: $52,792

Funding Source: U. S. Department of Energy through Battelle Memorial Institute, Pacific Northwest Laboratories

PROJECT SUMMARY

Project Title: University of Minnesota Aquifer Thermal Energy Storage Field Test Facility

Principal Investigators: Warren E. Soderberg and Matt Walton

Organization: University of Minnesota
319-15th Avenue S.E.
Minneapolis, MN 55455

Minnesota Geological Survey
1633 Eustis Street
St. Paul, MN 55108

Project Goals: The project goals are to construct a test facility with a nominal 5-megawatt thermal input/output capacity, perform a series of test cycles at temperatures up to 150°C, and acquire the basic hydrogeological, hydrogeochemical, and hydrogeothermal data to serve as design parameters for an applied ATES system using a major artesian bedrock aquifer.

Project Status: Construction of the facility is complete, except for some inoperative pressure transducers. Injection test cycles have begun. Problems during the first heat-injection cycle require redevelopment of the heat-storage well and the addition of water conditioning equipment to the system. Cycles are expected to be underway again in September 1982.

Contract Number: DE-AC06-76RLO 1830 Subcontract B97601-A-O

Contract Period: May 1980 to September 30 1982

Funding Level: 2,436,145

Funding Source: U.S. Department of Energy through Battelle Pacific Northwest Laboratories

PROJECT SUMMARY

Project Title:	Thermal Energy Storage in Confined Aquifers Using the Doublet Well Configuration
Principal Investigators:	Joel G. Melville, Fred J. Molz, Oktay Güven
Organization:	Civil Engineering Department Auburn University Auburn, Alabama 36849
Project Goals:	Conduct doublet field experiments in aquifer thermal energy storage. Three injection-storage-recovery cycles are planned to evaluate the doublet configuration and measure thermal efficiency for injection temperatures of 60°C, 90°C, and 125°C.
Project Status:	Preliminary aquifer testing and analysis has been completed. A paper, "Field Determination of Aquifer Thermal Energy Storage Parameters", has been submitted for publication in Ground Water. Based on the Mobile field experience and data analysis; hydraulic, thermodynamic, and geochemical parameters necessary for ATES are specified. Laboratory and field tests are described. Methods of analysis of test data are summarized. A paper, "ATES: A Well Doublet Experiment at Increased Temperatures", was submitted for publication in Water Resources Research. This paper presents the results of the second cycle of field experiments, 58,063m^3 of injected water at an average temperature of 81°C. The second cycle of injection was begun 6/12/81. Recovery pumping began 11/30/81 and was completed 1/23/82. The final, third cycle of experiments was begun 4/7/82 and the injection of 56,000m^3 was completed 7/14/82 at an average temperature of 81°C. The storage period will extend through August and recovery will begin in September 1982. The tasks for FY-83 will be to complete recovery in October, analyse data, and restore the site for completion of the project in December.
Contract Number:	Subcontract No. B-67770-A-0 Prime Contract DE-AC06-76RLO 1830
Contract Period:	03/26/80 through 12/31/82
Funding Level:	$1,087,000.
Funding Source:	U.S. Department of Energy through Battelle Pacific Norhtwest Laboratories

PROJECT SUMMARY

Project Title: Analysis of Reinjection Problems at the Stony Brook ATES Field Test Site.

Principal Investigator: Donald J. Supkow/James A. Shultz

Organization: Dames & Moore
6 Commerce Drive
Cranford, New Jersey 07016

Project Goals: To determine the causes of the reduction of pumping specific capacity and injection specific capacity of the pumping/injection well constructed for the Stony Brook, New York ATES chill storage field test site, and to restore the well to its original capacity.

Project Status: Well PI-2 had been constructed and screened in the Upper Magothy aquifer as part of an ATES chill storage field test. When the well was constructed it had a pumping specific capacity of about 13¼ gpm per foot of drawdown when pumped at a rate of 300 gpm. During the injection phase of the chill storage test, Well PI-2 would accept water at a rate of about only 100 gpm.

Suspected possible causes of reduction in injection capacity of Well PI-2 were clogging resulting from air entrainment, precipitation of iron or other compounds in the immediate well vicinity, injection of sediment derived from the pumped Well PI-1 and/or the interconnected plumbing system, and migration of fines within the immediate well vicinity.

Well PI-2 was redeveloped by pumping and surging with a deep well turbine pump during which time fine sediment was removed from the well. After the redevelopment work was completed, a step drawdown pumping test was conducted which showed that the pumping specific capacity had returned to the original value. No acid treatment was used for the well because the mechanical redevelopment proved to be adequate.

A step-injection test using normal temperature ground water from Well PI-1 was then performed on Well PI-2 in increments of 20 gpm to a maximum of 300 pgm. The test showed the injection specific capacity to be approximately equal to the pumping specific capacity. A cyclone filter and deaerator along with a 5 micron cartridge filter were used during the step-injection test. Some fine sediment was collected by the filtration system.

The project revealed that the original well clogging problems were caused primarily by introduction of sediment with the injection water and demonstrated the need for an effective filtration system to prevent sediment from being injected into the injection wells.

A short term chill injection test to test the injection specific capacity of chilled water in Well PI-2 is planned for the last phase of this project.

Contract Number: Subcontract No. B-C7296-A-O
Prime Contract DE-AC06-76RLO

Contract Period: June 8, 1982 through September 30, 1982

Funding Level: $97,200

Funding Source: U.S. Department of Energy through
Battelle Pacific Northwest Laboratories

PROJECT SUMMARY

Project Title: Investigation of Thermal Energy Storage and Heat Exchange Capacity of Water-Filled Mines--Ely, Minnesota

Principal Investigator: Matt Walton

Organization: Minnesota Geological Survey--University of Minnesota
1633 Eustis Street
St. Paul, Minnesota 55108

Project Goals: The project goals are to determine whether the water-filled iron mines at Ely, Minnesota, contain a large enough body of water in the underground workings at a suitable temperature for an efficient heat extraction by heat pumping to provide a major heat source for a community district heating system in the City of Ely, and also to determine if the lake which occupies the depression caused by subsidence over the mines can provide a sufficient volume of sun-warmed surface water during the summer to replace chilled water in the mine and replenish the heat source.

Project Status: Mine maps, acoustic depth profiles and aerial photographs have been collected to reconstruct the as-built configuration of the mine and the history of subsidence over the mine area. Temperature-depth profiles, downhole television scanner inspection and water samples have been collected from accessible shafts and the mine pond. Water analyses are in progress on different water masses identified in the mines, and arrangements for a pumping test are being made. Temperature-depth profiles will be repeated after the pumping test.

Contract Number: Sub B-D4459-A-O

Contract Period: May 28, 1982 to June 1, 1983

Funding Level: 34,820

Funding Source: U.S. Department of Energy through Battelle Pacific Northwest Laboratories

Project Summary

Project Title: Ice Production and Storage for Seasonal Applications Utilizing Heat Pipe Technology

Principal Investigator: A. J. Gorski

Organization: Argonne National Laboratory
9700 S. Cass Avenue
Argonne, IL 60439
(312) 972-6237

Project Goals: The main objective of this program is to characterize the technical features of formation, collection and storage of ice naturally grown during the winter months by means of innovative heat pipe technology.

Project Status: The tasks in this program include the development of theoretical models of heat pipe and system performance, and appropriate laboratory experiments on full size units to measure heat pipe performance as functions of ambient conditions. Accomplishments to date include design, construction and operation of three Roll-Bond™ and one coil evaporator type heat pipes. Ice yields and performance data have been obtained during actual winter conditions. A new system configuration is now under construction for the next winter season. Mathematical formalism has been developed for both types of heat pipe designs. Computer modeling for the one-dimensional case, rectangular coordinate system, for both the Roll-Bond™ and coil configuration will be completed. Additional effort will be required for the two dimensional analyses of the two designs.

Contract Number: B-B5248-A-0

Contract Period: March 1982 - September 1982

Funding Level: $85,000

Funding Source: Department of Energy, Pacific Northwest Laboratories

PROJECT SUMMARY

Project Title:	Seasonal Thermal Energy Storage Economic Assessment
Principal Investigator:	D. R. Brown
Organization:	Pacific Northwest Laboratory P. O. Box 999 Richland, Washington 99352 (509) 376-4453
Project Goals:	The principal objective of this task is to determine the economics of seasonal thermal energy storage technologies. The emphasis to date has been placed upon the investigation of aquifer thermal energy storage. Beginning this year, analysis of alternative seasonal storage technologies was included. In addition, this task is responsible for providing general support to the Underground Energy Storage Program.
Project Status:	Economic assessment activities completed in FY 1982 as part of this task include: 1) a detailed economic investigation of the cost of heat storage in aquifers, 2) documentation for AQUASTOR, a computer model for analyzing aquifer thermal energy storage coupled with district heating or cooling, and 3) an economic evaluation of several ice storage concepts. In addition, a detailed economic investigation of the cost of chill storage in aquifers is in progress.
Contract Number:	DE-AC06-76RLO 1830
Contract Period:	October 1981 - September 1982
Funding Level:	$85,000
Funding Source:	U.S. Department of Energy

PROJECT SUMMARY

Project Title:	Reservoir Stability Studies
• Principal Investigator:	T. J. Doherty
Organization:	Pacific Northwest Laboratory Richland, Washington 99352 Phone: (509) 375-3924
Project Goals:	The objective of the CAES Reservoir Stability Studies is to develop stability criteria for underground compressed air energy storage (CAES) reservoirs through literature, numerical, experimental and field studies as required.
Project Status:	Preliminary stability criteria have been completed and used as a basis for initiation of numerical and experimental studies. Reservoir types examined included compensated hard rock, solution-mined salt caverns, and anticlinal porous media structures. Numerical model development and experimental work were carried to completion by FY-1981. Porous media studies identified the need for combined effects laboratory studies and a field test involving air injection into an aquifer structure. Salt reservoir study in FY-1982 included coordinated laboratory and in-mine evaluations and finalization of salt stability criteria. This completed the work scope on Salt Cavern Reservoir Stability Studies. Hard rock cavern numerical and experimental evaluations were complete late in 1981 and a thoroughly reviewed version of the final stability criteria was published in 1982. This completed the work scope of the Hard Rock Reservoir Stability Studies. The numerical and experimental work in porous media continues in support of the field study. Exploration, placement of the major field study contract, and design of the facility for the aquifer field test were completed in FY 1982. Construction of the field test surface facilities is underway. Air injection is scheduled for the end of FY-1982.
Contract Number:	DE-AC06-76RLO 1830
Contract Period:	October 1981 to September 1982
Funding Level:	$1,426,000
Funding Source:	U.S. Department of Energy

PROJECT SUMMARY

Project Title:	Laboratory Tests of Salt Specimens Subjected to Loadings and Environmental Conditions Appropriate to a Compressed Air Energy Storage Reservoir.
Principal Investigator:	Robert L. Thoms
Organization:	Institute for Environmental Studies Louisiana State University Baton Rouge, LA 70803
Project Goals:	To test rock salt under conditions simulating effects of compressed air energy storage (CAES) in salt, and to formulate long-term stability criteria for CAES salt caverns.
Project Status:	Testing has been concluded, both in the laboratory and in south Louisiana salt mines. Contributions have been made to stability criteria document. Preparation of the final report on testing is in progress.
Contract Number:	B-67966-A-H
Contract Period:	1 October 1978 through 30 September 1982
Funding Level:	$460,633
Funding Source:	U.S. Department of Energy through Battelle-Pacific Northwest Laboratory

PROJECT SUMMARY

Project Title:	CAES Reservoir Stability Criteria Project: Hard Rock Caverns
Principal Investigator:	A. F. Fossum
Organization:	RE/SPEC Inc. P. O. Box 725 Rapid City, SD 57709 Phone: (605) 394-6400
Project Goals:	Develop design and stability criteria for long-term operation of underground reservoirs used for CAES to accelerate the commercialization of the concept.
Project Status:	All phases of the program have been completed. These phases included (1) a state-of-the-art survey to establish preliminary reservoir stability criteria and identify areas requiring research and development; (2) numerical modeling to evaluate the response and stability of CAES hard rock reservoirs parametrically under a wide variety of CAES operating and geotechnical conditions; (3) laboratory testing to investigate fundamental rock properties, examine issues not amenable to numerical modeling, and to provide data for use in numerical models; and (4) a confirmatory evaluation of the Acres American design for hard rock CAES caverns performed for Potomac Electric Power Company (PEPCO). A report was issued summarizing the geotechnical issues and guidelines for storage of compressed air in excavated hard rock caverns.
Contract Numbers:	Special Agreement Nos. B-51225-A-L, B-49407-A-H, B-51295-A-H, B-B5230-A-0/ Prime Contract EY-76-C-06-1830
Contract Period:	June, 1978 - August, 1982
Funding Level:	$579,205
Funding Source:	U.S. Department of Energy through Pacific Northwest Laboratory, Battelle Memorial Institute

PROJECT SUMMARY

Project Title:	Numerical Evaluation of the Field Test
Principal Investigator:	L. E. Wiles
Organization:	Pacific Northwest Laboratory P. O. Box 999 Richland, Washington 99352 (509) 375-2049
Project Goals:	The objective of this task was to use existing numerical models to support the CAES porous media field study. The models were used to develop "pretest" predictions of the thermohydraulic performance of the porous media reservoir. The model predictions were used to verify specifications for above ground equipment and instrumentation, define the time required to develop an air storage bubble of adequate size, develop and evaluate operational strategies for air cycling, and finally, to characterize the general performance of the field test reservoir.
Project Status:	The pretest analysis made use of our capability to evaluate four distinct problems: bubble development, water coning, thermal development, and near-wellbore desaturation. The analysis verified that the air compressor should be of adequate capacity to develop the air bubble in 60 to 75 days. Analysis using the latest permeability data and operational cycles suggest that water coning should not be a problem. The operational cycle should allow detectable thermal development at the instrumentation wells located 3 and 6 m from the injection/withdrawal well. Results of the desaturation analysis led to a redesign of the above-ground humidity measurement system. Future analysis will focus on application of actual reservoir performance data. Adjustment of model parameters that allow model predictions to match reservoir performance should improve our knowledge of reservoir properties as well as our ability to accurately predict reservoir performance.
Contract Number:	DE-AC06-76RLO 1830
Contract Period:	October 1981 - September 1982
Funding Level:	$35,000
Funding Source:	U.S. Department of Energy

PROJECT SUMMARY

Project Title:	Porous Media Experimental Task
Principal Investigator:	R. L. Erikson
Organization:	Pacific Northwest Laboratory PO Box 999 Richland, Washington 99352 (509) 376-8627
Project Goals:	The objective of this project is to investigate the physical stability of reservoir sandstone in the laboratory when subjected to CAES conditions. In particular, physical response of St. Peter sandstone taken from the CAES Aquifer Field Test is to be determined under anticipated test conditions.
Project Status:	The CAES Porous Media Flow Loop, a laboratory apparatus, is being used to simulate Aquifer Field Test conditions. Four samples of St. Peter sandstone from the injection/withdrawal borehole at the Pittsfield site have been tested in the facility to date. Each sample has hydrostatically confined to a pressure of 1200 psi, and ventilated with dry air maintained at a constant pressure of 275 psi. The experiments completed have concentrated on the effects of temperature and temperature cycling on the permeability of Pittsfield reservoir rock. Permeabilities for the four samples measured at room temperature range from 150 to 600 millidarcies. The effect of temperature (up to 180°C) on permeability is small; both small increases and decreases in permeability with temperature have been recorded. There appears to be, however, hysteresis when reservoir samples are cycled between 20° and 180°C. The data for 2 samples suggests that as the reservoir sample is heated and then cooled, the room temperature permeability at the end of the cycle is considerably smaller (10 to 15%) than the initial value. The magnitude of the permeability decrease is greatest for the first cycle and diminishes with subsequent cycling.
Contract Number:	DE-AC06-76RLO 1830
Contract Period:	October 1981 - September 1982
Funding Level:	$145,000
Funding Source:	U.S. Department of Energy

PROJECT SUMMARY

Project Title:	Pittsfield Porous Media Field Test - Field Studies Support and Analysis
Principal Investigators:	R. D. Allen and T. J. Doherty
Organization:	Pacific Northwest Laboratory P. O. Box 999 Richland, Washington 99352 (509) 375-3926
Project Goals:	The objectives of the Porous Media Field Test are 1) to demonstrate aquifer air storage, 2) to validate stability criteria, and 3) to correlate predictions with numerical and laboratory work. The specific objective of this subtask is to perform the necessary Pacific Northwest Laboratory management functions relating to organization and control of the field study activities in Pittsfield, Illinois.
Project Status:	During FY 1982 the following activities have been performed at PNL: . analysis of lithologic and geophysical logs . the Form B Operations Permit application submittal to IEPA . natural gas powered compressor system selection . liaison on final subsurface instrumentation design . QA plan modified and approved . detailed surface facility design finalized . final well development planning completed . geologic report reviewed; modeling data synthesized . formal design review held with contractor . "Experimental Test Plan for Aquifer Evaluation" reviewed and extensively revised . budget, schedule and work plan review, approval, and modifications.
Contract Number:	DE-AC06-76RLO 1830
Contract Period:	October 1981 - September 1982
Funding Level:	$55K
Funding Source:	U.S. Department of Energy

PROJECT SUMMARY

Project Title:	Compressed Air Energy Storage (CAES) Aquifer Field Test - Conceptual Design, Construction and Operation
Principal Investigator:	John A. Istvan
Organization:	PB-KBB Inc. Subsurface Systems and Technology Houston, Texas 77024
Project Goals:	Field evaluation of a typical aquifer for storing and cycling compressed air under conditions similar to those which would be obtained in a full scale CAES operation. Determine the effect of varying injection temperature from ambient to 200°C. Preliminary laboratory reservoir stability and simulation criteria will be modified based upon actual field data. Post injection core testing will determine the permanent effect of air injection on the formation.
Project Status:	The compressor and air processing skids have all been constructed and were delivered and installed at Pittsfield in August 1982. Final construction will be completed in September for initial air injection and bubble development before the end of FY-82. Subsurface instrumentation components are being calibrated and will be installed in Y-F and Y-G, the close-in instrument wells, in September 1982, prior to injection. Final hookup of sampling/logging wells back to the microcomputer in the building and installation of injection tubing and a thermal packer were completed this month. Completion of the building to house the air processing and instrumentation skid will be accomplished by early September.
Contract Number:	B-82313-A-0
Contract Period:	January 20, 1981 through March 1984
Funding Level:	$2.2MM
Funding Source:	U.S. Department of Energy through Pacific Northwest Laboratory, operated by Battelle Memorial Institute.

PROJECT SUMMARY

Project Title:	Second Generation CAES Studies
Principal Investigator:	J. A. Fort
Organization:	Pacific Northwest Laboratory P. O. Box 999 Richland, Washington 99352 (509) 375-2251
Project Goals:	The main objective of this study is to prepare a user's manual for the computer code, CAESCAP. This code is used at the Pacific Northwest Laboratory to perform thermodynamic simulations of second generation CAES cycles. The user's manual is to include a description of the code, an input guide and several CAES cycle simulations as user samples.
Project Status:	The tasks in this study include writing the user's manual and performing the sample simulations. To date a first draft of the code description has been completed, writing of the input guide is approximately 25% complete. The user sample simulations are approximately 30% complete. All work will be completed by the end of FY 1982.
Contract Number:	DE-AC06-76RLO 1830
Contract Period:	FY 1982
Funding Level:	$30K
Funding Source:	U.S. Department of Energy, Office of Energy Systems Research

PROJECT SUMMARY

Project Title:	An Evaluation of Thermal Energy Media for Advanced Compressed Air Energy Storage Systems
Principal Investigator:	F. R. Zaloudek
Organization:	Pacific Northwest Laboratory P. O. Box 999 Richland, Washington 99352 (509) 375-2155
Project Goals:	The objective of this study was to experimentally screen several thermal energy storage (TES) materials to determine which have the best chance of providing suitable long-term service in adiabatic and hybrid CAES systems. Materials considered included: • 3/8 in OD iron oxide pellets • 1/2 in OD Denstone pebbles • 1 in OD cast iron balls • crushed Dresser basalt rock The evaluation included subjecting samples of these materials to repeated thermal cycles, exposure to high temperature and pressure air and exposure to a moist, acidic environment such as would occur in a real CAES system.
Project Status:	All experimental work has been completed including both work performed at PNL and that subcontracted to FluiDyne Engineering Corporation and reported in another paper. Preparation of the final report is in progress and scheduled for completion by the end of FY 1982.
Contract Number:	DE-AC06-76RLO 1830
Contract Period:	October 1980 through September 1982
Funding Level:	$425K
Funding Source:	U. S. Department of Energy, Office of Energy Systems Research

PROJECT SUMMARY

Project Title: Thermomechanical Screening of Thermal Energy Storage Materials for Compressed Air Energy Storage

Project Manager: David G. DeCoursin

Organization: FluiDyne Engineering Corporation
5900 Olson Memorial Highway
Minneapolis, Minnesota 55422

Project Goals: Determine the thermal, hydraulic and mechanical performance of Beds of specified TES media. Measure and characterize comminution and particulate elutriation of these beds. Provide design data for full-scale beds at propsed Adiabatic CAES (ACAES) system design condition.

Project Status: The project is complete. Screening tests were successfully run on four materials: Denstone fireclay, iron ore, basalt rock, and cast iron. Each material was exposed to over 100 cycles at 4 hours per cycle between 100F and 900F. The most significant result was the good performance of the Dresser basalt rock, which is also the lowest cost material by a large margin.

Subcontract Number: B-B5473-A-0

Prime Contract Number: DE-AC06-76RL0 1830

Contract Period: March 12, 1981 through July 31, 1982

Funding Level: $320,000

Funding Source: U.S. Department of Energy
Additional funding was provided by the Electric Power Research Insititute, EPRI

PROJECT SUMMARY

Project Title: Technical and Economic Analysis of Storage Technologies

Principal Investigator: J.G. Asbury

Organization: Systems Evaluation Group
Electrochemical Technology Program
Argonne National Laboratory
Argonne, IL 60439

Project Goals: To perform technical and economic analyses of technologies and systems for the storage and transport of energy. Specific studies and associated goals are:

Assessment of Cool Storage Technologies: Evaluate the performance characteristic and economics of cool storage in commercial buildings for electric load leveling; identify R&D needs.

New Concepts Study: Identify and screen promising new concepts for the storage and transport of energy; define R&D needs.

Review of Storage Assessment: Critically review, update, and summarize the findings of recent assessments of energy storage technologies.

Energy Efficiency Study: Evaluate the direct economic benefits of improved round trip efficiency of energy storage technologies.

Project Status: The assessment of cool storage technology and the advanced concepts study were completed during FY82. The storage assessment review and the energy efficiency studies, begun during FY82, will be completed during FY83.

Contract Number: AL-10-15/49433

Contract Period: Oct. 1, 1979 through Sept. 30, 1982

Funding Level: 270K

Funding Source: U.S. Department of Energy, Office of Energy Systems Research, Energy Storage Systems Division

PROJECT SUMMARY

PROJECT TITLE: Superconducting Magnetic Energy Storage (SMES)

PRINCIPAL INVESTIGATOR: John D. Rogers

ORGANIZATION: University of California, Los Alamos National Laboratory
Los Alamos, NM 87545
(505) 667-5427; FTS 843-5427

PROJECT GOALS: The goal of the SMES program is to design, fabricate, and place into operation a 30 MJ, 10 MW SMES unit for electric utility transmission line stabilization on the Bonneville Power Administration (BPA) system in 1983.

PROJECT STATUS: The engineering of the BPA SMES transmission line stabilization system is almost entirely complete. All large hardware items are complete. The nonconducting dewar should be completed and tested by 7-25-82. The seismic mounting of the 30 MJ superconducting coil is complete. Software for control of the system is to be complete by 8-1-82 and all hardware at Los Alamos will have been verified by 8-1-82. The Tacoma Substation site engineering is to be complete by about 9-1-82.

This then sets the stage for FY 83 activities. Installation at the BPA Tacoma Substation is scheduled for 8/82 to 11/82 at which time experimental operation of the SMES system is to begin and continue until 3-1-83. At that time full utility operation is to commence and to run for many months. BPA is to make a decision by mid 9/83 to retain the 30 MJ SMES stabilizing system.

CONTRACT NUMBER: W-7405-ENG-36

CONTRACT PERIOD: Project Closed 9-30-83

FUNDING LEVEL: $1,245,000 FY 82

FUNDING SOURCE: Department of Energy

PROJECT SUMMARY

PROJECT TITLE:	Superconducting Magnetic Energy Storage (SMES)
PRINCIPAL INVESTIGATOR:	Barry Miller/Stig Annestrand
ORGANIZATION:	Bonneville Power Administration Portland, OR 97208 (503 234-3750; FTS 429-3750
PROJECT GOALS:	The goal of the SMES program is to design, fabricate, and place into operation a 30 MJ, 10 MW SMES unit for electric utility transmission line stabilization on the Bonneville Power Administration (BPA) system in 1983.
PROJECT STATUS:	The engineering of the BPA SMES transmission line stabilization system is almost entirely complete. All large hardware items are complete. The non-conducting dewar should be completed and tested by 7-25-82. The seismic mounting of the 30 MJ super-conducting coil is complete. Software for control of the system is to be complete by 8-1-82 and all hardware at Los Alamos will have been verified by 8-1-82. The Tacoma Substation site engineering is to be complete by 10-1-82. This then sets the stage for FY 83 activities. Installation at the BPA Tacoma Substation is scheduled for 8/82 to 11/82 at which time experimental operation of the SMES system is to begin and continue until 4-1-83. At that time full utility operation is to commence and to run for many months. BPA is to make a decision by mid 9/83 to retain the 30 MJ SMES stabilizing system. BPA will design all hardware and devise the software for the microwave telemetry between Ditmer, OR, and the Tacoma Substation for control of the SMES system. BPA is also performing all the substation site preparation and is providing the site power for the project.
FUNDING LEVEL:	estimated $700,000-$1,200,000
FUNDING SOURCE:	Bonneville Power Administration

PROJECT SUMMARY

Project Title:	Flywheel Rotor and Containment Technology Development
Principal Investigator:	S.V. Kulkarni
Organization:	Lawrence Livermore National Laboratory
Project Goals:	o To develop an efficient, economical, and practical composite flywheel for energy conservation applications. Current goal is the development by 1984 of a flywheel with an energy density of 88 Wh/kg at failure, an operational energy density of 44 to 55 Wh/kg, and an energy storage capacity of approximately 1 kWh. o To determine the suitability of various manufacturing processes for rotor fabrication. o To investigate flywheel and flywheel-systems dynamics. o To evaluate prototype rotor burst and cyclic test data. o To develop by 1984, a fail-safe, lightweight, and low-cost flywheel containment.
Project Status:	The following tasks have been accomplished: o Evaluated the GE and Avco containment designs and selected the GE design for prototype fabrication and testing (Task Milestone). o Demonstrated and evaluated flywheel rotor cyclic test capability at the Oak Ridge Flywheel Evaluation Laboratory (ORFEL) (Task Milestone). o LLNL designed Owens-Corning/Lord SMC disk/ring hybrid rotors were burst tested at ORFEL. o Fabricated prototype GE and Garrett flywheels and initated cyclic testing at ORFEL. o Completed the static/fatigue torsion tests of the rotor/hub elastomeric bond at room temperature. o Initiated prototype GE containment housing fabrication activity.
Contract Number:	W-7405-Eng-48
Contract Period:	October 1, 1981 to September 30, 1982
Funding Level:	$850K
Funding Source:	U.S. Department of Energy

PROJECT SUMMARY

Project Title: Flywheel Testing and Evaluation

Principal Investigator: R. S. Steele

Organization: Oak Ridge Y-12 Plant
Union Carbide Corporation, Nuclear Division
P.O. Box Y
Bldg. 9998, MS-2
Oak Ridge, TN 37830
(615) 574-1838

Project Goals: The objective of the testing program is to evaluate the performance of composite flywheels developed under the flywheel rotor and containment technology development project. The evaluations will determine the performance limiters in both ultimate energy storage and life under cyclic fatigue loading.

Project Status: Test data to date supports six general statements regarding the state-of-the-art regarding flywheel development.

a. Energy density performance exceeds metallic flywheels performance.
b. Containment requirements are less severe.
c. Fatigue life typically exceeds 1000 cycles.
d. Thermal considerations dictate low pressure environments.
e. Suspension system design must consider balance changes with speed.
f. Analytical models of the flywheels have increased confidence.

Testing supports the early proponents' predictions of composite flywheels' applicability. But the data also show that the risk of using this new technology may still be high. Composite flywheels have demonstrated energy density and total capacity sufficient to accomplish the automotive energy storage requirements. Testing must now address questions relating to lifetime, reliability, system design, and cost.

Contract Number: W-7405-eng-26

Contract Period: FY 1982

Funding Level: $365,000

Funding Source: Oak Ridge National Laboratory

PROJECT SUMMARY

Project Title: Manufacturing Cost/Design Trade-Studies for Flywheels

Principal Investigator: B. R. Noton

Organization: Battelle's Columbus Laboratories
505 King Avenue
Columbus, OH 43201
(614) 424-5608

Project Goals: The initial task of this program was to develop a methodology to enable comparisons of different flywheel designs based on performance ratings, manufacturing, and inspection costs. Development of the methodology required identification of all operational sequences in the manufacture and inspection of each design and specification of ground rules. The detailed manufacturing sequences need to be subsequently studied to reveal those which are cost-drivers and the results applied to three selected composite flywheel systems. The cost-drivers identified enable development requirements to be determined for acceptance of composite flywheels for production commitment.

Project Status: A methodology has been developed to calculate the recurring and nonrecurring tooling costs for the flywheel and containment. The manufacturing operational sequences have been specified in detail for each of the experimental flywheels developed and tested under the LLNL MEST program. The detailed manufacturing plans have been specified and the cost-drivers identified and prepared for review by industry. An approach for systems assessment and rating of the flywheels has been developed. In response to the cost-drivers in design, manufacturing and inspection of flywheels, a number of opportunities have been identified. Flywheel manufacturers have been visited to discuss modifications of the prototype designs to reduce cost in the production environment. Advanced manufacturing technologies, to significantly impact the cost-drivers, have been identified and these include aluminum sheet laminated-hubs and also pultrusion for spokes where required and RF curing for appropriate composites. Due to the high-cost of materials for composite flywheels compared with other state-of-the-art materials utilized in the automotive industry, forecasts have been prepared to the year 2000 on the approximate material costs for various fibers and matrices. Remaining tasks include analysis of cost estimates by various companies and the assessment of these with respect to data developed by the contractor.

Contract No.: W-7405-ENG-92 (SANL 108-002)
Funding Level: $41,210
Contract Period: 1/82 - 9/82
Funding Source: Dept. of Energy

PROJECT SUMMARY

Project Title: Development of Nondestructive Testing Techniques for Composite Material for Flywheels

Principal Investigator: W. A. Simpson, Jr.

Organization: Oak Ridge National Laboratory
Building 4500-S, Room D-61
P.O. Box X
Oak Ridge, TN 37830
(615) 574-4421

Project Goals: The objective of this program is to develop or modify NDT methods for inspecting a composite flywheel's material integrity and its variation due to service.

Project Status: An initial material characterization study of the composite has been completed. The behavior of the ultrasonic properties as functions of strain history were determined on tensile specimens of S-2 glass/epoxy. These measurements indicate a good correlation between the monitored parameters and the total strain. Measurements on actual flywheels before and after spin testing have also begun.

The tasks for FY 1983 will be the collection and assessment of data on flywheels subjected to spin testing and the monitoring of additional properties of composite tensile specimens.

Contract Number: W-7405-eng-26

Contract Period: October 1981—September 1982

Funding Level: $125,000

Funding Source: Department of Energy

PROJECT SUMMARY

Project Title:	Fiber Composite Materials Technology for Flywheel Energy Storage*
Principal Investigator:	T. T. Chiao
Organization:	Lawrence Livermore National Laboratory P.O. Box 808, L-338 Livermore, CA 94550 Telephone: 415/422-9271
Project Goals:	This project has three goals: 1) screen and evaluate new materials applicable to future flywheels; 2) generate materials data for design, and 3) disseminate materials information to industry.
Project Status:	In the area of new materials screening, we have completed preliminary evaluation of two high performance reinforcing fibers. They look very promising for future flywheel use. Work on materials data generation for design and the publication of Composites Technology Review magazine have all been closed out because of funding limitations.
Contract Number:	W-7405-Eng-48
Contract Period:	October 1979 - September 1980
Funding Level:	$200,000.00
Funding Source:	U. S. Department of Energy

---

*Work performed under the auspices of the U. S. Department of Energy by the Lawrence Livermore National Laboratory under contract number W-7405-ENG-48.

PROJECT SUMMARY

Project Title: Composite Hybrid Flywheel Rotor Design Optimization and Fabrication

Principal Investigator: Anthony P. Coppa

Organization: General Electric Company
Space Systems Division
P.O. Box 8555, Philadelphia, PA 19101
(215) 962-4904

Project Goals: The design and fabrication of complete hybrid type composite flywheels are the principal goals of this program. It is required to furnish at least 10 prototype rotors having an operational energy storage capacity and life time of 0.25 kwh and 10^5 idealized spin-up, spin-down cycles. It is also required to furnish an additional 6 to 9 rotors to provide needed engineering test data regarding material properties and elevated temperature operation. Another goal is to contribute cost data to a comprehensive analysis of hybrid rotor large quantity production cost that is being done by another contractor.

Project Status: General Electric composite hybrid flywheels have been optimized and fabricated under Tasks 13-15 of this program. Specifically, the optimization has consisted in applying the results of previously performed spin evaluation and containment tests and additional material strength data to defining rotor designs that offer high combined rotor/containment energy density, durability and acceptably low cost.

The program has called for the fabrication of 14 complete hybrid rotors and five complete disk rotors. The hybrid rotors are designed to have a nominal capacity of 0.25 kwh at maximum operational speed and the disk rotors a capacity that ranges between 0.20 and 0.40 kwh at burst speed. Thus far all rotor components have been fabricated. One disk rotor, has already been spin-tested and has exhibited excellent laminate strength.

Contract Number: Subcontract No. 6624409

Contract Period: September, 1981 to October, 1982

Funding Level: $152,900

Funding Source: U.S. Department of Energy through Lawrence Livermore National Laboratory

PROJECT SUMMARY

Project Title: Assessment of Flywheel System Benefits in Selected Vehicle Applications

Principal Investigator: Lester Forrest

Organization: The Aerospace Corporation
El Segundo, California 90245

Project Goals: Assess the value of the flywheel as a range extender or energy conservation device in passenger car applications.

Project Status: The technical work on this project has been completed. The final report is in the process of publication. The major conclusions of the work are as follows.

Heat engine/flywheel automobiles can provide substantial fuel economy benefits for driving duty cycles in which the potential for braking energy recovery is large. The benefits are essentially constant over a wide range of rotor energy storage capacities. Parasitic losses constitute a relatively small part of total powertrain losses; therefore, technological advances in flywheel design alone do not appear to offer worthwhile incremental fuel economy gains. Flywheel spindown loss can have a significant effect on short-trip energy efficiency. Therefore, it appears that the smallest wheel meeting the power requirements of the driving cycle and capable of absorbing cycle-available braking energy would be an ideal selection for the implementation of a practical vehicle system.

Battery/flywheel vehicle designs incorporating new technology flywheel systems (hermetically sealed flywheel/generators) do not provide measurable benefits in range relative to near-term all-electric vehicles equipped with the same battery pack. Redesign of the flywheel/battery system to trade off power for increased energy density provides no range advantage over the all-electric vehicle equipped with the same redesigned batteries. Properly configured, however, the flywheel system will provide improved performance in the execution of short-duration road maneuvers such as standing-start acceleration, merging, and passing.

Contract Number: DE-AC08-79ET26306

Contract Period: 1 October 1979 through 31 July 1981

Funding Level: $199,500

Funding Source: U. S. Department of Energy

PROJECT SUMMARY REPORT

Project Title: Flywheel Evaluation at ORFEL

Principal Investigator: E. F. Babelay, Jr.

Organization: Union Carbide Nuclear Division
Oak Ridge Y-12 Plant
P.O. Box Y
Oak Ridge, TN 37830

Project Goals: The primary goal is to provide comprehensive evaluation of flywheel rotors supplied by the ORNL/MES program. The rotors will be evaluated for ultimate speed, fatigue life, and containment requirements according to the needs of the program.

Project Status: The completion of a fatigue life test of a composite flywheel fabricated by the General Electric Company has verified the cyclic test capability of ORFEL. The test demonstrated the fatigue life of this rotor was in excess of 1400 cycles. Ultimate speed evaluations were performed for three flywheels fabricated by Owens-Corning Fiberglas and the Lord Kinematic Corporation. An additional ultimate speed test was provided for a modified design of the General Electric flywheel.

The remainder of the year's activity will involve the balancing and testing of flywheels fabricated by General Electric and Garrett-AiResearch for ultimate energy storage and fatigue life. Studies designed to measure strain in the rotor at speed are expected to begin in September.

Contract Number: W-7405-eng-26

Contract Period: October 1981 — September 1982

Funding Level: $265,000

Funding Source: Department of Energy

PROJECT SUMMARY

Project Title:	Regenerative Braking Through Elastomeric Engery Storage
Principal Investigator:	Lyle O. Hoppie
Organization:	Eaton Corporation Engineering & Research Center 26201 Northwestern Highway P. O. Box 766 Southfield, MI 48037
Project Goals:	To improve the energy density and fatigue life of the elastomeric units through elastomer formulations and fabrication technique research, and to verify that a compact method of attachment is feasible in full-size units.
Project Status:	• Samples of a new compound have shown an improvement of 100 percent in energy density as compared with the previous compound. The energy density, hysteresis loss, and fatigue life of full-size units fabricated with this compound will be measured during this project. • Molding techniques commonly used within the rubber industry give rise to surface flaws on the finished energy storage units, and these surface flaws have been identified as sources of subsequent fatigue failure. A molding technique aimed at minimizing surface flaws will be investigated during this project. • Small-scale energy storage units were used to carry out a comparison of compact attachment concepts. One concept has been selected and will be incorporated into full-size units for test and evaluation during this project.
Contract-Number:	Union Carbide Corporation, Subcontract 86X-17482C
Contract Period:	June 1982 - March 1983
Funding Level:	$140,000
Funding Source:	U.S. Department of Energy through Oak Ridge National Laboratory

PROJECT SUMMARY

Project Title:	Electric Hybrid Vehicle Simulation
Principal Investigator:	Dan C. Pasma
Organization:	Eaton Corporation Engineering & Research Center 26201 Northwestern Highway P.O. Box 766 Southfield, MI 48037
Project Goals:	To evaluate electric hybrid vehicle design configurations to determine the most efficient combination of currently available components.
Project Status:	The project plan includes the development of six electric hybrid vehicle design configurations. A baseline electric vehicle (EV) model will serve as the base of comparison. Other configurations will include EVs with electrically and mechanically controlled flywheels, and an elastomeric regenerative braking system. Inherent in the development of the propulsion system models is the development of the system component models. Component model development has commenced with the evaluation of the HEAVY program hybrid vehicle components. Those components which can accommodate experimental data will be used as is while others will be modified, and new components developed as required. Component models which have been developed at Eaton Corporation during previous analysis work are currently being converted to HEAVY format, and a new elastomeric regenerative braking system component has been completed. The development of all components required for the analysis are scheduled to be completed in August, 1982. The development of the propulsion system models will begin in September, 1982.
Contract Number:	Subcontract 86X-17480C
Contract Period:	June, 1982 - December, 1982
Funding Level:	$161,694
Funding Source:	Department of Energy

PROJECT SUMMARY

Project Title:	The SERI Solar Energy Storage Program
Principal Investigator:	Werner Luft
Organization:	Solar Energy Research Institute 1617 Cole Boulevard Golden, Colorado 80401 (303) 231-1823
Project Goals:	The overall objective of this program is to gain a better understanding of advanced thermal energy storage and transport technologies and obtain information that allows developers to select the most promising thermal energy storage technologies. The emphasis of the program is on thermal energy storage for solar thermal power and process heat applications and on thermal energy transport. Research is performed on direct contact heat exchange, thermocline maintenance, and thermochemical storage and transport processes to provide a basis for the selection of these promising technologies. Studies are subcontracted to investigate new thermal energy storage concepts. Research is also conducted to improve the cost and performance of thermal energy transport concepts. Systems analyses identify thermal energy storage concepts for solar thermal applications.
Project Status:	Experiments have been performed for direct contact heat exchange between oil and salt hydrates and between molten salt and air. Analyses have been completed of the economic and technical potential of thermochemical energy storage and transport in a large thermal utility and of thermochemical transport in a distributed collector solar process heat system. Rankings have been completed of thermal storage concepts for the focused TESSTA development program. Analyses have been made of molten-salt-to-air/rock long duration storage for solar process heat, and experiments have been made on a raft method of thermocline maintenance. Subcontracted work has been completed by the University of Washington on molten slag storage, by Grumman Aerospace on direct contact latent heat storage, by Institute of Gas Technology on composite latent/sensible heat storage, by Eureka Laboratories on internal pipe insulation, and by Rensselaer Polytechnic Institute on photochemical hydrogen production catalyst synthesis.
Contract Number:	EG-77-C-01-4042
Contract Period:	October 1981-September 1982
Funding Level:	$1,400,000
Funding Source:	Department of Energy, Division of Energy Storage Technology

PROJECT SUMMARY

Project Title: Analyses of Thermal Storage Systems

Principal Investigator: R. J. Copeland

Organization: Solar Energy Research Institute
1617 Cole Boulevard
Golden, CO 80401
(303) 231-1012 (FTS 327-1012)

Project Goals: The objective of this project is to identify promising thermal storage concepts for research and development. The value of thermal storage concepts in solar thermal applications is analyzed to establish cost goals. Thermal storage concepts are compared to each other using a consistent costing approach and accounting for the performance differences between the concepts. The best concept for specific applications is recommended for continued development. Analyses of new concepts and applications are also given to identify promising areas for research.

Project Status: During FY 1982 analyses were conducted on thermal storage for solar thermal applications. An in-depth study evaluated potential thermal storage technologies for a liquid metal solar thermal receiver in an electric power application. Both promising and nonpromising concepts were identified. An assessment of an advanced, high-temperature molten salt concept (1110°C maximum) was completed and the concept was shown to be promising. An assessment of thermal storage in a double-effect absorption chiller with a parabolic-trough collector was completed; that system was also promising. An assessment of long-duration storage with a molten nitrate salt, solar thermal central receiver is in progress. A very high-temperature (up to 1400°C) thermal storage concept was identified.

Contract Number: EG-77-C-01-4042

Contract Period: October 1981 - September 1982

Funding Level: $174,600

Funding Source: Department of Energy, Office of Advanced Conservation Technologies

PROJECT SUMMARY

Project Title: Advanced, High-Temperature Molten Salt Storage

Principal Investigator: R. J. Copeland

Organization: Solar Energy Research Institute
1617 Cole Blvd.
Golden, CO 80401
(303) 231-1012, (FTS-327-1012)

Project Goals: The objective of this project is to research key issues in advanced, high-temperature molten salt thermal storage. Applications have been identified for maximum temperatures of 900° and 1100°C; the highest potential temperature is 1100°C. A multiphase project is being conducted. Initially, the 900°C case is being explored since it has lower risk; the 1100°C case will be emphasized in the latter phases.

Project Status: During FY 1982, research is being conducted on two of the key issues: an insulated floating platform (raft) and materials compatibility. The insulated raft floats between hot molten salt (900° to 1100°C) and cold molten salt in a thermocline thermal storage tank. Experiments are being conducted in a water thermocline to evaluate raft stability and performance. Structural and insulating materials are in close contact with the molten salts (NaOH, carbonates, or chlorides). Literature survey and experiments on materials compatibility are being performed.

Contract Number: EG-77-C-01-4042

Contract Period: February 1982 - September 1982

Funding Level: $133,900

Funding Source: Department of Energy

Project Summary

Project Title: Thermochemical Energy System Research

Principal Investigator: R. G. Nix

Organization: Solar Energy Research Institute
1617 Cole Boulevard
Golden, CO 80401
(303) 231-1757

Project Goals: The objective is to gain a better understanding of the use of reversible chemical reactions for energy storage and transport. Specifically, we intend to define the potential of thermochemical energy systems, define research opportunities and appropriate research programs.

Project Status: Work to date has evaluated the use of thermochemical reactions to store and transport energy in both large and small scale applications. The systems evaluated were those most prominent in the literature. Results indicated these systems were not generally cost-effective, but there were special cases of cost-effectiveness.

Present work is emphasizing definition of more cost-effective thermochemical systems and definition and evaluation of thermochemical systems for renewable liquid fuels production using solar energy input.

Contract Number: EG-77-C-01-4042

Contract Period: October 1981 - September 1982

Funding Level: $250 K

Funding Source: Department of Energy

PROJECT SUMMARY

Project Title: Direct-Contact Thermal Storage Research

Principal Investigator: Mark S. Bohn

Organization: Solar Energy Research Institute
1617 Cole Blvd.
Golden, CO 80401
(303) 231-1755

Project Goals: The objective of this task is to reduce the heat-transfer related costs of thermal energy storage systems by performing research on direct-contact heat exchange.

Project Status: Research is focused on heat exchangers employing direct contact between air and molten nitrate salts. Such devices have cost advantages over conventional indirect fin-tube heat exchangers. Analyses have been conducted to determine favorable operating conditions and to identify important parameters. An experimental apparatus is now being assembled that will allow measurement of heat-transfer coefficients as a function of packing type and flow ratios, and provide a tool for verifying or developing heat-transfer models.

The work on low-temperature, direct-contact latent heat storage in salt hydrates has been concluded. The problem of oil distribution was satisfactorily resolved, but we could not solve the problem of salt hydrate carryover with the oil phase. Because of the carryover problem and because latent heat storage in salt hydrates shows only small volume reduction and little potential for cost reduction as compared with a water tank, further research is not recommended in salt hydrate, direct-contact systems.

Contract Number: EG-77-C-01-4042

Contract Period: October 1981 - September 1982

Funding Level: $195,900

Funding Source: Department of Energy, Division of Energy Storage Technology

PROJECT SUMMARY

Project Title: Internally Insulated Pipe Systems for Long Distance Transport of Thermal Energy

Principal Investigator: Steve K. Leung

Organization: Eureka Laboratories, Inc.
215 - 26th Street
Sacramento, CA 95816
(916) 443-3932

Project Goals: The main purpose of this project is to evaluate the preliminary feasibility of internally insulated pipe systems for the transport of thermal energy over distances of 5 to 50 km. The specific objectives were to screen technologically feasible concepts, to determine the incremental cost relative to conventional externally insulated pipe, and to recommend areas requiring further research and development to commercialize the long distance transport of thermal energy.

Project Status: The tasks in this project include screening of internal insulation concepts, stress analysis, economic feasibility analysis and recommendations of additional research and development work. Based on preliminary analysis, two internally insulated systems with "evacuated superinsulation (ESI)" and calcium silicate, were found to be technically feasible, from a standpoint of pressure induced stresses and thermal losses. At steam temperature range of 600°-1000°F and pressure range of 600 to 1800 psi, the internal insulation cases are shown to provide less expensive transport of energy than both conventional and ESI externally insulated pipes. For high temperature water (HTW) at temperature ranges between 250°-450°F for similar power levels, internal insulation is marginally cost effective as compared to external cases, depending on the maintenance cost benefits associated with plastic pipe.

Based on these preliminary feasibility data, it was recommended that experimental work on these two internal insulation concepts be conducted.

Contract Number: XP-1-1081-1

Contract Period: July 1981 - August 1982

Funding Level: $68,062.00

Funding Source: Department of Energy

PROJECT SUMMARY

Project Title: High Temperature Integrated Thermal Storage for Solar Thermal Applications

Principal Investigators: Adam P. Bruckner and A. Hertzberg

Organization: Aerospace and Energetics Research Program
University of Washington FL-10
Seattle, WA 98195
(206) 543-6321

Project Goals: Investigate the technical and economic feasibility of a high temperature (~1650°K) solar thermal conversion and storage system utilizing molten glass or slag as the storage medium and direct contact heat transfer between this medium and a working gas in a droplet heat exchanger. Study thermophysical and chemical properties of glasses and slags as potential thermal storage media and refractory materials for storage vessel construction. Investigate methods of storage material handling and transport and develop 1-D two-phase flow model of direct contact heat exchange between falling slag droplets and counterflowing gas, including radiative effects. Develop capital, operating and maintenance cost data for a 1100 MW-hr storage baseline design and compare to 2nd generation thermal storage concepts, using constant thermal storage capacity as basis for comparison.

Project Status: A silicate slag of composition 50% SiO_2, 30% CaO, 20% MgO by weight has been selected as the storage material for the baseline design. This material has a low melting temperature, low viscosity, high heat capacity, high surface tension, low vapor pressure and low cost.

Fused-cast alpha-alumina (99.3% Al_2O_3) has been determined to be the most suitable refractory liner material for the storage vessel. It exhibits the highest resistance of any available refractory to corrosion by basic slags and offers a number of other desirable high temperature properties. A 1710 m^3 molten slag storage vessel similar to glass melting tanks has been designed.

A 1-D model of the direct contact droplet heat exchanger, including radiative effects, has been developed and used in parametric studies aimed at optimizing the reference design used in the economic studies.

The capital, operating and maintenance cost data are presently being finalized. Preliminary estimates place the energy-related unit capital cost for our system at $6/kW-hr.

Contract Number: SERI XP-0-9371-1

Contract Period: 15 April, 1981 - 14 August 1982

Funding Level: $51,734

Funding Source: Solar Energy Research Institute

PROJECT SUMMARY

Project Title: Chemical Storage of Light Energy

Principal Investigator: K. T. Potts

Organization: Rensselaer Polytechnic Institute
Department of Chemistry
Troy, New York 12181
(518) 270-6355

Project Goals: The main objective of this program is to develop new 2,2'-bipyridinyl ligands with long-chain, electron donating substituents in the 4,4'-positions and study their complexation with ruthenium for ultimate use as catalysts in the generation of hydrogen by photoreduction of water.

Project Status: The tasks in this program focus initially on the development of new, practical syntheses of 2,2'-bipyridinyl derivatives. Accomplishments to date include the synthesis and characterization of 2,2'-bipyridinyl containing 4,4'-bis(ethylthio) substituents, 4,4'-bis(tetradecanamido) substituents, and 4,4'-bis(tetradecylamino) substituents. Synthons useful for the construction of bipyridinyl derivatives have also been developed.

Contract Number: XP-1-1101-1

Contract Period: April 15, 1981 - August 26, 1982

Funding Level: $77,315

Funding Source: Midwest Research Institute
Solar Energy Research Institute

PROJECT SUMMARY

Project Title:	High Temperature Active Heat Exchanger Research for Latent Heat Storage
Principal Investigator:	J. Alario, R. Haslett, and R. Brown
Organization:	Grumman Aerospace Corporation Bethpage, NY 11714 (516) 575-2433/3924
Project Objectives:	The objective of this program is to develop a high-temperature direct-contact latent heat exchange thermal energy storage system by demonstration and test evaluation of a suitable scale model.
Project Status:	Under an initial DOE/NASA-Lewis contract a modular test unit of 10 kW heat transfer rate and 10 kW-hr storage was designed and fabricated to investigate heat transfer by direct contact between molten salt and a liquid metal eutectic carrier fluid. The concept selection, evaluation, and design phases of that program have been published in Topical Report No. NASA CR 159726 (January 1980). The test evaluation phase was interrupted due to various technical difficulties with the hardware (leaks and corrosion). This current project is a three-phase, follow-on program which includes inspection and redesign of the existing equipment (Phase I), fabrication/assembly and checkout (Phase II), and experimentation (Phase III). At this time, Phase I is complete and we are into the assembly and instrumentation tasks of Phase II. All technical work is expected to be finished by 31 October 1982.
Conctact Number:	XP-0-9383-1
Contract Period:	1 October 1981 - 31 January 1983 (16 months)
Funding Level:	$143,326
Funding Source:	Solar Energy Research Institute

PROJECT SUMMARY

Project Title: Molten Salt Thermal Energy Storage Subsystem Research Experiment

Principle Investigator: W. C. Peila

Organization: Sandia National Laboratories
Division 8453
Livermore, CA 94550

Subcontractor:

Martin Marietta Aerospace
Denver Aerospace
P.O. Box 179
Denver, CO 80201

Project Goals: To minimize the cost of a molten salt sensible heat storage for solar thermal plants and to resolve the uncertainties associated with the design, fabrication, operation, and performance of such a system.

Project Status: The program is complete. The final report will be published in September, 1982.

Contract No: 20-2988

Contract Period: October, 1980 - September 1982

Funding Level: $2,490,427

Funding Source: Sandia National Laboratories

PROJECT SUMMARY

PROJECT TITLE: Manufacture, Distribution and Handling of Nitrate Salts for Solar Thermal Applications.

PRINCIPAL INVESTIGATOR: L. C. Fiorucci
S. L. Goldstein

ORGANIZATION: OLIN CORPORATION
Chemicals Group
275 Winchester Avenue
New Haven, Ct. 06511
(203) 789-5210

PROJECT GOALS: The main objective of this investigation is to provide the potential user of sodium and potassium nitrate salts with information relevant to the availabilitv, transport, handling, safety aspects, charging, salt maintenance and disposal, and utilization of these salts for commercial-size solar central receiver applications. The quantities of salt required range from 20,000 lbs. for a 1 MW_t industrial process heat application to $250^t \times 10^6$ lbs. for a 300 MW_e stand alone electric power plant with 18 hours storage.

PROJECT STATUS: The tasks in this program include investigation of current manufacturing technologies for Na/K nitrate salts and the associated handling and storage practices. Also, included is a survey of current industrial safety practices involving the utilization of dry and molten salt. Various handling and transportation modes are investigated along with on-site storage and initial charging of the solar plant, with solar assist. Specific operational problems including plant start-up, shutdown, and line freeze up are addressed.

CONTRACT NO: Sandia 84-3878

CONTRACT PERIOD: June 1981 - December 1981.

FUNDING LEVEL: $94,579

FUNDING SOURCE: Department of Energy - Sandia National Labs.

PROJECT SUMMARY

Project Title: The ORNL Thermal Energy Storage Program

Principal Investigator: James F. Martin

Organization: Oak Ridge National Laboratory
P.O. Box Y, 9204-1, MS-3
Oak Ridge, TN 37830

Project Goals: The overall goal of the program is the development of advanced thermal energy storage technologies directed towards residential and commercial building heating and cooling and industrial applications. Research and development is conducted to develop effective, low cost thermal storage materials and subsystems for defined application areas. Systems utilizing both latent and sensible heat storage will be developed. Thermal energy sources include industrial process reject heat, utility waste heat, solar energy, and electricity available off-peak or at reduced demand.

Project Status: Twenty-six projects were active during FY 1982. Sixteen projects were completed and eight new projects were started. An assessment of heat pump storage for heating and cooling was completed. A class of combined latent and sensible heat storage media are under development for recovery and storage of waste heat from industrial kilns. Gas clathrates of Freon were identified as potentially attractive candidates for direct contact heat exchange media for heat pump cool storage at 7°C. Computer modeling of a "solar room" was utilized to establish design criteria for the development of a passive solar building material. Development of a material consisting of a hollow channel plastic sheet with a melting/freezing salt hydrate sealed in is in progress. The earth-assisted heat pump concept was experimentally evaluated and found to have favorable electric energy conservation potential for residential heating use. Electric storage furnace brick fabrication technology was brought to the technology transfer stage. Experimental assessments of installations representing membrane, labyrinth, and naturally stratified water storage were conducted.

Contract Number: W-7405-eng-26

Contract Period: Oct. 1981 - Sept. 1982

Funding Level: $2,500,000

Funding Source: Department of Energy, Division of Energy Storage Systems

PROJECT SUMMARY

Project Title: PERFORMANCE OF LABYRINTH-STRATIFIED WATER STORAGE SYSTEM FOR HEATING AND COOLING

Principal Investigator: Maurice W. Wildin

Organization: The University of New Mexico
Department of Mechanical Engineering
Albuquerque, New Mexico 87131

Project Goals: To monitor the performance of labyrinth-type stratified water storage tanks installed in the Mechanical Engineering Building at the University of New Mexico, with a view to demonstrating the utility of this concept and to improving the performance of this type of stratified water storage.

Project Status: The project is approaching completion. Data have been collected for approximately a year and a half, including two heating seasons, one cooling season and the intermediate seasons. Data collection for a second cooling season is currently under way. The feasibility of using thermally stratified water tanks for storing both heating and cooling capacity in a system that operates on a diurnal cycle has been clearly demonstrated. Relatively sharp thermoclines, usually about three feet thick, have been obtained in both heated and chilled water tanks both with and without internal partitions. Internal partitions have been found to be unnecessary to achieve stratification in our tanks, for either heated or cooled storage for normal flow rates, if the water flowing through storage is introduced and withdrawn carefully. Linear diffusers have been developed which serve satisfactorily as inlets or outlets. The results obtained to date are all for relatively large overall Richardson numbers of 5 or more. It is planned that results will be obtained for overall Richardson numbers down to the critical range of 0.25 to 0.4, before the project ends.

Data collection will be terminated in September, and a final report will be prepared by the end of calendar year 1982.

Contract Number: UCC, ND Subcontract No. 7967

Contract Period: October 1, 1980 through December 31, 1982

PROJECT SUMMARY (continued)

Funding Level: $102,384

Funding Source: U.S. Department of Energy through Oak Ridge National Laboratory

PROJECT SUMMARY

Project Title: Olivine Heat Storage Media

Principal Investigator: O. J. Whittemore

Organization: University of Washington, FB-10
Mining, Metallurgical & Ceramic Engineering Dept.
Seattle, WA 98195
(206) 543-2012

Project Goals: The objective of this project is to develop olivine bricks for off-peak storage units which bricks do not require firing and which are made of Washingon olivine.

Project Status: This project is essentially completed. Olivine brick were developed from Washington olivine utilizing from 1 to 3% of either of two sodium phosphates. When molded in a heavy-duty friction press, these brick had a density of 2.8 g/cm^3 in comparison with brick now being used with densities from 2.4 to 2.6 g/cm^3. Without firing and with only 1% of sodium phosphate addition, these bricks are as strong as bricks now being used.

Contract Number: W-7405-eng-26(ORNL/Sub.9063).

Contract Period: August 1, 1981 - September 30, 1982

Funding Level: $26,210.

Funding Source: Union Carbide Corporation, Nuclear Division

PROJECT SUMMARY REPORT

Project Title: Development of Chemically Bonded Ceramic Materials For Use In Thermal Energy Storage Devices

Principal Investigator: D. A. Brosnan

Organization: Materials Consultant Associates, Inc. (MCA)
P. O. Box 23
Pell City, AL 35125
(205) 338-7932

Project Goals: The objective of this program is to develop phosphate and calcium aluminate cement bonded ceramic materials based on North Carolina olivine which are capable of serving as the heat storage media in electric furnaces using the "off peak" power heating concept. These compositions will be "castable" refractories formed without the conventional step of powder pressing and cured at temperatures below 315°C which eliminates the conventional ceramic firing step which requires temperatures in the range of 1370-1480°C for olivine bricks.

Project Status: New binder technologies have been developed for use with N.C. olivines whereby phosphate bonded materials may be produced with cured densities of 2.20 g/cm^3 (138 lb/ft^3) which can withstand heating rates of 140°C/hr to 1200°C without appreciable thermal shock damage. Calcium aluminate cement bonded compositions with densities of 2.30 g/cm^3 also appear capable of similar heating rates. Experiments with "gap-graded" castable compositions show further improvements in bulk density and are expected to improve thermal shock properties of the various compositions. Additions of iron oxide rich minerals to the compositions have produced cured densities of 2.58 g/cm^3 which is similar to the density of commercial fired olivine bricks. These iron oxide rich compositions may have higher volumetric heat capacities than fired olivine bricks.

Tasks for FY83 include: (1) continued optimization of compositions, (2) determination of thermal properties, and (3) a component test program using commercial storage heaters.

Contract Number: 40X-16953V

Contract Period: December 1981 - August 1983

Funding Level: $39,035

Funding Source: U. S. Department of Energy

PROJECT SUMMARY

Project Title: Thermal Energy Storage Testing Facility

Investigator: Robert J. Schoenhals

Organization: Ray W. Herrick Laboratories
School of Mechanical Engineering
Purdue University
West Lafayette, IN 47907

Project Goals: Develop and evaluate apparatus and test procedures for establishing thermal performance of electrically heated thermal energy storage (TES) units. Provide technical information to assist ASHRAE in its effort to establish a standard for this purpose. Obtain test results for evaluating performance associated with particular TES unit configurations and energy storage materials.

Project Status: Laboratory apparatus and procedures for testing of central TES units were evaluated and improved. A 30 kW central TES unit was tested in a typical laboratory environment and also in an environmentally-controlled room in order to determine the influence of ambient air temperature and humidity variations on the test results. In addition, test results were used to compare the performance of domestic olivine energy storage bricks with that of the English- manufactured olivine bricks currently supplied for this particular central TES unit. Final test results are currently being obtained for a second set of domestic olivine bricks fabricated using an unfired process.

A calorimeter chamber was designed, constructed and instrumented. Improvements in the apparatus and in the test procedures were incorporated in order to yield test results of acceptable quality, as determined in accordance with an overall energy balance and also an error analysis. Eight different room-size TES units were tested using this facility. A study of the radiative and convective heat transfer contributions to the total thermal output of a unit during testing was performed. Test results were used to compare the performance of domestic olivine energy storage bricks with that of European magnesite bricks for two TES units. Thermocouple measurements were employed to explain the comparisons.

Contract Number: W-7405-eng-26 (ORNL/Sub-7961)

Contract Period: November 1, 1980 through August 15, 1982

Funding Level: $89,255

Funding Source: Union Carbide Corporation, Nuclear Division

PROJECT SUMMARY

Project Title: Heat Pump Cool Storage in a Clathrate of Freon

Principal Investigator: J. J. Tomlinson

Organization: Oak Ridge National Laboratory
Engineering Technology Division
P. O. Box Y
Bldg. 9204-1, MS-3
Oak Ridge, Tennessee 37830

Project Goals: The objective of this program is to develop a heat pump/cool storage system capable of load management and improved operating efficiencies as well. The cool storage mechanism under study exploits the energetics in formation of a gas hydrate or clathrate with water and a heat pump refrigerant. Advantage of the system include: (1) a phase-change temperature of 4-7°C (40-45°F), (2) heat of formation comparable to that of ice, and (3) effective heat transfer by direct contact.

Project Status: A comprehensive literature survey of prior work on gas hydrates has been completed. An experimental loop has been designed, constructed and initial testing begun. Clathrate formation was seen to occur in the 45-50°F range with little agitation. The experimental loop is being modified to allow better control and measurement of refrigerant/water inventory, operating conditions and agitation rates.

Contract Number: W-7405-eng-26

Contract Period: Continuing

Funding Level: In-House

Funding Source: Department of Energy

PROJECT SUMMARY

Project Title: Natural Thermal Stratification in Tanks

Principal Investigator: Roger L. Cole

Organization: Argonne National Laboratory
Solar Energy Group
9700 South Cass Avenue
Argonne, IL 60439
(312) 972-6230

Project Goals:

(1) Develop a mathematical model of stratification in vertical tanks.

(2) Measure thermal stratification of water in tanks.

(3) Publish guidelines for tank designers and manufacturers.

Project Status: The project has been completed. The final report Natural Thermal Stratification in Tanks: Phase 1 Final Report, Argonne National Laboratory Report ANL-82-5 is available from the National Technical Information Service.

Contract Number: 85379

Contract Period: March 1981 - February 1982

Funding Level: $110K

Funding Source: Department of Energy (Oak Ridge National Laboratory)

PROJECT SUMMARY

Project Title: Development of Heat Storage Building Materials for Passive Solar Applications

Project Manager: J.W. Fletcher

Organization: Lockheed Missiles & Space Co., Inc.
Huntsville Research & Engineering Center
4800 Bradford Drive
Huntsville, Alabama 35805
(205) 837-1800

Project Goals: The main objective of this project is to develop a heat storage building material to be used for passive solar applications and general load leveling within building spaces. Specifically, PCM-filled plastic panels are to be developed as wallboard and ceiling panels. Three PCMs ($CaCl_2 \cdot 6H_2O$; $Na_2SO_4 \cdot 10H_2O$; $LiNO_3 \cdot 3H_2O$) are to be evaluated for use in the double-walled, hollow-channeled plastic panels of approximately 1/4-in. thickness. Laboratory development of the panels will include determination of filling and sealing techniques, behavior of the PCMs, container properties and materials compatibility. Testing will include vapor transmission, thermal cycle, dynamic performance, accelerated life and durability tests. In addition to development and testing, an applications analysis will be performed for specific passive solar applications. Conceptual design of a single family passive solar residence will be prepared and performance evaluated.

Project Status: Screening of the three PCM candidates is essentially complete. The behavior of the three has been observed in the selected polypropylene panels, and calcium chloride hexahydrate has been determined to behave the best. Considerable problems were encountered with sealing of the panels, however, a satisfactory sealing technique (pressure-heat seal) has been developed for the prototype panels. As anticipated, the PCM behaved much more reliably with the channels oriented horizontally during preliminary thermal cycling tests. The test chamber design, instrumentation and data reduction techniques have been determined, construction and check-out of the test chamber have been completed and formal thermal cycling tests are to begin in August. Vapor transmission tests for the panels were begun in April and will continue throughout the study.

Contract Number: 86X17460C

Contract Period: March 1982 - May 1983

Funding Level: $160,000

Funding Source: DOE through Union Carbide Corporation

PROJECT SUMMARY

Project Title: Effect of Additives on Performance of Hydrated Salt TES Systems

Principal Investigator: Calvin D. MacCracken

Organization: Calmac Manufacturing Corporation
150 S. Van Brunt Street
P.O. Box 710
Englewood, NJ 07631
(201) 569-0420

Project Goals: The objectives of this contract were 1) to evaluate the recently developed CALOR Group(England) gel as a means of preventing stratification in 89F Glauber Salt and its 45F eutectic and also in 115F hypo salt, 2) to evaluate glycerine and ethylene glycol addition as a means to control crystal growth rate, size and fusion point, and 3) to evaluate the effect of pH on subcooling of 115F PCM.

Project Status: Completed. Final report submitted and approved.

Contract Number: 86X-70522V

Contract Period: April 1981 to March 1982

Funding Level: $90,207.00

Funding Source: Department of Energy, Oak Ridge National Laboratory

PROJECT SUMMARY

Project Title: Earth Thermal Storage-Assisted Heat Pump

Principal Investigator: Mark P. Ternes

Organization: Oak Ridge National Laboratory
Engineering Technology Division
P.O. Box Y
Bldg., 9204-1, MS-3
Oak Ridge, TN 37830
(615) 574-0749

Project Goals: The objective of this program is to quantify the seasonal improvements in the heat pump efficiency and the energy savings which would result if the heat pump used the heat or "cool" stored in the earth under a house with a crawl space.

Project Status: A controlled test involving three "identical", unoccupied houses was begun, and data was collected over most of the heating season. Results indicate that significant improvements are realizable, but that increased house loads caused by the concept partially negate the benefits obtained from the improved performance.

Summer data collection is underway and solutions to the heating load problem are being studied. Data collection over a second heating season is planned.

Contract Number: W-7405-eng-26

Contract Period: Continuing

Funding Level: In-House

Funding Source: Department of Energy

PROJECT SUMMARY

Project Title:	Thermal Energy Storage Systems for Industrial Process and Reject Heat Applications
Principal Investigator:	T. D. Claar
Organization:	Institute of Gas Technology IIT Center Chicago, Illinois 60616
Project Goals:	Research and development of advanced composite carbonate salt/ceramic media for high-temperature industrial process TES applications
Project Status:	Carbonate/ceramic composite powder processing, shape fabrication, and materials stability tests have been performed. Salt compositions Na_2CO_3-Li_2CO_3, Na_2CO_3-K_2CO_3, Na_2CO_3-$BaCO_3$, and Na_2CO_3 have been evaluated with candidate ceramic support materials. Selected Na_2CO_3-$BaCO_3$/MgO as model system for further development. Cold-pressed and sintered pellets demonstrated excellent salt retention and structural integrity during 500-hour thermal cycling tests. Evaluated die pressing, extrusion, and molten salt impregnation as media fabrication processes. Room- and elevated-temperature mechanical property measurements in progress. Designed TES test facility for packed-bed charge/discharge experiments. Facility construction is in progress.
Contract Number:	ORNL/UCC 86X-9500-1C
Contract Period:	May 1981 through September 1982
Funding Level:	$755,000
Funding Source:	U.S. Department of Energy through Oak Ridge National Laboratory

PROJECT SUMMARY

Project Title:	New Thermal Energy Storage Concept for Solar Thermal Applications
Principal Investigator:	R. J. Petri
Organization:	Institute of Gas Technology IIT Center Chicago, Illinois 60616
Project Goals:	Assess the technical and economic feasibility of utilizing composite latent/sensible TES media for solar thermal storage applications. Conduct composite processing and materials behavior experiments, and lab-scale TES proof-of-concept tests.
Project Status:	Selected and tested Na_2CO_3-$BaCO_3$ salt and MgO and $NaAlO_2$ ceramic supports for materials compatibility. Developed spray drying and die pressing processes for fabrication of composite media shapes. Composite Na_2CO_3-$BaCO_3$/MgO pellets demonstrated good performance and stability in lab-scale packed-bed thermal cycling experiments. Concept shows potential for reduction in TES system volume and cost, relative to state-of-the-art sensible-heat media.
Contract Number:	SERI XP-0-0371-2
Contract Period:	June 1981 - August 1982
Funding Level:	$59,779
Funding Source:	U.S. Department of Energy through Solar Energy Research Institute

PROJECT SUMMARY

Project Title:	Application of Thermal Energy Storage to Process Heat Recovery, Phase III, Heat Exchanger Evaluation
Principal Investigator:	L. B. Katter
Organization:	Rocket Research Company 11441 Willows Road Redmond, Washington 98052
Project Goals:	The overall goals of the Phase III Heat Exchanger Evaluation are to develop data which will enable the design of a heat exchanger suitable for long-term continuous operation in the aluminum plant pollution control system environment and to assure that the installation of such a device will have no negative impact upon the existing processes.
Project Status:	The project is currently into the third phase of a four-phase program. First phase, Preliminary Investigation, and second phase, Technical and Economic Analyses, have been completed. A series of tests starting with small-scale experiments and expanding in magnitude to a production prototype is currently in process. The smallest scale testing is complete. Information gathered has been used to define a subscale heat exchanger. The subscale heat exchanger has been fabricated and installed and is currently being tested.
Contract Number:	86 X-61624C
Contract Period:	February 1, 1980 - May 31, 1984
Funding Level:	$1,277,488 (FY 1982)
Funding Source:	U.S. Department of Energy through Oak Ridge National Laboratories

PROJECT SUMMARY

Project Title: Identify Generic Thermal Energy Storage (TES) Needs for Industrial Applications

Principal Investigator: Donald R. Glenn

Organization: The Decision Research Group, Inc.
9101 Parliament Drive
Burke, Virginia 22015
(703) 978-1862

Project Goals: Based on the numerous studies of industrial applications for thermal energy storage, where real-time energy analyses were determined/synthesized/measured, derive patterns of thermal energy flows, mass flow and temperatures that might indicate common parametric relationships. Reconcile the available data and derive "standardized" TES conceptual designs using off-the-shelf equipment/techniques. Establish economic performance baseline(s) from which advanced TES systems can be compared.

Project Status: The tasks include reviewing previous applications studies, and other relevant reports where detailed energy flow data are provided, tabulate process thermal energy parameters and determine where commonality exists relative to process dynamics, conceptuali a baseline TES design capable of enveloping these applications, and finally, financially evaluate projected energy savings potentials, breakeven costs and markets(location and size estimates).

The first two tasks are completed and a second round of data reviews are underway to extend the review coverage to a larger portion of industrial processes. There are indications that a major segment of these processes can be equipped with modules of two fundamental design approaches/temperature levels; one operating between 750°-1000°F, and a second at 1000° - 1500°F. To cover the variety of process flow rates, each installation is expected to be satified by combinations of two basic sizes/capacities.

Contract Number: 86X-17459V

Contract Period: February 1982 - September 1982

Funding Level: $14,500

Funding Source: Oak Ridge National Laboratory/Union Carbide Corp.

PROJECT SUMMARY

Project Title: Analysis of Thermal Energy Storage in a Public School Facility in North Carolina

Principal Investigator: Tony W. Sigmon

Organization: Research Triangle Institute
Energy Systems Department
P. O. Box 12194
Research Triangle Park, North Carolina 27709
919/541-5878

Project Goals: To determine the performance characteristics of the TES system through an analysis of on-site operational data and to use this information to provide a broad guide for similar applications.

Project Status: The system under consideration consists of an electric chiller, electric boiler and two above-ground water thermal storage tanks. The system supplies space heating and cooling and domestic hot water to the school.

The study is currently in the eighth month of a twelve-month monitoring program. Prior efforts have included: (1) specification of data acquisition needs, (2) installation and check-out of data acquisition hardware, (3) development of data analysis software, and (4) continual monitoring of the system and analysis of data since January, 1982.

Preparations are now being made to restart the TES system for the beginning of the school year. This includes check-out of all monitoring equipment and making suggestions to school personnel that should improve the system's overall performance.

Contract Number: 62B-1385C

Contract Period: 5/81 - 5/83

Funding Level:
1. $51,883
2. $150,000

Funding Source:
1. U.S. Department of Energy
2. North Carolina Alternative Energy Corporation

PROJECT SUMMARY

Project Title:	Evaluation of Stratified Thermal Storage System for Oliver Springs Elementary School
Principal Investigators:	R. L. Reid and A. F. G. Bedinger
Organization:	The University of Tennessee Energy, Environment, and Resources Center 327 South Stadium Hall Knoxville, TN 37916 (615) 974-4251
Project Goals:	Determine estimated electrical demand savings potential of the TES using measured total building electric power consumption and measured cooling load. Determine tank efficiency for a cold tank and a hot tank and experimentally develop a tank temperature versus time profile for a hot tank and a cold tank. Determine by measurement and calculation the source of the thermal losses for hot water storage and the thermal gains for chilled water storage. These losses or gains can be categorized as either related to heat transfer through the tank walls or through the membrane.
Project Status:	Data collection will be terminated my mid-July 1982. Data reduction and writing of the final report will take place during the remainder of the contract period.
Contract Number:	7685 (Project Authorization X60)
Contract Period:	June 1, 1980, through August 31, 1982
Funding Level:	$110,506
Funding Source:	Union Carbide Corporation Nuclear Division

PROJECT SUMMARY

Project Title: Mathematical Modeling of TES Subsystems

Principal Investigator: A. D. Solomon

Organization: Mathematics and Statistics Research Department
Computer Sciences
Union Carbide Corporation, Nuclear Division
P. O. Box Y, Building 9704-1
Oak Ridge, Tennessee 37830
(615) 574-8696

Project Goals: To develop and apply mathematical methods to the solution of problems arising from the mathematical modeling of TES subsystems. This includes the development of analytical and approximate models, numerical simulations and other techniques of engineering and applied mathematics.

Project Status: At the present time we have taken the direction of moving towards the simulation of more realistic systems, using earlier results concerning the moving boundary problem and phase change heat transfer. During the past year, in this spirit, we have developed simulation models for passive systems incorporating phase change materials in various modes. Among other results has been the quantitative validation of the PCM concept for passive solar houses, to the extent justified by the modeling already done. The tools used have included earlier derived approximations and the full simulation tools available from finite difference calculations. Present plans call for extension of the simulation tool to increasingly realistic systems, and to the derivation of engineering "rules of thumb" for complex systems.

Contract Period: October 1981 - September 1982

Funding Source: Department of Energy

PROJECT SUMMARY

Project Title: Modeling the Moving Boundary Problem for TES with PCMs

Principal Investigator: Ralph M. Deal

Organization: Chemistry Department
Kalamazoo College
Kalamazoo, Michigan 49007

Project Goals: Experimental and theoretical modelling of the moving boundary problem in phase change materials used in thermal energy storage.

Project Status: Three phases have been completed.

Implementation of a simple graphics demonstration of temperature profiles for a melting PCM based on both an analytical solution and a Budak numerical solution for a one-dimensional slab.

The determination of the range of validity and optimal parameter criteria for the use of the Budak method for modeling heat transfer in PCMs.

Construction of a loop to control the temperature of one face of a 4"x4"x4" cell containing a PCM.

The fourth phase is being completed. Testing with that cell the feasibility of a simple method for measuring thermal gradients in the liquid portion of a PCM undergoing freezing/melting. The data will be tested against various models.

Contract Number: UCND 9038

Contract Period: April 1, 1981 through September 30, 1982

Funding Level: $41,613

Funding Source: U.S. Department of Energy through Oak Ridge National Laboratory

PROJECT SUMMARY

Project Title: Basic Chemical Studies Related to Low Temperature Thermal Energy Storage. Task I: Thermodynamic Properties and Interactions of Salt Hydrates Used as Phase Change Materials

Principal Investigator: J. Braunstein

Organization: Oak Ridge National Laboratory
Chemistry Division
P. O. Box X
Oak Ridge, TN 37830
(615) 574-5032

Project Goals: The purpose of this task is to critically review the state-of-the-art of salt hydrates as phase change materials. Areas for review include phase equilibria, nucleation and melting kinetics of the commonly used hydrates (e.g., $Na_2SO_4 \cdot 10H_2O$, $Na_2S_2O_3 \cdot 5H_2O$, $CaCl_2 \cdot 6H_2O$, $MgCl_2 \cdot 6H_2O$) with the objective of identifying research that would result in more practicable use of these materials.

Project Status: A survey of the literature has been made and a list of recommended basic chemical research has been prepared.

Contract Number: W-7405-eng-26

Contract Period: November 1981 - June 1982

Funding Level: In House

Funding Source: DOE

PROJECT SUMMARY

Project Title: New Physical-Chemical Reactions Useful for TES*

Principal Investigator: James S. Johnson, Jr.

Organization: Oak Ridge National Laboratory
P. O. Box X
Oak Ridge, TN 37830
(615) 574-4982

Project Goals: New options in materials for heat storage is the aim of the program. Chemical systems, including those having equilibria with high temperature coefficients, are tested by differential scanning calorimetry for evidence of enhanced heat capacity. The approach is high-risk and exploratory, and in the search for new classes of storage systems, relatively little weight is given the costs of members of the classes that are at present apparent.

Project Status: Several possibilities have been tested in a preliminary way. These include concentrated aqueous solutions of a hydrolyzable metal ion; aqueous solutions of polyethylene oxide-polypropylene oxide polymers, which when cross-linked take up or eject water in temperature cycles; and soluble partially fluorinated organic compounds, in hope that hydrates might be formed and be "melted" in temperature ranges of interest (analogous to clathrates). Certain petroleum ester waxes have also been tested. No promising embodiments have been found so far, but the survey is too incomplete as yet to rule any out.

Contract Number: W-7405-eng-26

Contract Period: January 1982 - September 1982

Funding Level: $50,000

Funding Source: Department of Energy

*Research sponsored by the Division of Energy Storage, U. S. Department of Energy, under contract W-7405-eng-26 with Union Carbide Corporation

REVIEW COMMITTEE

Mr. Frank Biancardi	United Technologies Research Center
Mr. James Calogeras	NASA Lewis Research Center
Mr. Rudolph Duscha	NASA Lewis Research Center
Mr. Elihue Fein	Futures Group Inc.
Mr. Mitch O. Hoenig	Francis Bitter National Magnet Laboratory
Mr. Howard E. Lowitt	Energetics Inc.
Mr. Marvin Malik	General Motors Corporation
Prof. George R. Newkome	Louisiana State University
Mr. Ernest G. Rodriguez	NASA Goddard Space Flight Center
Dr. Neilson Rudd	Consultant
Mr. C. J. Swet	Consultant
Mr. J. Brian Taylor	National Research Council of Canada
Dr. Charles E. Wyman	Badger Company Inc.

August 26, 1982

U.S. DOE PHYSICAL AND CHEMICAL ENERGY STORAGE

ANNUAL CONTRACTORS' REVIEW MEETING

Arlington, Virginia
August 23-26, 1982

Final Participant List

ALARIO, Joseph
Grumman Aerospace Corporation
M.S. B09-25
Bethpage, New York 11714
516/575-2433

ARGABRIGHT, Theresa A.
Solar Turbines Incorporated
P.O. Box 80966/Mail Zone R-1
San Diego, California 92138
714/288-6787

ASBURY, Joseph G.
Argonne National Laboratory
9700 South Cass Avenue
Argonne, Illinois 60439
312/972-3776

BELLER, Morris
Brookhaven National Laboratory
Building 475
Upton, New York 11973
516/282-2041

BESENBRUCH, G. E.
General Atomic Company
P.O. Box 81608
San Diego, California 92138
714/455-3079

BIANCARDI, Frank
United Technological Research Center
East Hartford, Connecticut 06108
203/723-7234

BONNER, Michael F.
Brookhaven National Laboratory
Building 120
Upton, New York 11973
516/282-3340

BRETT, C. Everett
The University of Alabama
Box 6282
University, Alabama 35486
205/348-4520

BROSNAN, Denis A.
MCA, Inc.
P.O. Box 23
Pell City, Alabama 35125
205/338-7932

BROWN, Daryl R.
Battelle Pacific Northwest Laboratories
P.O. Box 999
Richland, Washington 99352
509/376-4453

BRUCKNER, Adam P.
University of Washington, FL-10
Seattle, Washington 98195
206/543-6321

BURDICK, Patricia
Owens-Corning Fiberglas Technical Center
Box 415
Granville, Ohio 43023
614/587-8052

BURKE, Ken
Life Systems, Inc.
24755 Highpoint Road
Cleveland, Ohio 44122
216/464-3291

CALOGERAS, James E.
NASA Lewis Research Center
21000 Brookpark Road
Cleveland, Ohio 44135
216/433-4000, ext. 5215

CHANG, Ji Young
Westinghouse ARD
P.O. Box 158
Madison, Pennsylvania 15663
412/722-5471

CLAAR, Terry D.
Institute of Gas Technology
3424 S. State Street
Chicago, Illinois 60616
312/567-3672

CLARK, E. Charles
Rocket Research Company
11441 Willows Road
Redmond, Washington 98052
206/885-5000

CLINCH, Dr. J. Michael
Argonne National Laboratory
9700 S. Cass Avenue
Argonne, Illinois 60439
312/972-7693

COPELAND, Robert J.
SERI
1617 Cole Boulevard
Golden, Colorado 80401
303/231-1012

COPPA, Anthony P.
General Electric Company
Space Systems Division
M1223, VFSC, P.O. Box 8555
Philadelphia, Pennsylvania 19101
215/962-4904

DEHART, Arnold O.
General Motors Research Laboratories
GM Technical Center
Warren, Michigan 48090
313/575-3057

DOHERTY, T. J.
Battelle Northwest Laboratories, Inc.
P.O. Box 999
Richland, Washington 99352
509/375-3924

DUSCHA, Rudolph A.
NASA Lewis Research Center
21000 Brookpark Road
Cleveland, Ohio 44135
216/433-4000, ext. 5241

EDWARDS, Dick
Science Applications
1710 Goodridge Drive
McLean, Virginia 32102
703/821-4517

EGAN, Gregory J.
Ergenics Division MPD Tech. (INCO)
681 Lawlins Road
Wyckoff, New Jersey 07481
201/891-9103

ENGLAND, Christopher
Engineering Research Group
178 Vista Circle Drive
Sierra Madre, California 91024
213/355-2415

ESCHER, William J. D.
E. F. Technology, Inc.
P.O. Box 189
St. Johns, Michigan 48879
517/224-3268

FARQUHAR, Oswald C.
Dept. of Geology and Geography
University of Massachusetts
Amherst, Massachusetts 01003
413/545-2286

FEIN, Elihu
The Futures Group
76 Eastern Boulevard
Glastonburry, Connecticut 06033
203/633-3501

FIORUCCI, L. C.
Olin Chemicals Group
275 Winchester Avenue
New Haven, Connecticut 06511
203/789-5210

FLETCHER, James
Lockheed Missiles & Space Co., Inc.
4800 Bradford Drive
Huntsville, Alabama 35805
205/837-1800

FORREST, Lester
The Aerospace Corporation
P.O. Box 92957
Los Angeles, California 90009
213/648-5752

FOSSUM, Dr. Arlo F.
RE/SPEC Inc.
P.O. Box 725
Rapid City, South Dakota 57709
605/394-6400

GIESE, Robert F.
Argonne National Laboratory
9700 South Cass Avenue
Argonne, Illinois 60439
312/972-3282

GLENN, Donald R.
The Decision Research Group, Inc.
9101 Parliament Drive
Burke, Virginia 22015
703/978-1862

GODFREY, R. D.
Owens Corning Fiberglas
Technical Center
Granville, Ohio 43023
614/587-7085

GORSKI, Anthony J.
Argonne National Laboratory
9700 South Cass Avenue
Argonne, Illinois 60439
312/972-6237

GROSS, Robert J.
Sandia National Laboratories
Division 5513
P.O. Box 5800, Kirtland AFB East
Albuquerque, New Mexico 87115
505/846-0753

GUREVICH, Michael
U.S. Dept. of Energy
1000 Independence Avenue, S.W.
Washington, D.C. 20585
202/252-1507

GYUK, Imre
U.S. Department of Energy
1000 Independence Avenue, S.W.
Washington, D.C. 20585
202/252-1508

HAUER, John F.
Bonneville Power Administration
P.O. Box 3621
Portland, Oregon 97208
503/230-3904

HOENIG, Mitchell O.
MIT - Plasma Fusion Center
Building NW16-176
Cambridge, Massachusetts 02139
617/253-5503

HOLBROOK, John H.
Battelle Columbus Laboratories
505 King Avenue
Columbus, Ohio 43201
614/424-4357

HURWITCH, Jonathan W.
Battelle Washington Operations
2030 M Street, N.W.
Washington, D.C. 20036
202/785-8400

ISTVAN, John A.
PB-KBB, Inc.
P.O. Box 19672
Houston, Texas 77024
713/496-5590

JACKSON, A. W.
Brookhaven National Laboratory
444 North Capitol Street, Suite 611
Washington, D.C. 20001
202/376-4042

KANNBERG, Landis D.
Battelle Northwest Laboratories
P.O. Box 999
Richland, Washington 99352
509/375-3919

KOVACH, Andy
Life Systems, Inc.
24755 Highpoint Road
Cleveland, Ohio 44122
216/464-3291

KRISHNAN, Gopala
SRI International
333 Ravenswood Avenue
Menlo Park, California 94025
415/859-2627

KULKARNI, Dr. S. V.
Lawrence Livermore Laboratories
P.O. Box 808, L-338
Livermore, California 94550
415/422-7128

KWAN, Quon Y.
The Aerospace Corporation
955 L'Enfant Plaza, S.W.
Washington, D.C. 20024
202/488-6081

LANE, George A.
Dow Chemical Company
1776 Building 1
Midland, Michigan 48640
517/636-0292

LEUNG, Steve K.
Eureka Laboratories, Inc.
215 26th Street
Sacramento, California 95816
916/443-3932

LOWITT, Howard E.
Energetics, Inc.
2000 Century Plaza
Columbia, Maryland 21044
301/992-4000

LUCCI, Armando D.
Rockwell International Corp.
Rocketdyne Division
6633 Canoga Avenue
Canoga Park, California 91304
213/710-3460

LUFT, Werner
SERI
1617 Cole Boulevard
Golden, Colorado 80401
303/231-1823

MACCRACKEN, Calvin D.
Calmac Manufacturing Corporation
Box 710
Englewood, New Jersey 07631
201/569-0420

McBREEN, James
Brookhaven National Laboratory
Upton, New York 11973
516/286-4513

McCHESNEY, H.R.
United Technologies Research Center
M.S. 79, Silver Lane
East Hartford, Connecticut 06108
203/727-7340

McELROY, James F.
General Electric Company
50 Fordham Road
Wilmington, Massachusetts 01887
617/657-5277

MALIK, Marvin J.
General Motors Corporation
Engineering Staff Building
G.M. Technical Center
Warren, Michigan 48090
313/575-1239

MARKSBERRY, Lynn
FluiDyne Engineering Corporation
5900 Olson Memorial Highway
Minneapolis, Minnesota 55422
612/544-2721

MARTIN, James F.
Oak Ridge National Laboratory
Box Y
Oak Ridge, Tennessee 37830
615/576-3977

MEZZINA, Alessio
Brookhaven National Laboratory
Building 120
Upton, New York 11973
516/282-3920

MICHAELS, Allan I.
Argonne National Laboratory
9700 South Cass Avenue
Argonne, Illinois 60439
312/972-7785

MILLER, Barry L.
Bonneville Power Administration
1002 N.E. Holladay Street
P.O. Box 3621
Portland, Oregon 97236
503/230-3750

MIYASE, Dr. A.
University of Ottawa
Dept. of Mechanical Engineering
Ottawa, Ontario, Canada K1N 6N5
613/231-5730

MOLZ, Fred J.
Auburn University
Auburn, Alabama 36849
205/826-4326

MURRAY, John N.
Teledyne Energy Systems
110 West Timonium Road
Timonium, Maryland 21093
301/252-8220, ext. 303

NANNELLI, Piero
Pennwalt Corporation
900 First Avenue
King of Prussia, Pennsylvania 19406
215/337-6737

NEWKOME, George R.
Louisiana State University
Department of Chemistry
Baton Rouge, Louisiana 70803
504/388-2479

NIX, R. G.
SERI
1617 Cole Boulevard
Golden, Colorado 80401
303/231-1757

O'CONNELL, Lawrence C.
Lawrence Livermore National Laborator
P.O. Box 808
Livermore, California 94550
415/422-6419

OLSZEWSKI, Mitchell
Oak Ridge National Laboratory
P.O. Box Y
Oak Ridge, Tennessee 37830
615/574-0770

OSBURN, Jack
Doty Associates, Inc.
451 Hungerford Drive
Rockville, Maryland 20850
301/424-0270

OWEN, Dr. Lawrence B.
Terra Tek Research
420 Wakara Way
Salt Lake City, Utah 84108
801/584-2424

PASMA, Dan C.
Eaton Corporation
26201 Northwestern Highway
Southfield, Michigan 48037
313/354-6924

PEILA, Bill
Sandia Laboratories Livermore
P.O. Box 969, Div. 8453
Livermore, California 94550
415/422-2326

RABL, Veronika A.
EPRI
P.O. Box 10412
Palo Alto, California 94303
415/855-2401

RAYMOND, John R.
Battelle Northwest Laboratories
P.O. Box 999
Richland, Washington 99352
509/375-3929

REEVES, Robert R.
RPI/DOE
Rensselaer Polytechnic Institute
Troy, New York 12181
202/252-1503

RODRIGUEZ, G. Ernest
Goddard Space Flight Center/NASA
Code 711.2
Greenbelt, Maryland 20770
301/344-5541

ROESLER, Wilfrod J.
Johns Hopkins University
Applied Physics Laboratory
Johns Hopkins Road
Laurel, Maryland 20707
301/953-7100

ROGERS, John D.
Los Alamos National Laboratory
MS-D464
Los Alamos, New Mexico 87545
505/667-5427

ROHY, David A.
Solar Turbines, Inc.
P.O. Box 80966
San Diego, California 92138
714/238-5604

ROSE, Kathleen J.
Rockwell International Corporation
Rocketdyne Division
6633 Canoga Avenue
Canoga Park, California 91304
213/710-3070

ROSENZWEIG, Sol
The Aerospace Corporation
955 L'Enfant Plaza, S.W., Suite 4000
Washington, D.C. 20024
202/488-6192

ROSSO, Matt
Ergenics
681 Lawlins Road
Wyckoff, New Jersey 07481
201/891-9103

RUBY, Stan
U.S. Department of Energy
1000 Independence Avenue, S.W.
Room 1G066
Washington, D.C. 20585
202/252-1486

RUDD, Neilson
P.O. Box 176
Put-In-Bay, Ohio 43456
419/285-7001

RUFFINI, Alan
Rensselaer Polytechnic Institute
Department of Chemistry
Troy, New York 12181
518/250-6355

SCHAETZLE, Walter J.
W. J. Schaetzle & Associates, Inc.
P.O. Box 1523
Tuscaloosa, Alabama 35403
205/339-9587

SCHLUTER, Georg
General Atomic Company
P.O. Box 81608
San Diego, California 92138
714/455-3079

SCHOENHALS, Prof. Robert J.
School of Mechanical Engineering
Purdue University
West Lafayette, Indiana 47907
317/494-5626

SCHUBERT, Franz
Life Systems, Inc.
24755 Highpoint Road
Cleveland, Ohio 44122
216/464-3291

SCOTT, Dr. David S.
Mechanical Engineering
University of Toronto
5 King's College Road
Toronto, Ontario, Canada M5S 1A4
416/591-9367

SHAW, David
Rocket Research Company
11441 Willows Road
Redmond, Washington 98052
206/885-5000, ext. 495

SHEFT, Irving
Argonne National Laboratory
9700 S. Cass Avenue
Argonne, Illinois 60439
312/972-3522

SHIVERS, Rufus W.
U.S. Department of Energy
CE 141, Energy Storage Division
Washington, D.C. 20545
202/252-1476

SIGMON, Tony W.
Research Triangle Institute
P.O. Box 12194
Research Triangle Park,
North Carolina 27709
919/541-5878

SILVERSTEIN, Calvin C.
CCS Associates
P.O. Box 563
Bethel Park, Pennsylvania 15102
412/221-0999

SIMPSON, W. A., Jr.
Oak Ridge National Laboratory
P.O. Box X, Bldg. 45005
Oak Ridge, Tennessee 37830
615/574-4421

SKAPERDAS, George
Brookhaven National Laboratory
Building 120
Upton, New York 11973
516/282-2123

STANDLEY, Warren
TRW Energy Development Group
8301 Greensboro Drive
McLean, Virginia 22102
703/734-6412

STEELE, R. S.
Union Carbide Corporation
Nuclear Division
P.O. Box Y
Oak Ridge, Tennessee 37830
615/574-1838

STRICKLAND, Gerald
Brookhaven National Laboratory
Building 120
Upton, New York 11973
516/282-4091

SUNDLOF, Bertil
VBB AB Stockholm/Royal Institute
of Technology
Hagagatan 28
S-11347, Stockholm, Sweden

SUPKOW, Donald J.
Dames & Moore
6 Commerce Drive
Cranford, New Jersey 07016
201/272-8300

SWET, C. J.
7040 Woodville Road
Mt. Airy, Maryland 21771
301/831-7446

SWISHER, James H.
U.S. Department of Energy
Washington, D.C. 20858
202/252-1488

TANTON, Thomas F.
Eureka Laboratories, Inc.
215 26th Street
Sacramento, California 95816
916/443-3932

TAYLOR, Dr. J. B.
National Research Council of Canada
M-12, Montreal Road
Ottawa, Ontario, Canada K1A 0R9
613/993-2506

THOMS, Robert L.
Institute for Environmental Studies
Louisiana State University
Baton Rouge, Louisiana 70808
504/388-8521

TOMLINSON, John J.
Oak Ridge National Laboratory
P.O. Box Y
Oak Ridge, Tennessee 37830
615/574-0768

TOPPER, Leonard
2126 Connecticut Avenue, N.W.
Washington, D.C. 20008
202/234-5984

TSANG, Chin Fu
Lawrence Berkeley Laboratory
Earth Sciences Division
90/1106
Berkeley, California 94720
415/486-5782

WALTON, Matt
Minnesota Geological Survey
1633 Eustis Street
St. Paul, Minnesota 55108
612/373-3372

WHEELER, K. R.
Battelle Pacific Northwest Lab.
P.O. Box 999
Richland, Washington 99352
509/376-0830

WHITTEMORE, O. J.
University of Washington
Ceramic Engineering, FB 10
Seattle, Washington 98195
206/543-2012

WILDIN, Maurice W.
The University of New Mexico
Albuquerque, New Mexico 87131
505/277-6280

WILKINSON, William O.
Johns Hopkins University
Applied Physics Laboratory
11100 Johns Hopkins Road
Laurel, Maryland 20707
301/953-7100

WRIGHT, John D.
Solar Energy Research Institute
1617 Cole Boulevard
Golden, Colorado 80401
303/231-1756

WYMAN, Charles E.
Badger Co., Inc.
P.O. Box 119
E. Weymouth, Massachusetts 02189
617/337-6750

* U.S. GOVERNMENT PRINTING OFFICE 1982 381-060/4118

UNITED STATES
DEPARTMENT OF ENERGY
WASHINGTON, D.C. 20585

OFFICIAL BUSINESS
PENALTY FOR PRIVATE USE, $300

POSTAGE AND FEES PAID
U.S. DEPARTMENT OF ENERGY
DOE 350